

APPENDIX C

DATA TABULATION

Rev. 0

C.1 RADIONUCLIDE SCREENING AND TRIGGER LEVEL RESULTS

The screening calculations and trigger levels determined for each vault type at the EAV disposal facility are provided in Tables C.1-1 through C.1-4.

Table C.1-1. Screening calculations and trigger levels for the ILT vaults

Nuclide	T1/2 (year)	DCF (mrem/pCi)	Lambda (1/year)	Kd (cm**3/gm)	Rf	ILT GW Trigger (Ci/vault)	ILT Int Trigger (Ci/vault)
H-3	1.23e+01	6.3e-08	5.62e-02	0	1	1.3e+01	2.2e-01
Be-7	1.47e-01	1.1e-07	4.72e+00	0	1	>1E20	>1E20
Bc-10	1.60e+06	4.2e-06	4.33e-07	0	1	5.2e-04	8.0e-04
C-11	3.86e-05	1.2e-08	1.80e+04	2	11	>1E20	>1E20
C-14	5.73e+03	2.1e-06	1.21e-04	2	11	1.2e-02	8.1e-04
F-18	2.14e-04	1.0e-04	3.25e+03	0	1	>1E20	>1E20
Na-22	2.58e+00	1.2e-05	2.69e-01	0	1	3.3e+08	3.7e+08
Na-24	1.71e-03	1.4e-06	4.05e+02	0	1	>1E20	>1E20
Mg-28	2.40e-03	7.5e-06	2.89e+02	0	1	>1E20	>1E20
Al-26	7.40e+05	1.3e-05	9.37e-07	0	1	1.7e-04	8.0e-04
Si-31	2.99e-04	5.4e-07	2.32e+03	0	1	>1E20	>1E20
Si-32	6.50e+02	1.7e-06	1.07e-03	0	1	1.4e-03	8.9e-04
P-32	3.89e-02	7.7e-06	1.78e+01	0	1	>1E20	>1E20
P-33	6.84e-02	8.8e-07	1.01e+01	0	1	>1E20	>1E20
S-35	2.39e-01	4.3e-07	2.90e+00	0	1	>1E20	>1E20
Cl-36	3.01e+05	3.0e-06	2.30e-06	0	1	7.3e-04	8.0e-04
Cl-38	7.07e-05	2.0e-07	9.80e+03	0	1	>1E20	>1E20
Cl-39	1.06e-04	1.4e-07	6.57e+03	0	1	>1E20	>1E20
K-40	1.28e+09	1.9e-05	5.42e-10	0	1	1.2e-04	8.0e-04
K-42	1.41e-03	1.1e-06	4.92e+02	0	1	>1E20	>1E20
K-43	2.56e-03	7.8e-07	2.71e+02	0	1	>1E20	>1E20
K-44	4.18e-05	1.5e-07	1.66e+04	0	1	>1E20	>1E20
K-45	3.04e-05	9.3e-08	2.28e+04	0	1	>1E20	>1E20
Ca-41	1.30e+05	1.2e-06	5.33e-06	0	1	1.8e-03	8.0e-04
Ca-45	4.46e-01	3.0e-06	1.55e+00	0	1	>1E20	>1E20
Ca-47	1.24e-02	6.2e-06	5.58e+01	0	1	>1E20	>1E20
Sc-43	4.47e-04	7.3e-07	1.55e+03	0	1	>1E20	>1E20
Sc-44m	6.68e-03	9.9e-06	1.04e+02	0	1	>1E20	>1E20
Sc-44	4.47e-04	1.4e-06	1.55e+03	0	1	>1E20	>1E20
Sc-46	2.29e-01	5.6e-06	3.02e+00	0	1	>1E20	>1E20
Sc-47	9.39e-03	1.9e-06	7.38e+01	0	1	>1E20	>1E20
Sc-48	5.03e-03	6.4e-06	1.38e+02	0	1	>1E20	>1E20
Sc-49	1.09e-04	2.4e-07	6.34e+03	0	1	>1E20	>1E20

C-3
Table C.1-1. (continued)

WSRC-RP-94-218

Nuclide	T1/2 (year)	DCF (mrem/pCi)	Lambda (1/year)	Kd (cm ³ /gm)	Rf	ILT GW Trigger (Ci/vault)	ILT Int Trigger (Ci/vault)
Ti-44	4.80e+01	1.9e-05	1.44e-02	0	1	5.3e-04	3.4e-03
Ti-45	3.52e-04	5.7e-07	1.97e+03	0	1	>1E20	>1E20
V-47	6.27e-05	1.6e-07	1.10e+04	0	1	>1E20	>1E20
V-48	4.41e-02	7.5e-06	1.57e+01	0	1	>1E20	>1E20
V-49	9.03e-01	5.4e-08	7.67e-01	0	1	>1E20	>1E20
Cr-48	2.62e-03	8.2e-07	2.64e+02	40	201	>1E20	>1E20
Cr-49	7.97e-05	1.7e-07	8.70e+03	40	201	>1E20	>1E20
Cr-51	7.58e-02	1.3e-07	9.14e+00	40	201	>1E20	>1E20
Mn-51	8.56e-05	2.5e-07	8.10e+03	50	251	>1E20	>1E20
Mn-52m	3.99e-05	1.5e-07	1.74e+04	50	251	>1E20	>1E20
Mn-52	1.52e-02	6.9e-06	4.56e+01	50	251	>1E20	>1E20
Mn-53	2.00e+06	9.9e-08	3.47e-07	50	251	5.6e+00	8.0e-04
Mn-54	7.97e-01	2.7e-06	8.70e-01	50	251	>1E20	>1E20
Mn-56	2.94e-04	9.5e-07	2.36e+03	50	251	>1E20	>1E20
Fe-52	9.35e-04	5.4e-06	7.41e+02	0	1	>1E20	>1E20
Fe-55	2.70e+00	5.8e-07	2.57e-01	0	1	1.9e+09	1.1e+08
Fe-59	1.22e-01	6.6e-06	5.68e+00	0	1	>1E20	>1E20
Fe-60	3.00e+05	1.5e-04	2.31e-06	0	1	1.5e-05	8.0e-04
Co-55	2.08e-03	4.1e-06	3.34e+02	10	51	>1E20	>1E20
Co-56	2.11e-01	1.2e-05	3.29e+00	10	51	>1E20	>1E20
Co-57	7.39e-01	1.1e-05	9.38e-01	10	51	>1E20	>1E20
Co-58m	1.03e-03	8.8e-08	6.75e+02	10	51	>1E20	>1E20
Co-58	1.95e-01	3.5e-06	3.55e+00	10	51	>1E20	>1E20
Co-60m	2.00e-05	3.6e-09	3.47e+04	10	51	>1E20	>1E20
Co-60	5.27e+00	2.6e-05	1.32e-01	10	51	8.1e+17	4.1e+02
Co-61	1.88e-04	2.6e-07	3.68e+03	10	51	>1E20	>1E20
Co-62m	3.04e-06	9.6e-08	2.28e+05	10	51	>1E20	>1E20
Ni-56	1.67e-02	3.5e-06	4.15e+01	300	1501	>1E20	>1E20
Ni-57	4.11e-03	3.3e-06	1.69e+02	300	1501	>1E20	>1E20
Ni-59	8.00e+04	2.0e-07	8.66e-06	300	1501	1.8e+01	8.0e-04
Ni-63	1.00e+02	5.4e-07	6.93e-03	300	1501	>1E20	1.6e-03
Ni-65	2.87e-04	6.1e-07	2.41e+03	300	1501	>1E20	>1E20
Ni-66	6.23e-03	1.1e-05	1.11e+02	300	1501	>1E20	>1E20
Cu-60	4.37e-05	1.7e-07	1.59e+04	25	126	>1E20	>1E20

Rev. 0

C-4
Table C.1-1. (continued)

WSRC-RP-94-218

Nuclide	T1/2 (year)	DCF (mrem/pCi)	Lambda (1/year)	Kd (cm**3/gm)	Rf	ILT GW Trigger (Ci/vault)	ILT Int Trigger (Ci/vault)
Cu-61	3.89e-04	4.1e-07	1.78e+03	25	126	>1E20	>1E20
Cu-64	1.45e-03	4.3e-07	4.78e+02	25	126	>1E20	>1E20
Cu-67	7.06e-03	1.1e-06	9.82e+01	25	126	>1E20	>1E20
Zn-62	1.04e-03	3.4e-06	6.64e+02	16	81	>1E20	>1E20
Zn-63	7.30e-05	2.0e-07	9.49e+03	16	81	>1E20	>1E20
Zn-65	6.67e-01	1.4e-05	1.04e+00	16	81	>1E20	>1E20
Zn-69m	1.57e-03	1.2e-05	4.40e+02	16	81	>1E20	>1E20
Zn-69	1.08e-04	8.5e-08	6.40e+03	16	81	>1E20	>1E20
Zn-71m	4.56e-04	8.3e-07	1.52e+03	16	81	>1E20	>1E20
Zn-72	1.27e-01	4.9e-06	5.44e+00	16	81	>1E20	>1E20
Ga-65	2.89e-05	7.8e-08	2.40e+04	0	1	>1E20	>1E20
Ga-66	1.07e-03	4.7e-06	6.46e+02	0	1	>1E20	>1E20
Ga-67	8.91e-03	7.2e-07	7.78e+01	0	1	>1E20	>1E20
Ga-68	1.30e-04	3.3e-07	5.34e+03	0	1	>1E20	>1E20
Ga-70	4.01e-05	7.1e-08	1.73e+04	0	1	>1E20	>1E20
Ga-72	1.61e-03	4.4e-06	4.31e+02	0	1	>1E20	>1E20
Ga-73	1.34e-02	1.0e-06	5.19e+01	0	1	>1E20	>1E20
Ge-66	1.07e-03	2.1e-07	6.46e+02	0	1	>1E20	>1E20
Ge-67	3.61e-05	1.1e-07	1.92e+04	0	1	>1E20	>1E20
Ge-68	7.86e-01	1.1e-06	8.82e-01	0	1	>1E20	>1E20
Ge-69	4.45e-03	3.6e-07	1.56e+02	0	1	>1E20	>1E20
Ge-71	3.12e-02	9.6e-09	2.22e+01	0	1	>1E20	>1E20
Ge-75	1.57e-04	7.3e-08	4.40e+03	0	1	>1E20	>1E20
Ge-77	1.29e-03	5.6e-07	5.38e+02	0	1	>1E20	>1E20
Ge-78	1.65e-04	2.1e-07	4.19e+03	0	1	>1E20	>1E20
As-69	2.85e-05	1.1e-07	2.43e+04	3	16	>1E20	>1E20
As-70	1.01e-04	3.4e-07	6.88e+03	3	16	>1E20	>1E20
As-71	7.07e-03	1.3e-06	9.80e+01	3	16	>1E20	>1E20
As-72	2.97e-03	5.6e-06	2.34e+02	3	16	>1E20	>1E20
As-73	2.20e-01	6.1e-07	3.15e+00	3	16	>1E20	>1E20
As-74	3.29e-02	3.3e-06	2.11e+01	3	16	>1E20	>1E20
As-76	3.00e-03	4.8e-06	2.31e+02	3	16	>1E20	>1E20
As-77	1.06e-01	1.1e-06	6.53e+00	3	16	>1E20	>1E20
As-78	1.73e-04	6.5e-07	4.01e+03	3	16	>1E20	>1E20

Rev. 0

Table C1-1L (continued)

Nuclide	T1/2 (year)	DCF (mrem/yr)	Lambda (1/year)	Kd (cm ² /g)	Rf	ILT GW Trigger (Ci/haft)	ILT Int Trigger (Ci/haft)
Se-70	8.37e-05	4.8e-07	8.29e+03	5	26	>1E20	>1E20
Se-73m	7.99e-05	1.5e-07	8.68e+03	5	26	>1E20	>1E20
Se-73	8.10e-04	1.5e-06	8.56e+02	5	26	>1E20	>1E20
Se-75	3.30e-01	8.8e-06	2.10e+00	5	26	>1E20	>1E20
Se-79	6.50e+04	8.3e-06	1.07e-05	5	26	6.9e-03	8.0e-04
Se-81m	1.09e-04	2.1e-07	6.36e+03	5	26	>1E20	>1E20
Se-81	4.30e-05	6.1e-08	1.61e+04	5	26	>1E20	>1E20
Se-83	4.28e-05	1.5e-07	1.62e+04	5	26	>1E20	>1E20
Br-74m	7.89e-05	2.2e-07	8.78e+03	0	1	>1E20	>1E20
Br-74	6.84e-05	1.4e-07	1.01e+04	0	1	>1E20	>1E20
Br-75	1.94e-04	1.3e-07	3.57e+03	0	1	>1E20	>1E20
Br-76	1.84e-03	1.4e-06	3.77e+02	0	1	>1E20	>1E20
Br-77	6.50e-03	3.1e-07	1.07e+02	0	1	>1E20	>1E20
Br-80m	5.04e-04	2.3e-07	1.37e+03	0	1	>1E20	>1E20
Br-80	3.37e-05	5.5e-08	2.06e+04	0	1	>1E20	>1E20
Br-82	4.03e-03	1.7e-06	1.72e+02	0	1	>1E20	>1E20
Br-83	2.74e-04	7.3e-08	2.53e+03	0	1	>1E20	>1E20
Br-84	6.05e-05	1.5e-07	1.15e+04	0	1	>1E20	>1E20
Rb-79	3.99e-05	8.7e-08	1.74e+04	0	1	>1E20	>1E20
Rb-81m	6.08e-05	1.8e-08	1.14e+04	0	1	>1E20	>1E20
Rb-81	5.36e-04	1.3e-07	1.29e+03	0	1	>1E20	>1E20
Rb-82m	7.30e-04	4.2e-07	9.49e+02	0	1	>1E20	>1E20
Rb-83	2.27e-01	7.7e-06	3.05e+00	0	1	>1E20	>1E20
Rb-84	9.31e-02	1.0e-05	7.45e+00	0	1	>1E20	>1E20
Rb-86	5.09e-02	9.4e-06	1.36e+01	0	1	>1E20	>1E20
Rb-87	4.80e+10	4.8e-06	1.44e-11	0	1	4.6e-04	8.0e-04
Rb-88	3.37e-05	1.6e-07	2.06e+04	0	1	>1E20	>1E20
Rb-89	2.89e-05	8.0e-08	2.40e+04	0	1	>1E20	>1E20
Sr-80	1.94e-04	5.2e-09	3.57e+03	10	51	>1E20	>1E20
Sr-81	5.51e-05	2.2e-07	1.26e+04	10	51	>1E20	>1E20
Sr-83	3.76e-03	2.3e-06	1.84e+02	10	51	>1E20	>1E20
Sr-85m	1.29e-04	2.4e-08	5.39e+03	10	51	>1E20	>1E20
Sr-85	1.79e-01	1.9e-06	3.88e+00	10	51	>1E20	>1E20
Sr-87m	3.21e-04	1.2e-07	2.16e+03	10	51	>1E20	>1E20

Rev. 0

C-6
Table C.1-1. (continued)

WSRC-RP-94-218

Nuclide	T1/2 (year)	DCF (mrem/pCi)	Lambda (1/year)	Kd (cm**3/gm)	Rf	ILT GW Trigger (Ci/vault)	ILT Int Trigger (Ci/vault)
Sr-89	1.38e-01	8.7e-06	5.01e+00	10	51	>1E20	>1E20
Sr-90	2.86e+01	1.3e-04	2.42e-02	10	51	4.7e+00	9.1e-03
Sr-91	1.08e-03	3.0e-06	6.41e+02	10	51	>1E20	>1E20
Sr-92	3.09e-04	1.9e-06	2.24e+03	10	51	>1E20	>1E20
Y-86m	9.13e-05	2.4e-07	7.60e+03	10	51	>1E20	>1E20
Y-86	1.67e-03	4.1e-06	4.16e+02	10	51	>1E20	>1E20
Y-87	9.13e-03	2.2e-06	7.60e+01	10	51	>1E20	>1E20
Y-88	2.88e-01	5.2e-06	2.41e+00	10	51	>1E20	>1E20
Y-90m	3.64e-04	6.6e-07	1.90e+03	10	51	>1E20	>1E20
Y-90	2.86e+01	1.0e-05	2.42e-02	10	51	6.1e+01	9.1e-03
Y-91m	9.51e-05	3.9e-08	7.29e+03	10	51	>1E20	>1E20
Y-91	1.67e-01	8.9e-06	4.15e+00	10	51	>1E20	>1E20
Y-92	4.03e-04	1.9e-06	1.72e+03	10	51	>1E20	>1E20
Y-93	1.16e-03	4.5e-06	5.96e+02	10	51	>1E20	>1E20
Y-94	3.61e-05	1.8e-07	1.92e+04	10	51	>1E20	>1E20
Y-95	2.00e-05	9.7e-08	3.47e+04	10	51	>1E20	>1E20
Zr-86	1.88e-03	3.5e-06	3.68e+02	0	1	>1E20	>1E20
Zr-88	2.33e-01	1.3e-06	2.98e+00	0	1	>1E20	>1E20
Zr-89	8.94e-03	3.1e-06	7.75e+01	0	1	>1E20	>1E20
Zr-93	1.50e+06	1.6e-06	4.62e-07	0	1	1.4e-03	8.0e-04
Zr-95	1.75e-01	3.4e-06	3.96e+00	0	1	>1E20	>1E20
Zr-97	1.92e-03	8.0e-06	3.62e+02	0	1	>1E20	>1E20
Nb-88	2.66e-05	7.2e-08	2.60e+04	0	1	>1E20	>1E20
Nb-89(66m)	1.25e-04	4.6e-07	5.52e+03	0	1	>1E20	>1E20
Nb-89(122m)	2.32e-04	1.0e-06	2.99e+03	0	1	>1E20	>1E20
Nb-90	1.67e-03	4.9e-06	4.16e+02	0	1	>1E20	>1E20
Nb-93m	1.01e+01	5.3e-07	6.84e-02	0	1	5.5e+00	7.5e-01
Nb-94	2.00e+04	5.1e-06	3.47e-05	0	1	4.3e-04	8.1e-04
Nb-95m	9.88e-03	2.0e-06	7.02e+01	0	1	>1E20	>1E20
Nb-95	9.58e-02	2.2e-06	7.23e+00	0	1	>1E20	>1E20
Nb-96	2.67e-03	4.4e-06	2.60e+02	0	1	>1E20	>1E20
Nb-97	1.40e-04	2.3e-07	4.95e+03	0	1	>1E20	>1E20
Nb-98	8.87e-08	3.4e-07	7.81e+06	0	1	>1E20	>1E20
Mo-90	6.50e-04	2.5e-06	1.07e+03	0	1	>1E20	>1E20

Rev. 0

C-7
Table C.1-1. (continued)

WSRC-RP-94-218

Nuclide	T1/2 (year)	DCF (mrem/pCi)	Lambda (1/year)	Kd (cm**3/gm)	Rf	ILT GW Trigger (Ci/vault)	ILT Int Trigger (Ci/vault)
Mo-93m	7.87e-04	1.1e-06	8.81e+02	0	1	>1E20	>1E20
Mo-93	3.50e+03	1.3e-06	1.98e-04	0	1	1.7e-03	8.2e-04
Mo-99	7.53e-03	4.4e-06	9.20e+01	0	1	>1E20	>1E20
Mo-101	2.78e-05	9.2e-08	2.50e+04	0	1	>1E20	>1E20
Tc-93m	8.18e-05	7.1e-08	8.48e+03	0.36	2.8	>1E20	>1E20
Tc-93	3.08e-04	1.6e-07	2.25e+03	0.36	2.8	>1E20	>1E20
Tc-94m	1.01e-04	2.5e-07	6.88e+03	0.36	2.8	>1E20	>1E20
Tc-94	5.57e-04	5.8e-07	1.24e+03	0.36	2.8	>1E20	>1E20
Tc-96m	9.89e-05	3.1e-08	7.01e+03	0.36	2.8	>1E20	>1E20
Tc-96	1.18e-02	2.7e-06	5.89e+01	0.36	2.8	>1E20	>1E20
Tc-97m	2.46e-01	1.1e-06	2.81e+00	0.36	2.8	>1E20	>1E20
Tc-97	2.60e+06	1.5e-07	2.67e-07	0.36	2.8	4.1e-02	8.0e-04
Tc-98	1.50e+06	4.8e-06	4.62e-07	0.36	2.8	1.3e-03	8.0e-04
Tc-99m	6.87e-04	6.0e-08	1.01e+03	0.36	2.8	>1E20	>1E20
Tc-99	2.11e+05	1.3e-06	3.29e-06	0.36	2.8	4.7e-03	8.0e-04
Tc-101	2.70e-05	3.8e-08	2.57e+04	0.36	2.8	>1E20	>1E20
Tc-104	3.42e-05	1.6e-07	2.03e+04	0.36	2.8	>1E20	>1E20
Ru-94	1.08e-04	3.3e-07	6.40e+03	100	501	>1E20	>1E20
Ru-97	7.91e-03	6.4e-07	8.76e+01	100	501	>1E20	>1E20
Ru-103	1.08e-01	2.7e-06	6.43e+00	100	501	>1E20	>1E20
Ru-105	5.07e-04	1.0e-06	1.37e+03	100	501	>1E20	>1E20
Ru-106	9.99e-01	2.1e-05	6.94e-01	100	501	>1E20	>1E20
Rh-99m	5.36e-04	2.8e-07	1.29e+03	0	1	>1E20	>1E20
Rh-99	4.38e-02	2.0e-06	1.58e+01	0	1	>1E20	>1E20
Rh-100	2.28e-03	3.1e-06	3.04e+02	0	1	>1E20	>1E20
Rh-101m	1.23e-02	8.8e-07	5.63e+01	0	1	>1E20	>1E20
Rh-101	3.10e+00	2.3e-06	2.24e-01	0	1	1.5e+07	4.1e+06
Rh-102m	2.90e+00	3.5e-06	2.39e-01	0	1	5.0e+07	1.9e+07
Rh-102	5.75e-01	5.5e-06	1.21e+00	0	1	>1E20	>1E20
Rh-103m	1.06e-04	0.00000001	6.51e+03	0	1	>1E20	>1E20
Rh-105	4.05e-03	1.4e-06	1.71e+02	0	1	>1E20	>1E20
Rh-106m	2.49e-04	6.1e-07	2.79e+03	0	1	>1E20	>1E20
Rh-107	4.13e-05	5.4e-08	1.68e+04	0	1	>1E20	>1E20

Rev. 0

C-8
Table C.1-1. (continued)

WSRC-RP-94-218

Nuclide	T1/2 (year)	DCF (mrem/pCi)	Lambda (1/year)	Kd (cm**3/gm)	Rf	ILT GW Trigger (Ci/vault)	ILT Int Trigger (Ci/vault)
Pd-100	1.10e-02	3.8e-06	6.33e+01	0	1	>1E20	>1E20
Pd-101	9.58e-04	3.8e-07	7.23e+02	0	1	>1E20	>1E20
Pd-103	4.65e-02	6.9e-07	1.49e+01	0	1	>1E20	>1E20
Pd-107	6.50e+06	1.4e-07	1.07e-07	0	1	1.6e-02	8.0e-04
Pd-109	1.53e-03	2.1e-06	4.53e+02	0	1	>1E20	>1E20
Ag-102	2.85e-05	7.9e-08	2.43e+04	10	51	>1E20	>1E20
Ag-103	1.25e-04	1.4e-07	5.52e+03	10	51	>1E20	>1E20
Ag-104m	5.70e-05	1.5e-07	1.22e+04	10	51	>1E20	>1E20
Ag-104	1.27e-04	2.3e-07	5.44e+03	10	51	>1E20	>1E20
Ag-105	1.10e-01	1.9e-06	6.33e+00	10	51	>1E20	>1E20
Ag-106m	2.27e-02	6.1e-06	3.05e+01	10	51	>1E20	>1E20
Ag-106	4.56e-05	7.6e-08	1.52e+04	10	51	>1E20	>1E20
Ag-108m	1.30e+02	7.5e-06	5.33e-03	10	51	9.9e-02	1.4e-03
Ag-110m	6.90e-01	1.1e-05	1.00e+00	10	51	>1E20	>1E20
Ag-111	2.05e-02	4.5e-06	3.39e+01	10	51	>1E20	>1E20
Ag-112	3.57e-04	1.6e-06	1.94e+03	10	51	>1E20	>1E20
Ag-115	3.99e-05	1.5e-07	1.74e+04	10	51	>1E20	>1E20
Cd-104	1.08e-04	2.3e-07	6.40e+03	8	41	>1E20	>1E20
Cd-107	7.42e-04	2.4e-07	9.35e+02	8	41	>1E20	>1E20
Cd-109	1.24e+00	1.2e-05	5.59e-01	8	41	>1E20	>1E20
Cd-113m	1.46e+01	1.5e-04	4.75e-02	8	41	1.2e+03	9.3e-02
Cd-113	9.30e+15	1.6e-04	7.45e-17	8	41	5.6e-04	8.0e-04
Cd-115m	1.36e-01	1.5e-05	5.11e+00	8	41	>1E20	>1E20
Cd-115	6.10e-03	4.7e-06	1.14e+02	8	41	>1E20	>1E20
Cd-117m	3.88e-04	1.1e-06	1.79e+03	8	41	>1E20	>1E20
Cd-117	2.97e-04	1.1e-06	2.34e+03	8	41	>1E20	>1E20
In-109	4.91e-04	2.7e-07	1.41e+03	0	1	>1E20	>1E20
In-110(69m)	1.27e-04	3.3e-07	5.44e+03	0	1	>1E20	>1E20
In-111	7.69e-03	1.2e-06	9.01e+01	0	1	>1E20	>1E20
In-112	2.66e-05	0.00000002	2.60e+04	0	1	>1E20	>1E20
In-113m	1.89e-04	1.0e-07	3.66e+03	0	1	>1E20	>1E20
In-114m	1.36e-01	0.000015	5.11e+00	0	1	>1E20	>1E20
In-115m	5.13e-04	3.4e-07	1.35e+03	0	1	>1E20	>1E20
In-115	4.60e+15	1.4e-04	1.51e-16	0	1	1.6e-05	8.0e-04

Rev. 0

C-9
Table C.1-1. (continued)

WSRC-RP-94-218

Nuclide	T1/2 (year)	DCF (mrem/pCi)	Lambda (1/year)	Kd (cm ³ /gm)	Rf	ILT GW Trigger (Ci/vault)	ILT Int Trigger (Ci/vault)
In-116m	1.03e-04	2.1e-07	6.73e+03	0	1	>1E20	>1E20
In-117m	2.21e-04	4.2e-07	3.13e+03	0	1	>1E20	>1E20
In-117	8.37e-05	8.7e-08	8.29e+03	0	1	>1E20	>1E20
In-119m	3.42e-05	1.0e-07	2.03e+04	0	1	>1E20	>1E20
Sn-110	4.56e-04	1.5e-06	1.52e+03	130	651	>1E20	>1E20
Sn-111	6.65e-05	6.7e-08	1.04e+04	130	651	>1E20	>1E20
Sn-113	3.15e-01	2.7e-06	2.20e+00	130	651	>1E20	>1E20
Sn-117m	3.83e-02	2.6e-06	1.81e+01	130	651	>1E20	>1E20
Sn-119m	8.02e-01	1.2e-05	8.64e-01	130	651	>1E20	>1E20
Sn-121m	7.60e+01	1.3e-06	9.12e-03	130	651	2.1e+13	2.0e-03
Sn-121	3.08e-03	8.9e-07	2.25e+02	130	651	>1E20	>1E20
Sn-123m	7.61e-05	1.0e-07	9.11e+03	130	651	>1E20	>1E20
Sn-123	3.53e-01	7.7e-06	1.96e+00	130	651	>1E20	>1E20
Sn-125	2.64e-02	1.1e-05	2.62e+01	130	651	>1E20	>1E20
Sn-126	1.00e+05	1.7e-05	6.93e-06	130	651	8.6e-02	8.0e-04
Sn-127	2.42e-04	7.4e-07	2.87e+03	130	651	>1E20	>1E20
Sn-128	1.12e-04	5.2e-07	6.18e+03	130	651	>1E20	>1E20
Sb-115	5.89e-05	6.3e-08	1.18e+04	10	51	>1E20	>1E20
Sb-116m	1.14e-04	2.4e-07	6.08e+03	10	51	>1E20	>1E20
Sb-116	2.85e-05	5.6e-08	2.43e+04	10	51	>1E20	>1E20
Sb-117	3.19e-04	7.4e-08	2.17e+03	10	51	>1E20	>1E20
Sb-118m	5.82e-04	9.3e-07	1.19e+03	10	51	>1E20	>1E20
Sb-119	4.33e-03	3.4e-07	1.60e+02	10	51	>1E20	>1E20
Sb-120(16m)	3.04e-05	3.0e-08	2.28e+04	10	51	>1E20	>1E20
Sb-120(6d)	1.59e-02	5.4e-06	4.37e+01	10	51	>1E20	>1E20
Sb-122	7.45e-03	6.3e-06	9.31e+01	10	51	>1E20	>1E20
Sb-124m	1.77e-04	2.0e-08	3.92e+03	10	51	>1E20	>1E20
Sb-124	1.65e-01	9.3e-06	4.20e+00	10	51	>1E20	>1E20
Sb-125	2.40e+00	2.6e-06	2.89e-01	10	51	>1E20	2.8e+09
Sb-126m	3.61e-05	7.3e-08	1.92e+04	10	51	>1E20	>1E20
Sb-126	3.39e-02	9.6e-06	2.04e+01	10	51	>1E20	>1E20
Sb-127	1.04e-02	6.6e-06	6.66e+01	10	51	>1E20	>1E20
Sb-128(9h)	1.03e-03	4.3e-06	6.75e+02	10	51	>1E20	>1E20
Sb-128(10m)	1.90e-05	5.0e-08	3.65e+04	10	51	>1E20	>1E20

Rev. 0

C-10
Table C.1-1. (continued)

Nuclide	T1/2 (year)	DCF (mrem/pCi)	Lambda (1/year)	Kd (cm ³ /gm)	Rf	ILT GW Trigger (Ci/vault)	ILT Int Trigger (Ci/vault)
Sb-129	4.95e-04	1.7e-06	1.40e+03	10	51	>1E20	>1E20
Sb-130	1.25e-05	2.6e-07	5.52e+04	10	51	>1E20	>1E20
Sb-131	4.37e-05	2.9e-07	1.59e+04	10	51	>1E20	>1E20
Te-118	1.64e-02	6.7e-07	4.22e+01	0	1	>1E20	>1E20
Te-121m	4.11e-01	6.7e-06	1.69e+00	0	1	>1E20	>1E20
Te-121	4.65e-02	1.5e-06	1.49e+01	0	1	>1E20	>1E20
Te-123m	3.28e-01	5.1e-06	2.12e+00	0	1	>1E20	>1E20
Te-123	1.20e+13	4.1e-06	5.78e-14	0	1	5.4e-04	8.0e-04
Te-125m	1.59e-01	3.4e-06	4.37e+00	0	1	>1E20	>1E20
Te-127m	2.98e-01	7.9e-06	2.32e+00	0	1	>1E20	>1E20
Te-127	1.07e-03	6.9e-07	6.46e+02	0	1	>1E20	>1E20
Te-129m	9.14e-02	9.9e-06	7.58e+00	0	1	>1E20	>1E20
Te-129	1.33e-04	1.9e-07	5.21e+03	0	1	>1E20	>1E20
Te-131m	3.42e-03	1.5e-05	2.03e+02	0	1	>1E20	>1E20
Te-131	4.75e-05	2.0e-07	1.46e+04	0	1	>1E20	>1E20
Te-132	8.76e-03	7.4e-06	7.91e+01	0	1	>1E20	>1E20
Te-133m	1.05e-04	7.6e-07	6.58e+03	0	1	>1E20	>1E20
Te-133	2.38e-05	1.6e-07	2.92e+04	0	1	>1E20	>1E20
Te-134	7.99e-05	2.1e-07	8.68e+03	0	1	>1E20	>1E20
I-120m	1.01e-04	3.9e-07	6.88e+03	0.6	4	>1E20	>1E20
I-120	1.48e-04	6.7e-07	4.67e+03	0.6	4	>1E20	>1E20
I-121	2.40e-04	1.8e-07	2.89e+03	0.6	4	>1E20	>1E20
I-123	1.52e-03	4.9e-07	4.57e+02	0.6	4	>1E20	>1E20
I-124	1.15e-02	3.1e-05	6.03e+01	0.6	4	>1E20	>1E20
I-125	1.64e-01	3.8e-05	4.72e+00	0.6	4	>1E20	>1E20
I-126	3.64e-02	7.1e-05	1.90e+01	0.6	4	>1E20	>1E20
I-128	4.75e-05	8.5e-08	1.46e+04	0.6	4	>1E20	>1E20
I-129	1.72e+07	2.8e-04	4.02e-08	0.6	4	3.1e-05	8.0e-04
I-130	1.41e-03	4.3e-06	4.90e+02	0.6	4	>1E20	>1E20
I-131	2.22e-02	5.3e-05	3.13e+01	0.6	4	>1E20	>1E20
I-132m	1.58e-04	4.7e-07	4.39e+03	0.6	4	>1E20	>1E20
I-132	2.60e-04	3.3e-07	2.66e+03	0.6	4	>1E20	>1E20
I-133	2.37e-03	5.4e-06	2.92e+02	0.6	4	>1E20	>1E20
I-134	1.00e-04	1.9e-07	6.93e+03	0.6	4	>1E20	>1E20

C-11
Table C.1-1. (continued)

WSRC-RP-94-218

Nuclide	T1/2 (year)	DCF (mrem/pCi)	Lambda (1/year)	Kd (cm ³ /gm)	Rf	ILT GW Trigger (Ci/vault)	ILT Int Trigger (Ci/vault)
I-135	7.51e-04	2.0e-05	9.23e+02	0.6	4	>1E20	>1E20
Cs-125	8.56e-05	5.5e-08	8.10e+03	100	501	>1E20	>1E20
Cs-127	7.07e-04	8.0e-08	9.80e+02	100	501	>1E20	>1E20
Cs-129	3.65e-03	2.2e-07	1.90e+02	100	501	>1E20	>1E20
Cs-130	5.70e-05	4.9e-08	1.22e+04	100	501	>1E20	>1E20
Cs-131	2.66e-02	2.4e-07	2.61e+01	100	501	>1E20	>1E20
Cs-132	1.80e-02	1.9e-06	3.85e+01	100	501	>1E20	>1E20
Cs-134m	3.31e-04	4.2e-08	2.10e+03	100	501	>1E20	>1E20
Cs-134	2.06e+00	7.4e-05	3.36e-01	100	501	>1E20	3.3e+11
Cs-135m	1.01e-04	4.9e-08	6.88e+03	100	501	>1E20	>1E20
Cs-135	2.30e+06	7.1e-06	3.01e-07	100	501	1.6e-01	8.0e-04
Cs-136	3.53e-02	1.1e-05	1.96e+01	100	501	>1E20	>1E20
Cs-137	3.01e+01	5.0e-05	2.30e-02	100	501	>1E20	8.0e-03
Cs-138	6.12e-05	1.6e-07	1.13e+04	100	501	>1E20	>1E20
Ba-126	1.84e-04	9.0e-07	3.76e+03	5	26	>1E20	>1E20
Ba-128	6.57e-03	1.0e-05	1.05e+02	5	26	>1E20	>1E20
Ba-131m	2.78e-05	9.7e-07	2.50e+04	5	26	>1E20	>1E20
Ba-131	3.20e-02	1.6e-06	2.16e+01	5	26	>1E20	>1E20
Ba-133m	4.44e-03	2.0e-06	1.56e+02	5	26	>1E20	>1E20
Ba-133	1.07e+01	3.2e-06	6.48e-02	5	26	5.3e+04	5.2e-01
Ba-135m	3.27e-03	1.6e-06	2.12e+02	5	26	>1E20	>1E20
Ba-137m	4.85e-06	0.0	1.43e+05	5	26	>1E20	>1E20
Ba-139	1.58e-04	3.9e-07	4.38e+03	5	26	>1E20	>1E20
Ba-140	3.50e-02	8.4e-06	1.98e+01	5	26	>1E20	>1E20
Ba-141	3.48e-05	2.0e-07	1.99e+04	5	26	>1E20	>1E20
Ba-142	2.03e-05	1.0e-07	3.41e+04	5	26	>1E20	>1E20
La-131	1.12e-04	1.1e-07	6.18e+03	100	501	>1E20	>1E20
La-132	5.13e-04	1.5e-06	1.35e+03	100	501	>1E20	>1E20
La-135	2.22e-03	1.3e-07	3.12e+02	100	501	>1E20	>1E20
La-137	6.00e+04	4.3e-07	1.16e-05	100	501	2.6e+00	8.0e-04
La-138	1.06e+11	5.9e-06	6.54e-12	100	501	1.9e-01	8.0e-04
La-140	4.59e-03	7.7e-06	1.51e+02	100	501	>1E20	>1E20
La-141	4.41e-04	1.4e-06	1.57e+03	100	501	>1E20	>1E20
La-142	1.76e-04	8.3e-07	3.95e+03	100	501	>1E20	>1E20

Rev. 0

C-12
Table C.1-1. (continued)

WSRC-RP-94-218

Nuclide	T1/2 (year)	DCF (mrem/pCi)	Lambda (1/year)	Kd (cm ³ /gm)	Rf	ILT GW Trigger (Ci/vault)	ILT Int Trigger (Ci/vault)
La-143	2.66e-05	1.4e-07	2.60e+04	100	501	>1E20	>1E20
Ce-134	8.21e-03	8.9e-06	8.44e+01	10	51	>1E20	>1E20
Ce-135	1.96e-03	3.2e-06	3.53e+02	10	51	>1E20	>1E20
Ce-137m	3.92e-03	2.0e-06	1.77e+02	10	51	>1E20	>1E20
Ce-137	1.03e-03	9.8e-08	6.75e+02	10	51	>1E20	>1E20
Ce-139	3.77e-01	1.1e-06	1.84e+00	10	51	>1E20	>1E20
Ce-141	8.90e-02	2.6e-06	7.79e+00	10	51	>1E20	>1E20
Ce-143	3.76e-03	4.2e-06	1.84e+02	10	51	>1E20	>1E20
Ce-144	7.94e-01	2.0e-05	8.73e-01	10	51	>1E20	>1E20
Pr-136	1.25e-04	6.8e-08	5.52e+03	10	51	>1E20	>1E20
Pr-137	1.71e-04	1.3e-07	4.05e+03	100	501	>1E20	>1E20
Pr-138m	2.40e-04	4.9e-07	2.89e+03	100	501	>1E20	>1E20
Pr-139	5.13e-04	1.2e-07	1.35e+03	100	501	>1E20	>1E20
Pr-142m	2.72e-05	6.3e-08	2.55e+04	100	501	>1E20	>1E20
Pr-142	2.18e-03	5.1e-06	3.18e+02	100	501	>1E20	>1E20
Pr-143	3.75e-02	4.5e-06	1.85e+01	100	501	>1E20	>1E20
Pr-144	3.29e-05	1.1e-07	2.11e+04	100	501	>1E20	>1E20
Pr-145	6.82e-04	1.5e-06	1.02e+03	100	501	>1E20	>1E20
Pr-147	2.28e-05	5.7e-08	3.04e+04	100	501	>1E20	>1E20
Nd-136	9.64e-05	3.3e-07	7.19e+03	100	501	>1E20	>1E20
Nd-138	4.18e-05	2.5e-06	1.66e+04	100	501	>1E20	>1E20
Nd-139m	6.27e-04	1.0e-06	1.10e+03	100	501	>1E20	>1E20
Nd-139	5.93e-04	5.7e-08	1.17e+03	100	501	>1E20	>1E20
Nd-141	2.85e-04	3.2e-08	2.43e+03	100	501	>1E20	>1E20
Nd-147	3.01e-02	3.9e-06	2.30e+01	100	501	>1E20	>1E20
Nd-149	1.97e-03	4.6e-07	3.51e+02	100	501	>1E20	>1E20
Nd-151	2.36e-05	7.4e-08	2.94e+04	100	501	>1E20	>1E20
Pm-141	4.18e-05	8.4e-08	1.66e+04	100	501	>1E20	>1E20
Pm-143	7.26e-01	9.5e-07	9.55e-01	100	501	>1E20	>1E20
Pm-144	8.22e-01	3.9e-06	8.43e-01	100	501	>1E20	>1E20
Pm-145	1.77e+01	4.6e-07	3.92e-02	100	501	>1E20	4.0e-02
Pm-146	1.94e+00	3.2e-06	3.57e-01	100	501	>1E20	2.5e+12
Pm-147	2.52e+00	9.5e-07	2.75e-01	100	501	>1E20	7.2e+08
Pm-148m	1.14e-01	7.0e-06	6.06e+00	100	501	>1E20	>1E20

Rev. 0

C-13
Table C.1-1. (continued)

WSRC-RP-94-218

Nuclide	T1/2 (year)	DCF (mrem/pCi)	Lambda (1/year)	Kd (cm ³ /gm)	Rf	ILT GW Trigger (Ci/vault)	ILT Int Trigger (Ci/vault)
Pm-148	1.47e-02	9.5e-06	4.71e+01	100	501	>1E20	>1E20
Pm-149	6.06e-03	3.6e-06	1.14e+02	100	501	>1E20	>1E20
Pm-150	3.06e-04	9.8e-07	2.27e+03	100	501	>1E20	>1E20
Pm-151	3.24e-03	2.8e-06	2.14e+02	100	501	>1E20	>1E20
Sm-141m	4.30e-05	1.8e-07	1.61e+04	100	501	>1E20	>1E20
Sm-141	1.94e-05	8.4e-08	3.57e+04	100	501	>1E20	>1E20
Sm-142	1.37e-04	6.0e-07	5.06e+03	100	501	>1E20	>1E20
Sm-145	9.31e-01	8.5e-07	7.45e-01	100	501	>1E20	>1E20
Sm-146	7.00e+07	2.0e-04	9.90e-09	100	501	5.5e-03	8.0e-04
Sm-147	1.06e+11	1.8e-04	6.54e-12	100	501	6.1e-03	8.0e-04
Sm-151	9.00e+01	3.4e-07	7.70e-03	100	501	1.7e+09	1.7e-03
Sm-153	5.33e-03	2.6e-06	1.30e+02	100	501	>1E20	>1E20
Sm-155	4.22e-05	6.6e-08	1.64e+04	100	501	>1E20	>1E20
Sm-158	8.37e-05	1.0e-06	8.29e+03	100	501	>1E20	>1E20
Eu-145	1.62e-02	3.2e-05	4.29e+01	100	501	>1E20	>1E20
Eu-146	1.26e-02	5.1e-06	5.50e+01	100	501	>1E20	>1E20
Eu-147	6.02e-02	1.8e-06	1.15e+01	100	501	>1E20	>1E20
Eu-148	1.48e-01	5.2e-06	4.69e+00	100	501	>1E20	>1E20
Eu-149	2.90e-01	4.2e-07	2.39e+00	100	501	>1E20	>1E20
Eu-150(12h)	1.37e-03	1.5e-06	5.06e+02	100	501	>1E20	>1E20
Eu-150(34y)	3.40e+01	6.2e-06	2.04e-02	100	501	>1E20	6.2e-03
Eu-152m	1.07e-03	1.9e-06	6.51e+02	100	501	>1E20	>1E20
Eu-152	1.34e+01	6.0e-06	5.17e-02	100	501	>1E20	1.4e-01
Eu-154	8.20e+00	9.1e-06	8.45e-02	100	501	>1E20	3.8e+00
Eu-155	1.70e+00	1.3e-06	4.08e-01	100	501	>1E20	4.1e+14
Eu-156	4.22e-02	8.7e-06	1.64e+01	100	501	>1E20	>1E20
Eu-157	1.73e-03	2.3e-06	4.00e+02	100	501	>1E20	>1E20
Eu-158	8.73e-05	2.6e-07	7.94e+03	100	501	>1E20	>1E20
Gd-145	4.75e-05	1.1e-07	1.46e+04	100	501	>1E20	>1E20
Gd-146	1.26e-02	3.8e-06	5.50e+01	100	501	>1E20	>1E20
Gd-147	3.99e-03	2.6e-06	1.74e+02	100	501	>1E20	>1E20
Gd-148	1.30e+02	2.1e-04	5.33e-03	100	501	5.7e+03	1.4e-03
Gd-149	2.46e-02	1.8e-06	2.81e+01	100	501	>1E20	>1E20
Gd-151	3.29e-01	7.7e-07	2.11e+00	100	501	>1E20	>1E20

Rev. 0

C-14
Table C.1-1. (continued)

WSRC-RP-94-218

Nuclide	T1/2 (year)	DCF (mrem/pCi)	Lambda (1/year)	Kd (cm ³ /gm)	Rf	ILT GW Trigger (Ci/vault)	ILT Int Trigger (Ci/vault)
Gd-152	1.10e+14	1.5e-04	6.30e-15	100	501	7.4e-03	8.0e-04
Gd-153	6.61e-01	1.1e-06	1.05e+00	100	501	>1E20	>1E20
Gd-159	2.12e-03	1.9e-06	3.27e+02	100	501	>1E20	>1E20
Tb-147	4.56e-05	5.6e-07	1.52e+04	100	501	>1E20	>1E20
Tb-149	4.68e-04	9.5e-07	1.48e+03	100	501	>1E20	>1E20
Tb-150	3.54e-04	9.7e-07	1.96e+03	100	501	>1E20	>1E20
Tb-151	2.05e-03	1.4e-06	3.38e+02	100	501	>1E20	>1E20
Tb-153	6.27e-03	9.9e-07	1.10e+02	100	501	>1E20	>1E20
Tb-154	9.70e-04	2.8e-06	7.15e+02	100	501	>1E20	>1E20
Tb-155	1.53e-02	8.2e-07	4.52e+01	100	501	>1E20	>1E20
Tb-156m(24h)	2.74e-03	7.0e-07	2.53e+02	100	501	>1E20	>1E20
Tb-156m(5h)	6.27e-04	3.2e-07	1.10e+03	100	501	>1E20	>1E20
Tb-156	1.48e-02	4.6e-06	4.69e+01	100	501	>1E20	>1E20
Tb-157	1.50e+02	1.0e-07	4.62e-03	100	501	1.9e+06	1.3e-03
Tb-158	1.20e+03	4.0e-06	5.78e-04	100	501	1.2e+00	8.5e-04
Tb-160	1.98e-01	6.4e-06	3.50e+00	100	501	>1E20	>1E20
Tb-161	1.88e-02	2.6e-06	3.68e+01	100	501	>1E20	>1E20
Dy-155	1.20e-03	5.6e-07	5.79e+02	100	501	>1E20	>1E20
Dy-157	9.24e-04	2.7e-07	7.50e+02	100	501	>1E20	>1E20
Dy-159	3.94e-01	4.0e-07	1.76e+00	100	501	>1E20	>1E20
Dy-165	2.66e-04	3.6e-07	2.61e+03	100	501	>1E20	>1E20
Dy-166	9.31e-03	6.2e-06	7.45e+01	100	501	>1E20	>1E20
Ho-155	9.51e-05	1.2e-07	7.29e+03	100	501	>1E20	>1E20
Ho-157	2.66e-05	1.9e-08	2.60e+04	100	501	>1E20	>1E20
Ho-159	6.27e-05	2.3e-08	1.10e+04	100	501	>1E20	>1E20
Ho-161	2.85e-04	4.7e-08	2.43e+03	100	501	>1E20	>1E20
Ho-162m	1.29e-04	9.0e-08	5.36e+03	100	501	>1E20	>1E20
Ho-162	2.85e-05	6.7e-09	2.43e+04	100	501	>1E20	>1E20
Ho-164m	7.13e-05	4.9e-08	9.72e+03	100	501	>1E20	>1E20
Ho-164	7.03e-05	2.4e-08	9.85e+03	100	501	>1E20	>1E20
Ho-166m	1.20e+03	7.8e-06	5.78e-04	100	501	6.4e-01	8.5e-04
Ho-166	3.06e-03	5.5e-06	2.27e+02	100	501	>1E20	>1E20
Ho-167	3.54e-04	3.2e-07	1.96e+03	100	501	>1E20	>1E20
Er-161	3.54e-04	3.3e-07	1.96e+03	100	501	>1E20	>1E20

Rev. 0

C-15
Table C.1-1. (continued)

WSRC-RP-94-218

Nuclide	T1/2 (year)	DCF (mrem/pCi)	Lambda (1/year)	Kd (cm ³ /gm)	Rf	ILT GW Trigger (Ci/vault)	ILT Int Trigger (Ci/vault)
Er-165	1.18e-03	7.9e-08	5.86e+02	100	501	>1E20	>1E20
Er-169	2.57e-02	1.4e-06	2.69e+01	100	501	>1E20	>1E20
Er-171	8.58e-04	1.4e-06	8.08e+02	100	501	>1E20	>1E20
Er-172	5.59e-03	3.7e-06	1.24e+02	100	501	>1E20	>1E20
Tm-162	1.46e-04	7.0e-08	4.73e+03	100	501	>1E20	>1E20
Tm-166	8.78e-04	1.2e-06	7.89e+02	100	501	>1E20	>1E20
Tm-167	2.63e-02	2.1e-06	2.64e+01	100	501	>1E20	>1E20
Tm-170	3.53e-01	5.0e-06	1.96e+00	100	501	>1E20	>1E20
Tm-171	1.92e+00	3.9e-07	3.61e-01	100	501	>1E20	3.8e+12
Tm-172	7.26e-03	6.0e-06	9.55e+01	100	501	>1E20	>1E20
Tm-173	9.35e-04	1.2e-06	7.41e+02	100	501	>1E20	>1E20
Tm-175	3.80e-05	5.4e-08	1.82e+04	100	501	>1E20	>1E20
Yb-162	3.59e-05	7.0e-08	1.93e+04	100	501	>1E20	>1E20
Yb-165	1.90e-05	3.8e-06	3.65e+04	100	501	>1E20	>1E20
Yb-167	3.42e-05	1.7e-08	2.03e+04	100	501	>1E20	>1E20
Yb-169	8.76e-02	2.8e-06	7.91e+00	100	501	>1E20	>1E20
Yb-175	1.15e-02	1.6e-06	6.04e+01	100	501	>1E20	>1E20
Yb-177	2.17e-04	3.1e-07	3.20e+03	100	501	>1E20	>1E20
Yb-178	1.40e-04	3.9e-07	4.94e+03	100	501	>1E20	>1E20
Lu-169	3.88e-03	2.0e-06	1.79e+02	100	501	>1E20	>1E20
Lu-170	5.48e-03	4.3e-06	1.27e+02	100	501	>1E20	>1E20
Lu-171	2.27e-02	2.6e-06	3.05e+01	100	501	>1E20	>1E20
Lu-172	1.83e-02	5.0e-06	3.78e+01	100	501	>1E20	>1E20
Lu-173	1.37e+00	9.7e-07	5.06e-01	100	501	>1E20	>1E20
Lu-174m	3.83e-01	1.8e-06	1.81e+00	100	501	>1E20	>1E20
Lu-174	3.60e+00	9.9e-07	1.93e-01	100	501	>1E20	1.8e+05
Lu-176m	4.21e-04	6.3e-07	1.65e+03	100	501	>1E20	>1E20
Lu-176	3.00e+10	6.6e-06	2.31e-11	100	501	1.7e-01	8.0e-04
Lu-177m	4.41e-02	6.8e-06	1.57e+01	100	501	>1E20	>1E20
Lu-177	1.84e-02	2.0e-06	3.77e+01	100	501	>1E20	>1E20
Lu-178m	3.80e-05	8.8e-08	1.82e+04	100	501	>1E20	>1E20
Lu-178	5.70e-05	1.2e-07	1.22e+04	100	501	>1E20	>1E20
Lu-179	5.25e-04	8.1e-07	1.32e+03	100	501	>1E20	>1E20
Hf-170	1.39e-03	1.2e-05	4.98e+02	100	501	>1E20	>1E20

Rev. 0

C-16
Table C.1-1. (continued)

Nuclide	T1/2 (year)	DCF (mrem/pCi)	Lambda (1/year)	Kd (cm ² /gm)	Rf	ILT GW Trigger (Ci/vault)	ILT Int Trigger (Ci/vault)
Hf-172	5.00e+00	4.1e-06	1.39e-01	100	501	>1E20	8.4e+02
Hf-173	2.69e-03	9.6e-07	2.57e+02	100	501	>1E20	>1E20
Hf-175	1.92e-01	1.6e-06	3.62e+00	100	501	>1E20	>1E20
Hf-177m	9.77e-05	2.5e-07	7.09e+03	100	501	>1E20	>1E20
Hf-178m	3.10e+01	2.0e-05	2.24e-02	100	501	>1E20	7.5e-03
Hf-179m	6.87e-02	4.8e-06	1.01e+01	100	501	>1E20	>1E20
Hf-180m	6.27e-04	8.9e-07	1.10e+03	100	501	>1E20	>1E20
Hf-181	1.16e-01	4.3e-06	5.97e+00	100	501	>1E20	>1E20
Hf-182m	1.18e-04	1.4e-07	5.88e+03	100	501	>1E20	>1E20
Hf-182	9.00e+06	1.4e-05	7.70e-08	100	501	7.9e-02	8.0e-04
Hf-183	1.25e-04	2.5e-07	5.52e+03	100	501	>1E20	>1E20
Hf-184	4.68e-04	2.1e-06	1.48e+03	100	501	>1E20	>1E20
Ta-172	8.37e-05	1.4e-07	8.29e+03	0	1	>1E20	>1E20
Ta-173	4.22e-04	7.4e-07	1.64e+03	0	1	>1E20	>1E20
Ta-174	1.48e-04	1.9e-07	4.67e+03	0	1	>1E20	>1E20
Ta-175	1.20e-03	8.8e-07	5.79e+02	0	1	>1E20	>1E20
Ta-176	9.13e-04	1.3e-06	7.60e+02	0	1	>1E20	>1E20
Ta-177	6.46e-03	4.1e-07	1.07e+02	0	1	>1E20	>1E20
Ta-178	1.79e-05	2.9e-07	3.88e+04	0	1	>1E20	>1E20
Ta-179	2.40e-04	2.5e-07	2.89e+03	0	1	>1E20	>1E20
Ta-180m	9.24e-04	2.1e-07	7.50e+02	0	1	>1E20	>1E20
Ta-180	1.00e+13	3.3e-06	6.93e-14	0	1	6.7e-04	8.0e-04
Ta-182m	3.02e-05	2.4e-08	2.29e+04	0	1	>1E20	>1E20
Ta-182	3.15e-01	6.0e-06	2.20e+00	0	1	>1E20	>1E20
Ta-183	1.40e-02	4.6e-06	4.96e+01	0	1	>1E20	>1E20
Ta-184	9.92e-04	2.7e-06	6.98e+02	0	1	>1E20	>1E20
Ta-185	9.51e-05	2.0e-07	7.29e+03	0	1	>1E20	>1E20
Ta-186	2.00e-05	6.7e-08	3.47e+04	0	1	>1E20	>1E20
W-176	2.85e-04	4.8e-07	2.43e+03	0	1	>1E20	>1E20
W-177	2.57e-04	2.4e-07	2.70e+03	0	1	>1E20	>1E20
W-178	5.89e-02	9.3e-07	1.18e+01	0	1	>1E20	>1E20
W-179	7.22e-05	9.0e-09	9.59e+03	0	1	>1E20	>1E20
W-181	3.31e-01	3.1e-07	2.09e+00	0	1	>1E20	>1E20
W-185	2.06e-01	1.9e-06	3.37e+00	0	1	>1E20	>1E20

Rev. 0

Table C.1-1. (continued)

Nuclide	T _{1/2} (year)	DCF (mrem/pCi)	Lambda (1/year)	K _d (cm ² /g)	R _f	ILT GW Trigger (Ci/vault)	ILT Int Trigger (Ci/vault)
W-187	2.73e-03	2.6e-06	2.54e+02	0	1	>1E20	>1E20
W-188	1.89e-01	9.0e-06	3.67e+00	0	1	>1E20	>1E20
Re-177	3.23e-05	4.4e-08	2.14e+04	0	1	>1E20	>1E20
Re-178	2.85e-05	4.8e-08	2.43e+04	0	1	>1E20	>1E20
Re-181	2.05e-03	1.0e-06	3.38e+02	0	1	>1E20	>1E20
Re-182(64h)	7.30e-03	3.4e-06	9.49e+01	0	1	>1E20	>1E20
Re-182(12h)	1.45e-03	7.4e-07	4.78e+02	0	1	>1E20	>1E20
Re-184m	4.63e-01	2.4e-06	1.50e+00	0	1	>1E20	>1E20
Rm-184	1.04e-02	2.2e-06	6.66e+01	0	1	>1E20	>1E20
Re-186m	2.00e+05	3.3e-06	3.47e-06	0	1	6.7e-04	8.0e-04
Re-186	1.03e-02	2.6e-06	6.71e+01	0	1	>1E20	>1E20
Re-187	7.00e+10	8.3e-09	9.90e-12	0	1	2.7e-01	8.0e-04
Re-188m	3.54e-05	6.2e-08	1.96e+04	0	1	>1E20	>1E20
Re-188	1.91e-03	2.8e-06	3.64e+02	0	1	>1E20	>1E20
Re-189	2.74e-03	1.5e-06	2.53e+02	0	1	>1E20	>1E20
Os-180	4.13e-05	4.7e-08	1.68e+04	0	1	>1E20	>1E20
Os-181	4.37e-05	3.5e-07	1.59e+04	0	1	>1E20	>1E20
Os-182	2.51e-03	2.2e-06	2.76e+02	0	1	>1E20	>1E20
Os-185	2.57e-01	2.1e-06	2.69e+00	0	1	>1E20	>1E20
Os-189m	6.84e-04	6.6e-08	1.01e+03	0	1	>1E20	>1E20
Os-191m	1.48e-03	3.6e-07	4.67e+02	0	1	>1E20	>1E20
Os-191	4.19e-02	2.0e-06	1.65e+01	0	1	>1E20	>1E20
Os-193	3.48e-03	3.1e-06	1.99e+02	0	1	>1E20	>1E20
Os-194	6.00e+00	9.1e-06	1.16e-01	0	1	4.5e+01	8.4e+01
Ir-182	2.85e-05	1.2e-07	2.43e+04	0	1	>1E20	>1E20
Ir-184	3.65e-04	6.4e-07	1.90e+03	0	1	>1E20	>1E20
Ir-185	1.60e-03	1.1e-06	4.34e+02	0	1	>1E20	>1E20
Ir-186	1.83e-03	2.1e-06	3.80e+02	0	1	>1E20	>1E20
Ir-187	1.20e-03	4.8e-07	5.79e+02	0	1	>1E20	>1E20
Ir-188	4.68e-03	2.7e-06	1.48e+02	0	1	>1E20	>1E20
Ir-189	3.64e-02	9.3e-07	1.90e+01	0	1	>1E20	>1E20
Ir-190m	3.65e-04	3.0e-08	1.90e+03	0	1	>1E20	>1E20
Ir-190	3.01e-02	4.9e-06	2.30e+01	0	1	>1E20	>1E20
Ir-192m	2.74e-06	1.5e-06	2.53e+05	0	1	>1E20	>1E20

Rev. 0

Table C-1-1. (continued)

Nuclide	T _{1/2} (year)	DCF (mrem/pCi)	Lambda (1/year)	K _d (cm ³ /gm)	R _f	ILT GW Trigger (Ci/vault)	ILT Int Trigger (Ci/vault)
Ir-192	2.03e-01	5.3e-06	3.41e+00	0	1	>1E20	>1E20
Ir-194m	4.68e-01	8.1e-06	1.48e+00	0	1	>1E20	>1E20
Ir-194	2.22e-03	5.1e-06	3.12e+02	0	1	>1E20	>1E20
Ir-195m	4.45e-04	6.4e-07	1.56e+03	0	1	>1E20	>1E20
Ir-195	4.79e-04	3.4e-07	1.45e+03	0	1	>1E20	>1E20
Pt-186	3.42e-04	3.7e-07	2.03e+03	0	1	>1E20	>1E20
Pt-188	2.79e-02	3.0e-06	2.48e+01	0	1	>1E20	>1E20
Pt-189	1.24e-03	4.9e-07	5.57e+02	0	1	>1E20	>1E20
Pt-191	1.24e-03	1.3e-06	5.57e+02	0	1	>1E20	>1E20
Pt-193m	1.18e-02	1.7e-06	5.89e+01	0	1	>1E20	>1E20
Pt-193	5.00e+01	1.1e-07	1.39e-02	0	1	8.6e-02	3.2e-03
Pt-195m	1.10e-02	2.2e-06	6.30e+01	0	1	>1E20	>1E20
Pt-197m	1.79e-04	3.1e-07	3.88e+03	0	1	>1E20	>1E20
Pt-197	2.09e-03	1.5e-06	3.32e+02	0	1	>1E20	>1E20
Pt-199	5.86e-05	1.0e-07	1.18e+04	0	1	>1E20	>1E20
Pt-200	1.31e-03	4.5e-06	5.28e+02	0	1	>1E20	>1E20
Au-193	1.83e-03	6.0e-07	3.80e+02	0	1	>1E20	>1E20
Au-194	4.51e-03	2.0e-06	1.54e+02	0	1	>1E20	>1E20
Au-195	5.01e-01	1.1e-06	1.38e+00	0	1	>1E20	>1E20
Au-198m	6.30e-03	5.7e-06	1.10e+02	0	1	>1E20	>1E20
Au-198	7.38e-03	2.3e-06	9.39e+01	0	1	>1E20	>1E20
Au-199	8.60e-03	1.8e-06	8.06e+01	0	1	>1E20	>1E20
Au-200m	2.13e-03	4.6e-06	3.25e+02	0	1	>1E20	>1E20
Au-200	9.20e-05	1.9e-07	7.53e+03	0	1	>1E20	>1E20
Au-201	4.94e-05	5.7e-08	1.40e+04	0	1	>1E20	>1E20
Hg-193m	1.14e-03	1.6e-06	6.08e+02	1000	5001	>1E20	>1E20
Hg-193	6.84e-04	3.3e-07	1.01e+03	1000	5001	>1E20	>1E20
Hg-194	1.90e+00	6.0e-06	3.65e-01	1000	5001	>1E20	5.6e+12
Hg-195m	4.56e-03	2.2e-06	1.52e+02	1000	5001	>1E20	>1E20
Hg-195	1.08e-03	3.8e-07	6.40e+02	1000	5001	>1E20	>1E20
Hg-197m	2.72e-03	1.7e-06	2.55e+02	1000	5001	>1E20	>1E20
Hg-197	7.31e-03	9.1e-07	9.48e+01	1000	5001	>1E20	>1E20
Hg-199m	8.10e-05	8.5e-08	8.56e+03	1000	5001	>1E20	>1E20
Hg-203	1.28e-01	2.1e-06	5.43e+00	1000	5001	>1E20	>1E20

Rev. 0

Table C-1-1. (continued)

Nuclide	T1/2 (year)	DCF (mrem/PC)	Lambda (1/year)	Kd (cm ² /g)	Rf	LT GW Trigger (C/Vault)	LT Int Trigger (C/Vault)
Tl-194m	6.24e-05	7.1e-08	1.11e+04	0	1	>1E20	>1E20
Tl-194	6.27e-05	1.9e-08	1.10e+04	0	1	>1E20	>1E20
Tl-195	1.37e-04	7.7e-08	5.06e+03	0	1	>1E20	>1E20
Tl-197	3.19e-04	6.9e-08	2.17e+03	0	1	>1E20	>1E20
Tl-198m	2.13e-04	1.6e-07	3.25e+03	0	1	>1E20	>1E20
Tl-198	6.05e-04	2.6e-07	1.15e+03	0	1	>1E20	>1E20
Tl-199	8.44e-04	8.2e-08	8.21e+02	0	1	>1E20	>1E20
Tl-200	2.98e-03	6.7e-07	2.33e+02	0	1	>1E20	>1E20
Tl-201	8.33e-03	2.9e-07	8.32e+01	0	1	>1E20	>1E20
Tl-202	3.29e-02	1.5e-06	2.11e+01	0	1	>1E20	>1E20
Tl-204	3.77e+00	3.2e-06	1.84e-01	0	1	1.7e+05	7.8e+04
Pb-195m	2.85e-05	8.5e-08	2.43e+04	100	501	>1E20	>1E20
Pb-198	2.74e-04	1.6e-07	2.53e+03	100	501	>1E20	>1E20
Pb-199	1.71e-04	2.2e-07	4.05e+03	100	501	>1E20	>1E20
Pb-200	2.45e-03	1.5e-06	2.83e+02	100	501	>1E20	>1E20
Pb-201	1.07e-03	6.7e-07	6.46e+02	100	501	>1E20	>1E20
Pb-202m	4.13e-04	5.5e-07	1.68e+03	100	501	>1E20	>1E20
Pb-202	3.00e+05	3.9e-05	2.31e-06	100	501	2.8e-02	8.0e-04
Pb-203	5.94e-03	9.6e-07	1.17e+02	100	501	>1E20	>1E20
Pb-205	1.40e+07	1.5e-06	4.95e-08	100	501	7.4e-01	8.0e-04
Pb-209	6.24e-06	9.0e-08	1.11e+05	100	501	>1E20	>1E20
Pb-210	2.23e+01	5.1e-03	3.11e-02	100	501	>1E20	1.8e-02
Pb-211	6.88e-05	4.4e-07	1.01e+04	100	501	>1E20	>1E20
Pb-212	1.21e-03	4.1e-05	5.71e+02	100	501	>1E20	>1E20
Pb-214	5.10e-05	5.8e-07	1.36e+04	100	501	>1E20	>1E20
Bi-200	6.65e-05	1.7e-07	1.04e+04	0	1	>1E20	>1E20
Bi-201	2.05e-04	4.5e-07	3.38e+03	0	1	>1E20	>1E20
Bi-202	1.81e-04	3.6e-07	3.84e+03	0	1	>1E20	>1E20
Bi-203	1.35e-03	2.1e-06	5.15e+02	0	1	>1E20	>1E20
Bi-205	4.19e-02	3.7e-06	1.65e+01	0	1	>1E20	>1E20
Bi-206	1.71e-02	8.0e-06	4.06e+01	0	1	>1E20	>1E20
Bi-207	7.94e+00	4.9e-06	8.73e-02	0	1	4.3e+00	5.0e+00
Bi-210m	3.50e+06	8.6e-05	1.98e-07	0	1	2.6e-05	8.0e-04
Bi-210	1.37e-02	5.9e-06	5.06e+01	0	1	>1E20	>1E20

Rev. 0

C-20
Table C.1-1. (continued)

WSRC-RP-94-218

Nuclide	T1/2 (year)	DCF (mrem/pCi)	Lambda (1/year)	Kd (cm ³ /gm)	Rf	ILT GW Trigger (Ci/vault)	ILT Int Trigger (Ci/vault)
Bi-212	1.15e-04	9.9e-07	6.02e+03	0	1	>1E20	>1E20
Bi-213	8.68e-05	6.8e-07	7.99e+03	0	1	>1E20	>1E20
Bi-214	3.76e-05	2.4e-07	1.84e+04	0	1	>1E20	>1E20
Po-203	7.99e-05	2.0e-07	8.68e+03	0	1	>1E20	>1E20
Po-205	2.05e-04	2.4e-07	3.38e+03	0	1	>1E20	>1E20
Po-207	6.50e-04	6.1e-07	1.07e+03	0	1	>1E20	>1E20
Po-210	3.79e-01	1.6e-03	1.83e+00	0	1	>1E20	>1E20
At-207	2.05e-04	8.9e-07	3.38e+03	0	1	>1E20	>1E20
At-211	8.22e-04	4.1e-05	8.43e+02	0	1	>1E20	>1E20
Fr-222	2.81e-05	2.5e-06	2.46e+04	0	1	>1E20	>1E20
Fr-223	4.18e-05	8.6e-06	1.66e+04	0	1	>1E20	>1E20
Ra-223	3.13e-02	5.5e-04	2.21e+01	500	2501	>1E20	>1E20
Ra-224	9.91e-03	3.3e-04	6.99e+01	500	2501	>1E20	>1E20
Ra-225	4.05e-02	3.1e-04	1.71e+01	500	2501	>1E20	>1E20
Ra-226	1.62e+03	1.1e-03	4.27e-04	500	2501	1.1e+00	8.4e-04
Ra-227	7.83e-05	2.2e-07	8.85e+03	500	2501	>1E20	>1E20
Ra-228	5.75e+00	1.2e-03	1.21e-01	500	2501	>1E20	1.4e+02
Ac-224	3.31e-04	2.6e-06	2.10e+03	150	751	>1E20	>1E20
Ac-225	2.74e-02	9.5e-05	2.53e+01	150	751	>1E20	>1E20
Ac-226	3.31e-03	4.0e-05	2.10e+02	150	751	>1E20	>1E20
Ac-227	2.18e+01	1.4e-02	3.18e-02	150	751	>1E20	1.9e-02
Ac-228	6.99e-04	2.1e-06	9.91e+02	150	751	>1E20	>1E20
Th-226	5.87e-05	9.2e-07	1.18e+04	3000	15001	>1E20	>1E20
Th-227	5.13e-02	3.6e-05	1.35e+01	3000	15001	>1E20	>1E20
Th-228	1.91e+00	3.8e-04	3.62e-01	3000	15001	>1E20	4.4e+12
Th-229	7.43e+03	3.5e-03	9.33e-05	3000	15001	1.0e+01	8.1e-04
Th-230	7.70e+04	5.3e-04	9.00e-06	3000	15001	1.2e-01	8.0e-04
Th-231	2.91e-03	1.3e-06	2.38e+02	3000	15001	>1E20	>1E20
Th-232	1.41e+10	2.8e-03	4.93e-11	3000	15001	1.2e-02	8.0e-04
Th-234	6.60e-02	1.3e-05	1.05e+01	3000	15001	>1E20	>1E20
Pa-227	7.28e-05	1.3e-06	9.52e+03	10	51	>1E20	>1E20
Pa-228	2.97e-03	4.0e-06	2.34e+02	10	51	>1E20	>1E20
Pa-230	4.85e-02	5.6e-06	1.43e+01	10	51	>1E20	>1E20
Pa-231	3.28e+04	1.1e-02	2.12e-05	10	51	1.0e-05	8.1e-04

Rev. 0

C-21
Table C.1-1. (continued)

WSRC-RP-94-218

Nuclide	T1/2 (year)	DCF (mrem/pCi)	Lambda (1/year)	Kd (cm ³ /gm)	Rf	ILT GW Trigger (Ci/vault)	ILT Int Trigger (Ci/vault)
Pa-232	3.59e-03	3.4e-06	1.93e+02	10	51	>1E20	>1E20
Pa-233	7.39e-02	3.3e-06	9.38e+00	10	51	>1E20	>1E20
Pa-234	7.64e-04	2.1e-06	9.07e+02	10	51	>1E20	>1E20
U-230	5.69e-02	8.4e-04	1.22e+01	50	251	>1E20	>1E20
U-231	4.30e+00	1.1e-06	1.61e-01	50	251	>1E20	8.0e+03
U-232	7.20e+01	1.3e-03	9.63e-03	50	251	2.0e+02	2.1e-03
U-233	1.60e+05	2.7e-04	4.35e-06	50	251	2.1e-03	8.0e-04
U-234	2.45e+05	2.6e-04	2.83e-06	50	251	2.1e-03	8.0e-04
U-235	7.04e+08	2.5e-04	9.85e-10	50	251	2.2e-03	8.0e-04
U-236	2.34e+07	2.5e-04	2.96e-08	50	251	2.2e-03	8.0e-04
U-237	1.85e-02	2.7e-06	3.75e+01	50	251	>1E20	>1E20
U-238	4.47e+09	2.3e-04	1.55e-10	50	251	2.4e-03	8.0e-04
U-239	4.47e-05	7.6e-08	1.55e+04	50	251	>1E20	>1E20
U-240	1.61e-03	4.1e-06	4.31e+02	50	251	>1E20	>1E20
Np-232	2.47e-05	2.4e-08	2.80e+04	10	51	>1E20	>1E20
Np-233	6.65e-05	5.6e-09	1.04e+04	10	51	>1E20	>1E20
Np-234	1.20e-02	1.7e-06	5.75e+01	10	51	>1E20	>1E20
Np-235	1.12e+00	2.1e-07	6.17e-01	10	51	>1E20	>1E20
Np-236(1E5y)	1.10e+05	7.9e-04	6.30e-06	10	51	1.4e-04	8.0e-04
Np-236(22h)	2.51e-03	9.5e-07	2.76e+02	10	51	>1E20	>1E20
Np-237	2.14e+06	3.9e-03	3.24e-07	10	51	2.9e-05	8.0e-04
Np-238	5.80e-03	3.4e-06	1.20e+02	10	51	>1E20	>1E20
Np-239	6.38e-03	2.9e-06	1.09e+02	10	51	>1E20	>1E20
Np-240	1.20e-04	2.0e-07	5.79e+03	10	51	>1E20	>1E20
Pu-234	1.03e-03	1.2e-06	6.75e+02	100	501	>1E20	>1E20
Pu-235	4.94e-05	1.4e-08	1.40e+04	100	501	>1E20	>1E20
Pu-236	2.85e+00	1.3e-03	2.43e-01	100	501	>1E20	2.9e+07
Pu-237	1.24e-01	1.0e-06	5.58e+00	100	501	>1E20	>1E20
Pu-238	8.78e+01	3.8e-03	7.90e-03	100	501	2.5e+05	1.8e-03
Pu-239	2.41e+04	4.3e-03	2.87e-05	100	501	2.8e-04	8.1e-04
Pu-240	6.57e+03	4.3e-03	1.06e-04	100	501	3.4e-04	8.1e-04
Pu-241	1.44e+01	8.6e-05	4.81e-02	100	501	>1E20	9.9e-02
Pu-242	3.76e+05	4.1e-03	1.84e-06	100	501	2.7e-04	8.0e-04
Pu-243	5.65e-04	3.3e-07	1.23e+03	100	501	>1E20	>1E20

Rev. 0

C-22
Table C.1-1. (continued)

WSRC-RP-94-218

Nuclide	T1/2 (year)	DCF (mrem/pCi)	Lambda (1/year)	Kd (cm**3/gm)	Rf	ILT GW Trigger (Ci/vault)	ILT Int Trigger (Ci/vault)
Pu-244	8.10e+07	4.0e-03	8.56e-09	100	501	2.8e-04	8.0e-04
Pu-245	1.14e-03	2.4e-06	6.08e+02	100	501	>1E20	>1E20
Am-237	1.48e-04	7.4e-08	4.67e+03	150	751	>1E20	>1E20
Am-238	2.17e-04	1.7e-07	3.20e+03	150	751	>1E20	>1E20
Am-239	1.38e-03	1.0e-06	5.02e+02	150	751	>1E20	>1E20
Am-240	5.82e-03	2.9e-06	1.19e+02	150	751	>1E20	>1E20
Am-241	4.32e+02	4.5e-03	1.60e-03	150	751	1.8e-01	9.4e-04
Am-242m	1.52e+02	4.2e-03	4.56e-03	150	751	1.7e+04	1.3e-03
Am-242	1.83e-03	1.2e-06	3.80e+02	150	751	>1E20	>1E20
Am-243	7.37e+03	4.5e-03	9.40e-05	150	751	5.3e-04	8.1e-04
Am-244m	4.94e-05	6.8e-08	1.40e+04	150	751	>1E20	>1E20
Am-244	1.15e-03	2.0e-06	6.02e+02	150	751	>1E20	>1E20
Am-245	2.40e-04	1.8e-07	2.89e+03	150	751	>1E20	>1E20
Am-246m	4.75e-05	8.4e-08	1.46e+04	150	751	>1E20	>1E20
Am-246	4.75e-05	1.5e-07	1.46e+04	150	751	>1E20	>1E20
Cm-238	2.85e-04	3.6e-07	2.43e+03	100	501	>1E20	>1E20
Cm-240	7.34e-02	6.3e-05	9.45e+00	100	501	>1E20	>1E20
Cm-241	9.58e-02	4.6e-06	7.23e+00	100	501	>1E20	>1E20
Cm-242	4.46e-01	1.1e-04	1.56e+00	100	501	>1E20	>1E20
Cm-243	2.85e+01	2.9e-03	2.43e-02	100	501	>1E20	9.1e-03
Cm-244	1.81e+01	2.3e-03	3.83e-02	100	501	>1E20	3.7e-02
Cm-245	8.50e+03	4.5e-03	8.15e-05	100	501	3.0e-04	8.1e-04
Cm-246	4.70e+03	4.5e-03	1.47e-04	100	501	3.6e-04	8.2e-04
Cm-247	1.60e+07	4.1e-03	4.33e-08	100	501	2.7e-04	8.0e-04
Cm-248	3.50e+05	1.6e-02	1.98e-06	100	501	6.9e-05	8.0e-04
Cm-249	1.24e-04	9.5e-08	5.61e+03	100	501	>1E20	>1E20
Bk-245	1.36e-02	2.3e-06	5.08e+01	100	501	>1E20	>1E20
Bk-246	4.93e-03	1.9e-06	1.41e+02	100	501	>1E20	>1E20
Bk-247	1.40e+03	2.3e-03	4.95e-04	100	501	1.7e-03	8.4e-04
Bk-249	8.80e-01	6.0e-06	7.88e-01	100	501	>1E20	>1E20
Bk-250	3.67e-04	5.0e-07	1.89e+03	100	501	>1E20	>1E20
Cf-244	4.75e-05	1.5e-07	1.46e+04	100	501	>1E20	>1E20
Cf-246	4.11e-03	1.2e-05	1.69e+02	100	501	>1E20	>1E20
Cf-248	9.86e-01	2.8e-04	7.03e-01	100	501	>1E20	>1E20

Rev. 0

C-23
Table C.1-1. (continued)

WSRC-RP-94-218

Nuclide	T1/2 (year)	DCF (mrem/pCi)	Lambda (1/year)	Kd (cm ³ /gm)	Rf	ILT GW Trigger (Ci/vault)	ILT Int Trigger (Ci/vault)
Cf-249	3.51e+02	4.6e-03	1.97e-03	100	501	4.1e-02	9.8e-04
Cf-250	1.31e+01	1.9e-03	5.29e-02	100	501	>1E20	1.6e-01
Cf-251	9.00e+02	4.6e-03	7.70e-04	100	501	1.8e-03	8.7e-04
Cf-252	2.62e+00	9.4e-04	2.65e-01	100	501	>1E20	2.5e+08
Cf-253	4.87e-02	9.2e-06	1.42e+01	100	501	>1E20	>1E20
Cf-254	1.66e-01	2.5e-03	4.18e+00	100	501	>1E20	>1E20
Es-250	9.13e-04	9.5e-08	7.60e+02	100	501	>1E20	>1E20
Es-251	4.11e-03	6.7e-07	1.69e+02	100	501	>1E20	>1E20
Es-253	5.60e-02	2.4e-05	1.24e+01	100	501	>1E20	>1E20
Es-254m	4.48e-03	1.5e-05	1.55e+02	100	501	>1E20	>1E20
Es-254	7.56e-01	1.5e-04	9.17e-01	100	501	>1E20	>1E20
Fm-252	2.62e-03	9.9e-06	2.64e+02	100	501	>1E20	>1E20
Fm-253	8.21e-03	3.5e-06	8.44e+01	100	501	>1E20	>1E20
Fm-254	3.70e-04	1.6e-06	1.88e+03	100	501	>1E20	>1E20
Fm-255	2.29e-03	9.7e-06	3.02e+02	100	501	>1E20	>1E20
Fm-257	2.19e-01	7.3e-05	3.16e+00	100	501	>1E20	>1E20
Md-257	3.42e-04	5.4e-07	2.03e+03	100	501	>1E20	>1E20
Md-258	1.53e-01	6.1e-05	4.52e+00	100	501	>1E20	>1E20

Table C.1-2. Screening calculations and trigger levels for the ILNT vaults

Nuclide	T1/2 (year)	DCF (mrem/pCi)	Lambda (1/year)	Kd (cm ³ /gm)	Rf	ILNT GW Trigger (Ci/vault)	ILNT Int Trigger (Ci/vault)
H-3	1.23e+01	6.3e-08	5.62e-02	0	1	3.4e-01	1.6e+00
Bc-7	1.47e-01	1.1e-07	4.72e+00	0	1	2.6e+09	>1E20
Bc-10	1.60e+06	4.2e-06	4.33e-07	0	1	3.8e-03	5.9e-03
C-11	3.86e-05	1.2e-08	1.80e+04	2	11	>1E20	>1E20
C-14	5.73e+03	2.1e-06	1.21e-04	2	11	8.5e-02	6.0e-03
F-18	2.14e-04	1.0e-04	3.25e+03	0	1	>1E20	>1E20
Na-22	2.58e+00	1.2e-05	2.69e-01	0	1	5.1e-03	2.7e+09
Na-24	1.71e-03	1.4e-06	4.05e+02	0	1	>1E20	>1E20
Mg-28	2.40e-03	7.5e-06	2.89e+02	0	1	>1E20	>1E20
Al-26	7.40e+05	1.3e-05	9.37e-07	0	1	1.2e-03	5.9e-03
Si-31	2.99e-04	5.4e-07	2.32e+03	0	1	>1E20	>1E20
Si-32	6.50e+02	1.7e-06	1.07e-03	0	1	9.5e-03	6.5e-03
P-32	3.89e-02	7.7e-06	1.78e+01	0	1	>1E20	>1E20
P-33	6.84e-02	8.8e-07	1.01e+01	0	1	>1E20	>1E20
S-35	2.39e-01	4.3e-07	2.90e+00	0	1	7.6e+04	>1E20
Cl-36	3.01e+05	3.0e-06	2.30e-06	0	1	5.4e-03	5.9e-03
Cl-38	7.07e-05	2.0e-07	9.80e+03	0	1	>1E20	>1E20
Cl-39	1.06e-04	1.4e-07	6.57e+03	0	1	>1E20	>1E20
K-40	1.28e+09	1.9e-05	5.42e-10	0	1	8.5e-04	5.9e-03
K-42	1.41e-03	1.1e-06	4.92e+02	0	1	>1E20	>1E20
K-43	2.56e-03	7.8e-07	2.71e+02	0	1	>1E20	>1E20
K-44	4.18e-05	1.5e-07	1.66e+04	0	1	>1E20	>1E20
K-45	3.04e-05	9.3e-08	2.28e+04	0	1	>1E20	>1E20
Ca-41	1.30e+05	1.2e-06	5.33e-06	0	1	1.3e-02	5.9e-03
Ca-45	4.46e-01	3.0e-06	1.55e+00	0	1	1.3e+01	>1E20
Ca-47	1.24e-02	6.2e-06	5.58e+01	0	1	>1E20	>1E20
Sc-43	4.47e-04	7.3e-07	1.55e+03	0	1	>1E20	>1E20
Sc-44m	6.68e-03	9.9e-06	1.04e+02	0	1	>1E20	>1E20
Sc-44	4.47e-04	1.4e-06	1.55e+03	0	1	>1E20	>1E20
Sc-46	2.29e-01	5.6e-06	3.02e+00	0	1	1.0e+04	>1E20
Sc-47	9.39e-03	1.9e-06	7.38e+01	0	1	>1E20	>1E20
Sc-48	5.03e-03	6.4e-06	1.38e+02	0	1	>1E20	>1E20
Sc-49	1.09e-04	2.4e-07	6.34e+03	0	1	>1E20	>1E20

Rev. 0

C-25
Table C.1-2. (continued)

WSRC-RP-94-218

Nuclide	T1/2 (year)	DCF (mrem/pCi)	Lambda (1/year)	Kd (cm ³ /gm)	Rf	ILNT GW Trigger (Ci/vault)	ILNT Int Trigger (Ci/vault)
Ti-44	4.80e+01	1.9e-05	1.44e-02	0	1	9.1e-04	2.5e-02
Ti-45	3.52e-04	5.7e-07	1.97e+03	0	1	>1E20	>1E20
V-47	6.27e-05	1.6e-07	1.10e+04	0	1	>1E20	>1E20
V-48	4.41e-02	7.5e-06	1.57e+01	0	1	>1E20	>1E20
V-49	9.03e-01	5.4e-08	7.67e-01	0	1	1.4e+01	>1E20
Cr-48	2.62e-03	8.2e-07	2.64e+02	40	201	>1E20	>1E20
Cr-49	7.97e-05	1.7e-07	8.70e+03	40	201	>1E20	>1E20
Cr-51	7.58e-02	1.3e-07	9.14e+00	40	201	>1E20	>1E20
Mn-51	8.56e-05	2.5e-07	8.10e+03	50	251	>1E20	>1E20
Mn-52m	3.99e-05	1.5e-07	1.74e+04	50	251	>1E20	>1E20
Mn-52	1.52e-02	6.9e-06	4.56e+01	50	251	>1E20	>1E20
Mn-53	2.00e+06	9.9e-08	3.47e-07	50	251	4.1e+01	5.9e-03
Mn-54	7.97e-01	2.7e-06	8.70e-01	50	251	>1E20	>1E20
Mn-56	2.94e-04	9.5e-07	2.36e+03	50	251	>1E20	>1E20
Fe-52	9.35e-04	5.4e-06	7.41e+02	0	1	>1E20	>1E20
Fe-55	2.70e+00	5.8e-07	2.57e-01	0	1	1.0e-01	8.3e+08
Fe-59	1.22e-01	6.6e-06	5.68e+00	0	1	5.2e+09	>1E20
Fe-60	3.00e+05	1.5e-04	2.31e-06	0	1	1.1e-04	5.9e-03
Co-55	2.08e-03	4.1e-06	3.34e+02	10	51	>1E20	>1E20
Co-56	2.11e-01	1.2e-05	3.29e+00	10	51	>1E20	>1E20
Co-57	7.39e-01	1.1e-05	9.38e-01	10	51	>1E20	>1E20
Co-58m	1.03e-03	8.8e-08	6.75e+02	10	51	>1E20	>1E20
Co-58	1.95e-01	3.5e-06	3.55e+00	10	51	>1E20	>1E20
Co-60m	2.00e-05	3.6e-09	3.47e+04	10	51	>1E20	>1E20
Co-60	5.27e+00	2.6e-05	1.32e-01	10	51	1.2e+13	3.0e+03
Co-61	1.88e-04	2.6e-07	3.68e+03	10	51	>1E20	>1E20
Co-62m	3.04e-06	9.6e-08	2.28e+05	10	51	>1E20	>1E20
Ni-56	1.67e-02	3.5e-06	4.15e+01	300	1501	>1E20	>1E20
Ni-57	4.11e-03	3.3e-06	1.69e+02	300	1501	>1E20	>1E20
Ni-59	8.00e+04	2.0e-07	8.66e-06	300	1501	1.3e+02	5.9e-03
Ni-63	1.00e+02	5.4e-07	6.93e-03	300	1501	>1E20	1.2e-02
Ni-65	2.87e-04	6.1e-07	2.41e+03	300	1501	>1E20	>1E20
Ni-66	6.23e-03	1.1e-05	1.11e+02	300	1501	>1E20	>1E20
Cu-60	4.37e-05	1.7e-07	1.59e+04	25	126	>1E20	>1E20

Rev. 0

C-26
Table C.1-2 (continued)

WSRC-RP-94-218

Nuclide	T1/2 (year)	DCF (mrem/pCi)	Lambda (1/year)	Kd (cm ³ /gm)	Rf	ILNT GW Trigger (Ci/vault)	ILNT Int Trigger (Ci/vault)
Cu-61	3.89e-04	4.1e-07	1.78e+03	25	126	>1E20	>1E20
Cu-64	1.45e-03	4.3e-07	4.78e+02	25	126	>1E20	>1E20
Cu-67	7.06e-03	1.1e-06	9.82e+01	25	126	>1E20	>1E20
Zn-62	1.04e-03	3.4e-06	6.64e+02	16	81	>1E20	>1E20
Zn-63	7.30e-05	2.0e-07	9.49e+03	16	81	>1E20	>1E20
Zn-65	6.67e-01	1.4e-05	1.04e+00	16	81	>1E20	>1E20
Zn-69m	1.57e-03	1.2e-05	4.40e+02	16	81	>1E20	>1E20
Zn-69	1.08e-04	8.5e-08	6.40e+03	16	81	>1E20	>1E20
Zn-71m	4.56e-04	8.3e-07	1.52e+03	16	81	>1E20	>1E20
Zn-72	1.27e-01	4.9e-06	5.44e+00	16	81	>1E20	>1E20
Ga-65	2.89e-05	7.8e-08	2.40e+04	0	1	>1E20	>1E20
Ga-66	1.07e-03	4.7e-06	6.46e+02	0	1	>1E20	>1E20
Ga-67	8.91e-03	7.2e-07	7.78e+01	0	1	>1E20	>1E20
Ga-68	1.30e-04	3.3e-07	5.34e+03	0	1	>1E20	>1E20
Ga-70	4.01e-05	7.1e-08	1.73e+04	0	1	>1E20	>1E20
Ga-72	1.61e-03	4.4e-06	4.31e+02	0	1	>1E20	>1E20
Ga-73	1.34e-02	1.0e-06	5.19e+01	0	1	>1E20	>1E20
Ge-66	1.07e-03	2.1e-07	6.46e+02	0	1	>1E20	>1E20
Ge-67	3.61e-05	1.1e-07	1.92e+04	0	1	>1E20	>1E20
Ge-68	7.86e-01	1.1e-06	8.82e-01	0	1	1.2e+00	>1E20
Ge-69	4.45e-03	3.6e-07	1.56e+02	0	1	>1E20	>1E20
Ge-71	3.12e-02	9.6e-09	2.22e+01	0	1	>1E20	>1E20
Ge-75	1.57e-04	7.3e-08	4.40e+03	0	1	>1E20	>1E20
Ge-77	1.29e-03	5.6e-07	5.38e+02	0	1	>1E20	>1E20
Ge-78	1.65e-04	2.1e-07	4.19e+03	0	1	>1E20	>1E20
As-69	2.85e-05	1.1e-07	2.43e+04	3	16	>1E20	>1E20
As-70	1.01e-04	3.4e-07	6.88e+03	3	16	>1E20	>1E20
As-71	7.07e-03	1.3e-06	9.80e+01	3	16	>1E20	>1E20
As-72	2.97e-03	5.6e-06	2.34e+02	3	16	>1E20	>1E20
As-73	2.20e-01	6.1e-07	3.15e+00	3	16	>1E20	>1E20
As-74	3.29e-02	3.3e-06	2.11e+01	3	16	>1E20	>1E20
As-76	3.00e-03	4.8e-06	2.31e+02	3	16	>1E20	>1E20
As-77	1.06e-01	1.1e-06	6.53e+00	3	16	>1E20	>1E20
As-78	1.73e-04	6.5e-07	4.01e+03	3	16	>1E20	>1E20

Rev. 0

C-27
Table C.1-2 (continued)

WSRC-RP-94-218

Nuclide	T1/2 (year)	DCF (mrem/pCi)	Lambda (1/year)	Kd (cm ³ /gm)	Rf	ILNT GW Trigger (Ci/vault)	ILNT Int Trigger (Ci/vault)
Se-70	8.37e-05	4.8e-07	8.29e+03	5	26	>1E20	>1E20
Se-73m	7.99e-05	1.5e-07	8.68e+03	5	26	>1E20	>1E20
Se-73	8.10e-04	1.5e-06	8.56e+02	5	26	>1E20	>1E20
Se-75	3.30e-01	8.8e-06	2.10e+00	5	26	>1E20	>1E20
Se-79	6.50e+04	8.3e-06	1.07e-05	5	26	5.1e-02	5.9e-03
Se-81m	1.09e-04	2.1e-07	6.36e+03	5	26	>1E20	>1E20
Se-81	4.30e-05	6.1e-08	1.61e+04	5	26	>1E20	>1E20
Se-83	4.28e-05	1.5e-07	1.62e+04	5	26	>1E20	>1E20
Br-74m	7.89e-05	2.2e-07	8.78e+03	0	1	>1E20	>1E20
Br-74	6.84e-05	1.4e-07	1.01e+04	0	1	>1E20	>1E20
Br-75	1.94e-04	1.3e-07	3.57e+03	0	1	>1E20	>1E20
Br-76	1.84e-03	1.4e-06	3.77e+02	0	1	>1E20	>1E20
Br-77	6.50e-03	3.1e-07	1.07e+02	0	1	>1E20	>1E20
Br-80m	5.04e-04	2.3e-07	1.37e+03	0	1	>1E20	>1E20
Br-80	3.37e-05	5.5e-08	2.06e+04	0	1	>1E20	>1E20
Br-82	4.03e-03	1.7e-06	1.72e+02	0	1	>1E20	>1E20
Br-83	2.74e-04	7.3e-08	2.53e+03	0	1	>1E20	>1E20
Br-84	6.05e-05	1.5e-07	1.15e+04	0	1	>1E20	>1E20
Rb-79	3.99e-05	8.7e-08	1.74e+04	0	1	>1E20	>1E20
Rb-81m	6.08e-05	1.8e-08	1.14e+04	0	1	>1E20	>1E20
Rb-81	5.36e-04	1.3e-07	1.29e+03	0	1	>1E20	>1E20
Rb-82m	7.30e-04	4.2e-07	9.49e+02	0	1	>1E20	>1E20
Rb-83	2.27e-01	7.7e-06	3.05e+00	0	1	8.8e+03	>1E20
Rb-84	9.31e-02	1.0e-05	7.45e+00	0	1	2.4e+13	>1E20
Rb-86	5.09e-02	9.4e-06	1.36e+01	0	1	>1E20	>1E20
Rb-87	4.80e+10	4.8e-06	1.44e-11	0	1	3.4e-03	5.9e-03
Rb-88	3.37e-05	1.6e-07	2.06e+04	0	1	>1E20	>1E20
Rb-89	2.89e-05	8.0e-08	2.40e+04	0	1	>1E20	>1E20
Sr-80	1.94e-04	5.2e-09	3.57e+03	10	51	>1E20	>1E20
Sr-81	5.51e-05	2.2e-07	1.26e+04	10	51	>1E20	>1E20
Sr-83	3.76e-03	2.3e-06	1.84e+02	10	51	>1E20	>1E20
Sr-85m	1.29e-04	2.4e-08	5.39e+03	10	51	>1E20	>1E20
Sr-85	1.79e-01	1.9e-06	3.88e+00	10	51	>1E20	>1E20
Sr-87m	3.21e-04	1.2e-07	2.16e+03	10	51	>1E20	>1E20

Rev. 0

C-28
Table C.1-2 (continued)

WSRC-RP-94-218

Nuclide	T1/2 (year)	DCF (mrem/pCi)	Lambda (1/year)	Kd (cm ³ /gm)	Rf	ILNT GW Trigger (Ci/vault)	ILNT Int Trigger (Ci/vault)
Sr-89	1.38e-01	8.7e-06	5.01e+00	10	51	>1E20	>1E20
Sr-90	2.86e+01	1.3e-04	2.42e-02	10	51	3.1e+00	6.6e-02
Sr-91	1.08e-03	3.0e-06	6.41e+02	10	51	>1E20	>1E20
Sr-92	3.09e-04	1.9e-06	2.24e+03	10	51	>1E20	>1E20
Y-86m	9.13e-05	2.4e-07	7.60e+03	10	51	>1E20	>1E20
Y-86	1.67e-03	4.1e-06	4.16e+02	10	51	>1E20	>1E20
Y-87	9.13e-03	2.2e-06	7.60e+01	10	51	>1E20	>1E20
Y-88	2.88e-01	5.2e-06	2.41e+00	10	51	>1E20	>1E20
Y-90m	3.64e-04	6.6e-07	1.90e+03	10	51	>1E20	>1E20
Y-90	2.86e+01	1.0e-05	2.42e-02	10	51	4.0e+01	6.6e-02
Y-91m	9.51e-05	3.9e-08	7.29e+03	10	51	>1E20	>1E20
Y-91	1.67e-01	8.9e-06	4.15e+00	10	51	>1E20	>1E20
Y-92	4.03e-04	1.9e-06	1.72e+03	10	51	>1E20	>1E20
Y-93	1.16e-03	4.5e-06	5.96e+02	10	51	>1E20	>1E20
Y-94	3.61e-05	1.8e-07	1.92e+04	10	51	>1E20	>1E20
Y-95	2.00e-05	9.7e-08	3.47e+04	10	51	>1E20	>1E20
Zr-86	1.88e-03	3.5e-06	3.68e+02	0	1	>1E20	>1E20
Zr-88	2.33e-01	1.3e-06	2.98e+00	0	1	3.6e+04	>1E20
Zr-89	8.94e-03	3.1e-06	7.75e+01	0	1	>1E20	>1E20
Zr-93	1.50e+06	1.6e-06	4.62e-07	0	1	1.0e-02	5.9e-03
Zr-95	1.75e-01	3.4e-06	3.96e+00	0	1	1.8e+06	>1E20
Zr-97	1.92e-03	8.0e-06	3.62e+02	0	1	>1E20	>1E20
Nb-88	2.66e-05	7.2e-08	2.60e+04	0	1	>1E20	>1E20
Nb-89(66m)	1.25e-04	4.6e-07	5.52e+03	0	1	>1E20	>1E20
Nb-89(122m)	2.32e-04	1.0e-06	2.99e+03	0	1	>1E20	>1E20
Nb-90	1.67e-03	4.9e-06	4.16e+02	0	1	>1E20	>1E20
Nb-93m	1.01e+01	5.3e-07	6.84e-02	0	1	4.3e-02	5.5e+00
Nb-94	2.00e+04	5.1e-06	3.47e-05	0	1	3.2e-03	5.9e-03
Nb-95m	9.88e-03	2.0e-06	7.02e+01	0	1	>1E20	>1E20
Nb-95	9.58e-02	2.2e-06	7.23e+00	0	1	3.7e+13	>1E20
Nb-96	2.67e-03	4.4e-06	2.60e+02	0	1	>1E20	>1E20
Nb-97	1.40e-04	2.3e-07	4.95e+03	0	1	>1E20	>1E20
Nb-98	8.87e-08	3.4e-07	7.81e+06	0	1	>1E20	>1E20
Mo-90	6.50e-04	2.5e-06	1.07e+03	0	1	>1E20	>1E20

Rev. 0

C-29
Table C.1-2 (continued)

WSRC-RP-94-218

Nuclide	T1/2 (year)	DCF (mrem/pCi)	Lambda (1/year)	Kd (cm ³ /gm)	Rf	ILNT GW Trigger (Ci/vault)	ILNT Int Trigger (Ci/vault)
Mo-93m	7.87e-04	1.1e-06	8.81e+02	0	1	>1E20	>1E20
Mo-93	3.50e+03	1.3e-06	1.98e-04	0	1	1.2e-02	6.0e-03
Mo-99	7.53e-03	4.4e-06	9.20e+01	0	1	>1E20	>1E20
Mo-101	2.78e-05	9.2e-08	2.50e+04	0	1	>1E20	>1E20
Tc-93m	8.18e-05	7.1e-08	8.48e+03	0.36	2.8	>1E20	>1E20
Tc-93	3.08e-04	1.6e-07	2.25e+03	0.36	2.8	>1E20	>1E20
Tc-94m	1.01e-04	2.5e-07	6.88e+03	0.36	2.8	>1E20	>1E20
Tc-94	5.57e-04	5.8e-07	1.24e+03	0.36	2.8	>1E20	>1E20
Tc-96m	9.89e-05	3.1e-08	7.01e+03	0.36	2.8	>1E20	>1E20
Tc-96	1.18e-02	2.7e-06	5.89e+01	0.36	2.8	>1E20	>1E20
Tc-97m	2.46e-01	1.1e-06	2.81e+00	0.36	2.8	5.2e+15	>1E20
Tc-97	2.60e+06	1.5e-07	2.67e-07	0.36	2.8	3.0e-01	5.9e-03
Tc-98	1.50e+06	4.8e-06	4.62e-07	0.36	2.8	9.4e-03	5.9e-03
Tc-99m	6.87e-04	6.0e-08	1.01e+03	0.36	2.8	>1E20	>1E20
Tc-99	2.11e+05	1.3e-06	3.29e-06	0.36	2.8	3.5e-02	5.9e-03
Tc-101	2.70e-05	3.8e-08	2.57e+04	0.36	2.8	>1E20	>1E20
Tc-104	3.42e-05	1.6e-07	2.03e+04	0.36	2.8	>1E20	>1E20
Ru-94	1.08e-04	3.3e-07	6.40e+03	100	501	>1E20	>1E20
Ru-97	7.91e-03	6.4e-07	8.76e+01	100	501	>1E20	>1E20
Ru-103	1.08e-01	2.7e-06	6.43e+00	100	501	>1E20	>1E20
Ru-105	5.07e-04	1.0e-06	1.37e+03	100	501	>1E20	>1E20
Ru-106	9.99e-01	2.1e-05	6.94e-01	100	501	>1E20	>1E20
Rh-99m	5.36e-04	2.8e-07	1.29e+03	0	1	>1E20	>1E20
Rh-99	4.38e-02	2.0e-06	1.58e+01	0	1	>1E20	>1E20
Rh-100	2.28e-03	3.1e-06	3.04e+02	0	1	>1E20	>1E20
Rh-101m	1.23e-02	8.8e-07	5.63e+01	0	1	>1E20	>1E20
Rh-101	3.10e+00	2.3e-06	2.24e-01	0	1	2.1e-02	3.0e+07
Rh-102m	2.90e+00	3.5e-06	2.39e-01	0	1	1.5e-02	1.4e+08
Rh-102	5.75e-01	5.5e-06	1.21e+00	0	1	1.2e+00	>1E20
Rh-103m	1.06e-04	0.00000001	6.51e+03	0	1	>1E20	>1E20
Rh-105	4.05e-03	1.4e-06	1.71e+02	0	1	>1E20	>1E20
Rh-106m	2.49e-04	6.1e-07	2.79e+03	0	1	>1E20	>1E20
Rh-107	4.13e-05	5.4e-08	1.68e+04	0	1	>1E20	>1E20
Pd-100	1.10e-02	3.8e-06	6.33e+01	0	1	>1E20	>1E20

Rev. 0

Table C-1.2 (continued)

Nuclide	T _{1/2} (year)	DCF (mrem/pCi)	Lambda (1/year)	K _d (cm ² /g)	R _f	ILNT GW Trigger (Ci/vault)	ILNT Int Trigger (Ci/vault)
Pd-101	9.58e-04	3.8e-07	7.23e+02	0	1	>1E20	>1E20
Pd-103	4.65e-02	6.9e-07	1.49e+01	0	1	>1E20	>1E20
Pd-107	6.50e+06	1.4e-07	1.07e-07	0	1	1.2e-01	5.9e-03
Pd-109	1.53e-03	2.1e-06	4.53e+02	0	1	>1E20	>1E20
Ag-102	2.85e-05	7.9e-08	2.43e+04	10	51	>1E20	>1E20
Ag-103	1.25e-04	1.4e-07	5.52e+03	10	51	>1E20	>1E20
Ag-104m	5.70e-05	1.5e-07	1.22e+04	10	51	>1E20	>1E20
Ag-104	1.27e-04	2.3e-07	5.44e+03	10	51	>1E20	>1E20
Ag-105	1.10e-01	1.9e-06	6.33e+00	10	51	>1E20	>1E20
Ag-106m	2.27e-02	6.1e-06	3.05e+01	10	51	>1E20	>1E20
Ag-106	4.56e-05	7.6e-08	1.52e+04	10	51	>1E20	>1E20
Ag-108m	1.30e+02	7.5e-06	5.33e-03	10	51	4.3e-01	1.0e-02
Ag-110m	6.98e-01	1.1e-05	1.00e+00	10	51	>1E20	>1E20
Ag-111	2.05e-02	4.5e-06	3.39e+01	10	51	>1E20	>1E20
Ag-112	3.57e-04	1.6e-06	1.94e+03	10	51	>1E20	>1E20
Ag-115	3.99e-05	1.5e-07	1.74e+04	10	51	>1E20	>1E20
Cd-104	1.08e-04	2.3e-07	6.40e+03	8	41	>1E20	>1E20
Cd-107	7.42e-04	2.4e-07	9.35e+02	8	41	>1E20	>1E20
Cd-109	1.24e+00	1.2e-05	5.59e-01	8	41	>1E20	>1E20
Cd-113m	1.46e+01	1.5e-04	4.75e-02	8	41	7.4e+01	6.8e-01
Cd-113	9.30e+15	1.6e-04	7.45e-17	8	41	4.1e-03	5.9e-03
Cd-115m	1.36e-01	1.5e-05	5.11e+00	8	41	>1E20	>1E20
Cd-115	6.10e-03	4.7e-06	1.14e+02	8	41	>1E20	>1E20
Cd-117m	3.88e-04	1.1e-06	1.79e+03	8	41	>1E20	>1E20
Cd-117	2.97e-04	1.1e-06	2.34e+03	8	41	>1E20	>1E20
In-109	4.91e-04	2.7e-07	1.41e+03	0	1	>1E20	>1E20
In-110(69m)	1.27e-04	3.3e-07	5.44e+03	0	1	>1E20	>1E20
In-111	7.69e-03	1.2e-06	9.01e+01	0	1	>1E20	>1E20
In-112	2.66e-05	0.00000002	2.60e+04	0	1	>1E20	>1E20
In-113m	1.89e-04	1.0e-07	3.66e+03	0	1	>1E20	>1E20
In-114m	1.36e-01	0.000015	5.11e+00	0	1	1.4e+08	>1E20
In-115m	5.13e-04	3.4e-07	1.35e+03	0	1	>1E20	>1E20
In-115	4.60e+15	1.4e-04	1.51e-16	0	1	1.2e-04	5.9e-03
In-116m	1.03e-04	2.1e-07	6.73e+03	0	1	>1E20	>1E20

Rev. 0

C-31
Table C.1-2 (continued)

WSRC-RP-94-218

Nuclide	T1/2 (year)	DCF (mrem/pCi)	Lambda (1/year)	Kd (cm ² /gm)	Rf	ILNT GW Trigger (Ci/vault)	ILNT Int Trigger (Ci/vault)
In-117m	2.21e-04	4.2e-07	3.13e+03	0	1	>1E20	>1E20
In-117	8.37e-05	8.7e-08	8.29e+03	0	1	>1E20	>1E20
In-119m	3.42e-05	1.0e-07	2.03e+04	0	1	>1E20	>1E20
Sn-110	4.56e-04	1.5e-06	1.52e+03	130	651	>1E20	>1E20
Sn-111	6.65e-05	6.7e-08	1.04e+04	130	651	>1E20	>1E20
Sn-113	3.15e-01	2.7e-06	2.20e+00	130	651	>1E20	>1E20
Sn-117m	3.83e-02	2.6e-06	1.81e+01	130	651	>1E20	>1E20
Sn-119m	8.02e-01	1.2e-05	8.64e-01	130	651	>1E20	>1E20
Sn-121m	7.60e+01	1.3e-06	9.12e-03	130	651	6.3e+13	1.5e-02
Sn-121	3.08e-03	8.9e-07	2.25e+02	130	651	>1E20	>1E20
Sn-123m	7.61e-05	1.0e-07	9.11e+03	130	651	>1E20	>1E20
Sn-123	3.53e-01	7.7e-06	1.96e+00	130	651	>1E20	>1E20
Sn-125	2.64e-02	1.1e-05	2.62e+01	130	651	>1E20	>1E20
Sn-126	1.00e+05	1.7e-05	6.93e-06	130	651	6.3e-01	5.9e-03
Sn-127	2.42e-04	7.4e-07	2.87e+03	130	651	>1E20	>1E20
Sn-128	1.12e-04	5.2e-07	6.18e+03	130	651	>1E20	>1E20
Sb-115	5.89e-05	6.3e-08	1.18e+04	10	51	>1E20	>1E20
Sb-116m	1.14e-04	2.4e-07	6.08e+03	10	51	>1E20	>1E20
Sb-116	2.85e-05	5.6e-08	2.43e+04	10	51	>1E20	>1E20
Sb-117	3.19e-04	7.4e-08	2.17e+03	10	51	>1E20	>1E20
Sb-118m	5.82e-04	9.3e-07	1.19e+03	10	51	>1E20	>1E20
Sb-119	4.33e-03	3.4e-07	1.60e+02	10	51	>1E20	>1E20
Sb-120(16m)	3.04e-05	3.0e-08	2.28e+04	10	51	>1E20	>1E20
Sb-120(6d)	1.59e-02	5.4e-06	4.37e+01	10	51	>1E20	>1E20
Sb-122	7.45e-03	6.3e-06	9.31e+01	10	51	>1E20	>1E20
Sb-124m	1.77e-04	2.0e-08	3.92e+03	10	51	>1E20	>1E20
Sb-124	1.65e-01	9.3e-06	4.20e+00	10	51	>1E20	>1E20
Sb-125	2.40e+00	2.6e-06	2.89e-01	10	51	>1E20	2.0e+10
Sb-126m	3.61e-05	7.3e-08	1.92e+04	10	51	>1E20	>1E20
Sb-126	3.39e-02	9.6e-06	2.04e+01	10	51	>1E20	>1E20
Sb-127	1.04e-02	6.6e-06	6.66e+01	10	51	>1E20	>1E20
Sb-128(9h)	1.03e-03	4.3e-06	6.75e+02	10	51	>1E20	>1E20
Sb-128(10m)	1.90e-05	5.0e-08	3.65e+04	10	51	>1E20	>1E20
Sb-129	4.95e-04	1.7e-06	1.40e+03	10	51	>1E20	>1E20

Rev. 0

C-32
Table C.1-2. (continued)

Nuclide	T1/2 (year)	DCF (mrem/pCi)	Lambda (1/year)	Kd (cm ³ /gm)	Rf	ILNT GW Trigger (C/vault)	ILNT Int Trigger (C/vault)
Sb-130	1.25e-05	2.6e-07	5.52e+04	10	51	>1E20	>1E20
Sb-131	4.37e-05	2.9e-07	1.59e+04	10	51	>1E20	>1E20
Te-118	1.64e-02	6.7e-07	4.22e+01	0	1	>1E20	>1E20
Te-121m	4.11e-01	6.7e-06	1.69e+00	0	1	1.1e+01	>1E20
Te-121	4.65e-02	1.5e-06	1.49e+01	0	1	>1E20	>1E20
Te-123m	3.28e-01	5.1e-06	2.12e+00	0	1	1.2e+02	>1E20
Te-123	1.20e+13	4.1e-06	5.78e-14	0	1	3.9e-03	5.9e-03
Te-125m	1.59e-01	3.4e-06	4.37e+00	0	1	1.4e+07	>1E20
Te-127m	2.98e-01	7.9e-06	2.32e+00	0	1	2.3e+02	>1E20
Te-127	1.07e-03	6.9e-07	6.46e+02	0	1	>1E20	>1E20
Te-129m	9.14e-02	9.9e-06	7.58e+00	0	1	4.7e+13	>1E20
Te-129	1.33e-04	1.9e-07	5.21e+03	0	1	>1E20	>1E20
Te-131m	3.42e-03	1.5e-05	2.03e+02	0	1	>1E20	>1E20
Te-131	4.75e-05	2.0e-07	1.46e+04	0	1	>1E20	>1E20
Te-132	8.76e-03	7.4e-06	7.91e+01	0	1	>1E20	>1E20
Te-133m	1.05e-04	7.6e-07	6.58e+03	0	1	>1E20	>1E20
Te-133	2.38e-05	1.6e-07	2.92e+04	0	1	>1E20	>1E20
Te-134	7.99e-05	2.1e-07	8.68e+03	0	1	>1E20	>1E20
I-120m	1.01e-04	3.9e-07	6.88e+03	0.6	4	>1E20	>1E20
I-120	1.48e-04	6.7e-07	4.67e+03	0.6	4	>1E20	>1E20
I-121	2.40e-04	1.8e-07	2.89e+03	0.6	4	>1E20	>1E20
I-123	1.52e-03	4.9e-07	4.57e+02	0.6	4	>1E20	>1E20
I-124	1.15e-02	3.1e-05	6.03e+01	0.6	4	>1E20	>1E20
I-125	1.64e-01	3.8e-05	4.22e+00	0.6	4	>1E20	>1E20
I-126	3.64e-02	7.1e-05	1.90e+01	0.6	4	>1E20	>1E20
I-128	4.75e-05	8.5e-08	1.46e+04	0.6	4	>1E20	>1E20
I-129	1.72e+07	2.8e-04	4.02e-08	0.6	4	2.3e-04	5.9e-03
I-130	1.41e-03	4.3e-06	4.90e+02	0.6	4	>1E20	>1E20
I-131	2.22e-02	5.3e-05	3.13e+01	0.6	4	>1E20	>1E20
I-132m	1.58e-04	4.7e-07	4.39e+03	0.6	4	>1E20	>1E20
I-132	2.60e-04	3.3e-07	2.66e+03	0.6	4	>1E20	>1E20
I-133	2.37e-03	5.4e-06	2.92e+02	0.6	4	>1E20	>1E20
I-134	1.00e-04	1.9e-07	6.93e+03	0.6	4	>1E20	>1E20
I-135	7.51e-04	2.0e-05	9.23e+02	0.6	4	>1E20	>1E20

Rev. 0

C-33
Table C.1-2. (continued)

WSRC-RP-94-218

Nuclide	T1/2 (year)	DCF (mrem/pCi)	Lambda (1/year)	Kd (cm ³ /gm)	Rf	ILNT GW Trigger (Ci/vault)	ILNT Int Trigger (Ci/vault)
Cs-125	8.56e-05	5.5e-08	8.10e+03	100	501	>1E20	>1E20
Cs-127	7.07e-04	8.0e-08	9.80e+02	100	501	>1E20	>1E20
Cs-129	3.65e-03	2.2e-07	1.90e+02	100	501	>1E20	>1E20
Cs-130	5.70e-05	4.9e-08	1.22e+04	100	501	>1E20	>1E20
Cs-131	2.66e-02	2.4e-07	2.61e+01	100	501	>1E20	>1E20
Cs-132	1.80e-02	1.9e-06	3.85e+01	100	501	>1E20	>1E20
Cs-134m	3.31e-04	4.2e-08	2.10e+03	100	501	>1E20	>1E20
Cs-134	2.06e+00	7.4e-05	3.36e-01	100	501	>1E20	2.4e+12
Cs-135m	1.01e-04	4.9e-08	6.88e+03	100	501	>1E20	>1E20
Cs-135	2.30e+06	7.1e-06	3.01e-07	100	501	1.1e+00	5.9e-03
Cs-136	3.53e-02	1.1e-05	1.96e+01	100	501	>1E20	>1E20
Cs-137	3.01e+01	5.0e-05	2.30e-02	100	501	>1E20	5.9e-02
Cs-138	6.12e-05	1.6e-07	1.13e+04	100	501	>1E20	>1E20
Ba-126	1.84e-04	9.0e-07	3.76e+03	5	26	>1E20	>1E20
Ba-128	6.57e-03	1.0e-05	1.05e+02	5	26	>1E20	>1E20
Ba-131m	2.78e-05	9.7e-07	2.50e+04	5	26	>1E20	>1E20
Ba-131	3.20e-02	1.6e-06	2.16e+01	5	26	>1E20	>1E20
Ba-133m	4.44e-03	2.0e-06	1.56e+02	5	26	>1E20	>1E20
Ba-133	1.07e+01	3.2e-06	6.48e-02	5	26	5.9e+02	3.8e+00
Ba-135m	3.27e-03	1.6e-06	2.12e+02	5	26	>1E20	>1E20
Ba-137m	0.000005		1.43e+05	5	26	>1E20	>1E20
Ba-139	1.58e-04	3.9e-07	4.38e+03	5	26	>1E20	>1E20
Ba-140	3.50e-02	8.4e-06	1.98e+01	5	26	>1E20	>1E20
Ba-141	3.48e-05	2.0e-07	1.99e+04	5	26	>1E20	>1E20
Ba-142	2.03e-05	1.0e-07	3.41e+04	5	26	>1E20	>1E20
La-131	1.12e-04	1.1e-07	6.18e+03	100	501	>1E20	>1E20
La-132	5.13e-04	1.5e-06	1.35e+03	100	501	>1E20	>1E20
La-135	2.22e-03	1.3e-07	3.12e+02	100	501	>1E20	>1E20
La-137	6.00e+04	4.3e-07	1.16e-05	100	501	1.9e+01	5.9e-03
La-138	1.06e+11	5.9e-06	6.54e-12	100	501	1.4e+00	5.9e-03
La-140	4.59e-03	7.7e-06	1.51e+02	100	501	>1E20	>1E20
La-141	4.41e-04	1.4e-06	1.57e+03	100	501	>1E20	>1E20
La-142	1.76e-04	8.3e-07	3.95e+03	100	501	>1E20	>1E20
La-143	2.66e-05	1.4e-07	2.60e+04	100	501	>1E20	>1E20

Rev. 0

C-34
Table C.1-2. (continued)

WSRC-RP-94-218

Nuclide	T1/2 (year)	DCF (mrem/pCi)	Lambda (1/year)	Kd (cm ³ /gm)	Rf	ILNT GW Trigger (Ci/vault)	ILNT Int Trigger (Ci/vault)
Ce-134	8.21e-03	8.9e-06	8.44e+01	10	51	>1E20	>1E20
Ce-135	1.96e-03	3.2e-06	3.53e+02	10	51	>1E20	>1E20
Ce-137m	3.92e-03	2.0e-06	1.77e+02	10	51	>1E20	>1E20
Ce-137	1.03e-03	9.8e-08	6.75e+02	10	51	>1E20	>1E20
Ce-139	3.77e-01	1.1e-06	1.84e+00	10	51	>1E20	>1E20
Ce-141	8.90e-02	2.6e-06	7.79e+00	10	51	>1E20	>1E20
Ce-143	3.76e-03	4.2e-06	1.84e+02	10	51	>1E20	>1E20
Ce-144	7.94e-01	2.0e-05	8.73e-01	10	51	>1E20	>1E20
Pr-136	1.25e-04	6.8e-08	5.52e+03	10	51	>1E20	>1E20
Pr-137	1.71e-04	1.3e-07	4.05e+03	100	501	>1E20	>1E20
Pr-138m	2.40e-04	4.9e-07	2.89e+03	100	501	>1E20	>1E20
Pr-139	5.13e-04	1.2e-07	1.35e+03	100	501	>1E20	>1E20
Pr-142m	2.72e-05	6.3e-08	2.55e+04	100	501	>1E20	>1E20
Pr-142	2.18e-03	5.1e-06	3.18e+02	100	501	>1E20	>1E20
Pr-143	3.75e-02	4.5e-06	1.85e+01	100	501	>1E20	>1E20
Pr-144	3.29e-05	1.1e-07	2.11e+04	100	501	>1E20	>1E20
Pr-145	6.82e-04	1.5e-06	1.02e+03	100	501	>1E20	>1E20
Pr-147	2.28e-05	5.7e-08	3.04e+04	100	501	>1E20	>1E20
Nd-136	9.64e-05	3.3e-07	7.19e+03	100	501	>1E20	>1E20
Nd-138	4.18e-05	2.5e-06	1.66e+04	100	501	>1E20	>1E20
Nd-139m	6.27e-04	1.0e-06	1.10e+03	100	501	>1E20	>1E20
Nd-139	5.93e-04	5.7e-08	1.17e+03	100	501	>1E20	>1E20
Nd-141	2.85e-04	3.2e-08	2.43e+03	100	501	>1E20	>1E20
Nd-147	3.01e-02	3.9e-06	2.30e+01	100	501	>1E20	>1E20
Nd-149	1.97e-03	4.6e-07	3.51e+02	100	501	>1E20	>1E20
Nd-151	2.36e-05	7.4e-08	2.94e+04	100	501	>1E20	>1E20
Pm-141	4.18e-05	8.4e-08	1.66e+04	100	501	>1E20	>1E20
Pm-143	7.26e-01	9.5e-07	9.55e-01	100	501	>1E20	>1E20
Pm-144	8.22e-01	3.9e-06	8.43e-01	100	501	>1E20	>1E20
Pm-145	1.77e+01	4.6e-07	3.92e-02	100	501	>1E20	3.0e-01
Pm-146	1.94e+00	3.2e-06	3.57e-01	100	501	>1E20	1.8e+13
Pm-147	2.52e+00	9.5e-07	2.75e-01	100	501	>1E20	5.3e+09
Pm-148m	1.14e-01	7.0e-06	6.06e+00	100	501	>1E20	>1E20
Pm-148	1.47e-02	9.5e-06	4.71e+01	100	501	>1E20	>1E20

Rev. 0

C-35
Table C.1-2 (continued)

WSRC-RP-94-218

Nuclide	T1/2 (year)	DCF (mrem/pCi)	Lambda (1/year)	Kd (cm ³ /gm)	Rf	ILNT GW Trigger (Ci/vault)	ILNT Int Trigger (Ci/vault)
Pm-149	6.06e-03	3.6e-06	1.14e+02	100	501	>1E20	>1E20
Pm-150	3.06e-04	9.8e-07	2.27e+03	100	501	>1E20	>1E20
Pm-151	3.24e-03	2.8e-06	2.14e+02	100	501	>1E20	>1E20
Sm-141m	4.30e-05	1.8e-07	1.61e+04	100	501	>1E20	>1E20
Sm-141	1.94e-05	8.4e-08	3.57e+04	100	501	>1E20	>1E20
Sm-142	1.37e-04	6.0e-07	5.06e+03	100	501	>1E20	>1E20
Sm-145	9.31e-01	8.5e-07	7.45e-01	100	501	>1E20	>1E20
Sm-146	7.00e+07	2.0e-04	9.90e-09	100	501	4.0e-02	5.9e-03
Sm-147	1.06e+11	1.8e-04	6.54e-12	100	501	4.5e-02	5.9e-03
Sm-151	9.00e+01	3.4e-07	7.70e-03	100	501	5.7e+09	1.3e-02
Sm-153	5.33e-03	2.6e-06	1.30e+02	100	501	>1E20	>1E20
Sm-155	4.22e-05	6.6e-08	1.64e+04	100	501	>1E20	>1E20
Sm-158	8.37e-05	1.0e-06	8.29e+03	100	501	>1E20	>1E20
Eu-145	1.62e-02	3.2e-05	4.29e+01	100	501	>1E20	>1E20
Eu-146	1.26e-02	5.1e-06	5.50e+01	100	501	>1E20	>1E20
Eu-147	6.02e-02	1.8e-06	1.15e+01	100	501	>1E20	>1E20
Eu-148	1.48e-01	5.2e-06	4.69e+00	100	501	>1E20	>1E20
Eu-149	2.90e-01	4.2e-07	2.39e+00	100	501	>1E20	>1E20
Eu-150(12h)	1.37e-03	1.5e-06	5.06e+02	100	501	>1E20	>1E20
Eu-150(34y)	3.40e+01	6.2e-06	2.04e-02	100	501	>1E20	4.5e-02
Eu-152m	1.07e-03	1.9e-06	6.51e+02	100	501	>1E20	>1E20
Eu-152	1.34e+01	6.0e-06	5.17e-02	100	501	>1E20	1.0e+00
Eu-154	8.20e+00	9.1e-06	8.45e-02	100	501	>1E20	2.8e+01
Eu-155	1.70e+00	1.3e-06	4.08e-01	100	501	>1E20	>1E20
Eu-156	4.22e-02	8.7e-06	1.64e+01	100	501	>1E20	>1E20
Eu-157	1.73e-03	2.3e-06	4.00e+02	100	501	>1E20	>1E20
Eu-158	8.73e-05	2.6e-07	7.94e+03	100	501	>1E20	>1E20
Gd-145	4.75e-05	1.1e-07	1.46e+04	100	501	>1E20	>1E20
Gd-146	1.26e-02	3.8e-06	5.50e+01	100	501	>1E20	>1E20
Gd-147	3.99e-03	2.6e-06	1.74e+02	100	501	>1E20	>1E20
Gd-148	1.30e+02	2.1e-04	5.33e-03	100	501	2.4e+04	1.0e-02
Gd-149	2.46e-02	1.8e-06	2.81e+01	100	501	>1E20	>1E20
Gd-151	3.29e-01	7.7e-07	2.11e+00	100	501	>1E20	>1E20
Gd-152	1.10e+14	1.5e-04	6.30e-15	100	501	5.4e-02	5.9e-03

Rev. 0

C-36
Table C.1-2. (continued)

WSRC-RP-94-218

Nuclide	T1/2 (year)	DCF (mrem/pCi)	Lambda (1/year)	Kd (cm ³ /gm)	Rf	ILNT GW Trigger (Ci/vault)	ILNT Int Trigger (Ci/vault)
Gd-153	6.61e-01	1.1e-06	1.05e+00	100	501	>1E20	>1E20
Gd-159	2.12e-03	1.9e-06	3.27e+02	100	501	>1E20	>1E20
Tb-147	4.56e-05	5.6e-07	1.52e+04	100	501	>1E20	>1E20
Tb-149	4.68e-04	9.5e-07	1.48e+03	100	501	>1E20	>1E20
Tb-150	3.54e-04	9.7e-07	1.96e+03	100	501	>1E20	>1E20
Tb-151	2.05e-03	1.4e-06	3.38e+02	100	501	>1E20	>1E20
Tb-153	6.27e-03	9.9e-07	1.10e+02	100	501	>1E20	>1E20
Tb-154	9.70e-04	2.8e-06	7.15e+02	100	501	>1E20	>1E20
Tb-155	1.53e-02	8.2e-07	4.52e+01	100	501	>1E20	>1E20
Tb-156m(24h)	2.74e-03	7.0e-07	2.53e+02	100	501	>1E20	>1E20
Tb-156m(5h)	6.27e-04	3.2e-07	1.10e+03	100	501	>1E20	>1E20
Tb-156	1.48e-02	4.6e-06	4.69e+01	100	501	>1E20	>1E20
Tb-157	1.50e+02	1.0e-07	4.62e-03	100	501	8.6e+06	9.3e-03
Tb-158	1.20e+03	4.0e-06	5.78e-04	100	501	8.6e+00	6.2e-03
Tb-160	1.98e-01	6.4e-06	3.50e+00	100	501	>1E20	>1E20
Tb-161	1.88e-02	2.6e-06	3.68e+01	100	501	>1E20	>1E20
Dy-155	1.20e-03	5.6e-07	5.79e+02	100	501	>1E20	>1E20
Dy-157	9.24e-04	2.7e-07	7.50e+02	100	501	>1E20	>1E20
Dy-159	3.94e-01	4.0e-07	1.76e+00	100	501	>1E20	>1E20
Dy-165	2.66e-04	3.6e-07	2.61e+03	100	501	>1E20	>1E20
Dy-166	9.31e-03	6.2e-06	7.45e+01	100	501	>1E20	>1E20
Ho-155	9.51e-05	1.2e-07	7.29e+03	100	501	>1E20	>1E20
Ho-157	2.66e-05	1.9e-08	2.60e+04	100	501	>1E20	>1E20
Ho-159	6.27e-05	2.3e-08	1.10e+04	100	501	>1E20	>1E20
Ho-161	2.85e-04	4.7e-08	2.43e+03	100	501	>1E20	>1E20
Ho-162m	1.29e-04	9.0e-08	5.36e+03	100	501	>1E20	>1E20
Ho-162	2.85e-05	6.7e-09	2.43e+04	100	501	>1E20	>1E20
Ho-164m	7.13e-05	4.9e-08	9.72e+03	100	501	>1E20	>1E20
Ho-164	7.03e-05	2.4e-08	9.85e+03	100	501	>1E20	>1E20
Ho-166m	1.20e+03	7.8e-06	5.78e-04	100	501	4.4e+00	6.2e-03
Ho-166	3.06e-03	5.5e-06	2.27e+02	100	501	>1E20	>1E20
Ho-167	3.54e-04	3.2e-07	1.96e+03	100	501	>1E20	>1E20
Er-161	3.54e-04	3.3e-07	1.96e+03	100	501	>1E20	>1E20
Er-165	1.18e-03	7.9e-08	5.86e+02	100	501	>1E20	>1E20

Rev. 0

Table C-1-2 (continued)

Nuclide	T _{1/2} (year)	DCF (micro/pCi)	Lambda (1/year)	K _d (cm ³ /gm)	R _f	ILNT Trigger (Ci/vault)	GW	ILNT Trigger (Ci/vault)
Er-169	2.57e-02	1.4e-06	2.69e+01	100	501	>1E20		>1E20
Er-171	8.58e-04	1.4e-06	8.08e+02	100	501	>1E20		>1E20
Er-172	5.59e-03	3.7e-06	1.24e+02	100	501	>1E20		>1E20
Tm-162	1.46e-04	7.0e-08	4.73e+03	100	501	>1E20		>1E20
Tm-166	8.78e-04	1.2e-06	7.89e+02	100	501	>1E20		>1E20
Tm-167	2.63e-02	2.1e-06	2.64e+01	100	501	>1E20		>1E20
Tm-170	3.53e-01	5.0e-06	1.96e+00	100	501	>1E20		>1E20
Tm-171	1.92e+00	3.9e-07	3.61e-01	100	501	>1E20		2.8e+13
Tm-172	7.26e-03	6.0e-06	9.55e+01	100	501	>1E20		>1E20
Tm-173	9.35e-04	1.2e-06	7.41e+02	100	501	>1E20		>1E20
Tm-175	3.80e-05	5.4e-08	1.82e+04	100	501	>1E20		>1E20
Yb-162	3.59e-05	7.0e-08	1.93e+04	100	501	>1E20		>1E20
Yb-165	1.90e-05	3.8e-06	3.65e+04	100	501	>1E20		>1E20
Yb-167	3.42e-05	1.7e-08	2.03e+04	100	501	>1E20		>1E20
Yb-169	8.76e-02	2.8e-06	7.91e+00	100	501	>1E20		>1E20
Yb-175	1.15e-02	1.6e-06	6.04e+01	100	501	>1E20		>1E20
Yb-177	2.17e-04	3.1e-07	3.20e+03	100	501	>1E20		>1E20
Yb-178	1.40e-04	3.9e-07	4.94e+03	100	501	>1E20		>1E20
Lu-169	3.88e-03	2.0e-06	1.79e+02	100	501	>1E20		>1E20
Lu-170	5.48e-03	4.3e-06	1.27e+02	100	501	>1E20		>1E20
Lu-171	2.27e-02	2.6e-06	3.05e+01	100	501	>1E20		>1E20
Lu-172	1.83e-02	5.0e-06	3.78e+01	100	501	>1E20		>1E20
Lu-173	1.37e+00	9.7e-07	5.06e-01	100	501	>1E20		>1E20
Lu-174m	3.83e-01	1.8e-06	1.81e+00	100	501	>1E20		>1E20
Lu-174	3.60e+00	9.9e-07	1.93e-01	100	501	>1E20		1.4e+06
Lu-176m	4.21e-04	6.3e-07	1.65e+03	100	501	>1E20		>1E20
Lu-176	3.00e+10	6.6e-06	2.31e-11	100	501	1.2e+00		5.9e-03
Lu-177m	4.41e-02	6.8e-06	1.57e+01	100	501	>1E20		>1E20
Lu-177	1.84e-02	2.0e-06	3.77e+01	100	501	>1E20		>1E20
Lu-178m	3.80e-05	8.8e-08	1.82e+04	100	501	>1E20		>1E20
Lu-178	5.70e-05	1.2e-07	1.22e+04	100	501	>1E20		>1E20
Lu-179	5.25e-04	8.1e-07	1.32e+03	100	501	>1E20		>1E20
Hf-170	1.39e-03	1.2e-05	4.98e+02	100	501	>1E20		>1E20
Hf-172	5.00e+00	4.1e-06	1.39e-01	100	501	>1E20		6.2e+03

Rev. 0

C-38
Table C.1-2. (continued)

WSRC-RP-94-218

Nuclide	T1/2 (year)	DCF (mrem/pCi)	Lambda (1/year)	Kd (cm ³ /gm)	Rf	ILNT GW Trigger (Ci/vault)	ILNT Int Trigger (Ci/vault)
Hf-173	2.69e-03	9.6e-07	2.57e+02	100	501	>1E20	>1E20
Hf-175	1.92e-01	1.6e-06	3.62e+00	100	501	>1E20	>1E20
Hf-177m	9.77e-05	2.5e-07	7.09e+03	100	501	>1E20	>1E20
Hf-178m	3.10e+01	2.0e-05	2.24e-02	100	501	>1E20	5.5e-02
Hf-179m	6.87e-02	4.8e-06	1.01e+01	100	501	>1E20	>1E20
Hf-180m	6.27e-04	8.9e-07	1.10e+03	100	501	>1E20	>1E20
Hf-181	1.16e-01	4.3e-06	5.97e+00	100	501	>1E20	>1E20
Hf-182m	1.18e-04	1.4e-07	5.88e+03	100	501	>1E20	>1E20
Hf-182	9.00e+06	1.4e-05	7.70e-08	100	501	5.8e-01	5.9e-03
Hf-183	1.25e-04	2.5e-07	5.52e+03	100	501	>1E20	>1E20
Hf-184	4.68e-04	2.1e-06	1.48e+03	100	501	>1E20	>1E20
Ta-172	8.37e-05	1.4e-07	8.29e+03	0	1	>1E20	>1E20
Ta-173	4.22e-04	7.4e-07	1.64e+03	0	1	>1E20	>1E20
Ta-174	1.48e-04	1.9e-07	4.67e+03	0	1	>1E20	>1E20
Ta-175	1.20e-03	8.8e-07	5.79e+02	0	1	>1E20	>1E20
Ta-176	9.13e-04	1.3e-06	7.60e+02	0	1	>1E20	>1E20
Ta-177	6.46e-03	4.1e-07	1.07e+02	0	1	>1E20	>1E20
Ta-178	1.79e-05	2.9e-07	3.88e+04	0	1	>1E20	>1E20
Ta-179	2.40e-04	2.5e-07	2.89e+03	0	1	>1E20	>1E20
Ta-180m	9.24e-04	2.1e-07	7.50e+02	0	1	>1E20	>1E20
Ta-180	1.00e+13	3.3e-06	6.93e-14	0	1	4.9e-03	5.9e-03
Ta-182m	3.02e-05	2.4e-08	2.29e+04	0	1	>1E20	>1E20
Ta-182	3.15e-01	6.0e-06	2.20e+00	0	1	1.6e+02	>1E20
Ta-183	1.40e-02	4.6e-06	4.96e+01	0	1	>1E20	>1E20
Ta-184	9.92e-04	2.7e-06	6.98e+02	0	1	>1E20	>1E20
Ta-185	9.51e-05	2.0e-07	7.29e+03	0	1	>1E20	>1E20
Ta-186	2.00e-05	6.7e-08	3.47e+04	0	1	>1E20	>1E20
W-176	2.85e-04	4.8e-07	2.43e+03	0	1	>1E20	>1E20
W-177	2.57e-04	2.4e-07	2.70e+03	0	1	>1E20	>1E20
W-178	5.89e-02	9.3e-07	1.18e+01	0	1	>1E20	>1E20
W-179	7.22e-05	9.0e-09	9.59e+03	0	1	>1E20	>1E20
W-181	3.31e-01	3.1e-07	2.09e+00	0	1	1.8e+03	>1E20
W-185	2.06e-01	1.9e-06	3.37e+00	0	1	1.8e+05	>1E20
W-187	2.73e-03	2.6e-06	2.54e+02	0	1	>1E20	>1E20

Rev. 0

C-39
Table C.1-2. (continued)

Nuclide	T1/2 (year)	DCF (mrem/pCi)	Lambda (1/year)	Kd (cm ³ /gm)	RI	ILNT GW Trigger (C/vault)	ILNT Int Trigger (C/vault)
W-188	1.89e-01	9.0e-06	3.67e+00	0	1	1.7e+05	>1E20
Re-177	3.23e-05	4.4e-08	2.14e+04	0	1	>1E20	>1E20
Re-178	2.85e-05	4.8e-08	2.43e+04	0	1	>1E20	>1E20
Re-181	2.05e-03	1.0e-06	3.38e+02	0	1	>1E20	>1E20
Re-182(64h)	7.30e-03	3.4e-06	9.49e+01	0	1	>1E20	>1E20
Re-182(12h)	1.45e-03	7.4e-07	4.78e+02	0	1	>1E20	>1E20
Re-184m	4.63e-01	2.4e-06	1.50e+00	0	1	1.2e+01	>1E20
Rm-184	1.04e-02	2.2e-06	6.66e+01	0	1	>1E20	>1E20
Re-186m	2.00e+05	3.3e-06	3.47e-06	0	1	4.9e-03	5.9e-03
Re-186	1.03e-02	2.6e-06	6.71e+01	0	1	>1E20	>1E20
Re-187	7.00e+10	8.3e-09	9.90e-12	0	1	1.9e+00	5.9e-03
Re-188m	3.54e-05	6.2e-08	1.96e+04	0	1	>1E20	>1E20
Re-188	1.91e-03	2.8e-06	3.64e+02	0	1	>1E20	>1E20
Re-189	2.74e-03	1.5e-06	2.53e+02	0	1	>1E20	>1E20
Os-180	4.13e-05	4.7e-08	1.68e+04	0	1	>1E20	>1E20
Os-181	4.37e-05	3.5e-07	1.59e+04	0	1	>1E20	>1E20
Os-182	2.51e-03	2.2e-06	2.76e+02	0	1	>1E20	>1E20
Os-185	2.57e-01	2.1e-06	2.69e+00	0	1	5.4e+03	>1E20
Os-189m	6.84e-04	6.6e-08	1.01e+03	0	1	>1E20	>1E20
Os-191m	1.48e-03	3.6e-07	4.67e+02	0	1	>1E20	>1E20
Os-191	4.19e-02	2.0e-06	1.65e+01	0	1	>1E20	>1E20
Os-193	3.48e-03	3.1e-06	1.99e+02	0	1	>1E20	>1E20
Os-194	6.00e+00	9.1e-06	1.16e-01	0	1	3.2e-03	6.1e+02
Ir-182	2.85e-05	1.2e-07	2.43e+04	0	1	>1E20	>1E20
Ir-184	3.65e-04	6.4e-07	1.90e+03	0	1	>1E20	>1E20
Ir-185	1.60e-03	1.1e-06	4.34e+02	0	1	>1E20	>1E20
Ir-186	1.83e-03	2.1e-06	3.80e+02	0	1	>1E20	>1E20
Ir-187	1.20e-03	4.8e-07	5.79e+02	0	1	>1E20	>1E20
Ir-188	4.68e-03	2.7e-06	1.48e+02	0	1	>1E20	>1E20
Ir-189	3.64e-02	9.3e-07	1.90e+01	0	1	>1E20	>1E20
Ir-190m	3.65e-04	3.0e-08	1.90e+03	0	1	>1E20	>1E20
Ir-190	3.01e-02	4.9e-06	2.30e+01	0	1	>1E20	>1E20
Ir-192m	2.74e-06	1.5e-06	2.53e+05	0	1	>1E20	>1E20
Ir-192	2.03e-01	5.3e-06	3.41e+00	0	1	7.8e+04	>1E20

Rev. 0

C-40
Table C.1-2. (continued)

WSRC-RP-94-218

Nuclide	T _{1/2} (year)	DCF (mrem/pCi)	Lambda (1/year)	K _d (cm ² /3/gm)	Rf	PLNT GW Trigger (Ci/valut)	PLNT Int Trigger (Ci/valut)
Ir-194m	4.68e-01	8.1e-06	1.48e+00	0	1	3.3e+00	>1E20
Ir-194	2.22e-03	5.1e-06	3.12e+02	0	1	>1E20	>1E20
Ir-195m	4.45e-04	6.4e-07	1.56e+03	0	1	>1E20	>1E20
Ir-195	4.79e-04	3.4e-07	1.45e+03	0	1	>1E20	>1E20
Pt-186	3.42e-04	3.7e-07	2.03e+03	0	1	>1E20	>1E20
Pt-188	2.79e-02	3.0e-06	2.48e+01	0	1	>1E20	>1E20
Pt-189	1.24e-03	4.9e-07	5.57e+02	0	1	>1E20	>1E20
Pt-191	1.24e-03	1.3e-06	5.57e+02	0	1	>1E20	>1E20
Pt-193m	1.18e-02	1.7e-06	5.89e+01	0	1	>1E20	>1E20
Pt-193	5.00e+01	1.1e-07	1.39e-02	0	1	1.6e-01	2.4e-02
Pt-195m	1.10e-02	2.2e-06	6.30e+01	0	1	>1E20	>1E20
Pt-197m	1.79e-04	3.1e-07	3.88e+03	0	1	>1E20	>1E20
Pt-197	2.09e-03	1.5e-06	3.32e+02	0	1	>1E20	>1E20
Pt-199	5.86e-05	1.0e-07	1.18e+04	0	1	>1E20	>1E20
Pt-200	1.31e-03	4.5e-06	5.28e+02	0	1	>1E20	>1E20
Au-193	1.83e-03	6.0e-07	3.80e+02	0	1	>1E20	>1E20
Au-194	4.51e-03	2.0e-06	1.54e+02	0	1	>1E20	>1E20
Au-195	5.01e-01	1.1e-06	1.38e+00	0	1	1.5e+01	>1E20
Au-198m	6.30e-03	5.7e-06	1.10e+02	0	1	>1E20	>1E20
Au-198	7.38e-03	2.3e-06	9.39e+01	0	1	>1E20	>1E20
Au-199	8.60e-03	1.8e-06	8.06e+01	0	1	>1E20	>1E20
Au-200m	2.13e-03	4.6e-06	3.25e+02	0	1	>1E20	>1E20
Au-200	9.20e-05	1.9e-07	7.53e+03	0	1	>1E20	>1E20
Au-201	4.94e-05	5.7e-08	1.40e+04	0	1	>1E20	>1E20
Hg-193m	1.14e-03	1.6e-06	6.08e+02	1000	5001	>1E20	>1E20
Hg-193	6.84e-04	3.3e-07	1.01e+03	1000	5001	>1E20	>1E20
Hg-194	1.90e+00	6.0e-06	3.65e-01	1000	5001	>1E20	4.1e+13
Hg-195m	4.56e-03	2.2e-06	1.52e+02	1000	5001	>1E20	>1E20
Hg-195	1.08e-03	3.8e-07	6.40e+02	1000	5001	>1E20	>1E20
Hg-197m	2.72e-03	1.7e-06	2.55e+02	1000	5001	>1E20	>1E20
Hg-197	7.31e-03	9.1e-07	9.48e+01	1000	5001	>1E20	>1E20
Hg-199m	8.10e-05	8.5e-08	8.56e+03	1000	5001	>1E20	>1E20
Hg-203	1.28e-01	2.1e-06	5.43e+00	1000	5001	>1E20	>1E20
Tl-194m	6.24e-05	7.1e-08	1.11e+04	0	1	>1E20	>1E20

Rev. 0

Table C.1-2 (continued)

Nuclide	T1/2 (year)	DCF (mrem/pCi)	Lambda (1/year)	Kd (cm ³ /g)	Rf	ILNT GW Trigger (Ci/haul)	ILNT Inc Trigger (Ci/haul)
Tl-194	6.27e-05	1.9e-08	1.10e+04	0	1	>1E20	>1E20
Tl-195	1.37e-04	7.7e-08	5.06e+03	0	1	>1E20	>1E20
Tl-197	3.19e-04	6.9e-08	2.17e+03	0	1	>1E20	>1E20
Tl-198m	2.13e-04	1.6e-07	3.25e+03	0	1	>1E20	>1E20
Tl-198	6.05e-04	2.6e-07	1.15e+03	0	1	>1E20	>1E20
Tl-199	8.44e-04	8.2e-08	8.21e+02	0	1	>1E20	>1E20
Tl-200	2.98e-03	6.7e-07	2.33e+02	0	1	>1E20	>1E20
Tl-201	8.33e-03	2.9e-07	8.32e+01	0	1	>1E20	>1E20
Tl-202	3.29e-02	1.5e-06	2.11e+01	0	1	>1E20	>1E20
Tl-204	3.77e+00	3.2e-06	1.84e-01	0	1	1.3e-02	5.7e+05
Pb-195m	2.85e-05	8.5e-08	2.43e+04	100	501	>1E20	>1E20
Pb-198	2.74e-04	1.6e-07	2.53e+03	100	501	>1E20	>1E20
Pb-199	1.71e-04	2.2e-07	4.05e+03	100	501	>1E20	>1E20
Pb-200	2.45e-03	1.5e-06	2.83e+02	100	501	>1E20	>1E20
Pb-201	1.07e-03	6.7e-07	6.46e+02	100	501	>1E20	>1E20
Pb-202m	4.13e-04	5.5e-07	1.68e+03	100	501	>1E20	>1E20
Pb-202	3.00e+05	3.9e-05	2.31e-06	100	501	2.1e-01	5.9e-03
Pb-203	5.94e-03	9.6e-07	1.17e+02	100	501	>1E20	>1E20
Pb-205	1.40e+07	1.5e-06	4.95e-08	100	501	5.4e+00	5.9e-03
Pb-209	6.24e-06	9.0e-08	1.11e+05	100	501	>1E20	>1E20
Pb-210	2.23e+01	5.1e-03	3.11e-02	100	501	>1E20	1.3e-01
Pb-211	6.86e-05	4.4e-07	1.01e+04	100	501	>1E20	>1E20
Pb-212	1.21e-03	4.1e-05	5.71e+02	100	501	>1E20	>1E20
Pb-214	5.10e-05	5.8e-07	1.36e+04	100	501	>1E20	>1E20
Bi-200	6.65e-05	1.7e-07	1.04e+04	0	1	>1E20	>1E20
Bi-201	2.05e-04	4.5e-07	3.38e+03	0	1	>1E20	>1E20
Bi-202	1.61e-04	3.6e-07	3.84e+03	0	1	>1E20	>1E20
Bi-203	1.35e-03	2.1e-06	5.15e+02	0	1	>1E20	>1E20
Bi-205	4.19e-02	3.7e-06	1.65e+01	0	1	>1E20	>1E20
Bi-206	1.71e-02	8.0e-06	4.06e+01	0	1	>1E20	>1E20
Bi-207	7.94e+00	4.9e-06	8.73e-02	0	1	5.1e-03	3.6e+01
Bi-210m	3.50e+06	8.6e-05	1.98e-07	0	1	1.9e-04	5.9e-03
Bi-210	1.37e-02	5.9e-06	5.06e+01	0	1	>1E20	>1E20
Bi-212	1.15e-04	9.9e-07	6.02e+03	0	1	>1E20	>1E20

Rev. 0

Table C.1-2 (continued)

Nuclide	T1/2 (year)	DCF (mrem/pCi)	Lambda (1/year)	Kd (cm ² /gm)	Rf	ILNT GW Trigger (Ci/vault)	ILNT Int Trigger (Ci/vault)
Bi-213	8.68e-05	6.8e-07	7.99e+03	0	1	> 1E20	> 1E20
Bi-214	3.76e-05	2.4e-07	1.84e+04	0	1	> 1E20	> 1E20
Po-203	7.99e-05	2.0e-07	8.68e+03	0	1	> 1E20	> 1E20
Po-205	2.05e-04	2.4e-07	3.38e+03	0	1	> 1E20	> 1E20
Po-207	6.50e-04	6.1e-07	1.07e+03	0	1	> 1E20	> 1E20
Po-210	3.79e-01	1.6e-03	1.83e+00	0	1	9.5e-02	> 1E20
At-207	2.05e-04	8.9e-07	3.38e+03	0	1	> 1E20	> 1E20
At-211	8.22e-04	4.1e-05	8.43e+02	0	1	> 1E20	> 1E20
Fr-222	2.81e-05	2.5e-06	2.46e+04	0	1	> 1E20	> 1E20
Fr-223	4.18e-05	8.6e-06	1.66e+04	0	1	> 1E20	> 1E20
Ra-223	3.13e-02	5.5e-04	2.21e+01	500	2501	> 1E20	> 1E20
Ra-224	9.91e-03	3.3e-04	6.99e+01	500	2501	> 1E20	> 1E20
Ra-225	4.05e-02	3.1e-04	1.71e+01	500	2501	> 1E20	> 1E20
Ra-226	1.62e+03	1.1e-03	4.27e-04	500	2501	7.7e+00	6.1e-03
Ra-227	7.83e-05	2.2e-07	8.85e+03	500	2501	> 1E20	> 1E20
Ra-228	5.75e+00	1.2e-03	1.21e-01	500	2501	> 1E20	1.0e+03
Ac-224	3.31e-04	2.6e-06	2.10e+03	150	751	> 1E20	> 1E20
Ac-225	2.74e-02	9.5e-05	2.53e+01	150	751	> 1E20	> 1E20
Ac-226	3.31e-03	4.0e-05	2.10e+02	150	751	> 1E20	> 1E20
Ac-227	2.18e+01	1.4e-02	3.18e-02	150	751	> 1E20	1.4e-01
Ac-228	6.99e-04	2.1e-06	9.91e+02	150	751	> 1E20	> 1E20
Th-226	5.87e-05	9.2e-07	1.18e+04	3000	15001	> 1E20	> 1E20
Th-227	5.13e-02	3.6e-05	1.35e+01	3000	15001	> 1E20	> 1E20
Th-228	1.91e+00	3.8e-04	3.62e-01	3000	15001	> 1E20	3.2e+13
Th-229	7.43e+03	3.5e-03	9.33e-05	3000	15001	7.6e+01	5.9e-03
Th-230	7.70e+04	5.3e-04	9.00e-06	3000	15001	9.0e-01	5.9e-03
Th-231	2.91e-03	1.3e-06	2.38e+02	3000	15001	> 1E20	> 1E20
Th-232	1.41e+10	2.8e-03	4.93e-11	3000	15001	1.9e-02	5.9e-03
Th-234	6.60e-02	1.3e-05	1.05e+01	3000	15001	> 1E20	> 1E20
Pa-227	7.28e-05	1.3e-06	9.52e+03	10	51	> 1E20	> 1E20
Pa-228	2.97e-03	4.0e-06	2.34e+02	10	51	> 1E20	> 1E20
Pa-230	4.85e-02	5.6e-06	1.43e+01	10	51	> 1E20	> 1E20
Pa-231	3.28e+04	1.1e-02	2.12e-05	10	51	7.5e-05	5.9e-03
Pa-232	3.59e-03	3.4e-06	1.93e+02	10	51	> 1E20	> 1E20

Rev. 0

C-43
Table C.1-2. (continued)

WSRC-RP-94-218

Nuclide	T1/2 (year)	DCF (mrem/pCi)	Lambda (1/year)	Kd (cm ³ /gm)	Rf	ILNT GW Trigger (Ci/vault)	ILNT Int Trigger (Ci/vault)
Pa-233	7.39e-02	3.3e-06	9.38e+00	10	51	>1E20	>1E20
Pa-234	7.64e-04	2.1e-06	9.07e+02	10	51	>1E20	>1E20
U-230	5.69e-02	8.4e-04	1.22e+01	50	251	>1E20	>1E20
U-231	4.30e+00	1.1e-06	1.61e-01	50	251	>1E20	5.9e+04
U-232	7.20e+01	1.3e-03	9.63e-03	50	251	5.5e+02	1.5e-02
U-233	1.60e+05	2.7e-04	4.35e-06	50	251	1.5e-02	5.9e-03
U-234	2.45e+05	2.6e-04	2.83e-06	50	251	1.5e-02	5.9e-03
U-235	7.04e+08	2.5e-04	9.85e-10	50	251	7.7e-03	5.9e-03
U-236	2.34e+07	2.5e-04	2.96e-08	50	251	1.6e-02	5.9e-03
U-237	1.85e-02	2.7e-06	3.75e+01	50	251	>1E20	>1E20
U-238	4.47e+09	2.3e-04	1.55e-10	50	251	1.6e-02	5.9e-03
U-239	4.47e-05	7.6e-08	1.55e+04	50	251	>1E20	>1E20
U-240	1.61e-03	4.1e-06	4.31e+02	50	251	>1E20	>1E20
Np-232	2.47e-05	2.4e-08	2.80e+04	10	51	>1E20	>1E20
Np-233	6.65e-05	5.6e-09	1.04e+04	10	51	>1E20	>1E20
Np-234	1.20e-02	1.7e-06	5.75e+01	10	51	>1E20	>1E20
Np-235	1.12e+00	2.1e-07	6.17e-01	10	51	>1E20	>1E20
Np-236(1E5y)	1.10e+05	7.9e-04	6.30e-06	10	51	1.0e-03	5.9e-03
Np-236(22h)	2.51e-03	9.5e-07	2.76e+02	10	51	>1E20	>1E20
Np-237	2.14e+06	3.9e-03	3.24e-07	10	51	2.1e-04	5.9e-03
Np-238	5.80e-03	3.4e-06	1.20e+02	10	51	>1E20	>1E20
Np-239	6.38e-03	2.9e-06	1.09e+02	10	51	>1E20	>1E20
Np-240	1.20e-04	2.0e-07	5.79e+03	10	51	>1E20	>1E20
Pu-234	1.03e-03	1.2e-06	6.75e+02	100	501	>1E20	>1E20
Pu-235	4.94e-05	1.4e-08	1.40e+04	100	501	>1E20	>1E20
Pu-236	2.85e+00	1.3e-03	2.43e-01	100	501	>1E20	2.1e+08
Pu-237	1.24e-01	1.0e-06	5.58e+00	100	501	>1E20	>1E20
Pu-238	8.78e+01	3.8e-03	7.90e-03	100	501	3.9e+01	1.3e-02
Pu-239	2.41e+04	4.3e-03	2.87e-05	100	501	2.0e-03	5.9e-03
Pu-240	6.57e+03	4.3e-03	1.06e-04	100	501	2.4e-03	5.9e-03
Pu-241	1.44e+01	8.6e-05	4.81e-02	100	501	3.8e+00	7.2e-01
Pu-242	3.76e+05	4.1e-03	1.84e-06	100	501	2.0e-03	5.9e-03
Pu-243	5.65e-04	3.3e-07	1.23e+03	100	501	>1E20	>1E20
Pu-244	8.10e+07	4.0e-03	8.56e-09	100	501	2.0e-03	5.9e-03

Rev. 0

C-44
Table C.1-2 (continued)

WSRC-RP-94-218

Nuclide	T1/2 (year)	DCF (mrem/pCi)	Lambda (1/year)	Kd (cm ³ /gm)	Rf	ILNT GW Trigger (Ci/vault)	ILNT Int Trigger (Ci/vault)
Pu-245	1.14e-03	2.4e-06	6.08e+02	100	501	>1E20	>1E20
Am-237	1.48e-04	7.4e-08	4.67e+03	150	751	>1E20	>1E20
Am-238	2.17e-04	1.7e-07	3.20e+03	150	751	>1E20	>1E20
Am-239	1.38e-03	1.0e-06	5.02e+02	150	751	>1E20	>1E20
Am-240	5.82e-03	2.9e-06	1.19e+02	150	751	>1E20	>1E20
Am-241	4.32e+02	4.5e-03	1.60e-03	150	751	5.4e-01	6.9e-03
Am-242m	1.52e+02	4.2e-03	4.56e-03	150	751	7.9e+04	9.3e-03
Am-242	1.83e-03	1.2e-06	3.80e+02	150	751	>1E20	>1E20
Am-243	7.37e+03	4.5e-03	9.40e-05	150	751	3.3e-03	5.9e-03
Am-244m	4.94e-05	6.8e-08	1.40e+04	150	751	>1E20	>1E20
Am-244	1.15e-03	2.0e-06	6.02e+02	150	751	>1E20	>1E20
Am-245	2.40e-04	1.8e-07	2.89e+03	150	751	>1E20	>1E20
Am-246m	4.75e-05	8.4e-08	1.46e+04	150	751	>1E20	>1E20
Am-246	4.75e-05	1.5e-07	1.46e+04	150	751	>1E20	>1E20
Cm-238	2.85e-04	3.6e-07	2.43e+03	100	501	>1E20	>1E20
Cm-240	7.34e-02	6.3e-05	9.45e+00	100	501	>1E20	>1E20
Cm-241	9.58e-02	4.6e-06	7.23e+00	100	501	>1E20	>1E20
Cm-242	4.46e-01	1.1e-04	1.56e+00	100	501	>1E20	>1E20
Cm-243	2.85e+01	2.9e-03	2.43e-02	100	501	>1E20	6.7e-02
Cm-244	1.81e+01	2.3e-03	3.83e-02	100	501	9.0e-01	2.7e-01
Cm-245	8.50e+03	4.5e-03	8.15e-05	100	501	2.2e-03	5.9e-03
Cm-246	4.70e+03	4.5e-03	1.47e-04	100	501	2.6e-03	6.0e-03
Cm-247	1.60e+07	4.1e-03	4.33e-08	100	501	2.0e-03	5.9e-03
Cm-248	3.50e+05	1.6e-02	1.98e-06	100	501	5.1e-04	5.9e-03
Cm-249	1.24e-04	9.5e-08	5.61e+03	100	501	>1E20	>1E20
Bk-245	1.36e-02	2.3e-06	5.08e+01	100	501	>1E20	>1E20
Bk-246	4.93e-03	1.9e-06	1.41e+02	100	501	>1E20	>1E20
Bk-247	1.40e+03	2.3e-03	4.95e-04	100	501	1.2e-02	6.2e-03
Bk-249	8.80e-01	6.0e-06	7.88e-01	100	501	>1E20	>1E20
Bk-250	3.67e-04	5.0e-07	1.89e+03	100	501	>1E20	>1E20
Cf-244	4.75e-05	1.5e-07	1.46e+04	100	501	>1E20	>1E20
Cf-246	4.11e-03	1.2e-05	1.69e+02	100	501	>1E20	>1E20
Cf-248	9.86e-01	2.8e-04	7.03e-01	100	501	>1E20	>1E20
Cf-249	3.51e+02	4.6e-03	1.97e-03	100	501	2.5e-01	7.2e-03

Rev. 0

C-45
Table C.1-2 (continued)

WSRC-RP-94-218

Nuclide	T1/2 (year)	DCF (mrem/pCi)	Lambda (1/year)	Kd (cm ³ /gm)	Rf	ILNT GW Trigger (Ci/vault)	ILNT Int Trigger (Ci/vault)
Cf-250	1.31e+01	1.9e-03	5.29e-02	100	501	>1E20	1.2e+00
Cf-251	9.00e+02	4.6e-03	7.70e-04	100	501	1.2e-02	6.4e-03
Cf-252	2.62e+00	9.4e-04	2.65e-01	100	501	6.7e+01	1.8e+09
Cf-253	4.87e-02	9.2e-06	1.42e+01	100	501	>1E20	>1E20
Cf-254	1.66e-01	2.5e-03	4.18e+00	100	501	>1E20	>1E20
Es-250	9.13e-04	9.5e-08	7.60e+02	100	501	>1E20	>1E20
Es-251	4.11e-03	6.7e-07	1.69e+02	100	501	>1E20	>1E20
Es-253	5.60e-02	2.4e-05	1.24e+01	100	501	>1E20	>1E20
Es-254m	4.48e-03	1.5e-05	1.55e+02	100	501	>1E20	>1E20
Es-254	7.56e-01	1.5e-04	9.17e-01	100	501	>1E20	>1E20
Fm-252	2.62e-03	9.9e-06	2.64e+02	100	501	>1E20	>1E20
Fm-253	8.21e-03	3.5e-06	8.44e+01	100	501	>1E20	>1E20
Fm-254	3.70e-04	1.6e-06	1.88e+03	100	501	>1E20	>1E20
Fm-255	2.29e-03	9.7e-06	3.02e+02	100	501	>1E20	>1E20
Fm-257	2.19e-01	7.3e-05	3.16e+00	100	501	>1E20	>1E20
Md-257	3.42e-04	5.4e-07	2.03e+03	100	501	>1E20	>1E20
Md-258	1.53e-01	6.1e-05	4.52e+00	100	501	>1E20	>1E20

Rev. 0

Table C.1-3. Screening calculations and trigger levels for the LAW vaults

Nuclide	T1/2 (year)	DCF (mrem/pCi)	Lambda (1/year)	Kd (cm ³ /gm)	Rf	LAW GW Trigger (Ci/vault)	LAW Int Trigger (Ci/vault)
H-3	1.23e+01	6.3e-08	5.62e-02	0	1	2.8e+00	1.3e+01
Be-7	1.47e-01	1.1e-07	4.72e+00	0	1	2.2e+10	>1E20
Be-10	1.60e+06	4.2e-06	4.33e-07	0	1	3.1e-02	4.8e-02
C-11	3.86e-05	1.2e-08	1.80e+04	2	11	>1E20	>1E20
C-14	5.73e+03	2.1e-06	1.21e-04	2	11	7.0e-01	4.9e-02
F-18	2.14e-04	1.0e-04	3.25e+03	0	1	>1E20	>1E20
Na-22	2.58e+00	1.2e-05	2.69e-01	0	1	4.2e-02	2.2e+10
Na-24	1.71e-03	1.4e-06	4.05e+02	0	1	>1E20	>1E20
Mg-28	2.40e-03	7.5e-06	2.89e+02	0	1	>1E20	>1E20
Al-26	7.40e+05	1.3e-05	9.37e-07	0	1	1.0e-02	4.8e-02
Si-31	2.99e-04	5.4e-07	2.32e+03	0	1	>1E20	>1E20
Si-32	6.50e+02	1.7e-06	1.07e-03	0	1	7.8e-02	5.4e-02
P-32	3.89e-02	7.7e-06	1.78e+01	0	1	>1E20	>1E20
P-33	6.84e-02	8.8e-07	1.01e+01	0	1	>1E20	>1E20
S-35	2.39e-01	4.3e-07	2.90e+00	0	1	6.2e+05	>1E20
Cl-36	3.01e+05	3.0e-06	2.30e-06	0	1	4.4e-02	4.8e-02
Cl-38	7.07e-05	2.0e-07	9.80e+03	0	1	>1E20	>1E20
Cl-39	1.06e-04	1.4e-07	6.57e+03	0	1	>1E20	>1E20
K-40	1.28e+09	1.9e-05	5.42e-10	0	1	6.9e-03	4.8e-02
K-42	1.41e-03	1.1e-06	4.92e+02	0	1	>1E20	>1E20
K-43	2.56e-03	7.8e-07	2.71e+02	0	1	>1E20	>1E20
K-44	4.18e-05	1.5e-07	1.66e+04	0	1	>1E20	>1E20
K-45	3.04e-05	9.3e-08	2.28e+04	0	1	>1E20	>1E20
Ca-41	1.30e+05	1.2e-06	5.33e-06	0	1	1.1e-01	4.8e-02
Ca-45	4.46e-01	3.0e-06	1.55e+00	0	1	1.0e+02	>1E20
Ca-47	1.24e-02	6.2e-06	5.58e+01	0	1	>1E20	>1E20
Sc-43	4.47e-04	7.3e-07	1.55e+03	0	1	>1E20	>1E20
Sc-44m	6.68e-03	9.9e-06	1.04e+02	0	1	>1E20	>1E20
Sc-44	4.47e-04	1.4e-06	1.55e+03	0	1	>1E20	>1E20
Sc-46	2.29e-01	5.6e-06	3.02e+00	0	1	8.6e+04	>1E20
Sc-47	9.39e-03	1.9e-06	7.38e+01	0	1	>1E20	>1E20
Sc-48	5.03e-03	6.4e-06	1.38e+02	0	1	>1E20	>1E20
Sc-49	1.09e-04	2.4e-07	6.34e+03	0	1	>1E20	>1E20

C-47
Table C.1-3. (continued)

WSRC-RP-94-218

Nuclide	T1/2 (year)	DCF (mrem/pCi)	Lambda (1/year)	Kd (cm**3/gm)	Rf	LAW GW Trigger (Ci/vault)	LAW Int Trigger (Ci/vault)
Ti-44	4.80e+01	1.9e-05	1.44e-02	0	1	7.5e-03	2.0e-01
Ti-45	3.52e-04	5.7e-07	1.97e+03	0	1	>1E20	>1E20
V-47	6.27e-05	1.6e-07	1.10e+04	0	1	>1E20	>1E20
V-48	4.41e-02	7.5e-06	1.57e+01	0	1	>1E20	>1E20
V-49	9.03e-01	5.4e-08	7.67e-01	0	1	1.1e+02	>1E20
Cr-48	2.62e-03	8.2e-07	2.64e+02	40	201	>1E20	>1E20
Cr-49	7.97e-05	1.7e-07	8.70e+03	40	201	>1E20	>1E20
Cr-51	7.58e-02	1.3e-07	9.14e+00	40	201	>1E20	>1E20
Mn-51	8.56e-05	2.5e-07	8.10e+03	50	251	>1E20	>1E20
Mn-52m	3.99e-05	1.5e-07	1.74e+04	50	251	>1E20	>1E20
Mn-52	1.52e-02	6.9e-06	4.56e+01	50	251	>1E20	>1E20
Mn-53	2.00e+06	9.9e-08	3.47e-07	50	251	3.3e+02	4.8e-02
Mn-54	7.97e-01	2.7e-06	8.70e-01	50	251	>1E20	>1E20
Mn-56	2.94e-04	9.5e-07	2.36e+03	50	251	>1E20	>1E20
Fe-52	9.35e-04	5.4e-06	7.41e+02	0	1	>1E20	>1E20
Fe-55	2.70e+00	5.8e-07	2.57e-01	0	1	8.2e-01	6.8e+09
Fe-59	1.22e-01	6.6e-06	5.68e+00	0	1	4.2e+10	>1E20
Fe-60	3.00e+05	1.5e-04	2.31e-06	0	1	8.8e-04	4.8e-02
Co-55	2.08e-03	4.1e-06	3.34e+02	10	51	>1E20	>1E20
Co-56	2.11e-01	1.2e-05	3.29e+00	10	51	>1E20	>1E20
Co-57	7.39e-01	1.1e-05	9.38e-01	10	51	>1E20	>1E20
Co-58m	1.03e-03	8.8e-08	6.75e+02	10	51	>1E20	>1E20
Co-58	1.95e-01	3.5e-06	3.55e+00	10	51	>1E20	>1E20
Co-60m	2.00e-05	3.6e-09	3.47e+04	10	51	>1E20	>1E20
Co-60	5.27e+00	2.6e-05	1.32e-01	10	51	9.5e+13	2.5e+04
Co-61	1.88e-04	2.6e-07	3.68e+03	10	51	>1E20	>1E20
Co-62m	3.04e-06	9.6e-08	2.28e+05	10	51	>1E20	>1E20
Ni-56	1.67e-02	3.5e-06	4.15e+01	300	1501	>1E20	>1E20
Ni-57	4.11e-03	3.3e-06	1.69e+02	300	1501	>1E20	>1E20
Ni-59	8.00e+04	2.0e-07	8.66e-06	300	1501	1.1e+03	4.8e-02
Ni-63	1.00e+02	5.4e-07	6.93e-03	300	1501	>1E20	9.6e-02
Ni-65	2.87e-04	6.1e-07	2.41e+03	300	1501	>1E20	>1E20
Ni-66	6.23e-03	1.1e-05	1.11e+02	300	1501	>1E20	>1E20
Cu-60	4.37e-05	1.7e-07	1.59e+04	25	126	>1E20	>1E20

Rev. 0

C-48
Table C.I-3. (continued)

Nuclide	T _{1/2} (year)	DCF (mrem/pCi)	Lambda (1/year)	K _d (cm ² /g _m)	R _f	LAW GW Trigger (Ci/vault)	LAW Int Trigger (Ci/vault)
Cu-61	3.89e-04	4.1e-07	1.78e+03	25	126	>1E20	>1E20
Cu-64	1.45e-03	4.3e-07	4.78e+02	25	126	>1E20	>1E20
Cu-67	7.06e-03	1.1e-06	9.82e+01	25	126	>1E20	>1E20
Zn-62	1.04e-03	3.4e-06	6.64e+02	16	81	>1E20	>1E20
Zn-63	7.30e-05	2.0e-07	9.49e+03	16	81	>1E20	>1E20
Zn-65	6.67e-01	1.4e-05	1.04e+00	16	81	>1E20	>1E20
Zn-69m	1.57e-03	1.2e-05	4.40e+02	16	81	>1E20	>1E20
Zn-69	1.08e-04	8.5e-08	6.40e+03	16	81	>1E20	>1E20
Zn-71m	4.56e-04	8.3e-07	1.52e+03	16	81	>1E20	>1E20
Zn-72	1.27e-01	4.9e-06	5.44e+00	16	81	>1E20	>1E20
Ga-65	2.89e-05	7.8e-08	2.40e+04	0	1	>1E20	>1E20
Ga-66	1.07e-03	4.7e-06	6.46e+02	0	1	>1E20	>1E20
Ga-67	8.91e-03	7.2e-07	7.78e+01	0	1	>1E20	>1E20
Ga-68	1.30e-04	3.3e-07	5.34e+03	0	1	>1E20	>1E20
Ga-70	4.01e-05	7.1e-08	1.73e+04	0	1	>1E20	>1E20
Ga-72	1.61e-03	4.4e-06	4.31e+02	0	1	>1E20	>1E20
Ga-73	1.34e-02	1.0e-06	5.19e+01	0	1	>1E20	>1E20
Ge-66	1.07e-03	2.1e-07	6.46e+02	0	1	>1E20	>1E20
Ge-67	3.61e-05	1.1e-07	1.92e+04	0	1	>1E20	>1E20
Ge-68	7.86e-01	1.1e-06	8.82e-01	0	1	9.9e+00	>1E20
Ge-69	4.45e-03	3.6e-07	1.56e+02	0	1	>1E20	>1E20
Ge-71	3.12e-02	9.6e-09	2.22e+01	0	1	>1E20	>1E20
Ge-75	1.57e-04	7.3e-08	4.40e+03	0	1	>1E20	>1E20
Ge-77	1.29e-03	5.6e-07	5.38e+02	0	1	>1E20	>1E20
Ge-78	1.65e-04	2.1e-07	4.19e+03	0	1	>1E20	>1E20
As-69	2.85e-05	1.1e-07	2.43e+04	3	16	>1E20	>1E20
As-70	1.01e-04	3.4e-07	6.88e+03	3	16	>1E20	>1E20
As-71	7.07e-03	1.3e-06	9.80e+01	3	16	>1E20	>1E20
As-72	2.97e-03	5.6e-06	2.34e+02	3	16	>1E20	>1E20
As-73	2.20e-01	6.1e-07	3.15e+00	3	16	>1E20	>1E20
As-74	3.29e-02	3.3e-06	2.11e+01	3	16	>1E20	>1E20
As-76	3.00e-03	4.8e-06	2.31e+02	3	16	>1E20	>1E20
As-77	1.06e-01	1.1e-06	6.53e+00	3	16	>1E20	>1E20
As-78	1.73e-04	6.5e-07	4.01e+03	3	16	>1E20	>1E20

Rev. 0

C-49
Table C.1-3. (continued)

Nuclide	T1/2 (year)	DCF (mrem/pCi)	Lambda (1/year)	Kd (cm ³ /gm)	Rf	LAW GW Trigger (Ci/vault)	LAW Int Trigger (Ci/vault)
Se-70	8.37e-05	4.8e-07	8.29e+03	5	26	>1E20	>1E20
Se-73m	7.99e-05	1.5e-07	8.68e+03	5	26	>1E20	>1E20
Se-73	8.10e-04	1.5e-06	8.56e+02	5	26	>1E20	>1E20
Se-75	3.30e-01	8.8e-06	2.10e+00	5	26	>1E20	>1E20
Se-79	6.50e+04	8.3e-06	1.07e-05	5	26	4.1e-01	4.8e-02
Se-81m	1.09e-04	2.1e-07	6.36e+03	5	26	>1E20	>1E20
Se-81	4.30e-05	6.1e-08	1.61e+04	5	26	>1E20	>1E20
Se-83	4.28e-05	1.5e-07	1.62e+04	5	26	>1E20	>1E20
Br-74m	7.89e-05	2.2e-07	8.78e+03	0	1	>1E20	>1E20
Br-74	6.84e-05	1.4e-07	1.01e+04	0	1	>1E20	>1E20
Br-75	1.94e-04	1.3e-07	3.57e+03	0	1	>1E20	>1E20
Br-76	1.84e-03	1.4e-06	3.77e+02	0	1	>1E20	>1E20
Br-77	6.50e-03	3.1e-07	1.07e+02	0	1	>1E20	>1E20
Br-80m	5.04e-04	2.3e-07	1.37e+03	0	1	>1E20	>1E20
Br-80	3.37e-05	5.5e-08	2.06e+04	0	1	>1E20	>1E20
Br-82	4.03e-03	1.7e-06	1.72e+02	0	1	>1E20	>1E20
Br-83	2.74e-04	7.3e-08	2.53e+03	0	1	>1E20	>1E20
Br-84	6.05e-05	1.5e-07	1.15e+04	0	1	>1E20	>1E20
Rb-79	3.99e-05	8.7e-08	1.74e+04	0	1	>1E20	>1E20
Rb-81m	6.08e-05	1.8e-08	1.14e+04	0	1	>1E20	>1E20
Rb-81	5.36e-04	1.3e-07	1.29e+03	0	1	>1E20	>1E20
Rb-82m	7.30e-04	4.2e-07	9.49e+02	0	1	>1E20	>1E20
Rb-83	2.27e-01	7.7e-06	3.05e+00	0	1	7.2e+04	>1E20
Rb-84	9.31e-02	1.0e-05	7.45e+00	0	1	1.9e+14	>1E20
Rb-86	5.09e-02	9.4e-06	1.36e+01	0	1	>1E20	>1E20
Rb-87	4.80e+10	4.8e-06	1.44e-11	0	1	2.7e-02	4.8e-02
Rb-88	3.37e-05	1.6e-07	2.06e+04	0	1	>1E20	>1E20
Rb-89	2.89e-05	8.0e-08	2.40e+04	0	1	>1E20	>1E20
Sr-80	1.94e-04	5.2e-09	3.57e+03	10	51	>1E20	>1E20
Sr-81	5.51e-05	2.2e-07	1.26e+04	10	51	>1E20	>1E20
Sr-83	3.76e-03	2.3e-06	1.84e+02	10	51	>1E20	>1E20
Sr-85m	1.29e-04	2.4e-08	5.39e+03	10	51	>1E20	>1E20
Sr-85	1.79e-01	1.9e-06	3.88e+00	10	51	>1E20	>1E20
Sr-87m	3.21e-04	1.2e-07	2.16e+03	10	51	>1E20	>1E20

Rev. 0

C-50
Table C.1-3. (continued)

WSRC-RP-94-218

Nuclide	T1/2 (year)	DCF (mrem/pCi)	Lambda (1/year)	Kd (cm ³ /gm)	Rf	LAW GW Trigger (Ci/vault)	LAW Int Trigger (Ci/vault)
Sr-89	1.38e-01	8.7e-06	5.01e+00	10	51	>1E20	>1E20
Sr-90	2.86e+01	1.3e-04	2.42e-02	10	51	2.5e+01	5.4e-01
Sr-91	1.08e-03	3.0e-06	6.41e+02	10	51	>1E20	>1E20
Sr-92	3.09e-04	1.9e-06	2.24e+03	10	51	>1E20	>1E20
Y-86m	9.13e-05	2.4e-07	7.60e+03	10	51	>1E20	>1E20
Y-86	1.67e-03	4.1e-06	4.16e+02	10	51	>1E20	>1E20
Y-87	9.13e-03	2.2e-06	7.60e+01	10	51	>1E20	>1E20
Y-88	2.88e-01	5.2e-06	2.41e+00	10	51	>1E20	>1E20
Y-90m	3.64e-04	6.6e-07	1.90e+03	10	51	>1E20	>1E20
Y-90	2.86e+01	1.0e-05	2.42e-02	10	51	3.2e+02	5.4e-01
Y-91m	9.51e-05	3.9e-08	7.29e+03	10	51	>1E20	>1E20
Y-91	1.67e-01	8.9e-06	4.15e+00	10	51	>1E20	>1E20
Y-92	4.03e-04	1.9e-06	1.72e+03	10	51	>1E20	>1E20
Y-93	1.16e-03	4.5e-06	5.96e+02	10	51	>1E20	>1E20
Y-94	3.61e-05	1.8e-07	1.92e+04	10	51	>1E20	>1E20
Y-95	2.00e-05	9.7e-08	3.47e+04	10	51	>1E20	>1E20
Zr-86	1.88e-03	3.5e-06	3.68e+02	0	1	>1E20	>1E20
Zr-88	2.33e-01	1.3e-06	2.98e+00	0	1	3.0e+05	>1E20
Zr-89	8.94e-03	3.1e-06	7.75e+01	0	1	>1E20	>1E20
Zr-93	1.50e+06	1.6e-06	4.62e-07	0	1	8.2e-02	4.8e-02
Zr-95	1.75e-01	3.4e-06	3.96e+00	0	1	1.5e+07	>1E20
Zr-97	1.92e-03	8.0e-06	3.62e+02	0	1	>1E20	>1E20
Nb-88	2.66e-05	7.2e-08	2.60e+04	0	1	>1E20	>1E20
Nb-89(66m)	1.25e-04	4.6e-07	5.52e+03	0	1	>1E20	>1E20
Nb-89(122m)	2.32e-04	1.0e-06	2.99e+03	0	1	>1E20	>1E20
Nb-90	1.67e-03	4.9e-06	4.16e+02	0	1	>1E20	>1E20
Nb-93m	1.01e+01	5.3e-07	6.84e-02	0	1	3.5e-01	4.5e+01
Nb-94	2.00e+04	5.1e-06	3.47e-05	0	1	2.6e-02	4.8e-02
Nb-95m	9.88e-03	2.0e-06	7.02e+01	0	1	>1E20	>1E20
Nb-95	9.58e-02	2.2e-06	7.23e+00	0	1	3.1e+14	>1E20
Nb-96	2.67e-03	4.4e-06	2.60e+02	0	1	>1E20	>1E20
Nb-97	1.40e-04	2.3e-07	4.95e+03	0	1	>1E20	>1E20
Nb-98	8.87e-08	3.4e-07	7.81e+06	0	1	>1E20	>1E20
Mo-90	6.50e-04	2.5e-06	1.07e+03	0	1	>1E20	>1E20

Rev. 0

C-51
Table C.1-3. (continued)

WSRC-RP-94-218

Nuclide	T1/2 (year)	DCF (mrem/pCi)	Lambda (1/year)	Kd (cm ³ /gm)	Rf	LAW GW Trigger (Ci/vault)	LAW Int Trigger (Ci/vault)
Mo-93m	7.87e-04	1.1e-06	8.81e+02	0	1	>1E20	>1E20
Mo-93	3.50e+03	1.3e-06	1.98e-04	0	1	1.0e-01	4.9e-02
Mo-99	7.53e-03	4.4e-06	9.20e+01	0	1	>1E20	>1E20
Mo-101	2.78e-05	9.2e-08	2.50e+04	0	1	>1E20	>1E20
Tc-93m	8.18e-05	7.1e-08	8.48e+03	0.36	2.8	>1E20	>1E20
Tc-93	3.08e-04	1.6e-07	2.25e+03	0.36	2.8	>1E20	>1E20
Tc-94m	1.01e-04	2.5e-07	6.88e+03	0.36	2.8	>1E20	>1E20
Tc-94	5.57e-04	5.8e-07	1.24e+03	0.36	2.8	>1E20	>1E20
Tc-96m	9.89e-05	3.1e-08	7.01e+03	0.36	2.8	>1E20	>1E20
Tc-96	1.18e-02	2.7e-06	5.89e+01	0.36	2.8	>1E20	>1E20
Tc-97m	2.46e-01	1.1e-06	2.81e+00	0.36	2.8	4.3e+16	>1E20
Tc-97	2.60e+06	1.5e-07	2.67e-07	0.36	2.8	2.5e+00	4.8e-02
Tc-98	1.50e+06	4.8e-06	4.62e-07	0.36	2.8	7.7e-02	4.8e-02
Tc-99m	6.87e-04	6.0e-08	1.01e+03	0.36	2.8	>1E20	>1E20
Tc-99	2.11e+05	1.3e-06	3.29e-06	0.36	2.8	2.8e-01	4.8e-02
Tc-101	2.70e-05	3.8e-08	2.57e+04	0.36	2.8	>1E20	>1E20
Tc-104	3.42e-05	1.6e-07	2.03e+04	0.36	2.8	>1E20	>1E20
Ru-94	1.08e-04	3.3e-07	6.40e+03	100	501	>1E20	>1E20
Ru-97	7.91e-03	6.4e-07	8.76e+01	100	501	>1E20	>1E20
Ru-103	1.08e-01	2.7e-06	6.43e+00	100	501	>1E20	>1E20
Ru-105	5.07e-04	1.0e-06	1.37e+03	100	501	>1E20	>1E20
Ru-106	9.99e-01	2.1e-05	6.94e-01	100	501	>1E20	>1E20
Rh-99m	5.36e-04	2.8e-07	1.29e+03	0	1	>1E20	>1E20
Rh-99	4.38e-02	2.0e-06	1.58e+01	0	1	>1E20	>1E20
Rh-100	2.28e-03	3.1e-06	3.04e+02	0	1	>1E20	>1E20
Rh-101m	1.23e-02	8.8e-07	5.63e+01	0	1	>1E20	>1E20
Rh-101	3.10e+00	2.3e-06	2.24e-01	0	1	1.8e-01	2.5e+08
Rh-102m	2.90e+00	3.5e-06	2.39e-01	0	1	1.2e-01	1.2e+09
Rh-102	5.75e-01	5.5e-06	1.21e+00	0	1	9.9e+00	>1E20
Rh-103m	1.06e-04	0.00000001	6.51e+03	0	1	>1E20	>1E20
Rh-105	4.05e-03	1.4e-06	1.71e+02	0	1	>1E20	>1E20
Rh-106m	2.49e-04	6.1e-07	2.79e+03	0	1	>1E20	>1E20
Rh-107	4.13e-05	5.4e-08	1.68e+04	0	1	>1E20	>1E20
Pd-100	1.10e-02	3.8e-06	6.33e+01	0	1	>1E20	>1E20

Rev. 0

C-52
Table C.1-3. (continued)

WSRC-RP-94-218

Nuclide	T1/2 (year)	DCF (mrem/pCi)	Lambda (1/year)	Kd (cm ³ /gm)	Rf	LAW GW Trigger (Ci/vault)	LAW Int Trigger (Ci/vault)
Pd-101	9.58e-04	3.8e-07	7.23e+02	0	1	>1E20	>1E20
Pd-103	4.65e-02	6.9e-07	1.49e+01	0	1	>1E20	>1E20
Pd-107	6.50e+06	1.4e-07	1.07e-07	0	1	9.4e-01	4.8e-02
Pd-109	1.53e-03	2.1e-06	4.53e+02	0	1	>1E20	>1E20
Ag-102	2.85e-05	7.9e-08	2.43e+04	10	51	>1E20	>1E20
Ag-103	1.25e-04	1.4e-07	5.52e+03	10	51	>1E20	>1E20
Ag-104m	5.70e-05	1.5e-07	1.22e+04	10	51	>1E20	>1E20
Ag-104	1.27e-04	2.3e-07	5.44e+03	10	51	>1E20	>1E20
Ag-105	1.10e-01	1.9e-06	6.33e+00	10	51	>1E20	>1E20
Ag-106m	2.27e-02	6.1e-06	3.05e+01	10	51	>1E20	>1E20
Ag-106	4.56e-05	7.6e-08	1.52e+04	10	51	>1E20	>1E20
Ag-108m	1.30e+02	7.5e-06	5.33e-03	10	51	3.5e+00	8.2e-02
Ag-110m	6.90e-01	1.1e-05	1.00e+00	10	51	>1E20	>1E20
Ag-111	2.05e-02	4.5e-06	3.39e+01	10	51	>1E20	>1E20
Ag-112	3.57e-04	1.6e-06	1.94e+03	10	51	>1E20	>1E20
Ag-115	3.99e-05	1.5e-07	1.74e+04	10	51	>1E20	>1E20
Cd-104	1.08e-04	2.3e-07	6.40e+03	8	41	>1E20	>1E20
Cd-107	7.42e-04	2.4e-07	9.35e+02	8	41	>1E20	>1E20
Cd-109	1.24e+00	1.2e-05	5.59e-01	8	41	>1E20	>1E20
Cd-113m	1.46e+01	1.5e-04	4.75e-02	8	41	6.1e+02	5.6e+00
Cd-113	9.30e+15	1.6e-04	7.45e-17	8	41	3.4e-02	4.8e-02
Cd-115m	1.36e-01	1.5e-05	5.11e+00	8	41	>1E20	>1E20
Cd-115	6.10e-03	4.7e-06	1.14e+02	8	41	>1E20	>1E20
Cd-117m	3.88e-04	1.1e-06	1.79e+03	8	41	>1E20	>1E20
Cd-117	2.97e-04	1.1e-06	2.34e+03	8	41	>1E20	>1E20
In-109	4.91e-04	2.7e-07	1.41e+03	0	1	>1E20	>1E20
In-110(69m)	1.27e-04	3.3e-07	5.44e+03	0	1	>1E20	>1E20
In-111	7.69e-03	1.2e-06	9.01e+01	0	1	>1E20	>1E20
In-112	2.66e-05	0.00000002	2.60e+04	0	1	>1E20	>1E20
In-113m	1.89e-04	1.0e-07	3.66e+03	0	1	>1E20	>1E20
In-114m	1.36e-01	0.000015	5.11e+00	0	1	1.1e+09	>1E20
In-115m	5.13e-04	3.4e-07	1.35e+03	0	1	>1E20	>1E20
In-115	4.60e+15	1.4e-04	1.51e-16	0	1	9.4e-04	4.8e-02
In-116m	1.03e-04	2.1e-07	6.73e+03	0	1	>1E20	>1E20

Rev. 0

C-53
Table C.1-3. (continued)

Nuclide	T1/2 (year)	DCF (mrem/pCi)	Lambda (1/year)	Kd (cm ² /g)	Rf	LAW GW Trigger (Ci/vault)	LAW Int Trigger (Ci/vault)
In-117m	2.21e-04	4.2e-07	3.13e+03	0	1	>1E20	>1E20
In-117	8.37e-05	8.7e-08	8.29e+03	0	1	>1E20	>1E20
In-119m	3.42e-05	1.0e-07	2.03e+04	0	1	>1E20	>1E20
Sa-110	4.56e-04	1.5e-06	1.52e+03	130	651	>1E20	>1E20
Sa-111	6.65e-05	6.7e-08	1.04e+04	130	651	>1E20	>1E20
Sa-113	3.15e-01	2.7e-06	2.20e+00	130	651	>1E20	>1E20
Sa-117m	3.83e-02	2.6e-06	1.81e+01	130	651	>1E20	>1E20
Sa-119m	8.02e-01	1.2e-05	8.64e-01	130	651	>1E20	>1E20
Sa-121m	7.60e+01	1.3e-06	9.12e-03	130	651	5.2e+14	1.2e-01
Sn-121	3.08e-03	8.9e-07	2.25e+02	130	651	>1E20	>1E20
Sn-123m	7.61e-05	1.0e-07	9.11e+03	130	651	>1E20	>1E20
Sn-123	3.53e-01	7.7e-06	1.96e+00	130	651	>1E20	>1E20
Sn-125	2.64e-02	1.1e-05	2.62e+01	130	651	>1E20	>1E20
Sn-126	1.00e+05	1.7e-05	6.93e-06	130	651	5.2e+00	4.8e-02
Sn-127	2.42e-04	7.4e-07	2.87e+03	130	651	>1E20	>1E20
Sn-128	1.12e-04	5.2e-07	6.18e+03	130	651	>1E20	>1E20
Sb-115	5.89e-05	6.3e-08	1.18e+04	10	51	>1E20	>1E20
Sb-116m	1.14e-04	2.4e-07	6.08e+03	10	51	>1E20	>1E20
Sb-116	2.85e-05	5.6e-08	2.43e+04	10	51	>1E20	>1E20
Sb-117	3.19e-04	7.4e-08	2.17e+03	10	51	>1E20	>1E20
Sb-118m	5.82e-04	9.3e-07	1.19e+03	10	51	>1E20	>1E20
Sb-119	4.33e-03	3.4e-07	1.60e+02	10	51	>1E20	>1E20
Sb-120(16m)	3.04e-05	3.0e-08	2.28e+04	10	51	>1E20	>1E20
Sb-120(6d)	1.59e-02	5.4e-06	4.37e+01	10	51	>1E20	>1E20
Sb-122	7.45e-03	6.3e-06	9.31e+01	10	51	>1E20	>1E20
Sb-124m	1.77e-04	2.0e-08	3.92e+03	10	51	>1E20	>1E20
Sb-124	1.65e-01	9.3e-06	4.20e+00	10	51	>1E20	>1E20
Sb-125	2.40e+00	2.6e-06	2.89e-01	10	51	>1E20	1.7e+11
Sb-126m	3.61e-05	7.3e-08	1.92e+04	10	51	>1E20	>1E20
Sb-126	3.39e-02	9.6e-06	2.04e+01	10	51	>1E20	>1E20
Sb-127	1.04e-02	6.6e-06	6.66e+01	10	51	>1E20	>1E20
Sb-128(9h)	1.03e-03	4.3e-06	6.75e+02	10	51	>1E20	>1E20
Sb-128(10m)	1.90e-05	5.0e-08	3.65e+04	10	51	>1E20	>1E20
Sb-129	4.95e-04	1.7e-06	1.40e+03	10	51	>1E20	>1E20

Rev. 0

C-54
Table C.1-3. (continued)

WSRC-RP-94-218

Nuclide	T1/2 (year)	DCF (mrem/pCi)	Lambda (1/year)	Kd (cm ³ /gm)	Rf	LAW GW Trigger (Ci/vault)	LAW Int Trigger (Ci/vault)
Sb-130	1.25e-05	2.6e-07	5.52e+04	10	51	>1E20	>1E20
Sb-131	4.37e-05	2.9e-07	1.59e+04	10	51	>1E20	>1E20
Te-118	1.64e-02	6.7e-07	4.22e+01	0	1	>1E20	>1E20
Te-121m	4.11e-01	6.7e-06	1.69e+00	0	1	9.1e+01	>1E20
Te-121	4.65e-02	1.5e-06	1.49e+01	0	1	>1E20	>1E20
Te-123m	3.28e-01	5.1e-06	2.12e+00	0	1	1.0e+03	>1E20
Te-123	1.20e+13	4.1e-06	5.78e-14	0	1	3.2e-02	4.8e-02
Te-125m	1.59e-01	3.4e-06	4.37e+00	0	1	1.2e+08	>1E20
Te-127m	2.98e-01	7.9e-06	2.32e+00	0	1	1.8e+03	>1E20
Te-127	1.07e-03	6.9e-07	6.46e+02	0	1	>1E20	>1E20
Te-129m	9.14e-02	9.9e-06	7.58e+00	0	1	3.8e+14	>1E20
Te-129	1.33e-04	1.9e-07	5.21e+03	0	1	>1E20	>1E20
Te-131m	3.42e-03	1.5e-05	2.03e+02	0	1	>1E20	>1E20
Te-131	4.75e-05	2.0e-07	1.46e+04	0	1	>1E20	>1E20
Te-132	8.76e-03	7.4e-06	7.91e+01	0	1	>1E20	>1E20
Te-133m	1.05e-04	7.6e-07	6.58e+03	0	1	>1E20	>1E20
Te-133	2.38e-05	1.6e-07	2.92e+04	0	1	>1E20	>1E20
Te-134	7.99e-05	2.1e-07	8.68e+03	0	1	>1E20	>1E20
I-120m	1.01e-04	3.9e-07	6.88e+03	0.6	4	>1E20	>1E20
I-120	1.48e-04	6.7e-07	4.67e+03	0.6	4	>1E20	>1E20
I-121	2.40e-04	1.8e-07	2.89e+03	0.6	4	>1E20	>1E20
I-123	1.52e-03	4.9e-07	4.57e+02	0.6	4	>1E20	>1E20
I-124	1.15e-02	3.1e-05	6.03e+01	0.6	4	>1E20	>1E20
I-125	1.64e-01	3.8e-05	4.22e+00	0.6	4	>1E20	>1E20
I-126	3.64e-02	7.1e-05	1.90e+01	0.6	4	>1E20	>1E20
I-128	4.75e-05	8.5e-08	1.46e+04	0.6	4	>1E20	>1E20
I-129	1.72e+07	2.8e-04	4.02e-08	0.6	4	1.9e-03	4.8e-02
I-130	1.41e-03	4.3e-06	4.90e+02	0.6	4	>1E20	>1E20
I-131	2.22e-02	5.3e-05	3.13e+01	0.6	4	>1E20	>1E20
I-132m	1.58e-04	4.7e-07	4.39e+03	0.6	4	>1E20	>1E20
I-132	2.60e-04	3.3e-07	2.66e+03	0.6	4	>1E20	>1E20
I-133	2.37e-03	5.4e-06	2.92e+02	0.6	4	>1E20	>1E20
I-134	1.00e-04	1.9e-07	6.93e+03	0.6	4	>1E20	>1E20
I-135	7.51e-04	2.0e-05	9.23e+02	0.6	4	>1E20	>1E20

Rev. 0

C-55
Table C.1-3. (continued)

WSRC-RP-94-218

Nuclide	T1/2 (year)	DCF (mrem/pCi)	Lambda (1/year)	Kd (cm**3/gm)	Rf	LAW GW Trigger (Ci/vault)	LAW Int Trigger (Ci/vault)
Cs-125	8.56e-05	5.5e-08	8.10e+03	100	501	>1E20	>1E20
Cs-127	7.07e-04	8.0e-08	9.80e+02	100	501	>1E20	>1E20
Cs-129	3.65e-03	2.2e-07	1.90e+02	100	501	>1E20	>1E20
Cs-130	5.70e-05	4.9e-08	1.22e+04	100	501	>1E20	>1E20
Cs-131	2.66e-02	2.4e-07	2.61e+01	100	501	>1E20	>1E20
Cs-132	1.80e-02	1.9e-06	3.85e+01	100	501	>1E20	>1E20
Cs-134m	3.31e-04	4.2e-08	2.10e+03	100	501	>1E20	>1E20
Cs-134	2.06e+00	7.4e-05	3.36e-01	100	501	>1E20	2.0e+13
Cs-135m	1.01e-04	4.9e-08	6.88e+03	100	501	>1E20	>1E20
Cs-135	2.30e+06	7.1e-06	3.01e-07	100	501	9.3e+00	4.8e-02
Cs-136	3.53e-02	1.1e-05	1.96e+01	100	501	>1E20	>1E20
Cs-137	3.01e+01	5.0e-05	2.30e-02	100	501	>1E20	4.8e-01
Cs-138	6.12e-05	1.6e-07	1.13e+04	100	501	>1E20	>1E20
Ba-126	1.84e-04	9.0e-07	3.76e+03	5	26	>1E20	>1E20
Ba-128	6.57e-03	1.0e-05	1.05e+02	5	26	>1E20	>1E20
Ba-131m	2.78e-05	9.7e-07	2.50e+04	5	26	>1E20	>1E20
Ba-131	3.20e-02	1.6e-06	2.16e+01	5	26	>1E20	>1E20
Ba-133m	4.44e-03	2.0e-06	1.56e+02	5	26	>1E20	>1E20
Ba-133	1.07e+01	3.2e-06	6.48e-02	5	26	4.9e+03	3.1e+01
Ba-135m	3.27e-03	1.6e-06	2.12e+02	5	26	>1E20	>1E20
Ba-137m	0.000005		1.43e+05	5	26	>1E20	>1E20
Ba-139	1.58e-04	3.9e-07	4.38e+03	5	26	>1E20	>1E20
Ba-140	3.50e-02	8.4e-06	1.98e+01	5	26	>1E20	>1E20
Ba-141	3.48e-05	2.0e-07	1.99e+04	5	26	>1E20	>1E20
Ba-142	2.03e-05	1.0e-07	3.41e+04	5	26	>1E20	>1E20
La-131	1.12e-04	1.1e-07	6.18e+03	100	501	>1E20	>1E20
La-132	5.13e-04	1.5e-06	1.35e+03	100	501	>1E20	>1E20
La-135	2.22e-03	1.3e-07	3.12e+02	100	501	>1E20	>1E20
La-137	6.00e+04	4.3e-07	1.16e-05	100	501	1.6e+02	4.8e-02
La-138	1.06e+11	5.9e-06	6.54e-12	100	501	1.1e+01	4.8e-02
La-140	4.59e-03	7.7e-06	1.51e+02	100	501	>1E20	>1E20
La-141	4.41e-04	1.4e-06	1.57e+03	100	501	>1E20	>1E20
La-142	1.76e-04	8.3e-07	3.95e+03	100	501	>1E20	>1E20
La-143	2.66e-05	1.4e-07	2.60e+04	100	501	>1E20	>1E20

Rev. 0

C-56
Table C.1-3. (continued)

WSRC-RP-94-218

Nuclide	T1/2 (year)	DCF (mrem/pCi)	Lambda (1/year)	Kd (cm**3/gm)	Rf	LAW GW Trigger (Ci/vault)	LAW Int Trigger (Ci/vault)
Ce-134	8.21e-03	8.9e-06	8.44e+01	10	51	>1E20	>1E20
Ce-135	1.96e-03	3.2e-06	3.53e+02	10	51	>1E20	>1E20
Ce-137m	3.92e-03	2.0e-06	1.77e+02	10	51	>1E20	>1E20
Ce-137	1.03e-03	9.8e-08	6.75e+02	10	51	>1E20	>1E20
Ce-139	3.77e-01	1.1e-06	1.84e+00	10	51	>1E20	>1E20
Ce-141	8.90e-02	2.6e-06	7.79e+00	10	51	>1E20	>1E20
Ce-143	3.76e-03	4.2e-06	1.84e+02	10	51	>1E20	>1E20
Ce-144	7.94e-01	2.0e-05	8.73e-01	10	51	>1E20	>1E20
Pr-136	1.25e-04	6.8e-08	5.52e+03	10	51	>1E20	>1E20
Pr-137	1.71e-04	1.3e-07	4.05e+03	100	501	>1E20	>1E20
Pr-138m	2.40e-04	4.9e-07	2.89e+03	100	501	>1E20	>1E20
Pr-139	5.13e-04	1.2e-07	1.35e+03	100	501	>1E20	>1E20
Pr-142m	2.72e-05	6.3e-08	2.55e+04	100	501	>1E20	>1E20
Pr-142	2.18e-03	5.1e-06	3.18e+02	100	501	>1E20	>1E20
Pr-143	3.75e-02	4.5e-06	1.85e+01	100	501	>1E20	>1E20
Pr-144	3.29e-05	1.1e-07	2.11e+04	100	501	>1E20	>1E20
Pr-145	6.82e-04	1.5e-06	1.02e+03	100	501	>1E20	>1E20
Pr-147	2.28e-05	5.7e-08	3.04e+04	100	501	>1E20	>1E20
Nd-136	9.64e-05	3.3e-07	7.19e+03	100	501	>1E20	>1E20
Nd-138	4.18e-05	2.5e-06	1.66e+04	100	501	>1E20	>1E20
Nd-139m	6.27e-04	1.0e-06	1.10e+03	100	501	>1E20	>1E20
Nd-139	5.93e-04	5.7e-08	1.17e+03	100	501	>1E20	>1E20
Nd-141	2.85e-04	3.2e-08	2.43e+03	100	501	>1E20	>1E20
Nd-147	3.01e-02	3.9e-06	2.30e+01	100	501	>1E20	>1E20
Nd-149	1.97e-03	4.6e-07	3.51e+02	100	501	>1E20	>1E20
Nd-151	2.36e-05	7.4e-08	2.94e+04	100	501	>1E20	>1E20
Pm-141	4.18e-05	8.4e-08	1.66e+04	100	501	>1E20	>1E20
Pm-143	7.26e-01	9.5e-07	9.55e-01	100	501	>1E20	>1E20
Pm-144	8.22e-01	3.9e-06	8.43e-01	100	501	>1E20	>1E20
Pm-145	1.77e+01	4.6e-07	3.92e-02	100	501	>1E20	2.4e+00
Pm-146	1.94e+00	3.2e-06	3.57e-01	100	501	>1E20	1.5e+14
Pm-147	2.52e+00	9.5e-07	2.75e-01	100	501	>1E20	4.3e+10
Pm-148m	1.14e-01	7.0e-06	6.06e+00	100	501	>1E20	>1E20
Pm-148	1.47e-02	9.5e-06	4.71e+01	100	501	>1E20	>1E20

Rev. 0

Table C.1-3. (continued)

Nuclide	T1/2 (year)	DCF (mmrem/pCi)	Lambda (1/year)	Kd (cm**3/gm)	Rf	LAW GW Trigger (Civault)	LAW Int Trigger (Civault)
Pm-149	6.06e-03	3.6e-06	1.14e+02	100	501	>1E20	>1E20
Pm-150	3.06e-04	9.8e-07	2.27e+03	100	501	>1E20	>1E20
Pm-151	3.24e-03	2.8e-06	2.14e+02	100	501	>1E20	>1E20
Sm-141m	4.30e-05	1.8e-07	1.61e+04	100	501	>1E20	>1E20
Sm-141	1.94e-05	8.4e-08	3.57e+04	100	501	>1E20	>1E20
Sm-142	1.37e-04	6.0e-07	5.06e+03	100	501	>1E20	>1E20
Sm-145	9.31e-01	8.5e-07	7.45e-01	100	501	>1E20	>1E20
Sm-146	7.00e+07	2.0e-04	9.90e-09	100	501	3.3e-01	4.8e-02
Sm-147	1.06e+11	1.8e-04	6.54e-12	100	501	3.7e-01	4.8e-02
Sm-151	9.00e+01	3.4e-07	7.70e-03	100	501	4.6e+10	1.0e-01
Sm-153	5.33e-03	2.6e-06	1.30e+02	100	501	>1E20	>1E20
Sm-155	4.22e-05	6.6e-08	1.64e+04	100	501	>1E20	>1E20
Sm-158	8.37e-05	1.0e-06	8.29e+03	100	501	>1E20	>1E20
Eu-145	1.62e-02	3.2e-05	4.29e+01	100	501	>1E20	>1E20
Eu-146	1.26e-02	5.1e-06	5.50e+01	100	501	>1E20	>1E20
Eu-147	6.02e-02	1.8e-06	1.15e+01	100	501	>1E20	>1E20
Eu-148	1.48e-01	5.2e-06	4.69e+00	100	501	>1E20	>1E20
Eu-149	2.90e-01	4.2e-07	2.39e+00	100	501	>1E20	>1E20
Eu-150(12h)	1.37e-03	1.5e-06	5.06e+02	100	501	>1E20	>1E20
Eu-150(34y)	3.40e+01	6.2e-06	2.04e-02	100	501	>1E20	3.7e-01
Eu-152m	1.07e-03	1.9e-06	6.51e+02	100	501	>1E20	>1E20
Eu-152	1.34e+01	6.0e-06	5.17e-02	100	501	>1E20	8.5e+00
Eu-154	8.20e+00	9.1e-06	8.45e-02	100	501	>1E20	2.3e+02
Eu-155	1.70e+00	1.3e-06	4.08e-01	100	501	>1E20	>1E20
Eu-156	4.22e-02	8.7e-06	1.64e+01	100	501	>1E20	>1E20
Eu-157	1.73e-03	2.3e-06	4.00e+02	100	501	>1E20	>1E20
Eu-158	8.73e-05	2.6e-07	7.94e+03	100	501	>1E20	>1E20
Gd-145	4.75e-05	1.1e-07	1.46e+04	100	501	>1E20	>1E20
Gd-146	1.26e-02	3.8e-06	5.50e+01	100	501	>1E20	>1E20
Gd-147	3.99e-03	2.6e-06	1.74e+02	100	501	>1E20	>1E20
Gd-148	1.30e+02	2.1e-04	5.33e-03	100	501	2.0e+05	8.2e-02
Gd-149	2.46e-02	1.8e-06	2.81e+01	100	501	>1E20	>1E20
Gd-151	3.29e-01	7.7e-07	2.11e+00	100	501	>1E20	>1E20
Gd-152	1.10e+14	1.5e-04	6.30e-15	100	501	4.4e-01	4.8e-02

Rev. 0

C-58
Table C.1-3. (continued)

WSRC-RP-94-218

Nuclide	T1/2 (year)	DCF (mrem/pCi)	Lambda (1/year)	Kd (cm**3/gm)	Rf	LAW GW Trigger (Ci/vault)	LAW Int Trigger (Ci/vault)
Gd-153	6.61e-01	1.1e-06	1.05e+00	100	501	>1E20	>1E20
Gd-159	2.12e-03	1.9e-06	3.27e+02	100	501	>1E20	>1E20
Tb-147	4.56e-05	5.6e-07	1.52e+04	100	501	>1E20	>1E20
Tb-149	4.68e-04	9.5e-07	1.48e+03	100	501	>1E20	>1E20
Tb-150	3.54e-04	9.7e-07	1.96e+03	100	501	>1E20	>1E20
Tb-151	2.05e-03	1.4e-06	3.38e+02	100	501	>1E20	>1E20
Tb-153	6.27e-03	9.9e-07	1.10e+02	100	501	>1E20	>1E20
Tb-154	9.70e-04	2.8e-06	7.15e+02	100	501	>1E20	>1E20
Tb-155	1.53e-02	8.2e-07	4.52e+01	100	501	>1E20	>1E20
Tb-156m(24h)	2.74e-03	7.0e-07	2.53e+02	100	501	>1E20	>1E20
Tb-156m(5h)	6.27e-04	3.2e-07	1.10e+03	100	501	>1E20	>1E20
Tb-156	1.48e-02	4.6e-06	4.69e+01	100	501	>1E20	>1E20
Tb-157	1.50e+02	1.0e-07	4.62e-03	100	501	7.0e+07	7.6e-02
Tb-158	1.20e+03	4.0e-06	5.78e-04	100	501	7.0e+01	5.1e-02
Tb-160	1.98e-01	6.4e-06	3.50e+00	100	501	>1E20	>1E20
Tb-161	1.88e-02	2.6e-06	3.68e+01	100	501	>1E20	>1E20
Dy-155	1.20e-03	5.6e-07	5.79e+02	100	501	>1E20	>1E20
Dy-157	9.24e-04	2.7e-07	7.50e+02	100	501	>1E20	>1E20
Dy-159	3.94e-01	4.0e-07	1.76e+00	100	501	>1E20	>1E20
Dy-165	2.66e-04	3.6e-07	2.61e+03	100	501	>1E20	>1E20
Dy-166	9.31e-03	6.2e-06	7.45e+01	100	501	>1E20	>1E20
Ho-155	9.51e-05	1.2e-07	7.29e+03	100	501	>1E20	>1E20
Ho-157	2.66e-05	1.9e-08	2.60e+04	100	501	>1E20	>1E20
Ho-159	6.27e-05	2.3e-08	1.10e+04	100	501	>1E20	>1E20
Ho-161	2.85e-04	4.7e-08	2.43e+03	100	501	>1E20	>1E20
Ho-162m	1.29e-04	9.0e-08	5.36e+03	100	501	>1E20	>1E20
Ho-162	2.85e-05	6.7e-09	2.43e+04	100	501	>1E20	>1E20
Ho-164m	7.13e-05	4.9e-08	9.72e+03	100	501	>1E20	>1E20
Ho-164	7.03e-05	2.4e-08	9.85e+03	100	501	>1E20	>1E20
Ho-166m	1.20e+03	7.8e-06	5.78e-04	100	501	3.6e+01	5.1e-02
Ho-166	3.06e-03	5.5e-06	2.27e+02	100	501	>1E20	>1E20
Ho-167	3.54e-04	3.2e-07	1.96e+03	100	501	>1E20	>1E20
Er-161	3.54e-04	3.3e-07	1.96e+03	100	501	>1E20	>1E20
Er-165	1.18e-03	7.9e-08	5.86e+02	100	501	>1E20	>1E20

Rev. 0

C-59
Table C.1-3. (continued)

WSRC-RP-94-218

Nuclide	T1/2 (year)	DCF (mrem/pCi)	Lambda (1/year)	Kd (cm ³ /gm)	Rf	LAW GW Trigger (Ci/vault)	LAW Int Trigger (Ci/vault)
Er-169	2.57e-02	1.4e-06	2.69e+01	100	501	>1E20	>1E20
Er-171	8.58e-04	1.4e-06	8.08e+02	100	501	>1E20	>1E20
Er-172	5.59e-03	3.7e-06	1.24e+02	100	501	>1E20	>1E20
Tm-162	1.46e-04	7.0e-08	4.73e+03	100	501	>1E20	>1E20
Tm-166	8.78e-04	1.2e-06	7.89e+02	100	501	>1E20	>1E20
Tm-167	2.63e-02	2.1e-06	2.64e+01	100	501	>1E20	>1E20
Tm-170	3.53e-01	5.0e-06	1.96e+00	100	501	>1E20	>1E20
Tm-171	1.92e+00	3.9e-07	3.61e-01	100	501	>1E20	2.3e+14
Tm-172	7.26e-03	6.0e-06	9.55e+01	100	501	>1E20	>1E20
Tm-173	9.35e-04	1.2e-06	7.41e+02	100	501	>1E20	>1E20
Tm-175	3.80e-05	5.4e-08	1.82e+04	100	501	>1E20	>1E20
Yb-162	3.59e-05	7.0e-08	1.93e+04	100	501	>1E20	>1E20
Yb-165	1.90e-05	3.8e-06	3.65e+04	100	501	>1E20	>1E20
Yb-167	3.42e-05	1.7e-08	2.03e+04	100	501	>1E20	>1E20
Yb-169	8.76e-02	2.8e-06	7.91e+00	100	501	>1E20	>1E20
Yb-175	1.15e-02	1.6e-06	6.04e+01	100	501	>1E20	>1E20
Yb-177	2.17e-04	3.1e-07	3.20e+03	100	501	>1E20	>1E20
Yb-178	1.40e-04	3.9e-07	4.94e+03	100	501	>1E20	>1E20
Lu-169	3.88e-03	2.0e-06	1.79e+02	100	501	>1E20	>1E20
Lu-170	5.48e-03	4.3e-06	1.27e+02	100	501	>1E20	>1E20
Lu-171	2.27e-02	2.6e-06	3.05e+01	100	501	>1E20	>1E20
Lu-172	1.83e-02	5.0e-06	3.78e+01	100	501	>1E20	>1E20
Lu-173	1.37e+00	9.7e-07	5.06e-01	100	501	>1E20	>1E20
Lu-174m	3.83e-01	1.8e-06	1.81e+00	100	501	>1E20	>1E20
Lu-174	3.60e+00	9.9e-07	1.93e-01	100	501	>1E20	1.1e+07
Lu-176m	4.21e-04	6.3e-07	1.65e+03	100	501	>1E20	>1E20
Lu-176	3.00e+10	6.6e-06	2.31e-11	100	501	1.0e+01	4.8e-02
Lu-177m	4.41e-02	6.8e-06	1.57e+01	100	501	>1E20	>1E20
Lu-177	1.84e-02	2.0e-06	3.77e+01	100	501	>1E20	>1E20
Lu-178m	3.80e-05	8.8e-08	1.82e+04	100	501	>1E20	>1E20
Lu-178	5.70e-05	1.2e-07	1.22e+04	100	501	>1E20	>1E20
Lu-179	5.25e-04	8.1e-07	1.32e+03	100	501	>1E20	>1E20
Hf-170	1.39e-03	1.2e-05	4.98e+02	100	501	>1E20	>1E20
Hf-172	5.00e+00	4.1e-06	1.39e-01	100	501	>1E20	5.0e+04

Rev. 0

C-60
Table C.1-3. (continued)

WSRC-RP-94-218

Nuclide	T1/2 (year)	DCF (mrem/pCi)	Lambda (1/year)	Kd (cm ³ /gm)	Rf	LAW GW Trigger (Ci/vault)	LAW Int Trigger (Ci/vault)
Hf-173	2.69e-03	9.6e-07	2.57e+02	100	501	>1E20	>1E20
Hf-175	1.92e-01	1.6e-06	3.62e+00	100	501	>1E20	>1E20
Hf-177m	9.77e-05	2.5e-07	7.09e+03	100	501	>1E20	>1E20
Hf-178m	3.10e+01	2.0e-05	2.24e-02	100	501	>1E20	4.5e-01
Hf-179m	6.87e-02	4.8e-06	1.01e+01	100	501	>1E20	>1E20
Hf-180m	6.27e-04	8.9e-07	1.10e+03	100	501	>1E20	>1E20
Hf-181	1.16e-01	4.3e-06	5.97e+00	100	501	>1E20	>1E20
Hf-182m	1.18e-04	1.4e-07	5.88e+03	100	501	>1E20	>1E20
Hf-182	9.00e+06	1.4e-05	7.70e-08	100	501	4.7e+00	4.8e-02
Hf-183	1.25e-04	2.5e-07	5.52e+03	100	501	>1E20	>1E20
Hf-184	4.68e-04	2.1e-06	1.48e+03	100	501	>1E20	>1E20
Ta-172	8.37e-05	1.4e-07	8.29e+03	0	1	>1E20	>1E20
Ta-173	4.22e-04	7.4e-07	1.64e+03	0	1	>1E20	>1E20
Ta-174	1.48e-04	1.9e-07	4.67e+03	0	1	>1E20	>1E20
Ta-175	1.20e-03	8.8e-07	5.79e+02	0	1	>1E20	>1E20
Ta-176	9.13e-04	1.3e-06	7.60e+02	0	1	>1E20	>1E20
Ta-177	6.46e-03	4.1e-07	1.07e+02	0	1	>1E20	>1E20
Ta-178	1.79e-05	2.9e-07	3.88e+04	0	1	>1E20	>1E20
Ta-179	2.40e-04	2.5e-07	2.89e+03	0	1	>1E20	>1E20
Ta-180m	9.24e-04	2.1e-07	7.50e+02	0	1	>1E20	>1E20
Ta-180	1.00e+13	3.3e-06	6.93e-14	0	1	4.0e-02	4.8e-02
Ta-182m	3.02e-05	2.4e-08	2.29e+04	0	1	>1E20	>1E20
Ta-182	3.15e-01	6.0e-06	2.20e+00	0	1	1.3e+03	>1E20
Ta-183	1.40e-02	4.6e-06	4.96e+01	0	1	>1E20	>1E20
Ta-184	9.92e-04	2.7e-06	6.98e+02	0	1	>1E20	>1E20
Ta-185	9.51e-05	2.0e-07	7.29e+03	0	1	>1E20	>1E20
Ta-186	2.00e-05	6.7e-08	3.47e+04	0	1	>1E20	>1E20
W-176	2.85e-04	4.8e-07	2.43e+03	0	1	>1E20	>1E20
W-177	2.57e-04	2.4e-07	2.70e+03	0	1	>1E20	>1E20
W-178	5.89e-02	9.3e-07	1.18e+01	0	1	>1E20	>1E20
W-179	7.22e-05	9.0e-09	9.59e+03	0	1	>1E20	>1E20
W-181	3.31e-01	3.1e-07	2.09e+00	0	1	1.5e+04	>1E20
W-185	2.06e-01	1.9e-06	3.37e+00	0	1	1.5e+06	>1E20
W-187	2.73e-03	2.6e-06	2.54e+02	0	1	>1E20	>1E20

Rev. 0

C-61
Table C.1-3. (continued)

WSRC-RP-94-218

Nuclide	T1/2 (year)	DCF (mrem/pCi)	Lambda (1/year)	Kd (cm ³ /gm)	Rf	LAW GW Trigger (Ci/vault)	LAW Int Trigger (Ci/vault)
W-188	1.89e-01	9.0e-06	3.67e+00	0	1	1.4e+06	>1E20
Re-177	3.23e-05	4.4e-08	2.14e+04	0	1	>1E20	>1E20
Re-178	2.85e-05	4.8e-08	2.43e+04	0	1	>1E20	>1E20
Re-181	2.05e-03	1.0e-06	3.38e+02	0	1	>1E20	>1E20
Re-182(64h)	7.30e-03	3.4e-06	9.49e+01	0	1	>1E20	>1E20
Re-182(12h)	1.45e-03	7.4e-07	4.78e+02	0	1	>1E20	>1E20
Re-184m	4.63e-01	2.4e-06	1.50e+00	0	1	9.8e+01	>1E20
Rm-184	1.04e-02	2.2e-06	6.66e+01	0	1	>1E20	>1E20
Re-186m	2.00e+05	3.3e-06	3.47e-06	0	1	4.0e-02	4.8e-02
Re-186	1.03e-02	2.6e-06	6.71e+01	0	1	>1E20	>1E20
Re-187	7.00e+10	8.3e-09	9.90e-12	0	1	1.6e+01	4.8e-02
Re-188m	3.54e-05	6.2e-08	1.96e+04	0	1	>1E20	>1E20
Re-188	1.91e-03	2.8e-06	3.64e+02	0	1	>1E20	>1E20
Re-189	2.74e-03	1.5e-06	2.53e+02	0	1	>1E20	>1E20
Os-180	4.13e-05	4.7e-08	1.68e+04	0	1	>1E20	>1E20
Os-181	4.37e-05	3.5e-07	1.59e+04	0	1	>1E20	>1E20
Os-182	2.51e-03	2.2e-06	2.76e+02	0	1	>1E20	>1E20
Os-185	2.57e-01	2.1e-06	2.69e+00	0	1	4.4e+04	>1E20
Os-189m	6.84e-04	6.6e-08	1.01e+03	0	1	>1E20	>1E20
Os-191m	1.48e-03	3.6e-07	4.67e+02	0	1	>1E20	>1E20
Os-191	4.19e-02	2.0e-06	1.65e+01	0	1	>1E20	>1E20
Os-193	3.48e-03	3.1e-06	1.99e+02	0	1	>1E20	>1E20
Os-194	6.00e+00	9.1e-06	1.16e-01	0	1	2.6e-02	5.0e+03
Ir-182	2.85e-05	1.2e-07	2.43e+04	0	1	>1E20	>1E20
Ir-184	3.65e-04	6.4e-07	1.90e+03	0	1	>1E20	>1E20
Ir-185	1.60e-03	1.1e-06	4.34e+02	0	1	>1E20	>1E20
Ir-186	1.83e-03	2.1e-06	3.80e+02	0	1	>1E20	>1E20
Ir-187	1.20e-03	4.8e-07	5.79e+02	0	1	>1E20	>1E20
Ir-188	4.68e-03	2.7e-06	1.48e+02	0	1	>1E20	>1E20
Ir-189	3.64e-02	9.3e-07	1.90e+01	0	1	>1E20	>1E20
Ir-190m	3.65e-04	3.0e-08	1.90e+03	0	1	>1E20	>1E20
Ir-190	3.01e-02	4.9e-06	2.30e+01	0	1	>1E20	>1E20
Ir-192m	2.74e-06	1.5e-06	2.53e+05	0	1	>1E20	>1E20
Ir-192	2.03e-01	5.3e-06	3.41e+00	0	1	6.4e+05	>1E20

Rev. 0

Table C1-3. (continued)

Nuclide	T1/2 (year)	DCF (mrem/pCi)	Lambda (1/year)	Kd (cm ² /gm)	Rf	LAW GW Trigger (C/Nault)	LAW Int Trigger (C/Nault)
Ir-194m	4.68e-01	8.1e-06	1.48e+00	0	1	2.7e+01	>1E20
Ir-194	2.22e-03	5.1e-06	3.12e+02	0	1	>1E20	>1E20
Ir-195m	4.45e-04	6.4e-07	1.56e+03	0	1	>1E20	>1E20
Ir-195	4.79e-04	3.4e-07	1.45e+03	0	1	>1E20	>1E20
Pt-186	3.42e-04	3.7e-07	2.03e+03	0	1	>1E20	>1E20
Pt-188	2.79e-02	3.0e-06	2.48e+01	0	1	>1E20	>1E20
Pt-189	1.24e-03	4.9e-07	5.57e+02	0	1	>1E20	>1E20
Pt-191	1.24e-03	1.3e-06	5.57e+02	0	1	>1E20	>1E20
Pt-193m	1.18e-02	1.7e-06	5.89e+01	0	1	>1E20	>1E20
Pt-193	5.00e+01	1.1e-07	1.39e-02	0	1	1.3e+00	1.9e-01
Pt-195m	1.10e-02	2.2e-06	6.30e+01	0	1	>1E20	>1E20
Pt-197m	1.79e-04	3.1e-07	3.88e+03	0	1	>1E20	>1E20
Pt-197	2.09e-03	1.5e-06	3.32e+02	0	1	>1E20	>1E20
Pt-199	5.86e-05	1.0e-07	1.18e+04	0	1	>1E20	>1E20
Pt-200	1.31e-03	4.5e-06	5.28e+02	0	1	>1E20	>1E20
Au-193	1.83e-03	6.0e-07	3.80e+02	0	1	>1E20	>1E20
Au-194	4.51e-03	2.0e-06	1.54e+02	0	1	>1E20	>1E20
Au-195	5.01e-01	1.1e-06	1.38e+00	0	1	1.2e+02	>1E20
Au-198m	6.30e-03	5.7e-06	1.10e+02	0	1	>1E20	>1E20
Au-198	7.38e-03	2.3e-06	9.39e+01	0	1	>1E20	>1E20
Au-199	8.60e-03	1.8e-06	8.06e+01	0	1	>1E20	>1E20
Au-200m	2.13e-03	4.6e-06	3.25e+02	0	1	>1E20	>1E20
Au-200	9.20e-05	1.9e-07	7.53e+03	0	1	>1E20	>1E20
Au-201	4.94e-05	5.7e-08	1.40e+04	0	1	>1E20	>1E20
Hg-193m	1.14e-03	1.6e-06	6.08e+02	1000	5001	>1E20	>1E20
Hg-193	6.84e-04	3.3e-07	1.01e+03	1000	5001	>1E20	>1E20
Hg-194	1.90e+00	6.0e-06	3.65e-01	1000	5001	>1E20	3.4e+14
Hg-195m	4.56e-03	2.2e-06	1.52e+02	1000	5001	>1E20	>1E20
Hg-195	1.08e-03	3.8e-07	6.40e+02	1000	5001	>1E20	>1E20
Hg-197m	2.72e-03	1.7e-06	2.55e+02	1000	5001	>1E20	>1E20
Hg-197	7.31e-03	9.1e-07	9.48e+01	1000	5001	>1E20	>1E20
Hg-199m	8.10e-05	8.5e-08	8.56e+03	1000	5001	>1E20	>1E20
Hg-203	1.28e-01	2.1e-06	5.43e+00	1000	5001	>1E20	>1E20
Tl-194m	6.24e-05	7.1e-08	1.11e+04	0	1	>1E20	>1E20

Rev. 0

C-63
Table C.1-3. (continued)

WSRC-RP-94-218

Nuclide	T1/2 (year)	DCF (mrem/pCi)	Lambda (1/year)	Kd (cm**3/gm)	Rf	LAW GW Trigger (Ci/vault)	LAW Int Trigger (Ci/vault)
Tl-194	6.27e-05	1.9e-08	1.10e+04	0	1	>1E20	>1E20
Tl-195	1.37e-04	7.7e-08	5.06e+03	0	1	>1E20	>1E20
Tl-197	3.19e-04	6.9e-08	2.17e+03	0	1	>1E20	>1E20
Tl-198m	2.13e-04	1.6e-07	3.25e+03	0	1	>1E20	>1E20
Tl-198	6.05e-04	2.6e-07	1.15e+03	0	1	>1E20	>1E20
Tl-199	8.44e-04	8.2e-08	8.21e+02	0	1	>1E20	>1E20
Tl-200	2.98e-03	6.7e-07	2.33e+02	0	1	>1E20	>1E20
Tl-201	8.33e-03	2.9e-07	8.32e+01	0	1	>1E20	>1E20
Tl-202	3.29e-02	1.5e-06	2.11e+01	0	1	>1E20	>1E20
Tl-204	3.77e+00	3.2e-06	1.84e-01	0	1	1.0e-01	4.6e+06
Pb-195m	2.85e-05	8.5e-08	2.43e+04	100	501	>1E20	>1E20
Pb-198	2.74e-04	1.6e-07	2.53e+03	100	501	>1E20	>1E20
Pb-199	1.71e-04	2.2e-07	4.05e+03	100	501	>1E20	>1E20
Pb-200	2.45e-03	1.5e-06	2.83e+02	100	501	>1E20	>1E20
Pb-201	1.07e-03	6.7e-07	6.46e+02	100	501	>1E20	>1E20
Pb-202m	4.13e-04	5.5e-07	1.68e+03	100	501	>1E20	>1E20
Pb-202	3.00e+05	3.9e-05	2.31e-06	100	501	1.7e+00	4.8e-02
Pb-203	5.94e-03	9.6e-07	1.17e+02	100	501	>1E20	>1E20
Pb-205	1.40e+07	1.5e-06	4.95e-08	100	501	4.4e+01	4.8e-02
Pb-209	6.24e-06	9.0e-08	1.11e+05	100	501	>1E20	>1E20
Pb-210	2.23e+01	5.1e-03	3.11e-02	100	501	>1E20	1.1e+00
Pb-211	6.86e-05	4.4e-07	1.01e+04	100	501	>1E20	>1E20
Pb-212	1.21e-03	4.1e-05	5.71e+02	100	501	>1E20	>1E20
Pb-214	5.10e-05	5.8e-07	1.36e+04	100	501	>1E20	>1E20
Bi-200	6.65e-05	1.7e-07	1.04e+04	0	1	>1E20	>1E20
Bi-201	2.05e-04	4.5e-07	3.38e+03	0	1	>1E20	>1E20
Bi-202	1.81e-04	3.6e-07	3.84e+03	0	1	>1E20	>1E20
Bi-203	1.35e-03	2.1e-06	5.15e+02	0	1	>1E20	>1E20
Bi-205	4.19e-02	3.7e-06	1.65e+01	0	1	>1E20	>1E20
Bi-206	1.71e-02	8.0e-06	4.06e+01	0	1	>1E20	>1E20
Bi-207	7.94e+00	4.9e-06	8.73e-02	0	1	4.2e-02	3.0e+02
Bi-210m	3.50e+06	8.6e-05	1.98e-07	0	1	1.5e-03	4.8e-02
Bi-210	1.37e-02	5.9e-06	5.06e+01	0	1	>1E20	>1E20
Bi-212	1.15e-04	9.9e-07	6.02e+03	0	1	>1E20	>1E20

Rev. 0

C-64
Table C.1-3. (continued)

WSRC-RP-94-218

Nuclide	T1/2 (year)	DCF (mrem/pCi)	Lambda (1/year)	Kd (cm**3/gm)	Rf	LAW GW Trigger (Ci/vault)	LAW Int Trigger (Ci/vault)
Bi-213	8.68e-05	6.8e-07	7.99e+03	0	1	>1E20	>1E20
Bi-214	3.76e-05	2.4e-07	1.84e+04	0	1	>1E20	>1E20
Po-203	7.99e-05	2.0e-07	8.68e+03	0	1	>1E20	>1E20
Po-205	2.05e-04	2.4e-07	3.38e+03	0	1	>1E20	>1E20
Po-207	6.50e-04	6.1e-07	1.07e+03	0	1	>1E20	>1E20
Po-210	3.79e-01	1.6e-03	1.83e+00	0	1	7.7e-01	>1E20
At-207	2.05e-04	8.9e-07	3.38e+03	0	1	>1E20	>1E20
At-211	8.22e-04	4.1e-05	8.43e+02	0	1	>1E20	>1E20
Fr-222	2.81e-05	2.5e-06	2.46e+04	0	1	>1E20	>1E20
Fr-223	4.18e-05	8.6e-06	1.66e+04	0	1	>1E20	>1E20
Ra-223	3.13e-02	5.5e-04	2.21e+01	500	2501	>1E20	>1E20
Ra-224	9.91e-03	3.3e-04	6.99e+01	500	2501	>1E20	>1E20
Ra-225	4.05e-02	3.1e-04	1.71e+01	500	2501	>1E20	>1E20
Ra-226	1.62e+03	1.1e-03	4.27e-04	500	2501	6.3e+01	5.0e-02
Ra-227	7.83e-05	2.2e-07	8.85e+03	500	2501	>1E20	>1E20
Ra-228	5.75e+00	1.2e-03	1.21e-01	500	2501	>1E20	8.3e+03
Ac-224	3.31e-04	2.6e-06	2.10e+03	150	751	>1E20	>1E20
Ac-225	2.74e-02	9.5e-05	2.53e+01	150	751	>1E20	>1E20
Ac-226	3.31e-03	4.0e-05	2.10e+02	150	751	>1E20	>1E20
Ac-227	2.18e+01	1.4e-02	3.18e-02	150	751	>1E20	1.2e+00
Ac-228	6.99e-04	2.1e-06	9.91e+02	150	751	>1E20	>1E20
Th-226	5.87e-05	9.2e-07	1.18e+04	3000	15001	>1E20	>1E20
Th-227	5.13e-02	3.6e-05	1.35e+01	3000	15001	>1E20	>1E20
Th-228	1.91e+00	3.8e-04	3.62e-01	3000	15001	>1E20	2.6e+14
Th-229	7.43e+03	3.5e-03	9.33e-05	3000	15001	6.2e+02	4.9e-02
Th-230	7.70e+04	5.3e-04	9.00e-06	3000	15001	7.3e+00	4.8e-02
Th-231	2.91e-03	1.3e-06	2.38e+02	3000	15001	>1E20	>1E20
Th-232	1.41e+10	2.8e-03	4.93e-11	3000	15001	1.6e-01	4.8e-02
Th-234	6.60e-02	1.3e-05	1.05e+01	3000	15001	>1E20	>1E20
Pa-227	7.28e-05	1.3e-06	9.52e+03	10	51	>1E20	>1E20
Pa-228	2.97e-03	4.0e-06	2.34e+02	10	51	>1E20	>1E20
Pa-230	4.85e-02	5.6e-06	1.43e+01	10	51	>1E20	>1E20
Pa-231	3.28e+04	1.1e-02	2.12e-05	10	51	6.1e-04	4.8e-02
Pa-232	3.59e-03	3.4e-06	1.93e+02	10	51	>1E20	>1E20

Rev. 0

C-65
Table C.1-3. (continued)

WSRC-RP-94-218

Nuclide	T1/2 (year)	DCF (mrem/pCi)	Lambda (1/year)	Kd (cm**3/gm)	Rf	LAW GW Trigger (Ci/vault)	LAW Int Trigger (Ci/vault)
Pa-233	7.39e-02	3.3e-06	9.38e+00	10	51	>1E20	>1E20
Pa-234	7.64e-04	2.1e-06	9.07e+02	10	51	>1E20	>1E20
U-230	5.69e-02	8.4e-04	1.22e+01	50	251	>1E20	>1E20
U-231	4.30e+00	1.1e-06	1.61e-01	50	251	>1E20	4.8e+05
U-232	7.20e+01	1.3e-03	9.63e-03	50	251	4.5e+03	1.3e-01
U-233	1.60e+05	2.7e-04	4.35e-06	50	251	1.2e-01	4.8e-02
U-234	2.45e+05	2.6e-04	2.83e-06	50	251	1.2e-01	4.8e-02
U-235	7.04e+08	2.5e-04	9.85e-10	50	251	6.3e-02	4.8e-02
U-236	2.34e+07	2.5e-04	2.96e-08	50	251	1.3e-01	4.8e-02
U-237	1.85e-02	2.7e-06	3.75e+01	50	251	>1E20	>1E20
U-238	4.47e+09	2.3e-04	1.55e-10	50	251	1.3e-01	4.8e-02
U-239	4.47e-05	7.6e-08	1.55e+04	50	251	>1E20	>1E20
U-240	1.61e-03	4.1e-06	4.31e+02	50	251	>1E20	>1E20
Np-232	2.47e-05	2.4e-08	2.80e+04	10	51	>1E20	>1E20
Np-233	6.65e-05	5.6e-09	1.04e+04	10	51	>1E20	>1E20
Np-234	1.20e-02	1.7e-06	5.75e+01	10	51	>1E20	>1E20
Np-235	1.12e+00	2.1e-07	6.17e-01	10	51	>1E20	>1E20
Np-236(1E5y)	1.10e+05	7.9e-04	6.30e-06	10	51	8.5e-03	4.8e-02
Np-236(22h)	2.51e-03	9.5e-07	2.76e+02	10	51	>1E20	>1E20
Np-237	2.14e+06	3.9e-03	3.24e-07	10	51	1.7e-03	4.8e-02
Np-238	5.80e-03	3.4e-06	1.20e+02	10	51	>1E20	>1E20
Np-239	6.38e-03	2.9e-06	1.09e+02	10	51	>1E20	>1E20
Np-240	1.20e-04	2.0e-07	5.79e+03	10	51	>1E20	>1E20
Pu-234	1.03e-03	1.2e-06	6.75e+02	100	501	>1E20	>1E20
Pu-235	4.94e-05	1.4e-08	1.40e+04	100	501	>1E20	>1E20
Pu-236	2.85e+00	1.3e-03	2.43e-01	100	501	>1E20	1.8e+09
Pu-237	1.24e-01	1.0e-06	5.58e+00	100	501	>1E20	>1E20
Pu-238	8.78e+01	3.8e-03	7.90e-03	100	501	3.2e+02	1.1e-01
Pu-239	2.41e+04	4.3e-03	2.87e-05	100	501	1.6e-02	4.8e-02
Pu-240	6.57e+03	4.3e-03	1.06e-04	100	501	2.0e-02	4.9e-02
Pu-241	1.44e+01	8.6e-05	4.81e-02	100	501	3.1e+01	5.9e+00
Pu-242	3.76e+05	4.1e-03	1.84e-06	100	501	1.6e-02	4.8e-02
Pu-243	5.65e-04	3.3e-07	1.23e+03	100	501	>1E20	>1E20
Pu-244	8.10e+07	4.0e-03	8.56e-09	100	501	1.7e-02	4.8e-02

Rev. 0

C-66
Table C.1-3. (continued)

Nuclide	T1/2 (year)	DCF (mrem/pCi)	Lambda (1/year)	Kd (cm ² /gm)	Rf	LAW GW Trigger (Ci/vault)	LAW Int Trigger (Ci/vault)
Pu-245	1.14e-03	2.4e-06	6.08e+02	100	501	>1E20	>1E20
Am-237	1.48e-04	7.4e-08	4.67e+03	150	751	>1E20	>1E20
Am-238	2.17e-04	1.7e-07	3.20e+03	150	751	>1E20	>1E20
Am-239	1.38e-03	1.0e-06	5.02e+02	150	751	>1E20	>1E20
Am-240	5.82e-03	2.9e-06	1.19e+02	150	751	>1E20	>1E20
Am-241	4.32e+02	4.5e-03	1.60e-03	150	751	4.4e+00	5.7e-02
Am-242m	1.52e+02	4.2e-03	4.56e-03	150	751	6.4e+05	7.6e-02
Am-242	1.83e-03	1.2e-06	3.80e+02	150	751	>1E20	>1E20
Am-243	7.37e+03	4.5e-03	9.40e-05	150	751	2.7e-02	4.9e-02
Am-244m	4.94e-05	6.8e-08	1.40e+04	150	751	>1E20	>1E20
Am-244	1.15e-03	2.0e-06	6.02e+02	150	751	>1E20	>1E20
Am-245	2.40e-04	1.8e-07	2.89e+03	150	751	>1E20	>1E20
Am-246m	4.75e-05	8.4e-08	1.46e+04	150	751	>1E20	>1E20
Am-246	4.75e-05	1.5e-07	1.46e+04	150	751	>1E20	>1E20
Cm-238	2.85e-04	3.6e-07	2.43e+03	100	501	>1E20	>1E20
Cm-240	7.34e-02	6.3e-05	9.45e+00	100	501	>1E20	>1E20
Cm-241	9.58e-02	4.6e-06	7.23e+00	100	501	>1E20	>1E20
Cm-242	4.46e-01	1.1e-04	1.56e+00	100	501	>1E20	>1E20
Cm-243	2.85e+01	2.9e-03	2.43e-02	100	501	>1E20	5.5e-01
Cm-244	1.81e+01	2.3e-03	3.83e-02	100	501	7.3e+00	2.2e+00
Cm-245	8.50e+03	4.5e-03	8.15e-05	100	501	1.8e-02	4.9e-02
Cm-246	4.70e+03	4.5e-03	1.47e-04	100	501	2.1e-02	4.9e-02
Cm-247	1.60e+07	4.1e-03	4.93e-08	100	501	1.6e-02	4.8e-02
Cm-248	3.50e+05	1.6e-02	1.98e-06	100	501	4.2e-03	4.8e-02
Cm-249	1.24e-04	9.5e-08	5.61e+03	100	501	>1E20	>1E20
Bk-245	1.36e-02	2.3e-06	5.08e+01	100	501	>1E20	>1E20
Bk-246	4.93e-03	1.9e-06	1.41e+02	100	501	>1E20	>1E20
Bk-247	1.40e+03	2.3e-03	4.95e-04	100	501	9.9e-02	5.1e-02
Bk-249	8.80e-01	6.0e-06	7.88e-01	100	501	>1E20	>1E20
Bk-250	3.67e-04	5.0e-07	1.89e+03	100	501	>1E20	>1E20
Cf-244	4.75e-05	1.5e-07	1.46e+04	100	501	>1E20	>1E20
Cf-246	4.11e-03	1.2e-05	1.69e+02	100	501	>1E20	>1E20
Cf-248	9.86e-01	2.8e-04	7.03e-01	100	501	>1E20	>1E20
Cf-249	3.51e+02	4.6e-03	1.97e-03	100	501	2.0e+00	5.9e-02

Rev. 0

Table C.1-3. (continued)

Nuclide	T _{1/2} (year)	DCF (mrem/pCi)	Lambda (1/year)	Kd (cm ³ /gm)	Rf	LAW GW Trigger (Ci/vault)	LAW Int Trigger (Ci/vault)
Cf-250	1.31e+01	1.9e-03	5.29e-02	100	501	>1E20	9.6e+00
Cf-251	9.00e+02	4.6e-03	7.70e-04	100	501	9.9e-02	5.2e-02
Cf-252	2.62e+00	9.4e-04	2.65e-01	100	501	5.5e+02	1.5e+10
Cf-253	4.87e-02	9.2e-06	1.42e+01	100	501	>1E20	>1E20
Cf-254	1.66e-01	2.5e-03	4.18e+00	100	501	>1E20	>1E20
Es-250	9.13e-04	9.5e-08	7.60e+02	100	501	>1E20	>1E20
Es-251	4.11e-03	6.7e-07	1.69e+02	100	501	>1E20	>1E20
Es-253	5.60e-02	2.4e-05	1.24e+01	100	501	>1E20	>1E20
Es-254m	4.48e-03	1.5e-05	1.55e+02	100	501	>1E20	>1E20
Es-254	7.56e-01	1.5e-04	9.17e-01	100	501	>1E20	>1E20
Fm-252	2.62e-03	9.9e-06	2.64e+02	100	501	>1E20	>1E20
Fm-253	8.21e-03	3.5e-06	8.44e+01	100	501	>1E20	>1E20
Fm-254	3.70e-04	1.6e-06	1.88e+03	100	501	>1E20	>1E20
Fm-255	2.29e-03	9.7e-06	3.02e+02	100	501	>1E20	>1E20
Fm-257	2.19e-01	7.3e-05	3.16e+00	100	501	>1E20	>1E20
Md-257	3.42e-04	5.4e-07	2.03e+03	100	501	>1E20	>1E20
Md-258	1.53e-01	6.1e-05	4.52e+00	100	501	>1E20	>1E20

Table C.1-4. Weighted dose conversion factors for radionuclides with multiple daughters

Parent	Progeny	DCF rem/uCi	Rf	Time (year)	Arrival Time	Fraction @ Ar. Time	Weighted DCF
Th-232		2.8E+00	15001	75005	1.0E+00	1.9E-04	
	Ra-228	1.5E+00	2501		1.0E+00	6.0E-04	
	Tb-228	7.2E-01	15001	1.0E+00	4.8E-05		
Th-232 Ingrowth Factor (rem/uCi) = >							8.3E-04
U-234		2.6E-01	251	1255	1.0E+00	1.0E-03	
	Th-230	5.3E-01	15001	1.1E-01	3.9E-06		
	Ra-226	1.1E+00	2501		2.6E-03	1.1E-06	
	Pb-210	6.7E+00	501		2.5E-03	3.3E-05	
U-234 Ingrowth Factor (rem/uCi) =>							1.1E-03
U-235		2.6E-01	251	1255	1.0E+00	1.0E-03	
	Pa-231	1.1E+00	51		2.6E-02	5.7E-04	
	Ac-227	1.5E+01	751		2.6E-02	5.0E-04	
U-235 Ingrowth Factor (rem/uCi) =>							2.1E-03
U-236		2.5E-01	251	1255	1.0E+00	1.0E-03	
	Tb-232	2.8E+00	15001	6.2E-08	1.2E-11		
	Ra-228	1.2E+00	2501		6.2E-08	3.0E-11	
	Th-228	7.5E-01	15001	6.1E-08	3.1E-12		
U-236 Ingrowth Factor (rem/uCi) =>							1.0E-03
U-238		2.5E-01	251	1255	1.0E+00	9.8E-04	
	U-234	2.6E-01	251		3.6E-03	3.7E-06	
	Th-230	5.3E-01	15001	2.0E-05	7.1E-10		
	Ra-226	1.1E+00	2501		3.2E-06	1.4E-09	
	Pb-210	6.7E+00	501		3.0E-06	4.0E-08	
U-238 Ingrowth Factor (rem/uCi) =>							9.8E-04
Np-237		3.9E+00	51	255	1.0E+00	7.6E-02	
	U-233	2.7E-01	251		1.1E-03	1.2E-06	
	Th-229	3.9E+00	15001	1.3E-05	3.4E-09		
Np-237 Ingrowth Factor (rem/uCi) =>							7.6E-02
Pu-238		3.8E+00	501	2505	2.6E-09	1.9E-11	
	U-234	2.6E-01	251		3.6E-04	3.7E-07	
	Th-230	5.3E-01	15001	7.6E-06	2.7E-10		
	Ra-226	1.1E+00	2501		2.9E-06	1.3E-09	
	Pb-210	6.7E+00	501		2.8E-06	3.8E-08	
Pu-238 Ingrowth Factor (rem/uCi) =>							4.1E-07

Table C.1-4. (continued)

Parent	Progeny	DCF rem/uCi	Rf	Time (year)	Arrival Fraction @ Ar. Time	Weighted DCF
Pu-239		4.3E+00	501	2505	9.3E-01	8.0E-03
	U-235	2.6E-01	251		2.4E-06	2.4E-09
	Pa-231	1.1E+00	51		6.3E-08	1.4E-08
	Ac-227	1.5E+01	751		6.1E-08	1.2E-09
Pu-239 Ingrowth Factor (rem/uCi) =>						8.0E-03
Pu-241		8.6E-02	501	2505	4.3E-53	7.4E-57
	Am-241	4.5E+00	751		6.2E-04	3.7E-06
	Np-237	3.9E+00	51		6.2E-04	3.7E-06
	U-233	2.7E-01	251		5.5E-08	5.9E-11
	Th-229	3.9E+00	15001	5.0E-09	1.3E-12	
Pu-241 Ingrowth Factor (rem/uCi) =>						4.2E-06
Pu-242		4.1E+00	501	2505	1.0E+00	8.1E-03
	U-238	2.5E-01	251		3.9E-07	3.8E-10
	U-234	2.6E-01	251		1.4E-09	1.4E-12
	Th-230	5.3E-01	15001	1.0E-11	3.6E-16	
	Ra-226	1.1E+00	2501		2.3E-12	1.0E-15
	Pb-210	6.7E+00	501		2.2E-12	2.9E-14
Pu-242 Ingrowth Factor (rem/uCi) =>						8.1E-03
Am-241		4.5E+00	751	3755	2.4E-03	1.5E-05
	Np-237	3.9E+00	51		2.0E-04	1.5E-05
	U-233	2.7E-01	251		2.7E-06	2.9E-09
	Th-229	3.9E+00	15001	3.8E-07	9.9E-11	
Am-241 Ingrowth Factor (rem/uCi) =>						3.0E-05
Am-243		4.5E+00	751	3755	7.0E-01	4.2E-03
	Pu-239	4.3E+00	501		8.6E-02	7.4E-04
	U-235	2.6E-01	251		1.7E-07	1.7E-10
	Pa-231	1.1E+00	51		4.6E-09	1.0E-09
	Ac-227	1.5E+01	751		4.5E-09	8.8E-11
Am-243 Ingrowth Factor (rem/uCi) =>						4.9E-03
Cm-244		2.3E+00	501	2505	2.3E-42	1.1E-44
	Pu-240	2.1E-03	501		2.1E-03	1.8E-05
	U-236	2.5E-01	251		1.8E-07	1.8E-10
	Th-232	2.8E+00	15001	1.1E-14	2.1E-18	
	Ra-228	1.2E+00	2501		1.1E-14	5.4E-18
	Th-228	7.5E-01	15001	1.1E-14	5.7E-19	
Cm-244 Ingrowth Factor (rem/uCi) =>						1.8E-05

Table C.1-4. (continued)

Parent	Progeny	DCF rem/uCi	Rf	Arrival Time (year)	Fraction @ Ar. Time	Weighted DCF
Cf-252		9.4E-01	501	2505	0.0E+00	0.0E+00
	Cm-248	1.6E+01	501		7.5E-06	2.4E-07
	Pu-244	4.0E+00	501		1.5E-10	1.2E-12
	Pu-240	2.1E-03	501		1.8E-11	1.5E-13
	U-236	2.5E-01	251		4.4E-16	4.4E-19
	Th-232	2.8E+00	15001	1.4E-23	6.5E-27	
	Ra-228	1.2E+00	2501		1.4E-23	6.5E-27
	Th-228	7.5E-01	15001	1.4E-23	6.8E-28	
Cf-252 Ingrowth Factor (rem/uCi) =>						2.4E-07

C2 E-AREA STREAM FLOW DATA

The gauging results for SRS creeks in the vicinity of E-Area are presented in Table C2-1. In Fig. C.2-1, the location of stream flow measurements supporting these results is shown.

**Table C2-1. Stream gaging results for SRS creeks in the vicinity of E-Area
(field measurements taken on January 27, 1993 by Peter Kearl)**

Location Number	Location Description (refer to Fig. C2-1)	Flow, cfs
1	Crouch, near Upper Three Runs	1.78
2	Tributary to Crouch, near Upper Three Runs	1.42
3	Crouch, just above confluence with tributary	0.15
12	Crouch, 50 ft from stream stage measurement station	1.21
13	Crouch, upstream from station 12	0.78
14	Crouch, upstream from station 13	0.44
15	Crouch, upstream from station 14	0.014
16	Crouch, upstream from station 15	0.48
4	Crouch, just below road and NPDES sample site	0.137
17	Lower end of tributary to Upper Three Runs	0.33
18	Unnamed branch, just upstream from railroad crossing near Upper Three Runs	0.68
19	Unnamed branch, upstream from station 18	0.44
20	Unnamed branch, upstream from station 19	0.10

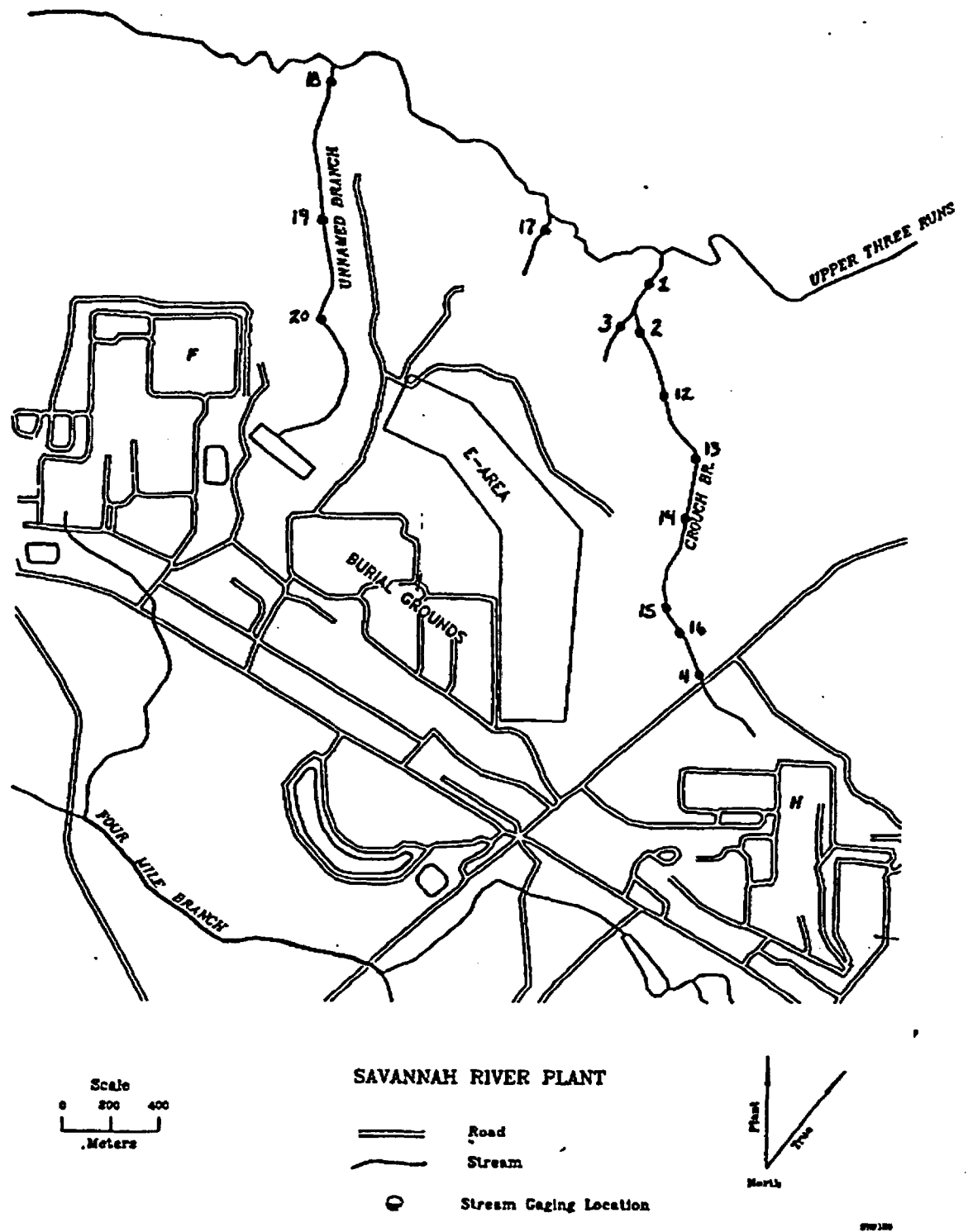


Fig. C.2-1. Locations of stream-gaging stations in creeks near E-Area.

C3 RADIONUCLIDE SCREENING RESULTS FOR SUSPECT SOIL

The screening results for radionuclides potentially present suspect soil are given in Table C.3-1.

Table C3-1. Screening calculations and trigger values for the suspect soil trenches

Nuclide	T1/2 (year)	DCF (mrem/pCi)	Lambda (1/year)	Kd (cm**3/gm)	Rf	SUSP GW Trigger (Ci/trench)	SUSP Int Trigger (Ci/trench)
H-3	1.23e+01	6.3e-08	5.62e-02	0	1	3.3e-01	2.4e-03
Be-7	1.47e-01	1.1e-07	4.72e+00	0	1	2.6e+09	>1E20
Be-10	1.60e+06	4.2e-06	4.33e-07	0	1	3.8e-03	8.6e-06
C-11	3.86e-05	1.2e-08	1.80e+04	2	11	>1E20	>1E20
C-14	5.73e+03	2.1e-06	1.21e-04	2	11	8.3e-02	8.7e-06
F-18	2.14e-04	1.0e-04	3.25e+03	0	1	>1E20	>1E20
Na-22	2.58e+00	1.2e-05	2.69e-01	0	1	5.0e-03	4.0e+06
Na-24	1.71e-03	1.4e-06	4.05e+02	0	1	>1E20	>1E20
Mg-28	2.40e-03	7.5e-06	2.89e+02	0	1	>1E20	>1E20
Al-26	7.40e+05	1.3e-05	9.37e-07	0	1	1.2e-03	8.6e-06
Si-31	2.99e-04	5.4e-07	2.32e+03	0	1	>1E20	>1E20
Si-32	6.50e+02	1.7e-06	1.07e-03	0	1	9.3e-03	9.6e-06
P-32	3.89e-02	7.7e-06	1.78e+01	0	1	>1E20	>1E20
P-33	6.84e-02	8.8e-07	1.01e+01	0	1	>1E20	>1E20
S-35	2.39e-01	4.3e-07	2.90e+00	0	1	7.4e+04	>1E20
Cl-36	3.01e+05	3.0e-06	2.30e-06	0	1	5.3e-03	8.6e-06
Cl-38	7.07e-05	2.0e-07	9.80e+03	0	1	>1E20	>1E20
Cl-39	1.06e-04	1.4e-07	6.57e+03	0	1	>1E20	>1E20
K-40	1.28e+09	1.9e-05	5.42e-10	0	1	8.3e-04	8.6e-06
K-42	1.41e-03	1.1e-06	4.92e+02	0	1	>1E20	>1E20
K-43	2.56e-03	7.8e-07	2.71e+02	0	1	>1E20	>1E20
K-44	4.18e-05	1.5e-07	1.66e+04	0	1	>1E20	>1E20
K-45	3.04e-05	9.3e-08	2.28e+04	0	1	>1E20	>1E20
Ca-41	1.30e+05	1.2e-06	5.33e-06	0	1	1.3e-02	8.6e-06
Ca-45	4.46e-01	3.0e-06	1.55e+00	0	1	1.2e+01	>1E20
Ca-47	1.24e-02	6.2e-06	5.58e+01	0	1	>1E20	>1E20
Sc-43	4.47e-04	7.3e-07	1.55e+03	0	1	>1E20	>1E20
Sc-44m	6.68e-03	9.9e-06	1.04e+02	0	1	>1E20	>1E20
Sc-44	4.47e-04	1.4e-06	1.55e+03	0	1	>1E20	>1E20
Sc-46	2.29e-01	5.6e-06	3.02e+00	0	1	1.0e+04	>1E20
Sc-47	9.39e-03	1.9e-06	7.38e+01	0	1	>1E20	>1E20
Sc-48	5.03e-03	6.4e-06	1.38e+02	0	1	>1E20	>1E20
Sc-49	1.09e-04	2.4e-07	6.34e+03	0	1	>1E20	>1E20

Rev. 0

C-76
Table C.3-1. (continued)

WSRC-RP-94-218

Nuclide	T1/2 (year)	DCF (mrem/pCi)	Lambda (1/year)	Kd (cm ³ /gm)	Rf	SUSP GW Trigger (Ci/trench)	SUSP Int Trigger (Ci/trench)
Ti-44	4.80e+01	1.9e-05	1.44e-02	0	1	8.9e-04	3.7e-05
Ti-45	3.52e-04	5.7e-07	1.97e+03	0	1	>1E20	>1E20
V-47	6.27e-05	1.6e-07	1.10e+04	0	1	>1E20	>1E20
V-48	4.41e-02	7.5e-06	1.57e+01	0	1	>1E20	>1E20
V-49	9.03e-01	5.4e-08	7.67e-01	0	1	1.4e+01	>1E20
Cr-48	2.62e-03	8.2e-07	2.64e+02	40	201	>1E20	>1E20
Cr-49	7.97e-05	1.7e-07	8.70e+03	40	201	>1E20	>1E20
Cr-51	7.58e-02	1.3e-07	9.14e+00	40	201	>1E20	>1E20
Mn-51	8.56e-05	2.5e-07	8.10e+03	50	251	>1E20	>1E20
Mn-52m	3.99e-05	1.5e-07	1.74e+04	50	251	>1E20	>1E20
Mn-52	1.52e-02	6.9e-06	4.56e+01	50	251	>1E20	>1E20
Mn-53	2.00e+06	9.9e-08	3.47e-07	50	251	4.0e+01	8.6e-06
Mn-54	7.97e-01	2.7e-06	8.70e-01	50	251	>1E20	>1E20
Mn-56	2.94e-04	9.5e-07	2.36e+03	50	251	>1E20	>1E20
Fe-52	9.35e-04	5.4e-06	7.41e+02	0	1	>1E20	>1E20
Fe-55	2.70e+00	5.8e-07	2.57e-01	0	1	9.8e-02	1.2e+06
Fe-59	1.22e-01	6.6e-06	5.68e+00	0	1	5.1e+09	>1E20
Fe-60	3.00e+05	1.5e-04	2.31e-06	0	1	1.1e-04	8.6e-06
Co-55	2.08e-03	4.1e-06	3.34e+02	10	51	>1E20	>1E20
Co-56	2.11e-01	1.2e-05	3.29e+00	10	51	>1E20	>1E20
Co-57	7.39e-01	1.1e-05	9.38e-01	10	51	>1E20	>1E20
Co-58m	1.03e-03	8.8e-08	6.75e+02	10	51	>1E20	>1E20
Co-58	1.95e-01	3.5e-06	3.55e+00	10	51	>1E20	>1E20
Co-60m	2.00e-05	3.6e-09	3.47e+04	10	51	>1E20	>1E20
Co-60	5.27e+00	2.6e-05	1.32e-01	10	51	1.1e+13	4.4e+00
Co-61	1.88e-04	2.6e-07	3.68e+03	10	51	>1E20	>1E20
Co-62m	3.04e-06	9.6e-08	2.28e+05	10	51	>1E20	>1E20
Ni-56	1.67e-02	3.5e-06	4.15e+01	300	1501	>1E20	>1E20
Ni-57	4.11e-03	3.3e-06	1.69e+02	300	1501	>1E20	>1E20
Ni-59	8.00e+04	2.0e-07	8.66e-06	300	1501	1.3e+02	8.6e-06
Ni-63	1.00e+02	5.4e-07	6.93e-03	300	1501	>1E20	1.7e-05
Ni-65	2.87e-04	6.1e-07	2.41e+03	300	1501	>1E20	>1E20
Ni-66	6.23e-03	1.1e-05	1.11e+02	300	1501	>1E20	>1E20
Cu-60	4.37e-05	1.7e-07	1.59e+04	25	126	>1E20	>1E20

Rev. 0

C-77
Table C-3-1. (continued)

WSRC-RP-94-218

Nuclide	T _{1/2} (year)	DCF (mrem/pCi)	Lambda (1/year)	K _d (cm ³ /gm)	R _f	SUSP GW Trigger (Ci/trench)	SUSP Int Trigger (Ci/trench)
Cu-61	3.89e-04	4.1e-07	1.78e+03	25	126	>1E20	>1E20
Cu-64	1.45e-03	4.3e-07	4.78e+02	25	126	>1E20	>1E20
Cu-67	7.06e-03	1.1e-06	9.82e+01	25	126	>1E20	>1E20
Zn-62	1.04e-03	3.4e-06	6.64e+02	16	81	>1E20	>1E20
Zn-63	7.30e-05	2.0e-07	9.49e+03	16	81	>1E20	>1E20
Zn-65	6.67e-01	1.4e-05	1.04e+00	16	81	>1E20	>1E20
Zn-69m	1.57e-03	1.2e-05	4.40e+02	16	81	>1E20	>1E20
Zn-69	1.08e-04	8.5e-08	6.40e+03	16	81	>1E20	>1E20
Zn-71m	4.56e-04	8.9e-07	1.52e+03	16	81	>1E20	>1E20
Zn-72	1.27e-01	4.9e-06	5.44e+00	16	81	>1E20	>1E20
Ga-65	2.89e-05	7.8e-08	2.40e+04	0	1	>1E20	>1E20
Ga-66	1.07e-03	4.7e-06	6.46e+02	0	1	>1E20	>1E20
Ga-67	8.91e-03	7.2e-07	7.78e+01	0	1	>1E20	>1E20
Ga-68	1.30e-04	3.3e-07	5.34e+03	0	1	>1E20	>1E20
Ga-70	4.01e-05	7.1e-08	1.73e+04	0	1	>1E20	>1E20
Ga-72	1.61e-03	4.4e-06	4.31e+02	0	1	>1E20	>1E20
Ga-73	1.34e-02	1.0e-06	5.19e+01	0	1	>1E20	>1E20
Ge-66	1.07e-03	2.1e-07	6.46e+02	0	1	>1E20	>1E20
Ge-67	3.61e-05	1.1e-07	1.92e+04	0	1	>1E20	>1E20
Ge-68	7.86e-01	1.1e-06	8.82e-01	0	1	1.2e+00	>1E20
Ge-69	4.45e-03	3.6e-07	1.56e+02	0	1	>1E20	>1E20
Ge-71	3.12e-02	9.6e-09	2.22e+01	0	1	>1E20	>1E20
Ge-75	1.57e-04	7.3e-08	4.40e+03	0	1	>1E20	>1E20
Ge-77	1.29e-03	5.6e-07	5.38e+02	0	1	>1E20	>1E20
Ge-78	1.65e-04	2.1e-07	4.19e+03	0	1	>1E20	>1E20
As-69	2.85e-05	1.1e-07	2.43e+04	3	16	>1E20	>1E20
As-70	1.01e-04	3.4e-07	6.88e+03	3	16	>1E20	>1E20
As-71	7.07e-03	1.3e-06	9.80e+01	3	16	>1E20	>1E20
As-72	2.97e-03	5.6e-06	2.34e+02	3	16	>1E20	>1E20
As-73	2.20e-01	6.1e-07	3.15e+00	3	16	>1E20	>1E20
As-74	3.29e-02	3.3e-06	2.11e+01	3	16	>1E20	>1E20
As-76	3.00e-03	4.8e-06	2.31e+02	3	16	>1E20	>1E20
As-77	1.06e-01	1.1e-06	6.53e+00	3	16	>1E20	>1E20
As-78	1.73e-04	6.5e-07	4.01e+03	3	16	>1E20	>1E20

Rev. 0

C-78
Table C3-1. (continued)

Nuclide	T1/2 (year)	DCF (mrem/pCi)	Lambda (1/year)	Kd (cm ³ /gm)	Rf	SUSP GW Trigger (Cl/trench)	SUSP Int Trigger (Cl/trench)
Se-70	8.37e-05	4.8e-07	8.29e+03	5	26	>1E20	>1E20
Se-73m	7.99e-05	1.5e-07	8.68e+03	5	26	>1E20	>1E20
Se-73	8.10e-04	1.5e-06	8.56e+02	5	26	>1E20	>1E20
Se-75	3.30e-01	8.8e-06	2.10e+00	5	26	>1E20	>1E20
Se-79	6.50e+04	8.3e-06	1.07e-05	5	26	5.0e-02	8.6e-06
Se-81m	1.09e-04	2.1e-07	6.36e+03	5	26	>1E20	>1E20
Se-81	4.30e-05	6.1e-08	1.61e+04	5	26	>1E20	>1E20
Se-83	4.28e-05	1.5e-07	1.62e+04	5	26	>1E20	>1E20
Br-74m	7.89e-05	2.2e-07	8.78e+03	0	1	>1E20	>1E20
Br-74	6.84e-05	1.4e-07	1.01e+04	0	1	>1E20	>1E20
Br-75	1.94e-04	1.3e-07	3.57e+03	0	1	>1E20	>1E20
Br-76	1.84e-03	1.4e-06	3.77e+02	0	1	>1E20	>1E20
Br-77	6.50e-03	3.1e-07	1.07e+02	0	1	>1E20	>1E20
Br-80m	5.04e-04	2.3e-07	1.37e+03	0	1	>1E20	>1E20
Br-80	3.37e-05	5.5e-08	2.06e+04	0	1	>1E20	>1E20
Br-82	4.03e-03	1.7e-06	1.72e+02	0	1	>1E20	>1E20
Br-83	2.74e-04	7.3e-08	2.53e+03	0	1	>1E20	>1E20
Br-84	6.05e-05	1.5e-07	1.15e+04	0	1	>1E20	>1E20
Rb-79	3.99e-05	8.7e-08	1.74e+04	0	1	>1E20	>1E20
Rb-81m	6.08e-05	1.8e-08	1.14e+04	0	1	>1E20	>1E20
Rb-81	5.36e-04	1.3e-07	1.29e+03	0	1	>1E20	>1E20
Rb-82m	7.30e-04	4.2e-07	9.49e+02	0	1	>1E20	>1E20
Rb-83	2.27e-01	7.7e-06	3.05e+00	0	1	8.6e+03	>1E20
Rb-84	9.31e-02	1.0e-05	7.45e+00	0	1	2.3e+13	>1E20
Rb-86	5.09e-02	9.4e-06	1.36e+01	0	1	>1E20	>1E20
Rb-87	4.80e+10	4.8e-06	1.44e-11	0	1	3.3e-03	8.6e-06
Rb-88	3.37e-05	1.6e-07	2.06e+04	0	1	>1E20	>1E20
Rb-89	2.89e-05	8.0e-08	2.40e+04	0	1	>1E20	>1E20
Sr-80	1.94e-04	5.2e-09	3.57e+03	10	51	>1E20	>1E20
Sr-81	5.51e-05	2.2e-07	1.26e+04	10	51	>1E20	>1E20
Sr-83	3.76e-03	2.3e-06	1.84e+02	10	51	>1E20	>1E20
Sr-85m	1.29e-04	2.4e-08	5.39e+03	10	51	>1E20	>1E20
Sr-85	1.79e-01	1.9e-06	3.88e+00	10	51	>1E20	>1E20
Sr-87m	3.21e-04	1.2e-07	2.16e+03	10	51	>1E20	>1E20

Rev. 0

C-79
Table C3-1. (continued)

WSRC-RP-94-218

Nuclide	T1/2 (year)	DCF (mrem/pCi)	Lambda (1/year)	Kd (cm**3/gm)	Rf	SUSP GW Trigger (Ci/trench)	SUSP Int Trigger (Ci/trench)
Sr-89	1.38e-01	8.7e-06	5.01e+00	10	51	>1E20	>1E20
Sr-90	2.86e+01	1.3e-04	2.42e-02	10	51	3.0e+00	9.8e-05
Sr-91	1.08e-03	3.0e-06	6.41e+02	10	51	>1E20	>1E20
Sr-92	3.09e-04	1.9e-06	2.24e+03	10	51	>1E20	>1E20
Y-86m	9.13e-05	2.4e-07	7.60e+03	10	51	>1E20	>1E20
Y-86	1.67e-03	4.1e-06	4.16e+02	10	51	>1E20	>1E20
Y-87	9.13e-03	2.2e-06	7.60e+01	10	51	>1E20	>1E20
Y-88	2.88e-01	5.2e-06	2.41e+00	10	51	>1E20	>1E20
Y-90m	3.64e-04	6.6e-07	1.90e+03	10	51	>1E20	>1E20
Y-90	2.86e+01	1.0e-05	2.42e-02	10	51	3.9e+01	9.8e-05
Y-91m	9.51e-05	3.9e-08	7.29e+03	10	51	>1E20	>1E20
Y-91	1.67e-01	8.9e-06	4.15e+00	10	51	>1E20	>1E20
Y-92	4.03e-04	1.9e-06	1.72e+03	10	51	>1E20	>1E20
Y-93	1.16e-03	4.5e-06	5.96e+02	10	51	>1E20	>1E20
Y-94	3.61e-05	1.8e-07	1.92e+04	10	51	>1E20	>1E20
Y-95	2.00e-05	9.7e-08	3.47e+04	10	51	>1E20	>1E20
Zr-86	1.88e-03	3.5e-06	3.68e+02	0	1	>1E20	>1E20
Zr-88	2.33e-01	1.3e-06	2.98e+00	0	1	3.6e+04	>1E20
Zr-89	8.94e-03	3.1e-06	7.75e+01	0	1	>1E20	>1E20
Zr-93	1.50e+06	1.6e-06	4.62e-07	0	1	9.9e-03	8.6e-06
Zr-95	1.75e-01	3.4e-06	3.96e+00	0	1	1.8e+06	>1E20
Zr-97	1.92e-03	8.0e-06	3.62e+02	0	1	>1E20	>1E20
Nb-88	2.66e-05	7.2e-08	2.60e+04	0	1	>1E20	>1E20
Nb-89(66m)	1.25e-04	4.6e-07	5.52e+03	0	1	>1E20	>1E20
Nb-89(122m)	2.32e-04	1.0e-06	2.99e+03	0	1	>1E20	>1E20
Nb-90	1.67e-03	4.9e-06	4.16e+02	0	1	>1E20	>1E20
Nb-93m	1.01e+01	5.3e-07	6.84e-02	0	1	4.2e-02	8.1e-03
Nb-94	2.00e+04	5.1e-06	3.47e-05	0	1	3.1e-03	8.7e-06
Nb-95m	9.88e-03	2.0e-06	7.02e+01	0	1	>1E20	>1E20
Nb-95	9.58e-02	2.2e-06	7.23e+00	0	1	3.7e+13	>1E20
Nb-96	2.67e-03	4.4e-06	2.60e+02	0	1	>1E20	>1E20
Nb-97	1.40e-04	2.3e-07	4.95e+03	0	1	>1E20	>1E20
Nb-98	8.87e-08	3.4e-07	7.81e+06	0	1	>1E20	>1E20
Mo-90	6.50e-04	2.5e-06	1.07e+03	0	1	>1E20	>1E20

Rev. 0

C-80
Table C.3-1. (continued)

WSRC-RP-94-218

Nuclide	T _{1/2} (year)	DCF (mrem/pCi)	Lambda (1/year)	K _d (cm ³ /gm)	R _f	SUSP GW Trigger (Ci/trench)	SUSP Int Trigger (Ci/trench)
Mo-93m	7.87e-04	1.1e-06	8.81e+02	0	1	>1E20	>1E20
Mo-93	3.50e+03	1.3e-06	1.98e-04	0	1	1.2e-02	8.8e-06
Mo-99	7.53e-03	4.4e-06	9.20e+01	0	1	>1E20	>1E20
Mo-101	2.78e-05	9.2e-08	2.50e+04	0	1	>1E20	>1E20
Tc-93m	8.18e-05	7.1e-08	8.48e+03	0.36	2.8	>1E20	>1E20
Tc-93	3.08e-04	1.6e-07	2.25e+03	0.36	2.8	>1E20	>1E20
Tc-94m	1.01e-04	2.5e-07	6.88e+03	0.36	2.8	>1E20	>1E20
Tc-94	5.57e-04	5.8e-07	1.24e+03	0.36	2.8	>1E20	>1E20
Tc-96m	9.89e-05	3.1e-08	7.01e+03	0.36	2.8	>1E20	>1E20
Tc-96	1.18e-02	2.7e-06	5.89e+01	0.36	2.8	>1E20	>1E20
Tc-97m	2.46e-01	1.1e-06	2.81e+00	0.36	2.8	5.1e+15	>1E20
Tc-97	2.60e+06	1.5e-07	2.67e-07	0.36	2.8	2.9e-01	8.6e-06
Tc-98	1.50e+06	4.8e-06	4.62e-07	0.36	2.8	9.2e-03	8.6e-06
Tc-99m	6.87e-04	6.0e-08	1.01e+03	0.36	2.8	>1E20	>1E20
Tc-99	2.11e+05	1.3e-06	3.29e-06	0.36	2.8	3.4e-02	8.6e-06
Tc-101	2.70e-05	3.8e-08	2.57e+04	0.36	2.8	>1E20	>1E20
Tc-104	3.42e-05	1.6e-07	2.03e+04	0.36	2.8	>1E20	>1E20
Ru-94	1.08e-04	3.3e-07	6.40e+03	100	501	>1E20	>1E20
Ru-97	7.91e-03	6.4e-07	8.76e+01	100	501	>1E20	>1E20
Ru-103	1.08e-01	2.7e-06	6.43e+00	100	501	>1E20	>1E20
Ru-105	5.07e-04	1.0e-06	1.37e+03	100	501	>1E20	>1E20
Ru-106	9.99e-01	2.1e-05	6.94e-01	100	501	>1E20	>1E20
Rh-99m	5.36e-04	2.8e-07	1.29e+03	0	1	>1E20	>1E20
Rh-99	4.38e-02	2.0e-06	1.58e+01	0	1	>1E20	>1E20
Rh-100	2.28e-03	3.1e-06	3.04e+02	0	1	>1E20	>1E20
Rh-101m	1.23e-02	8.8e-07	5.63e+01	0	1	>1E20	>1E20
Rh-101	3.10e+00	2.3e-06	2.24e-01	0	1	2.1e-02	4.4e+04
Rh-102m	2.90e+00	3.5e-06	2.39e-01	0	1	1.5e-02	2.1e+05
Rh-102	5.75e-01	5.5e-06	1.21e+00	0	1	1.2e+00	>1E20
Rh-103m	1.06e-04	0.00000001	6.51e+03	0	1	>1E20	>1E20
Rh-105	4.05e-03	1.4e-06	1.71e+02	0	1	>1E20	>1E20
Rh-106m	2.49e-04	6.1e-07	2.79e+03	0	1	>1E20	>1E20
Rh-107	4.13e-05	5.4e-08	1.68e+04	0	1	>1E20	>1E20
Pd-100	1.10e-02	3.8e-06	6.33e+01	0	1	>1E20	>1E20

Rev. 0

C-81
Table C3-1. (continued)

WSRC-RP-94-218

Nuclide	T1/2 (year)	DCF (mrem/pCi)	Lambda (1/year)	Kd (cm ³ /gm)	Rf	SUSP GW Trigger (Ci/trench)	SUSP Int Trigger (Ci/trench)
Pd-101	9.58e-04	3.8e-07	7.23e+02	0	1	>1E20	>1E20
Pd-103	4.65e-02	6.9e-07	1.49e+01	0	1	>1E20	>1E20
Pd-107	6.50e+06	1.4e-07	1.07e-07	0	1	1.1e-01	8.6e-06
Pd-109	1.53e-03	2.1e-06	4.53e+02	0	1	>1E20	>1E20
Ag-102	2.85e-05	7.9e-08	2.43e+04	10	51	>1E20	>1E20
Ag-103	1.25e-04	1.4e-07	5.52e+03	10	51	>1E20	>1E20
Ag-104m	5.70e-05	1.5e-07	1.22e+04	10	51	>1E20	>1E20
Ag-104	1.27e-04	2.3e-07	5.44e+03	10	51	>1E20	>1E20
Ag-105	1.10e-01	1.9e-06	6.33e+00	10	51	>1E20	>1E20
Ag-106m	2.27e-02	6.1e-06	3.05e+01	10	51	>1E20	>1E20
Ag-106	4.56e-05	7.6e-08	1.52e+04	10	51	>1E20	>1E20
Ag-108m	1.30e+02	7.5e-06	5.33e-03	10	51	4.2e-01	1.5e-05
Ag-110m	6.90e-01	1.1e-05	1.00e+00	10	51	>1E20	>1E20
Ag-111	2.05e-02	4.5e-06	3.39e+01	10	51	>1E20	>1E20
Ag-112	3.57e-04	1.6e-06	1.94e+03	10	51	>1E20	>1E20
Ag-115	3.99e-05	1.5e-07	1.74e+04	10	51	>1E20	>1E20
Cd-104	1.08e-04	2.3e-07	6.40e+03	8	41	>1E20	>1E20
Cd-107	7.42e-04	2.4e-07	9.35e+02	8	41	>1E20	>1E20
Cd-109	1.24e+00	1.2e-05	5.59e-01	8	41	>1E20	>1E20
Cd-113m	1.46e+01	1.5e-04	4.75e-02	8	41	7.3e+01	1.0e-03
Cd-113	9.30e+15	1.6e-04	7.45e-17	8	41	4.0e-03	8.6e-06
Cd-115m	1.36e-01	1.5e-05	5.11e+00	8	41	>1E20	>1E20
Cd-115	6.10e-03	4.7e-06	1.14e+02	8	41	>1E20	>1E20
Cd-117m	3.88e-04	1.1e-06	1.79e+03	8	41	>1E20	>1E20
Cd-117	2.97e-04	1.1e-06	2.34e+03	8	41	>1E20	>1E20
In-109	4.91e-04	2.7e-07	1.41e+03	0	1	>1E20	>1E20
In-110(69m)	1.27e-04	3.3e-07	5.44e+03	0	1	>1E20	>1E20
In-111	7.69e-03	1.2e-06	9.01e+01	0	1	>1E20	>1E20
In-112	2.66e-05	0.00000002	2.60e+04	0	1	>1E20	>1E20
In-113m	1.89e-04	1.0e-07	3.66e+03	0	1	>1E20	>1E20
In-114m	1.36e-01	0.000015	5.11e+00	0	1	1.3e+08	>1E20
In-115m	5.13e-04	3.4e-07	1.35e+03	0	1	>1E20	>1E20
In-115	4.60e+15	1.4e-04	1.51e-16	0	1	1.1e-04	8.6e-06
In-116m	1.03e-04	2.1e-07	6.73e+03	0	1	>1E20	>1E20

Rev. 0

C-82
Table C3-1. (continued)

WSRC-RP-94-218

Nuclide	T1/2 (year)	DCF (mrem/pCi)	Lambda (1/year)	Kd (cm ³ /gm)	Rf	SUSP GW Trigger (Ci/trench)	SUSP Int Trigger (Ci/trench)
In-117m	2.21e-04	4.2e-07	3.13e+03	0	1	>1E20	>1E20
In-117	8.37e-05	8.7e-08	8.29e+03	0	1	>1E20	>1E20
In-119m	3.42e-05	1.0e-07	2.03e+04	0	1	>1E20	>1E20
Sn-110	4.56e-04	1.5e-06	1.52e+03	130	651	>1E20	>1E20
Sn-111	6.65e-05	6.7e-08	1.04e+04	130	651	>1E20	>1E20
Sn-113	3.15e-01	2.7e-06	2.20e+00	130	651	>1E20	>1E20
Sn-117m	3.83e-02	2.6e-06	1.81e+01	130	651	>1E20	>1E20
Sn-119m	8.02e-01	1.2e-05	8.64e-01	130	651	>1E20	>1E20
Sn-121m	7.60e+01	1.3e-06	9.12e-03	130	651	6.2e+13	2.2e-05
Sn-121	3.08e-03	8.9e-07	2.25e+02	130	651	>1E20	>1E20
Sn-123m	7.61e-05	1.0e-07	9.11e+03	130	651	>1E20	>1E20
Sn-123	3.53e-01	7.7e-06	1.96e+00	130	651	>1E20	>1E20
Sn-125	2.64e-02	1.1e-05	2.62e+01	130	651	>1E20	>1E20
Sn-126	1.00e+05	1.7e-05	6.93e-06	130	651	6.2e-01	8.6e-06
Sn-127	2.42e-04	7.4e-07	2.87e+03	130	651	>1E20	>1E20
Sn-128	1.12e-04	5.2e-07	6.18e+03	130	651	>1E20	>1E20
Sb-115	5.89e-05	6.3e-08	1.18e+04	10	51	>1E20	>1E20
Sb-116m	1.14e-04	2.4e-07	6.08e+03	10	51	>1E20	>1E20
Sb-116	2.85e-05	5.6e-08	2.43e+04	10	51	>1E20	>1E20
Sb-117	3.19e-04	7.4e-08	2.17e+03	10	51	>1E20	>1E20
Sb-118m	5.82e-04	9.3e-07	1.19e+03	10	51	>1E20	>1E20
Sb-119	4.33e-03	3.4e-07	1.60e+02	10	51	>1E20	>1E20
Sb-120(16m)	3.04e-05	3.0e-08	2.28e+04	10	51	>1E20	>1E20
Sb-120(6d)	1.59e-02	5.4e-06	4.37e+01	10	51	>1E20	>1E20
Sb-122	7.45e-03	6.3e-06	9.31e+01	10	51	>1E20	>1E20
Sb-124m	1.77e-04	2.0e-08	3.92e+03	10	51	>1E20	>1E20
Sb-124	1.65e-01	9.3e-06	4.20e+00	10	51	>1E20	>1E20
Sb-125	2.40e+00	2.6e-06	2.89e-01	10	51	>1E20	3.0e+07
Sb-126m	3.61e-05	7.3e-08	1.92e+04	10	51	>1E20	>1E20
Sb-126	3.39e-02	9.6e-06	2.04e+01	10	51	>1E20	>1E20
Sb-127	1.04e-02	6.6e-06	6.66e+01	10	51	>1E20	>1E20
Sb-128(9h)	1.03e-03	4.3e-06	6.75e+02	10	51	>1E20	>1E20
Sb-128(10m)	1.90e-05	5.0e-08	3.65e+04	10	51	>1E20	>1E20
Sb-129	4.95e-04	1.7e-06	1.40e+03	10	51	>1E20	>1E20

Rev. 0

Table C.3-1. (continued)

Nuclide	T _{1/2} (year)	DCF (mrem/pCi)	Lambda (1/year)	K _d (cm ² /gm)	R _f	SUSP GW Trigger (Ci/trench)	SUSP Int Trigger (Ci/trench)
Sb-130	1.25e-05	2.6e-07	5.52e+04	10	51	>1E20	>1E20
Sb-131	4.37e-05	2.9e-07	1.59e+04	10	51	>1E20	>1E20
Te-118	1.64e-02	6.7e-07	4.22e+01	0	1	>1E20	>1E20
Te-121m	4.11e-01	6.7e-06	1.69e+00	0	1	1.1e+01	>1E20
Te-121	4.65e-02	1.5e-06	1.49e+01	0	1	>1E20	>1E20
Te-123m	3.28e-01	5.1e-06	2.12e+00	0	1	1.2e+02	>1E20
Te-123	1.20e+13	4.1e-06	5.78e-14	0	1	3.8e-03	8.6e-06
Te-125m	1.59e-01	3.4e-06	4.37e+00	0	1	1.4e+07	>1E20
Te-127m	2.98e-01	7.9e-06	2.32e+00	0	1	2.2e+02	>1E20
Te-127	1.07e-03	6.9e-07	6.46e+02	0	1	>1E20	>1E20
Te-129m	9.14e-02	9.9e-06	7.58e+00	0	1	4.6e+13	>1E20
Te-129	1.33e-04	1.9e-07	5.21e+03	0	1	>1E20	>1E20
Te-131m	3.42e-03	1.5e-05	2.03e+02	0	1	>1E20	>1E20
Te-131	4.75e-05	2.0e-07	1.46e+04	0	1	>1E20	>1E20
Te-132	8.76e-03	7.4e-06	7.91e+01	0	1	>1E20	>1E20
Te-133m	1.05e-04	7.6e-07	6.58e+03	0	1	>1E20	>1E20
Te-133	2.38e-05	1.6e-07	2.92e+04	0	1	>1E20	>1E20
Te-134	7.99e-05	2.1e-07	8.68e+03	0	1	>1E20	>1E20
I-120m	1.01e-04	3.9e-07	6.88e+03	0.6	4	>1E20	>1E20
I-120	1.48e-04	6.7e-07	4.67e+03	0.6	4	>1E20	>1E20
I-121	2.40e-04	1.8e-07	2.89e+03	0.6	4	>1E20	>1E20
I-123	1.52e-03	4.9e-07	4.57e+02	0.6	4	>1E20	>1E20
I-124	1.15e-02	3.1e-05	6.03e+01	0.6	4	>1E20	>1E20
I-125	1.64e-01	3.8e-05	4.22e+00	0.6	4	>1E20	>1E20
I-126	3.64e-02	7.1e-05	1.90e+01	0.6	4	>1E20	>1E20
I-128	4.75e-05	8.5e-08	1.46e+04	0.6	4	>1E20	>1E20
I-129	1.72e+07	2.8e-04	4.02e-08	0.6	4	2.3e-04	8.6e-06
I-130	1.41e-03	4.3e-06	4.90e+02	0.6	4	>1E20	>1E20
I-131	2.22e-02	5.3e-05	3.13e+01	0.6	4	>1E20	>1E20
I-132m	1.58e-04	4.7e-07	4.39e+03	0.6	4	>1E20	>1E20
I-132	2.60e-04	3.3e-07	2.66e+03	0.6	4	>1E20	>1E20
I-133	2.37e-03	5.4e-06	2.92e+02	0.6	4	>1E20	>1E20
I-134	1.00e-04	1.9e-07	6.93e+03	0.6	4	>1E20	>1E20
I-135	7.51e-04	2.0e-05	9.23e+02	0.6	4	>1E20	>1E20

Rev. 0

C-84
Table C3-1. (continued)

WSRC-RP-94-218

Nuclide	T1/2 (year)	DCF (mrem/pCi)	Lambda (1/year)	Kd (cm ³ /gm)	Rf	SUSP GW Trigger (Ci/trench)	SUSP Int Trigger (Ci/trench)
Cs-125	8.56e-05	5.5e-08	8.10e+03	100	501	>1E20	>1E20
Cs-127	7.07e-04	8.0e-08	9.80e+02	100	501	>1E20	>1E20
Cs-129	3.65e-03	2.2e-07	1.90e+02	100	501	>1E20	>1E20
Cs-130	5.70e-05	4.9e-08	1.22e+04	100	501	>1E20	>1E20
Cs-131	2.66e-02	2.4e-07	2.61e+01	100	501	>1E20	>1E20
Cs-132	1.80e-02	1.9e-06	3.85e+01	100	501	>1E20	>1E20
Cs-134m	3.31e-04	4.2e-08	2.10e+03	100	501	>1E20	>1E20
Cs-134	2.06e+00	7.4e-05	3.36e-01	100	501	>1E20	3.5e+09
Cs-135m	1.01e-04	4.9e-08	6.88e+03	100	501	>1E20	>1E20
Cs-135	2.30e+06	7.1e-06	3.01e-07	100	501	1.1e+00	8.6e-06
Cs-136	3.53e-02	1.1e-05	1.96e+01	100	501	>1E20	>1E20
Cs-137	3.01e+01	5.0e-05	2.30e-02	100	501	>1E20	8.6e-05
Cs-138	6.12e-05	1.6e-07	1.13e+04	100	501	>1E20	>1E20
Ba-126	1.84e-04	9.0e-07	3.76e+03	5	26	>1E20	>1E20
Ba-128	6.57e-03	1.0e-05	1.05e+02	5	26	>1E20	>1E20
Ba-131m	2.78e-05	9.7e-07	2.50e+04	5	26	>1E20	>1E20
Ba-131	3.20e-02	1.6e-06	2.16e+01	5	26	>1E20	>1E20
Ba-133m	4.44e-03	2.0e-06	1.56e+02	5	26	>1E20	>1E20
Ba-133	1.07e+01	3.2e-06	6.48e-02	5	26	5.8e+02	5.6e-03
Ba-135m	3.27e-03	1.6e-06	2.12e+02	5	26	>1E20	>1E20
Ba-137m	0.000005		1.43e+05	5	26	>1E20	>1E20
Ba-139	1.58e-04	3.9e-07	4.38e+03	5	26	>1E20	>1E20
Ba-140	3.50e-02	8.4e-06	1.98e+01	5	26	>1E20	>1E20
Ba-141	3.48e-05	2.0e-07	1.99e+04	5	26	>1E20	>1E20
Ba-142	2.03e-05	1.0e-07	3.41e+04	5	26	>1E20	>1E20
La-131	1.12e-04	1.1e-07	6.18e+03	100	501	>1E20	>1E20
La-132	5.13e-04	1.5e-06	1.35e+03	100	501	>1E20	>1E20
La-135	2.22e-03	1.3e-07	3.12e+02	100	501	>1E20	>1E20
La-137	6.00e+04	4.3e-07	1.16e-05	100	501	1.9e+01	8.6e-06
La-138	1.06e+11	5.9e-06	6.54e-12	100	501	1.3e+00	8.6e-06
La-140	4.59e-03	7.7e-06	1.51e+02	100	501	>1E20	>1E20
La-141	4.41e-04	1.4e-06	1.57e+03	100	501	>1E20	>1E20
La-142	1.76e-04	8.3e-07	3.95e+03	100	501	>1E20	>1E20
La-143	2.66e-05	1.4e-07	2.60e+04	100	501	>1E20	>1E20

Rev. 0

Table C3-1. (continued)

Nuclide	T1/2 (year)	DCF (mrem/pCi)	Lambda (1/year)	Kd (cm ³ /gm)	Rf	SUSP GW Trigger (Ci/trench)	SUSP lat Trigger (Ci/trench)
Ce-134	8.21e-03	8.9e-06	8.44e+01	10	51	>1E20	>1E20
Ce-135	1.96e-03	3.2e-06	3.53e+02	10	51	>1E20	>1E20
Ce-137m	3.92e-03	2.0e-06	1.77e+02	10	51	>1E20	>1E20
Ce-137	1.03e-03	9.8e-08	6.75e+02	10	51	>1E20	>1E20
Ce-139	3.77e-01	1.1e-06	1.84e+00	10	51	>1E20	>1E20
Ce-141	8.90e-02	2.6e-06	7.79e+00	10	51	>1E20	>1E20
Ce-143	3.76e-03	4.2e-06	1.84e+02	10	51	>1E20	>1E20
Ce-144	7.94e-01	2.0e-05	8.73e-01	10	51	>1E20	>1E20
Pr-136	1.25e-04	6.8e-08	5.52e+03	10	51	>1E20	>1E20
Pr-137	1.71e-04	1.3e-07	4.05e+03	100	501	>1E20	>1E20
Pr-138m	2.40e-04	4.9e-07	2.89e+03	100	501	>1E20	>1E20
Pr-139	5.13e-04	1.2e-07	1.35e+03	100	501	>1E20	>1E20
Pr-142m	2.72e-05	6.3e-08	2.55e+04	100	501	>1E20	>1E20
Pr-142	2.18e-03	5.1e-06	3.18e+02	100	501	>1E20	>1E20
Pr-143	3.75e-02	4.5e-06	1.85e+01	100	501	>1E20	>1E20
Pr-144	3.29e-05	1.1e-07	2.11e+04	100	501	>1E20	>1E20
Pr-145	6.82e-04	1.5e-06	1.02e+03	100	501	>1E20	>1E20
Pr-147	2.28e-05	5.7e-08	3.04e+04	100	501	>1E20	>1E20
Nd-136	9.64e-05	3.3e-07	7.19e+03	100	501	>1E20	>1E20
Nd-138	4.18e-05	2.5e-06	1.66e+04	100	501	>1E20	>1E20
Nd-139m	6.27e-04	1.0e-06	1.10e+03	100	501	>1E20	>1E20
Nd-139	5.93e-04	5.7e-08	1.17e+03	100	501	>1E20	>1E20
Nd-141	2.85e-04	3.2e-08	2.43e+03	100	501	>1E20	>1E20
Nd-147	3.01e-02	3.9e-06	2.30e+01	100	501	>1E20	>1E20
Nd-149	1.97e-03	4.6e-07	3.51e+02	100	501	>1E20	>1E20
Nd-151	2.36e-05	7.4e-08	2.94e+04	100	501	>1E20	>1E20
Pm-141	4.18e-05	8.4e-08	1.66e+04	100	501	>1E20	>1E20
Pm-143	7.26e-01	9.5e-07	9.55e-01	100	501	>1E20	>1E20
Pm-144	8.22e-01	3.9e-06	8.43e-01	100	501	>1E20	>1E20
Pm-145	1.77e+01	4.6e-07	3.92e-02	100	501	>1E20	4.3e-04
Pm-146	1.94e+00	3.2e-06	3.57e-01	100	501	>1E20	2.6e+10
Pm-147	2.52e+00	9.5e-07	2.75e-01	100	501	>1E20	7.7e+06
Pm-148m	1.14e-01	7.0e-06	6.06e+00	100	501	>1E20	>1E20
Pm-148	1.47e-02	9.5e-06	4.71e+01	100	501	>1E20	>1E20

Rev. 0

C-86
Table C3-1. (continued)

WSRC-RP-94-218

Nuclide	T1/2 (year)	DCF (mrem/pCi)	Lambda (1/year)	Kd (cm ³ /gm)	Rf	SUSP GW Trigger (Ci/french)	SUSP Int Trigger (Ci/french)
Pm-149	6.06e-03	3.6e-06	1.14e+02	100	501	>1E20	>1E20
Pm-150	3.06e-04	9.8e-07	2.27e+03	100	501	>1E20	>1E20
Pm-151	3.24e-03	2.8e-06	2.14e+02	100	501	>1E20	>1E20
Sm-141m	4.30e-05	1.8e-07	1.61e+04	100	501	>1E20	>1E20
Sm-141	1.94e-05	8.4e-08	3.57e+04	100	501	>1E20	>1E20
Sm-142	1.37e-04	6.0e-07	5.06e+03	100	501	>1E20	>1E20
Sm-145	9.31e-01	8.5e-07	7.45e-01	100	501	>1E20	>1E20
Sm-146	7.00e+07	2.0e-04	9.90e-09	100	501	4.0e-02	8.6e-06
Sm-147	1.06e+11	1.8e-04	6.54e-12	100	501	4.4e-02	8.6e-06
Sm-151	9.00e+01	3.4e-07	7.70e-03	100	501	5.6e+09	1.9e-05
Sm-153	5.33e-03	2.6e-06	1.30e+02	100	501	>1E20	>1E20
Sm-155	4.22e-05	6.6e-08	1.64e+04	100	501	>1E20	>1E20
Sm-158	8.37e-05	1.0e-06	8.29e+03	100	501	>1E20	>1E20
Eu-145	1.62e-02	3.2e-05	4.29e+01	100	501	>1E20	>1E20
Eu-146	1.26e-02	5.1e-06	5.50e+01	100	501	>1E20	>1E20
Eu-147	6.02e-02	1.8e-06	1.15e+01	100	501	>1E20	>1E20
Eu-148	1.48e-01	5.2e-06	4.69e+00	100	501	>1E20	>1E20
Eu-149	2.90e-01	4.2e-07	2.39e+00	100	501	>1E20	>1E20
Eu-150(12h)	1.37e-03	1.5e-06	5.06e+02	100	501	>1E20	>1E20
Eu-150(34y)	3.40e+01	6.2e-06	2.04e-02	100	501	>1E20	6.6e-05
Eu-152m	1.07e-03	1.9e-06	6.51e+02	100	501	>1E20	>1E20
Eu-152	1.34e+01	6.0e-06	5.17e-02	100	501	>1E20	1.5e-03
Eu-154	8.20e+00	9.1e-06	8.45e-02	100	501	>1E20	4.1e-02
Eu-155	1.70e+00	1.3e-06	4.08e-01	100	501	>1E20	>1E20
Eu-156	4.22e-02	8.7e-06	1.64e+01	100	501	>1E20	>1E20
Eu-157	1.73e-03	2.3e-06	4.00e+02	100	501	>1E20	>1E20
Eu-158	8.73e-05	2.6e-07	7.94e+03	100	501	>1E20	>1E20
Gd-145	4.75e-05	1.1e-07	1.46e+04	100	501	>1E20	>1E20
Gd-146	1.26e-02	3.8e-06	5.50e+01	100	501	>1E20	>1E20
Gd-147	3.99e-03	2.6e-06	1.74e+02	100	501	>1E20	>1E20
Gd-148	1.30e+02	2.1e-04	5.33e-03	100	501	2.4e+04	1.5e-05
Gd-149	2.46e-02	1.8e-06	2.81e+01	100	501	>1E20	>1E20
Gd-151	3.29e-01	7.7e-07	2.11e+00	100	501	>1E20	>1E20
Gd-152	1.10e+14	1.5e-04	6.30e-15	100	501	5.3e-02	8.6e-06

Rev. 0

C-87
Table C3-1. (continued)

WSRC-RP-94-218

Nuclide	T1/2 (year)	DCF (mrem/pCi)	Lambda (1/year)	Kd (cm**3/gm)	Rf	SUSP GW Trigger (Ci/trench)	SUSP Int Trigger (Ci/trench)
Gd-153	6.61e-01	1.1e-06	1.05e+00	100	501	>1E20	>1E20
Gd-159	2.12e-03	1.9e-06	3.27e+02	100	501	>1E20	>1E20
Tb-147	4.56e-05	5.6e-07	1.52e+04	100	501	>1E20	>1E20
Tb-149	4.68e-04	9.5e-07	1.48e+03	100	501	>1E20	>1E20
Tb-150	3.54e-04	9.7e-07	1.96e+03	100	501	>1E20	>1E20
Tb-151	2.05e-03	1.4e-06	3.38e+02	100	501	>1E20	>1E20
Tb-153	6.27e-03	9.9e-07	1.10e+02	100	501	>1E20	>1E20
Tb-154	9.70e-04	2.8e-06	7.15e+02	100	501	>1E20	>1E20
Tb-155	1.53e-02	8.2e-07	4.52e+01	100	501	>1E20	>1E20
Tb-156m(24h)	2.74e-03	7.0e-07	2.53e+02	100	501	>1E20	>1E20
Tb-156m(5h)	6.27e-04	3.2e-07	1.10e+03	100	501	>1E20	>1E20
Tb-156	1.48e-02	4.6e-06	4.69e+01	100	501	>1E20	>1E20
Tb-157	1.50e+02	1.0e-07	4.62e-03	100	501	8.4e+06	1.4e-05
Tb-158	1.20e+03	4.0e-06	5.78e-04	100	501	8.4e+00	9.2e-06
Tb-160	1.98e-01	6.4e-06	3.50e+00	100	501	>1E20	>1E20
Tb-161	1.88e-02	2.6e-06	3.68e+01	100	501	>1E20	>1E20
Dy-155	1.20e-03	5.6e-07	5.79e+02	100	501	>1E20	>1E20
Dy-157	9.24e-04	2.7e-07	7.50e+02	100	501	>1E20	>1E20
Dy-159	3.94e-01	4.0e-07	1.76e+00	100	501	>1E20	>1E20
Dy-165	2.66e-04	3.6e-07	2.61e+03	100	501	>1E20	>1E20
Dy-166	9.31e-03	6.2e-06	7.45e+01	100	501	>1E20	>1E20
Ho-155	9.51e-05	1.2e-07	7.29e+03	100	501	>1E20	>1E20
Ho-157	2.66e-05	1.9e-08	2.60e+04	100	501	>1E20	>1E20
Ho-159	6.27e-05	2.3e-08	1.10e+04	100	501	>1E20	>1E20
Ho-161	2.85e-04	4.7e-08	2.43e+03	100	501	>1E20	>1E20
Ho-162m	1.29e-04	9.0e-08	5.36e+03	100	501	>1E20	>1E20
Ho-162	2.85e-05	6.7e-09	2.43e+04	100	501	>1E20	>1E20
Ho-164m	7.13e-05	4.9e-08	9.72e+03	100	501	>1E20	>1E20
Ho-164	7.03e-05	2.4e-08	9.85e+03	100	501	>1E20	>1E20
Ho-166m	1.20e+03	7.8e-06	5.78e-04	100	501	4.3e+00	9.2e-06
Ho-166	3.06e-03	5.5e-06	2.27e+02	100	501	>1E20	>1E20
Ho-167	3.54e-04	3.2e-07	1.96e+03	100	501	>1E20	>1E20
Er-161	3.54e-04	3.3e-07	1.96e+03	100	501	>1E20	>1E20
Er-165	1.18e-03	7.9e-08	5.86e+02	100	501	>1E20	>1E20

Rev. 0

C-88
Table C3-1. (continued)

WSRC-RP-94-218

Nuclide	T1/2 (year)	DCF (mrem/pCi)	Lambda (1/year)	Kd (cm ³ /gm)	Rf	SUSP GW Trigger (Ci/trench)	SUSP Int Trigger (Ci/trench)
Er-169	2.57e-02	1.4e-06	2.69e+01	100	501	>1E20	>1E20
Er-171	8.58e-04	1.4e-06	8.08e+02	100	501	>1E20	>1E20
Er-172	5.59e-03	3.7e-06	1.24e+02	100	501	>1E20	>1E20
Tm-162	1.46e-04	7.0e-08	4.73e+03	100	501	>1E20	>1E20
Tm-166	8.78e-04	1.2e-06	7.89e+02	100	501	>1E20	>1E20
Tm-167	2.63e-02	2.1e-06	2.64e+01	100	501	>1E20	>1E20
Tm-170	3.53e-01	5.0e-06	1.96e+00	100	501	>1E20	>1E20
Tm-171	1.92e+00	3.9e-07	3.61e-01	100	501	>1E20	4.1e+10
Tm-172	7.26e-03	6.0e-06	9.55e+01	100	501	>1E20	>1E20
Tm-173	9.35e-04	1.2e-06	7.41e+02	100	501	>1E20	>1E20
Tm-175	3.80e-05	5.4e-08	1.82e+04	100	501	>1E20	>1E20
Yb-162	3.59e-05	7.0e-08	1.93e+04	100	501	>1E20	>1E20
Yb-165	1.90e-05	3.8e-06	3.65e+04	100	501	>1E20	>1E20
Yb-167	3.42e-05	1.7e-08	2.03e+04	100	501	>1E20	>1E20
Yb-169	8.76e-02	2.8e-06	7.91e+00	100	501	>1E20	>1E20
Yb-175	1.15e-02	1.6e-06	6.04e+01	100	501	>1E20	>1E20
Yb-177	2.17e-04	3.1e-07	3.20e+03	100	501	>1E20	>1E20
Yb-178	1.40e-04	3.9e-07	4.94e+03	100	501	>1E20	>1E20
Lu-169	3.88e-03	2.0e-06	1.79e+02	100	501	>1E20	>1E20
Lu-170	5.48e-03	4.3e-06	1.27e+02	100	501	>1E20	>1E20
Lu-171	2.27e-02	2.6e-06	3.05e+01	100	501	>1E20	>1E20
Lu-172	1.83e-02	5.0e-06	3.78e+01	100	501	>1E20	>1E20
Lu-173	1.37e+00	9.7e-07	5.06e-01	100	501	>1E20	>1E20
Lu-174m	3.83e-01	1.8e-06	1.81e+00	100	501	>1E20	>1E20
Lu-174	3.60e+00	9.9e-07	1.93e-01	100	501	>1E20	2.0e+03
Lu-176m	4.21e-04	6.3e-07	1.65e+03	100	501	>1E20	>1E20
Lu-176	3.00e+10	6.6e-06	2.31e-11	100	501	1.2e+00	8.6e-06
Lu-177m	4.41e-02	6.8e-06	1.57e+01	100	501	>1E20	>1E20
Lu-177	1.84e-02	2.0e-06	3.77e+01	100	501	>1E20	>1E20
Lu-178m	3.80e-05	8.8e-08	1.82e+04	100	501	>1E20	>1E20
Lu-178	5.70e-05	1.2e-07	1.22e+04	100	501	>1E20	>1E20
Lu-179	5.25e-04	8.1e-07	1.32e+03	100	501	>1E20	>1E20
Hf-170	1.39e-03	1.2e-05	4.98e+02	100	501	>1E20	>1E20
Hf-172	5.00e+00	4.1e-06	1.39e-01	100	501	>1E20	9.1e+00

Rev. 0

C-89
Table C3-1. (continued)

WSRC-RP-94-218

Nuclide	T1/2 (year)	DCF (mrem/pCi)	Lambda (1/year)	Kd (cm ³ /gm)	Rf	SUSP GW Trigger (Ci/trench)	SUSP Int Trigger (Ci/trench)
Hf-173	2.69e-03	9.6e-07	2.57e+02	100	501	>1E20	>1E20
Hf-175	1.92e-01	1.6e-06	3.62e+00	100	501	>1E20	>1E20
Hf-177m	9.77e-05	2.5e-07	7.09e+03	100	501	>1E20	>1E20
Hf-178m	3.10e+01	2.0e-05	2.24e-02	100	501	>1E20	8.1e-05
Hf-179m	6.87e-02	4.8e-06	1.01e+01	100	501	>1E20	>1E20
Hf-180m	6.27e-04	8.9e-07	1.10e+03	100	501	>1E20	>1E20
Hf-181	1.16e-01	4.3e-06	5.97e+00	100	501	>1E20	>1E20
Hf-182m	1.18e-04	1.4e-07	5.88e+03	100	501	>1E20	>1E20
Hf-182	9.00e+06	1.4e-05	7.70e-08	100	501	5.6e-01	8.6e-06
Hf-183	1.25e-04	2.5e-07	5.52e+03	100	501	>1E20	>1E20
Hf-184	4.68e-04	2.1e-06	1.48e+03	100	501	>1E20	>1E20
Ta-172	8.37e-05	1.4e-07	8.29e+03	0	1	>1E20	>1E20
Ta-173	4.22e-04	7.4e-07	1.64e+03	0	1	>1E20	>1E20
Ta-174	1.48e-04	1.9e-07	4.67e+03	0	1	>1E20	>1E20
Ta-175	1.20e-03	8.8e-07	5.79e+02	0	1	>1E20	>1E20
Ta-176	9.13e-04	1.3e-06	7.60e+02	0	1	>1E20	>1E20
Ta-177	6.46e-03	4.1e-07	1.07e+02	0	1	>1E20	>1E20
Ta-178	1.79e-05	2.9e-07	3.88e+04	0	1	>1E20	>1E20
Ta-179	2.40e-04	2.5e-07	2.89e+03	0	1	>1E20	>1E20
Ta-180m	9.24e-04	2.1e-07	7.50e+02	0	1	>1E20	>1E20
Ta-180	1.00e+13	3.3e-06	6.93e-14	0	1	4.8e-03	8.6e-06
Ta-182m	3.02e-05	2.4e-08	2.29e+04	0	1	>1E20	>1E20
Ta-182	3.15e-01	6.0e-06	2.20e+00	0	1	1.6e+02	>1E20
Ta-183	1.40e-02	4.6e-06	4.96e+01	0	1	>1E20	>1E20
Ta-184	9.92e-04	2.7e-06	6.98e+02	0	1	>1E20	>1E20
Ta-185	9.51e-05	2.0e-07	7.29e+03	0	1	>1E20	>1E20
Ta-186	2.00e-05	6.7e-08	3.47e+04	0	1	>1E20	>1E20
W-176	2.85e-04	4.8e-07	2.43e+03	0	1	>1E20	>1E20
W-177	2.57e-04	2.4e-07	2.70e+03	0	1	>1E20	>1E20
W-178	5.89e-02	9.3e-07	1.18e+01	0	1	>1E20	>1E20
W-179	7.22e-05	9.0e-09	9.59e+03	0	1	>1E20	>1E20
W-181	3.31e-01	3.1e-07	2.09e+00	0	1	1.8e+03	>1E20
W-185	2.06e-01	1.9e-06	3.37e+00	0	1	1.7e+05	>1E20
W-187	2.73e-03	2.6e-06	2.54e+02	0	1	>1E20	>1E20

Rev. 0

C-90
Table C3-1. (continued)

WSRC-RP-94-218

Nuclide	T1/2 (year)	DCF (mrem/pCi)	Lambda (1/year)	Kd (cm**3/gm)	Rf	SUSP GW Trigger (Ci/trench)	SUSP Int Trigger (Ci/trench)
W-188	1.89e-01	9.0e-06	3.67e+00	0	1	1.6e+05	>1E20
Re-177	3.23e-05	4.4e-08	2.14e+04	0	1	>1E20	>1E20
Re-178	2.85e-05	4.8e-08	2.43e+04	0	1	>1E20	>1E20
Re-181	2.05e-03	1.0e-06	3.38e+02	0	1	>1E20	>1E20
Re-182(64h)	7.30e-03	3.4e-06	9.49e+01	0	1	>1E20	>1E20
Re-182(12h)	1.45e-03	7.4e-07	4.78e+02	0	1	>1E20	>1E20
Re-184m	4.63e-01	2.4e-06	1.50e+00	0	1	1.2e+01	>1E20
Rm-184	1.04e-02	2.2e-06	6.66e+01	0	1	>1E20	>1E20
Re-186m	2.00e+05	3.3e-06	3.47e-06	0	1	4.8e-03	8.6e-06
Re-186	1.03e-02	2.6e-06	6.71e+01	0	1	>1E20	>1E20
Re-187	7.00e+10	8.3e-09	9.90e-12	0	1	1.9e+00	8.6e-06
Re-188m	3.54e-05	6.2e-08	1.96e+04	0	1	>1E20	>1E20
Re-188	1.91e-03	2.8e-06	3.64e+02	0	1	>1E20	>1E20
Re-189	2.74e-03	1.5e-06	2.53e+02	0	1	>1E20	>1E20
Os-180	4.13e-05	4.7e-08	1.68e+04	0	1	>1E20	>1E20
Os-181	4.37e-05	3.5e-07	1.59e+04	0	1	>1E20	>1E20
Os-182	2.51e-03	2.2e-06	2.76e+02	0	1	>1E20	>1E20
Os-185	2.57e-01	2.1e-06	2.69e+00	0	1	5.3e+03	>1E20
Os-189m	6.84e-04	6.6e-08	1.01e+03	0	1	>1E20	>1E20
Os-191m	1.48e-03	3.6e-07	4.67e+02	0	1	>1E20	>1E20
Os-191	4.19e-02	2.0e-06	1.65e+01	0	1	>1E20	>1E20
Os-193	3.48e-03	3.1e-06	1.99e+02	0	1	>1E20	>1E20
Os-194	6.00e+00	9.1e-06	1.16e-01	0	1	3.1e-03	9.0e-01
Ir-182	2.85e-05	1.2e-07	2.43e+04	0	1	>1E20	>1E20
Ir-183	3.65e-04	6.4e-07	1.90e+03	0	1	>1E20	>1E20
Ir-	1.60e-03	1.1e-06	4.34e+02	0	1	>1E20	>1E20
Ir-186	1.83e-03	2.1e-06	3.80e+02	0	1	>1E20	>1E20
Ir-187	1.20e-03	4.8e-07	5.79e+02	0	1	>1E20	>1E20
Ir-188	4.68e-03	2.7e-06	1.48e+02	0	1	>1E20	>1E20
Ir-189	3.64e-02	9.3e-07	1.90e+01	0	1	>1E20	>1E20
Ir-190m	3.65e-04	3.0e-08	1.90e+03	0	1	>1E20	>1E20
Ir-190	3.01e-02	4.9e-06	2.30e+01	0	1	>1E20	>1E20
Ir-192m	2.74e-06	1.5e-06	2.53e+05	0	1	>1E20	>1E20
Ir-192	2.03e-01	5.3e-06	3.41e+00	0	1	7.6e+04	>1E20

Rev. 0

C-91
Table C3-1. (continued)

WSRC-RP-94-218

Nuclide	T1/2 (year)	DCF (mrem/pCi)	Lambda (1/year)	Kd (cm ³ /gm)	Rf	SUSP GW Trigger (Ci/trench)	SUSP Int Trigger (Ci/trench)
Ir-194m	4.68e-01	8.1e-06	1.48e+00	0	1	3.2e+00	>1E20
Ir-194	2.22e-03	5.1e-06	3.12e+02	0	1	>1E20	>1E20
Ir-195m	4.45e-04	6.4e-07	1.56e+03	0	1	>1E20	>1E20
Ir-195	4.79e-04	3.4e-07	1.45e+03	0	1	>1E20	>1E20
Pt-186	3.42e-04	3.7e-07	2.03e+03	0	1	>1E20	>1E20
Pt-188	2.79e-02	3.0e-06	2.48e+01	0	1	>1E20	>1E20
Pt-189	1.24e-03	4.9e-07	5.57e+02	0	1	>1E20	>1E20
Pt-191	1.24e-03	1.3e-06	5.57e+02	0	1	>1E20	>1E20
Pt-193m	1.18e-02	1.7e-06	5.89e+01	0	1	>1E20	>1E20
Pt-193	5.00e+01	1.1e-07	1.39e-02	0	1	1.5e-01	3.5e-05
Pt-195m	1.10e-02	2.2e-06	6.30e+01	0	1	>1E20	>1E20
Pt-197m	1.79e-04	3.1e-07	3.88e+03	0	1	>1E20	>1E20
Pt-197	2.09e-03	1.5e-06	3.32e+02	0	1	>1E20	>1E20
Pt-199	5.86e-05	1.0e-07	1.18e+04	0	1	>1E20	>1E20
Pt-200	1.31e-03	4.5e-06	5.28e+02	0	1	>1E20	>1E20
Au-193	1.83e-03	6.0e-07	3.80e+02	0	1	>1E20	>1E20
Au-194	4.51e-03	2.0e-06	1.54e+02	0	1	>1E20	>1E20
Au-195	5.01e-01	1.1e-06	1.38e+00	0	1	1.4e+01	>1E20
Au-198m	6.30e-03	5.7e-06	1.10e+02	0	1	>1E20	>1E20
Au-198	7.38e-03	2.3e-06	9.39e+01	0	1	>1E20	>1E20
Au-199	8.60e-03	1.8e-06	8.06e+01	0	1	>1E20	>1E20
Au-200m	2.13e-03	4.6e-06	3.25e+02	0	1	>1E20	>1E20
Au-200	9.20e-05	1.9e-07	7.53e+03	0	1	>1E20	>1E20
Au-201	4.94e-05	5.7e-08	1.40e+04	0	1	>1E20	>1E20
Hg-193m	1.14e-03	1.6e-06	6.08e+02	1000	5001	>1E20	>1E20
Hg-193	6.84e-04	3.3e-07	1.01e+03	1000	5001	>1E20	>1E20
Hg-194	1.90e+00	6.0e-06	3.65e-01	1000	5001	>1E20	6.0e+10
Hg-195m	4.56e-03	2.2e-06	1.52e+02	1000	5001	>1E20	>1E20
Hg-195	1.08e-03	3.8e-07	6.40e+02	1000	5001	>1E20	>1E20
Hg-197m	2.72e-03	1.7e-06	2.55e+02	1000	5001	>1E20	>1E20
Hg-197	7.31e-03	9.1e-07	9.48e+01	1000	5001	>1E20	>1E20
Hg-199m	8.10e-05	8.5e-08	8.56e+03	1000	5001	>1E20	>1E20
Hg-203	1.28e-01	2.1e-06	5.43e+00	1000	5001	>1E20	>1E20
Tl-194m	6.24e-05	7.1e-08	1.11e+04	0	1	>1E20	>1E20

Rev. 0

C-92
Table C3-1. (continued)

Nuclide	T1/2 (year)	DCF (mrem/pCi)	Lambda (1/year)	Kd (cm ³ /gm)	Rf	SUSP GW Trigger (Ci/trench)	SUSP Int Trigger (Ci/trench)
Tl-194	6.27e-05	1.9e-08	1.10e+04	0	1	>1E20	>1E20
Tl-195	1.37e-04	7.7e-08	5.06e+03	0	1	>1E20	>1E20
Tl-197	3.19e-04	6.9e-08	2.17e+03	0	1	>1E20	>1E20
Tl-198m	2.13e-04	1.6e-07	3.25e+03	0	1	>1E20	>1E20
Tl-198	6.05e-04	2.6e-07	1.15e+03	0	1	>1E20	>1E20
Tl-199	8.44e-04	8.2e-08	8.21e+02	0	1	>1E20	>1E20
Tl-200	2.98e-03	6.7e-07	2.33e+02	0	1	>1E20	>1E20
Tl-201	8.33e-03	2.9e-07	8.32e+01	0	1	>1E20	>1E20
Tl-202	3.29e-02	1.5e-06	2.11e+01	0	1	>1E20	>1E20
Tl-204	3.77e+00	3.2e-06	1.84e-01	0	1	1.2e-02	8.3e+02
Pb-195m	2.85e-05	8.5e-08	2.43e+04	100	501	>1E20	>1E20
Pb-198	2.74e-04	1.6e-07	2.53e+03	100	501	>1E20	>1E20
Pb-199	1.71e-04	2.2e-07	4.05e+03	100	501	>1E20	>1E20
Pb-200	2.45e-03	1.5e-06	2.83e+02	100	501	>1E20	>1E20
Pb-201	1.07e-03	6.7e-07	6.46e+02	100	501	>1E20	>1E20
Pb-202m	4.13e-04	5.5e-07	1.68e+03	100	501	>1E20	>1E20
Pb-202	3.00e+05	3.9e-05	2.31e-06	100	501	2.0e-01	8.6e-06
Pb-203	5.94e-03	9.6e-07	1.17e+02	100	501	>1E20	>1E20
Pb-205	1.40e+07	1.5e-06	4.95e-08	100	501	5.3e+00	8.6e-06
Pb-209	6.24e-06	9.0e-08	1.11e+05	100	501	>1E20	>1E20
Pb-210	2.23e+01	5.1e-03	3.11e-02	100	501	>1E20	1.9e-04
Pb-211	6.86e-05	4.4e-07	1.01e+04	100	501	>1E20	>1E20
Pb-212	1.21e-03	4.1e-05	5.71e+02	100	501	>1E20	>1E20
Pb-214	5.10e-05	5.8e-07	1.36e+04	100	501	>1E20	>1E20
Bi-200	6.65e-05	1.7e-07	1.04e+04	0	1	>1E20	>1E20
Bi-201	2.05e-04	4.5e-07	3.38e+03	0	1	>1E20	>1E20
Bi-202	1.81e-04	3.6e-07	3.84e+03	0	1	>1E20	>1E20
Bi-203	1.35e-03	2.1e-06	5.15e+02	0	1	>1E20	>1E20
Bi-205	4.19e-02	3.7e-06	1.65e+01	0	1	>1E20	>1E20
Bi-206	1.71e-02	8.0e-06	4.06e+01	-0	1	>1E20	>1E20
Bi-207	7.94e+00	4.9e-06	8.73e-02	0	1	5.0e-03	5.3e-02
Bi-210m	3.50e+06	8.6e-05	1.98e-07	0	1	1.8e-04	8.6e-06
Bi-210	1.37e-02	5.9e-06	5.06e+01	0	1	>1E20	>1E20
Bi-212	1.15e-04	9.9e-07	6.02e+03	0	1	>1E20	>1E20

C-93
Table C3-1. (continued)

WSRC-RP-94-218

Nuclide	T1/2 (year)	DCF (mrem/pCi)	Lambda (1/year)	Kd (cm ³ /gm)	Rf	SUSP GW Trigger (Ci/trench)	SUSP Int Trigger (Ci/trench)
Bi-213	8.68e-05	6.8e-07	7.99e+03	0	1	>1E20	>1E20
Bi-214	3.76e-05	2.4e-07	1.84e+04	0	1	>1E20	>1E20
Po-203	7.99e-05	2.0e-07	8.68e+03	0	1	>1E20	>1E20
Po-205	2.05e-04	2.4e-07	3.38e+03	0	1	>1E20	>1E20
Po-207	6.50e-04	6.1e-07	1.07e+03	0	1	>1E20	>1E20
Po-210	3.79e-01	1.6e-03	1.83e+00	0	1	9.3e-02	>1E20
At-207	2.05e-04	8.9e-07	3.38e+03	0	1	>1E20	>1E20
At-211	8.22e-04	4.1e-05	8.43e+02	0	1	>1E20	>1E20
Fr-222	2.81e-05	2.5e-06	2.46e+04	0	1	>1E20	>1E20
Fr-223	4.18e-05	8.6e-06	1.66e+04	0	1	>1E20	>1E20
Ra-223	3.13e-02	5.5e-04	2.21e+01	500	2501	>1E20	>1E20
Ra-224	9.91e-03	3.3e-04	6.99e+01	500	2501	>1E20	>1E20
Ra-225	4.05e-02	3.1e-04	1.71e+01	500	2501	>1E20	>1E20
Ra-226	1.62e+03	1.1e-03	4.27e-04	500	2501	7.5e+00	9.0e-06
Ra-227	7.83e-05	2.2e-07	8.85e+03	500	2501	>1E20	>1E20
Ra-228	5.75e+00	1.2e-03	1.21e-01	500	2501	>1E20	1.5e+00
Ac-224	3.31e-04	2.6e-06	2.10e+03	150	751	>1E20	>1E20
Ac-225	2.74e-02	9.5e-05	2.53e+01	150	751	>1E20	>1E20
Ac-226	3.31e-03	4.0e-05	2.10e+02	150	751	>1E20	>1E20
Ac-227	2.18e+01	1.4e-02	3.18e-02	150	751	>1E20	2.1e-04
Ac-228	6.99e-04	2.1e-06	9.91e+02	150	751	>1E20	>1E20
Th-226	5.87e-05	9.2e-07	1.18e+04	3000	15001	>1E20	>1E20
Th-227	5.13e-02	3.6e-05	1.35e+01	3000	15001	>1E20	>1E20
Th-228	1.91e+00	3.8e-04	3.62e-01	3000	15001	>1E20	4.7e+10
Th-229	7.43e+03	3.5e-03	9.33e-05	3000	15001	7.4e+01	8.7e-06
Th-230	7.70e+04	5.3e-04	9.00e-06	3000	15001	8.8e-01	8.6e-06
Th-231	2.91e-03	1.3e-06	2.38e+02	3000	15001	>1E20	>1E20
Th-232	1.41e+10	2.8e-03	4.93e-11	3000	15001	8.5e-02	8.6e-06
Th-234	6.60e-02	1.3e-05	1.05e+01	3000	15001	>1E20	>1E20
Pa-227	7.28e-05	1.3e-06	9.52e+03	10	51	>1E20	>1E20
Pa-228	2.97e-03	4.0e-06	2.34e+02	10	51	>1E20	>1E20
Pa-230	4.85e-02	5.6e-06	1.43e+01	10	51	>1E20	>1E20
Pa-231	3.28e+04	1.1e-02	2.12e-05	10	51	7.4e-05	8.7e-06
Pa-232	3.59e-03	3.4e-06	1.93e+02	10	51	>1E20	>1E20

Rev. 0

C-94
Table C3-1. (continued)

WSRC-RP-94-218

Nuclide	T1/2 (year)	DCF (mrem/pCi)	Lambda (1/year)	Kd (cm ³ /gm)	Rf	SUSP GW Trigger (Ci/trench)	SUSP Int Trigger (Ci/trench)
Pa-233	7.39e-02	3.3e-06	9.38e+00	10	51	>1E20	>1E20
Pa-234	7.64e-04	2.1e-06	9.07e+02	10	51	>1E20	>1E20
U-230	5.69e-02	8.4e-04	1.22e+01	50	251	>1E20	>1E20
U-231	4.30e+00	1.1e-06	1.61e-01	50	251	>1E20	8.7e+01
U-232	7.20e+01	1.3e-03	9.63e-03	50	251	5.4e+02	2.3e-05
U-233	1.60e+05	2.7e-04	4.35e-06	50	251	1.5e-02	8.6e-06
U-234	2.45e+05	2.6e-04	2.83e-06	50	251	1.5e-02	8.6e-06
U-235	7.04e+08	2.5e-04	9.85e-10	50	251	1.6e-02	8.6e-06
U-236	2.34e+07	2.5e-04	2.96e-08	50	251	1.6e-02	8.6e-06
U-237	1.85e-02	2.7e-06	3.75e+01	50	251	>1E20	>1E20
U-238	4.47e+09	2.3e-04	1.55e-10	50	251	1.7e-02	8.6e-06
U-239	4.47e-05	7.6e-08	1.55e+04	50	251	>1E20	>1E20
U-240	1.61e-03	4.1e-06	4.31e+02	50	251	>1E20	>1E20
Np-232	2.47e-05	2.4e-08	2.80e+04	10	51	>1E20	>1E20
Np-233	6.65e-05	5.6e-09	1.04e+04	10	51	>1E20	>1E20
Np-234	1.20e-02	1.7e-06	5.75e+01	10	51	>1E20	>1E20
Np-235	1.12e+00	2.1e-07	6.17e-01	10	51	>1E20	>1E20
Np-236(1E5y)	1.10e+05	7.9e-04	6.30e-06	10	51	1.0e-03	8.6e-06
Np-236(22h)	2.51e-03	9.5e-07	2.76e+02	10	51	>1E20	>1E20
Np-237	2.14e+06	3.9e-03	3.24e-07	10	51	2.1e-04	8.6e-06
Np-238	5.80e-03	3.4e-06	1.20e+02	10	51	>1E20	>1E20
Np-239	6.38e-03	2.9e-06	1.09e+02	10	51	>1E20	>1E20
Np-240	1.20e-04	2.0e-07	5.79e+03	10	51	>1E20	>1E20
Pu-234	1.03e-03	1.2e-06	6.75e+02	100	501	>1E20	>1E20
Pu-235	4.94e-05	1.4e-08	1.40e+04	100	501	>1E20	>1E20
Pu-236	2.85e+00	1.3e-03	2.43e-01	100	501	>1E20	3.2e+05
Pu-237	1.24e-01	1.0e-06	5.58e+00	100	501	>1E20	>1E20
Pu-238	8.78e+01	3.8e-03	7.90e-03	100	501	8.2e+05	1.9e-05
Pu-239	2.41e+04	4.3e-03	2.87e-05	100	501	2.0e-03	8.7e-06
Pu-240	6.57e+03	4.3e-03	1.06e-04	100	501	2.4e-03	8.7e-06
Pu-241	1.44e+01	8.6e-05	4.81e-02	100	501	>1E20	1.1e-03
Pu-242	3.76e+05	4.1e-03	1.84e-06	100	501	1.9e-03	8.6e-06
Pu-243	5.65e-04	3.3e-07	1.23e+03	100	501	>1E20	>1E20
Pu-244	8.10e+07	4.0e-03	8.56e-09	100	501	2.0e-03	8.6e-06

Rev. 0

C-95
Table C3-1. (continued)

WSRC-RP-94-218

Nuclide	T1/2 (year)	DCF (mrem/pCi)	Lambda (1/year)	Kd (cm**3/gm)	Rf	SUSP GW Trigger (Ci/trench)	SUSP Int Trigger (Ci/trench)
Pu-245	1.14e-03	2.4e-06	6.08e+02	100	501	>1E20	>1E20
Am-237	1.48e-04	7.4e-08	4.67e+03	150	751	>1E20	>1E20
Am-238	2.17e-04	1.7e-07	3.20e+03	150	751	>1E20	>1E20
Am-239	1.38e-03	1.0e-06	5.02e+02	150	751	>1E20	>1E20
Am-240	5.82e-03	2.9e-06	1.19e+02	150	751	>1E20	>1E20
Am-241	4.32e+02	4.5e-03	1.60e-03	150	751	1.1e+00	1.0e-05
Am-242m	1.52e+02	4.2e-03	4.56e-03	150	751	7.7e+04	1.4e-05
Am-242	1.83e-03	1.2e-06	3.80e+02	150	751	>1E20	>1E20
Am-243	7.37e+03	4.5e-03	9.40e-05	150	751	3.7e-03	8.7e-06
Am-244m	4.94e-05	6.8e-08	1.40e+04	150	751	>1E20	>1E20
Am-244	1.15e-03	2.0e-06	6.02e+02	150	751	>1E20	>1E20
Am-245	2.40e-04	1.8e-07	2.89e+03	150	751	>1E20	>1E20
Am-246m	4.75e-05	8.4e-08	1.46e+04	150	751	>1E20	>1E20
Am-246	4.75e-05	1.5e-07	1.46e+04	150	751	>1E20	>1E20
Cm-238	2.85e-04	3.6e-07	2.43e+03	100	501	>1E20	>1E20
Cm-240	7.34e-02	6.3e-05	9.45e+00	100	501	>1E20	>1E20
Cm-241	9.58e-02	4.6e-06	7.23e+00	100	501	>1E20	>1E20
Cm-242	4.46e-01	1.1e-04	1.56e+00	100	501	>1E20	>1E20
Cm-243	2.85e+01	2.9e-03	2.43e-02	100	501	>1E20	9.8e-05
Cm-244	1.81e+01	2.3e-03	3.83e-02	100	501	>1E20	4.0e-04
Cm-245	8.50e+03	4.5e-03	8.15e-05	100	501	2.2e-03	8.7e-06
Cm-246	4.70e+03	4.5e-03	1.47e-04	100	501	2.5e-03	8.8e-06
Cm-247	1.60e+07	4.1e-03	4.33e-08	100	501	1.9e-03	8.6e-06
Cm-248	3.50e+05	1.6e-02	1.98e-06	100	501	5.0e-04	8.6e-06
Cm-249	1.24e-04	9.5e-08	5.61e+03	100	501	>1E20	>1E20
Bk-245	1.36e-02	2.3e-06	5.08e+01	100	501	>1E20	>1E20
Bk-246	4.93e-03	1.9e-06	1.41e+02	100	501	>1E20	>1E20
Bk-247	1.40e+03	2.3e-03	4.95e-04	100	501	1.2e-02	9.1e-06
Bk-249	8.80e-01	6.0e-06	7.88e-01	100	501	>1E20	>1E20
Bk-250	3.67e-04	5.0e-07	1.89e+03	100	501	>1E20	>1E20
Cf-244	4.75e-05	1.5e-07	1.46e+04	100	501	>1E20	>1E20
Cf-246	4.11e-03	1.2e-05	1.69e+02	100	501	>1E20	>1E20
Cf-248	9.86e-01	2.8e-04	7.03e-01	100	501	>1E20	>1E20
Cf-249	3.51e+02	4.6e-03	1.97e-03	100	501	2.4e-01	1.1e-05

Rev. 0

C-96
Table C.3-1. (continued)

WSRC-RP-94-218

Nuclide	T1/2 (year)	DCF (mrem/pCi)	Lambda (1/year)	Kd (cm ³ /gm)	Rf	SUSP GW Trigger (Ci/trench)	SUSP Int Trigger (Ci/trench)
Cf-250	1.31e+01	1.9e-03	5.29e-02	100	501	>1E20	1.7e-03
Cf-251	9.00e+02	4.6e-03	7.70e-04	100	501	1.2e-02	9.3e-06
Cf-252	2.62e+00	9.4e-04	2.65e-01	100	501	>1E20	2.7e+06
Cf-253	4.87e-02	9.2e-06	1.42e+01	100	501	>1E20	>1E20
Cf-254	1.66e-01	2.5e-03	4.18e+00	100	501	>1E20	>1E20
Es-250	9.13e-04	9.5e-08	7.60e+02	100	501	>1E20	>1E20
Es-251	4.11e-03	6.7e-07	1.69e+02	100	501	>1E20	>1E20
Es-253	5.60e-02	2.4e-05	1.24e+01	100	501	>1E20	>1E20
Es-254m	4.48e-03	1.5e-05	1.55e+02	100	501	>1E20	>1E20
Es-254	7.56e-01	1.5e-04	9.17e-01	100	501	>1E20	>1E20
Fm-252	2.62e-03	9.9e-06	2.64e+02	100	501	>1E20	>1E20
Fm-253	8.21e-03	3.5e-06	8.44e+01	100	501	>1E20	>1E20
Fm-254	3.70e-04	1.6e-06	1.88e+03	100	501	>1E20	>1E20
Fm-255	2.29e-03	9.7e-06	3.02e+02	100	501	>1E20	>1E20
Fm-257	2.19e-01	7.3e-05	3.16e+00	100	501	>1E20	>1E20
Md-257	3.42e-04	5.4e-07	2.03e+03	100	501	>1E20	>1E20
Md-258	1.53e-01	6.1e-05	4.52e+00	100	501	>1E20	>1E20

C.4 NEAR-FIELD RESULTS

Figures C.4-1 through C.4-12 show the time histories of fluxes to the water table. The fluxes are given in the yearly fraction of a unit inventory in each vault released to the water table.

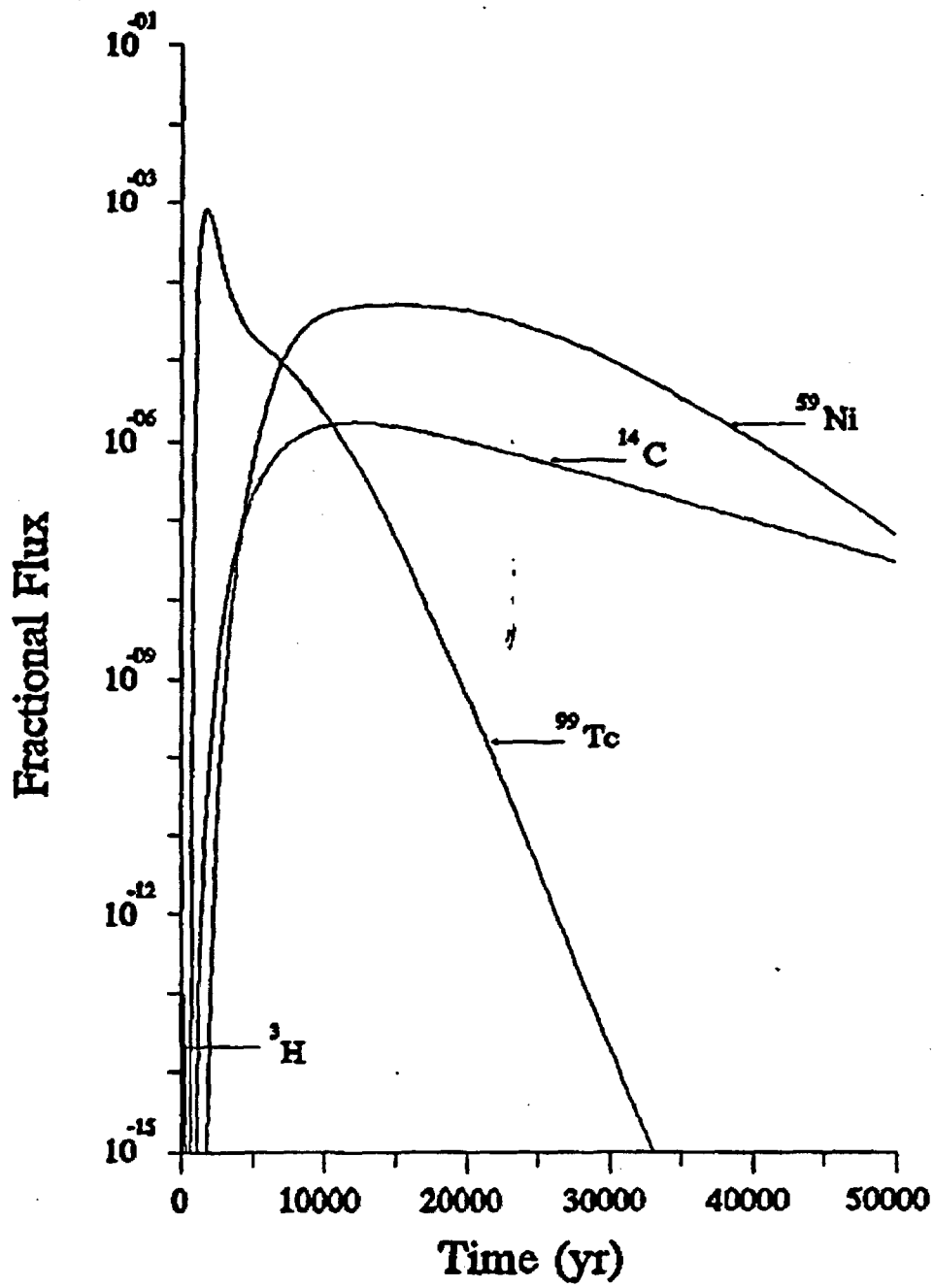


Fig. C.4-1. Fractional flux to the water table from the ILNT vaults.

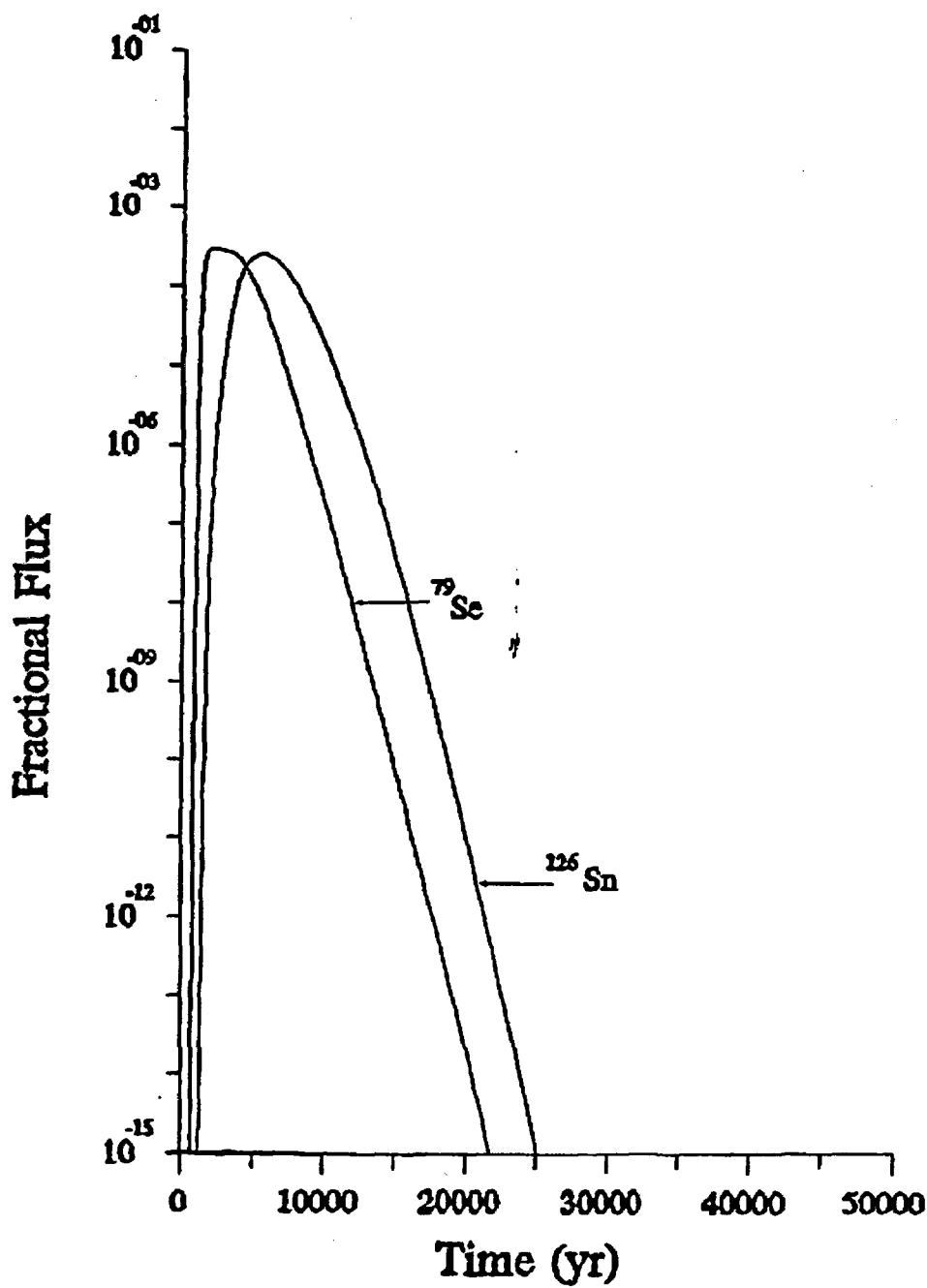


Fig. C.4-2. Fractional flux to the water table from the ILNT vaults.

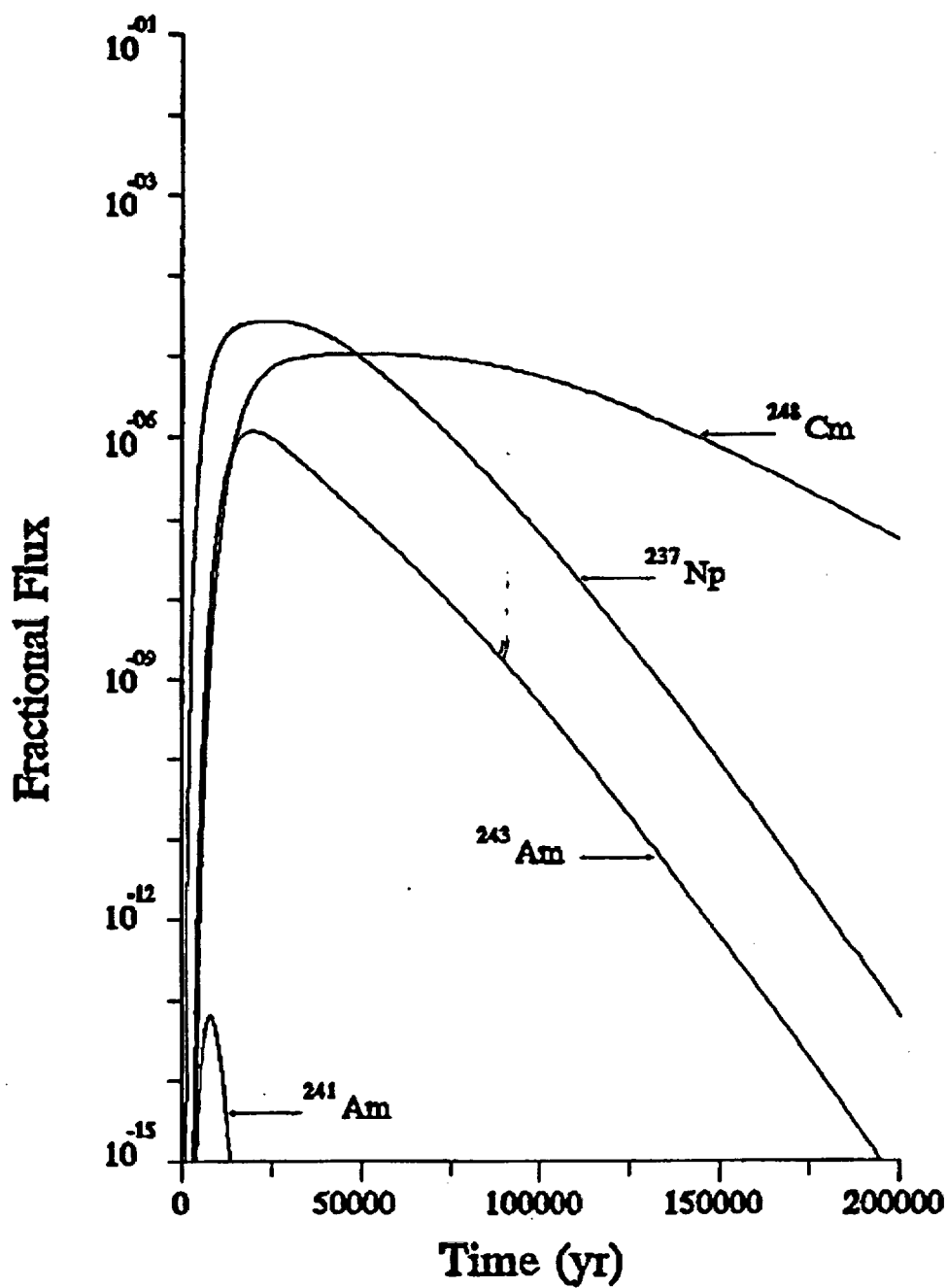


Fig. C.4-3. Fractional flux to the water table from the ILNT vaults.

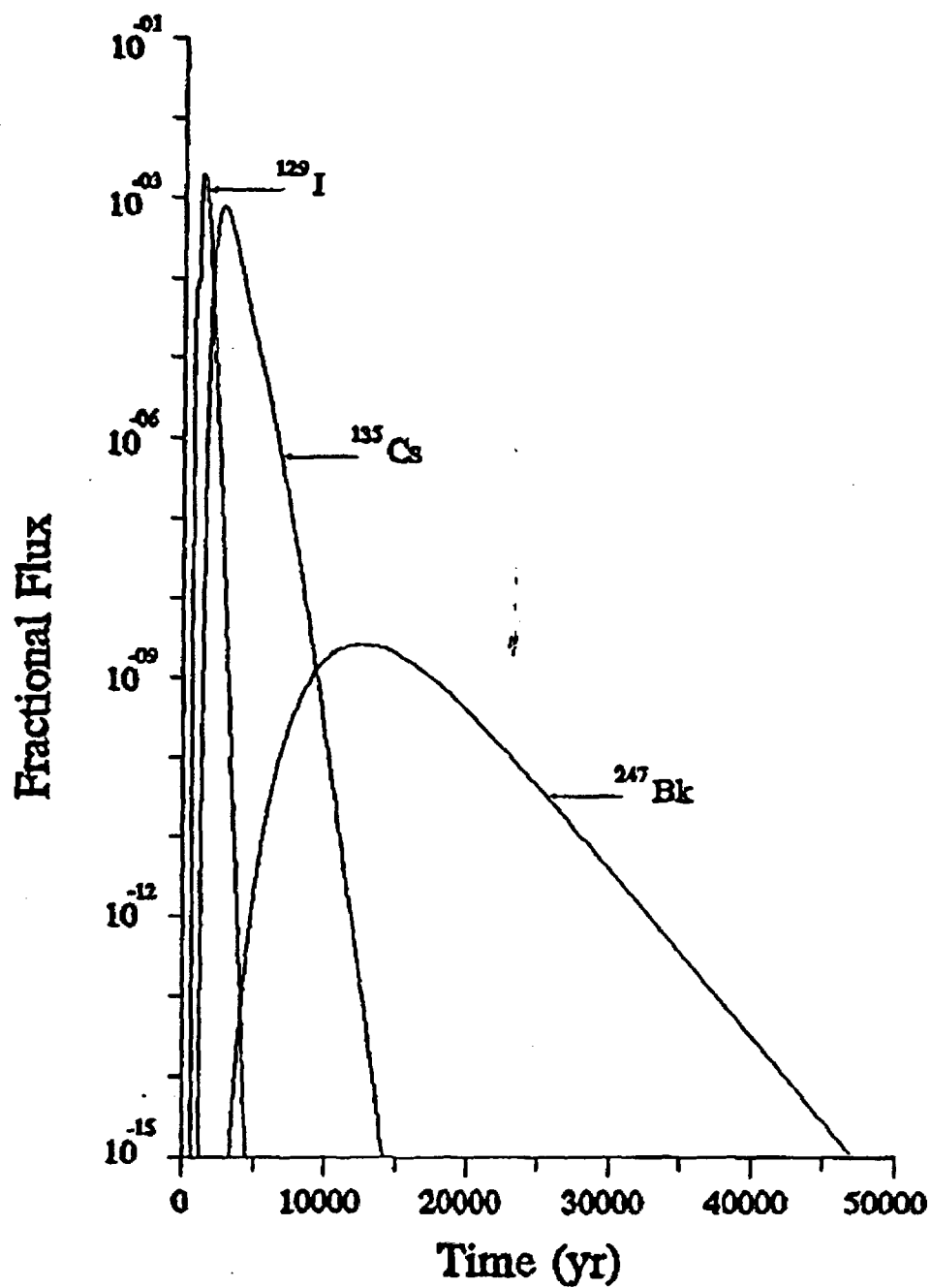


Fig. C.4-4. Fractional flux to the water table from the ILNT vaults.

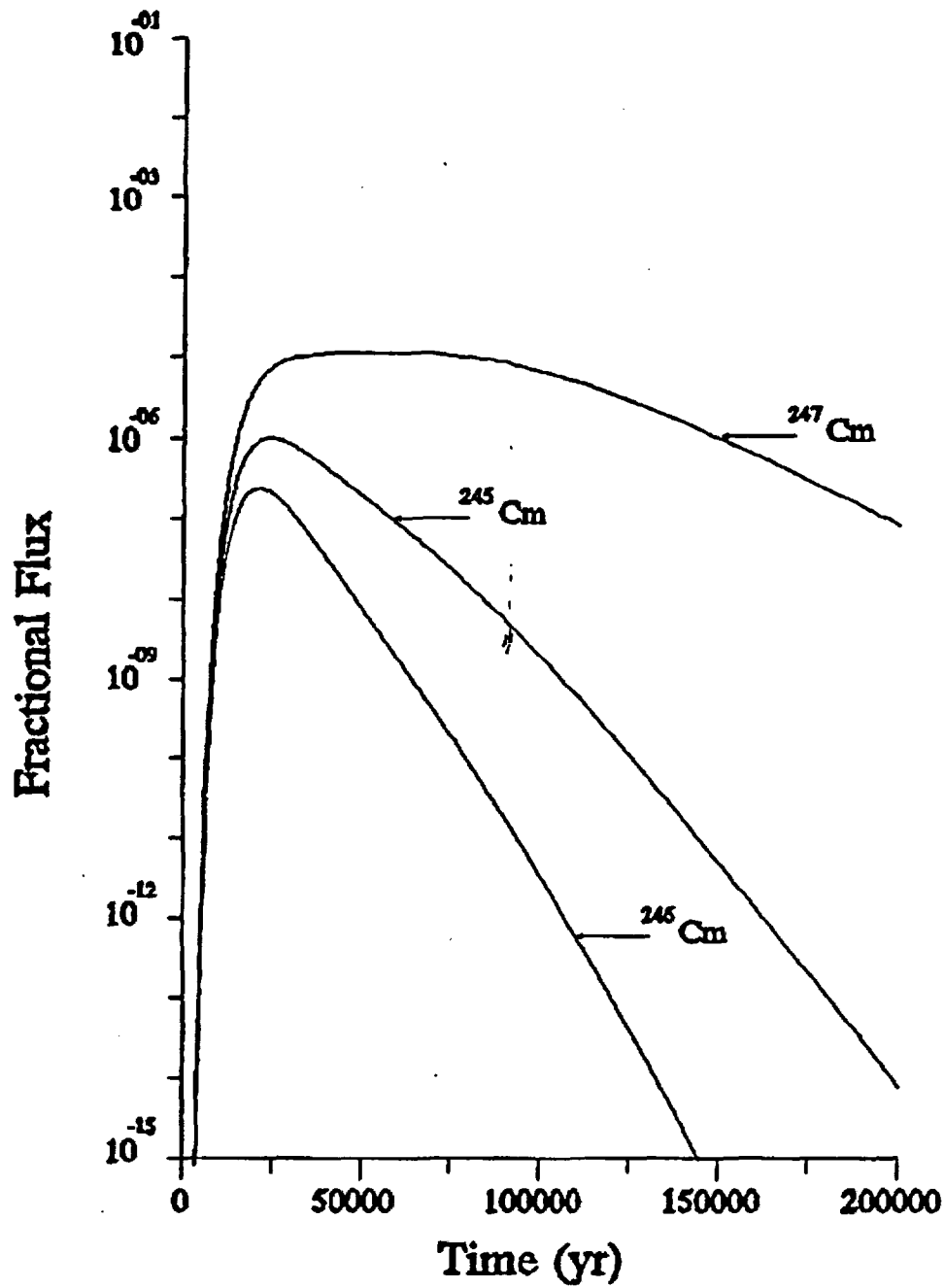


Fig. C4-5. Fractional flux to the water table from the ILNT vaults.

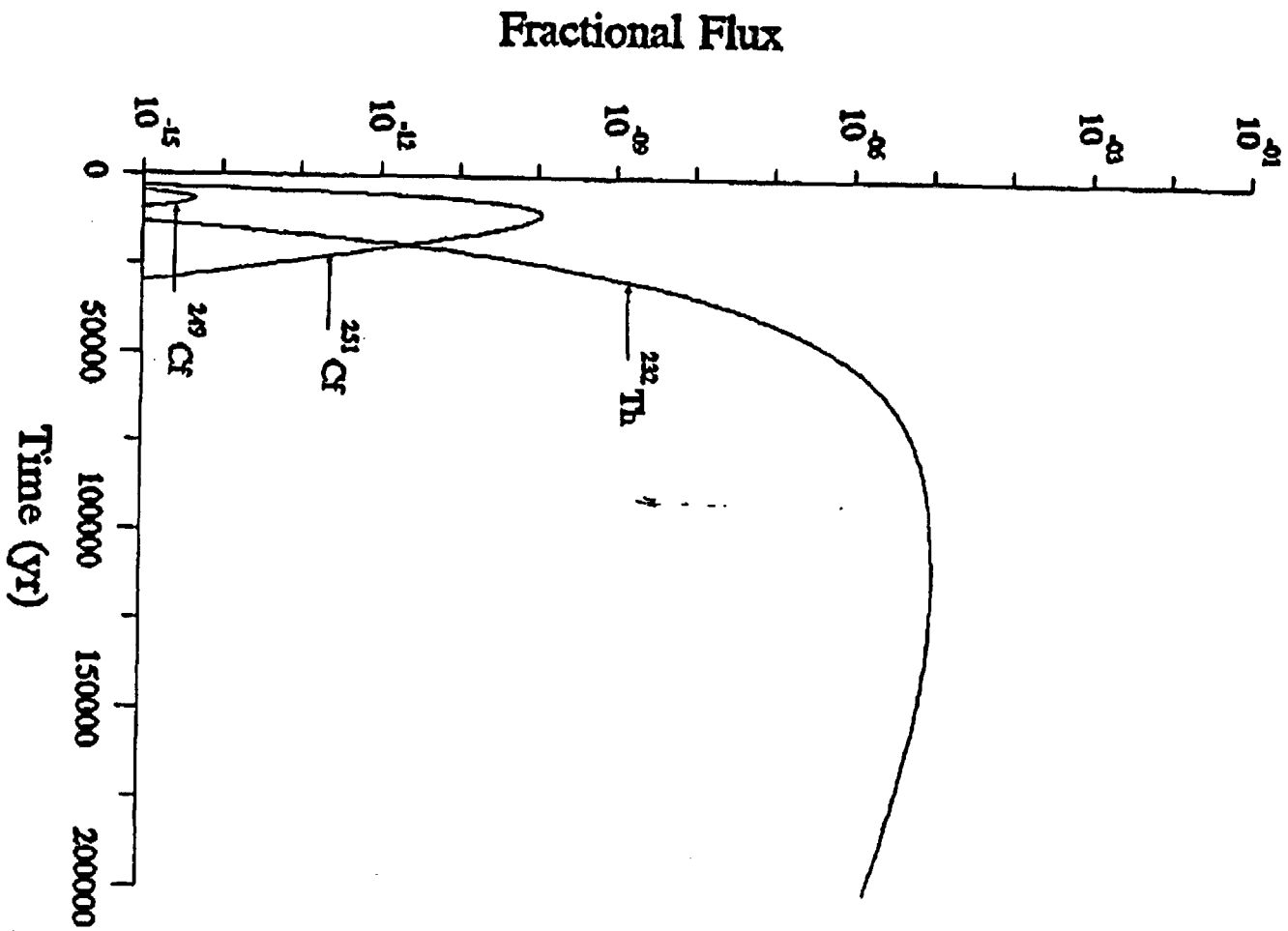


Fig. C-4-6. Fractional flux to the water table from the LLNT vaults.

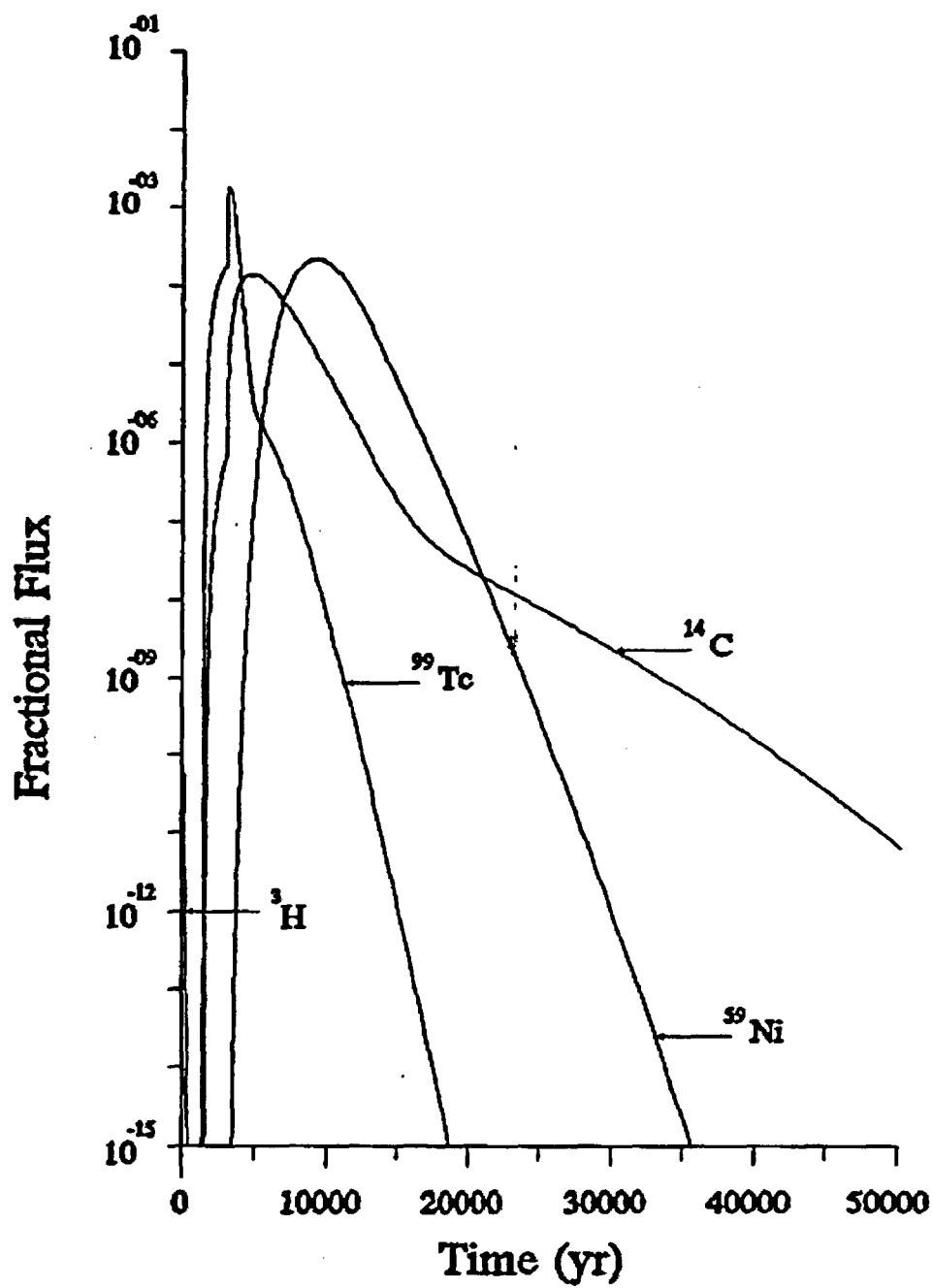


Fig. C.4-7. Fractional flux to the water table from the LAW vaults.

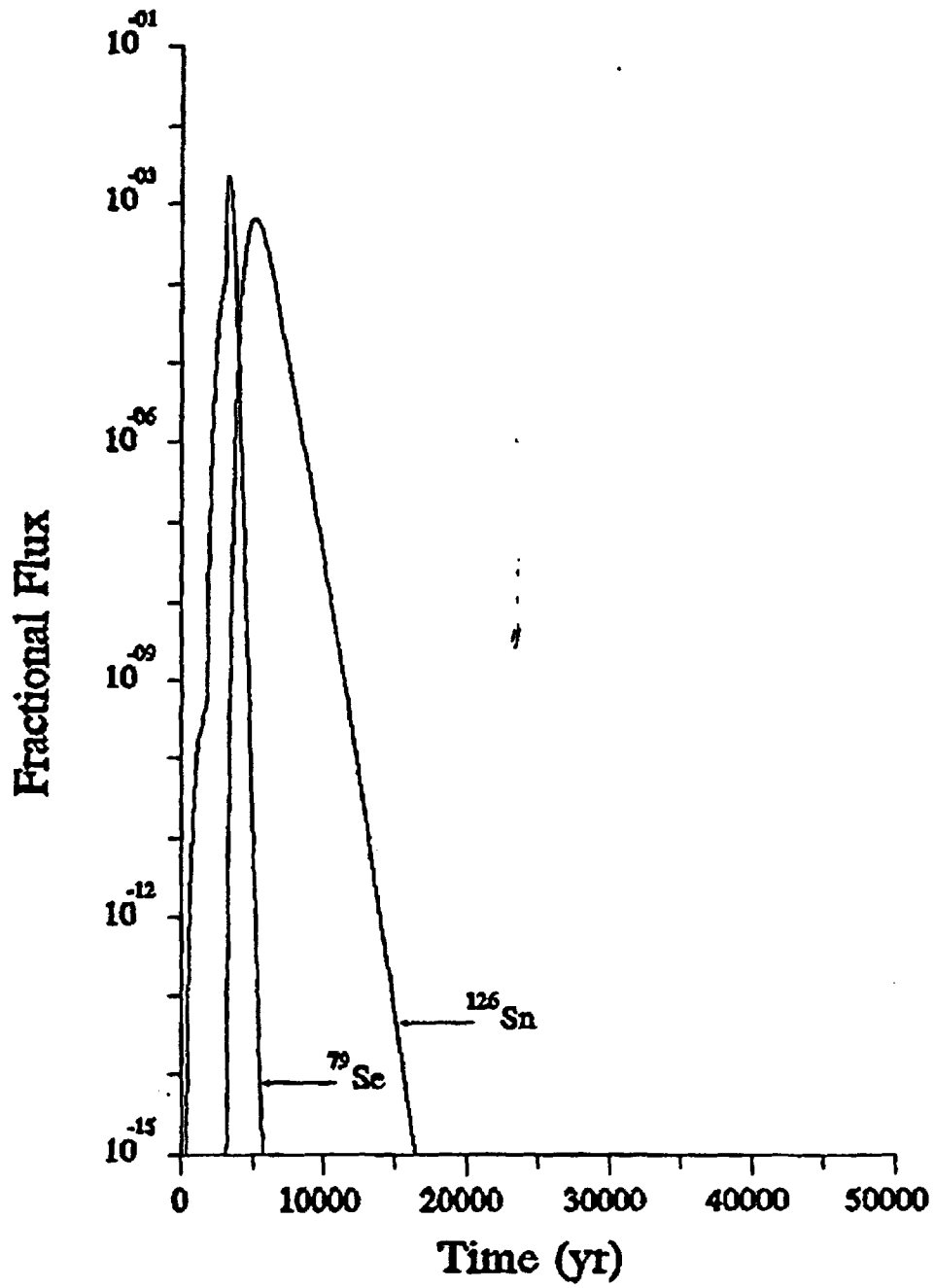


Fig. C.4-8. Fractional flux to the water table from the LAW vaults.

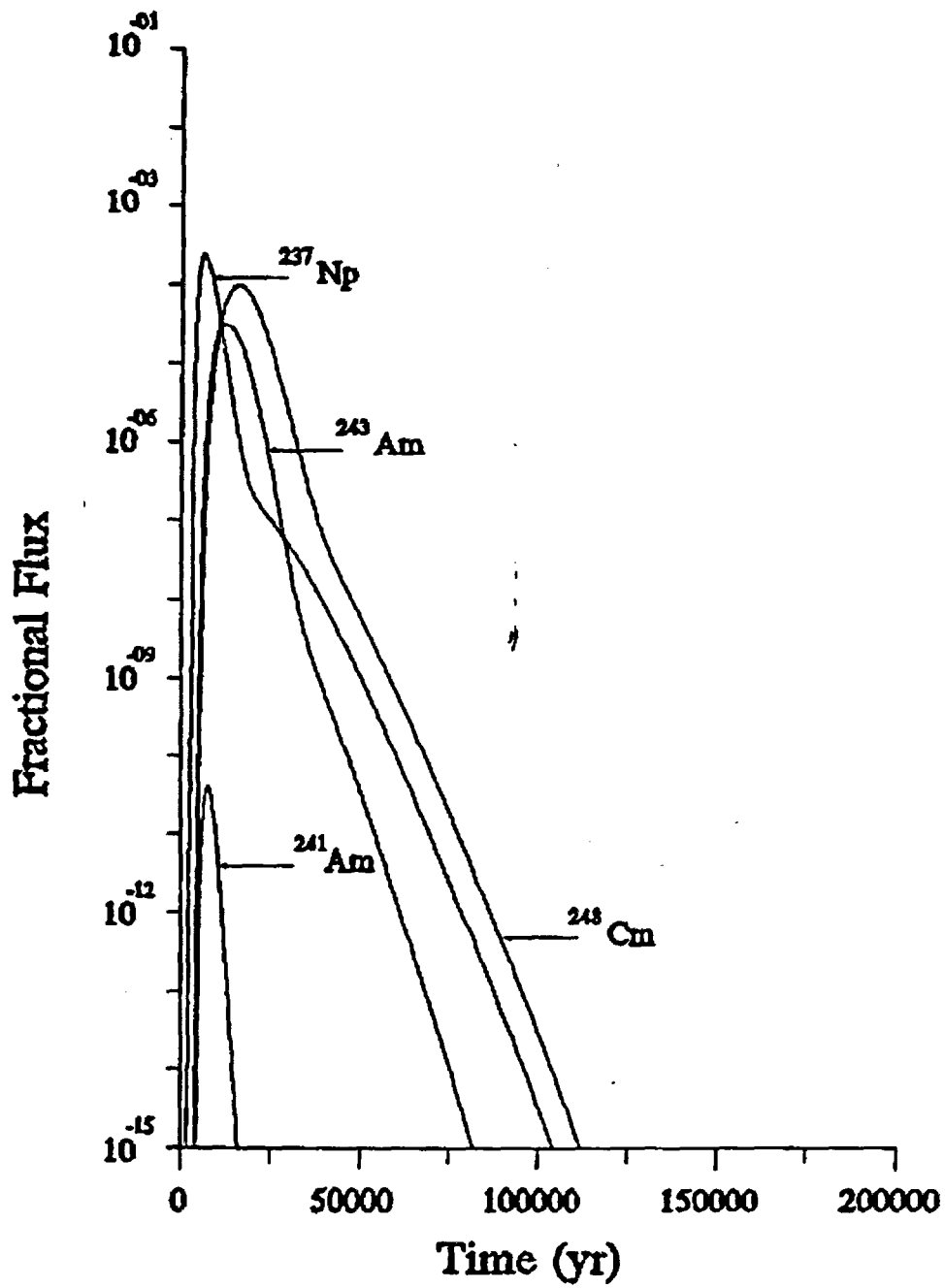


Fig. C.4-9. Fractional flux to the water table from the LAW vaults.

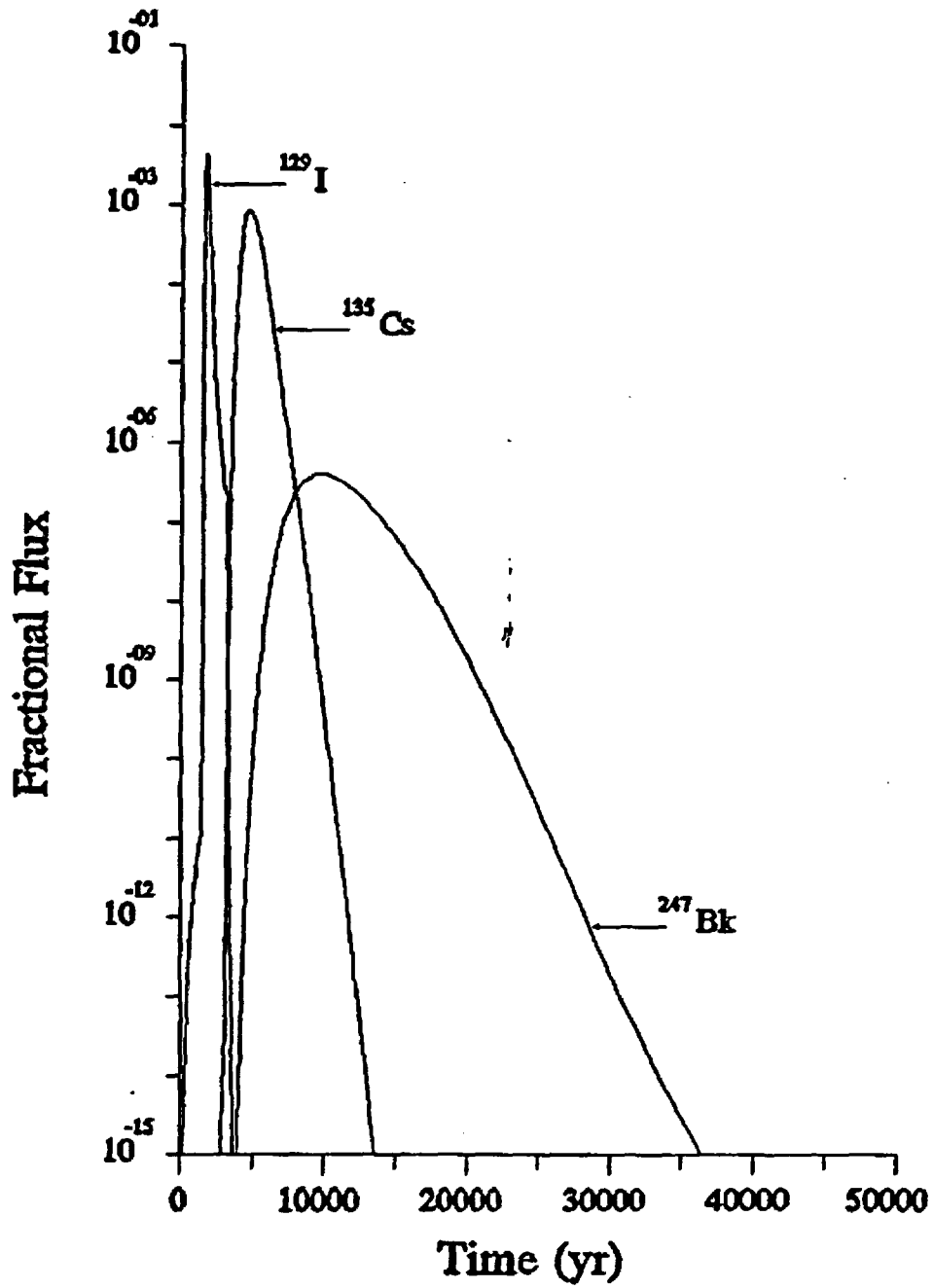


Fig. C.4-10. Fractional flux to the water table from the LAW vaults.

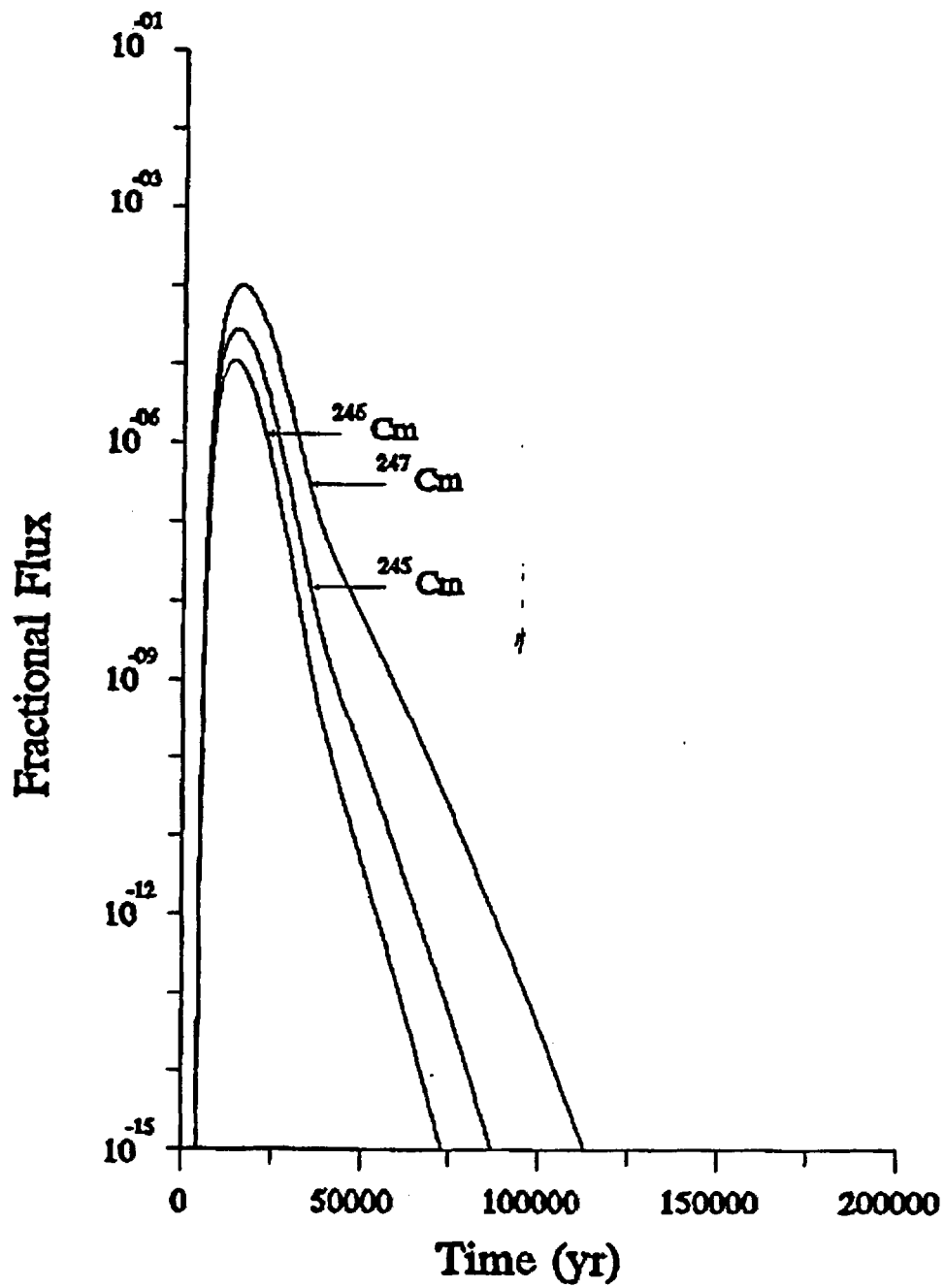


Fig. C4-11. Fractional flux to the water table from the LAW vaults.

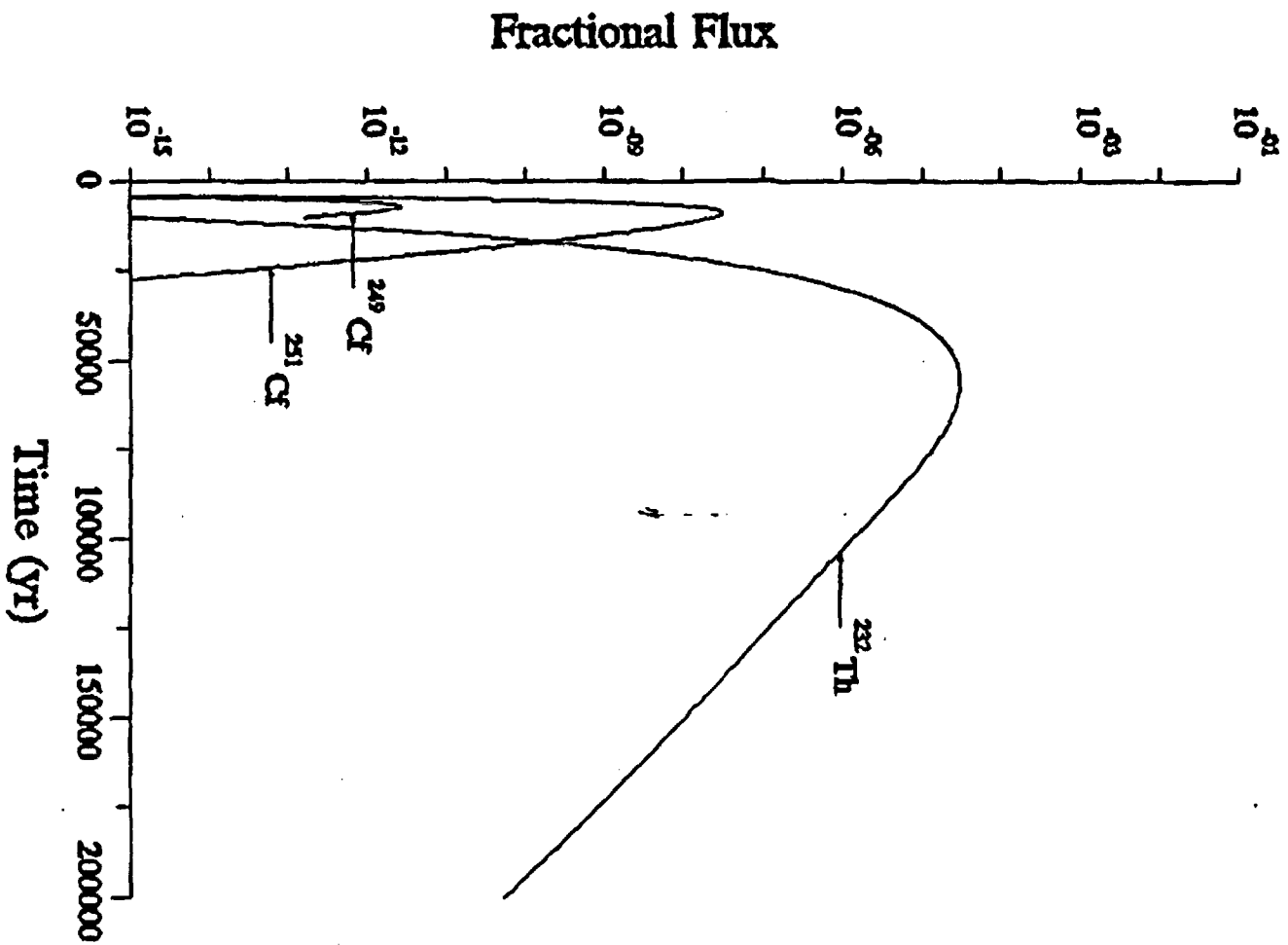
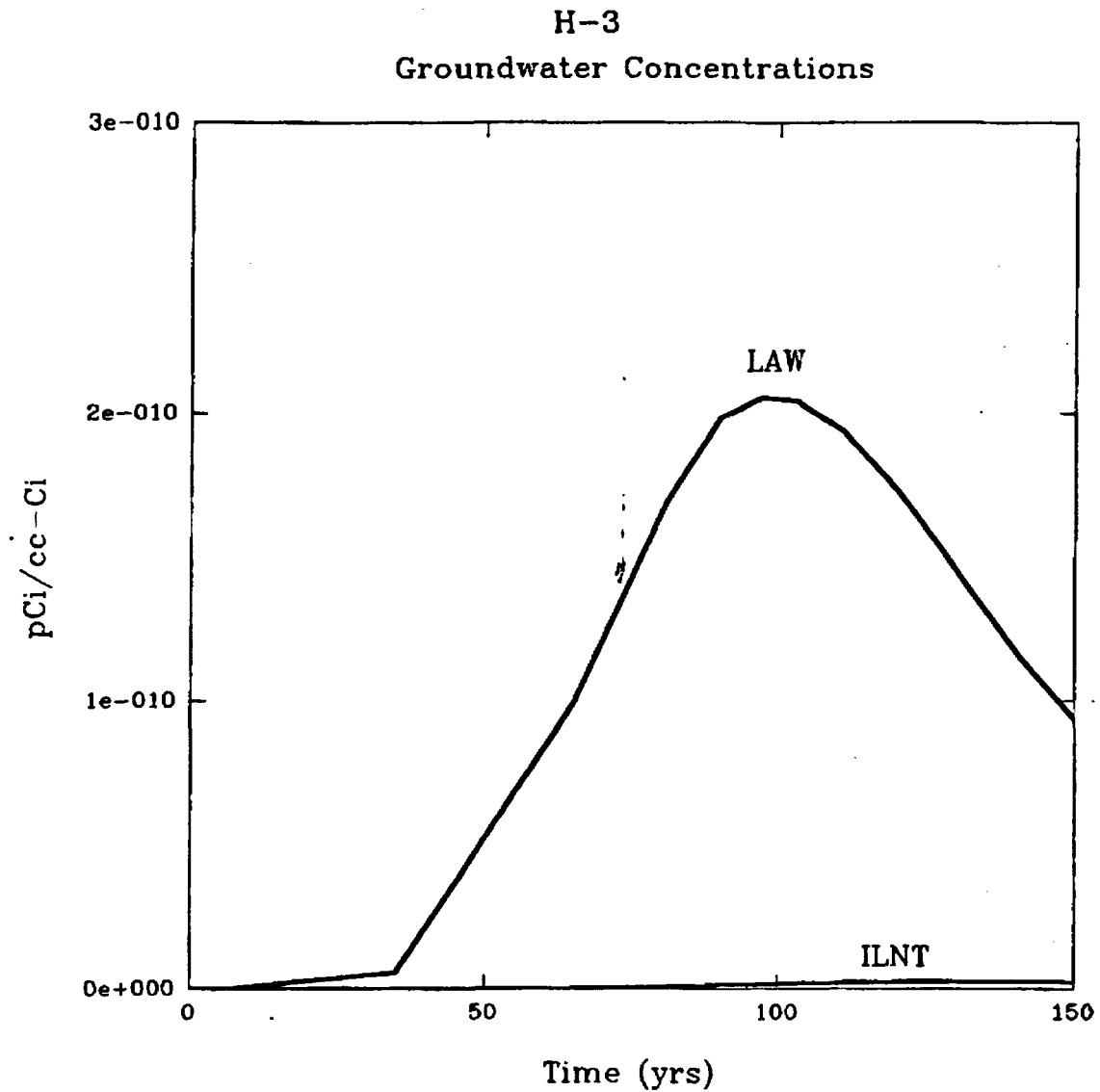


Fig. C-4-12. Fractional flux to the water table from the LAW vaults.

C.5 GROUNDWATER RESULTS

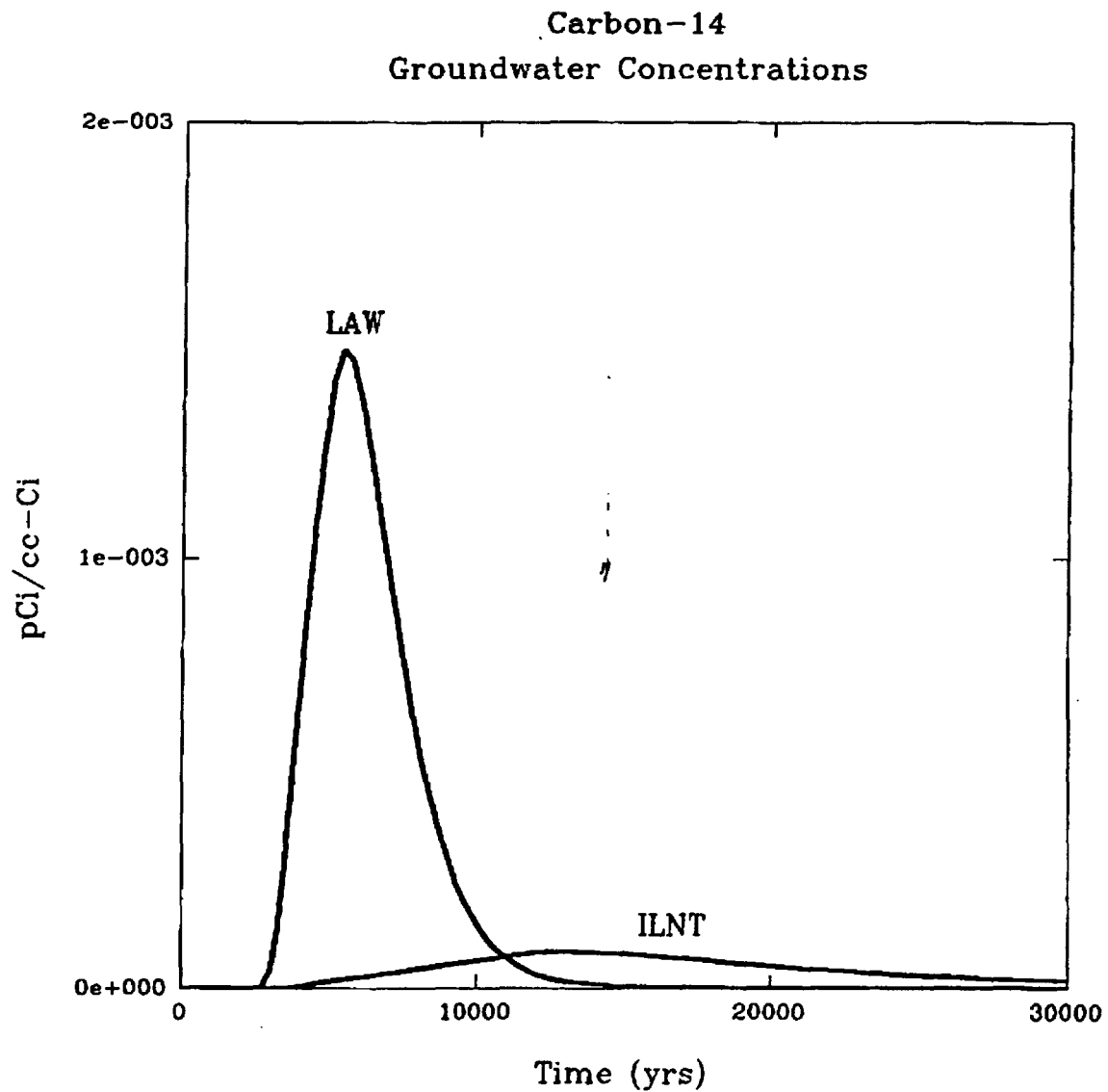
The fluxes given in Sect. C.4 were used in the groundwater transport simulations to estimate groundwater concentrations at the compliance point for groundwater protection. The groundwater concentrations are given in Figs. C.5-1 through C.5-31. The groundwater concentrations are given in units of concentration (pCi/cc) per Ci in each vault except for uranium and plutonium isotopes, which are solubility limited; for these isotopes, concentrations are given in units of pCi/cc.



	Peak Concentration	Time (yrs)
LAW	2.10 e-010	9.7 e+001
ILNT	2.70 e-012	1.30 e+002

h3.spg

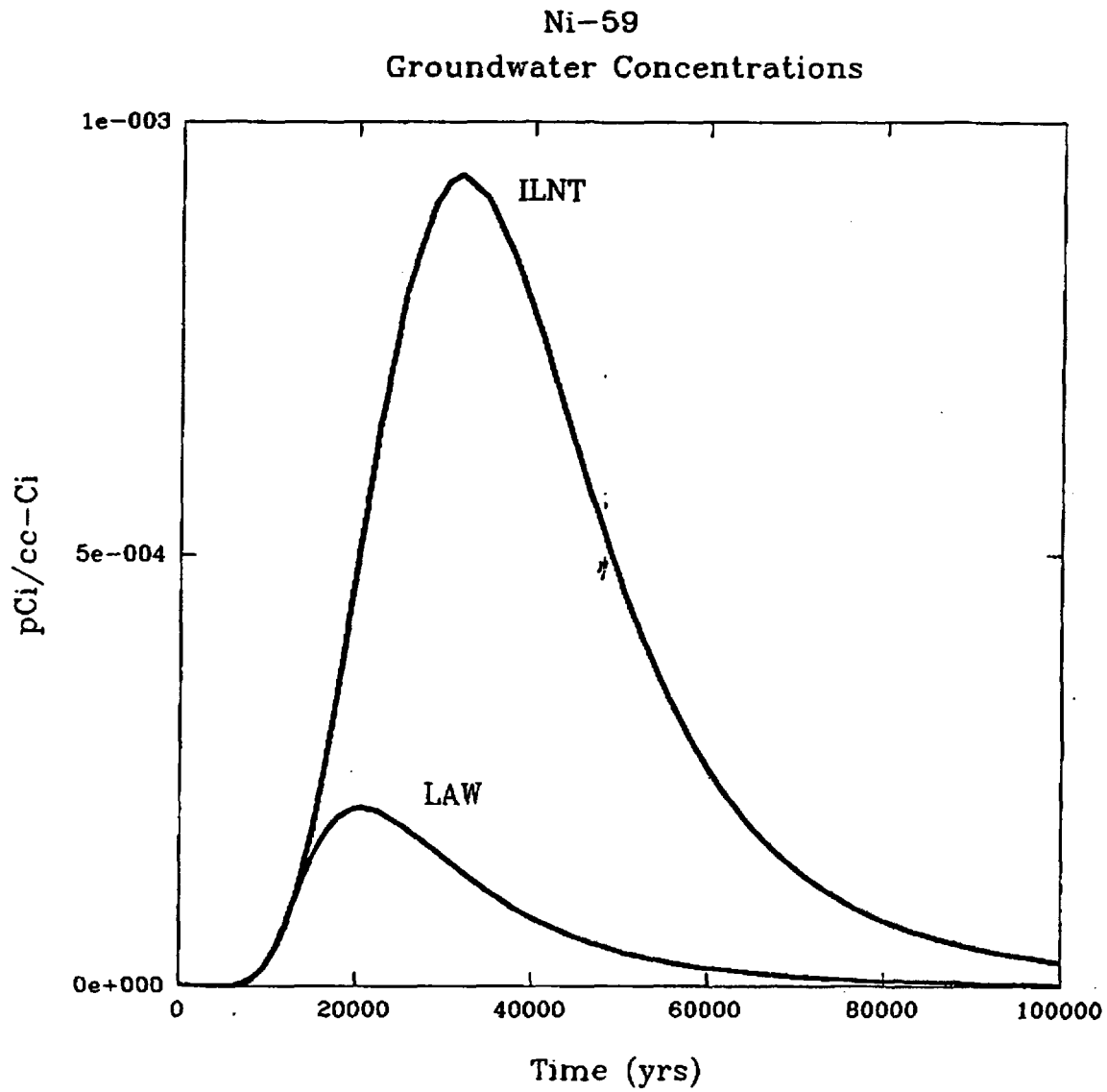
Fig. C.5-1. Predicted groundwater concentration of H-3 as a function of time.



	Peak Concentration	Time (yrs)
LAW	1.50 e-003	5.40 e+003
ILNT	8.70 e-005	1.20 e+004

c14.spg

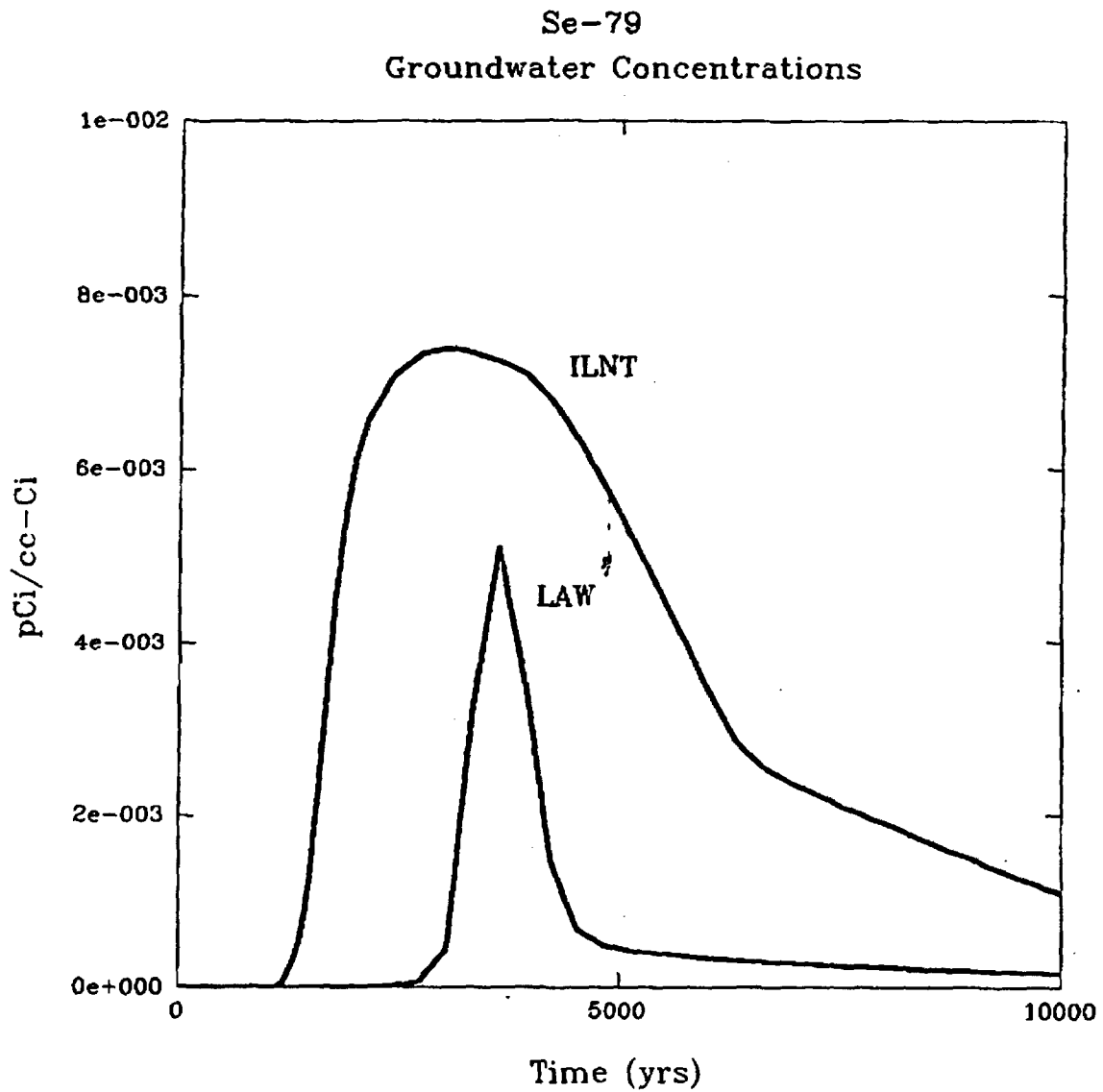
Fig. C.5-2. Predicted groundwater concentration of C-14 as a function of time.



	Peak Concentration	Time (yrs)
LAW	2.10 e-004	2.10 e+004
ILNT	9.4 e-004	3.20 e+004

ni59.spg

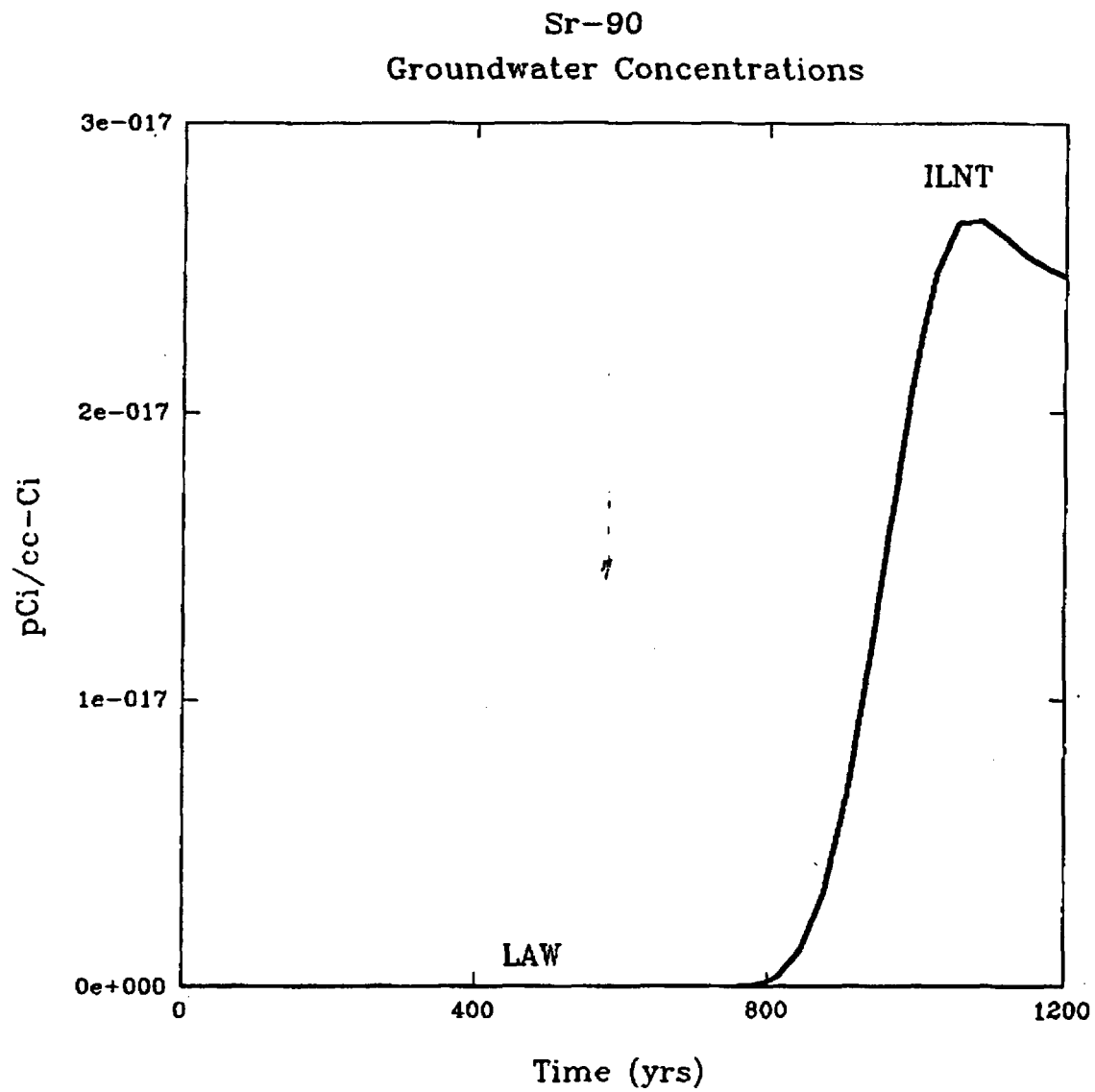
Fig. C5-3. Predicted groundwater concentration of Ni-59 as a function of time.



	Peak Concentration	Time (yrs)
LAW	5.10 e-003	3.60 e+003
ILNT	7.40 e-003	3.00 e+003

se79.spg

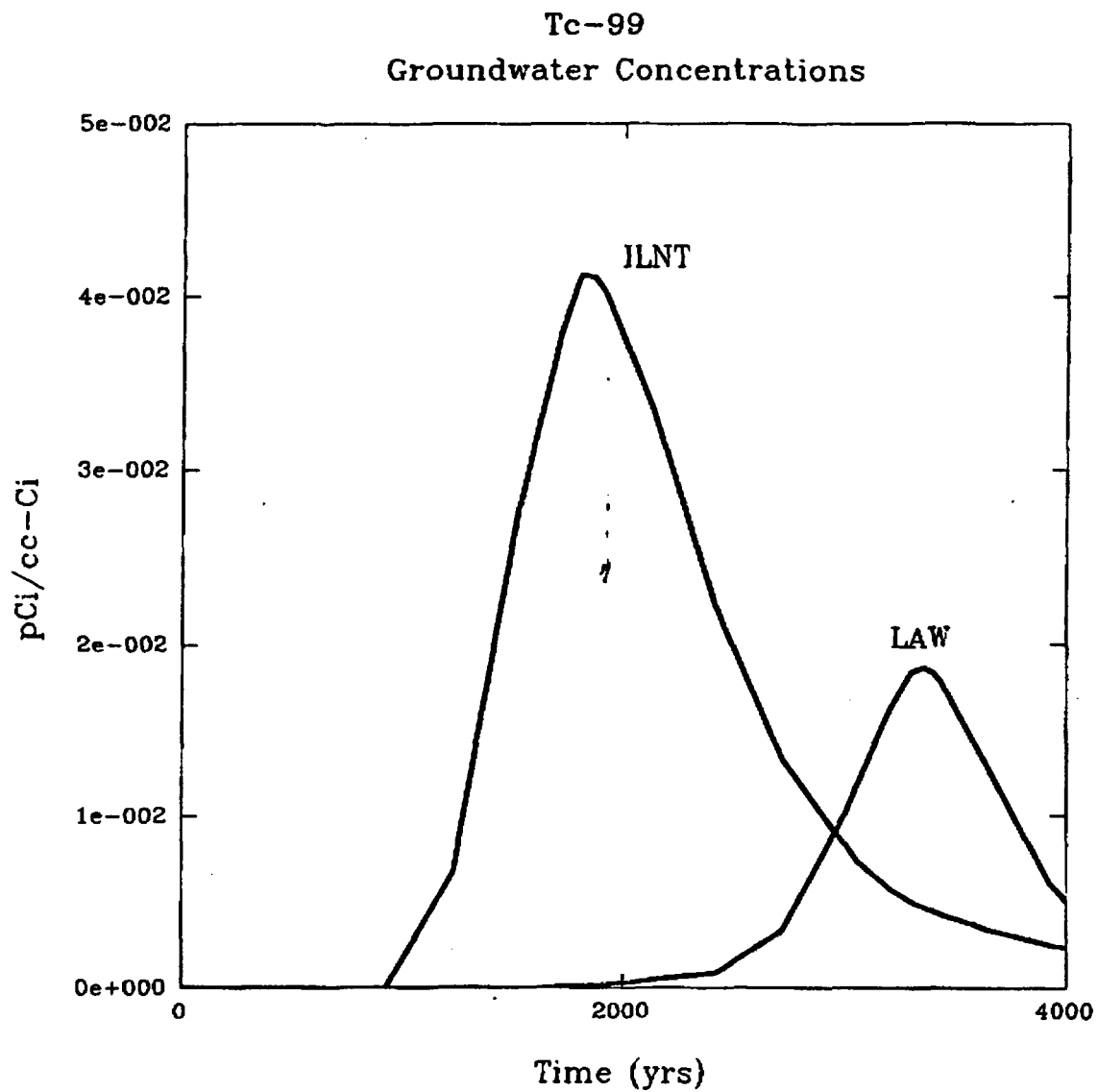
Fig. C.5-4. Predicted groundwater concentration of Se-79 as a function of time.



	Peak Concentration	Time (yrs)
LAW	1.50 e-022	5.20 e+002
ILNT	2.70 e-017	1.10 e+003

sr90.spg

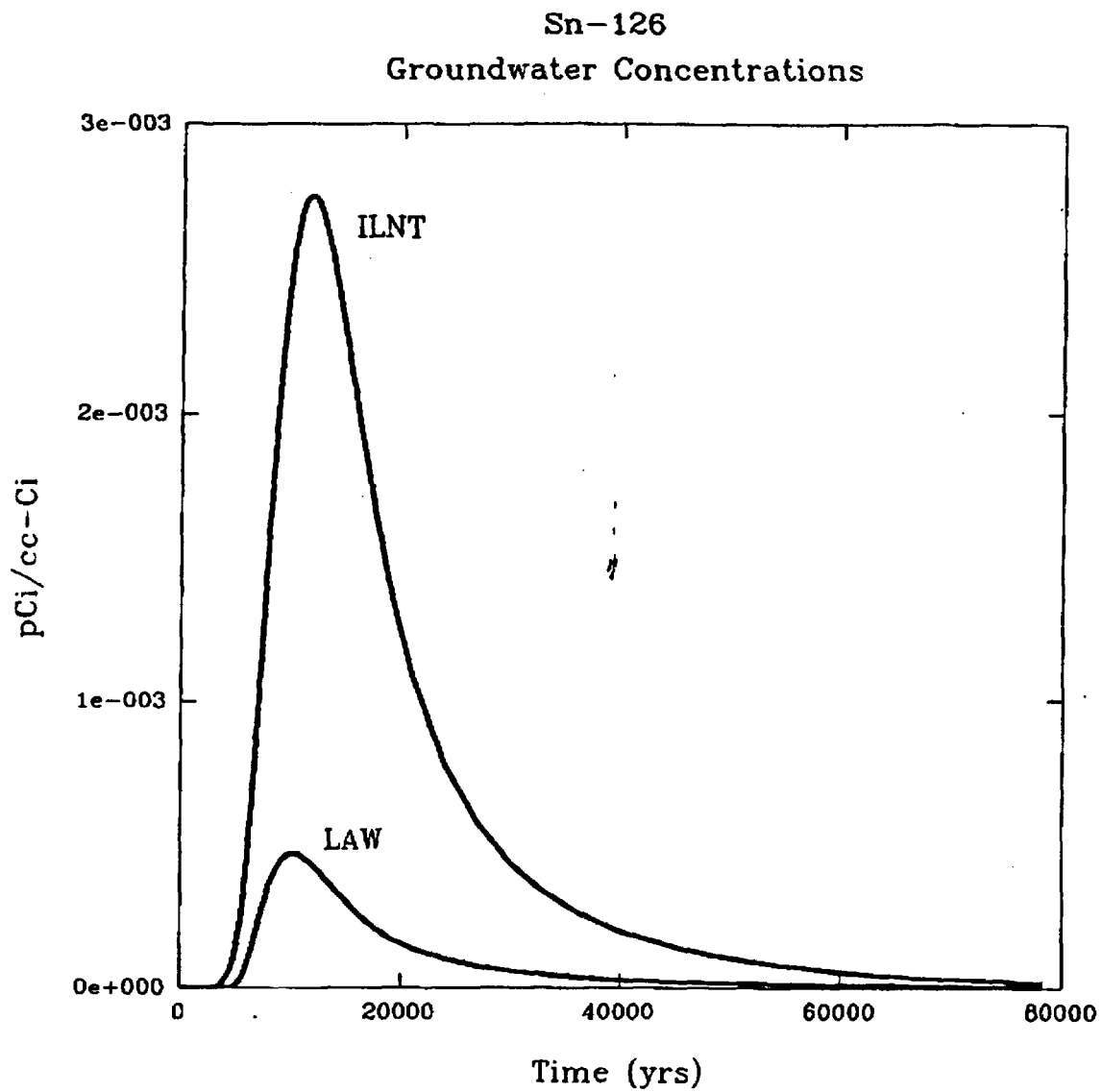
Fig. C.5-5. Predicted groundwater concentration of Sr-90 as a function of time.



	Peak Concentration	Time (yrs)
LAW	1.90 e-002	3.30 e+003
ILNT	4.10 e-002	1.80 e+003

tc99.spg

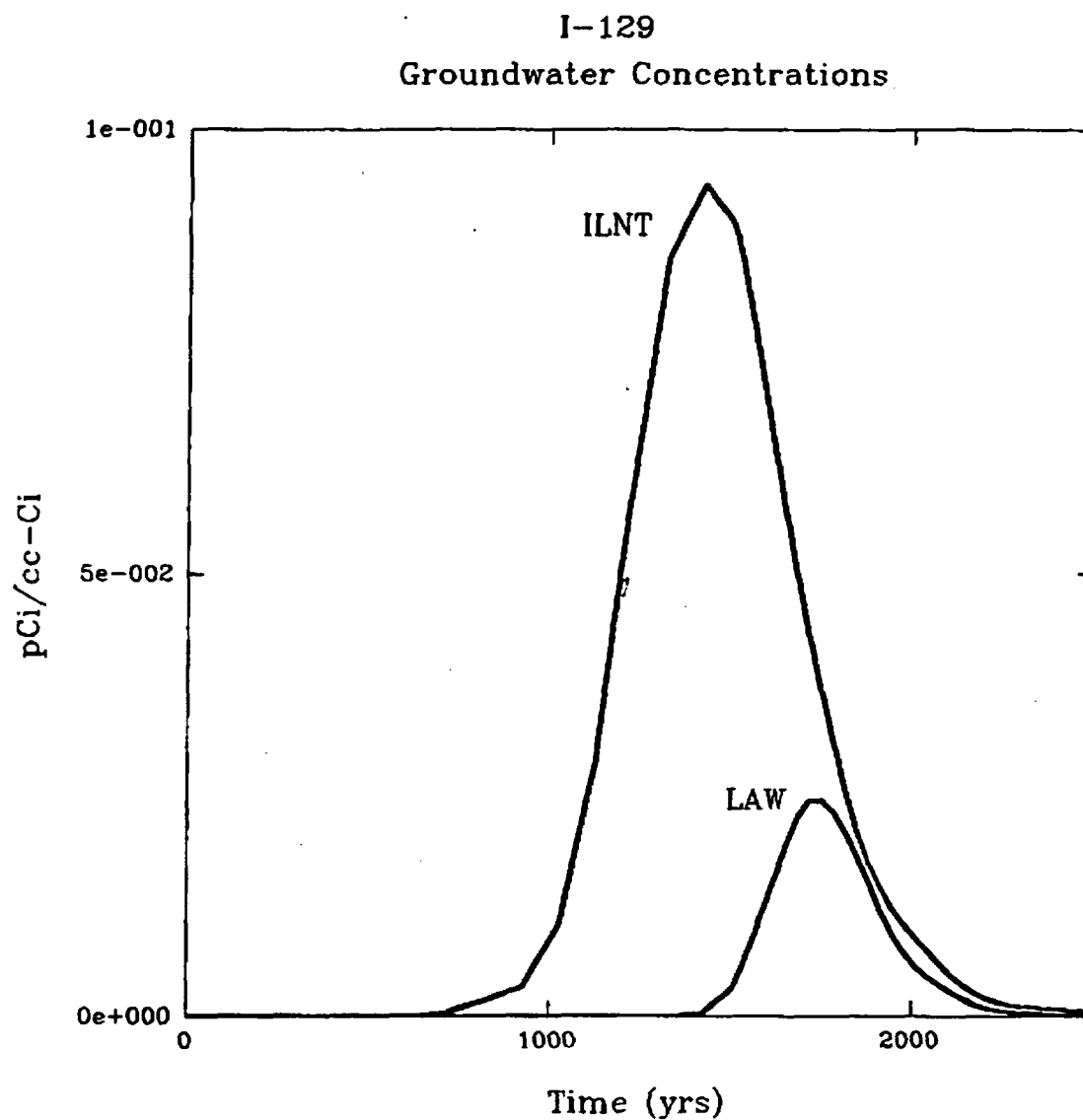
Fig. C.5-6. Predicted groundwater concentration of Tc-99 as a function of time.



	Peak Concentration	Time (yrs)
LAW	4.70 e-004	1.00 e+004
ILNT	2.80 e-003	1.20 e+004

sn126.spg

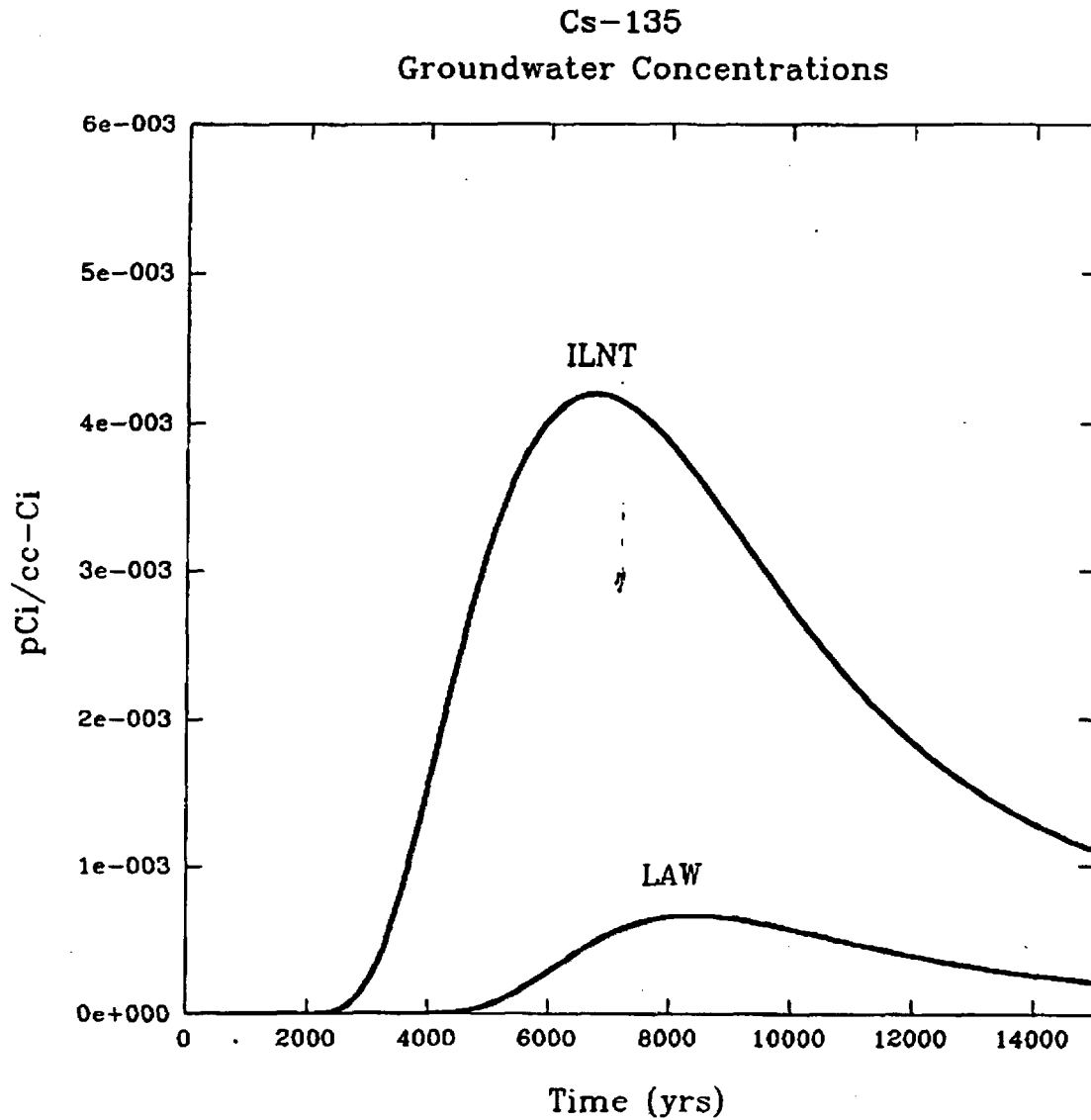
Fig. C.5-7. Predicted groundwater concentration of Sn-126 as a function of time.



	Peak Concentration	Time (yrs)
LAW	2.40 e-002	1.70 e+003
ILNT	9.40 e-002	1.40 e+003

i129.spg

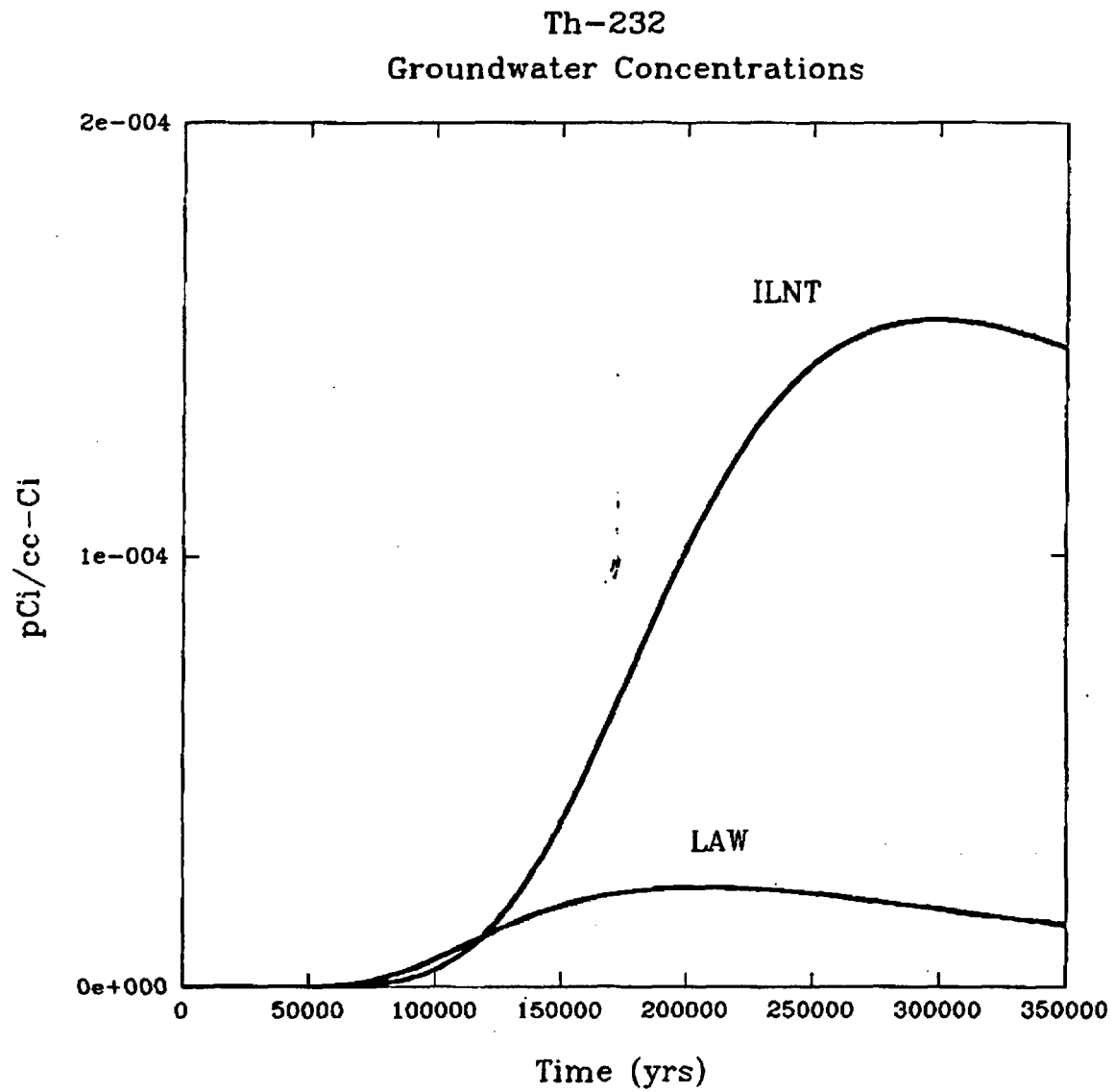
Fig. C.5-8. Predicted groundwater concentration of I-129 as a function of time.



	Peak Concentration	Time (yrs)
LAW	6.70 e-004	8.40 e+003
ILNT	4.20 e-003	6.70 e+003

cs135.spg

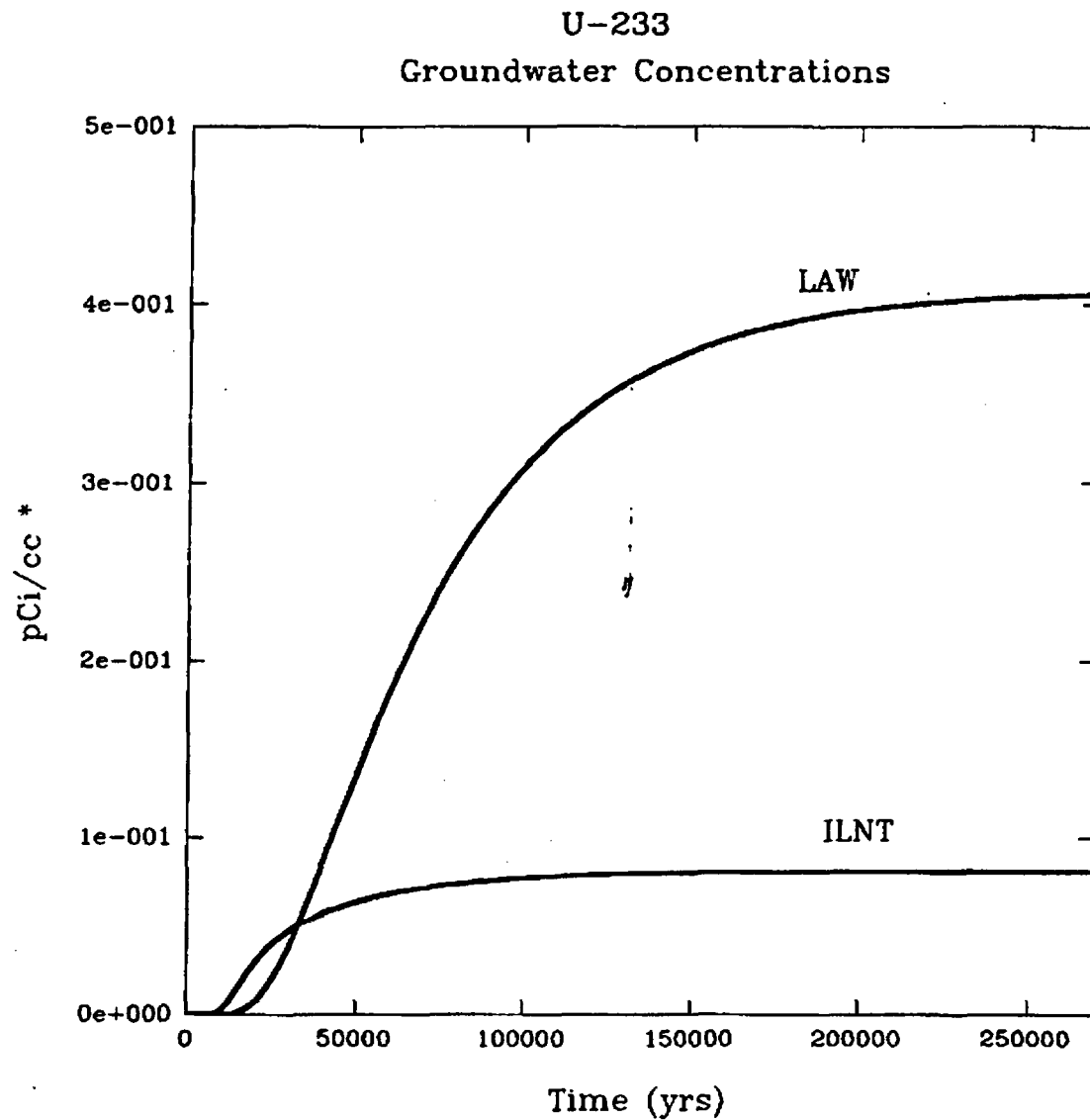
Fig. C.5-9. Predicted groundwater concentration of Cs-135 as a function of time.



	Peak Concentration	Time (yrs)
LAW	2.30 e-005	2.10 e+005
ILNT	1.50 e-004	3.00 e+005

th232.spg

Fig. C.5-10. Predicted groundwater concentration of Th-232 as a function of time.

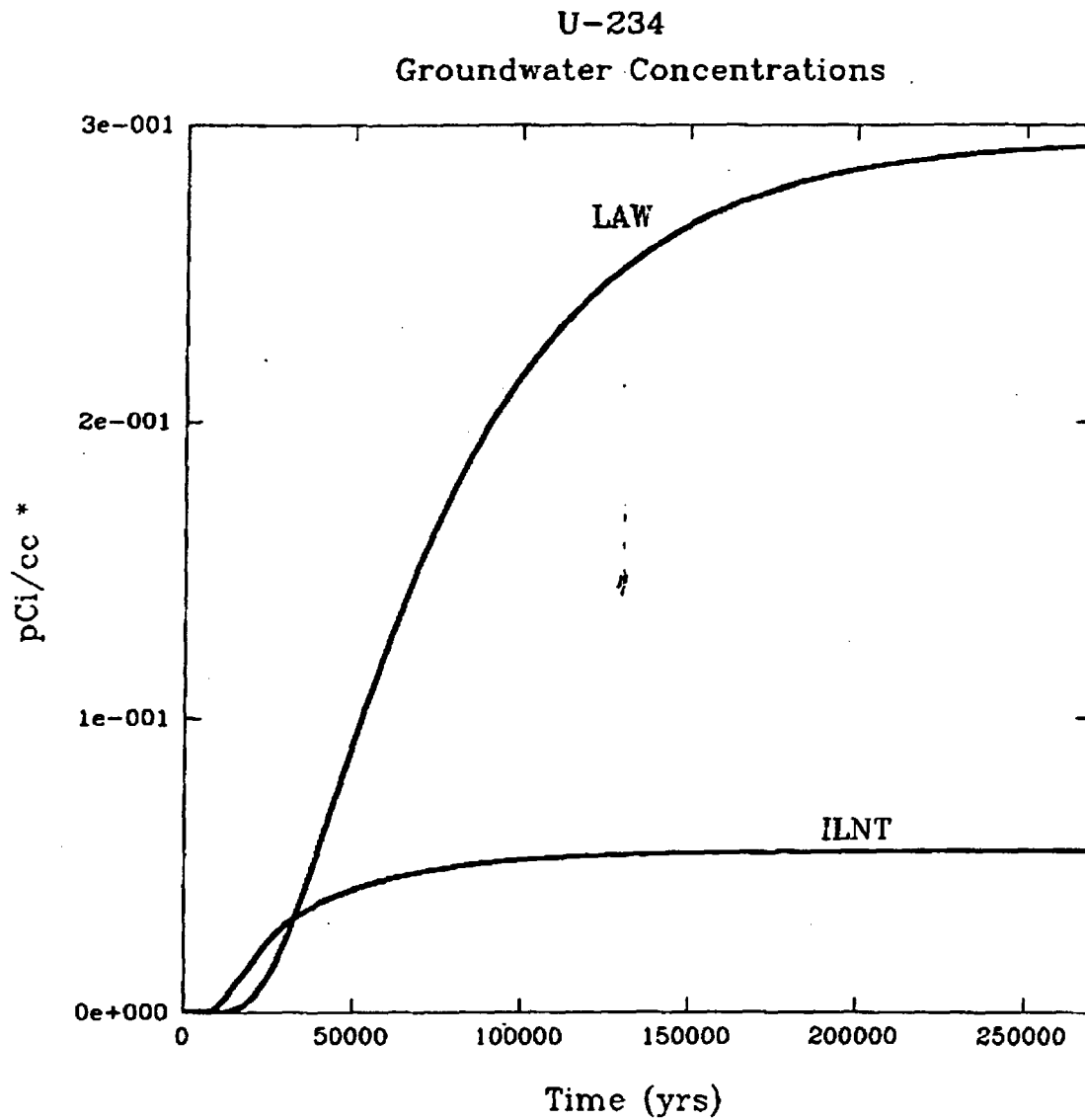


	Peak Concentration	Time (yrs)
LAW	4.10 e-001	2.61 e+005
ILNT	8.10 e-002	1.62 e+005

* Based on 10,000 kg U-233 per vault

u233.spg

Fig. C.5-11. Predicted groundwater concentration of U-233 as a function of time.

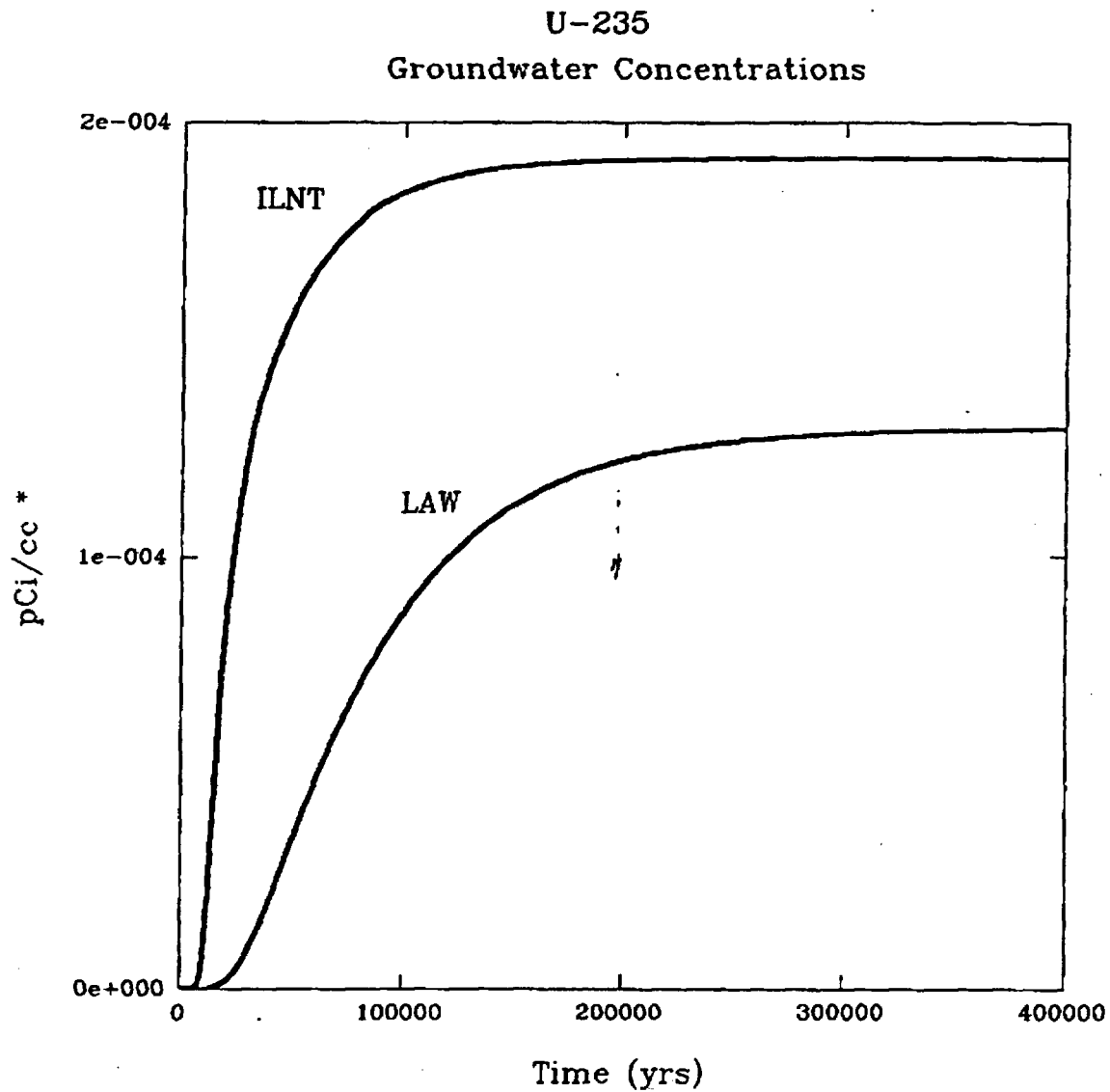


	Peak Concentration	Time (yrs)
LAW	2.90 e-001	2.01 e+005
ILNT	5.50 e-002	1.53 e+005

* Based on 10,000 kg U-234 per vault

u234.spg

Fig. C.5-12. Predicted groundwater concentration of U-234 as a function of time.

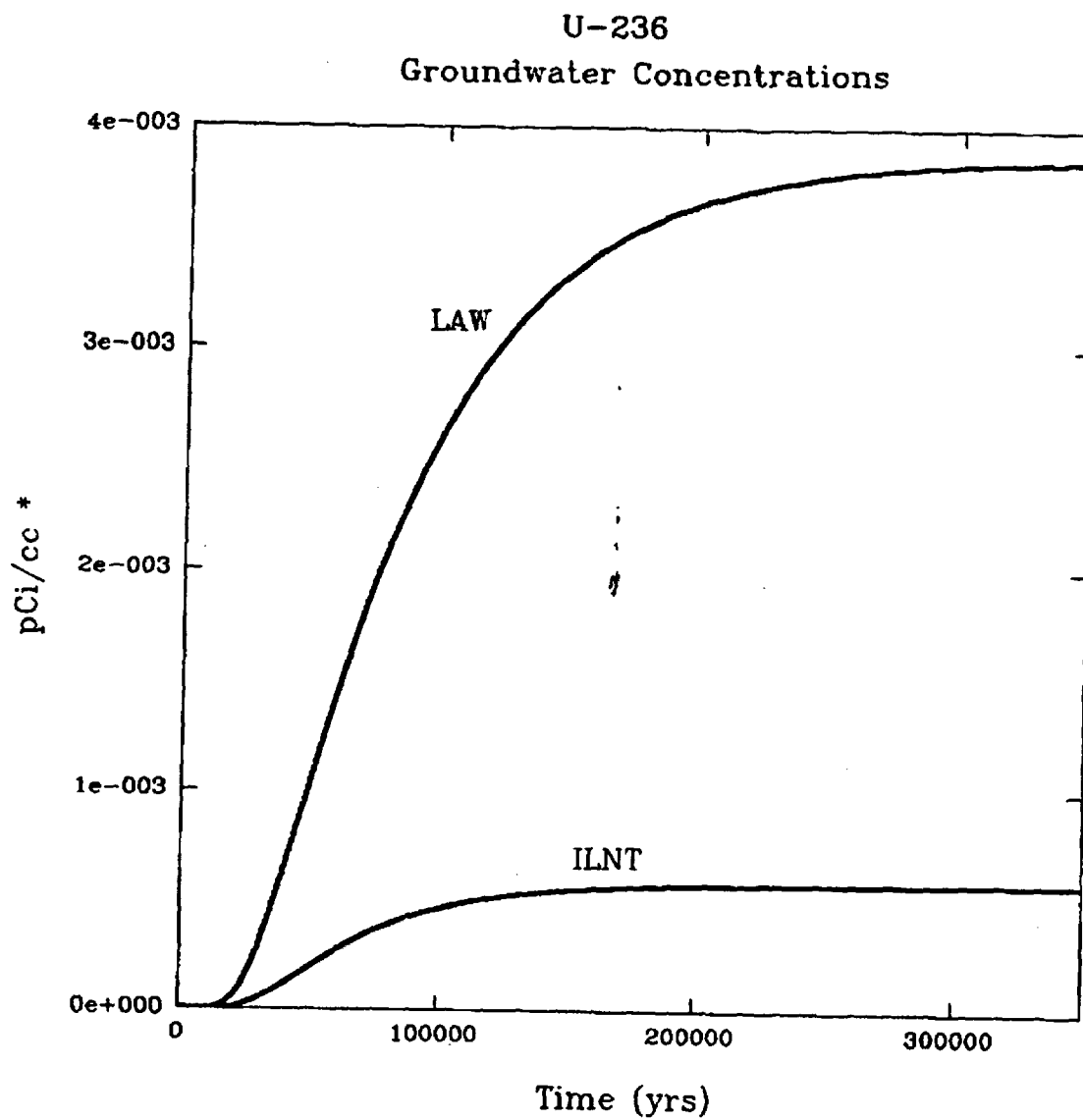


	Peak Concentration	Time (yrs)
LAW	1.30 e-004	2.30 e+005
ILNT	1.90 e-004	1.10 e+005

* Based on 10,000 kg U-235 per vault

U235.SPG

Fig. C.5-13. Predicted groundwater concentration of U-235 as a function of time.

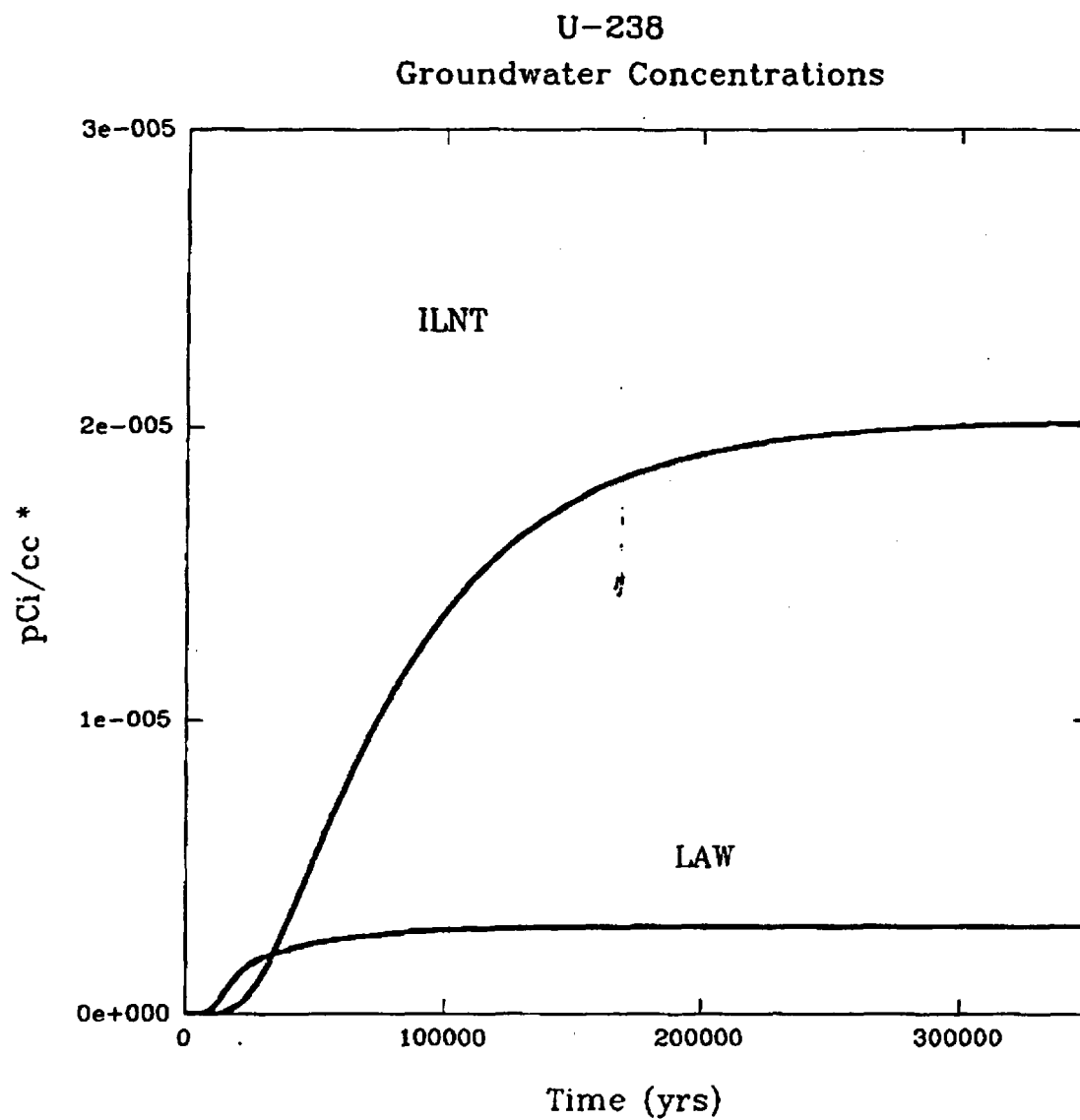


	Peak Concentration	Time (yrs)
LAW	3.90 e-003	3.24 e+005
ILNT	5.80 e-004	2.28 e+005

* Based on 10.000 kg U-236 per vault

u236.spg

Fig. C.5-14. Predicted groundwater concentration of U-236 as a function of time.

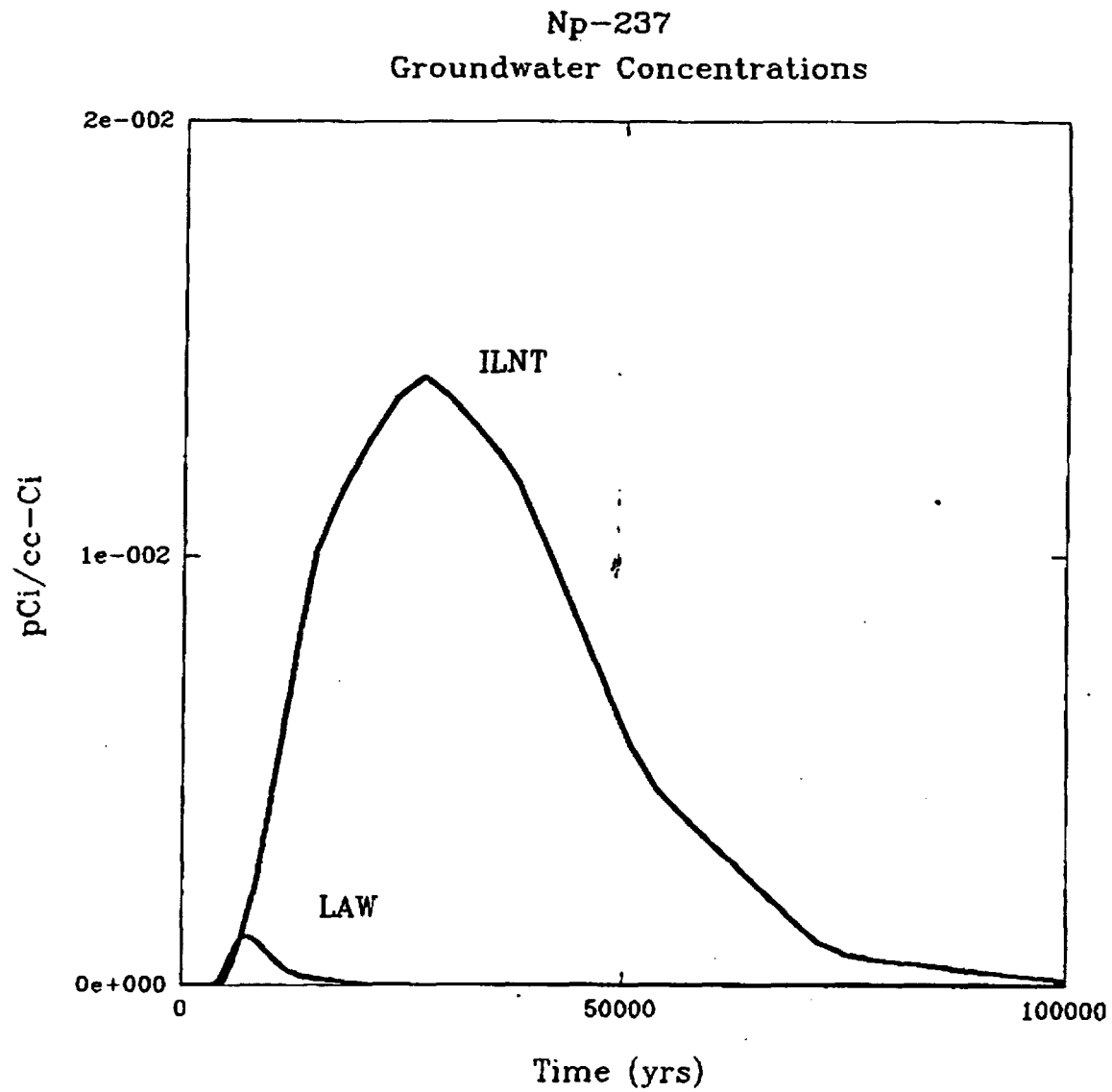


	Peak Concentration	Time (yrs)
LAW	2.00 e-005	2.31 e+005
ILNT	3.00 e-006	1.44 e+005

* Based on 10,000 kg U-238 per vault

u238.spg

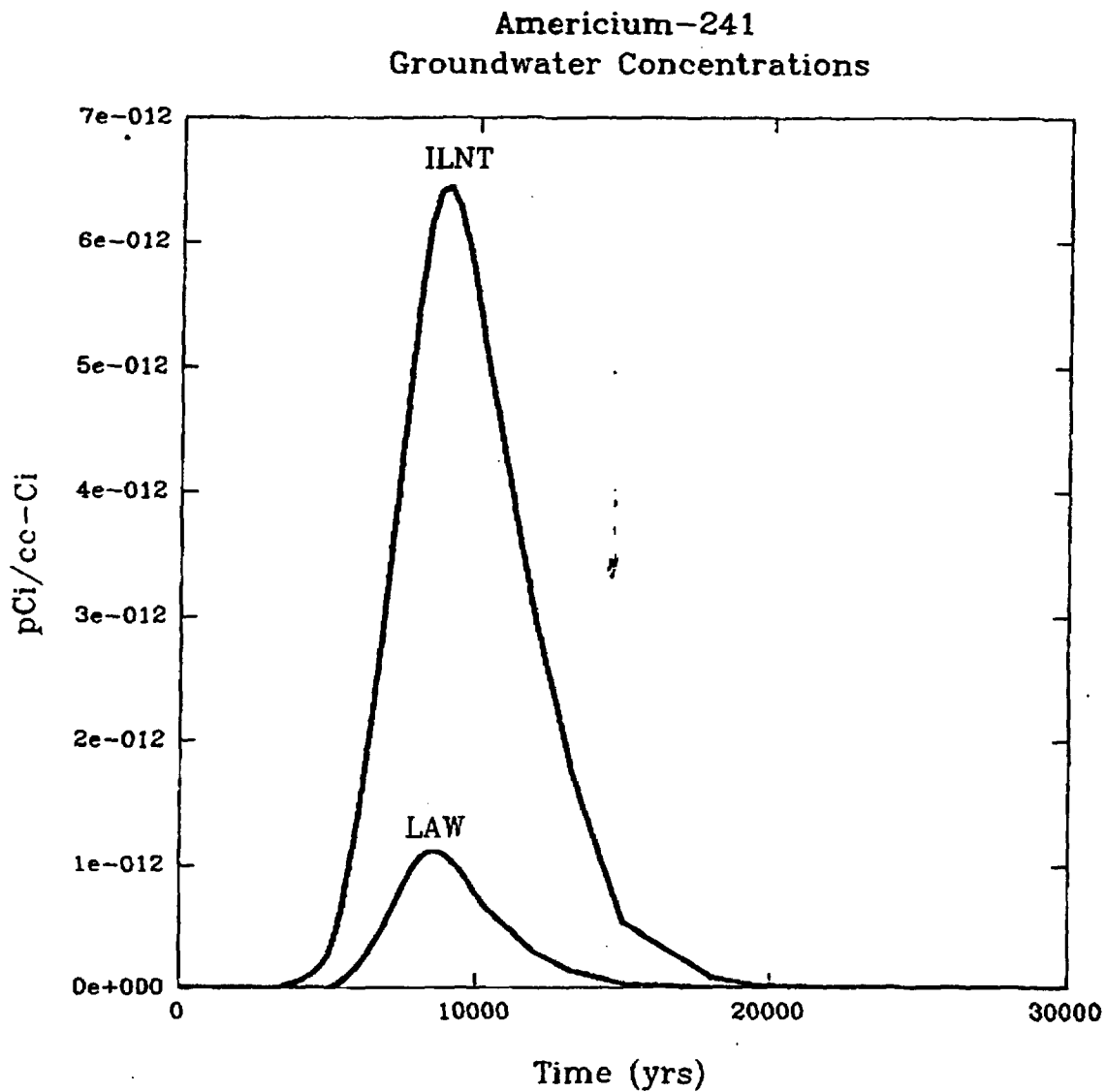
Fig. C-5-15. Predicted groundwater concentration of U-238 as a function of time.



	Peak Concentration	Time (yrs)
LAW	1.60 e-003	1.00 e+004
ILNT	1.40 e-002	2.70 e+004

np237.spg

Fig. C.5-16. Predicted groundwater concentration of Np-237 as a function of time.

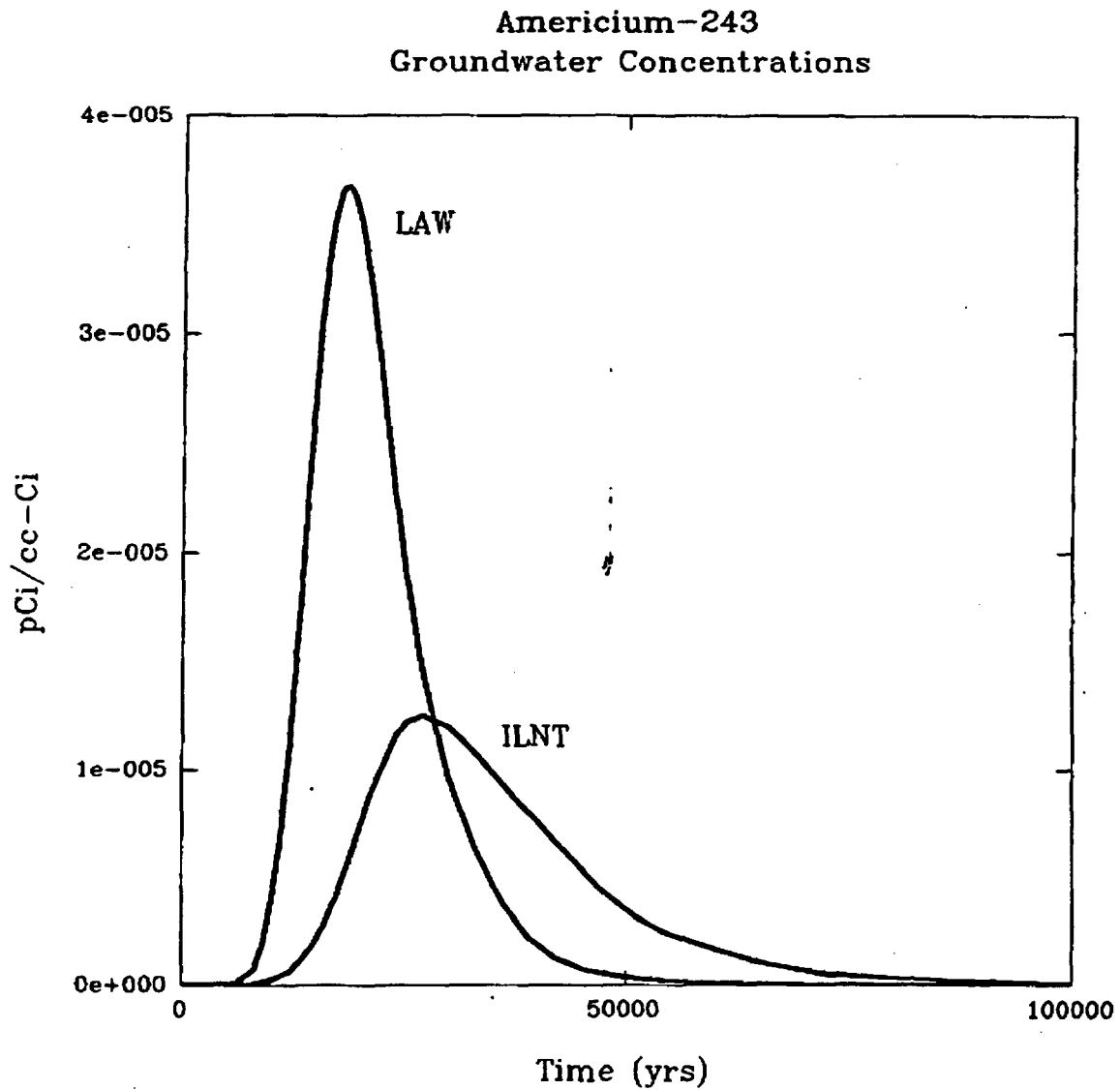


	Peak Concentration	Time (yrs)
LAW	1.10 e-012	8.70 e+003
ILNT	6.40 e-012	9.00 e+003

* Without radioactive daughter contributions.

am241.spg

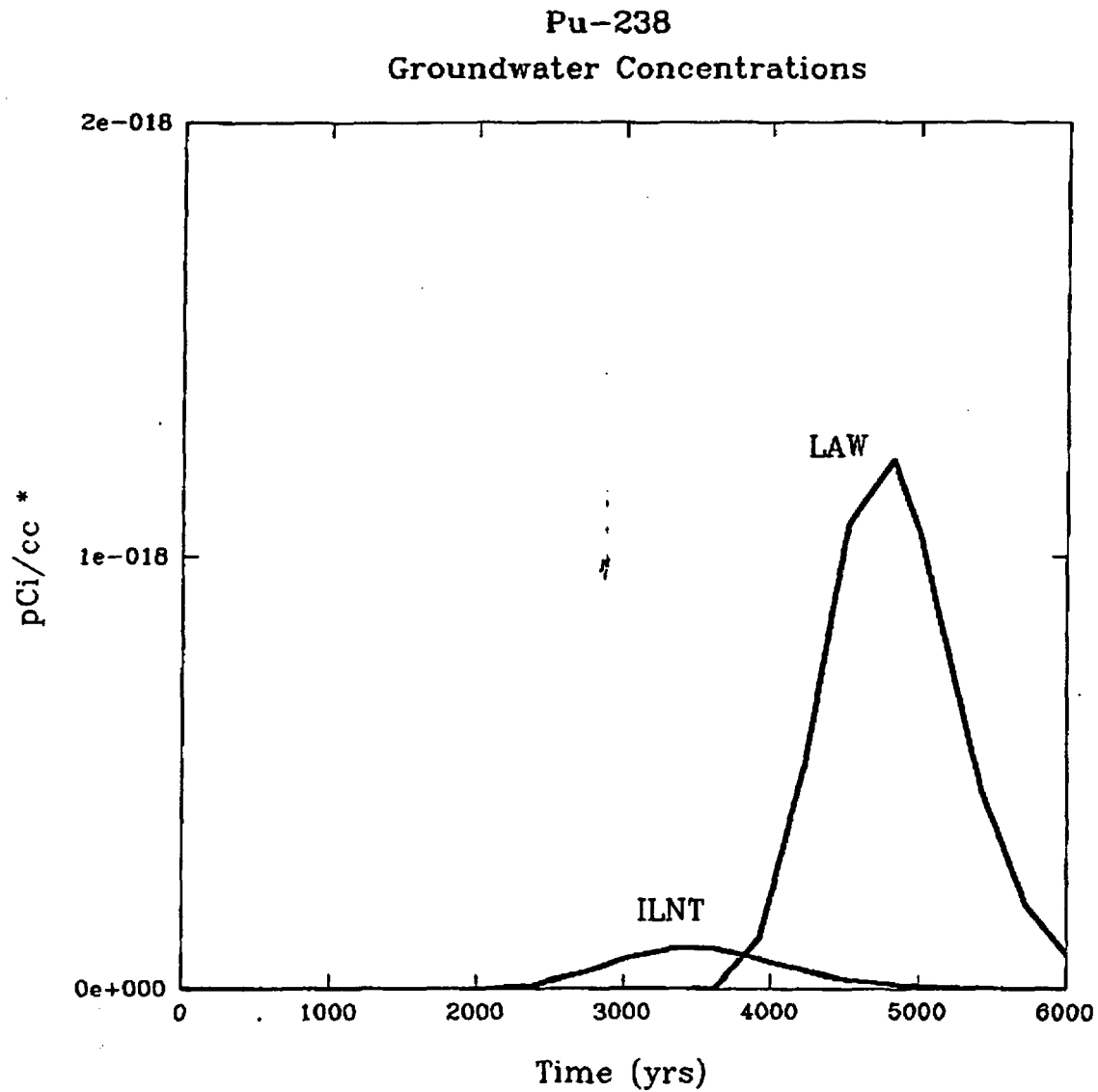
Fig. C5-17. Predicted groundwater concentration of Am-241 as a function of time.



	Peak Concentration	Time (yrs)
LAW	3.70 e-005	1.80 e+004
ILNT	1.20 e-005	2.70 e+004

am243.spg

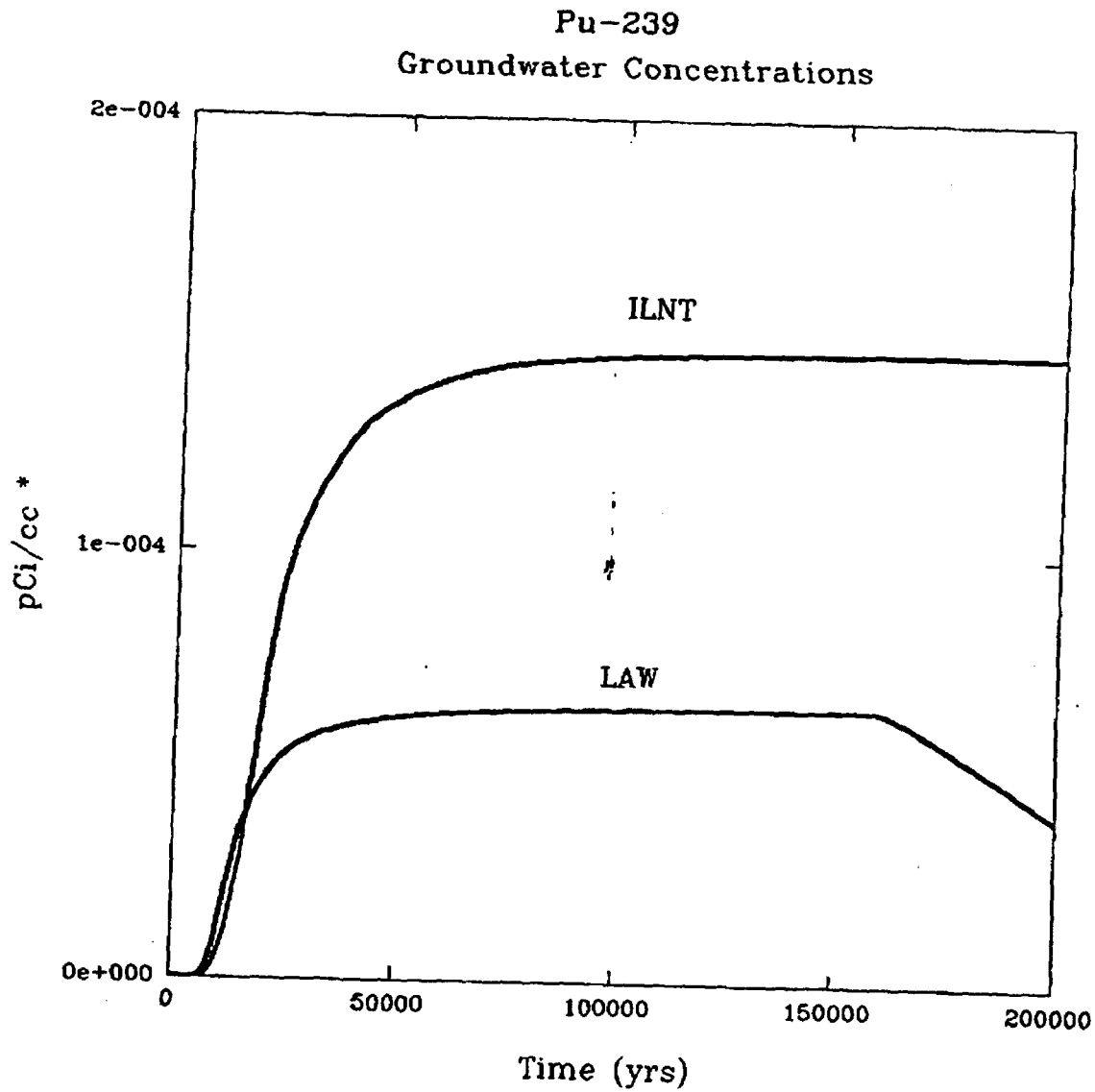
Fig. C.5-18. Predicted groundwater concentration of Am-243 as a function of time.



	Peak Concentration	Time (yrs)
LAW	1.20 e-018	4.83 e+003
ILNT	9.70 e-020	3.33 e+003

* Based on 150 Ci Pu-238 per vault

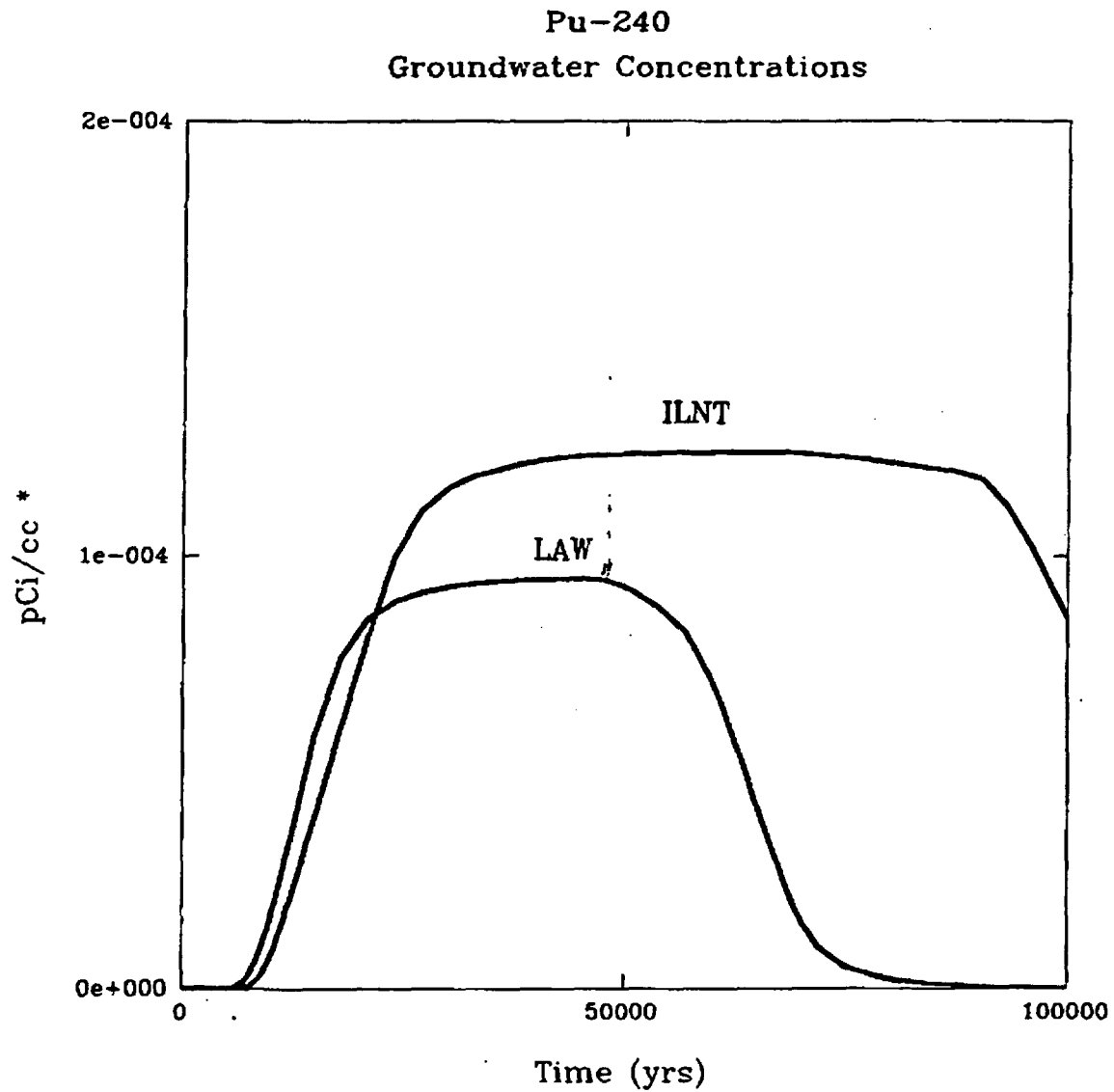
Fig. C.5-19. Predicted groundwater concentration of Pu-238 as a function of time. pu238.spg



	Peak Concentration	Time (yrs)
LAW	6.40 e-005	1.60 e+005
ILNT	1.50 e-004	2.20 e+005

* Based on 150 Ci Pu-239 per vault

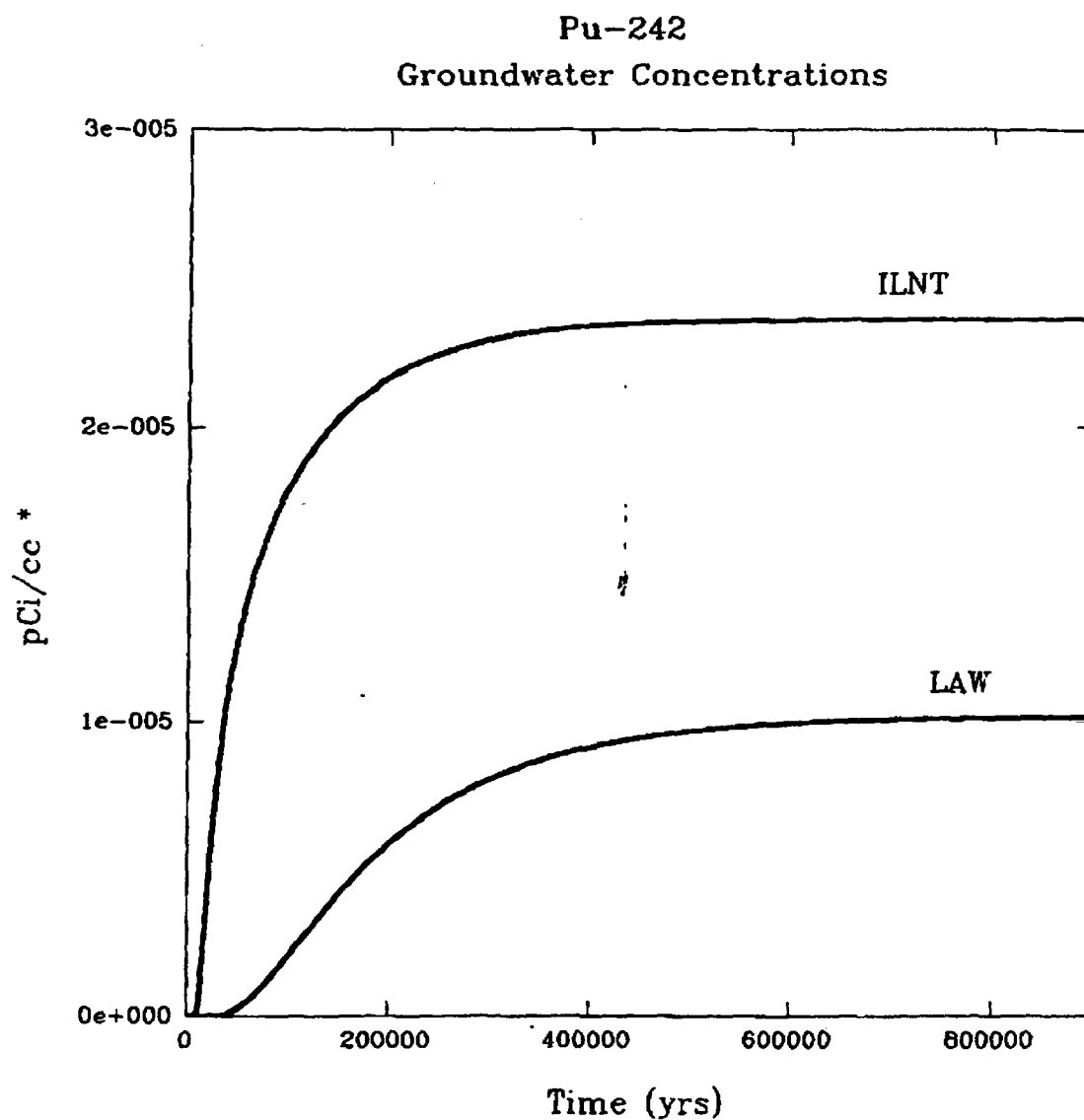
Fig. C.5-20. Predicted groundwater concentration of Pu-239 as a function of time.



	Peak Concentration	Time (yrs)
LAW	9.50 e-005	4.50 e+004
ILNT	1.20 e-004	6.60 e+004

* Based on 150 Ci Pu-240 per vault

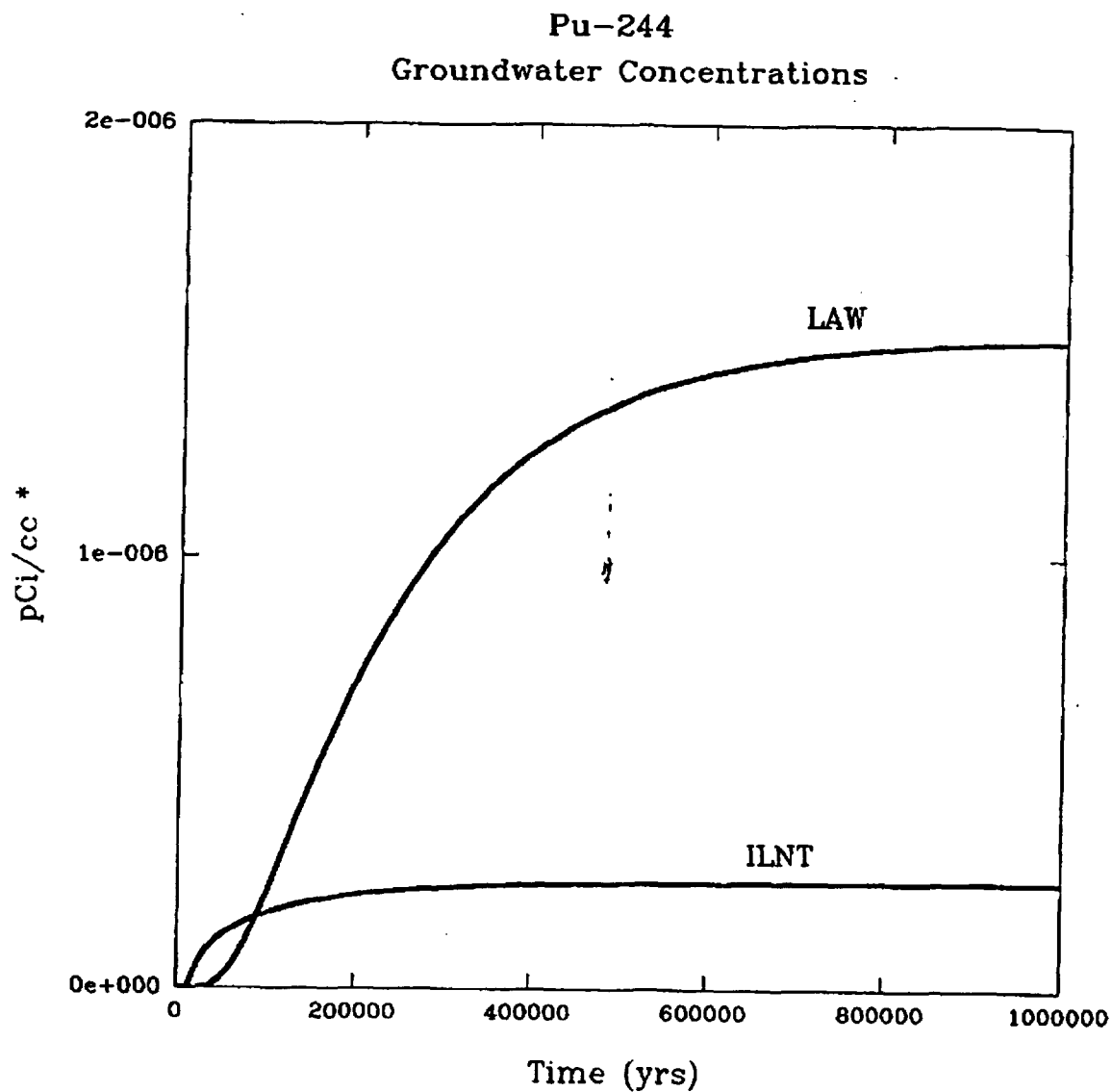
Fig. C.5-21. Predicted groundwater concentration of Pu-240 as a function of time.



	Peak Concentration	Time (yrs)
LAW	1.00 e-005	6.15 e+005
ILNT	2.40 e-005	4.98 e+005

* Based on 150 Ci Pu-242 per vault

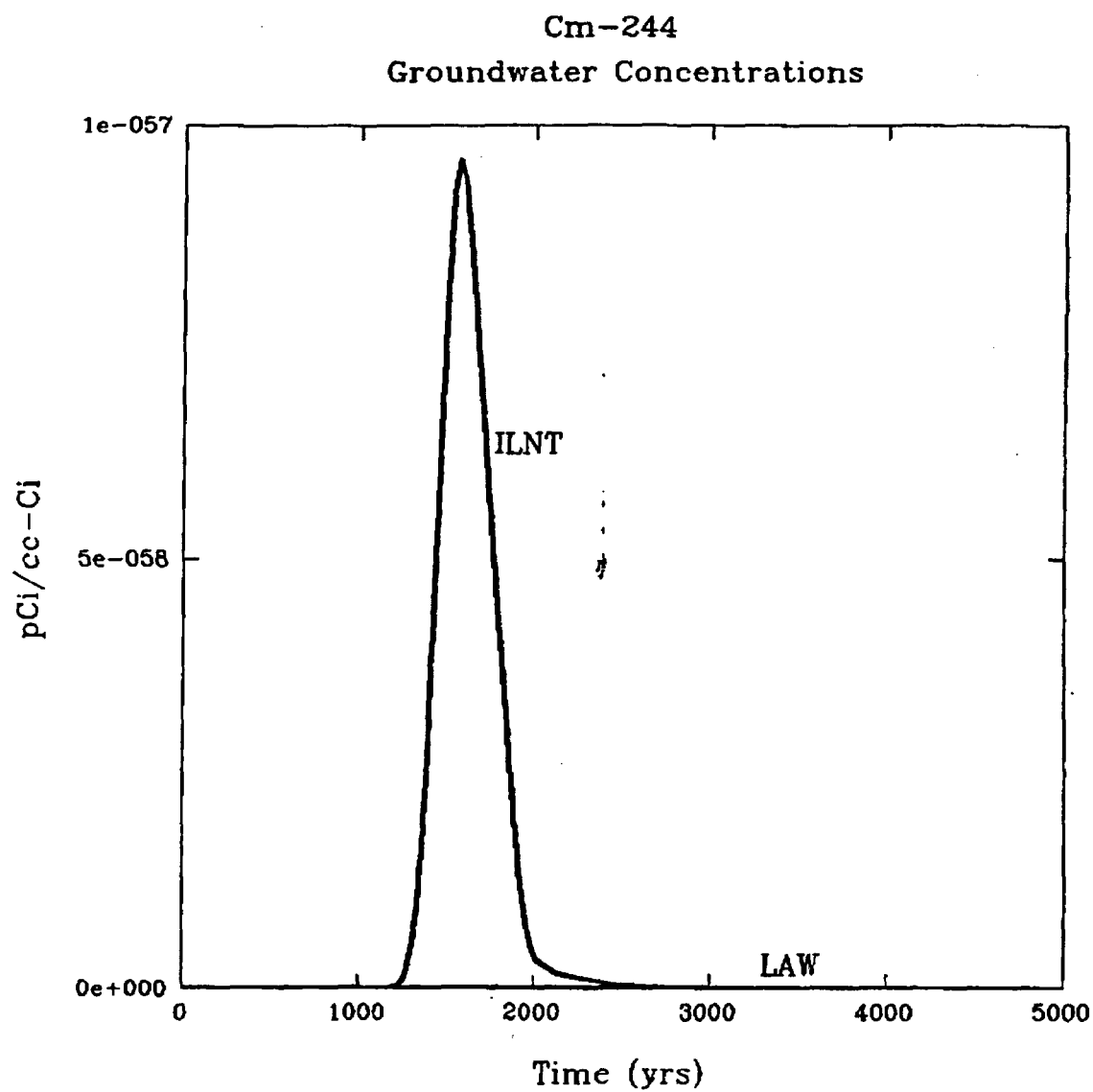
Fig. C.5-22. Predicted groundwater concentration of Pu-242 as a function of time.



	Peak Concentration	Time (yrs)
LAW	1.50 e-006	6.60 e+005
ILNT	2.50 e-007	4.08 e+005

* Based on 150 Ci Pu-244 per vault

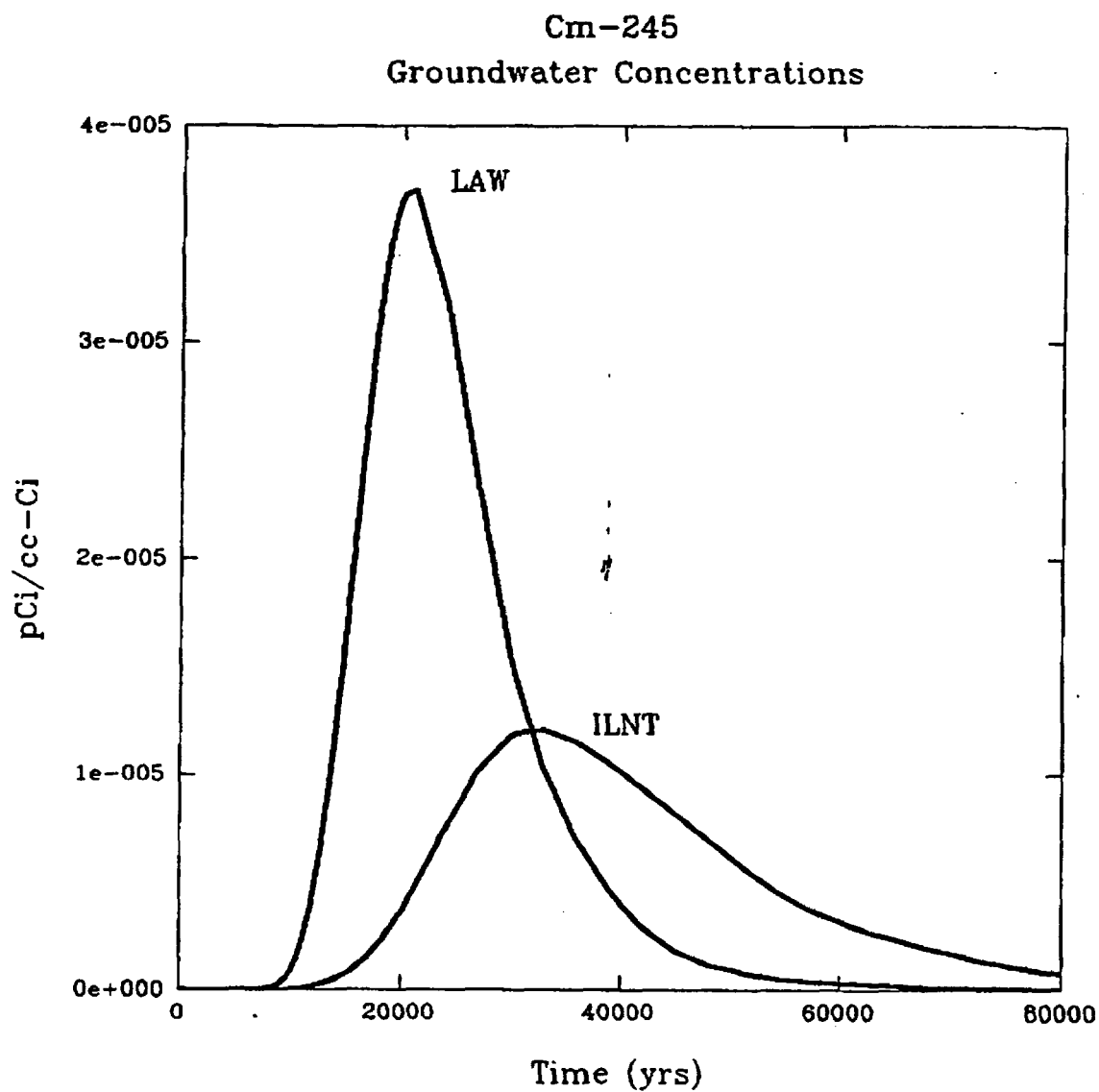
Fig. C.5-23. Predicted groundwater concentration of Pu-244 as a function of time.



	Peak Concentration	Time (yrs)
LAW	1.10 e-066	7.30 e+002
ILNT	9.60 e-058	1.60 e+003

cm244.spg

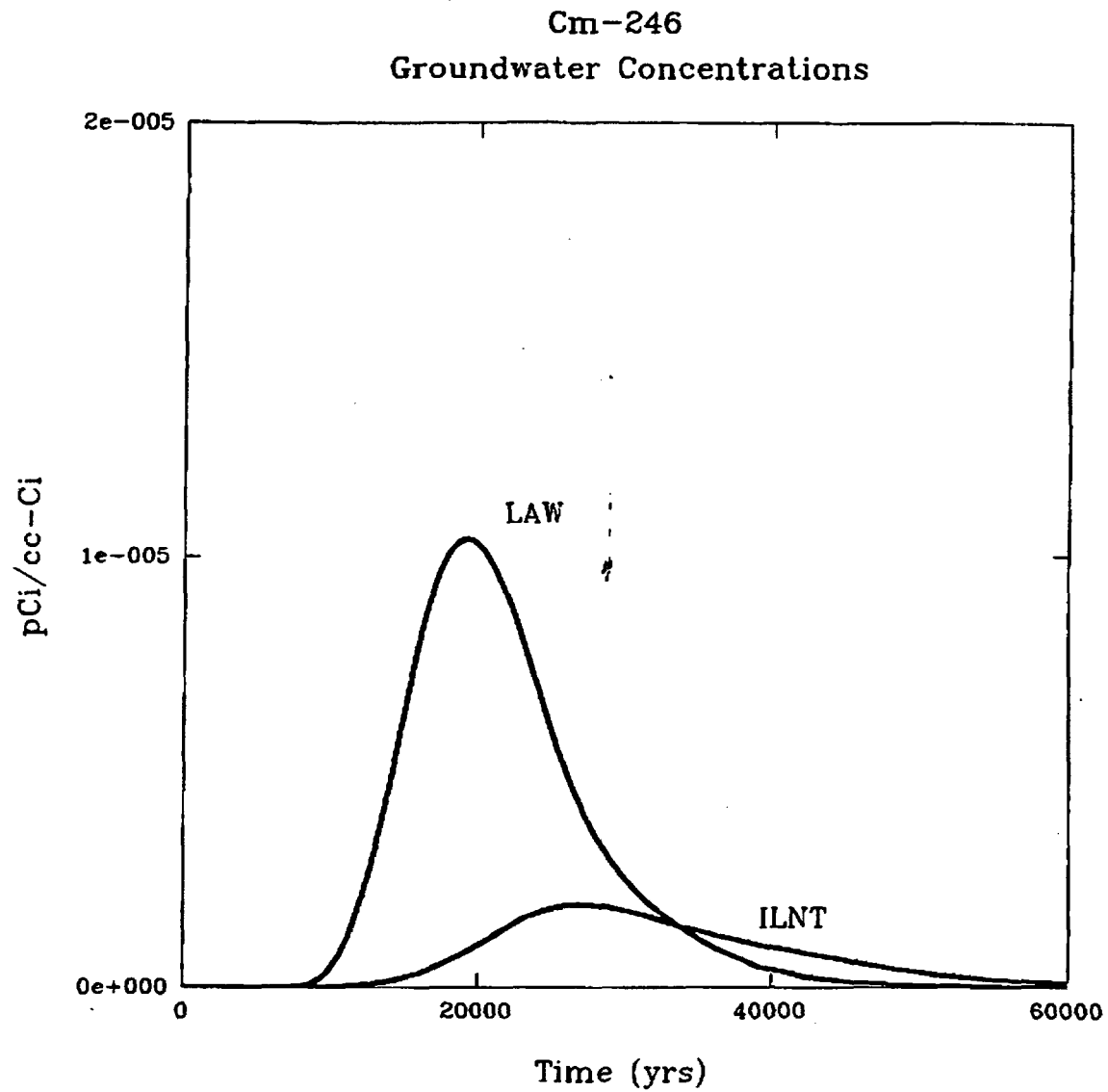
Fig. C.5-24. Predicted groundwater concentration of Cm-244 as a function of time.



	Peak Concentration	Time (yrs)
LAW	3.70 e-005	2.10 e+004
ILNT	1.20 e-005	3.30 e+004

cm245.spg

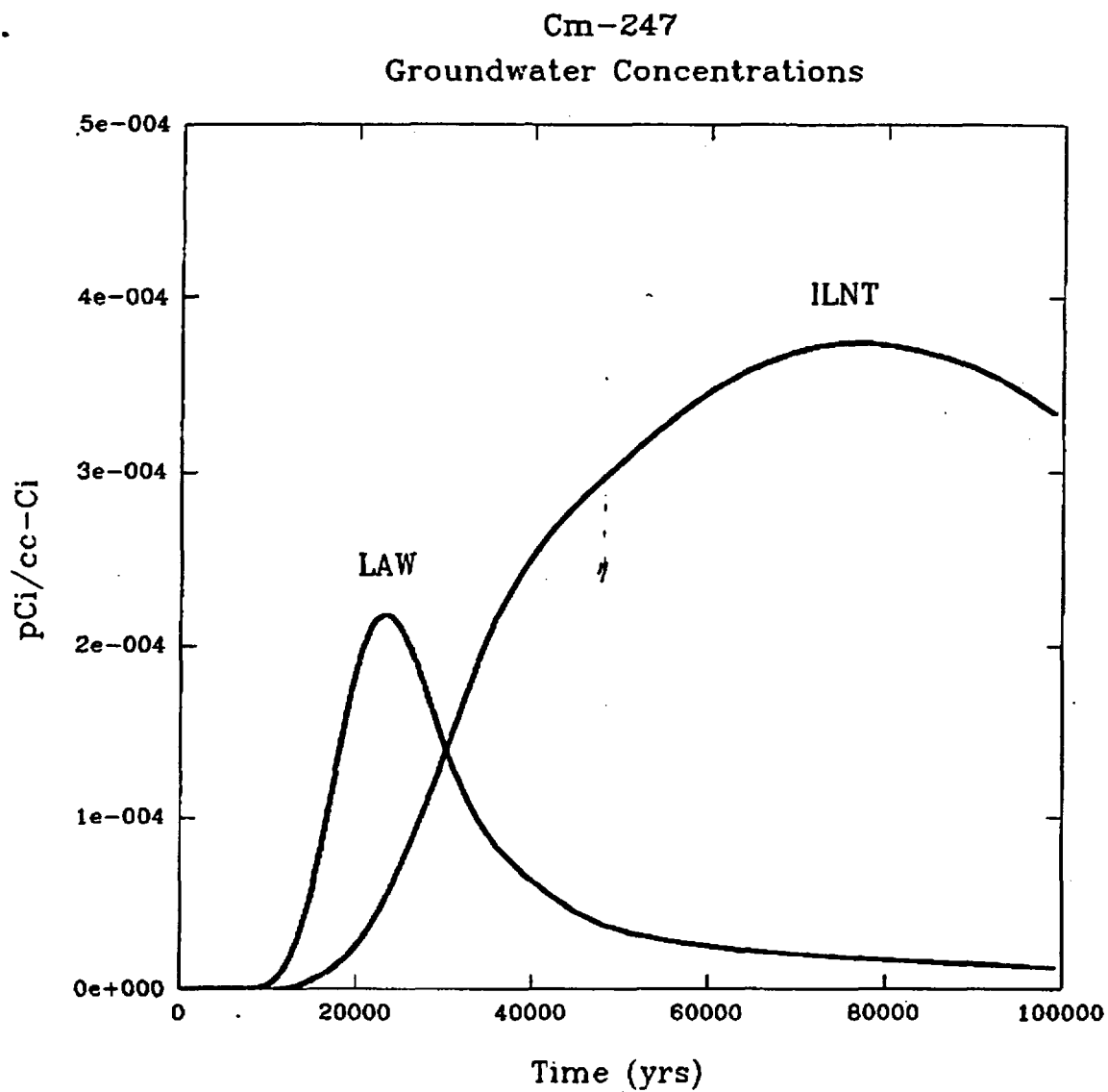
Fig. C.5-25. Predicted groundwater concentration of Cm-245 as a function of time.



	Peak Concentration	Time (yrs)
LAW	1.00 e-005	2.00 e+004
ILNT	1.90 e-006	2.70 e+004

cm246.spg

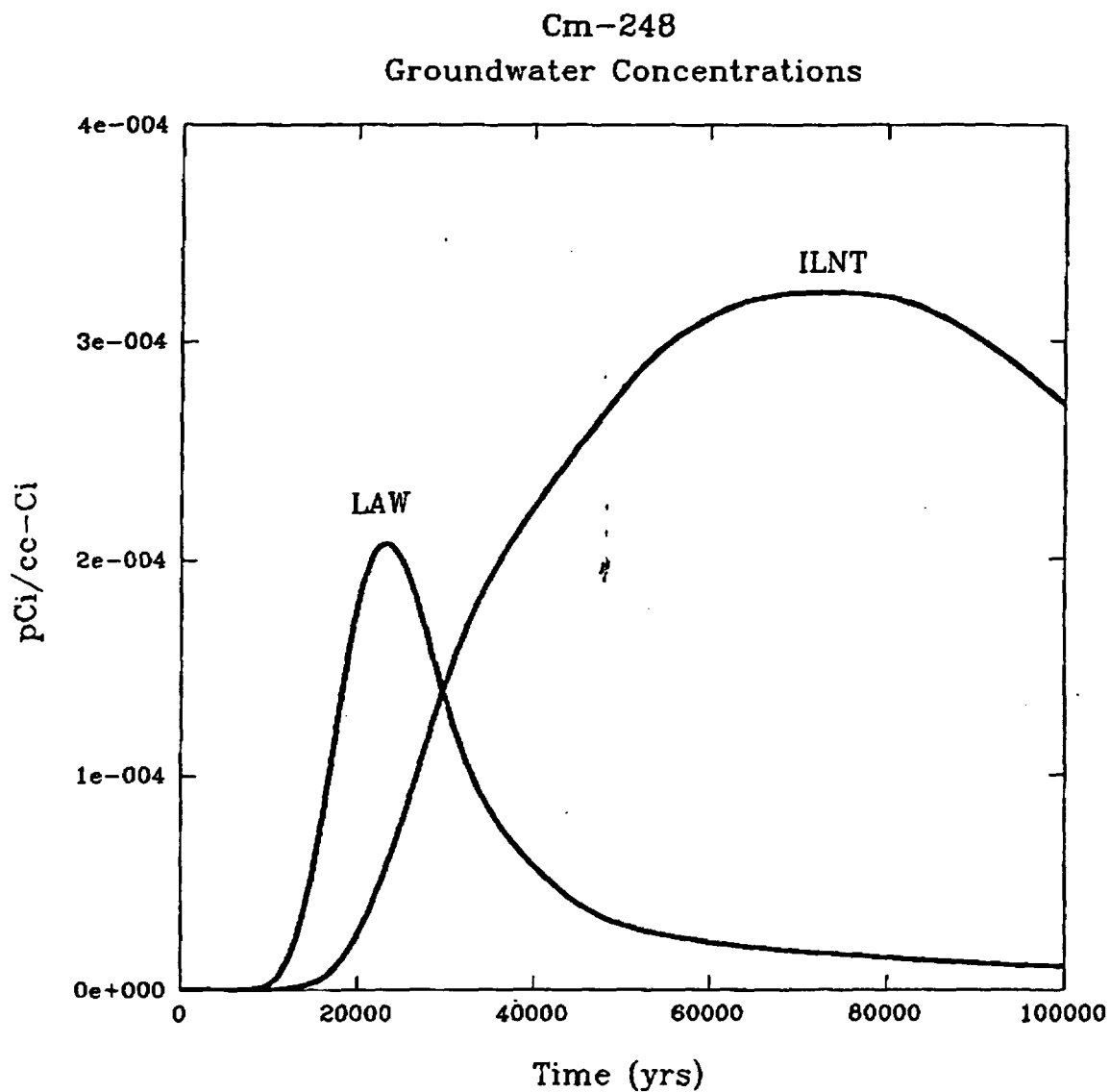
Fig. C.5-26. Predicted groundwater concentration of Cm-246 as a function of time.



	Peak Concentration	Time (yrs)
LAW	2.20 e-004	2.30 e+004
ILNT	3.70 e-004	7.60 e+004

cm247.spg

Fig. C.5-27. Predicted groundwater concentration of Cm-247 as a function of time.

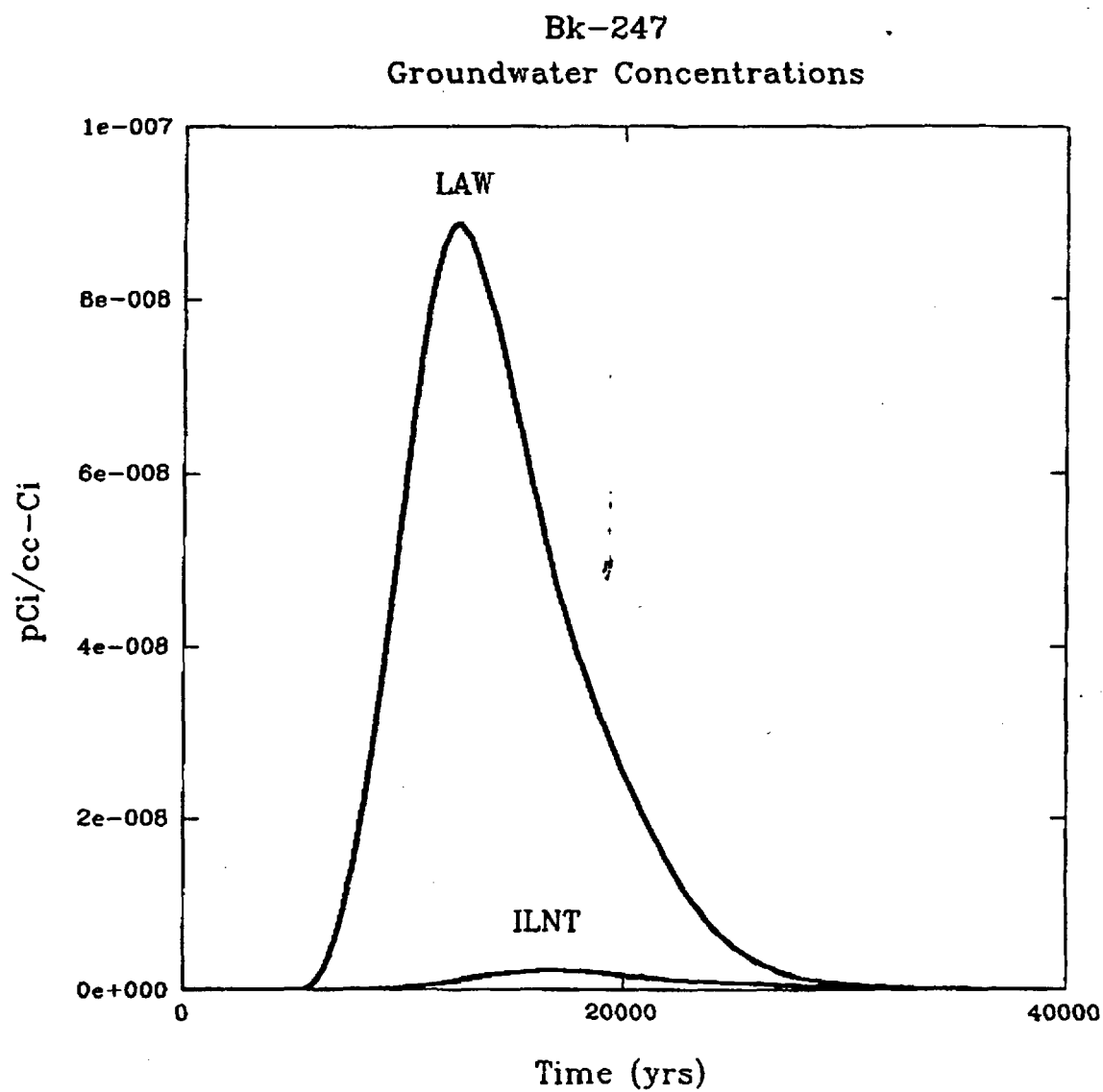


	Peak Concentration	Time (yrs)
LAW	2.10 e-004	2.30 e+004
ILNT	3.20 e-004	7.20 e+004

* Without radioactive daughter contributions.

cm248.spg

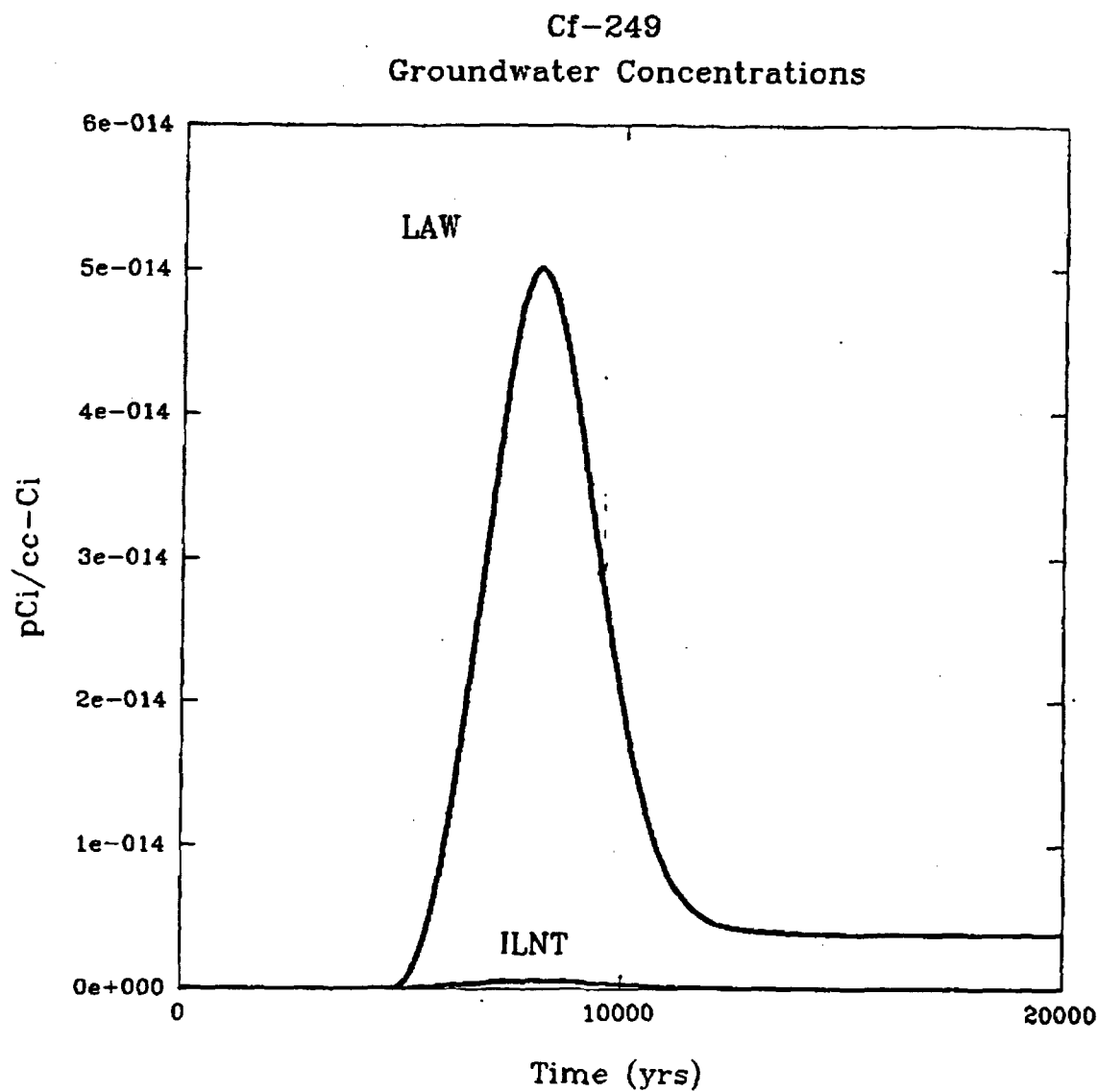
Fig. C.5-28. Predicted groundwater concentration of Cm-248 as a function of time.



	Peak Concentration	Time (yrs)
LAW	8.90 e-008	1.30 e+004
ILNT	4.40 e-009	1.60 e+004

bk247.spg

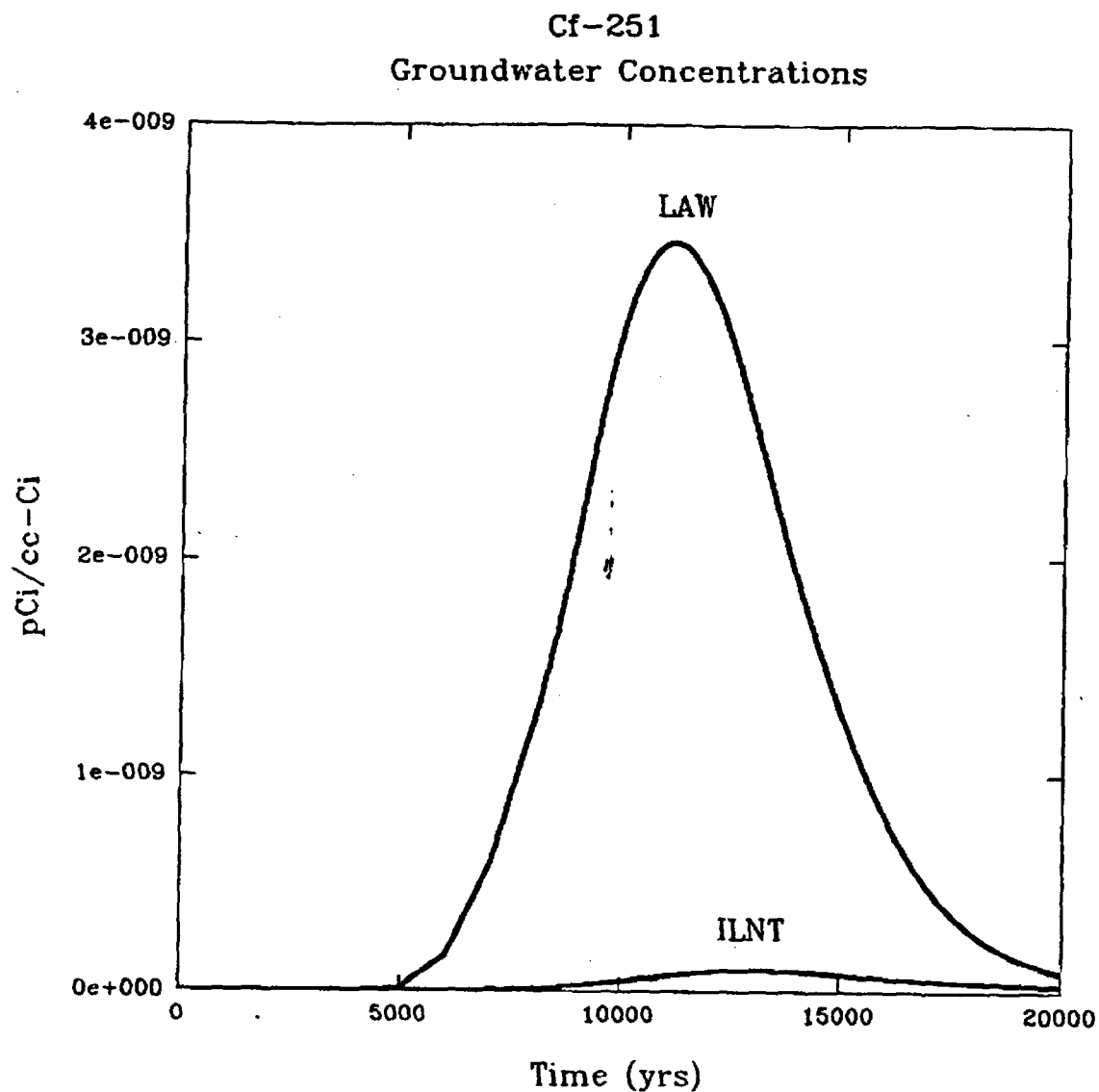
Fig. C.5-29. Predicted groundwater concentration of Bk-247 as a function of time.



	Peak Concentration	Time (yrs)
LAW	5.00 e-014	8.10 e+003
ILNT	5.90 e-016	7.90 e+003

cf249.spg

Fig. C.5-30. Predicted groundwater concentration of Cf-249 as a function of time.



	Peak Concentration	Time (yrs)
LAW	3.50 e-009	1.10 e+004
ILNT	9.40 e-011	1.30 e+004

cf251.spg

Fig. C.5-31. Predicted groundwater concentration of Cf-251 as a function of time.

C.6 ATMOSPHERIC TRANSPORT

The atmospheric transport and dose results are given in Table C.6-1.

Table C.6-1. AIRDOS-PC data for the volatile radionuclide pathway

FREQUENCIES OF WIND DIRECTIONS AND TRUE-AVERAGE WIND SPEEDS

WIND TOWARD	FREQUENCY	WIND SPEEDS FOR EACH STABILITY CLASS (METERS/SEC)						
		A	B	C	D	E	F	G
N	0.089	1.77	2.21	3.56	4.14	3.08	1.71	0.77
NNW	0.048	1.93	2.08	3.04	3.76	2.87	1.65	0.77
NW	0.084	1.95	2.34	3.24	3.69	3.03	1.72	0.77
WNW	0.043	1.85	2.35	3.25	3.64	2.71	1.59	0.77
W	0.052	2.00	2.40	3.55	3.60	2.74	1.69	0.77
WSW	0.041	2.09	2.21	3.12	3.21	2.87	1.73	0.77
SW	0.056	2.39	2.46	3.57	3.79	3.23	1.80	0.77
SSW	0.052	1.49	2.23	3.48	3.88	3.31	1.47	0.77
S	0.068	2.08	2.28	3.36	3.41	3.05	1.68	0.77
SSE	0.049	1.65	2.36	3.54	3.34	3.06	2.02	0.77
SE	0.058	1.87	2.21	3.56	4.39	3.44	1.94	0.77
ESE	0.060	2.42	2.85	3.86	5.71	4.02	1.96	0.77
E	0.101	1.93	2.54	4.15	5.82	3.95	1.88	0.77
ENE	0.080	2.39	2.35	3.98	4.97	3.57	1.91	0.77
NE	0.072	2.09	2.65	4.00	4.65	3.25	1.63	0.77
NNE	0.049	2.35	2.67	3.52	4.42	3.28	1.68	0.77

FREQUENCY OF ATMOSPHERIC STABILITY CLASSES FOR EACH DIRECTION

SECTOR	FRACTION OF TIME IN EACH STABILITY CLASS						
	A	B	C	D	E	F	G
N	0.0043	0.0560	0.0920	0.3666	0.1142	0.1839	0.1831
NNW	0.0110	0.0664	0.0922	0.3408	0.1281	0.1663	0.1953
NW	0.0162	0.1169	0.0898	0.3789	0.1055	0.1513	0.1415
WNW	0.0105	0.1247	0.1462	0.4085	0.1026	0.1092	0.0982
W	0.0176	0.1525	0.1478	0.3968	0.0690	0.1192	0.0971
WSW	0.0090	0.1421	0.1606	0.4678	0.0719	0.0814	0.0673
SW	0.0109	0.1324	0.1330	0.4765	0.0975	0.0915	0.0582
SSW	0.0103	0.1296	0.1377	0.5041	0.0745	0.0725	0.0714
S	0.0113	0.1266	0.1486	0.4282	0.0762	0.1303	0.0789
SSE	0.0201	0.1049	0.1135	0.2989	0.1086	0.2111	0.1429
SE	0.0040	0.0892	0.1217	0.3122	0.1215	0.2218	0.1297
ESE	0.0038	0.0666	0.1185	0.4218	0.1329	0.1122	0.1440
E	0.0053	0.0545	0.1103	0.4107	0.1405	0.1257	0.1530
ENE	0.0037	0.0797	0.1222	0.3300	0.1316	0.1669	0.1658
NE	0.0052	0.0761	0.1172	0.3445	0.0918	0.1541	0.2112
NNE	0.0016	0.0644	0.0822	0.3732	0.1302	0.1622	0.1863

Table C.6-1. (continued)

CLEAN AIR ACT COMPLIANCE REPORT

12/28/93 10:57 AM

Facility: ILT H-3 crucibles

Address:

City:

State:

Comments: H-3 releases to the off-site individual for ILT crucible vaults.

Year:

Dose Equivalent Rates to Nearby
Individuals (mrem/year)Effective
Dose Equivalent

0.0580

Highest Organ
Dose is to
REMAINDER

0.0680

-----EMISSION INFORMATION-----

Radio-nuclide	Class	Amad	Stack #1 (Ci/y)
H-3	*	0.0	2.6E+02
Stack Height (m)			1.00
Stack Diameter (m)			0.03
Buoyant (cal/s)			0.0E-01

-----SITE INFORMATION-----

Wind Data	AGS1018.WND	Temperature (C)	20
Food Source	LOCAL	Rainfall (cm/y)	100
Distance to	5000	Lid Height (m)	1000
Individuals (m)			

*NOTE: The results of this computer model are dose estimates.
They are only to be used for the purpose of determining
compliance and reporting per 40 CFR 61.93 and 40 CFR 61.94.

Table C.6-1. (continued)

CLEAN AIR ACT COMPLIANCE REPORT

2/ 9/94 10:40 AM

Facility: ILT Vaults JCV

Address:

City:

State:

Comments: H-3 releases to the off-site individual for the ILT vaults.

Year:

Dose Equivalent Rates to Nearby
Individuals (mrem/year)

Effective Dose Equivalent	2.46E-06
Highest Organ Dose is to REMAINDER	2.90E-06

-----EMISSION INFORMATION-----

Radio- nuclide	Class	Amad	Area #1 (Cf/y)
H-3	*	0.0	1.1E-02
Total Area (m**2)			6.4E+02

-----SITE INFORMATION-----

Wind Data	AGS1018.WND	Temperature (C)	20
Food Source	LOCAL	Rainfall (cm/y)	100
Distance to Individuals (m)	5000	Lid Height (m)	1000

*NOTE: The results of this computer model are dose estimates.
They are only to be used for the purpose of determining
compliance and reporting per 40 CFR 61.93 and 40 CFR 61.94.

Table C.6-1. (continued)

CLEAN AIR ACT COMPLIANCE REPORT

2/ 9/94 10:43 AM

Facility: ILNT Vaults JCW

Address:

City:

State:

Comments: K-3 releases to the off-site individual for the ILNT vaults.

Year:

Dose Equivalent Rates to Nearby
Individuals (mrem/year)

Effective Dose Equivalent	4.47E-06
Highest Organ Dose is to REMAINDER	5.27E-06

-----EMISSION INFORMATION-----

Radio- nuclide	Class	Area #1 (Ci/y)
K-3	*	0.0 2.0E-02
Total Area (m**2)		8.7E+03

-----SITE INFORMATION-----

Wind Data	AGS1018.WND	Temperature (C)	20
Food Source	LOCAL	Rainfall (cm/y)	100
Distance to Individuals (m)	5000	Lid Height (m)	1000

*NOTE: The results of this computer model are dose estimates.
They are only to be used for the purpose of determining
compliance and reporting per 40 CFR 61.93 and 40 CFR 61.94.

Table C.6-1. (continued)

CLEAN AIR ACT COMPLIANCE REPORT

2/ 9/94 2:30 PM

Facility: ILNT Vaults JCV

Address:

City:

State:

Comments: C-14 releases to the off-site individual for the ILNT vaults.

Year:

Dose Equivalent Rates to Nearby
Individuals (mrem/year)

Effective			
Dose Equivalent		0.1200	
Highest Organ			
Dose is to		0.5100	
ENDOSTEUM			

-----EMISSION INFORMATION-----

Radio-			Area
nuclide	Class	Amad	#1
			(Ci/y)
C-14	*	0.0	1.0E+01
Total Area (m**2)			8.7E+03

-----SITE INFORMATION-----

Wind Data	AGS1018.WND	Temperature (C)	20
Food Source	LOCAL	Rainfall (cm/y)	100
Distance to	5000	Lid Height (m)	1000
Individuals (m)			

*NOTE: The results of this computer model are dose estimates.
They are only to be used for the purpose of determining
compliance and reporting per 40 CFR 61.93 and 40 CFR 61.94.

Table C.6-1. (continued)

CLEAN AIR ACT COMPLIANCE REPORT

2/ 9/94 2:32 PM

Facility: LAW Vaults JCW

Address:

City:

State:

Comments: H-3 releases to the off-site individual for the LAW vaults.

Year:

Dose Equivalent Rates to Nearby Individuals (mrem/year)	
Effective Dose Equivalent	1.17E-05
Highest Organ Dose is to REMAINDER	1.37E-05

-----EMISSION INFORMATION-----

Radio- nuclide	Class	Area #1 (Ci/y)
H-3	*	0.0 5.2E-02
Total Area (m**2)		1.8E+05

-----SITE INFORMATION-----

Wind Data	AGS1018.WND	Temperature (C)	20
Food Source	LOCAL	Rainfall (cm/y)	100
Distance to Individuals (m)	5000	Lid Height (m)	1000

*NOTE: The results of this computer model are dose estimates.
They are only to be used for the purpose of determining
compliance and reporting per 40 CFR 61.93 and 40 CFR 61.94.

Table C.6-1. (continued)

CLEAN AIR ACT COMPLIANCE REPORT

2/ 9/94 2:34 PM

Facility: LAW Vaults C-14

Address:

City:

State:

Comments: C-14 releases to the off-site individual for the LAW vaults.

Year:

Dose Equivalent Rates to Nearby
Individuals (mrem/year)

Effective Dose Equivalent	0.2600
Highest Organ Dose is to ENDOSTEUM	1.1

-----EMISSION INFORMATION-----

Radio- nuclide	Class	Area #1 (Ci/y)
C-14	*	0.0
Total Area (m**2)		1.8E+05

-----SITE INFORMATION-----

Wind Data	AGS1018.WND	Temperature (C)	20
Food Source	LOCAL	Rainfall (cm/y)	100
Distance to Individuals (m)	5000	Lid Height (m)	1000

*NOTE: The results of this computer model are dose estimates.
They are only to be used for the purpose of determining
compliance and reporting per 40 CFR 61.93 and 40 CFR 61.94.

Table C.6-1. (continued)

CLEAN AIR ACT COMPLIANCE REPORT

2/ 9/94 2:37 PM

Facility: Suspect Soil Trenches

Address:

City:

State:

Comments: H-3 releases for the suspect soil trenches (off-site individual)

Year:

Dose Equivalent Rates to Nearby
Individuals (mrem/year)

Effective Dose Equivalent	6.48E-06
Highest Organ Dose is to REMAINDER	7.64E-06

-----EMISSION INFORMATION-----

Radio- nuclide	Class	Amad	Area #1 (Ci/y)
H-3	*	0.0	2.9E-02
Total Area (m**2)			6.0E+03

-----SITE INFORMATION-----

Wind Data	AGS1018.WND	Temperature (C)	20
Food Source	LOCAL	Rainfall (cm/y)	100
Distance to Individuals (m)	5000	Lid Height (m)	1000

*NOTE: The results of this computer model are dose estimates.
They are only to be used for the purpose of determining
compliance and reporting per 40 CFR 61.93 and 40 CFR 61.94.

Table C.6-1. (continued)

CLEAN AIR ACT COMPLIANCE REPORT

2/ 9/94 2:39 PM

Facility: Suspect Soil Trenches

Address:

City:

State:

Comments: C-14 releases for the suspect soil trenches (off-site individual)

Year:

Dose Equivalent Rates to Nearby
Individuals (mrem/year)

Effective Dose Equivalent	0.0120
Highest Organ Dose is to ENDOSTEUM	0.0510

-----EMISSION INFORMATION-----

Radio- nuclide	Class	Amad	Area #1 (Ci/y)
C-14	*	0.0	1.0E+00
Total Area (m**2)			6.0E+03

-----SITE INFORMATION-----

Wind Data	AGS101B.WND	Temperature (C)	20
Food Source	LOCAL	Rainfall (cm/y)	100
Distance to Individuals (m)	5000	Lid Height (m)	1000

*NOTE: The results of this computer model are dose estimates.
They are only to be used for the purpose of determining
compliance and reporting per 40 CFR 61.93 and 40 CFR 61.94.

Table C.6-1. (continued)

CLEAN AIR ACT COMPLIANCE REPORT

2/ 9/94 2:41 PM

Facility: Naval Reactor Waste

Address:

City:

State:

Comments: H-3 releases for the Naval Reactor Waste (off-site individual)

Year:

Dose Equivalent Rates to Nearby
Individuals (mrem/year)

Effective Dose Equivalent	0.0002
Highest Organ Dose is to REMAINDER	0.0002

-----EMISSION INFORMATION-----

Radio- nuclide	Class	Area #1 (Ci/y)
H-3	*	0.0
Total Area (m**2)		8.0E+02

-----SITE INFORMATION-----

Wind Data	AGS1018.WND	Temperature (C)	20
Food Source	LOCAL	Rainfall (m/y)	100
Distance to Individuals (m)	5000	Lid Height (m)	1000

*NOTE: The results of this computer model are dose estimates.
They are only to be used for the purpose of determining
compliance and reporting per 40 CFR 61.93 and 40 CFR 61.94.

Table C.6-1. (continued)

CLEAN AIR ACT COMPLIANCE REPORT

2/ 9/94 2:43 PM

Facility: Naval Reactor Waste

Address:

City:

State:

Comments: C-14 releases for the Naval Reactor Waste (off-site individual)

Year:

Dose Equivalent Rates to Nearby Individuals (mrem/year)	
Effective Dose Equivalent	1.2
Highest Organ Dose is to ENDOSTEUM	5.1

-----EMISSION INFORMATION-----

Radio- nuclide	Class	Area #1 (Ci/y)
C-14	*	0.0
Total Area (m**2)		8.0E+02

-----SITE INFORMATION-----

Wind Data	AGS1018.WND	Temperature (C)	20
Food Source	LOCAL	Rainfall (cm/y)	100
Distance to Individuals (m)	5000	Lid Height (m)	1000

*NOTE: The results of this computer model are dose estimates.
They are only to be used for the purpose of determining
compliance and reporting per 40 CFR 61.93 and 40 CFR 61.94.

APPENDIX D
GEOCHEMICAL INTERACTIONS

Rev. 0

D.1 INTRODUCTION

Predicting the release of radionuclides from the E-Area disposal facility is difficult because of the large variety of contaminated material that will be disposed of in the vaults. Conceptually, waste within steel boxes (B-12 and B-25) or activated metals disposed in the vaults will remain immobile until contacted by water that has leaked into the vaults. Defensible prediction of water and contaminant movement in the vaults and the effectiveness of boxes and activated metals in retarding waste release is not possible without development of a conservative simplified conceptual model. The key features of the conceptual model are summarized below.

Waste is immobile until contacted by water.

- 1) Water entering the vault will have a composition that can be represented as a mixture of concrete pore fluid and local groundwater equilibrated with soil levels of carbon dioxide gas.
- 2) Steel and activated metals present in the vaults will result in the formation of corrosion products (i.e., hydrous Fe[III] oxides) and lead to reducing conditions inside the vaults.
- 3) Entire vault inventory is available to react with the reducing water inside the vault.
- 4) Aqueous radionuclide concentrations are controlled by sorption (represented with a K_d or isotherm) onto corrosion products (LAW vault) or grout (ILT and ILNT vaults) with a solubility limited (oxide and hydroxide phases) upper concentration limit.
- 5) Contaminated water exiting the vault will interact with the concrete vault and radionuclides will be chemically retarded by the vault wall.

D.2 RADIONUCLIDES CONSIDERED

The radionuclides considered in detail for the LAW vaults are H-3, C-14, Ni-59, Se-79, Ra-226, Th-232, Sn-126, Tc-99, I-129, Cs-135, Sr-90, Y-90, Am-241, 243, Cm-244, 245, 246, 247, 248, Bk-247, 249, Cf-249, 251, 252, Np-237, Pu-238, 239, 240, 241, 242, 244, and U-234, 235, 236, 238. These radionuclides were selected for detailed numerical transport simulations based on the screening calculations discussed in Sect. 4.1.1. The anionic radionuclides C, Tc, and I, as well as tritium are weakly sorbed to corrosion products. If conditions in the vault are reducing enough, the anion Tc(VII) may be reduced to insoluble Tc(IV). Tritium release from tritium crucibles in the ILT vaults was found to be limited by transport through the vault sufficiently that no leach rate calculations were required to reach adequate performance. Distribution coefficients for the remaining radionuclides were developed based on hydrous ferric oxide (HFO) adsorption.

D.3 VAULT WATER COMPOSITION

Water compositions inside the vaults will reflect the interaction of concrete pore water and vadose water. The composition of the vault water will be dominated by concrete interactions even under conditions of fracture flow through the vault shell. The presence of CO₂ gas in the soil and calcite present as a weathering product in the cement will buffer the pH of the vault water to between 7 and 8.

D.4 RADIONUCLIDE SORPTION BEHAVIOR

Wastes disposed of in the LAW vaults will be contained in steel boxes (B-12 and B-25). The basic assumption of the method used to derive distribution coefficients for the LAW vault waste form is that the corrosion of the boxes will result in the formation of HFO, (e.g., goethite) and that any water contaminated with radionuclides must pass over the corroded area of the box.

Distribution coefficients (K_d) based on surface area of the adsorbent for the selected radionuclides were estimated by assuming that adsorption occurs exclusively on the corrosion products (HFO) of these boxes. The total potential concentration of HFO in the vault is 0.07 g/cm^3 [based on 9730 B-25 at 350 lbs and 4330 B-12 boxes at 300 lbs in a $1,700,000 \text{ ft}^3$ vault (Harley 1990a,b)]. The surface area of goethite in the vault is predicted to be $32,000 \text{ cm}^2/\text{cm}^3$ based on a specific surface area of goethite of $450,000 \text{ cm}^2/\text{g}$ (Hsi and Langmuir 1985).

Numerous adsorption studies of metal and radionuclides onto hydrous metal oxides are reported in the literature (see Dzombak and Morel 1990). Specific studies for key radionuclides (summarized below) were used to estimate K_d values at pH 8 for the waste assuming HFO is the only reactive phase. Distribution coefficients for radionuclides that lack adsorption experiments were estimated using elemental analogs. The K_d is calculated by relating the experimental data (i.e. fraction adsorbed and suspension concentration) to the waste in the vaults (i.e. surface area and bulk density of waste). This is accomplished by using the following equation.

$$K_d = SA \cdot X / r \cdot SA_{\text{exp}} (1-X) \quad (\text{Eq. 1})$$

where

SA is the specific surface area of the waste ($32,000 \text{ cm}^2/\text{cm}^3$)

X is the fraction adsorbed

r is the bulk density of the waste (1.6 g/cm^3)

SA_{exp} is the concentration of solid in the adsorption experiment (cm^2/mL)

Estimated K_d values for the LAW vaults are summarized below (Table D.4-1).

Table D.4-1. Summary of distribution coefficients for selected radionuclides on goethite (pH =8.0).

Radionuclide	Chemical Form	Distribution Coefficient (mL/g)
H-3	HTO	0
C-14	CO ₃ ²⁻	0
Tc-99	TcO ₄ ⁻	0
I-129	I ⁻	0
Cs-135	Cs ⁺	0
Sr-90	Sr ²⁺	3
Y-90	Y ³⁺	3
Sn-126	Sn ²⁺	55
Ra-226	Ra ²⁺	60
Se-79	SeO ₃ ²⁻	170
Ni-59	Ni ²⁺	1200
Th-232	Th ⁴⁺	2200
U-234, 235, 236, 238	UO ₂ ²⁺	6000
Np-237	NpO ₂ ⁺	750
Pu-238, 239, 240, 241, 242, 244	Pu ⁴⁺	2000
Am-241, 243	Am ³⁺	3700
Cm-244, 245, 246, 247, 248	Cm ³⁺	3700
Bk-247, 249	Bk ³⁺	3700
Cf-249, 251, 252	Cf ³⁺	3700

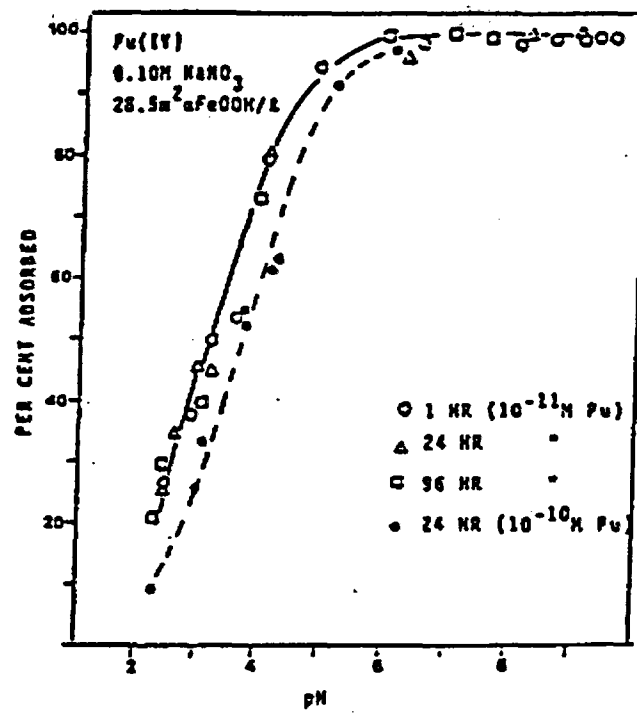
Plutonium

Aqueous plutonium speciation is a very complex because it may be simultaneously present in four oxidation states (III, IV, V, VI). The dominant oxidation states of plutonium in oxygenated waters are Pu(V) and Pu(VI) based on calculations and analyses (Nelson and Lovett 1978 and 1981; Nelson and Orlandini 1979; Bondietti and Trabalka 1980). Because of the large amount of reducing material, conditions inside the E-Area vaults will not be oxidizing enough to support Pu(VI) species. The predominant oxidation states expected are Pu(V) and Pu(IV).

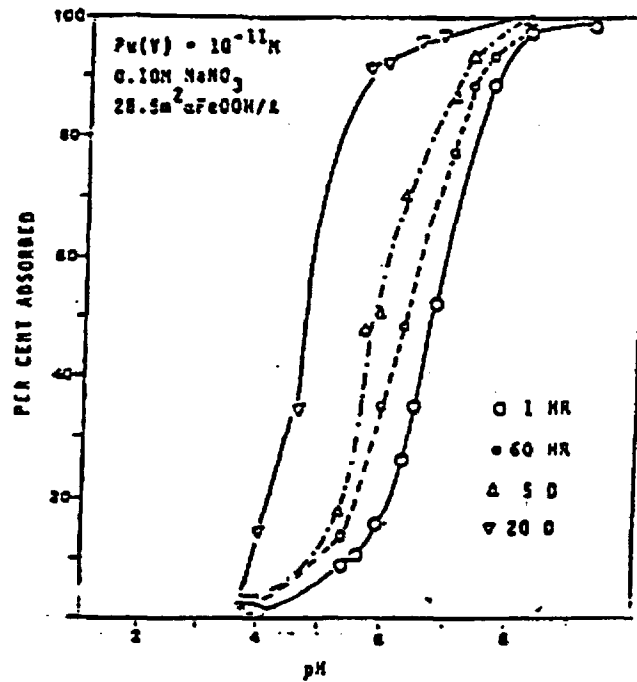
Plutonium adsorption on synthetic goethite as functions of pH, ionic strength, carbonate alkalinity, and dissolved organic carbon was measured by Sanchez et al. (1985). The experiments consisted of a synthetic goethite suspension with a surface area of 285 cm²/mL in a borosilicate glass reaction vessel. Hydrogen activity was controlled using HCl or NaOH. Adsorption of Pu(IV) is much stronger than Pu(V) on goethite because it is more strongly hydrolyzed. The adsorption edge for Pu(IV) occurs from pH 3 to 5 (Fig. D.4-1a) with relatively rapid kinetics (equilibrium reached in 1 h). Pu(V) adsorption is much slower and equilibrium was not achieved after 20 days (Fig. D.4-1b). The Pu(V) adsorption edge changes with time from pH 7 to pH 5 over the 20 day period. Although Pu(V) is predicted to be stable based on thermodynamic calculations the slow shift of the adsorption edge toward that of Pu(IV) suggests that Pu(V) may be reduced to Pu(IV). The reduction may take place on the goethite surface after adsorption of the Pu(V) or Pu(V) may be reduced as it nears the goethite surface and the Pu(IV) state is adsorbed (Sanchez et al. 1985).

Adsorption of Pu(IV) or Pu(V) was not significantly affected by ionic strength in the range of 0.1 to 3 M NaNO₃ or NaCl (see Table D.4-2). A decrease in Pu adsorption on goethite occurs with increased carbonate alkalinity. However, this occurs at much higher alkalinity levels than will be found in the E-Area vaults (Fig. D.4-2).

The data used to estimate Pu adsorption for the LAW vault waste is for a pH of 7 (negligible change from pH 7 to 8) and a total Pu concentration of 10⁻¹¹ M. At these conditions 97.1% of the Pu is on the solid (Table D.4-2). This sorption fraction is consistent with a K_d of 2,000 mL/g for expected bulk density and HFO content in the vaults using Eq. 1.



a)



b)

Fig. D.4-1. Adsorption of Pu on goethite as a function of pH at two plutonium concentrations (from Sanchez et al. 1985). a) Pu(IV), b) Pu(V).

Table D.4-2. Adsorption of Pu(IV) on goethite as a function of ionic strength
(pH = 7.0, Total Pu = 10^{-11} M) from Sanchez et al. 1985

Electrolyte Solution	Percent Adsorbed at Equilibrium
0.1 M NaNO ₃	97
0.5 M NaNO ₃	97
1.0 M NaNO ₃	98
3.0 M NaNO ₃	98
0.5 M NaNO ₃	98
3.0 M NaNO ₃	97
0.03 M NaNO ₃	97
0.15 M NaNO ₃	97
0.30 M NaNO ₃	95
Mean	97.1

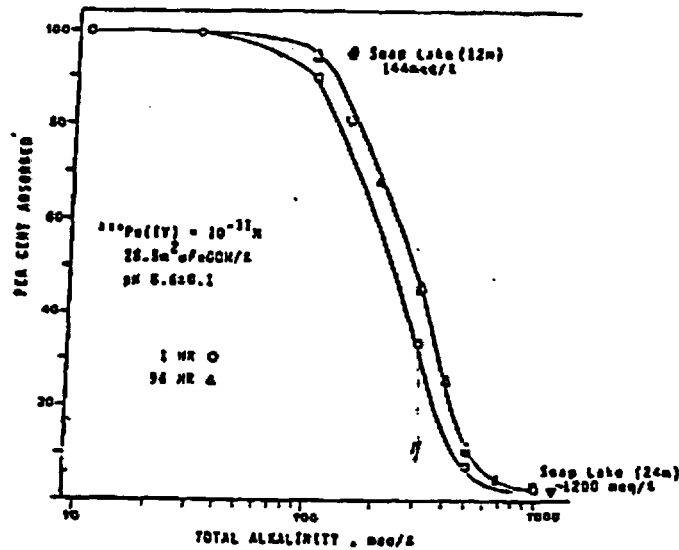


Fig. D.4-2. The effect of carbonate alkalinity on the adsorption of Pu(IV) on goethite (from Sanchez et al. 1985). Alkalinity in the vault will be approximately 60 meq/L.

Uranium

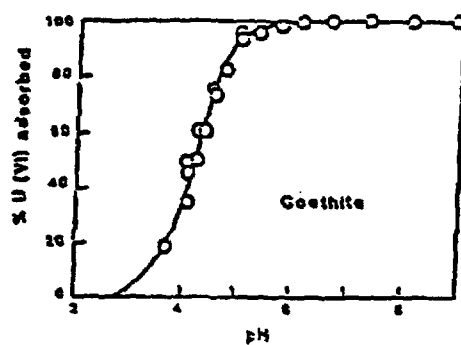
Uranium partitioning onto HFO under varying pH, ionic strength, competing cation and complexing anions is described by Hsi and Langmuir (1985). The HFO used by Hsi and Langmuir were amorphous ferric oxyhydroxide, goethite, and hematite. Uranyl species were strongly adsorbed to all three of the iron oxides considered at pHs above 5 to 6. The most adsorptive oxide considered was the amorphous ferric oxyhydroxide with natural hematite providing the least amount of adsorption. These differences in adsorption result from the difference in specific surface area of the polymorphs. We have calculated the adsorption of uranium in the waste based on goethite representing the steel corrosion product.

The surface area of the goethite suspension was 450 cm²/mL. HNO₃ and NaOH were used to maintain pH with a total uranyl concentration of 10⁻⁵ M. Goethite removes over 99% of the U from solution above pH 6 (Fig. D.4-3a). Uranyl adsorption was not affected by the presence of calcium and magnesium at total solution concentrations of 10⁻³ M. The vault pore fluid concentrations of Ca²⁺ and Mg²⁺ are anticipated to be lower than this and therefore should not result in reduced uranyl adsorption.

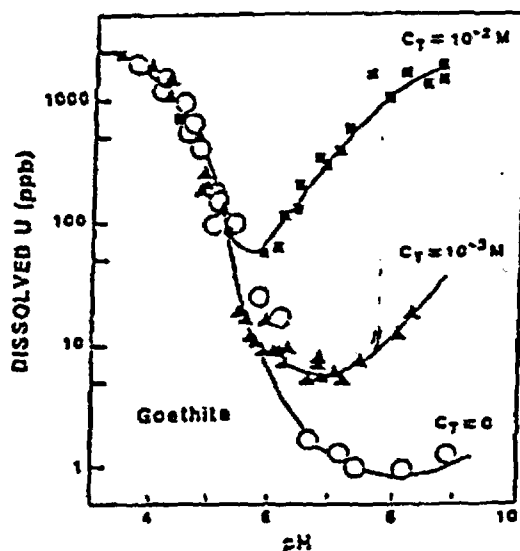
Total carbonate concentration influences the adsorption of uranium (VII) on goethite. Higher CO₃²⁻ content in solution results in increased uranyl carbonate complexation, predominantly UO₂(CO₃)₂²⁻ and UO₂(CO₃)₃⁴⁻, and decreases adsorption of UO₂²⁺ above pH 6 (Fig. D.4-3b). The affect of total carbonate on the adsorption of UO₂²⁺ is very evident in plots of soluble uranium versus pH with varying carbonate concentrations (Fig. D.4-3c). The dissolved uranium concentration at pH 7 for a carbonate concentration of 10⁻³ M was selected for use in the K_d estimation because this carbonate concentration and pH match the expected vault pore fluid conditions. A K_d for the LAW vault waste of 6000 mL/g was calculated using Eq. 1.

Strontium

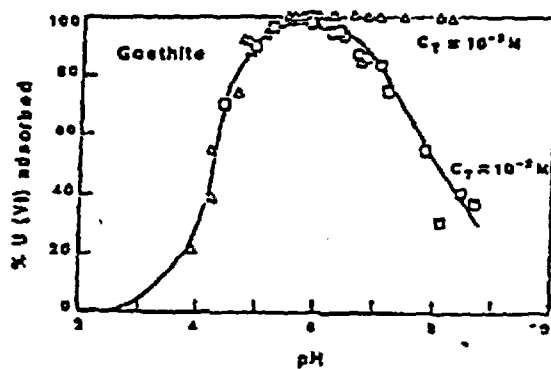
Adsorption of strontium onto hydrous ferric oxides has been studied by Kolarik (1961), Kinniburgh et al. (1975), and Kinniburgh et al. (1976). These experiments indicate that strontium ion adsorbs rapidly and is not significantly impacted by variations in the Na⁺



a)



b)



c)

Fig. D.4-3. Adsorption of uranyl on a 1 g/L goethite suspension as a function of pH in a 0.1 M NaNO_3 solution (from Hsi and Langmuir 1985). a) uranyl at 10^{-5} M, b) dissolved uranium at 10^{-5} M and varying total carbonate, c) effect of changes in total carbonate on the adsorption of uranyl.

concentration in the solution. These experiments also show that there is no selectivity for Ca^{2+} over Sr^{2+} (Kinniburgh et al. 1975). The adsorption edge for Sr^{2+} on the iron oxide (Kinniburgh et al. 1975) was between pH 6 and 7.5.

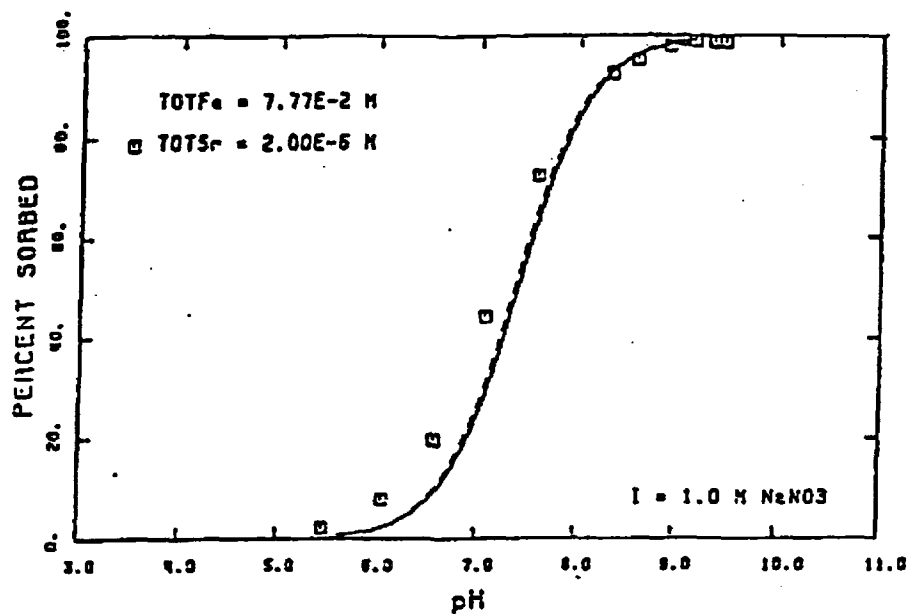
Dzombak and Morel (1990) provide a summary of adsorption data for Sr^{2+} on HFO. The experiments used to determine the adsorption of strontium on HFO are from Kinniburgh et al. (1975) and Kolarik (1961). The HFO was prepared by the addition of NaOH to $\text{Fe}(\text{NO}_3)_3$ solution and the ionic strength of the solution was held at 1.0 M NaNO_3 . The adsorption curves used to estimate strontium adsorption at pH 8 are shown in Fig. D.4-4a to k and the data are summarized in Table D.4-3. The total strontium in the experiments ranged from 10^{-2} to 10^{-7} M and HFO surface area ranged from 10700 to 106620 cm^2/mL . An average Sr^{2+} K_d for LAW vault waste of 3 mL/g was calculated from Eq. 1.

Nickel

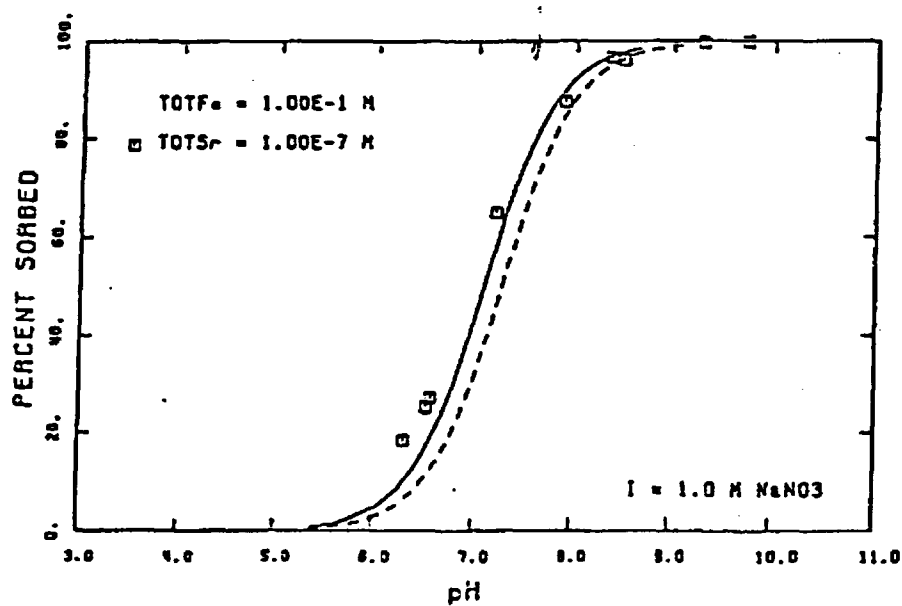
Dzombak and Morel (1990) provide a summary of adsorption data for Ni^{2+} on HFO. The experiment used to determine the adsorption curve for nickel on HFO is from Leckie et al. (1984). The HFO was prepared by the addition of NaOH to $\text{Fe}(\text{NO}_3)_3$ solution and the ionic strength of the solution was held at 0.1 M NaNO_3 . The adsorption edge is located between pH 6.5 and 7.5 (Fig. D.4-5) for the experiment used to estimate nickel adsorption. The total nickel in the system is 10^{-7} M and HFO surface area is 533 cm^2/mL . Approximately 97% of the nickel is adsorbed to the goethite surface at pH 8. A Ni^{2+} K_d for LAW vault waste of 1200 mL/g was calculated from Eq. 1.

Selenite

Selenium geochemistry is strongly controlled by the geochemistry of iron (Howard 1977). In the pH range from 2 to 8 selenite (SeO_3^{2-}) is strongly adsorbed and decreases from pH 8 to 11. Dzombak and Morel (1990) provide a summary of adsorption data for SeO_3^{2-} on HFO. The experiment used to determine the adsorption curve for selenite on HFO is from Plotnikov (1958). The HFO was prepared by the addition of NH_4OH to $\text{Fe}(\text{NO}_3)_3$ solution

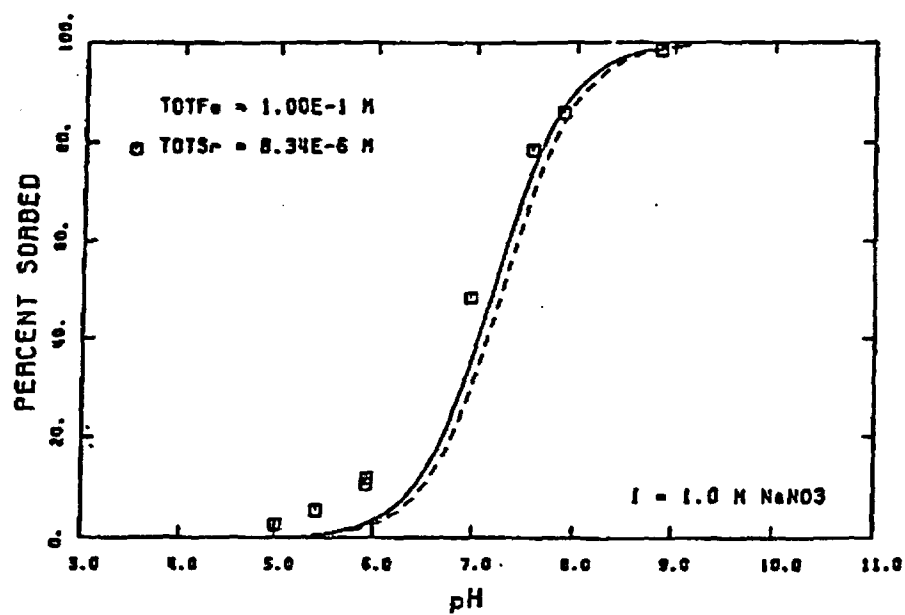


a)

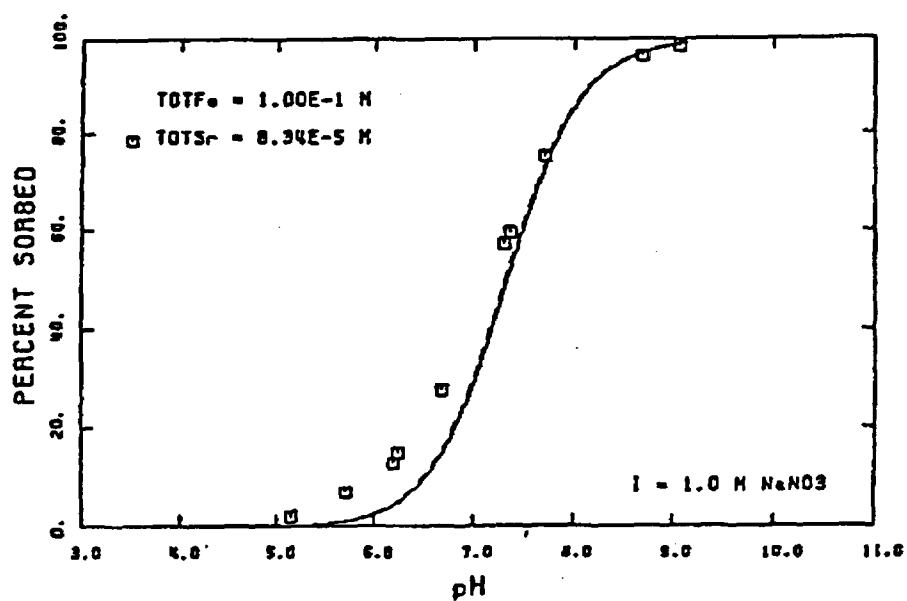


b)

Fig. D.4-4. Adsorption of Sr^{2+} on goethite as a function of pH in a 1.0 M NaNO_3 solution (from Dzombak and Morel 1990). a) 6.9 g goethite/L, b) 8.9 g goethite/L, c) 8.9 g goethite/L, d) 8.9 g goethite/L, e) 8.9 g goethite/L, f) 8.9 g goethite/L, g) 8.9 g goethite/L, h) 1.8 g goethite/L, i) 4.4 g goethite/L, j) 8.9 g goethite/L, k) 17.8 g goethite/L.

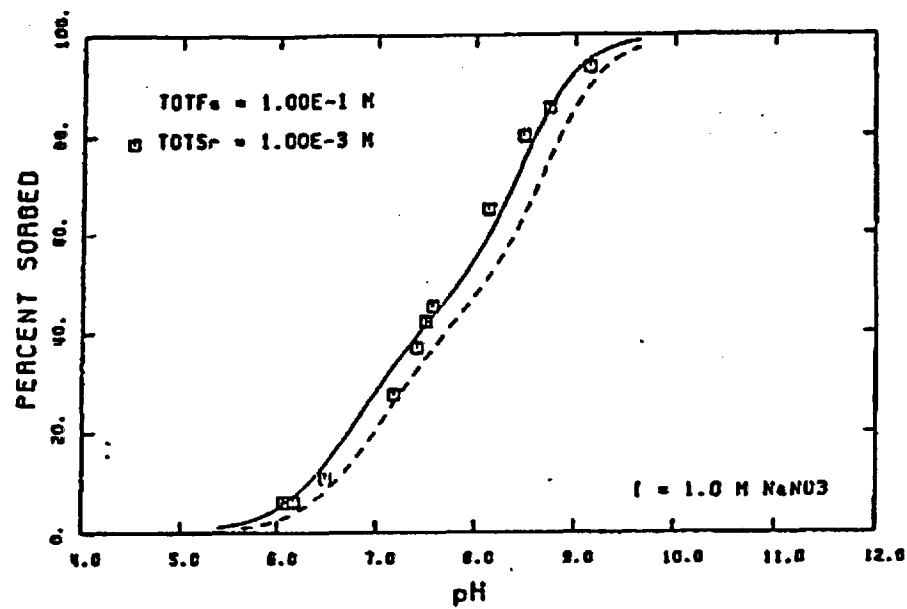


c)

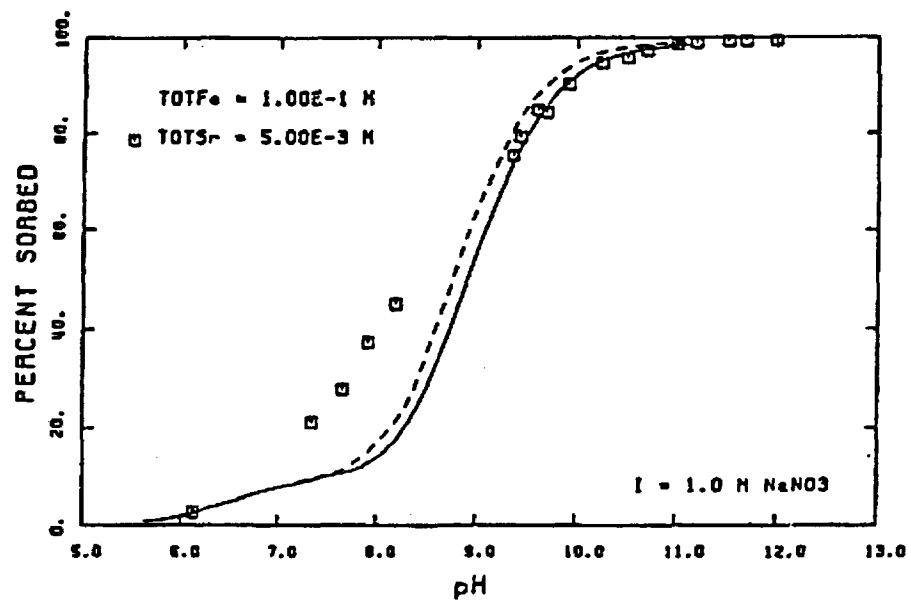


d)

Fig. D.4-4. (continued).

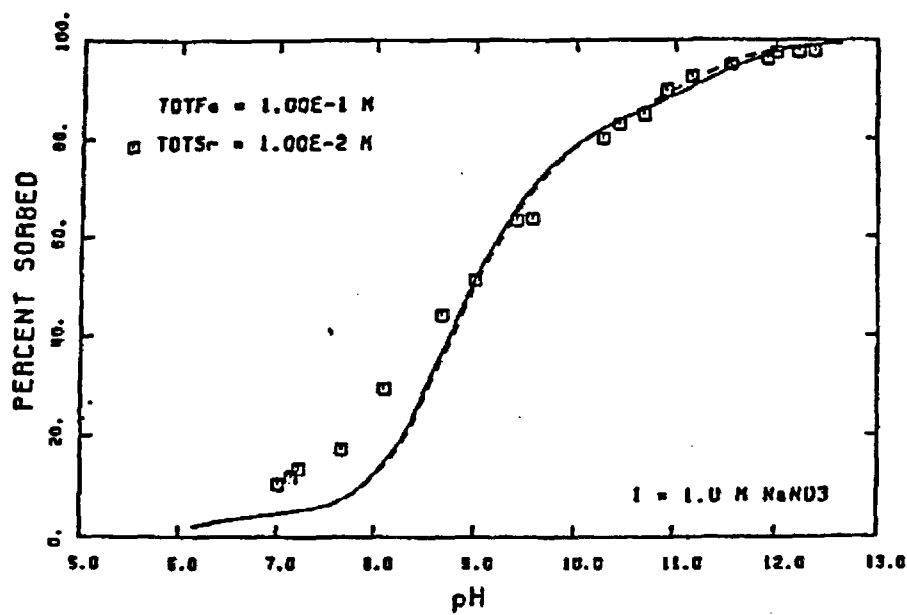


e)

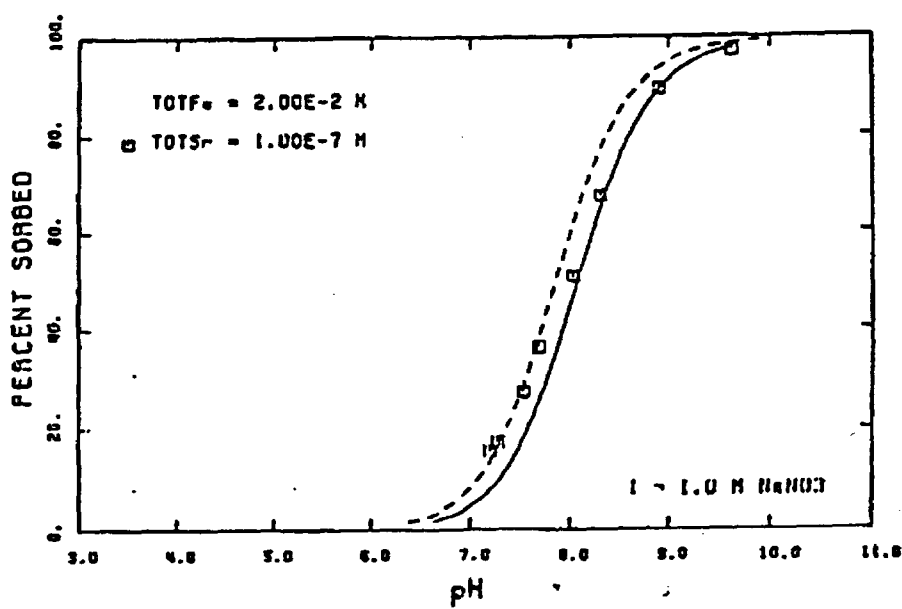


f)

Fig. D.4-4. (continued).

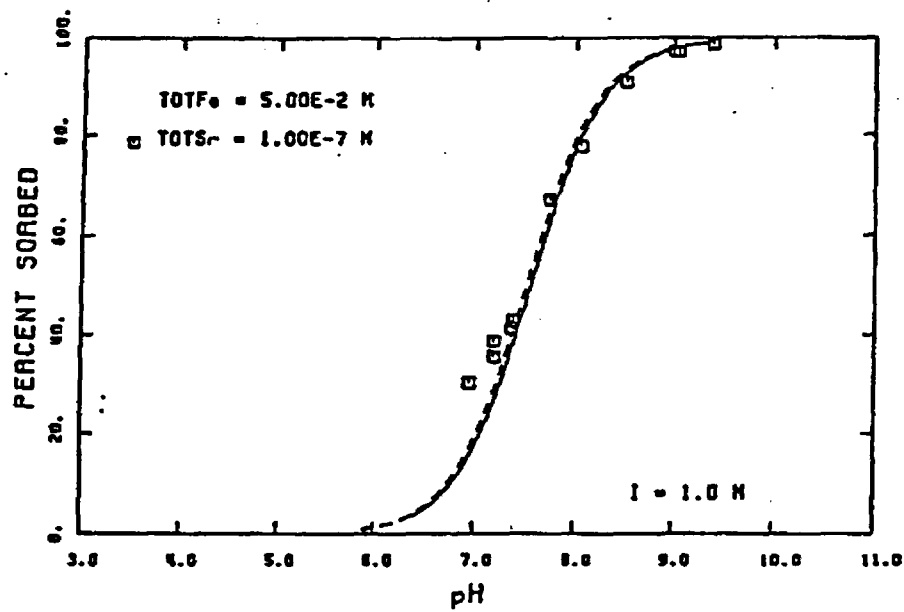


g)

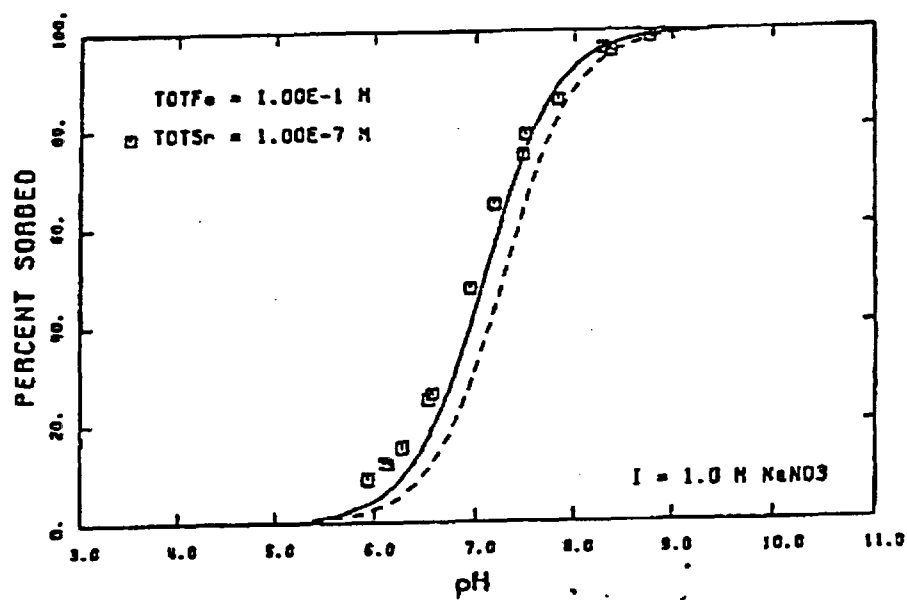


h)

Fig. D.4-4. (continued).

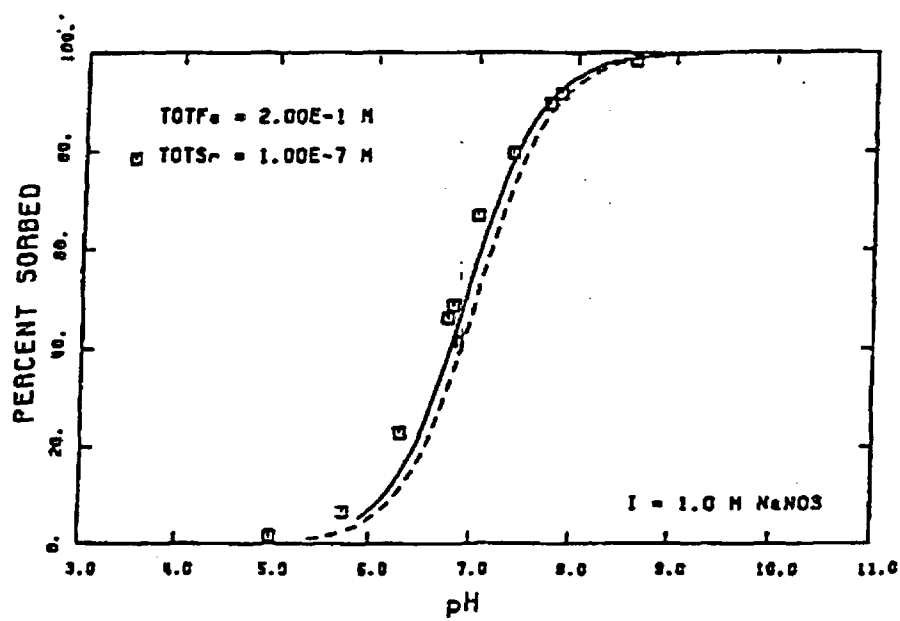


i)



j)

Fig. D.4.4. (continued).



k)

Fig. D.44. (continued).

Rev. 0

Table D.4-3. Adsorption data for strontium used to estimate K_d

Total Sr (M)	Surface Area (cm ² /mL)	Percent Adsorbed	K_d (mL/g)
2.00 10 ⁻⁶	41,420	87	3.2
1.00 10 ⁻⁷	53,000	90	3.4
8.34 10 ⁻⁶	53,000	90	3.4
8.34 10 ⁻⁵	53,000	88	2.8
1.00 10 ⁻³	53,000	58	0.5
5.00 10 ⁻³	53,000	40	0.3
1.00 10 ⁻²	53,000	30	0.2
1.00 10 ⁻⁷	10,700	51	1.9
1.00 10 ⁻⁷	26,700	80	3.0
1.00 10 ⁻⁷	53,300	93	5.0
1.00 10 ⁻⁷	106,620	95	3.6

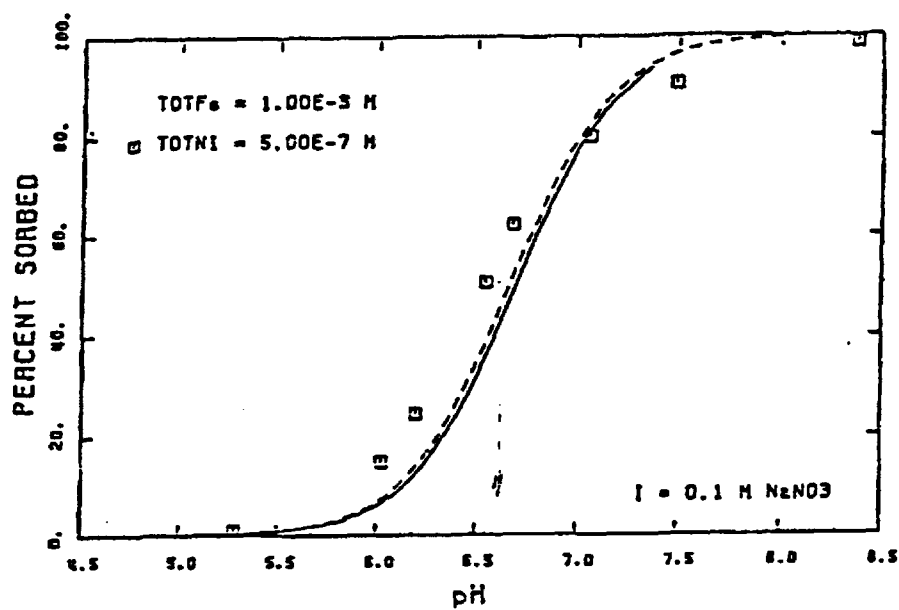


Fig. D.4-5. Adsorption of nickel on goethite as a function of pH in a 0.1 M NaNO₃ solution (from Dzombak and Morel 1990).

Rev. 0

and the ionic strength of the solution was held at 0.5 M NH_4NO_3 . The adsorption curve (Fig. D.4-6) was used to estimate selenite adsorption at pH 8. The total selenite in the system is $1.27 \cdot 10^{-5}$ M and HFO surface area is $3806 \text{ cm}^2/\text{mL}$. At this pH, 97% of the selenite is adsorbed to the goethite surface. A Se^{4+} K_d for LAW vault waste of 170 mL/g was calculated from Eq. 1.

Radium

No information is available for radium adsorption on HFO. However, Dzombak and Morel (1990) provide a summary of adsorption data for barium ion on HFO. This barium data will be used as an analog for radium. The experiments used to determine the adsorption curves for barium on HFO are from Kurbatov (1949) and Duval and Kurbatov (1952). Kurbatov (1949) prepared HFO by the addition of NH_4OH to FeCl_3 solution at ionic strengths of 0.0038, 0.033, and 0.3 M NH_4Cl . Duval and Kurbatov (1952) prepared HFO by the addition of NH_4OH to FeCl_3 solution at an ionic strength of 0.0087 N NH_4Cl . The adsorption curves (Fig. D.4-7a,b,c,d,e) were used to estimate barium adsorption at pH 8. The total barium, HFO surface areas, and percentage Ba^{2+} adsorbed at pH 8 are shown in Table D.4-4. An average Ba^{2+} K_d for LAW vault waste of 60 mL/g was calculated for radium from Eq. 1.

Thorium

Hunter et al. (1988) conducted Th adsorption studies on goethite that show the characteristic adsorption edge of hydrolyzable metal ions on oxides. Adsorption was found to involve $\text{Th}(\text{OH})_2(2+)$, $\text{Th}(\text{OH})_3(+)$, and $\text{Th}(\text{OH})_4$. Experiments were focused on determining the effects of the major ions Mg^{2+} , Ca^{2+} , and SO_4^{2-} on the adsorption of Th on goethite as compared to adsorption in a NaCl electrolyte. Adsorbent and adsorbate concentrations were also varied to determine if these concentrations effect Th adsorption.

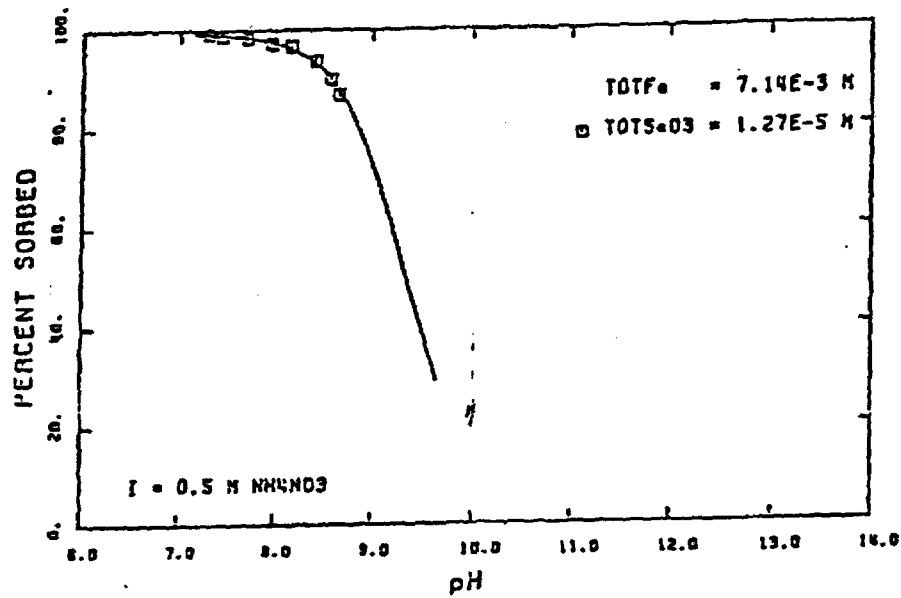
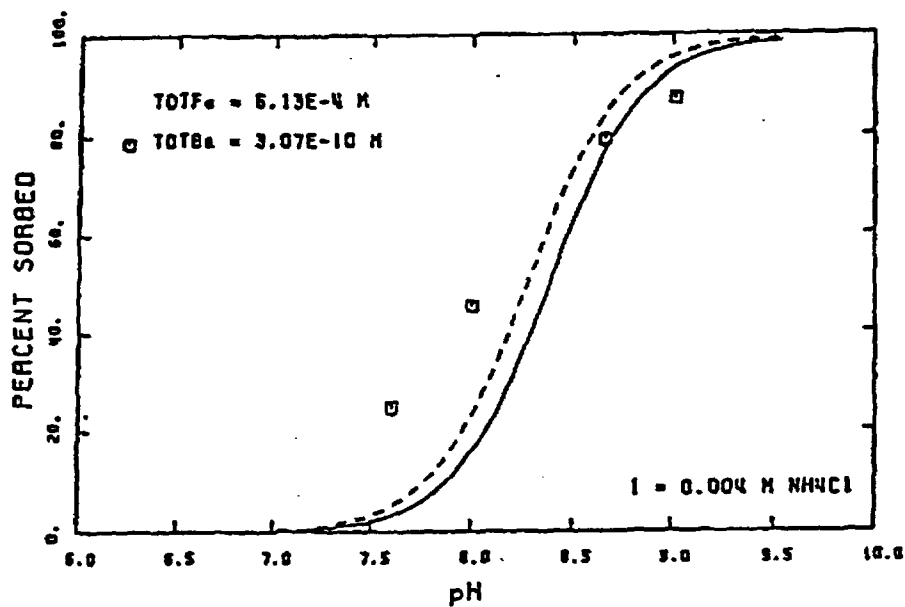
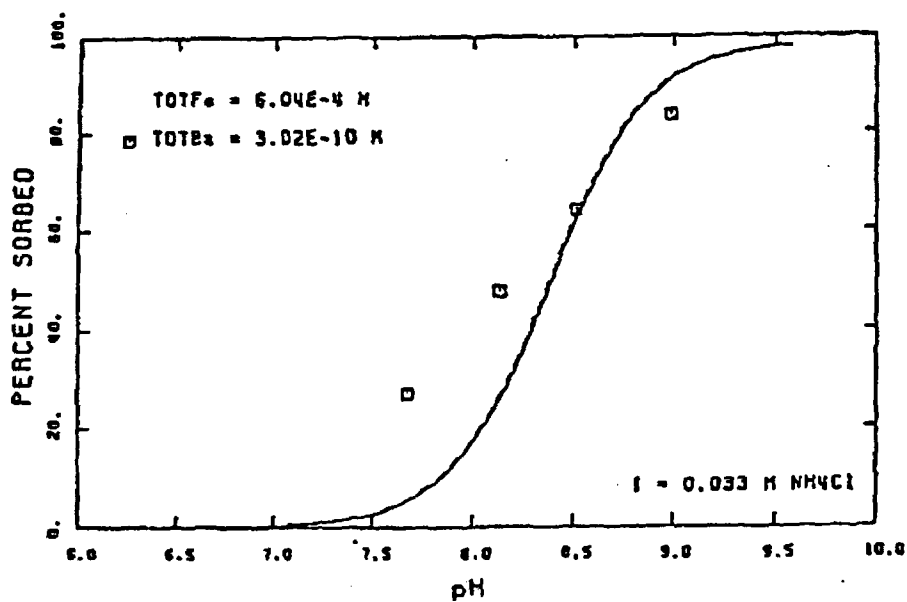


Fig. D.4-6. Adsorption of selenite on goethite as a function of pH in a 0.5 M NH_4NO_3 solution (from Dzombak and Morel 1990).

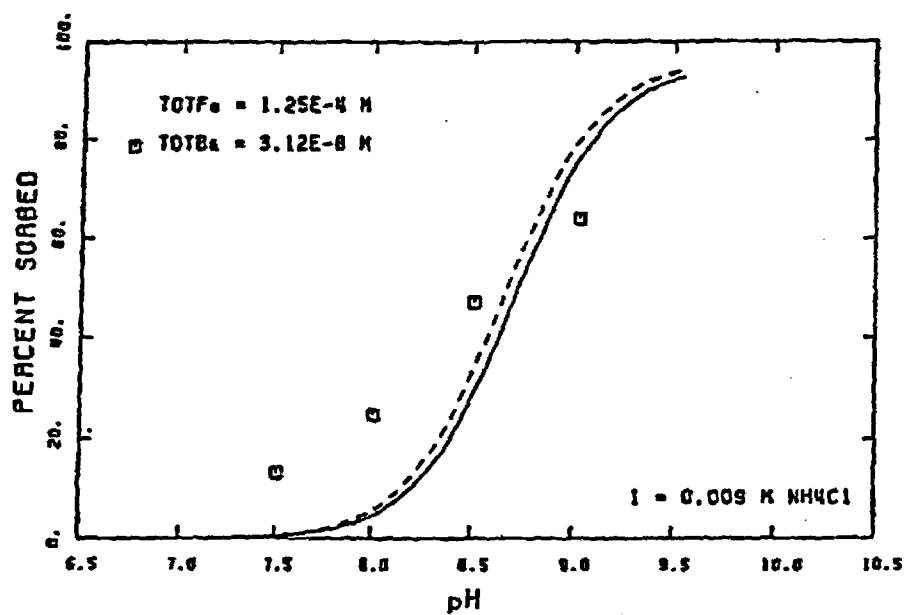


a)

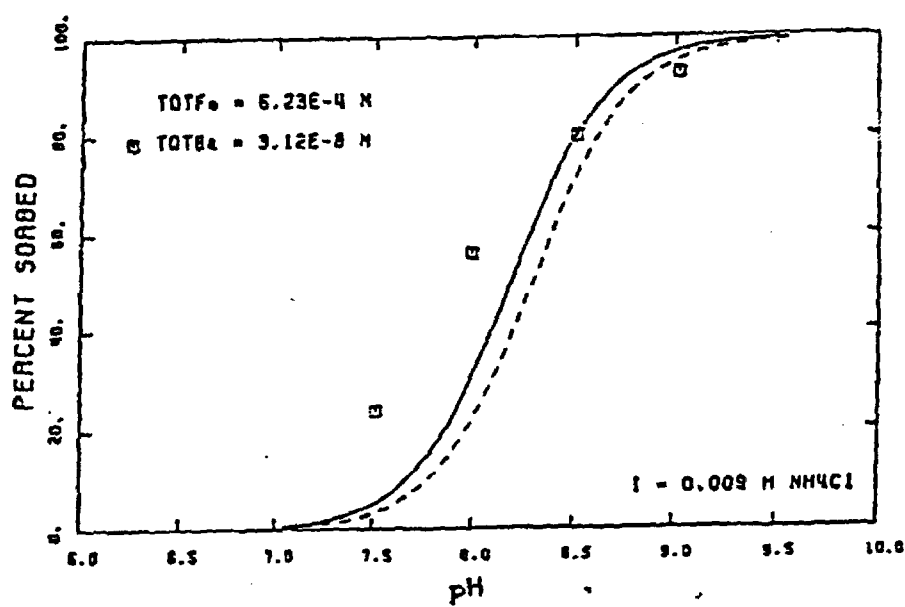


b)

Fig. D.4-7. Adsorption of barium on goethite as a function of pH as an analog for radium (from Dzombak and Morel 1990). a) 0.05 g goethite/L, b) 0.05 g goethite/L, c) 0.01 g goethite/L, d) 0.06 g goethite/L, e) 0.2 g goethite/L.



c)



d)

Fig. D.4-7. (continued).

Rev. 0

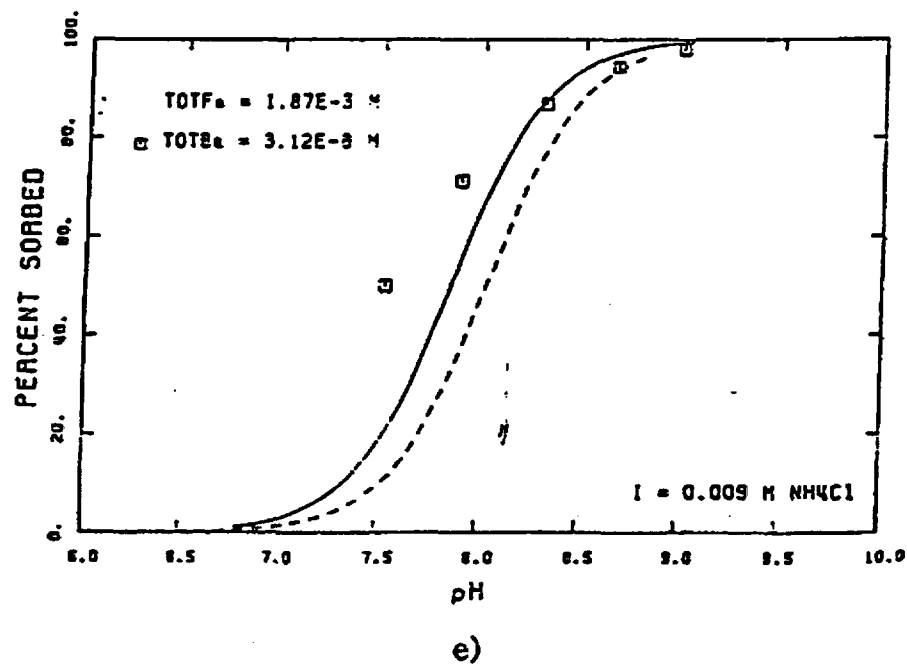


Fig. D.4-7. (continued).

Rev. 0

Table D.4-4. Adsorption data for barium used to estimate radium K_d

Total Ba (M)	Surface Area (cm ² /mL)	Percent Adsorbed	K_d (mL/g)
$3.07 \cdot 10^{-10}$	330	46	52
$3.02 \cdot 10^{-10}$	320	39	40
$3.12 \cdot 10^{-8}$	70	23	85
$3.12 \cdot 10^{-8}$	330	53	68
$3.12 \cdot 10^{-8}$	1000	74	57

The HFO was prepared by the addition of KOH to $\text{Fe}(\text{NO}_3)_3$ solution and the ionic strength of the solution was held at 0.1 M NaNO_3 . The adsorption curve (Fig. D.4-8) was used to estimate thorium adsorption at pH 8. The total thorium in the system is 6.6×10^{-5} M and HFO surface area is $80 \text{ cm}^2/\text{mL}$. At this pH, 90% of the thorium is adsorbed to the goethite surface. A Th K_d for LAW vault waste of 2200 mL/g was calculated from Eq. 1.

Neptunium

Neptunium has been identified in the aqueous phase in the IV, V, and VI oxidation states with Np(V) being most common for waters in contact with atmospheric oxygen between pH 5 and 11. Girvin et al. (1991) conducted Np(V) adsorption studies on synthetic iron oxyhydroxide. The HFO was prepared by the addition of NaOH to $\text{Fe}(\text{NO}_3)_3$ solution and the ionic strength of the solution was held at 0.1 M NaNO_3 . The adsorption curve (Fig. D.4-9) was used to estimate neptunium adsorption at pH 8. The total neptunium in the system is 4.7×10^{-12} M and HFO surface area is $5330 \text{ cm}^2/\text{mL}$. At this pH, 99.5% of the Np is adsorbed to the goethite surface. A Np K_d for LAW vault waste of 750 mL/g was calculated from Eq. 1.

Tin

No tin adsorption data is available for iron oxides. However, Dzombak and Morel (1990) provide a summary of adsorption data for Hg on HFO. The Hg experimental data of Avotins (1975) was used to determine the analog adsorption curve for tin on HFO. The HFO was prepared by the addition of NaOH to $\text{Fe}(\text{ClO}_4)_3$ solution and the ionic strength of the solution was held at 0.1 M NaClO_4 . The adsorption curves (Fig. D.4-10a,b) for mercury were used to estimate tin adsorption at pH 8. The total Hg in the system is 3.41×10^{-5} M and HFO surface area is $300 \text{ cm}^2/\text{mL}$. At this pH, 97% of the mercury is adsorbed to the goethite surface.

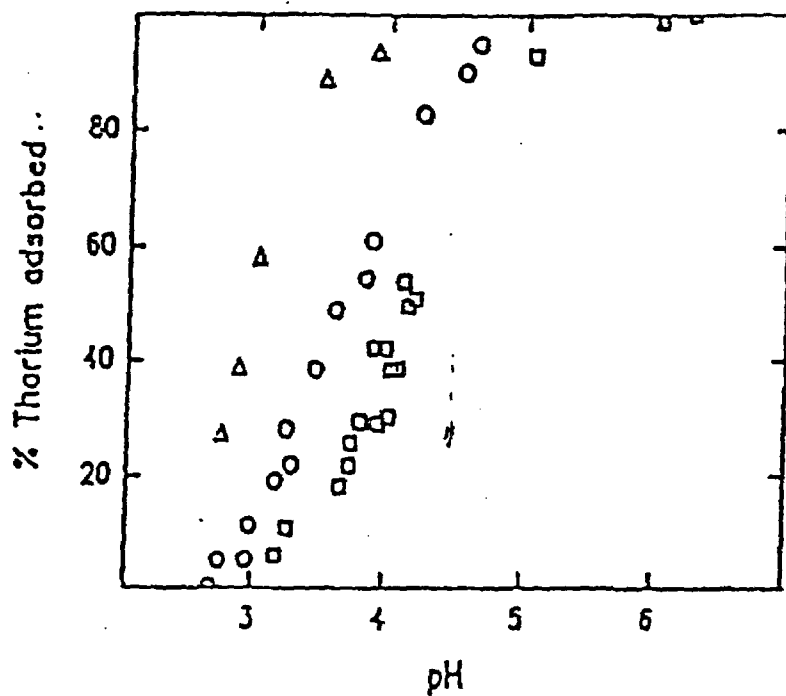


Fig. D.4-8. Adsorption of thorium on goethite as function of pH in 0.422 mol/Kg NaCl electrolyte at different thorium/oxide ratios (Hunter et al. 1988). Triangles: 9 micromol/L Th, 8.6 g/L goethite; Circles: 9 micromol/L Th, 0.54 g/L goethite; Squares: 45 micromol/L Th, 0.54 g/L goethite.

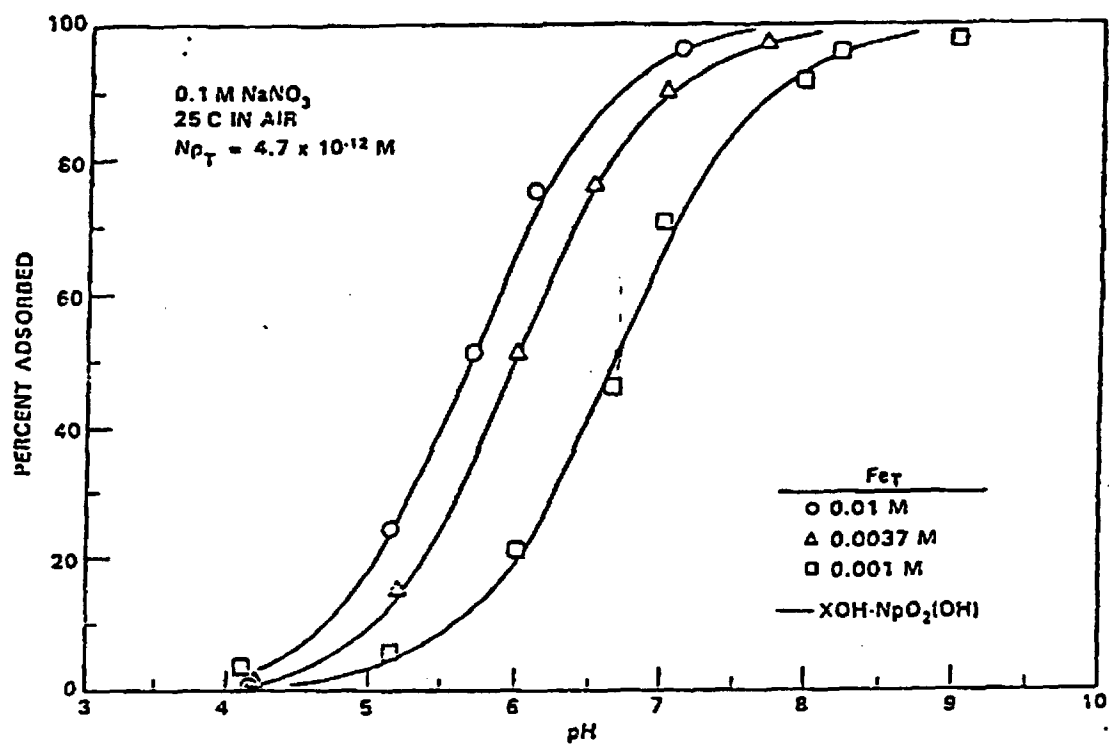
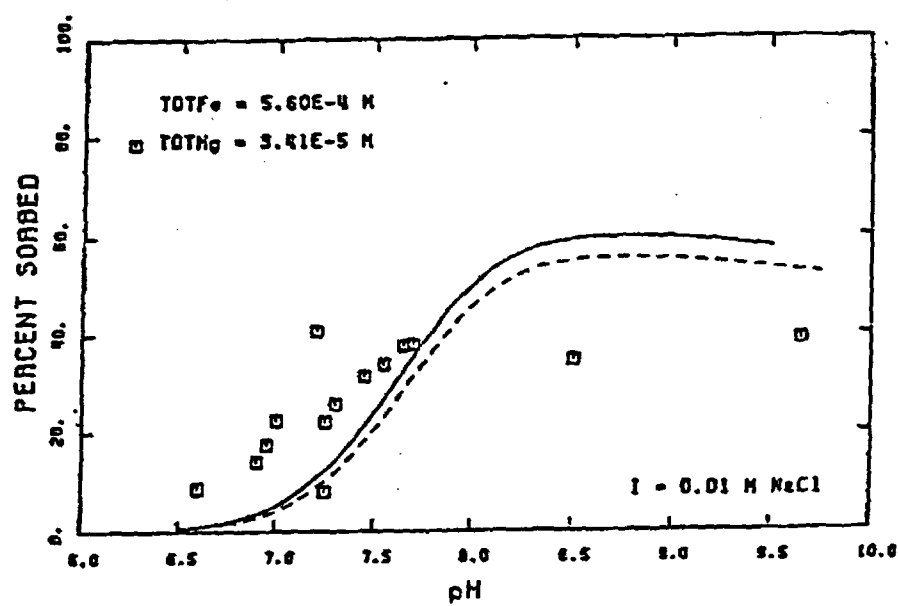
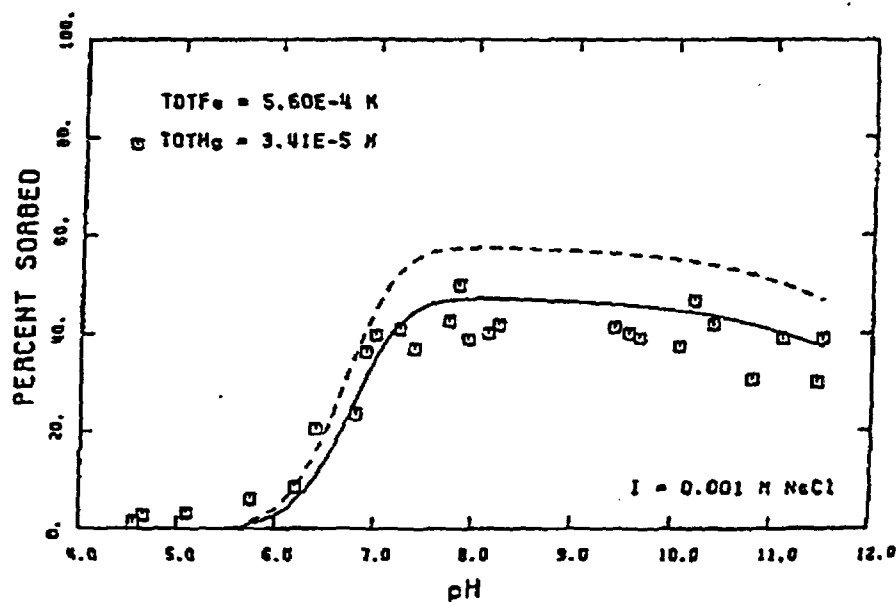


Fig. D.4-9. Adsorption of neptunium on goethite as function of pH (Girvin et al. 1991).
Triangles: 0.3 g/L goethite; Circles: 0.9 g/L goethite; Squares: 0.09 g/L goethite.



a)



b)

Fig. D.4-10. Adsorption of mercury on goethite as function of pH as an analog for tin (from Dzombak and Morel 1990). a) 0.05 g/L goethite, b) 0.05 g/L goethite.

An average tin K_d for LAW vault waste of 55 mL/g was calculated from Eq. 1.

Americium and Other Transplutonic Elements

Americium in aqueous environments can be found in the III, IV, V, and VI oxidation states. Am (III) is the most predominant oxidation state. No americium adsorption data was available for HFO so Cr(III) adsorption data summarized by Dzombak and Morel (1990) was used as an analog for americium. The HFO was used by prepared by the addition of NaOH to $\text{Fe}(\text{NO}_3)_3$ solution and the ionic strength of the solution was held at 0.1 M NaNO_3 (Leckie et al. 1980). The adsorption curve (Fig. D.4-11) was used to estimate Am adsorption at pH 8. The total Cr in the system is 5.0×10^{-6} M and HFO surface area is $530 \text{ cm}^2/\text{mL}$. At this pH, 99% of the chromium is adsorbed to the goethite surface. An americium K_d for LAW vault waste of 3700 mL/g was calculated from Eq. 1. Due to chemical similarities of the transplutonic elements, this K_d was also used for Cm(III), Bk(III), and Cf(III).

D.5 RADIONUCLIDE SOLUBILITY LIMITS

The release of radionuclides from the ILNT and ILT vaults will depend on the vault aqueous chemistry, solubility, and sorption behavior of the relevant radionuclides. The chemical conditions in the vaults will be controlled by the dissolution of the soluble constituents of the cement and by the corrosion of the iron waste containers and activated metals (Ewart et al. 1992). Corrosion of the waste containers and infiltration of water through the vaults will cause slow changes in the vault chemical conditions. Work conducted by Ewart et al. (1992) has shown that the pH of concrete repositories will remain above 10.5 for extended periods of time and Sharland et al. (1986) have shown that the oxidation potential throughout the near field will become reducing approximately 100 years after saturation. Ewart et al. (1992) have shown that the carbonate concentration in the near-field groundwater remain at a constant level of about 10^{-4} M to 10^{-5} M by the relatively high calcium concentration. These conditions provide low solubilities for actinides and provide

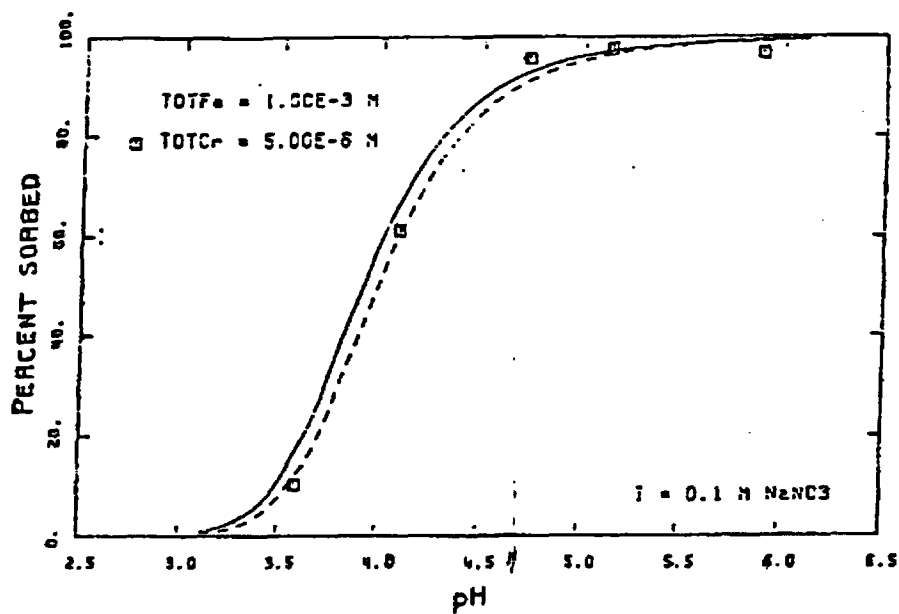


Fig. D.4-11. Adsorption of chromium III on goethite as function of pH as an analog for americium (from Dzombak and Morel 1990).

Rev. 0

a valuable chemical component of the multi-barrier containment of the waste. This section discusses the solubility limits for plutonium and uranium in the ILNT and ILT vault environments. Adsorption has been discussed in previous sections.

Plutonium

The tetravalent state of plutonium will predominate under the chemical conditions in the vaults. Solubility of plutonium was estimated assuming the controlling solid phase is amorphous $\text{Pu}(\text{OH})_4$ with the plutonium hydroxides (i.e. $\text{Pu}(\text{OH})^{3+}$, $\text{Pu}(\text{OH})_2^{2+}$, $\text{Pu}(\text{OH})_3^+$, and $\text{Pu}(\text{OH})_4^0$) comprising the soluble species.

A large variance, up to 16 orders of magnitude, in the solubility product values has been shown in experimental or theoretical techniques. Kim and Kanellakopulos (1989) have redone the experiments in order to provide a more substantiated solubility product value. A solubility product of $\log K_{sp} = -57.85 \pm 0.05$ for amorphous $\text{Pu}(\text{OH})_4$ was determined in a 1 M HClO_4 solution (Kim and Kanellakopulos 1989). This is the lowest value ever measured for amorphous $\text{Pu}(\text{OH})_4$ because the experiment includes the spectroscopic speciation to measure only the Pu^{4+} concentration (Kim and Kanellakopulos 1989). The formation constants for $\text{Pu}(\text{OH})^{3+}$, $\text{Pu}(\text{OH})_2^{2+}$, $\text{Pu}(\text{OH})_3^+$, and $\text{Pu}(\text{OH})_4^0$ were taken from Ewart et al. (1992). The reactions and constants used in the model are listed below in Table D.5-1.

Solubility calculations based on these thermodynamic data show a solubility limit of approximately 4.4×10^{-13} M for Pu(IV) at pH greater than 7. This value was used in the PORFLOW transport simulations. The solubility limit value does not change significantly above pH 7 (Fig. D.5-1). The solubility limit calculated here is lower than the average value reported by Ewart et al. (1992) of 7×10^{-11} M at high pH because a lower solubility product was used. The $\text{Pu}(\text{OH})_5^-$ species was not considered in the solubility calculations. Experimental observations by Ewart et al. (1992) indicate that this should not impact the calculations because $\text{Pu}(\text{OH})_5^-$ does not form to a significant extent.

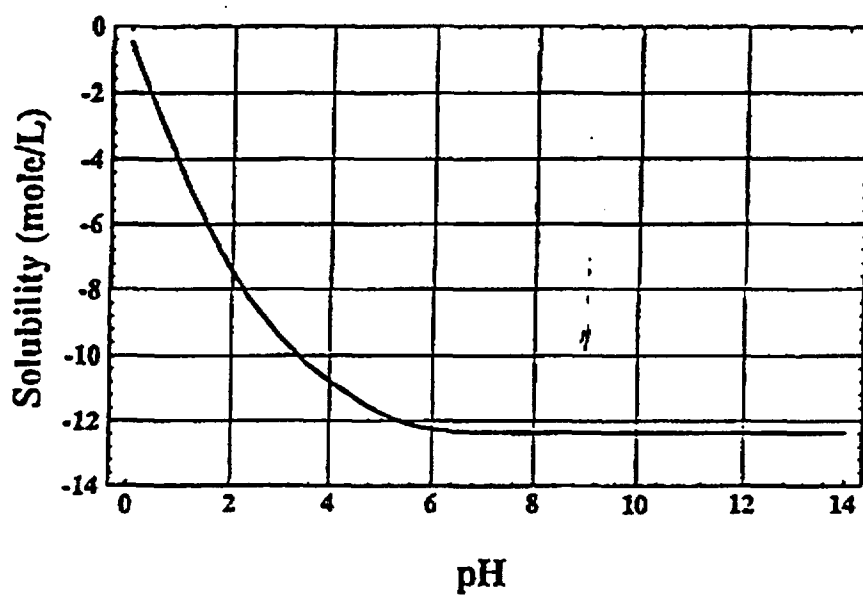


Fig. D.5-1. Estimated Pu(IV) solubility under E-Area conditions.

Rev. 0

Table D.5-1. Plutonium reactions considered

Reactions	log K	Reference
$\text{Pu}(\text{OH})_4 + 4\text{H}^+ \rightleftharpoons \text{Pu}^{4+} + 4\text{H}_2\text{O}$	-1.86	Kim and Kanellakopoulos 1989
$\text{Pu}^{4+} + \text{H}_2\text{O} \rightleftharpoons \text{PuOH}^{3+} + \text{H}^+$	-0.9	Ewart et al. 1992
$\text{Pu}^{4+} + 2\text{H}_2\text{O} \rightleftharpoons \text{Pu}(\text{OH})_2^{2+} + 2\text{H}^+$	-2.2	Ewart et al. 1992
$\text{Pu}^{4+} + 3\text{H}_2\text{O} \rightleftharpoons \text{Pu}(\text{OH})_3^+ + 3\text{H}^+$	-5.1	Ewart et al. 1992
$\text{Pu}^{4+} + 4\text{H}_2\text{O} \rightleftharpoons \text{Pu}(\text{OH})_4^0 + 4\text{H}^+$	-10.54	Ewart et al. 1992

Uranium

Uranium may be present in more than one oxidation state under the conditions found in the vaults. The solubility of uranium for both tetravalent and hexavalent states has been studied. The dominant oxidation state in the high pH and reducing conditions in the vault will be U(IV). The controlling solid selected for the calculations is uraninite, crystalline UO_2 , which is stable under the vault conditions (Brookins 1988) and is also present in nature. The value used for solubility limited transport calculations were generated by Orebaugh (1993) and confirmed for higher pH.

Orebaugh modeled uranium solubility using version 3.0 of ESP software from OLI Systems (OLI 1993). The calculations were based on the thermodynamic data provided with the software (based on Phillips et al., 1988). The oxidation state of the uranium was assumed to be reducing based on the presence of large amounts of iron in the vaults. The calculations were made for the major species U(IV) and U(VI) at concentrations of 10^{-6} M for each oxidation state at pH's between 4 and 8. Iron was present in equal amounts of 10^{-4} M for Fe(II) and Fe(III) and the redox couple is described by the equation:



Above pH 7 the solubility is controlled primarily by $\text{U}(\text{OH})_4$ in equilibrium with crystalline UO_2 . A total solubility for uranium of 3×10^{-10} M at pH 7 was used to model the release of uranium from the vaults in PORFLOW (Fig. D.5-2).

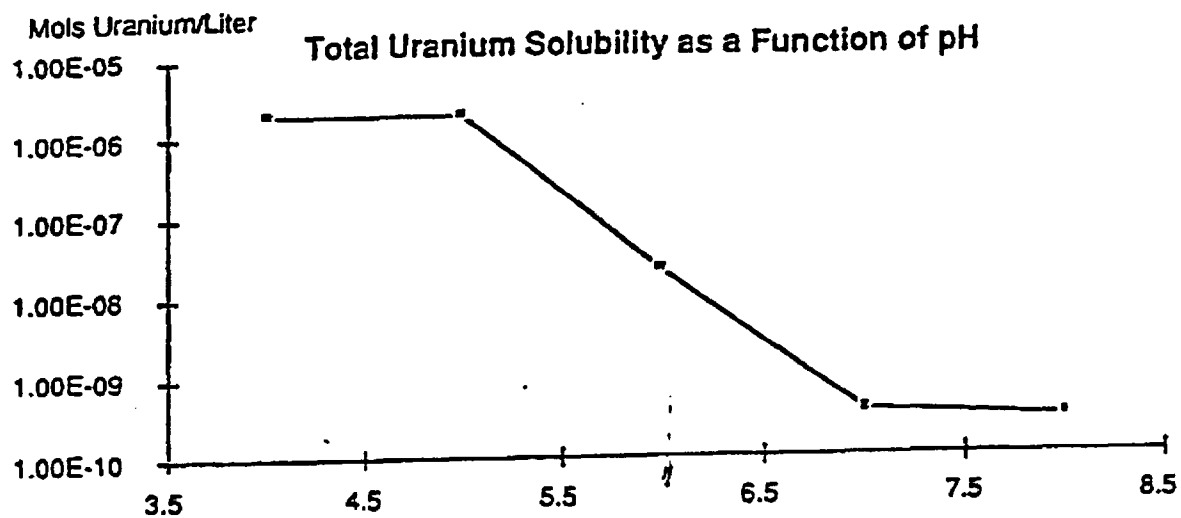


Fig. D.5-2. Estimated total uranium solubility under E-Area conditions (Source: Orebaugh 1993).

Solubility calculations conducted for U(IV) using Mathematica with uraninite as the controlling solid phase gave a similar solubility to that calculated by Orebaugh (1993) for the pH range of 7 to 12. Using the formation constants of Rai et al. (1990) and solubility product from Parks and Pohl (1988) a solubility of 3×10^{-10} M was calculated (Table D.5-2).

Table D.5-2. Uranium reactions considered

Reactions	log K	Reference
$\text{UO}_2 + 4\text{H}^+ \rightleftharpoons \text{U}^{4+} + 2(\text{H}_2\text{O})$	2.5	Parks and Pohl 1988
$\text{U}^{4+} + \text{H}_2\text{O} \rightleftharpoons \text{UOH}^{3+} + \text{H}^+$	-0.5	Rai et al. 1990
$\text{U}^{4+} + 2\text{H}_2\text{O} \rightleftharpoons \text{U}(\text{OH})_2^{2+} + 2\text{H}^+$	-4.0	Rai et al. 1990
$\text{U}^{4+} + 3\text{H}_2\text{O} \rightleftharpoons \text{U}(\text{OH})_3^+ + 3\text{H}^+$	-8.0	Rai et al. 1990
$\text{U}^{4+} + 4\text{H}_2\text{O} \rightleftharpoons \text{U}(\text{OH})_4^0 + 4\text{H}^+$	-12.0	Rai et al. 1990
$\text{U}^{4+} + 5\text{H}_2\text{O} \rightleftharpoons \text{U}(\text{OH})_5^- + 5\text{H}^+$	-26.0	Rai et al. 1990

The Orebaugh (1993) solubility calculations and Mathematica solubility calculations based on the thermodynamic data for U(IV) from Rai et al. (1990) and Parks and Pohl (1988) are in good agreement (Fig. D.5-3) above pH 7. Variation in the results below pH 7 is due to disregarding U(VI) in the Mathematica solubility calculation. This is not significant because the pH in the vaults should remain above pH 7 due to the high alkalinity of the concrete.

D.6 SORPTION IN SOILS

There has not been a need to generate K_d 's using iron oxide content of the soils. The K_d 's used in the PA are documented in tables within the text. Additional material may be added as required during the course of the PA.

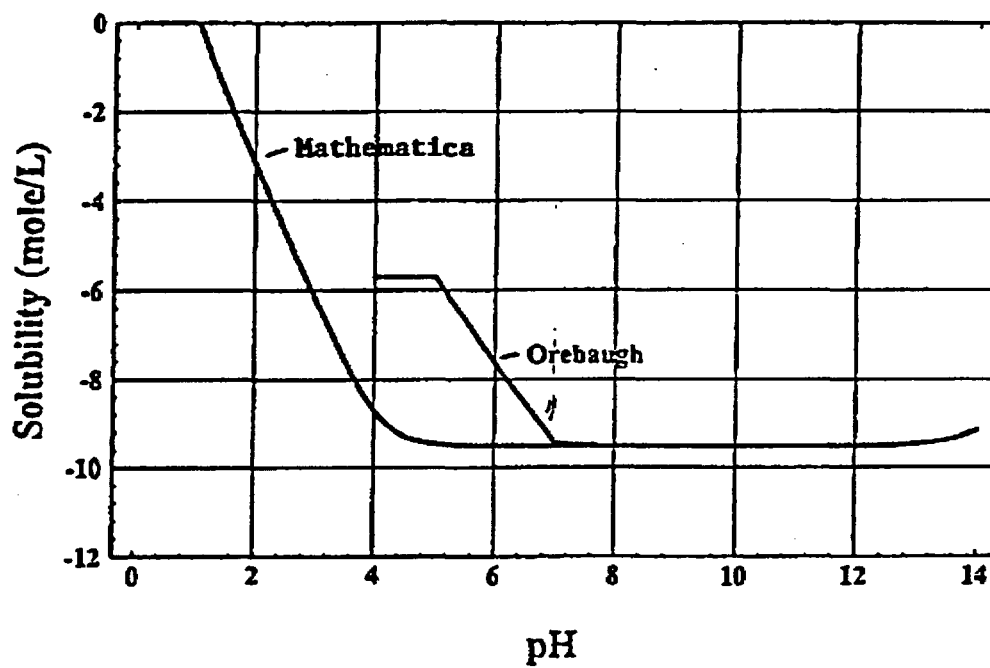


Fig. D.5-3. Comparison of uranium solubilities under E-Area conditions.

APPENDIX D

REFERENCES

- Avotins, P. V. 1975. *Adsorption and Coprecipitation Studies of Mercury on Hydrous Iron Oxide*. Ph.D. thesis. Stanford University, Stanford, Calif.
- Bondietti, E. A., and J. R. Trabalka. 1980. Evidence for Plutonium(V) in an Alkaline, Freshwater Pond. *Radiochem. Radioanal. Letters*, 42:169-176.
- Brookins, D. G. 1988. *Eh-pH Diagrams for Geochemistry*. Springer-Verlag, New York. p. 176.
- Duval, J. E., and M. H. Kurbatov. 1952. The Adsorption of Cobalt and Barium Ions by Hydrous Ferric Oxide at Equilibrium. *J. Phys. Chem*, 56(982-984).
- Dzombak, D. A., and F. M. M. Morel. 1990. *Surface Complexation Modeling: Hydrous Ferric Oxide*. Wiley-Interscience Publication, John Wiley & Sons, Inc.
- Ewart, F. T., J. L. Smith-Briggs, H. P. Thomason, and S. J. Williams. 1992. The Solubility of Actinides in a Cementitious Near-Field Environment. *Waste Management*, 12:241-252.
- Girvin, D. C., L. L. Ames, A. P. Schwab, and J. E. McGarrah. 1991. Neptunium Adsorption on Synthetic Amorphous Iron Oxyhydroxide. *Journal of Colloid and Interface Science*, 141:67-78.
- Harley, J. P., Jr. 1990a. *Specifications for Procurement of Low-Level Waste Burial Box*. Procurement Specification No. S4-G-183.
- Harley, J. P., Jr. 1990b. *Specifications for Procurement of 45 ft³ Disposal/Storage Box*. Procurement Specification No. S4-G-858.
- Hingston, F. J., A. M. Posner, and J. P. Quirk. 1968. *Adsorption of Selenite by Goethite*. In *Adsorption from Aqueous Solution*, Advances in Chemistry Series, American Chemical Society, pp. 82-90.
- Howard, J. H., III. 1977. Geochemistry of Selenium: Formation of Ferroselite and Selenium Behavior in the Vicinity of Oxidizing Sulfide and Uranium Deposits. *Geochimica et Cosmochimica Acta*, 41(1665-1678).

- Hsi, C. K. D., and D. Langmuir. 1985. Adsorption of Uranyl onto Ferric Oxyhydroxides: Application of the Surface Complexation Site-Binding Model. *Geochimica et Cosmochimica Acta*, 49(1931-1941).
- Hunter, K. A., D. J. Hawke, and L. K. Choo. 1988. Equilibrium Adsorption of Thorium by Metal Oxides in Marine Electrolytes. *Geochimica et Cosmochimica Acta*, 52(627-636).
- Kim, J. I., and B. Kanellakopulos. 1989. Solubility Products of Plutonium(IV) Oxide and Hydroxide. *Radiochimica Acta*, 48:145-150.
- Kinniburgh, D. G., J. K. Syers, and M. L. Jackson. 1975. Specific Adsorption of Trace Amounts of Calcium and Strontium by Hydrous Oxides of Iron and Aluminum. *Soil Science Society of America Proceedings*, 39(464-470).
- Kinniburgh, D. G., M. L. Jackson, and J. K. Syers. 1976. Adsorption of Alkaline Earth, Transition, and Heavy Metal Cations by Hydrous Oxide Gels of Iron and Aluminum. *Soil Science Society of America Proceedings*, 40(796-799).
- Kolarik, Z. 1961. Sorption Radioaktiver Isotopen an Niederschlagen. VI. System Eisen(II)-Hydroxyd-Strontiumnitratlösung und die allgemeinen gesetzmässigkeiten der Sorption am Eisen(III)-Hydroxyd. *Collection Czech. Chem. Commun.*, 27(938-949).
- Kurbatov, M. H. 1949. Rate of Adsorption of Barium Ions in Extreme Dilution by Hydrous Ferric Oxide. *Journal of American Chemical Society*, 71(858-863).
- Leckie, J. O., M. M. Benjamin, K. F. Hayes, G. Kaufman, and S. Altamann. 1980. *Adsorption/Coprecipitation of Trace Elements from Water with Iron Oxyhydroxide*. EPRI RP-910-1. Electric Power Research Institute, Palo Alto, CA.
- Leckie, J. O., A. R. Appleton, N. B. Ball, K. F. Hayes, and B. D. Honeyman. 1984. *Adsorptive Removal of Trace Elements from Fly-Ash Pond Effluents onto Iron Oxyhydroxide*. EPRI RP-910-1. Electric Power Research Institute, Palo Alto, CA.
- Nelson, D. M., and M. B. Lovett. 1978. Oxidation State of Plutonium in the Irish Sea. *Nature*, 236(599-601).

- Nelson, D. M., and M. B. Lovett. 1981. Measurements of the Oxidation State and Concentration of Plutonium in Interstitial Waters of the Irish Sea. In *Impacts of Radionuclide Releases into the Marine Environment*, Proc., Symp., Otaniemi, June 30-July 4, 1975. IAEA, Vienna.
- Nelson, D. M., and K. A. Orlandini. 1979. Identification of Pu(V) in Natural Waters. In *Radiological and Environmental Research Division Annual Report*, ANL-79-65, Part III, pp. 57-59.
- OLI. 1993. *ESP Version 3 Manual*. OLI Systems, Inc., Morris Plains, NJ.
- Orebaugh, E. G. 1993. *Modeling Uranium Solubility in Aged Vault Disposal*. WSRC-RP-93-1318. E. I. du Pont de Nemours and Company, Savannah River Laboratory, Aiken, SC.
- Parks, G. A., and Pohl, D. C. 1988. Hydrothermal solubility of uraninite. *Geochimica et Cosmochimica Acta*, 52:863-875.
- Phillips, S. L., Hale, F. V., Silvester, L. F., and Siegel, M. D. 1988. *Thermodynamic Tables for Nuclear Waste Isolation*. Aqueous Solution Database, NUREG/CR-4864, p. 138.
- Plotnikov, V. I. 1958. *Coprecipitation of Small Quantities of Selenium with Ferric Hydroxide*. Russian Journal of Inorganic Chemicals, 3(8):1761-1766.
- Rai, D., Felmy, A. R., and Ryan, J. L. 1990. Uranium(IV) Hydrolysis Constants and Solubility Product of $\text{UO}_2 \cdot x\text{H}_2\text{O}(\text{am})$. *Inorganic Chemistry*, 29:260-264.
- Sanchez, A. L., J. W. Murray, and T. H. Sibley. 1985. The Adsorption of Plutonium IV and V on Goethite. *Geochemica et Cosmochimica Acta*, 49(2297-2307).
- Sharland, S. M., P. W. Tasker, and C. I. Tweed. 1986. *The Evolution of Eh in the Pore Water of a Model Nuclear Waste Repository*. UKAEA Report AERE-R12442. Harwell Laboratory, UK.

APPENDIX E
HYDROGEOLOGY OF THE SRS

E.1 GEOLOGY

The surface of the Upper Atlantic Coastal Plain on which SRS is located slopes gently seaward. The province is underlain by a seaward dipping wedge of unconsolidated and semi-consolidated sediments that extends from the Fall Line to the seaward edge of the continental shelf. Sediment thickness increases from zero at the Fall Line, where the crystalline Piedmont province gives way to the Coastal Plain, to more than 1.2 km near the coast of South Carolina. The SRS is underlain by about 180 to 370 m of Coastal Plain sediments. The Coastal Plain sediments vary in age from Late Cretaceous to Recent. The Coastal Plain sediments are divided into several groups based principally on age and lithology. These groups are described briefly below. An in-depth treatment of the stratigraphy of the SRS is given in the Replacement Tritium Facility Draft Safety Analysis Report (WSRC 1992).

E.1.1 Late Cretaceous Lumbee Group

The Late Cretaceous sediments constitute the Lumbee Group, which includes, from oldest to youngest, the Cape Fear, Middendorf, Black Creek, and Peedee Formations (Fig. E.1-1). This group has also been referred to as the Tuscaloosa Formation (INTERA 1986). The thickness of the Lumbee Group varies across SRS from 120 m in the northwest to more than 230 m near the southeastern boundary.

The Cape Fear Formation is composed of poorly sorted silty-to-clayey quartz sands and interbedded clays. Bedding thicknesses range from 1.5 to 6 m, with sand beds being thicker than clay beds. The formation is about 9 m thick at the northwestern boundary of SRS, and it increases to more than 55 m near the southeastern boundary. This formation has not been observed to outcrop in the vicinity of the SRS.

The Middendorf Formation, which overlies the Cape Fear Formation, is composed mostly of medium and coarse quartz sand that is cleaner and less indurated than the underlying sediments. Clay casts and pebbly zones occur in several places in the

Rev. 0

COMPARISION OF HYDROSTRATIGRAPHIC UNITS USED AT SRS							
GEOLOGIC AGE	PRESENT NOMENCLATURE	SRP BASELINE HYDROGEOLOGIC STUDY		PROPOSED NOMENCLATURE AADLAND (1990)			
UNKNOWN	UPLAND	UPLAND UNIT			AQUIFER UNIT IIB ZONE 2	AQUIFER SYSTEM II	
TERTIARY	TOBACCO ROAD SAND	GROUP BARNWELL	TOBACCO ROAD	AQUIFER UNIT I/IIC	CONFINING ZONE IIB ₁ - IIB ₂		SYSTEMS BOUNDARY
	IRWINTON SAND MBR.		DRY BRANCH		7		
	TWIGGS CLAY MBR.		Tan clay				
	DRY BRANCH FM. (Griffins Landing Mbr.)						
	SANTEE FORMATION	McDEAN FORMATION			AQUIFER UNIT IIB ZONE 1	SYSTEM I-II CONFINING	
	CAWCAW MEMBER	Green clay			CONFINING UNIT IIA - IIB		
	CONGAREE FM.	CONGAREE			AQUIFER UNIT IIA		
	FISHBURNE FM. (Four Mile Mbr.)	WILLIAMSBURG FM			SYSTEM I-II CONFINING		
	WILLIAMSBURG FM. (Snapp Member)						
	REHMS FORMATION (Ellenton Mbr.)	ELLENTON FM			SYSTEM I AQUIFER		
CRETACEOUS	PEEDEE FM. (Steel Creek Mbr.)	PEEDEE FORMATION		CONFINING UNIT I/IIB-I/IIC			
	BLACK CREEK FM.	BLACK CREEK FM		CONFINING UNIT I/IIA - I/IIb		CONFINING UNIT IA-B	
	MIDDENDORF FM.	MIDDENDORF FM		AQUIFER UNIT I/IIA		AQUIFER UNIT IA	
	CAPE FEAR FM.	CAPE FEAR FM		CONFINING SYSTEM I			
TRIASSIC OR PALEOZOIC BASEMENT				PALEOZOIC - TRIASSIC BASEMENT HYDROLOGIC SYSTEM			

SRS111

Fig. E.1-1. Hydrologic and stratigraphic units underlying the SRS.

E2

WSRC-RP-94-218

Middendorf Formation. A clay zone up to 24 m thick forms the top of this formation over much of the SRS. In total, the Middendorf Formation ranges from approximately 40 to 55 m thick from the northwestern to southeastern boundary of the SRS. Outcrops of this formation have been identified northwest of the SRS.

The Black Creek Formation consists of quartz sands, silts and clays. The lower section consists of fine- to coarse-grained sands, with layers of pebbles and clay casts. The upper section changes in composition as it crosses the SRS from northwest to southeast; from massive clay to silty sand with interbeds of clay. Thickness of the Black Creek Formation under the SRS ranges from 34 m in the northwest to 76 m in the southeast. Outcropping in the vicinity of the SRS has not been confirmed.

The uppermost formation in the Lumbee Group is the Peedee Formation, which consists of fine-grained sandstone and siltstone with marine fossils. This formation is subtitled as the Steel Creek Member in Fig. E.1-1 to distinguish this formation from the Peedee Formation in southwestern South Carolina that is comparable in age, but lithologically distinct. The lower portion of this formation consists of fine- to coarse-grained quartz sand and silty sand, with a pebble-rich zone at its base. Pebbly zones and clay casts are common throughout the lower portion of the Peedee Formation. The upper portion of this formation is a clay that varies from more than 15 m to less than 1 m in thickness at the SRS. The Peedee Formation is about 34 m thick at the northwestern SRS boundary, and about 40 m thick at the southeastern boundary. No nearby outcropping has been identified.

E.1.2 Paleocene-Eocene Black Mingo Group

The Paleocene-Early Eocene sediments make up the Black Mingo Group. This group consists of the Early Paleocene Rhems Formation, the Late Paleocene Williamsburg Formation, and the Early Eocene Fishburne Formation (Fig. E.1-1). This group is about 21 m thick at the northwestern SRS boundary, thickens to about 46 m near the southeastern boundary, and is about 210 m thick at the coast.

The Rhems Formation has also been called the Ellenton Formation (INTERA 1986), but is now believed to be the time-equivalent to the Rhems Formation with some lithological differences in the vicinity of SRS. Thus, it is now designated as the Ellenton Member of the Rhems Formation (Fig. E.1-1). The Ellenton Member consists mostly of gray, poorly sorted, micaceous, lignitic, silty and clayey quartz sand interbedded with gray clays. It is approximately 12 m thick at the northwestern boundary of the SRS and thickens to about 30 m near the southeastern boundary. This formation outcrops about four miles northwest of the SRS.

The deposits near the SRS that are time equivalent to the Williamsburg Formation differ from the type Williamsburg and are designated as the Snapp Member of the Williamsburg Formation. The sediments are typically silty, medium- to coarse-grained quartz sand interbedded with clay. The Snapp Member is about 9 m thick at the northwestern SRS boundary and thickens to about 15 m near the southeastern boundary. Sediments of this formation have not been identified to outcrop northwest of the SRS. Although the Fishburne Formation exists in southwestern South Carolina, only one Early Eocene fossil assemblage has been found at the SRS. The distribution of any Fishburne equivalent at the SRS is not known at this time.

E.1.3 Middle Eocene Orangeburg Group

The Middle Eocene sediments make up the Orangeburg Group, which consists of the lower Middle Eocene Congaree Formation and the upper Middle Eocene Santee Limestone Formation. The sediments thicken from about 30 m at the northwestern SRS boundary to about 49 m near the southeastern boundary. The dip of the upper surface of this formation is about .002 m/m to the southeast across the site. The Orangeburg Group is about 100 m thick at the coast. The group outcrops at lower elevations in many places near and on the SRS.

The Congaree Formation consists of fine to coarse quartz sands. Thin clay laminae occur throughout with pebbly layers, clay casts, and glauconite present in places. A glauconitic clay encountered in some wells on the SRS may be at or near the base of this formation. In many places at the SRS, the upper part of the Congaree Formation is

cemented with silica, while in other places it is slightly calcareous. The well-sorted sands, glauconite, and a few fossils indicate that the Congaree is a shallow marine deposit. The formation is about 18 m thick at the northwestern boundary of the SRS and about 26 m thick near the southeastern boundary.

The Santee Limestone Formation consists of carbonates, calcareous quartz sands, quartz sands, glauconitic sands, and clays. The sediments comprising this formation have been referred to in the past as the McBean and Lisbon Formations. However, more recently (WSRC 1992), these sediments are considered to be one of three members of the Santee Limestone Formation. A fine-grained sandstone occurs at the base of the Santee Limestone Formation at several locations across the SRS. This sandstone is referred to as the Warley Hill Member. Green clay, which also occurs near the base of this formation, is referred to as the Caw Caw Member of the Santee Limestone. The remainder of the Santee Limestone Formation is assigned to the McBean Member, which dominates the formation and is made up of micritic, calcarenitic, and shelly limestone, calcareous quartz sand, and noncalcareous, generally fine-grained quartz sand. Previous investigations in the nearby vicinity (Z-Area) indicate that the green clay is not a discrete clay bed, but rather a series of thin clays interlayered with sandy clays (Dennehy et al. 1989). Therefore, the green clay tends to thicken and thin, and grade laterally into the sands of the overlying McBean Member (Dennehy et al. 1989).

Above the green clay, the McBean Member is comprised of 13 m of poorly sorted multi-colored clayey sand with clay lenses. Calcareous components of the McBean Member are rare in the northwestern part of the SRS, more abundant in central portions, and increase to the southeast across the SRS where they are widespread and thick. Siple (1967) noted that voids and loosely compacted sediments were encountered during well drilling and mentioned that large amounts of cement grout were used to stabilize the subsurface before construction of heavy structures, suggesting that dissolution of calcareous material in the Santee Limestone has occurred at the SRS. The Formation is about 12 m thick at the northwestern boundary and thickens to more than 24 m near the southeastern boundary. All three members of the Santee Limestone Formation outcrop within the SRS boundary.

E.1.4 Late Eocene Barnwell Group

The Late Eocene sediments make up the Barnwell Group, which consists of the Clinchfield, Dry Branch, and Tobacco Road Sand Formations (Fig. E.1-1). The Clinchfield Formation, the oldest of the three, is made up of quartz sand and has been identified only when the contrasting carbonates of the Dry Branch and Santee Limestone Formations are present, with the sand of the Clinchfield Formation sandwiched between them. It has been identified at several areas within the SRS, where it is up to 8 m thick, but it cannot be mapped with available data.

The Dry Branch Formation consists of three distinguishable members: the Griffins Landing Member, the Irwinton Sand Member and the Twiggs Clay Member. The latter member does not appear to be mappable within the SRS, but lithologically similar clay is present at various levels within this formation. The composition of the tan clay, varies from a dark brown to tan clayey sand to a red to dark brown sandy clay. There is no geologic evidence suggesting a discrete clay layer for the Twiggs Clay Member. Rather, this member is apparently a series of intercalated clay and sand layers.

The carbonate of the Griffins Landing Member is up to 14 m thick in the southeastern part of the SRS. This member consists mostly of calcilutite and calcarenite, calcareous quartz sand, and slightly calcareous clay. It occurs sporadically at the SRS and is not known to be present northwest of Tinker Creek and UTR Creek within the SRS boundaries. The Griffins Landing Member has previously been considered to be part of the "McBean Formation" (Siple 1967; INTERA 1986). The remainder of the Dry Branch Formation within the SRS is made up of the Irwinton Sand Member, which is composed of moderately sorted quartz sand, with interlaminated clays abundant in places. The Dry Branch formation is about 15 m thick at the northwestern SRS boundary, and thickens to 24 m near the southeastern boundary. It outcrops in many places around and within the SRS.

The Tobacco Road Sand overlies the Dry Branch Formation. The base of this unit is marked by a coarse layer that can contain flat quartz pebbles. The rest of the formation is made up of moderately to poorly sorted quartz sands. The sediments have the characteristics of a shallow marine deposit. The upper surface of this formation is irregular due to an incision that accompanied deposition of the overlying "Upland" unit and later erosion. The

thickness is variable as a result of erosive processes, but is at least 15 m in places. The Tobacco Road Sand of Barnwell Group (INTERA 1986), is widely exposed at the SRS. The combined thickness of the Dry Branch and Tobacco Road formations at the coast is almost 120 m.

E.1.5 "Upland Unit"

The "Upland Unit" is an informal stratigraphic term applied to terrestrial deposits that occur at higher elevations in some places in the southwestern South Carolina Coastal Plain. This unit occurs at the surface at higher elevations in many places around and within the SRS, but it is not present at all higher elevations. The sediments are poorly sorted, clayey-to-silty sands, with lenses and layers of conglomerates, pebbly sands, and clays. Clay casts are abundant. The "Upland" unit is up to 21 m thick in parts of the SRS. Much of this unit corresponds to the Hawthorne Formation and the Tertiary alluvial gravels identified in previous documents (INTERA 1986).

E.1.6 Quaternary Deposits

Cooke (1936) identified seven marine terraces in the region near the SRS, although the highest three are extensively eroded and are not easily recognized. The terrace deposits are a few tens of feet thick. The origin of these deposits is not definitive. Recent alluvium occurs in the main and tributary channels of the Savannah River and other streams in the vicinity of the SRS.

E2 GROUNDWATER HYDROLOGY

An alpha-numeric system of hydrostratigraphic nomenclature was developed by Aadland (1990) for SRS. Figure E.1-1 illustrates the alphanumeric system and compares it to other systems developed in previous studies.

E.2.1 Aquifer System I

The lowermost aquifer system, referred to as Aquifer System I, is regional in nature and includes the Middendorf Formation, the Black Creek Formation, and the Peedee Formation (Fig. E.1.1). These formations are of Cretaceous age and consists of beds of sands, silts, and clays. Aquifer System I is further divided into aquifer zones and confining zones depending upon hydraulic properties. This system serves as a major source of water for SRS and the region.

E.2.2 Confining System I-II

Confining System I-II separates Aquifer System I from Aquifer System II (Fig. E.1.1). Greater than 30 m thick, it is comprised of the Ellenton Clays. Hydraulically, it restricts flow between Aquifer System I and Aquifer System II.

E.2.3 Aquifer System II

Because of relative hydrologic isolation due to Confining System I, only the uppermost system of the two major aquifer systems is of interest for contamination studies at E-Area. This aquifer system, referred to as Aquifer System II, is divided into individual units and further subdivided into zones. These units and zones primarily relate to hydrogeological characteristics. The units and zones which comprise the aquifer system are as follows:

<u>Nomenclature of Aadland (1990)</u>	<u>Common Nomenclature</u>
Aquifer System II	
Aquifer Unit IIB, Zone 2	Water Table Aquifer
Confining Unit IIB1-IIB2	Tan Clay
Aquifer Unit IIB, Zone 1	Barnwell/McBean Aquifer
Confining Unit IIA-IIB	Green Clay
Aquifer Unit IIA	Congaree Aquifer
Confining System I-II	Ellenton Clays

E-Area is located within the GSA of the SRS. The GSA includes the present burial grounds and E-Area.

E23.1 Confining System I-II

Confining System I-II (Ellenton Clays) is a silty to sandy lignitic, micaceous clay interbedded with fine to coarse quartz sand. Individual layers of clays, silts, and sandy clays range in thickness from 0.6 to 6.7 m. Individual layers of clayey sands range in thickness from 0.3 to 4.6 m. Clay and silt lenses of Confining System I-II consist of buff and light gray to black clay and sandy clay. The interbeds of clayey sands and sands are generally fine to coarse grained and range from moderate to very poorly sorted. Grains are subangular to angular (GeoTrans 1992).

Confining System I-II attains a thickness of over 30 m in the GSA. The unit appears to occur no further northwest than the northwest boundary of SRS where it is about 12 m in thickness. Regionally, the unit thickens to the southeast.

E23.2 Aquifer Unit IIA

Aquifer Unit IIA (Congaree Aquifer) unconformably overlies Confining System I-II (Ellenton Clays) and ranges from 15.8 to 32.6 m thick within the GSA. The unit dips at 1.5 to 1.7 m per km to the south and southeast. Additionally, the unit thickens in the western portion of the GSA and to a minor extent, thickens to the southeast.

Clayey layers are encountered to some degree at all depths throughout the formation. However, by far the majority of such layers occur below an elevation of 24 m MSL which corresponds to the lower and middle portions of the formation. The unit consists predominantly of sands and clayey sands with small interbeds of sandy clays, clays, and calcareous sands. The sands and clayey sands range in thickness from 0.6 to 25.6 m while the sandy clays and clays range in thickness from 0.3 to 2.7 m. Calcareous sands range in thickness from 0.6 to 0.9 m. Sands and clayey sands of Aquifer Unit IIA are largely yellow to orange in color and consists of fine to coarse grained, subangular to subrounded quartz. The sands vary from well to poorly sorted.

Groundwater flow in the aquifer at E-Area is to the west toward UTR Creek (Fig. E.2-1). A local potentiometric map of Aquifer Unit IIA was developed based upon water level data from E-Area wells (Fig. E.2-2) which indicates the flow direction. A regional potentiometric map of Aquifer Unit IIA is provided in Fig. E.2-3 for comparison purposes. The horizontal gradient of the aquifer is estimated to be 0.006 in the GSA area. Based on a slug test (WSRC 1991) the hydraulic conductivity of the aquifer was estimated to be 6.46×10^{-4} cm/s in the GSA area.

E.2.3.3 Confining Unit IIA-IIB

Confining Unit IIA-IIB (Green Clay) separates Aquifer Unit IIA and Aquifer Unit IIB. This confining unit is locally known as the Green Clay. Recent investigations have indicated that this unit is comprised of several lenses of green clay that thicken, thin, and pinch out abruptly. Thickness can be variable, from 0.6 to 9 m. Although Confining Unit IIA-IIB does not always appear during drilling to be a significant geologic feature, wells screened above and below the layer routinely have very different heads. Thus, Confining Unit IIA-IIB retards downward vertical leakage from Aquifer Unit IIB, Zone 1 (Barnwell/McBean Aquifer), into Aquifer Unit IIA (Congaree Aquifer). The unit is thin to the west and southeast, becoming thicker to the north. Structural lows in the unit tend to correspond to areas of carbonate accumulation in the overlying sediments. In addition, the clays of the unit thin or truncate in these areas.

Confining Unit IIA-IIB consists predominantly of clays, sandy clays, and clayey sands. Locally, beds of calcareous mud contribute significant thickness to the unit. Minor interbeds of sands are also present. The clay and sandy clay lenses in the unit range in thickness from 0.6 to 3.6 m. The clayey sand beds range in thickness from 0.3 to 4.2 m. Calcareous muds range in thickness from 0.9 to 3.3 m and the sand beds range in thickness from 0.3 to 1.8 m (GeoTrans 1992).

The clayey sands are generally moderately to poorly sorted with grain sizes ranging from medium to very coarse. They are described as light tan to orange in color, fine to very fine grained, well sorted and occasionally indurated. Grains are usually subangular and in some layers cemented with silica.

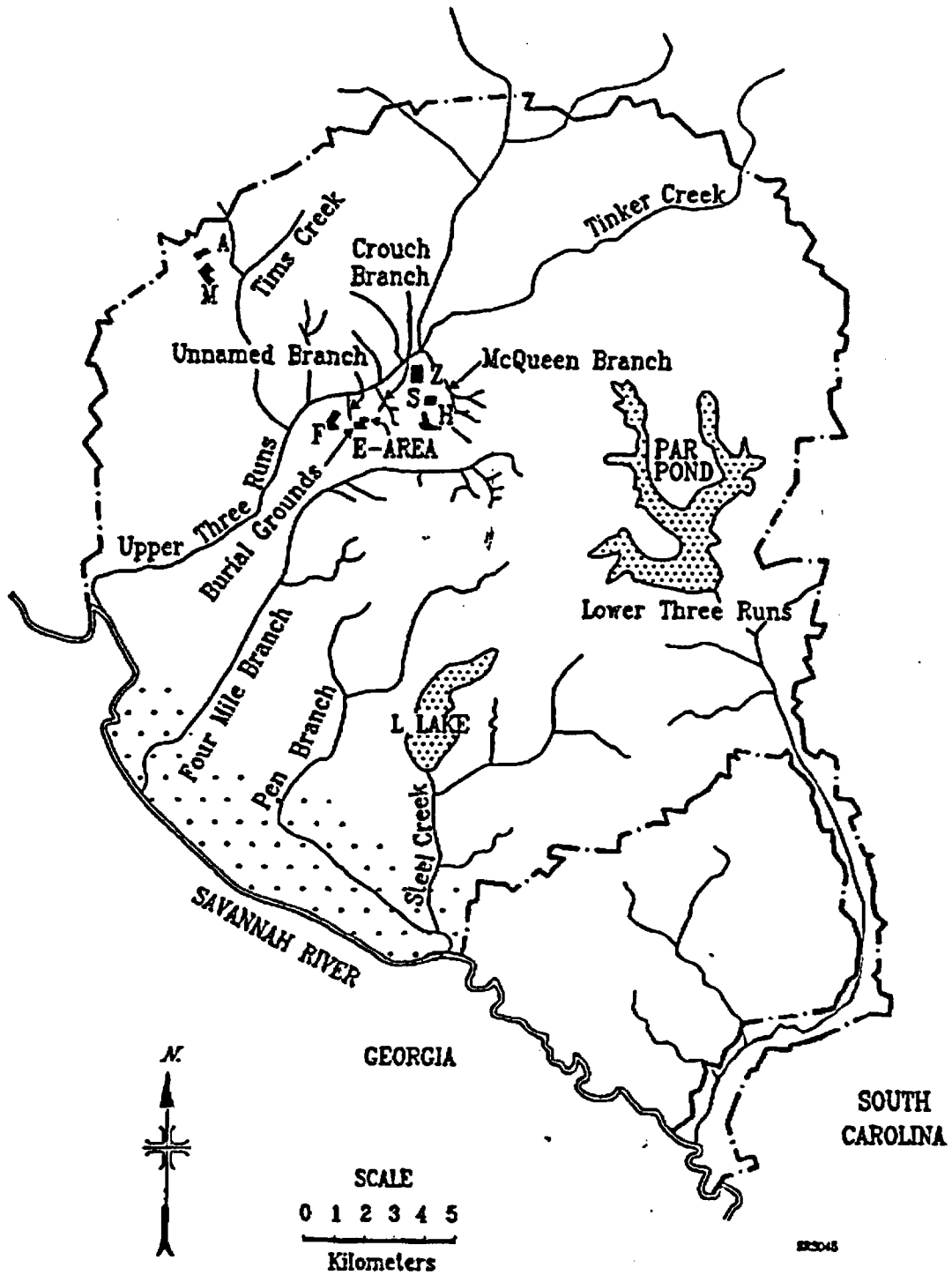


Fig. E.2-1. Surface drainage map of the SRS.

Rev. 0

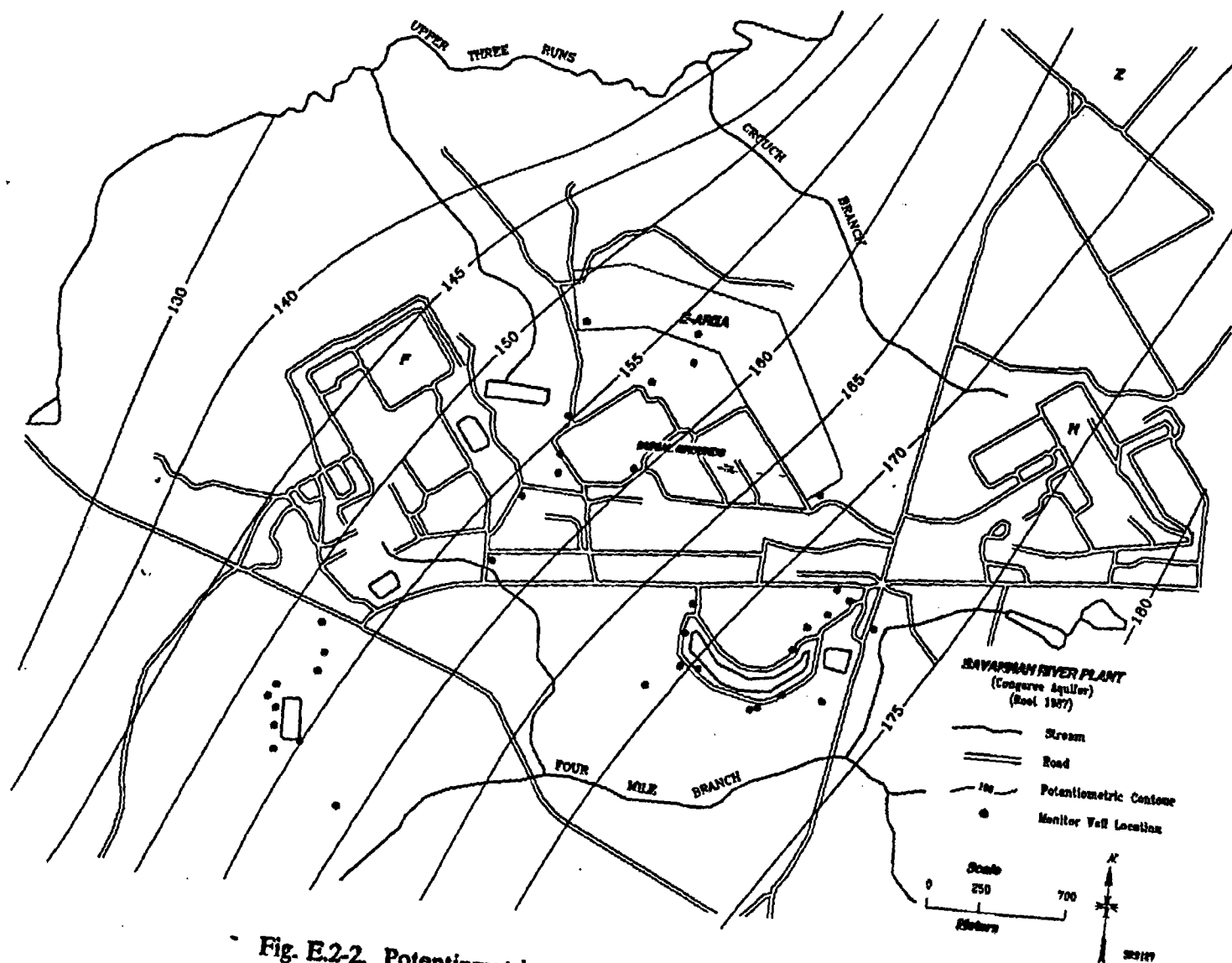


Fig. E.2-2. Potentiometric surface of Aquifer Unit IIA at E-Area.

E-12

WSRC-RP-94-218

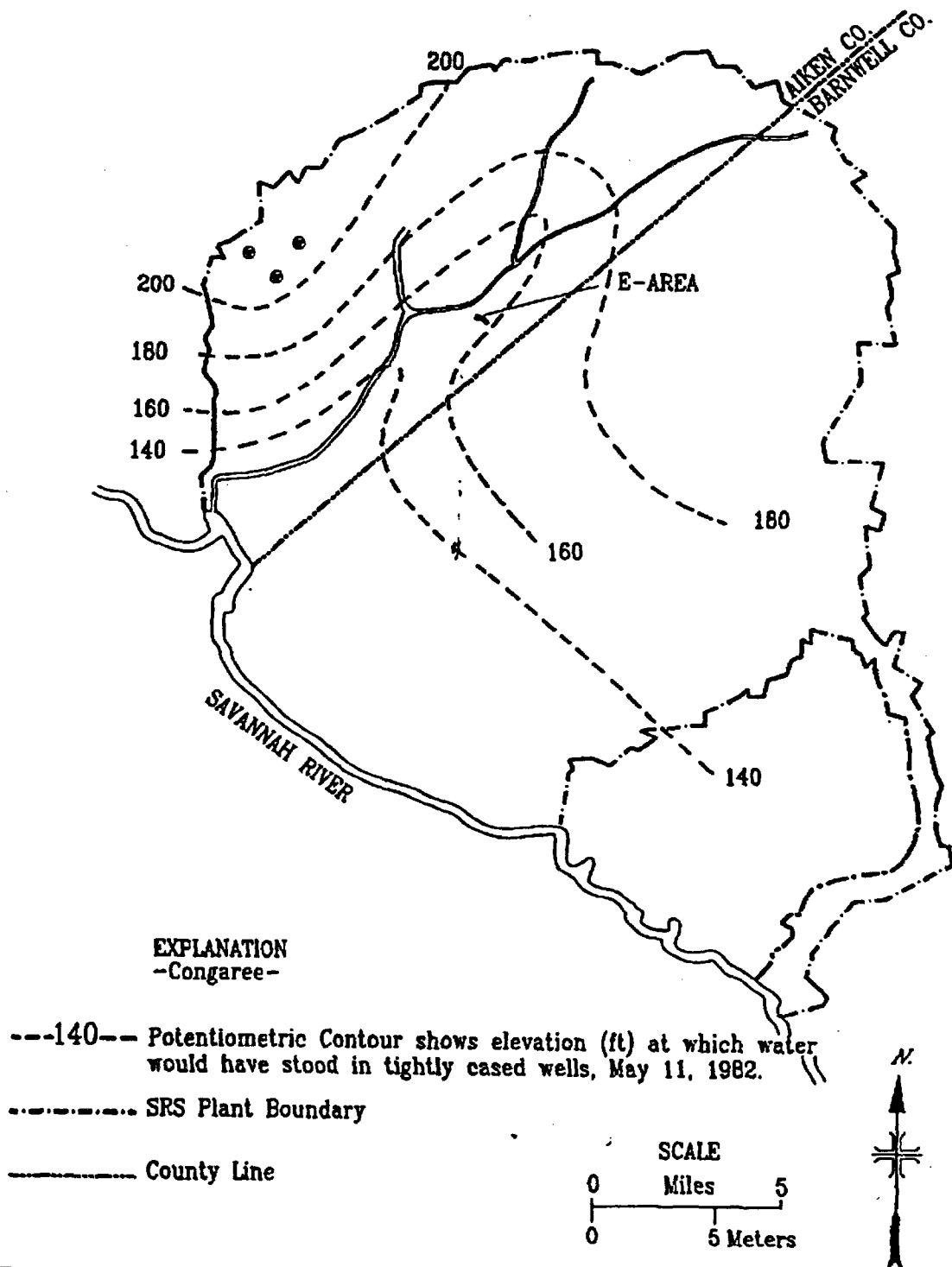


Fig. E.2-3. Regional potentiometric surface of Aquifer Unit IIA (Christensen and Gordon 1983).

SRS077

From laboratory tests of undisturbed samples, the hydraulic conductivity of Confining Unit IIA-IIB has been determined to range from 1.4×10^{-8} to 1.6×10^{-7} cm/s (horizontal) and 6.5×10^{-9} to 4.4×10^{-8} cm/s (vertical). The vertical gradient has been estimated to be 5.5 m/m (WSRC 1991).

E2.3.4 Aquifer Unit IIB1

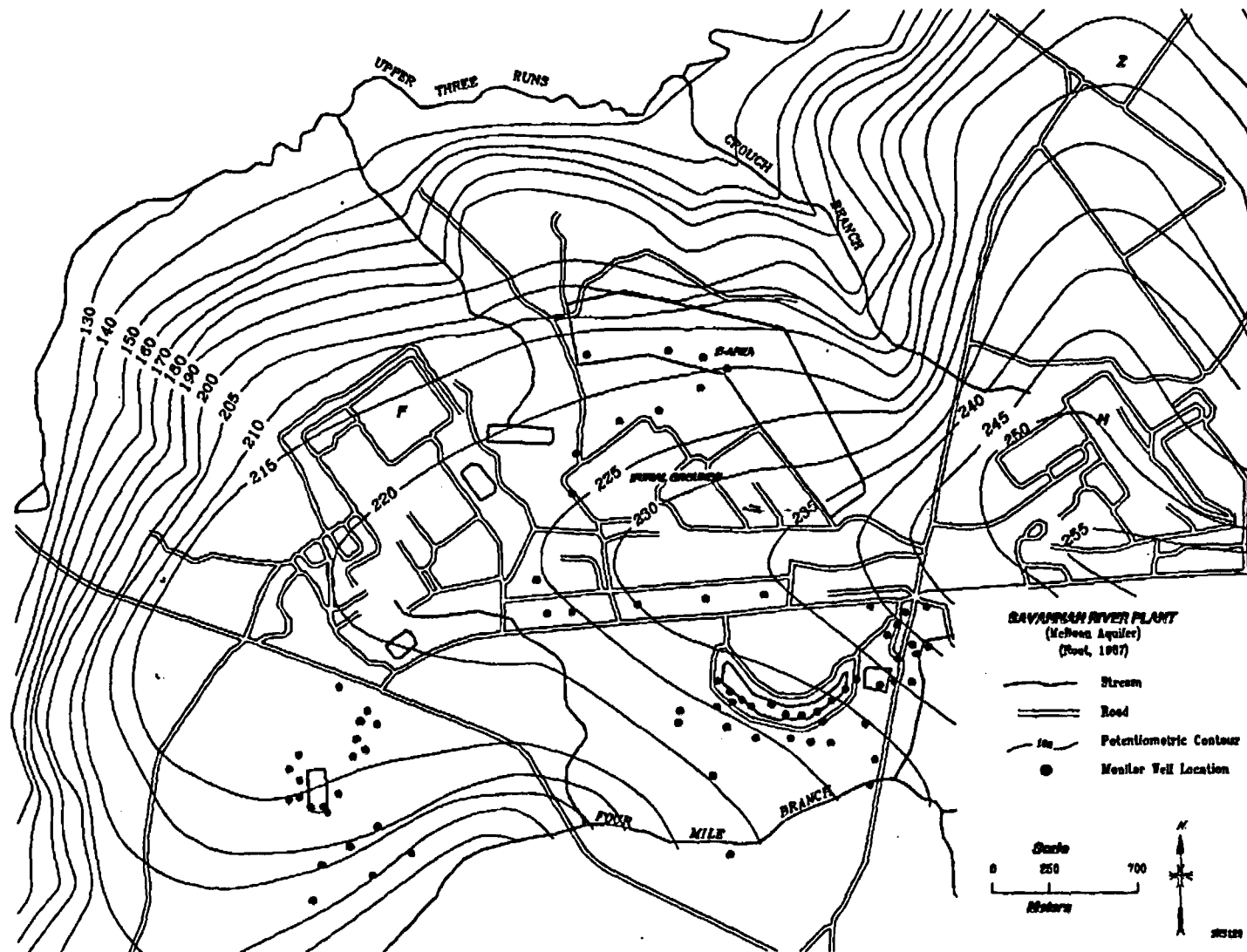
Aquifer Unit IIB, Zone 1 (Barnwell/McBean Aquifer), overlies Confining Unit IIA-IIB (Green Clay) and underlies Confining Unit IIB1-IIB2 (Tan Clay). This zone ranges in thickness from 11.9 to 27.7 m. It thins toward the western portion of the GSA, in the vicinity of the F-Area Seepage Basins. Thickening of the zone occurs to the southeast, in the vicinity of the H-Area Seepage Basins. Aquifer Unit IIB, Zone 1, dips approximately 1.5 to 1.7 m/km to the southeast (GeoTrans 1992).

This aquifer zone consists predominantly of sand and clayey sand sequences with localized zones of abundant calcareous sands, sandy and muddy limestones, and limestones. Minor interbeds of clay and sandy clay are also present. Sands and clayey sands within the zone range in thickness from 0.6 to 18 m. Calcareous sands range in thickness from 0.6 to 10 m. Sandy and muddy limestones, and limestones range in thickness from 0.9 to 9 m.

The sand and clayey sand beds are generally yellow to tan, occasionally greenish brown to light brown. The sand is fine to coarse grained, moderately to well sorted, and generally subangular. The calcareous sands are white to buff in color and contain up to 50% calcareous materials. The sandy and muddy limestones and limestones are white to buff in color and contain greater than 80 percent calcareous material. The interbeds of the clays and sandy clays in this unit are light tan to orange in color. Sand is quartz, fine to medium grained, subangular, and well to moderately sorted.

The hydraulic conductivity of the zone ranges from 7.39×10^{-5} to 7.2×10^{-3} cm/s. The horizontal hydraulic gradient within the zone is estimated to be 0.01 m/m. The vertical gradient in Aquifer Unit IIB1 is estimated to be 0.058 m/m (WSRC 1991). A potentiometric surface for Aquifer Unit IIB, Zone 1, was developed based upon water level data taken from E-Area wells and is provided in Fig. E.2-4.

Rev. 0



E-15

WSRC-RP-94-218

Fig. E.2-4. Potentiometric surface of Aquifer Unit IIB, Zone 1, at E-Area.

E.2.3.5 Confining Zone IIB1-IIB2

Confining Zone IIB1-IIB2 (Tan Clay) consists of multiple, discontinuous clay layers, which separates underlying Aquifer Unit IIB, Zone 1 (Barnwell/McBean), from overlying Aquifer Unit IIB, Zone 2 (water table). The two aquifer zones are in direct contact where this confining zone is absent. Thickness varies from 0 to 10 m. Confining Zone IIB1-IIB2 is not always clearly observed during drilling. Where the zone is present in the GSA, however, head differences between wells screened above and below the zone range from 0.9 to 1.5 m (GeoTrans 1992).

Confining Zone IIB1-IIB2 consists predominantly of clays and sandy clay with minor to equal interbeds of clayey sands and sands. Clays and sandy clays range in thickness from 0.3 to 3.3 m. Clayey sands and sands range in thickness from 0.3 to 2.4 m.

The clays, clayey sands, and sands within Confining Zone IIB1-IIB2 are light tan to light orange in color. The sands are predominantly medium to coarse grained with a moderate degree of sorting. Grain size tends to coarsen upward.

Laboratory analyses of undisturbed samples of Confining Zone IIB1-IIB2 yielded a range of hydraulic conductivities from 6.0×10^{-9} to 1.2×10^{-7} cm/s in the horizontal direction and 1.2×10^{-9} to 4.0×10^{-7} cm/s in the vertical direction (WSRC 1991).

E.2.3.6 Aquifer Unit IIB, Zone 2

Aquifer Unit IIB, Zone 2 (water table), is the uppermost aquifer. Although sometimes referred to as "water table", it is defined stratigraphically, not by the degree of saturation. In portions of the GSA this aquifer is completely desaturated. It overlies Confining Zone IIB1-IIB2 (Tan Clay) where the confining zone is present and Aquifer Unit IIB, Zone 1 (Barnwell/McBean), where the confining zone is absent. This aquifer zone attains a maximum thickness of 33.5 m within the GSA. The aquifer zone ranges from 0 to 20 m in thickness along Four Mile Branch which partially incises it within the GSA. Additionally, the aquifer zone dips at a rate of 1.5 to 1.7 m/km to the southeast (GeoTrans 1992).

Aquifer Unit IIB, Zone 2, consists predominantly of sands and clayey sands with lesser or equal amount of clay and sandy clay. Gravel and pebble layers occur locally. The sands and clayey sands within the zone range in thickness from 6.1 to 32.6 m while the clays and

sandy clays range in thickness from 0.3 to 5.4 m. Gravel and pebble layers range in thickness from 0.3 to 1.5 m.

Sands and clayey sands are tan to red to purple and are often highly variegated in color. Sands are fine to very coarse, subangular to angular and moderately to poorly sorted.

Hydraulic conductivities for Aquifer Unit IIB, Zone 2, range from 1.3×10^{-4} to 5.8×10^{-4} cm/s. The horizontal gradient ranges from 0.0035 to 0.018 m/m with the flow direction to the north and northwest toward UTR Creek (WSRC 1991). A potentiometric surface based upon water level data from wells located at E-Area is provided in Fig. E.2-5 for Aquifer Unit IIB, Zone 2.

E.2.4 Hydrologic Characteristics of the Unsaturated Zone

Hydraulic characteristics of unsaturated soil in E-Area were investigated by Gruber (1980) and in nearby Z-Area, by Quisenberry (1985). Soil water content - soil water pressure relationships for soil in both areas were developed, as were relationships between hydraulic conductivity and water content. Characteristic curves illustrating the relationship between moisture content and soil pressure head (m), and between moisture content and hydraulic conductivity (m s^{-1}), for soils in E-Area are presented in Fig. E.2-6 and E.2-7. The plotted data were obtained by Gruber for undisturbed soil cores. Saturated hydraulic conductivity of these soils was estimated by Gruber to be on the order of 1×10^{-6} m s^{-1} , with porosity on the order of 0.47 to 0.52, and bulk density on the order of 1.6 g cm^{-3} .

Results for the undisturbed soil in Z-Area are presented in Figs. E.2-8 and E.2-9. A relationship similar to that depicted in Fig. E.2-8 for undisturbed soil cores was found for disturbed soil, with a somewhat steeper gradient as soil water pressure approached zero. For the undisturbed soil cores, at pressures less than -1 m, little additional decrease in soilwater content was measured as pressures were decreased to -5 m. Saturated hydraulic conductivity of the Z-Area soils tested was estimated by Quisenberry to be 2×10^{-7} m s^{-1} , with a porosity of 0.37 and corresponding bulk density of 1.7 g cm^{-3} . It is noted by Quisenberry that the field measurements were made in three well-drained areas. The difference between both investigator's curves illustrate the heterogeneous nature of soils in the vicinity of E-Area.

REV. 0

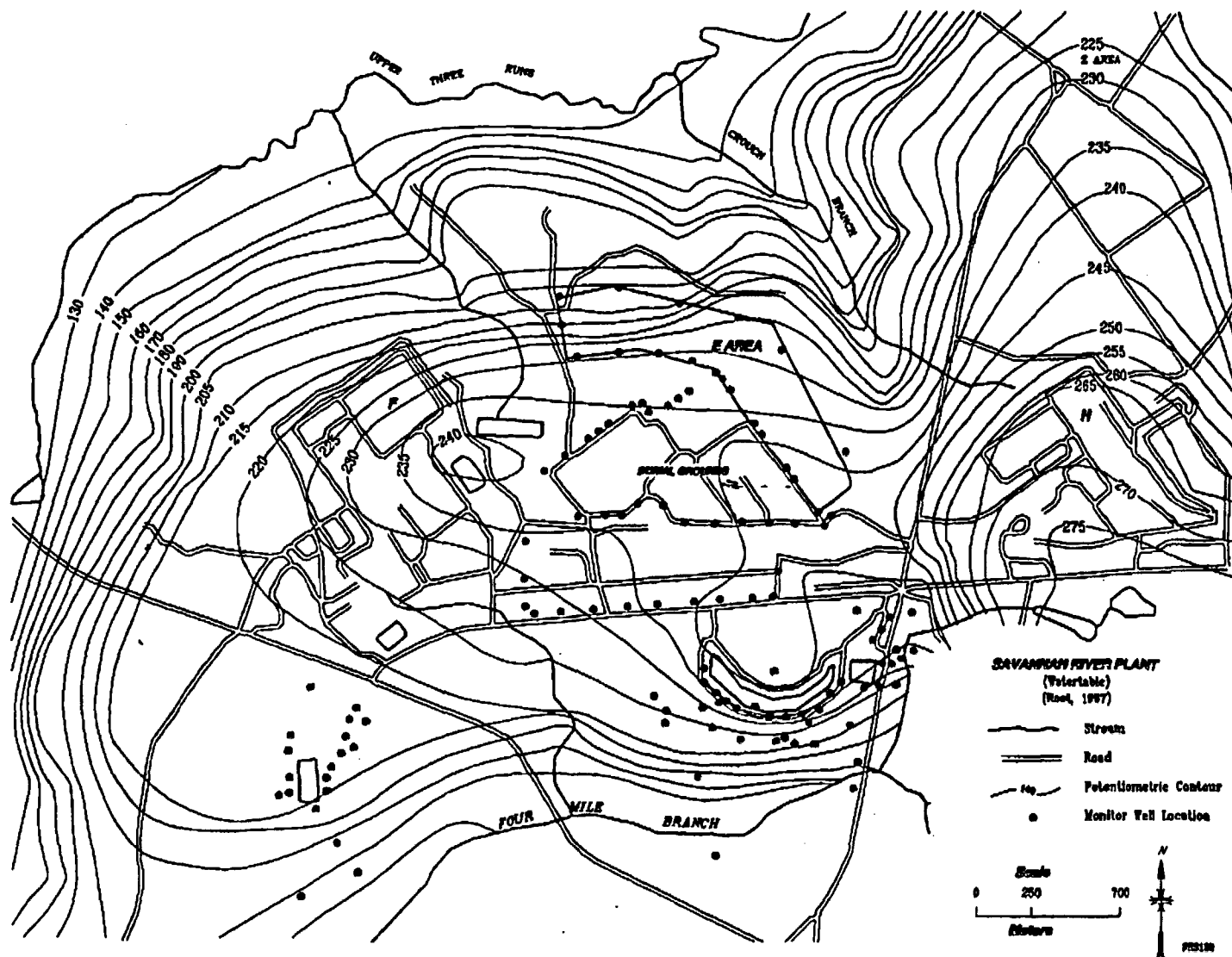


Fig. E.2-5. Potentiometric surface for Aquifer Unit IIB, Zone 2, at E-Area.

E-18

WSRC-RP-94-218

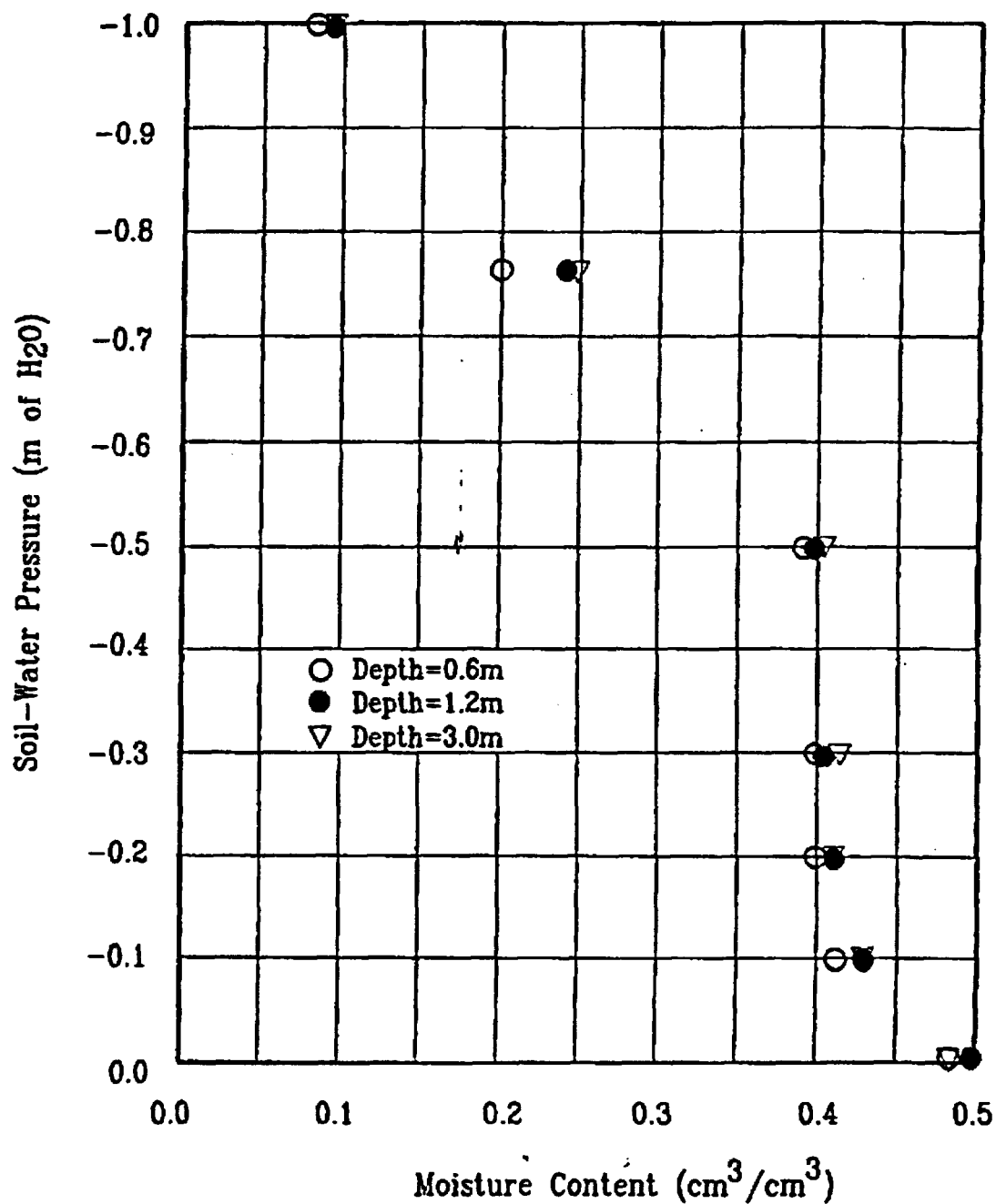


Fig. E.2-6. Soil water content - pressure relationships for undisturbed soils at SRS burial grounds (Gruber 1980).

SRS075

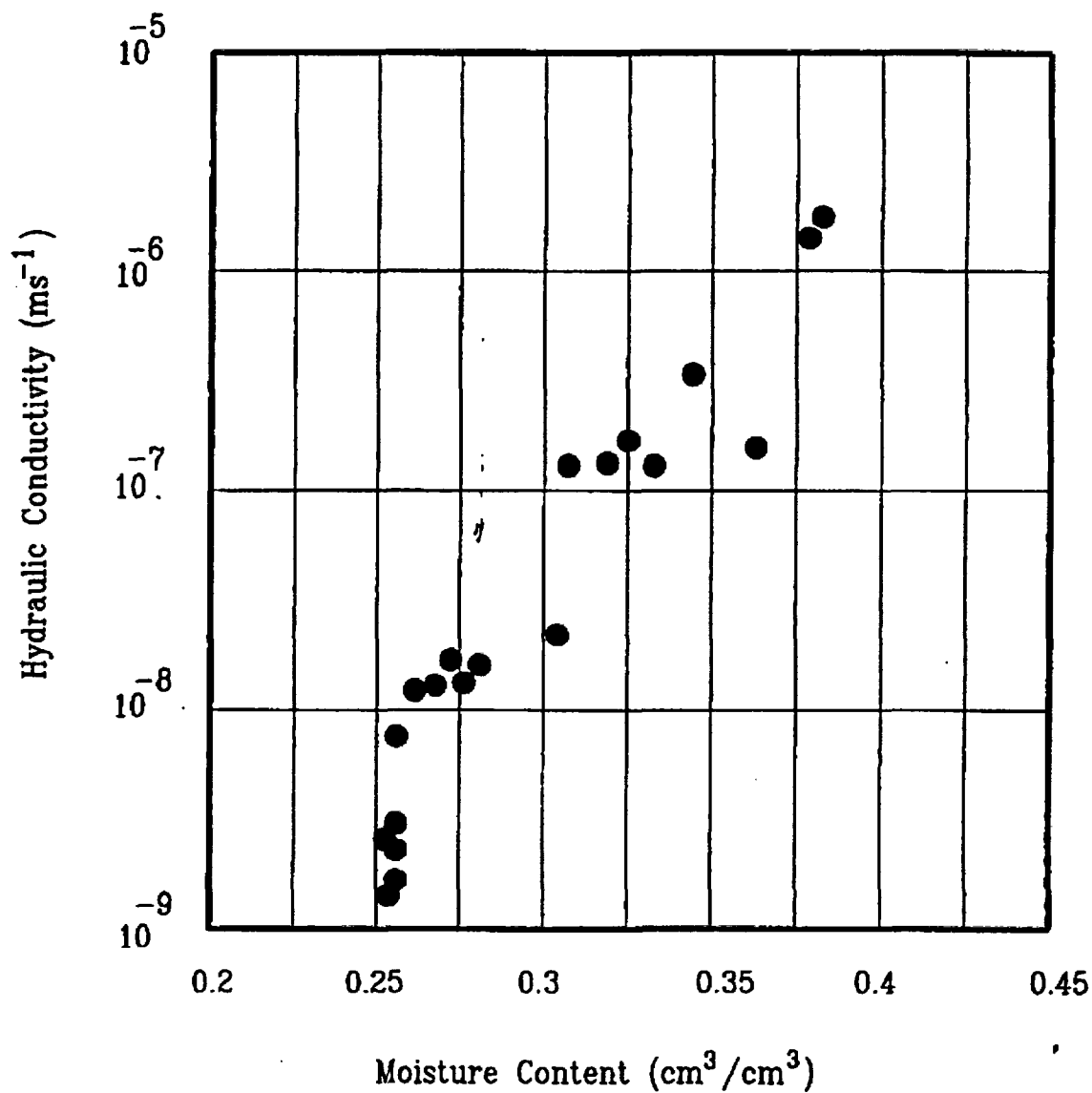
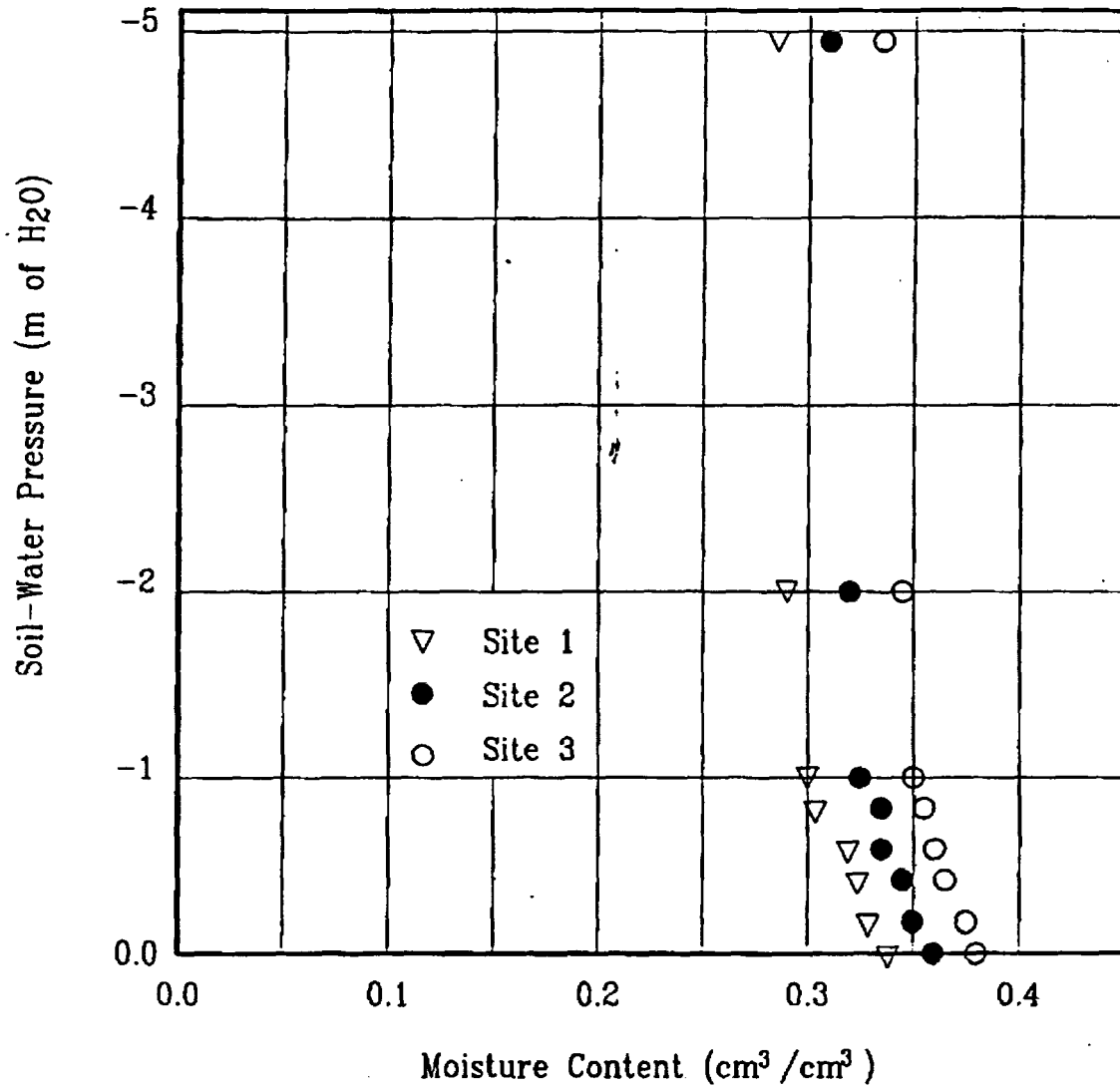


Fig. E.2-7. Unsaturated hydraulic conductivity as a function of moisture content at SRS burial grounds (Gruber 1980).

SRS076



SRS040

Fig. E.2-8. Soil water content-pressure relationships for undisturbed soils in Z-Area (Quisenberry 1985).

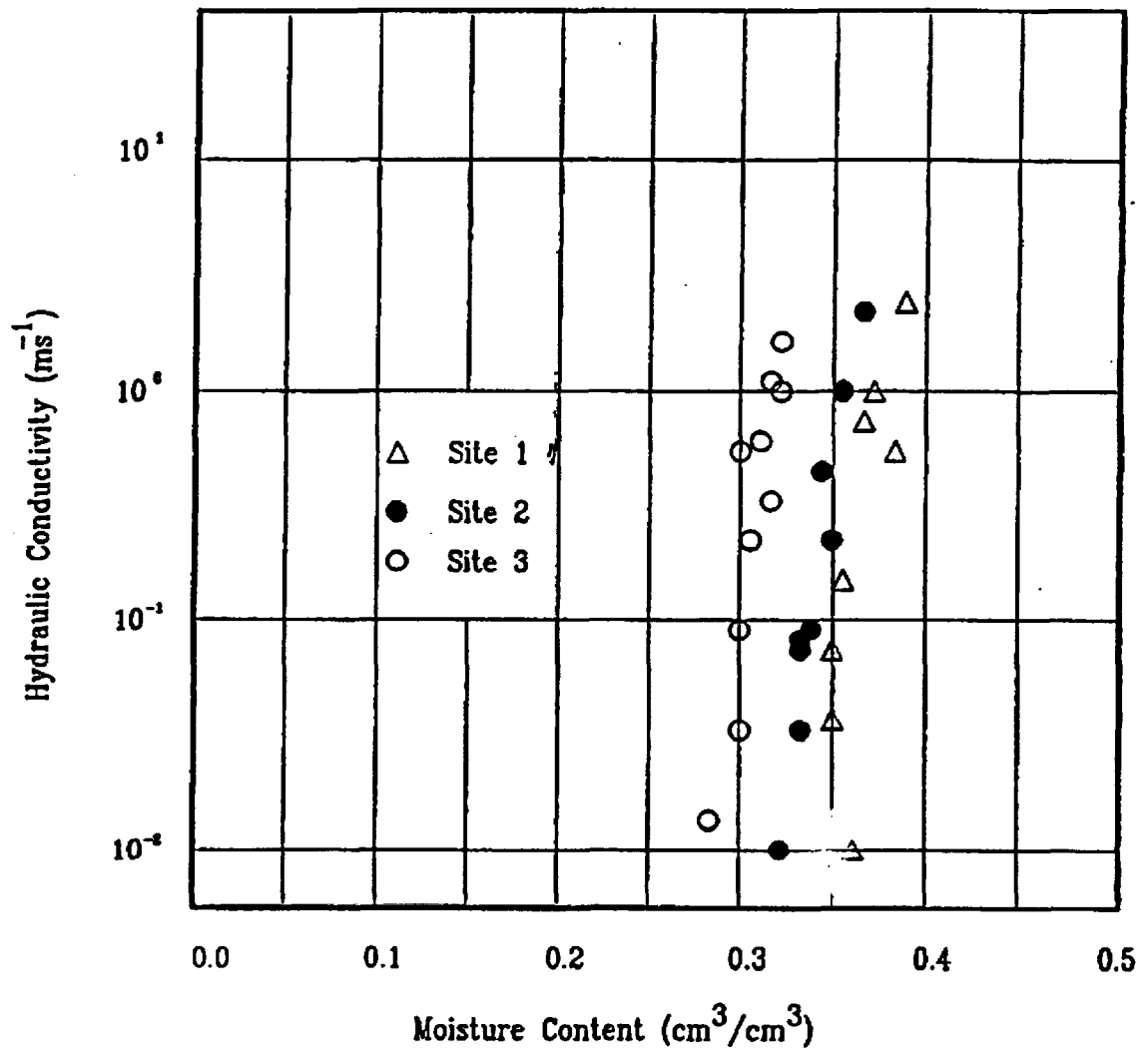


Fig. E.2-9. Unsaturated hydraulic conductivity as a function of moisture content at Z-Area (Quisenberry 1985).

APPENDIX E REFERENCES

- Aadland, R. K. 1990. *Classification of Hydrostratigraphic Units at Savannah River Site, South Carolina*. Savannah River Laboratory, WSRC-RP-90-987, Westinghouse Savannah River Company, Aiken, SC.
- Christensen, E. J., and D. E. Gordon. 1983. *Technical Summary of Groundwater Quality Protection Program at Savannah River Plant, Volume I*. DPST-83-829. Savannah River Laboratory, E. I. du Pont de Nemours & Co., Inc., Aiken, South Carolina.
- Cooke, C. W. 1936. *Geology of the Coastal Plain of South Carolina*. U. S. Geological Survey Bull. 867, U. S. Geological Survey.
- Dennehy, K. F., D. C. Prowell, and P. B. McMahon. 1989. *Reconnaissance Hydrological Investigation of the Defense Waste Processing Facility and Vicinity*. E. I. du Pont de Nemours & Co., Inc., Savannah River Laboratory, Aiken, SC.
- GeoTrans. 1992. *Groundwater Flow Model for the General Separations Area, Savannah River Site*. GeoTrans Project No. 3017-003, GeoTrans Inc., Sterling, Va.
- Gruber, P. 1980. *A Hydrologic Study of the Unsaturated Zone Adjacent to a Radioactive-Waste Disposal Site at the Savannah River Plant, Aiken, South Carolina*. M. S. Thesis, University of Georgia, Athens, Ga.
- INTERA. 1986. *Z-Area Site Assessment*. INTERA Technologies, Inc., for E. I. du Pont de Nemours & Co., Inc., Savannah Research Laboratory, Aiken, SC.

- Quisenberry, V. 1985. *Hydraulic Properties of Saltstone and Z-Area Soil*. DPST-86-268. Savannah River Laboratory, E. I. du Pont de Nemours & Co., Inc., Aiken, SC.
- Siple, G. E. 1967. *Geology and Ground Water of the Savannah River Plant and Vicinity, South Carolina*. Geological Survey Water-Supply Paper 1984, U. S. Atomic Energy Commission.
- WSRC. 1991. *Burial Grounds Expansion (U) - Hydrogeologic Characterization, Savannah River Site*. WSCR-RP-91-866. Prepared by Sirrine Environmental, Inc. for Westinghouse Savannah River Company, Aiken, SC.
- WSRC. 1992. *Safety Analysis 200 Area Replacement Tritium Facility*. WSRC-SA-1-1. Savannah River Laboratory, Aiken, SC.

APPENDIX F

SOFTWARE QA PLANS

Rev. 0

OAK RIDGE NATIONAL LABORATORY/GRAND JUNCTION OFFICE**SOFTWARE QUALITY ASSURANCE PLAN FOR PORFLOW-3D****1.0 PURPOSE**

This plan describes the steps taken by Oak Ridge National Laboratory's (ORNL) Pollutants Assessment Group (PAG) to implement software quality assurance (SQA) procedures, developed with consideration of the ORNL Quality Assurance Manual (ref. 10.1), the Martin Marietta Automated Data Processing Systems Development Methodology (ref. 10.2), and ASME NQA-2a (ref. 10.3) for the acquired computer code PORFLOW-3D (ref. 10.4).

2.0 SCOPE

The SQA plan applies to life-cycle phases of PORFLOW-3D as it is used in conducting radiological performance assessments at the Savannah River Site (SRS), including identification and acquisition, installation, testing, operation and maintenance, and retirement of this pre-existing custom software. Configuration control and quality control procedures are also included in the plan.

3.0 TERMS/DEFINITIONS**COMPUTER PROGRAMMING ASSISTANT**

The Computer Programming Assistant assists the Computer Services Manager in assignment and management of software.

COMPUTER SECURITY OFFICER (CSO)

The Computer Security Officer is the person who ensures computer and software security, and passwords.

COMPUTER SERVICES MANAGER (CSM)

The Computer Services Manager is the person who oversees procurement and assignment of computer hardware and software, who works to ensure compatibility of existing and newly acquired products, and who ensures systems have adequate backup.

CONFIGURATION CONTROL

Configuration control is the process of identifying and defining the configuration items in the PORFLOW-3D software system, controlling the release and change of these items throughout the system life cycle, and recording and reporting the status of configuration items and change requests.

PERFORMANCE ASSESSMENT PRINCIPAL INVESTIGATOR (PI)

The Principal Investigator is the person having overall technical responsibility for the radiological performance assessment (PA) project.

PORFLOW-3D

PORFLOW-3D is a commercially-available computer code acquired by ORNL for use in simulating unsaturated and saturated flow of mass transport in the subsurface. Simulation results will provide concentrations of radionuclides originating in low-level waste (LLW) facilities in groundwater. By sponsor (Westinghouse Savannah River Company) directive, it is subject to NQA-2a, and thus is considered a Category 4 software, from QA Procedure No. QA-L-19-100 entitled "Software Quality Assurance" in the ORNL QA Program.

SOFTWARE

Computer programs, procedures, associated procedure manuals, computer source codes and program disks.

CUSTOM SOFTWARE

Software developed to address a specific technical problem, as opposed to commercially-available wide-usage software such as a word processor or database manager.

SOFTWARE VALIDATION

Validation of software refers to the testing of the software with respect to the accuracy of decisions or assumptions incorporated into the software.

SOFTWARE VERIFICATION

Verification of software refers to the testing of the software with respect to accuracy of numerical algorithms.

4.0 RESPONSIBILITIES FOR SQA

PERFORMANCE ASSESSMENT PRINCIPAL INVESTIGATOR

The principal investigator (PI) for the radiological performance assessments for which PORFLOW-3D was acquired is responsible for defining software needs. Upon acquisition, the PI is responsible for overseeing that the software life cycle procedures are correctly implemented and for overseeing configuration control and quality control procedures. The PI is also responsible for maintaining documentation of SQA procedures.

COMPUTER SERVICES MANAGER

The Computer Services Manager (CSM) is responsible for assisting the PI, when requested, with identifying software needs, as well as determining software compatibility with existing or acquired hardware, the operating system, network system and other software that it may have to interface with.

COMPUTER SECURITY OFFICER

Software protection measures are defined by and overseen by the Computer Security Officer (CSO).

5.0 SOFTWARE LIFE CYCLE

5.1 Identification of Software Requirements

The PI shall examine, in detail, the performance assessment problem(s) that necessitate software acquisition, and define the purpose, objectives, scope and constraints of the software need. A feasibility study shall be done to identify alternative pre-existing custom software solutions.

When a code, such as PORFLOW-3D, is identified as a solution, the PI must define all significant requirements of PORFLOW-3D pertinent to its:

- 1) Function - verifiable simulations to be accomplished,
- 2) Performance - time efficiency,
- 3) External Interfaces - interactions with hardware, other software, and available trained operators,
- 4) Attributes - adequacy of documentation, security, particular attributes specified by sponsor.

Documentation of identified requirements of PORFLOW-3D will be provided in the Procedural Logbook, and in an appendix of the performance assessment report.

5.2 Software Installation

Because PORFLOW-3D is pre-existing software, installation must be preceded by tests to assure the software is complete and free of viruses that may infect the computer system on which it is installed. Backup copies of the original software shall be made, and used for installation. Installation will take place in accordance with the installation instructions provided by the provider of PORFLOW-3D.

Once installed, the original software and the backup copy is stored and protected from theft, loss and environmental damage. The Configuration Control Logbook shall be initiated, in which date of installation, version installed, and installation notes are recorded. This Logbook shall contain the name and telephone number of the PI responsible for PORFLOW-3D and the name of the performance assessment project for which it was acquired. Source code listing, software documentation and user's manuals will be stored in a location accessible to designated users of the software, and shall not be removed without permission of the PI.

5.3 Software Testing

Testing is required to confirm that PORFLOW-3D satisfies the objectives and requirements defined in Section 5.1, Identification of Software Requirements. Verification testing, described in Section 5.3.1, below, is a demonstration of whether PORFLOW-3D meets the requirements specified regarding function, performance, external interfaces and attributes.

5.3.1 Verification

The capabilities of PORFLOW-3D must be verified by comparing analytical solutions of the desired simulation equations for a defined problem to PORFLOW-3D output to evaluate the accuracy of numerical algorithms. Comparison of software simulation results with results from previously verified versions or codes (termed benchmarking) is acceptable.

5.3.2 Validation or Benchmarking

Validation of PORFLOW-3D requires data from SRS that are not available in sufficient quantity or quality to provide meaningful results. Benchmarking of PORFLOW-3D will therefore be carried out by comparing the results to software that has gained high acceptability by acknowledged experts.

5.3.3 Documentation of Testing

Results of verification and benchmarking of PORFLOW-3D shall be recorded in the Procedural Logbook which is initiated when requirements are identified (Sect. 5.1), and in an appendix of the performance assessment report.

5.4 Software Operation and Maintenance

5.4.1 Operation

Operation of PORFLOW-3D will be conducted by personnel approved by the PI, who in the PI's judgement, are appropriately trained. These individuals will have access to the user's manual of the code, the Procedural Logbook, and the Configuration Control Logbook.

Operational tests will be performed whenever PORFLOW-3D is installed on a different computer, or when configurational changes are made to the software or hardware system. The results of these tests will be documented in the Configuration Control Logbook.

5.4.2 Maintenance

Maintenance to correct software errors or adapt to changes in requirements or the operating environments will be made only with the PI's approval, documented in the Procedural Logbook. Written requests for maintenance actions will be kept in a specified location by the PI.

5.5 Software Retirement

Once the life cycle of PORFLOW-3D is over, it will be retired according to the developer's requirements, in order to assure future use is in accord with applicable licensing agreements. All documents pertaining to the life cycle of PORFLOW-3D will be archived, and a caretaker will be designated by the PI to ensure that the retired software is not made available for unrestricted use. Documentation of retirement procedures followed will be made in the Procedural Logbook.

6.0 CONFIGURATION CONTROL

6.1 Configuration Identification

A configuration baseline shall be defined for PORFLOW-3D, in input data sets including test cases, simulation results, and hardware as the tested and approved configuration. A labeling system will be implemented for each of these components of the system, such that each item is uniquely identified and that configurations resulting from revisions of each item are uniquely identified.

6.2 Configuration Change Control

Changes to configuration items, including the PORFLOW-3D code, input data sets, simulation results and hardware shall be formally documented under the following guidelines.

6.2.1 Changes to PORFLOW-3D

Changes to the baseline version of PORFLOW-3D must be approved by the PI. Verification shall be performed to ensure that changes are properly reflected in documentation of the code, and that the changed document is properly archived.

6.2.2 Changes to /Creation of Data Sets and Simulation Results

Changes to, or creation of new, data sets must be documented in a manner that uniquely identifies each set and corresponding simulation results set.

6.2.3 Changes in Hardware Configuration

Changes to hardware may affect the operation of PORFLOW-3D. Therefore, such changes shall be reflected in the archiving, or tracking procedure, and in the documentation.

6.3 Configuration Control Documentation

Configuration control documentation shall contain the information needed to manage the PORFLOW-3D configuration and accompanying data sets, simulation results and hardware requirements. This information shall identify the approved configuration (via a well documented naming conventions for software, data sets, and simulation results) and will be kept in the Configuration Control Logbook. This Logbook shall be easily decipherable with respect to reflecting modifications made to the various configurations.

7.0 QUALITY CONTROL

7.1 Technical Review of Software

The PI shall periodically review the approach and key assumptions, and evaluate input data sets to assure that QA procedures have been applied and that proper documentation is being generated throughout the life cycle of PORFLOW-3D. When necessary, the PI will call on others to review assumptions and input data to verify their appropriateness and accuracy.

7.2 Sign-off and Approvals

The sign-off and formal approvals on key assumptions and input data will be accomplished with cover letters transmitting the information being approved. Individuals whose approval is sought will be identified by the PI, and will include QA personnel from ORNL and from SRS, as well as those with particular knowledge of the specific information from both organizations, and appropriate managers.

7.3 Quality Control Documentation

Documentation of Quality Control procedures will be kept in the form of the sign-off and approval cover letters that transmit information that has submitted to these procedures. These signature forms and attached information will be kept in a separate notebook, entitled Quality Control Notebook.

8.0 PROBLEM REPORTING AND CORRECTIVE ACTION

A formal procedure of software problems and corrective action reporting shall be established by the PI for PORFLOW-3D errors and failures. The reporting system shall assure that problems and corrective actions taken are promptly reported to affected organizations, such as Idaho National Engineering Laboratory and SRS. Problems and corrective actions shall be reported in the form of letters to affected individuals and organizations, and will be described in the Procedural Logbook.

9.0 RECORDS

The following documents will be retained as records:

- 1) SQA Plan;
- 2) Procedural Logbook containing information on software requirements, code testing results, maintenance actions, and retirement procedures followed;
- 3) Configuration Control Logbook containing installation information, results of testing when configurational changes are made, and identification of approved or defined configuration items, including the PORFLOW-3D version, input data sets, simulation results and hardware;
- 4) Documentation of PORFLOW-3D, including user's manual; and
- 5) Quality Control Notebook including documentation of approvals on input data and major assumptions made.

10.0 REFERENCES

- Oak Ridge National Laboratory. *Quality Assurance Manual*. Current Edition. Oak Ridge National Laboratory, Oak Ridge, Tenn.
- Martin Marietta for Department of Energy. 1987. *Automated Data Processing Systems Development Methodology Volume I*. K/CSD/INF/86-3, Vol. 1 & 2, R3, (ADP SDM), August.
- ASME NQA-2a. Part 2.6, *Quality Assurance Requirements of Computer Software for Nuclear Facility Applications*.
- Runchal, A. K., and B. Saggarr. 1991. *PORFLOW: A Model For Fluid Flow, Heat and Mass Transport in Multifluid, Multiphase Fractured or Porous Media; User's Manual - Version 2.34*. Analytic and Computational Research, Inc., West Los Angeles, Calif.

F-9

WSRC-RP-94-218

EGG-EELS-10666

EG&G Idaho, Inc.
SOFTWARE QUALITY ASSURANCE PLAN FOR PORFLOW-3D

Steven J. Maheras

March 1993

Rev. 0

SOFTWARE QUALITY ASSURANCE PLAN FOR PORFLOW-3D

1. PURPOSE

This plan describes the steps taken by the Idaho National Engineering Laboratory (INEL) Subsurface and Environmental Modeling (SEM) Unit personnel to implement software quality assurance procedures consistent with the EG&G Idaho Quality Manual Section QP-21 "Computer Software Configuration Management," and ASME NQA-2a-1990 Part 2.7 "Quality Assurance Requirements of Computer Software for Nuclear Facility Applications," for the computer code PORFLOW-3D (Runchal and Saggar 1991).

2. SCOPE

The software quality assurance plan applies to life-cycle phases of PORFLOW-3D as it is used in conducting radiological performance assessments at the Savannah River Site (SRS) including acquisition, installation, testing, operation, maintenance, and retirement. Configuration control and quality assurance procedures are also included or referenced in this plan.

3. TERMS/DEFINITIONS

COMPUTER CODE CUSTODIAN - The designated individual with responsibility for coordinating the control of computer codes and related documentation.

CONFIGURATION CONTROL - Configuration control is the process of identifying and defining the configuration items in the PORFLOW-3D software system, controlling the release and change of these items throughout the system life cycle, and recording and reporting the status of configuration items and change requests.

PERFORMANCE ASSESSMENT PRINCIPAL INVESTIGATOR - The Principal Investigator (PI) is the person having overall technical responsibility for the radiological performance assessment project.

PORFLOW-3D - PORFLOW-3D is a commercially-available computer code acquired by the INEL for use in simulating unsaturated and saturated flow and mass transport in the subsurface. Simulation results will provide concentrations of radionuclides originating the low-level waste facilities in ground water. By sponsor [Westinghouse Savannah River Company (WSRC)] directive, it is considered "High Impact" software (QAP-20-1, Rev 1., 10/01/90). This is equivalent to EG&G Idaho Quality Level B software".

SOFTWARE - Computer programs, procedures, associated procedure manuals, computer source code, and program disks.

SOFTWARE VALIDATION - Software validation refers to the testing of the accuracy of decisions or assumptions incorporated into the software.

SOFTWARE VERIFICATION - Software verification refers to testing the accuracy of numerical algorithms contained in the software.

4. RESPONSIBILITIES FOR SQA

PERFORMANCE ASSESSMENT PRINCIPAL INVESTIGATOR - The PI for the radiological performance assessment for which PORFLOW-3D was acquired is responsible for software quality assurance. Upon acquisition, the PI is responsible for overseeing that the software life-cycle procedures are correctly implemented and for overseeing configuration control and quality control procedures. The PI is also responsible for maintaining documentation of software quality assurance procedures. The PI may delegate the configuration control responsibility to the computer code custodian.

-
- a. Quality Level B software failure would degrade the performance or reliability of operations, data acquisition, or deliverables.

5. SOFTWARE LIFE CYCLE

5.1 Software Installation

Because PORFLOW-3D is pre-existing, commercially available software, life cycle steps associated with the development of the software are the responsibility of the computer code vendor. Installation will take place in accordance with the instructions provided by the PORFLOW-3D vendor. A backup copy of the original software shall be made and stored under version control. Because PORFLOW-3D is stored under version control on the INEL CRAY, it is protected against theft, loss, and environmental damage.

After installation, PORFLOW-3D will be installed in the INEL Version Control System (Miller et al. 1991). The INEL Version Control System provides for automated change control and logging, therefore, a separate configuration control logbook is not required.

5.2 Software Testing

Testing is required to confirm that PORFLOW-3D functions as the code vendors assert. Once installed, a FORTRAN analyzer is typically run on the code to look for potential programming errors. Marshall and Marwil (1991) contains a description of a typical FORTRAN analyzer. No programming errors were identified in PORFLOW-3D.

5.2.1 Verification

The capabilities of PORFLOW-3D must be verified by comparing analytical solutions of the desired simulation equations for a defined problem to PORFLOW-3D output to evaluate the accuracy of numerical algorithms. Comparison of software simulation results with results from previously verified versions or codes (termed benchmarking) is acceptable. An independent verification of an earlier version of PORFLOW has been performed (Magnuson et al. 1990).

5.2.2 Validation or Benchmarking

Validation of PORFLOW-3D requires data from SRS that are not available in sufficient quantity or quality to provide meaningful results. Therefore, PORFLOW-3D will be benchmarked by comparing PORFLOW-3D results to results obtained using other software that has gained high acceptability from acknowledged experts. An independent benchmarking of an earlier version of PORFLOW has been performed (Magnuson et al. 1990).

5.2.3 Documentation of Testing

The results of the verification and benchmarking of PORFLOW-3D are documented in Magnuson et al. (1990). The verification and benchmark testing of PORFLOW was conducted using Version 1. However, the version of PORFLOW used on this project was PORFLOW-3D. The test problems used to verify and benchmark Version 1 have been run using PORFLOW-3D and equivalent results were obtained.

5.3 Software Operation and Maintenance

5.3.1 Operation

Operation of PORFLOW-3D will be conducted by personnel approved by the PI, who in the PI's judgement, are appropriately trained. These individuals will have access to the user's manual of the code.

Operational tests will be performed whenever PORFLOW-3D is installed on a computer with a different operating system, or when configuration changes are made to the software or hardware system.

5.3.2 Maintenance

Maintenance to correct software errors or adapt to changes in requirements or the operating environments will be made only with the PI's approval. However, the PI may delegate this authority to the code custodian.

The changes will be logged in the Version Control System. Because the Version Control System provides an automated log of changes to the source code, no separate maintenance log will be required.

5.4 Software Retirement

Once the life cycle of PORFLOW-3D is over, it will be retired according to the code developer's requirements in order to assure future use is in accordance with applicable licensing agreements. All documents pertaining to the life cycle of PORFLOW-3D at the INEL will be archived. During the retirement phase of the software life cycle, the routine use of PORFLOW-3D will be prevented. The retirement procedures followed will be documented.

6. CONFIGURATION CONTROL

PORFLOW-3D is maintained under configuration control using the INEL Version Control System. The Configuration Management Plan for PORFLOW-3D is part of a larger Configuration Management Plan documented in Matthews (1992), that meets the requirements of the EG&G Idaho Quality Manual, QP-21, "Computer Software Configuration Management".

7. QUALITY ASSURANCE

The PI shall periodically review the approach and assumptions and evaluate input data sets to ensure that quality assurance procedures have been applied and that proper documentation is being generated throughout the life cycle of PORFLOW-3D. When necessary, the PI will call on others to review assumptions and input data to verify their appropriateness and accuracy.

Key assumptions (those critical to the project) will be evaluated by WSRC, Oak Ridge National Laboratory - Grand Junction (ORNL-GJ), and INEL; a consensus on each key assumption will be reached.

Project notebooks will be used to document day-to-day project activities. Formal documentation of analyses conducted using PORFLOW-3D will

be accomplished using the EG&G Idaho Engineering Design File (EDF) format. The EDF format provides for formal approval of input data, assumptions, and output by the author, reviewer (technical), and approver (managerial) of the calculations. The EG&G Idaho Quality Manual, "Design Control," QP-3, Section 4.2.15, describes the elements required in the documentation of a design analysis. The EDF's generated during this project will be transmitted to SRS as part of the project documentation.

8. ERROR REPORTING AND CORRECTIVE ACTION

Any errors found in the code will be reported to the code author and other affected organizations such as SRS and ORNL-GJ. The error and its corrective action will be documented in the project logbook maintained by the analyst.

9. RECORDS

The following documents will be retained as records that will be turned over to WSRC:

1. Software Quality Assurance
2. Version Control System change log for PORFLOW-3D.
3. Documentation of PORFLOW-3D, including user's manual.
4. EDFs containing results generated using PORFLOW-3D.
5. Project notebooks.

10. REFERENCES

ASME NQA-2a-1990, Part 2.7, Quality Assurance Requirements of Computer Software for Nuclear Facility Applications.

EG&G Idaho, Inc., 1992, Quality Manual, Sections QP-3, "Design Control," and QP-21, "Computer Software Configuration Management".

Magnuson, S. O., R. G. Baca, A. J. Sondrup, 1990, Independent Verification and Benchmark Testing of the PORFLO-3 Computer Code, Version 1.0, EGG-BG-9175.

Marshall, N. H. and E. S. Marwil, 1991, Cross Reference Analysis of FORTRAN (CRAFT), EGG-CATT-9198.

Matthews, S. D., 1992, Software Configuration Management Plan for Controlled Code Support System, EGG-CATT-10196.

Miller, G. V., D. G. Barber, E. S. Marwil, 1991, Software Quality Assurance Plan for the Version Control System, Release 2, EGG-CATT-9821.

Runchal, A. K. and B. Saggat, 1991, PORFLOW: A Model for Flow, Heat and Mass Transport in Multifluid, Multiphase Fractured or Porous Media; User's Manual - Version 2.34, Analytic and Computational Research, Inc., West Los Angeles, CA.

APPENDIX G
COMPLETENESS REVIEW GUIDE

APPENDIX G
COMPLETENESS REVIEW GUIDE

An attempt was made to address all items identified in DOE/LLW-93 Performance Assessment Review Guide for DOE Low-Level Radioactive Waste Disposal Facilities and to specifically address these items in the E-Area Disposal Facility Performance Assessment. A table has been prepared which summarizes all items identified within the guidance document and connects each item with the appropriate section(s) of the Performance Assessment. In some cases the required items are addressed in two or more sections of the report. Additional details are sometimes presented in an Appendix. This table is provided as an aid to the reviewers in their completeness review of the E-Area Performance Assessment.

**DOE/LLW-93
REVIEW GUIDE SECTIONS**

**E-AREA PERFORMANCE
ASSESSMENT SECTIONS**

DISPOSAL FACILITY DESCRIPTION

Sect. 2

Site Characteristics

Sect. 2.1 and Sect. 2.2

Hydrogeology (Regional/Site Specific)

Sect. 2.1.4, Sect. 2.2.2, and Appendix E.2

Ecology and Biotic Conditions

Sect. 2.1.9

Natural Resources, Land and Water Use

Sect. 2.1.6 and Sect. 2.2.1

Geography and Demography

Sect. 2.1.1 and Sect. 2.1.2

Climate and Meteorology

Sect. 2.1.3

Geology (Regional/Site Specific)

Sect. 2.1.4, Sect. 2.2.2, and Appendix E.1

Seismology

Sect. 2.1.5

Natural Radiation Background

Sect. 2.1.10 and Sect. 2.2.5

Waste Generation Process

Sect. 2.3 and Sect. 2.4

Waste Characteristics

Sect. 2.4

Volumes

Sect. 2.4

Radionuclide Concentration and Inventory

Sect. 2.4.3 and Sect. 2.6

Chemical and Physical Form

Sect. 2.4

Packaging

Sect. 2.4.2

ANALYSIS OF PERFORMANCE

Sect. 3

Background

Source Term

Sect. 3.1

Transport/Pathways/Scenarios

Sect. 3.2

Assumptions/Methodologies

Sect. 3.3 and Sect. 3.4

Dose Conversion Factors

Sect. 3.4.3

Computer Modeling Codes

Sect. 3.4.1, Sect. 3.4.2, Appendix A
and B

RESULTS OF ANALYSIS

Sect. 4

Dose to Public and Intruder

Sect. 4.1.4 and Sect. 4.1.5

Sensitivity and Uncertainty Analysis

Sect. 4.2

QUALITY ASSURANCE/QUALITY CONTROL Appendix F

APPENDIX H

**PERFORMANCE ASSESSMENT PEER REVIEW
PANEL RECOMMENDATIONS**

HL1 INTRODUCTION

The Performance Assessment Peer Review Panel met on May 26-27, 1993 at the Savannah River Site to conduct a preliminary review of the radiological performance assessment (RPA) for the Savannah River Site E-Area Vaults Disposal Facility. Recommendations for improving this assessment were made by the Panel based on a review of an earlier version of the draft of this report and on presentations that were made to the Panel during the review. The Panel reached consensus on 19 recommendations which were presented to SRS, and are listed verbatim in Sect. H.2. How those recommendations which suggested action were adopted for improving this report are discussed immediately below each recommendation.

HL2 RECOMMENDATIONS OF THE PERFORMANCE ASSESSMENT PEER REVIEW PANEL

Recommendation #1

"The Peer Review Panel (PRP) is once again very appreciative of the courteous reception, generous hospitality, and openness of discussion provided by DOE's Savannah River Field Office, the Westinghouse Savannah River Company, and all review contributors."

Response:

No action requested.

Recommendation #2

"The PRP would like to commend the fine efforts of Westinghouse Savannah River Company for producing a high quality preliminary draft report, of comparable high quality to the Saltstone preliminary draft report. The basic elements of establishing a conceptual model, the early application of screening methods to establish the significant radionuclides, pathways, and scenarios, and the effort to establish waste acceptance criteria consistent with the PA methods and data are noteworthy."

Response:

No action requested.

Recommendation #3

"Again, the multidisciplinary 'teamwork' approach has been applied and is credited with the production of this high quality draft. The PRP feels that this preliminary review successfully met its expectations and objectives and hopes that our comments will be useful to the development of the final PA."

Response:

No action requested.

Recommendation #4

"The PRP notes that our final review of the Saltstone PA suffered because of the decision by the preparers to defer a final editorial review until after distribution to the PRP. The resulting errata pages and additional analyses that must be considered during the final review are somewhat awkward to handle. The PRP recommends that the time be spent on the E-Area PA to conduct a final internal editorial and technical review prior to release to the Panel."

Response:

The schedule of issuance of the final E-Area PA was adjusted to provide time to conduct a final internal editorial and technical review. The review included two separate reviews by WSRC and the PA Team and a review by DOE-SR and their subcontractor. Results of these reviews have been incorporated in this final PA.

Recommendation #5

"The PRP is concerned that no mention has been made in this PA of the disposal of post 1988 waste in the existing burial ground."

Response:

In the Implementation Plan for DOE Order 5820.2A, DOE-SR indicated that, for continuity of SRS operations, shallow land burial of low-level waste would continue until the E-Area vault disposal facility was available. The Implementation Plan also indicated that a radiological performance assessment would be conducted only for the E-Area vault facility. Consistent with this decision, no mention of post-1988 waste disposal in the existing burial ground is in the E-Area Vaults Performance Assessment.

Recommendation #6

"How are existing plumes and future E-Area plumes covered by this PA going to be differentiated by the near-term monitoring program?"

Response:

Differentiating future EAV Facility (EAVF) contaminant plumes from previously existing plumes will be based upon deviation from groundwater quality trends that will previously have been established.

Numerous groundwater monitoring wells have been installed in the vicinity of the EAVF to permit monitoring of contaminant plumes emanating from existing facilities. These wells are currently being sampled on a routine basis to define the current extent of contaminant plumes and to establish groundwater quality trends.

Several of these wells are situated close to the EAVF, both in the upgradient and downgradient directions. These wells are capable of detecting the presence of contaminants in the groundwater which might originate upgradient of the EAVF and flow beneath it. Data obtained from these wells indicates that contaminants originating at other facilities has already migrated beneath the EAVF (see Sect. 2.2.5).

Continued monitoring of these wells will allow establishment of future trends such that deviations due to EAVF operation will be apparent. Statistical analysis methodology will form the basis for making such a determination. An adequate methodology has not yet been developed, but is expected to be developed for analysis of groundwater at the Z-Area. The methodology will be described in a "Statistical Analysis Plan" which is required to obtain an Industrial Waste Permit from SCDHEC for operation of the Saltstone Facility. When the methodology is developed it will serve as a precedent that can be utilized at the EAVF.

Recommendation #7

"The PRP is concerned that the cumulative effects of the future hazardous waste/mixed waste disposal facility must be integrated with those in the E-Area PA."

Response:

The cumulative effects of the planned Hazardous Waste/Mixed Waste Disposal Facility and the E-Area Vaults will be addressed in the Performance Assessment for the HWMW facility. The HWMW PA is currently in the planning stage, but the actual project to design and construct the facility has not received funding. Integration of the HWMW and EAV PA results will be an important part of the analysis.

Recommendation #8

"The screening analysis used to determine significant radionuclides seems to focus on near term effects important during operations and the first few hundred years. By contrast, radionuclides important to low-level waste PAs are often long-lived mobile radionuclides that may be present in trace quantities (i.e., less than 1% of the total inventory) at the time of disposal. Efforts should be made to confirm, document, and justify the results of the inventory screening analysis. This is especially important in light of the changing mission with future inclusion of decommissioning wastes containing long-lived activation products."

Response:

The screening analysis, for both groundwater and intruder scenarios, was revised to include all 730 radionuclides assigned dose conversion factors in the DOE Compendium of dose conversion factors (DOE/EH-0071, "Internal Dose Conversion Factors for Calculation of Dose to the Public", July, 1988). This approach assures that any radionuclide with the potential to have an impact, either long-term or short-term, would be identified. The screening analyses are discussed in Sects. 3.2.3.4 and 3.2.4.4.

Recommendation #9

"Provide a discussion and justification of the methodology and criteria used to select the radionuclides considered in the initial inventory. For example, why were Fe-59, Fe-55, and Eu-152 not included?"

Response:

See the response to comment #8, above.

Recommendation #10

"The PRP is concerned about the allocation of activity in the inventory for the 'other' alpha and beta-gamma categories of Pu-239 and Sr-90/Cs-137. A review of the groundwater screening results presented indicates that Np-237 and Sn-126 should not be excluded."

Response:

The "Other Alpha" and "Other Beta-Gamma" categories have been removed from the Performance Assessment. The comprehensive screening analysis eliminated the need for these categories.

Recommendation #11

"The presentation material implied that the ILNT and LAW waste could contain less than 10 Ci of H-3 per package. However, table 2.4-1 shows relatively low H-3 activity levels for the ILNT and LAW vault categories (i.e., 1,000 and 5,000 Ci, respectively). It is not clear if H-3 is being assigned a value of zero for a portion of these inventories."

Response:

The present analysis no longer relies on estimated initial radionuclide inventories, which were presented in Table 2.4-1 in the original draft report. The methodology in the present RPA uses unit activity inventories or concentrations of radionuclides to determine the allowable inventory in a given vault type based upon the performance objectives for dose. Details of this methodology are provided in Sect. 3.1.1., 3.3, 3.4, and 4.1.

The reference inventories for the non-tritium vaults (ILNT and LAW) were increased based on 10 curies per B-25 container, 12,000 Ci for LAW vaults and 10,000 Ci for ILNT vaults.

Recommendation #12

"Although the PRP applauds the early application of screening methods to make decisions regarding design features and the choice of data and analysis methods for conducting the PA, we caution that efforts must be made to replace the screening methods with a justified site-specific approach. The current analysis may be overly conservative and is likely to be of little use beyond making initial decisions. For example, the high groundwater concentrations are apparently a result of conservative assumptions regarding degraded performance and attempts to simplify a complicated transport analysis. For the final PA, a more site-specific approach must be developed, justified and applied."

Response:

The preparers agree that a site-specific approach must be developed, justified, and applied. This has been done. A more rigorous analysis of vault degradation has been performed (Appendix K) and incorporated into the near-field conceptual model (Sect. 3.3.1, 3.4.1, and 4.1.2). A detailed site-specific three dimensional groundwater flow and transport model to determine the groundwater contaminant concentrations at the compliance point. Details of this model are presented in Sect. 3.3.2, 3.4.2, and 4.1.3.

Recommendation #13

"Provide a description of the conceptual model of how the vaults degrade and the environment evolves to provide an envelope of degraded conditions. The application of the conceptual model to the numerical methods must be described."

Response:

A special modeling study was conducted on the degradation of the concrete vaults in E-Area and the study is provided in Appendix K. The incorporation of this detailed site-specific degradation study into the near-field conceptual model is described in Sect. 3.3.1, 3.4.1, and 4.1.2.

Recommendation #14

"Consider the effects of increased infiltration beyond 40 cm/yr in the degraded scenario for the LAW vault facility after the subsidence event (roof collapse) has occurred."

Response:

An additional run of the unsaturated zone model of the LAW vault was made with the infiltration rate set at 120 cm/year, the total average annual precipitation at SRS, at the time of vault failure. Cs-135 and Th-232 were selected for this analysis. The calculated flux to the water table increased by a factor of about 3, the amount of increase in the infiltration. The results, in fractional flux to the water table, were:

	40 cm/year	120 cm/year
Cs-135	8.6E-04	2.6E-03
Th-232	3.0E-05	9.5E-05

Recommendation #15

"The treatment of the waste in the LAW vaults needs to be better described (i.e., the lifetime of the waste boxes, the void spaces, and the assignment of soil properties to the degraded waste forms)."

Response:

Additional detail has been added to the report to address treatment of the void (see Sect. 3.3.1.1 and Appendix A.1.2.2). Essentially, the boxes are assumed to collapse to a height assuming that the voids in the waste are no longer present, thus increasing the void above the

waste. The void above the boxes is assumed to behave as a high permeability porous media. No effective life is assumed for the waste boxes as it is assumed that the boxes will fail before the vault significantly increases in permeability and the boxes provide no structural support. The degraded boxes are also assumed to be a source of iron oxides (rust) that are used to determine K_d s for selected radionuclides.

A sensitivity analysis was conducted for the hydraulic conductivity of the waste and grout in the ILNT vault. Increases in hydraulic conductivity of the waste form of 4 orders of magnitude initially and a 2 order of magnitude increase for the degraded conditions were considered based on the reference waste form values for the different time periods specified by Andy Yu. These changes yielded an increase of roughly 3 orders of magnitude in the peak release rate for H-3. The impact was minimal on releases of C-14, Tc-99, and Ni-59. The results for the ILNT vault described above suggest that the properties of the waste form can have a significant impact on the release rate of H-3. Additional sensitivity cases for the LAW vault are being conducted, but are proving to be difficult to run. Work is continuing on the additional cases as time permits.

Recommendation #16

"The intruder scenario assumptions need to be further discussed. In particular, there needs to be clear descriptions and justifications of the construction of the house foundation or basement with respect to the waste material, the potential dilution factors applied, and the geometry selected for external dose calculations."

Response:

The assumptions for the intruder scenarios are described qualitatively in Sect. 3.2.4. and in more detail, including a description of the parameter values, in Appendix A.4. As described in the appendix, the assumptions regarding construction of a house foundation or basement that extends into the waste itself and the dilution factor for mixing of exhumed waste into native soil in an intruder's vegetable garden, essentially are the same as those used by the NRC in developing its regulations for low-level waste disposal in 10 CFR Part 61. The geometry selected for the external dose calculations also was used by the NRC. The assumption in estimating external dose of a uniform distribution of activity over the source region is reasonable for the kinds of disposal units in E-Area, particularly when one considers that intrusion onto the site will occur at random locations. It should also be borne in mind that while the assumptions for an intruder dose analysis should be reasonable for the conditions of the site and disposal facility, the primary purpose of the analysis is to establish waste acceptance criteria in the form of limits on concentrations, rather than to provide realistic estimates of dose that might be experienced by future inadvertent intruders. Therefore, it is entirely appropriate to develop simplifying assumptions for idealized exposure situations for inadvertent intruders as long as the assumptions are reasonably credible. This is particularly the case when one realizes that most assumptions will tend to result in estimates of dose that would exceed those that likely would be experienced by most individuals who might intrude onto the disposal site.

Recommendation #17

"The intruder scenarios should be evaluated using an inventory corrected for both decay and leaching. This correction may reduce the importance of radon in the long-term dose assessment."

Response:

The preparers agree that a leaching correction should be applied to reduce the concentrations of radionuclides to which an inadvertent intruder would be exposed at times long after disposal. The dose analysis in Sect. 4.1.5 has been recast to display this correction explicitly (see page 4-30). However, because the engineered barriers to be used in the disposal units are expected to maintain their integrity and preclude direct intrusion into the waste for long time periods after disposal (e.g., for perhaps thousands of years or more), uranium is probably the only radionuclide for which consideration of leaching would be important in increasing significantly the concentration limit for acceptable disposals. As noted by the Peer Review Panel, consideration of leaching for uranium is potentially important in reducing the dose estimates from radon at times long after disposal. However, a solubility limit for uranium has also been implemented (see Sect. 4.1.2.2 and Appendix D). This results in minimal leaching of uranium over the 10,000-year compliance period.

Recommendation #18

"The methods used to estimate doses from radon should be evaluated and justified. For example, the computed ratio of household radon concentration to the radium concentration is highly variable (not a fixed value). In addition, the concentration in basements is generally higher than in upper floors. Finally, a comparison of household radon to the concentrations derived using the ratio to radium in soil should be compared to concentrations estimated using diffusion models."

Response:

The fundamental difficulty with performance assessment for low-level waste disposal is the paucity of data that can be used to validate or justify the assumptions for the various aspects of system behavior. Therefore, when there are opportunities to use real environmental data in a dose analysis, these opportunities clearly should be embraced. Data on exposures of the public to radon due to radium in soil represent such an opportunity. As noted by the Peer Review Panel, the ratio of indoor radon exposure to radium concentration in soil is a variable quantity, depending on many factors, and the concentration of indoor radon varies with location within a house. However, the assumptions used in the dose analysis for the E-Area vaults take this variability into account; i.e., the assumptions represent average conditions taking into account a large body of data. Since it is not the purpose of a dose analysis for low-level waste disposal to estimate the real dose that might result from

a dose analysis for low-level waste disposal to estimate the real dose that might result from placing a real house on top of waste at the Savannah River Site, the use of average assumptions clearly is reasonable. It would be desirable to base the analysis for radon on average levels of indoor radon and average levels of radium in surface soil in the vicinity of the Savannah River Site, but the existence of such a data base is not known to the preparers. Regarding the request by the Peer Review Panel to use a diffusion model to estimate indoor radon levels, it is difficult for the preparers to see how this approach could produce a useful result for the purposes of this analysis. A diffusion model would involve many highly uncertain assumptions that could only be validated by direct comparison with the type of natural analog model used in this analysis. If a diffusion model could be justified only by comparison with existing environmental data, then there is no reason not to use the environment data as the model as in the present analysis.

It should also be noted (see Sect. 1.2 and Appendix A.3) that, although doses from radon and its decay products are presented in the results of intruder analyses, they are no longer considered in assessing compliance to the intruder performance objective. Rather, a radon exhalation rate is estimated and compared with the performance objective of 20 pCi/m²s.

Recommendation #19

"The likelihood of the long-term intruder scenario will be influenced by the depression in the ground surface resulting from subsidence of the LAW vault roof structure. This should be considered and discussed in the final analysis."

Response:

The development of a significant depression in the ground surface due to collapse of the LAW vault roof could affect the likelihood that an inadvertent intruder would excavate at the site. However, even after the roof collapses, the concrete presumably would be in the form of large, relatively intact pieces, in which case excavation into the waste would be precluded until most of the concrete has degraded to soil-like material. This process presumably would require at least a few hundred years, by which time the ground surface could assume a more normal contour due to normal weathering at the site. Therefore, the preparers believe it is reasonable to assume that collapse of the LAW vault roof should not effect the assumptions used in the intruder dose analysis, especially since exposure to longer-lived radionuclides at times long after disposal is the primary concern. Again, it must be borne in the mind that the primary purpose of the intruder dose analysis is to establish waste acceptance criteria, and the assumptions used in this process need not replicate actual exposure situations that might occur. Of course, collapse of the vault roof is potentially quite important in estimating releases from the vaults, and this factor is taken into account in the analysis.

APPENDIX I

SUSPECT SOIL PERFORMANCE ANALYSIS

APPENDIX I

SUSPECT SOIL PERFORMANCE ANALYSIS

I.1 DESCRIPTION OF SUSPECT SOIL TRENCHES

Between 2800 and 5600 m³ of soil from regulated areas at the SRS is designated annually as potentially contaminated soil (henceforth referred to in this appendix as "suspect soil", Cook 1991). Disposal of a portion of this soil in unlined trenches is being considered for the EAV facility. The performance of these proposed suspect soil trenches is analyzed in this appendix.

I.1.1 Physical Characteristics of Suspect Soil

The suspect soil at the SRS has not specifically been characterized, but can be assumed to have general characteristics similar to the soil horizons across the site. The SRS soils were described in Sect. 2.1.8. In general, the SRS soils are sandy, and underlain by a loamy or clayey subsoil. Excavation activities may result in mixing of the sandy soils with the subsoil. Therefore, it is likely that the suspect soil characteristics are representative of a mixture of the soil horizons present at the SRS.

I.1.2 Layout and Capacity of the Trenches

For this performance analysis, it is assumed that five below-grade trenches exist within the EAV facility. The conceptual configuration and dimensions of the trenches are shown in Fig. I.1-1. The width of the top of each trench is 6 m, and the bottom is 4.8 m wide. Each trench is 200 m long and 6 m deep, but the top 1.2 m of soil in each trench will be clean soil. The disposal capacity of each of the five trenches is approximately 5200 m³ of suspect soil. The base of the trenches is assumed to lie approximately 9 m above the water table at an elevation similar to that of the base of the LAW vaults.

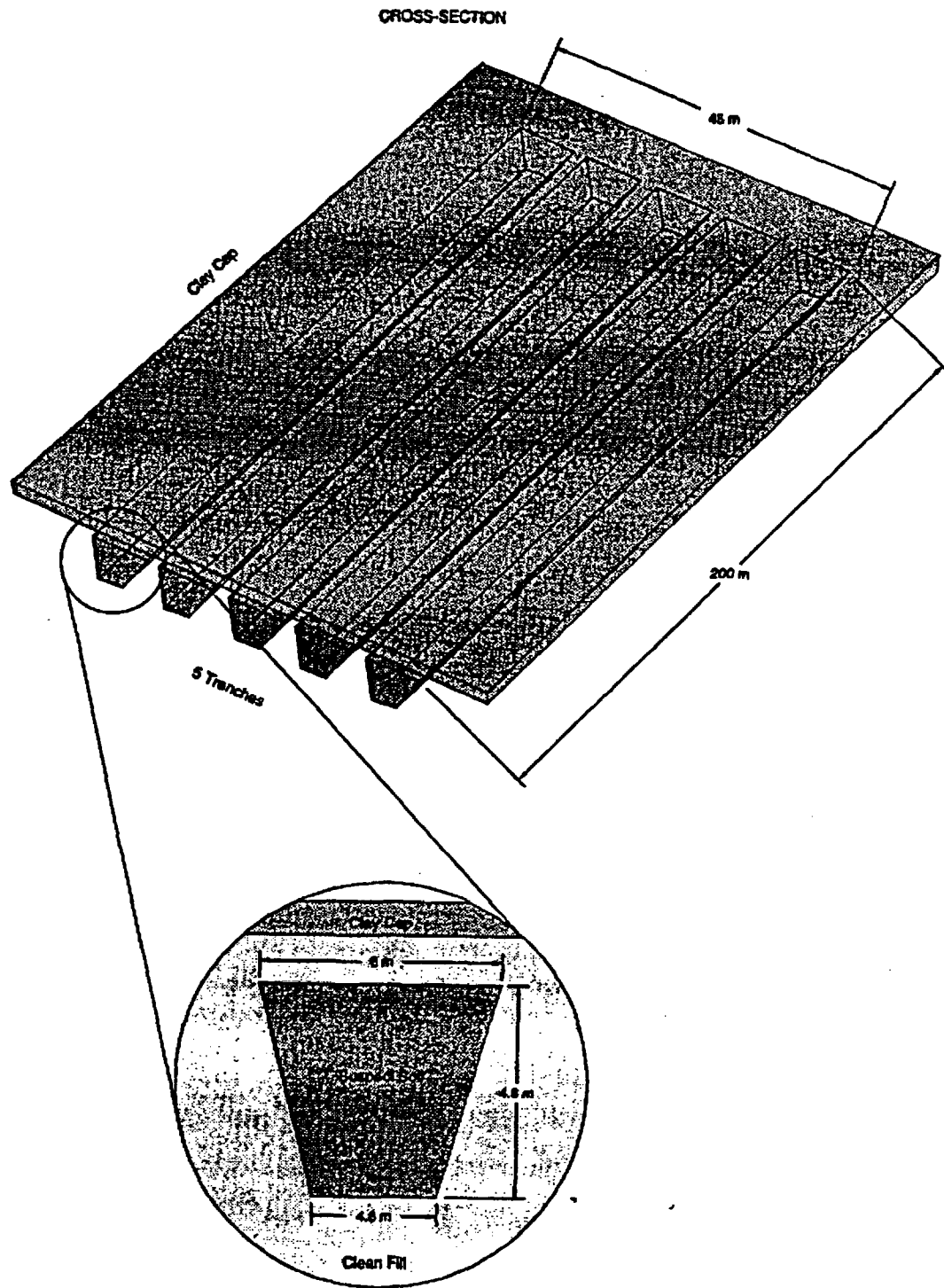


Fig. L1-1. Conceptual drawing of proposed suspect soil trenches.

Rev. 0

I.1.3 Radioactive Inventory of Suspect Soil

The inventory of radionuclides in suspect soil is not known. Therefore, a list of radionuclides that are possibly present was generated. These 730 radionuclides are listed in Table C.3-1. The level of contamination of suspect soil is unknown; therefore, the performance assessment of the suspect soil trenches will address allowable inventories that will meet performance objectives described in Sect. 1.2.

I.1.4 Closure Concept

Because the suspect soil trenches will be placed within the EAV facility, final closure will be the same as that for the entire facility. For the purposes of this assessment, the same closure concept as for the EAVs (Sect. 2.9) is assumed. Briefly, backfill of Burma Road sand is assumed to be placed over the filled trenches, above which a laterally extensive moisture barrier is assumed to be placed. The moisture barrier consists of 0.76 m of clay overlain by 0.3 m of gravel and a geotextile fabric. Over this moisture barrier, 0.76 m of backfill is assumed, followed by 0.15 m of topsoil. As a result, a minimum of 2.9 m of cover material is assumed to overlie the suspect soil trenches at closure. Revegetation and drainage ditches are assumed to constitute final closure, for the purposes of stabilizing soil, preventing pine tree growth, and diverting excess water from the gravel layer.

I.2 ANALYSIS OF PERFORMANCE OF SUSPECT SOIL

The methods used to analyze the long-term performance of the suspect soil trenches within the EAV facility are described in this section. A description of the radionuclide source term posed by the trenches is provided in Sect. I.2.1. Pathways to exposure of human receptors are considered in Sect. I.2.2. The conceptual models developed and computational approach used to assess the performance of the suspect soil trenches are described in Sect. I.2.3.

I2.1 Source Term

The suspect soil trenches provide a source of radionuclides to the geosphere. To characterize this source, it is necessary to evaluate the mechanisms of release. Release of radionuclides from the soil matrix may result from desorption from soil particles, dissolution of precipitated material within the soil matrix, or volatilization into soil gas. Subsequent release to the geosphere occurs as a result of advective and diffusive processes. Advective processes arise as a consequence of the infiltration of water through the trenches. Diffusive processes are driven by the concentration gradient that exists between pore fluids of the trenches and pores of the surrounding uncontaminated soil.

Degradation of the engineered cover will affect release to the geosphere through the effect on infiltration of water into the trenches. As was described in Sect. 3.1.3.1, a reasonable scenario for degradation of the cover is that the cover may be degraded to the gravel layer approximately 900 years after closure of the E-Area facility. Before that time, it is possible that infiltration may increase through the clay layer as a result of head buildup in the gravel layer, if for example the drains fail to divert sufficient water, or disturbance of the clay layer by roots or burrowing animals.

I2.2 Pathways and Scenarios

In this section, the pathways to human exposure to potential suspect soil constituents are addressed. The time periods of concern for human exposure are identical to those described in Sect. 3.2.1.

I2.2.1 Transport Pathways

Radionuclides released from the suspect soil trenches to the geosphere have the potential of reaching humans through numerous pathways. Most conceivable pathways for a buried LLW source such as the suspect soil trenches are described in Sect. 3.2.2.1. The same rationale as was applied in pathway screening for the EAVs applies to the suspect soil

trenches, with the result that only pathways related to contaminated air and groundwater are considered to be of potential consequence. These pathways include volatilization of H-3, C-14, and Rn-222, leaching of suspect soil, resulting in contamination of groundwater local to E-Area, and contamination of agricultural crops and animals as a result of irrigation with contaminated groundwater.

I.2.2.2 Exposures of Off-Site Members of the Public and Protection of Groundwater

According to the discussion in Sect. 3.2.3.3, the drinking water pathway is the only pathway that needs to be considered for off-site releases of radionuclides in groundwater. In cases where the MCL in groundwater corresponds to a dose equivalent less than the performance objective for off-site individuals of 25 mrem per year from all exposure pathways, compliance with the MCL would ensure that the dose to off-site individuals would be substantially less than the performance objective. In cases where the MCL in groundwater corresponds to a dose equivalent greater than the performance objective for off-site individuals, the dose from all exposure pathways other than drinking water would be insignificant compared with the dose from the drinking water pathway, particularly when the uncertainties in estimating maximum concentrations of radionuclides in groundwater at locations more than 100 m from any disposal units are taken into account.

In order to reduce the number of radionuclides for which a detailed analysis of potential groundwater concentrations is necessary, a screening analysis was carried out with respect to groundwater protection requirements. This analysis is essentially the same analysis that was applied to the list of radionuclides that was screened for the EAVs. The screening analysis is described in Sect. 3.2.3.4. Of the 730 radionuclides originally listed in Table C.3-1 of that report, 50 radionuclides were identified for which a more detailed analysis was needed. Radioactive daughters were considered in the screening analysis. These radionuclides are listed in Table I.2-1.

Radionuclides for which radioactive progeny were considered in the detailed groundwater analysis were selected based on the potential for significant ingrowth and mobilization of the progeny. For example, radioactive daughters of Pu-239 were not considered significant for several reasons, including: 1) decay of the parent is slow enough to limit the daughter activities available for transport to less than 0.001% of the initial Pu-239 activity during the first

Table L2-1. Radionuclides considered in the detailed groundwater analysis for suspect soil trenches

H-3	U-235 (Pa-231) ^a
C-14	U-236
Al-26	U-238
Ni-59	Np-237
Ni-63	Pu-238 (U-234) ^b
Se-79	Pu-239
Rb-87	Pu-240
Sr-90	Pu-241 (Am-241, Np-237) ^b
Zr-93	Pu-242
Tc-99	Pu-244
Pd-107	Am-241 (Np-237) ^b
Cd-113m	Am-242m (U-234) ^b
Sn-121m	Am-243 (Pu-239) ^a
Sn-126	Cm-242 (Pu-238) ^a
I-129	Cm-243 (Pu-239) ^a
Cs-135	Cm-244 (Pu-240) ^a
Sm-151	Cm-245
Ra-226	Cm-246 (Pu-242) ^a
Th-229	Cm-247 (Am-243, Pu-239) ^a
Th-230 (Ra-226) ^a	Cm-248
Th-232	Bk-249 (Cf-249) ^b
Pa-231	Cf-249 (Cm-245) ^b
U-232	Cf-250 (Cm-246) ^b
U-233 (Th-229) ^a	Cf-251 (Cm-247, Am-243, Pu-239) ^a
U-234 (Th-230, Ra-226) ^a	Cf-252 (Cm-248) ^b

- ^a Radioactive daughter(s), in parentheses, are potentially significant and are considered, along with their differential transport, in the groundwater analysis.
- ^b Radioactive daughter(s), in parentheses, are longer-lived than the relatively short-lived parent, and the groundwater analysis considers the daughter concentrations.

10,000 years, even when leaching of Pu-239 is neglected; 2) progeny of Pu-239 are generally less mobile than Pu-239, with the exception of U-238; and 3) although U-238 is more mobile (i.e., has a lower K_d), U-238 has a very low specific activity relative to that of Pu-239 and, thus, is not radiologically significant in this decay chain. For Np-237, the activity of the U-233 daughter fairly quickly approaches that of Np-237 if leaching of Np-237 from the suspect soil trenches is neglected. However, Np-237 is fairly mobile ($K_d = 5 \text{ mL/g}$), and is leached from the trenches before significant ingrowth can occur, based on groundwater transport simulations for the Np-237 parent.

The radionuclides for which ingrowth of daughters is believed to be insignificant, either up to 10,000 years or before the parent radionuclide has been leached from the trenches, are Np-237, Pu-239, Pu-240, Pu-242, Pu-244, U-236, U-238, Cm-245, and Cm-248. Radioactive progeny of other radionuclides listed in Table I.2.1 are included in the effective dose equivalents for the parent radionuclides, from which allowable concentrations in groundwater are calculated.

I.2.2.3 Exposure Scenarios for Inadvertent Intruders

Chronic and acute exposure scenarios were developed in Sect. 3.2.4 for inadvertent intruders. The scenarios developed were based on low-level radioactive waste disposal in vaults. The conclusions of Sect. 3.2.4 were that chronic exposure scenarios will always be more restrictive than acute scenarios in terms of compliance with performance objectives for protection of intruders, and that an agriculture scenario, a resident scenario and a post-drilling scenario should be considered. The same arguments apply for the suspect soil trenches, but only the agriculture scenario needs to be considered here according to the following reasoning.

The suspect soil trenches will be constructed without engineered barriers that could preclude excavation or drilling into the waste. Therefore, only the agriculture and post-drilling scenarios for inadvertent intruders are relevant. However, since both scenarios could occur beginning at 100 years after disposal, when active institutional control over the disposal site is assumed to be lost, and since the dose per unit concentration of radionuclides always

is greater for the agriculture scenario than for the post-drilling scenario, only the agriculture scenario needs to be considered in estimating dose to an inadvertent intruder and limits on concentrations and inventories of radionuclides that would be acceptable for disposal.

The agriculture scenario is described in detail in Sect. 3.2.4.1. This scenario assumes that an intruder comes onto the site after active institutional control ceases and establishes a permanent homestead, including on-site sources of water and foodstuffs. Suspect soil is assumed to be accessed when an intruder constructs a home directly on top of a disposal trench, with the foundation of the home extending into the trench itself, and some waste is assumed to be mixed with native soil in the intruder's vegetable garden. Ingestion, inhalation, and external exposure pathways are evaluated.

Screening of the list of 730 radionuclides listed in Table C.3-1 with respect to intruder doses was conducted in the manner described in Sect. 3.2.4.4. In addition to the radionuclides listed in Table L2-1, Co-60, Nb-93m, Cs-137, Eu-154, Eu-155, Pb-210, Ra-228, and Ac-227 were considered in the intruder analysis. Radionuclides not on the list could not pose a significant dose with respect to any performance objectives, due to their short half-lives and/or other factors affecting intruder exposures.

L2.3 Models and Assumptions

In Sect. L2.1 and L2.2, the potential mechanisms of release of radionuclides from the suspect soil trenches were defined, the radionuclides believed to be most significant to this RPA identified, and the relevant human exposure scenarios were described. In this section, the models adopted, and assumptions made, to carry out the computations necessary to estimate doses are described.

L2.3.1 Near-Field Model

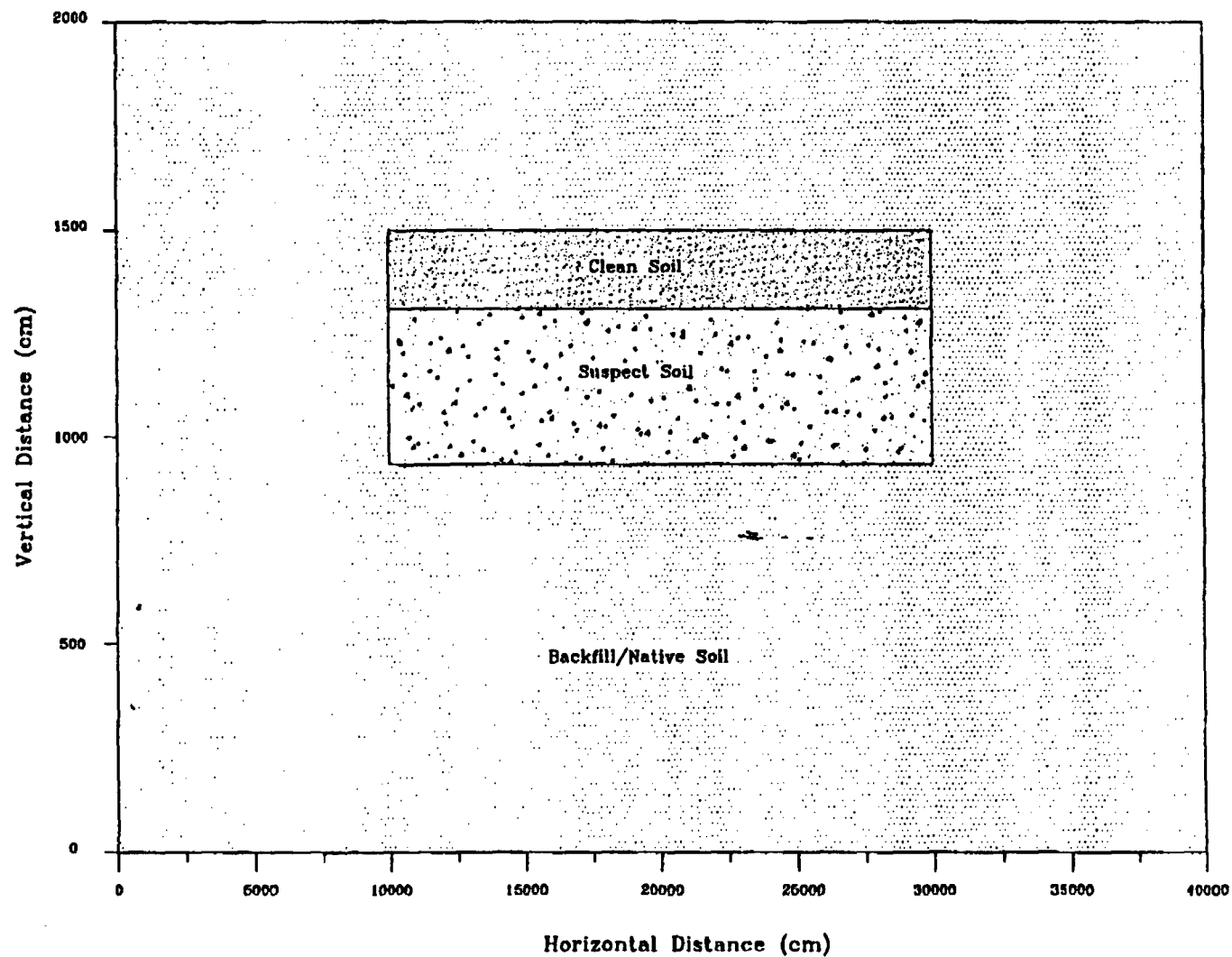
The near-field model for the suspect soil trenches addresses release of radionuclides from the trenches to the surrounding unsaturated soils of the vadose zone, and subsequent transport to the water table. The conceptual models implemented to describe flow and transport are described below.

Flow of water through the trenches is limited by the amount of infiltration through the overlying cover and the characteristics of the suspect soil and surrounding soil. Using the trench design described in Sect. I.1.2, a two-dimensional computational grid was designed to represent the trenches and surrounding soil for simulations carried out with PORFLOW, Version 2.5 (ACRI 1993). The model domain is shown in Fig. I.2-1, and represents a vertical, longitudinal slice through the trenches and surrounding soil. The domain extends vertically from the water table to the ground surface. The trenches are represented within this domain by a zone which is 200 m long and 4.8 m high. In two dimensions, the thickness of the slice is assumed to be of unit thickness, or 1 cm in this case.

The amount of infiltration entering the top of the domain shown in Fig. I.2-1 was assumed to be 40 cm per year, which represents the average infiltration without an engineered cover over the trenches. Although the cover will likely limit infiltration for hundreds of years if undisturbed, there is considerable uncertainty in the timing and extent of degradation. Therefore, for this analysis, no credit was taken for reductions in infiltration brought about by the cover. This is a conservative approach, because flux of radionuclides to the water table is directly proportional to the amount of water available to flow through the system. Therefore, with an intact cover, and the resulting 4 cm per year infiltration (Sect. 4.1.2.1), the flux to the water table is expected to be an order of magnitude lower than the fluxes estimated with a fully degraded cover. Test simulations were carried out at the lower infiltration rate, and confirmation of this proportional reduction in the flux rate was achieved.

Simulation of the path of water through the domain necessitated assumptions of moisture profiles in the suspect soil and surrounding soil. For this analysis, it was assumed that the suspect soil and surrounding soil were essentially the same hydraulically, and that the hydraulic properties described in Sect. 3.3.1.1 for native soil at the SRS are appropriate for these soils. The moisture characteristic data tabulated by Gruber (1980) were used to define the unsaturated hydraulic conductivity and matrix potential as a function of moisture content (Fig. E.2-6, Appendix E). Because the trench soil and surrounding backfill and native soil were assumed to have identical hydraulic properties, water is assumed to be neither diverted

Rev. 0



SRS160

Fig. I.2-1. Simulation domain for the suspect soil trenches in the vadose zone.

into or out of the trenches, but to flow vertically through. Under steady-state hydrologic conditions, the amount of water flowing out of the domain at the water table is equal to the amount of water entering via infiltration; thus, the steady-state flux of water through the suspect soil trenches and surrounding soil was 40 cm/year. Flow simulations were carried out with the computer code PORFLOW, for the two-dimensional domain described above. The PORFLOW input file for these simulations is provided in Fig. I.5-1. The steady-state flow field was subsequently used in mass transport simulations to analyze the advective flux from the trenches.

Release of radionuclides to the geosphere may result from desorption or dissolution processes, as noted in Sect. I.2.1. Advective and diffusive processes act to mobilize the radionuclides in the pore waters of the trenches. For the suspect soil analysis, radionuclides were assumed to be completely soluble, and sorption was considered to be a fully-reversible linear process at equilibrium. Equilibrium partitioning between solid (sorbed) and liquid phases was characterized by the elemental distribution coefficients (K_d 's) listed in Table I.2-2. The K_d values in this table are average values taken from site-specific literature, when available, and from a review article by Sheppard and Thibault (1990).

The computer code, PORFLOW, was used to simulate advection and diffusion from the trenches. The steady-state flow field provided flow rates through the trenches and to the water table (at the bottom of the domain, Fig. I.2-1), and K_d 's, effective diffusion and dispersion coefficients, and radioactive decay constants provided the necessary information for simulating advective-diffusive transport. An example input file is shown in Fig. I.5-2. Effective diffusion (i.e., molecular diffusion corrected for tortuosity of a porous medium) and dispersion coefficients are not radionuclide-specific, and the values used for these parameters in the PORFLOW simulations were: 1) longitudinal dispersivity = 3 m; 2) transverse dispersivity = 0.3 cm; and 3) effective diffusion coefficient = $158 \text{ cm}^2 \text{ yr}^{-1}$. No data are available for dispersivities in the unconsolidated sediments of the SRS. In the unsaturated zone, where flow velocities are very low, dispersion, which is directly proportional to flow velocity, is likely to be fairly insignificant with respect to plume movement. The values chosen for these simulations are believed to be reasonable based on a discussion of field-scale dispersivity in a reputable groundwater textbook (Freeze and Cherry 1979). Small values of dispersivity are

Table I2-2. Distribution coefficients assumed for elements in suspect soil trenches

Radionuclide	K _d Value Assumed (mL/g)		Literature Source	
	Soil	Clay	Soil	Clay
Al	1500	1500	Bacs and Sharp 1983	assumed same as soil
Am	1900	8400	Hoeffner 1985	Sheppard and Thibault 1990
Bk	1900	8400	same as Americium	same as Americium
C	2	1	McIntyre 1988	Sheppard and Thibault 1990
Cd	80	560	Sheppard and Thibault 1990	Sheppard and Thibault 1990
Cf	1900	8400	same as Americium	same as Americium
Cm	1900	6000	same as Americium	Sheppard and Thibault 1990
Co	10	550	Hoeffner 1985	Sheppard and Thibault 1990
Cs	330	1900	Hoeffner 1985	Sheppard and Thibault 1990
Eu	245	—	assumed the same as Sm	—
H	0	0	Sheppard and Thibault 1990	Sheppard and Thibault 1990
I	0.6	1	Hoeffner 1984	Sheppard and Thibault 1990
Nb	160	900	Sheppard and Thibault 1990	Sheppard and Thibault 1990
Ni	400	650	Sheppard and Thibault 1990	Sheppard and Thibault 1990
Np	5	55	Sheppard and Thibault 1990	Sheppard and Thibault 1990
Pa	550	2700	Sheppard and Thibault 1990	Sheppard and Thibault 1990
Pb	270	550	Sheppard and Thibault 1990	Sheppard and Thibault 1990
Pd	55	270	Sheppard and Thibault 1990	Sheppard and Thibault 1990
Pu	100	5100	Hoeffner 1985	Sheppard and Thibault 1990
Ra	500	9100	Sheppard and Thibault 1990	Sheppard and Thibault 1990
Rb	55	270	Sheppard and Thibault 1990	Sheppard and Thibault 1990
Se	5	740	Ticknor and Rucgger 1989	Sheppard and Thibault 1990
Sm	245	1300	Sheppard and Thibault 1990	Sheppard and Thibault 1990
Sn	130	670	Sheppard and Thibault 1990	Sheppard and Thibault 1990
Sr	10	110	Hoeffner 1985	Sheppard and Thibault 1990
Tc	0.36	1	Oblath 1982	Sheppard and Thibault 1990
Th	3000	5800	Sheppard and Thibault 1990	Sheppard and Thibault 1990
U	35	1600	Sheppard and Thibault 1990	Sheppard and Thibault 1990
Zr	600	3300	Sheppard and Thibault 1990	Sheppard and Thibault 1990

conservative for radionuclides which do not decay significantly before reaching the water table, as is the case with the great majority of radionuclides in the suspect soil analysis, because less spreading of the plume occurs with small values and the intruder exposures are maximized with the smaller loss from the trenches. Large values of dispersivity are conservative for radionuclides that decay significantly during transport to the water table, as the arrival time at the water table will be earlier and thus less radioactive decay can occur.

I2.3.2 Groundwater Transport Model

To simulate transport of radionuclides that are released from the suspect soil trenches to the water table, the conceptual saturated zone transport model described in Sect. 3.3.2 was adopted. The flow field established by PORFLOW simulations, which implemented this conceptual model, was used in the suspect soil analysis. Therefore, the groundwater transport model was identical to that described in Sect. 3.3.2 with the exception that the source zone was smaller (2 suspect soil source nodes versus 4 nodes for the ILNT vaults and 35 nodes for the LAW vaults). The smaller source zone represents the relatively smaller source area presented by the suspect soil trenches. An example PORFLOW input file for four radionuclides is shown in Fig. I5-3.

I2.3.3 Atmospheric Release Model for Volatile Components

Potential atmospheric release of volatile forms of H-3 and C-14 must be considered in order to consider all potentially significant pathways of exposure to radionuclides from the suspect soil trenches. Inadvertent intruders may be exposed to air within residences built on top of the soil above the trenches, and off-site individuals may be exposed to concentrations transported to or beyond the SRS boundary. The model described below was used to screen this pathway, with the purpose of determining whether a more detailed analysis of the potential significance of this pathway with respect to the 100 mrem per year performance objective for inadvertent intruders and the 10 mrem per year performance objective for off-site individuals (Sect. 1.2) was necessary.

To estimate fluxes of potentially volatile radionuclides, H-3 and C-14, from the suspect soil trenches, the model developed to conservatively estimate fluxes of these radionuclides arising from the LAW vaults (Sect. A.3.5 and A.3.6) was used. For H-3, the vapor phase concentration in the trenches is first calculated by assuming that the concentration of H-3 in water vapor in the trenches is the same as the H-3 concentration in the pore water of the suspect soil. The ideal gas law is used to estimate the ambient concentration of water vapor in air in the trenches, the result being 9.2 g m^{-3} at 10°C and 100% relative humidity. Converting to activity concentration units, the H-3 concentration in air in the trenches, in Ci m^{-3} , is 9.2×10^{-6} times the H-3 concentration in pore water. For C-14, all of this radionuclide was conservatively assumed to exist as $^{14}\text{CO}_2$ in the air in the trenches.

For off-site individuals, diffusion of H-3, C-14, and Rn-222 through soil overlying the suspect soil trenches, and subsequent transport to the site boundary were considered. One meter of soil was assumed to cover the suspect soil, although initially approximately 4 m of soil will overly the trenches with the engineered cover in place. Per Ci of H-3 initially in the trenches, the concentration in the air-filled voids of the trenches is calculated from:

$$C_{T\text{H-3}} = \frac{1 \text{ Ci}}{1460 \text{ m}^3} \times \frac{9.2 \times 10^{-6} \text{ Ci/m}^3_{(\text{air})}}{1 \text{ Ci/m}^3_{(\text{H}_2\text{O})}}$$

where 1460 m^3 represents the amount of pore fluid in the trenches. This pore fluid content is based on the 5200 m^3 disposal capacity of the trenches (Sect. I.1.2), a total assumed porosity of 0.40, and a saturation of approximately 0.7 in the trenches, based on flow simulations with PORFLOW. The resulting trench air concentration is $6.3 \times 10^{-9} \text{ Ci m}^{-3}$. The flux of H-3 at the soil surface ($J_{\text{H-3}}$ in $\text{Ci m}^{-2} \text{ yr}^{-1}$) is calculated from:

$$J_{\text{H-3}} = D_a \left(\frac{C_{T\text{H-3}}}{x} \right)$$

where D_a is the molecular diffusion coefficient in air ($754 \text{ m}^2 \text{ yr}^{-1}$ for water vapor, CRC 1981) and x is the soil thickness, assumed to be one meter. The initial flux of H-3 (i.e., at closure) from the soil is conservatively estimated to be $4.8 \times 10^{-6} \text{ Ci m}^{-2} \text{ yr}^{-1}$ over an area of 6000 m^2 , per Ci of H-3 disposed of in the suspect soil trenches.

For inadvertent intruders, a similar calculation of H-3 flux from soil above the trenches can be made, but 100-year radioactive decay is first considered because institutional control is assumed to preclude intrusion before 100 years. Per Ci of H-3 in the trenches, no more than 3.6×10^3 Ci would remain at 100 years after closure based on consideration of radioactive decay alone. Leaching is neglected. At 100 years, the concentration of H-3 in the trench air is calculated to be 2.3×10^{-11} Ci m³. The flux of H-3 at the soil surface (J_{H-3} in Ci m² yr⁻¹) at 100 years is estimated to be 1.7×10^{-8} Ci m² yr⁻¹ over an area of 6000 m².

Similarly, for C-14, the concentration in the trench air ($C_{T,C-14}$), in Ci m³ per Ci C-14 in the suspect soil trenches, is calculated based on a 100-year Ci content of the trenches of one; that is, decay has been insignificant and leaching is neglected. The trench air concentration of 1.6×10^3 Ci m³ was derived from the assumption of an unwetted void space of 624 m³ in the trenches. The flux at the surface, J_{C-14} , is calculated in the same manner as was done for H-3, using a diffusion coefficient in air of 440 m² yr⁻¹ (CRC 1981). The flux of C-14 from the soil overlying the suspect soil trenches is conservatively estimated to be 7.0×10^{-1} Ci m² yr⁻¹ over an area of 6000 m². A C-14 flux of 7.0×10^{-1} Ci m² yr⁻¹ over an area of 6000 m² corresponds to loss of the initial 1 Ci inventory in much less than one year. Therefore, the annual flux of C-14 was assumed to be 1 Ci per 6000 m², or 1.6×10^{-4} Ci m² yr⁻¹ for every Ci of C-14 initially in the suspect soil trenches. This flux represents both the initial flux for determining off-site exposures and the 100-year flux, for estimating intruder exposures.

The flux of Rn-222 through one meter of overlying soil was considered in Sect. A.3.7. The estimated Rn-222 flux, per Ci of U-234 in the trenches, is 2.3 pCi m² s⁻¹.

I.2.3.4 Models for Dose Estimation

Doses to off-site members of the public resulting from use of contaminated groundwater beyond the 100-m buffer zone around the suspect soil trenches were not directly estimated. Rather, comparisons of maximum predicted groundwater concentrations with the more restrictive of either MCLs or allowable concentrations based on 25-mrem per year performance objective were made. The allowable concentrations were calculated by dividing 25 mrem per year by the EDE per unit concentration in drinking water (Table A.4-6, Sect. A.4). These calculations are simple, were performed by hand, and checked several times for accuracy.

Other than the contaminated groundwater, the air pathway is the only potentially significant means of exposure that is considered for off-site individuals in the suspect soil analysis (Sect. I.2.2.2). Doses to off-site individuals were calculated in the manner described in Sect. A.3.1.3. This methodology utilizes the source term described in Sect. I.2.3.3 above, in Ci yr^{-1} of H-3 or C-14, and the AIRDOS-PC atmospheric dispersion model to estimate the all-pathway dose to an individual residing continuously at the SRS site boundary located 5 km from E-Area. The AIRDOS-PC input and output file information is provided in Appendix C.

To estimate dose to the intruder from potentially volatile H-3 and C-14 compounds released from the suspect soil trenches, the same procedure described in Sect. A.3.1.2 was used. Assuming that the intruder's house resides directly on top of soil, 1 m in thickness, overlying the suspect soil trenches, the steady-state air concentration (C_a), in Ci m^{-3} , of H-3 or C-14 to which the intruder is exposed is estimated from:

$$C_a = \frac{J/a}{h}$$

where

- J = flux rate of volatile H-3 or C-14 from soil and into house, $\text{Ci m}^{-2} \text{yr}^{-1}$,
- a = air exchange rate in house, assumed to be 8760 yr^{-1} , and
- h = height of the ceiling in house, 2.4 m.

Conservative estimates of the flux rates were provided in Sect. I.2.3.3 above. The inhalation dose to the intruder (D_H) was calculated from:

$$D_H = C_a \times B_r \times DCF_i$$

where

- B_r = breathing rate ($8000 \text{ m}^3 \text{yr}^{-1}$), and
- DCF_i = inhalation dose conversion factor for H-3 or C-14, (mrem Ci^{-1}).

Doses to inadvertent intruders from the agriculture scenario were estimated according to the procedures described in Sect. A.4.5.2.

I.2.4 Performance Analysis Methodology

The models and assumptions described in Sect. I.2.3 were applied to analyze the performance of the suspect soil trenches. Doses to off-site individuals and inadvertent intruders and groundwater concentrations at the compliance point for groundwater resource protection per Ci of each radionuclide listed in Table I.2-1 were estimated. Because inventories of radionuclides are not known for the suspect soil trenches, the computational results are used to calculate inventory limits for each radionuclide based on performance objectives of the RPA.

Specifically, the near-field model was implemented, using the PORFLOW computer code, to estimate fluxes of radionuclides to the water table over time and to track the inventory in the trenches as a function of time. The results of the two-dimensional PORFLOW simulations were obtained in terms of fraction of the initial inventory in the simulation domain that leaves the bottom boundary of the domain over time, the bottom boundary representing the water table. Because the simulation domain represents a "slice" through the trenches and surrounding soil, a correction was made to the results to account for losses of radionuclides through the faces at the sides of the trenches. This correction assumes that the radionuclide loss from the trenches through these faces is geometrically related to the loss through the ends of the trenches. The losses through the ends are accounted for in the PORFLOW simulations. By calculating the ratio of the side planes (or faces) to the area of the end planes of the trenches, and multiplying this ratio by the PORFLOW-simulated losses through the end planes, the results are corrected by adding this additional amount to the flux at the bottom of the domain. This correction, although necessary, did not significantly alter the flux results for the near-field model because the overwhelmingly significant losses from the trenches are from the base.

Following estimation of flux to the water table for the trenches, the groundwater model was implemented, again using PORFLOW, to estimate the time-dependent groundwater concentrations of each radionuclide at the compliance point for groundwater resource protection. The compliance point was selected from the groundwater simulation results as the node with the highest concentration which is at least 100 m from the edge of the suspect soil trenches. For radionuclides that are relatively short-lived (with half-lives less than 1000 years) and that decay to longer-lived radioactive progeny, daughter contributions to groundwater radioactivity per Ci of parent activity originally in the suspect soil trenches were estimated in the manner described in Sect. 4.1.3. The parent radionuclide is assumed to decay completely to the daughter in the trenches. Loss of the parent through leaching during the decay process is neglected. The initial activity of the daughter per Ci of original inventory of parent

is calculated from:

$$A_{D0} = A_{P0} \frac{\lambda_D}{\lambda_P} = \frac{\lambda_D}{\lambda_P}$$

where

A_{D0} = initial activity of the daughter, Ci,

A_{P0} = initial activity of the parent (= 1 Ci),

λ_D = radioactive decay constant ($0.693/T_{1/2}$) of the daughter (yr^{-1}), and

λ_P = radioactive decay constant of the parent (yr^{-1}).

The peak concentration of the daughter, per Ci of parent radionuclide, is calculated by multiplying the initial activity of the daughter per Ci of parent activity (A_{D0}) by the 10,000-year and peak groundwater concentration of the daughter (pCi/cc-Ci), which is determined with PORFLOW simulations. Inventory limits based on groundwater protection requirements and on the 25 mrem per year performance objective for off-site individuals were calculated for the most restrictive requirement. For other radionuclides for which daughters were considered (Table I.2-1), daughter ingrowth and transport were considered explicitly in the vadose zone and groundwater simulations. Again, the results are expressed as pCi/cc of daughter radionuclide per Ci of parent originally in the trenches.

The air pathway was considered by carrying out the calculations described in Sect. I.2.3.3 to calculate fluxes of H-3, C-14, and Rn-222 from the top of the trenches, assuming the approximately 3-m engineered moisture barrier had been removed or eroded away. For H-3 and C-14, these fluxes were then used to conservatively estimate doses to intruders residing over the trenches, or doses to off-site individuals per unit activity in the trenches. Inventory limits were calculated for the air pathway for H-3 and C-14 based on the performance objectives of 10 mrem per year for off-site individuals, and 100 mrem per year for inadvertent intruders. For U-234, inventory limits are based on the performance objective of 20 pCi/m²-s of Rn-222 in addition to consideration of groundwater concentrations of U-234, Th-230, and Ra-226.

Intruder doses from the agriculture scenario were calculated using the models referenced in Sect. I.2.3.4 above, for a unit inventory of each radionuclide. Inventory limits were calculated for intruders based on the performance objective of 100 mrem per year chronic exposure.

I.2.5 Quality Assurance

As described in Sect. 3.5, this analysis was conducted under the guidance of the provision of the ANSI/ASME NQA-1 Program Requirements for Nuclear Facilities (NRC 1989), as required by DOE Order 5820.2A (U.S.DOE 1988a). Pertinent elements of NQA-1 and relevant documentation are cited in that section of the RPA, and apply directly to the suspect soil analysis.

I.3 RESULTS OF SUSPECT SOIL ANALYSIS

In this section, the results of the analysis of performance of the suspect soil trenches are presented. Predicted releases to the environment (atmospheric releases and releases to the water table), resulting concentrations, results of dose analyses, and allowable inventories in the suspect soil trenches are presented in Sect. I.3.1. The results are interpreted in Sect. I.3.2.

I3.1 Analysis Results

I3.1.1 Near-Field Model Results

Table I3-1 lists the PORFLOW simulation results for the near-field model. The fluxes provided represent the peak flux to the water table per pCi inventory of radionuclide in the suspect soil trenches (i.e., peak fractional flux). These fluxes are based on a 40 cm per year infiltration rate through the trenches, as was noted in Sect. I2.3.1.

I3.1.2 Groundwater Concentrations

The results of the groundwater transport simulations are listed in Table I3-2. The values listed in this table represent peak groundwater concentration per Ci of radionuclide in the suspect soil trenches, at the compliance point for groundwater protection. If the peak occurs at a time greater than 10,000 years after closure, the 10,000 year compliance point concentration is also provided. The compliance point is considered to be the point of maximum groundwater concentration at least 100 m from the edge of the suspect soil trenches.

I3.1.3 Dose Analysis for Off-Site Releases of Radionuclides

As described in Sect. 3.2.3.3, the only performance objective of concern for off-site release of radionuclides are those pertinent to consumption of groundwater, provided doses from airborne release of radionuclides are insignificant.

The groundwater concentrations per Ci inventory in the trenches are compared to allowable groundwater concentrations to derive inventory limits based on consideration of groundwater resource protection and the 25 mrem-per-year performance objective for off-site individuals. Inventory limits are based on the more restrictive of the two requirements. In order to determine which performance objective is more restrictive for each radionuclide, the MCLs from Table 3.2-1 were compared to the results of the model for estimating dose from the drinking water pathway for off-site individuals. The annual EDEs, in rem per year, from the drinking water pathway per unit concentration (1 μ Ci/L) of radionuclide in groundwater are summarized in Table 4.1-7.

Table L3-1. Peak flux to the water table from suspect soil trenches

Radionuclide	Predicted Peak Fractional Flux (pCi/year-pCi)	Time of Peak Flux (year)
H-3	1.0×10^{-1}	3.4
C-14	8.3×10^{-3}	65
Al-26	1.3×10^{-5}	34,000
Ni-59	4.7×10^{-5}	8,900
Ni-63	1.7×10^{-10}	840
Se-79	3.7×10^{-3}	140
Rb-87	3.7×10^{-4}	1,300
Sr-90	6.7×10^{-5}	100
Zr-93	3.3×10^{-5}	14,000
Tc-99	3.4×10^{-2}	15
Pd-107	3.7×10^{-4}	1,300
Cd-113m	7.4×10^{-11}	130
Sn-121m	8.4×10^{-9}	400
Sn-126	1.5×10^{-4}	3,000
I-129	2.3×10^{-2}	23
Cs-135	6.2×10^{-5}	7,700
Sm-151	2.3×10^{-9}	680
Ra-226	2.2×10^{-6}	4,600
Th-229	2.0×10^{-7}	25,000
Th-230 Ra-226 ^a	3.8×10^{-6} 5.3×10^{-7}	56,000 45,000
Th-232	6.7×10^{-6}	71,000
Pa-231	2.9×10^{-5}	11,000
U-232	1.0×10^{-5}	280
U-233 Th-229 ^a	5.7×10^{-4} 4.1×10^{-2}	840 3,200
U-234 Th-230 ^a Ra-226 ^a	5.7×10^{-4} 3.1×10^{-8} 3.9×10^{-9}	840 5,000 9,700

Table I3-1. (continued)

Radionuclide	Predicted Peak Fractional Flux (pCi/year-pCi)	Time of Peak Flux (year)
U-235 Pa-231 ^a	5.7×10^{-4} 6.3×10^{-11}	840 3,900
U-236	5.7×10^{-4}	840
U-238	5.7×10^{-4}	840
Np-237	3.7×10^{-3}	140
Pu-238 U-234 ^a	2.6×10^{-7} 2.0×10^{-7}	480 840
Pu-239	1.9×10^{-3}	2,300
Pu-240	1.6×10^{-4}	2,100
Pu-241 Am-241 ^a Np-237 ^a	1.7×10^{-11} 7.0×10^{-13} 2.5×10^{-8}	140 3,700 140
Pu-242	2.0×10^{-4}	2,300
Pu-244	2.0×10^{-4}	2,300
Am-241 Np-237 ^a	2.1×10^{-11} 7.5×10^{-7}	3,700 140
Am-242m U-234 ^a	1.7×10^{-14} 3.5×10^{-7}	1,700 840
Am-243 Pu-239 ^a	8.5×10^{-7} 5.5×10^{-5}	19,000 6,600
Cm-242 Pu-238 ^a	4.2×10^{-40} 1.3×10^{-9}	7.6 480
Cm-243 Pu-239 ^a	9.0×10^{-21} 2.2×10^{-6}	400 2,300
Cm-244 Pu-240 ^a	1.4×10^{-22} 4.4×10^{-7}	250 2,100
Cm-245	1.1×10^{-6}	21,000
Cm-246 Pu-242 ^a	3.4×10^{-7} 8.1×10^{-5}	16,000 6,000
Cm-247 Am-243 ^a Pu-239 ^a	1.1×10^{-5} 5.0×10^{-9} 3.6×10^{-8}	44,000 45,000 29,000
Cm-248	9.8×10^{-6}	42,000
Bk-249 Cf-249 ^a	5.4×10^{-37} 1.5×10^{-14}	18 3,200

Table L3-1. (continued)

Radionuclide	Predicted Peak Fractional Flux (pCi/year-pCi)	Time of Peak Flux (year)
Cf-249	5.8×10^{-12}	3,200
Cf-250 Cm-246 ^a	5.8×10^{-24} 9.4×10^{-10}	190 16,000
Cf-251 Cm-247 ^a Am-243 ^a Pu-239 ^a	1.1×10^{-9} 1.1×10^{-5} 5.0×10^{-9} 3.5×10^{-8}	6,100 44,000 46,000 30,000
Cf-252 Cm-248 ^a	2.7×10^{-31} 7.6×10^{-11}	42 42,000

^a Fractional Flux and Time of Peak Flux given for radioactive daughter is per pCi of parent radionuclide.

Table I3-2. Predicted groundwater compliance concentration for the suspect soil trenches

Radionuclide	Groundwater Concentration at 10,000 years (pCi/cc-Ci)	Peak Groundwater Concentration	
		pCi/cc-Ci	Time of peak (year)
H-3	— ^a	1.8	13
C-14	— ^a	3.2×10^{-1}	185
Al-26	9.6×10^{-2}	3.4×10^{-4}	130,000
Ni-59	1.9×10^{-4}	1.3×10^{-3}	30,000
Ni-63	— ^a	1.8×10^{-16}	1,800
Se-79	— ^a	9.2×10^{-2}	370
Rb-87	— ^a	9.2×10^{-3}	4,400
Sr-90	— ^a	2.6×10^{-5}	190
Zr-93	3.3×10^{-5}	9.4×10^{-4}	45,000
Tc-99	— ^a	8.8×10^{-1}	35
Pd-107	— ^a	9.8×10^{-3}	3,900
Cd-113m	— ^a	1.0×10^{-10}	2,400
Sn-121m	— ^a	3.4×10^{-11}	610
Sn-126	— ^a	4.3×10^{-3}	9,600
I-129	— ^a	7.6×10^{-1}	65
Cs-135	4.4×10^{-4}	1.7×10^{-3}	24,000
Sm-151	— ^a	7.7×10^{-12}	1,000
Ra-226	— ^a	4.1×10^{-5}	2,700
Th-229	1.4×10^{-10}	5.7×10^{-4}	45,000
Th-230 Ra-226 ^b	3.4×10^{-10} 2.0×10^{-6}	3.3×10^{-5} 2.3×10^{-4}	180,000 160,000
Th-232	3.6×10^{-10}	2.2×10^{-4}	240,000
Pa-231	4.1×10^{-5}	4.8×10^{-4}	33,000
U-232	— ^a	2.1×10^{-6}	500

I-25
Table L3-2 (continued)

WSRC-RP-94-218

Radionuclide	Groundwater Concentration at 10,000 years (pCi/cc-Ci)	Peak Groundwater Concentration	
		pCi/cc-Ci	Time of peak (year)
U-233 Th-229 ^b	--- ^a 8.8×10^{-5}	1.2×10^{-2} 1.1×10^{-4}	2,400 16,000
U-234 Th-230 ^b Ra-226 ^b	--- ^a 1.2×10^{-5} 3.8×10^{-5}	1.2×10^{-2} 2.9×10^{-5} 9.7×10^{-5}	2,400 43,000 49,000
U-235 Pa-231 ^b	--- ^a 1.3×10^{-4}	1.2×10^{-2} 1.7×10^{-4}	2,400 25,000
U-236	--- ^a	1.2×10^{-2}	2,400
U-238	--- ^a	1.2×10^{-2}	2,400
Np-237	--- ^a	8.1×10^{-2}	330
Pu-238 U-234 ^b	--- ^a --- ^a	8.1×10^{-9} 5.0×10^{-6}	790 2,400
Pu-239	--- ^a	4.2×10^{-3}	6,600
Pu-240	--- ^a	2.6×10^{-3}	6,000
Pu-241 Am-241 ^b Np-237 ^b	--- ^a --- ^a --- ^a	4.8×10^{-15} 6.7×10^{-16} 5.5×10^{-7}	220 5,400 330
Pu-242	--- ^a	5.0×10^{-3}	6,900
Pu-244	--- ^a	5.1×10^{-3}	6,900
Am-241 Np-237 ^b	--- ^a --- ^a	2.0×10^{-14} 1.6×10^{-5}	5,400 330
Am-242m U-234 ^b	--- ^a --- ^a	8.3×10^{-19} 8.7×10^{-6}	2,400 2,400
Am-243 Pu-239 ^b	5.0×10^{-9} 4.6×10^{-4}	4.0×10^{-7} 5.1×10^{-4}	40,000 13,000
Cm-242 Pu-238 ^b	--- ^a --- ^a	--- ^c 4.1×10^{-11}	--- 790
Cm-243 Pu-239 ^b	--- ^a --- ^a	3.6×10^{-27} 5.0×10^{-6}	520 6,600
Cm-244 Pu-240 ^b	--- ^a --- ^a	1.4×10^{-29} 7.2×10^{-6}	340 6,000
Cm-245	7.6×10^{-9}	7.4×10^{-7}	48,000

I-26
Table L3-2. (continued)

WSRC-RP-94-218

Radionuclide	Groundwater Concentration at 10,000 years (pCi/cc-Ci)	Peak Groundwater Concentration	
		pCi/cc-Ci	Time of peak (year)
Cm-246 Pu-242 ^b	2.9×10^{-9} 3.0×10^{-5}	6.4×10^{-8} 3.3×10^{-5}	31,000 13,000
Cm-247 Am-243 ^b Pu-239 ^b	1.3×10^{-8} 7.8×10^{-9} 1.6×10^{-4}	2.8×10^{-4} 2.8×10^{-4} 8.7×10^{-4}	150,000 160,000 40,000
Cm-248	1.9×10^{-8}	2.6×10^{-4}	170,000
Bk-249 Cf-249 ^b Cm-245 ^b	--- ^a --- ^a 7.8×10^{-13}	--- ^a 7.8×10^{-18} 7.6×10^{-11}	--- 4,500 48,000
Cf-249 Cm-245 ^c	--- ^a 3.1×10^{-10}	3.1×10^{-15} 3.1×10^{-8}	4,500 48,000
Cf-250 Cm-246 ^b	--- ^a 1.1×10^{-11}	2.2×10^{-31} 2.7×10^{-10}	280 30,000
Cf-251 Cm-247 ^b Am-243 ^b Pu-239 ^b	--- ^a 7.6×10^{-13} 4.1×10^{-13} 6.3×10^{-9}	5.7×10^{-12} 1.6×10^{-8} 1.5×10^{-8} 4.7×10^{-8}	9,300 160,000 160,000 40,000
Cf-252 Cm-248 ^b	--- ^a 1.5×10^{-13}	--- ^a 2.0×10^{-9}	--- 170,000

^a Peak occurs before 10,000 years.

^b Concentration given is pCi/cc of the daughter per Ci of the parent. Time of peak applies to that of the daughter.

^c Fractional flux less than 10^{-30} per year; groundwater concentration not calculated.

For comparison to MCLs, the performance objective of 25 mrem per year for off-site individuals is divided by the EDEs in Table 4.1-7 to derive the concentration limit in drinking water of each radionuclide based on this dose limit. The results of this calculation, converted to appropriate units, and the appropriate MCLs from Table 3.2-1 are listed in Table I.3-3 for comparison. These results indicate that the 25 mrem per year performance objective is more restrictive for most of the alpha-emitting radionuclides, with the exception of Ra-226, Th-230, Am-242m, U-235, and U-238.

The allowable inventories derived for the drinking water pathway from off-site releases of radionuclides are given in Table I.3-4. These inventories (Ci) are calculated in the following manner. First, the most restrictive performance objective from Table I.3-3 is selected by choosing the lowest allowable groundwater concentration of the two values given for each radionuclide. Second, the lowest allowable groundwater concentration is divided by the maximum groundwater concentration up to 10,000 years, per Ci of inventory in the suspect soil trenches.

In order to evaluate the significance of the air pathway for the potentially volatile H-3 and C-14 radionuclides, doses were estimated using the fluxes derived in Sect. I.2.3.3 and the inhalation exposure model described in Sect. I.2.3.4. For Rn-222, the flux derived in Sect. A.3.7 was compared to the performance objective of $20 \text{ pCi m}^{-2} \text{ s}^{-1}$ for Rn-222 to calculate a disposal limit for U-234. The disposal limit of 8.8 Ci per trench (Sect. A.3.7) translates to a total of 44 Ci in all five trenches. The estimated fluxes from the soil per Ci of H-3, C-14, and U-234 present in the trenches, the corresponding inhalation doses per unit activity (mrem/Ci), the appropriate performance objectives (mrem/year) and the inventory limits (Ci) based on the air pathway are given in Table I.3-5. The doses for H-3 and C-14 are based on 50-year committed dose equivalent factors for inhalation of 6.3×10^4 mrem per Ci for $^3\text{H}_2\text{O}$ and 2.4×10^4 mrem per Ci for $^{14}\text{CO}_2$ (U.S.DOE 1988b).

I.3.1.4 Dose Analysis for Inadvertent Intruders

The results of the dose analysis for the agriculture scenario for the suspect soil trenches are given in Table I.3-6. The limits on concentrations and inventories of radionuclides are

Table I3-3. Comparison of MCLs and allowable groundwater concentrations based on the 25 mrem per year performance objective for off-site individuals

Radionuclide	MCL, ^c pCi/L	Allowable Concentration Based on 25 mrem per year, ^a pCi/L
H-3	20,000	540,000
C-14	6,400	16,000
Al-26	420 ^c	2,600
Ni-59	530	160,000
Ni-63	80	64,000
Se-79	660 ^c	4,100
Rb-87	270	7,100
Sr-90	8	250
Zr-93	2,100	21,000
Tc-99	800	26,000
Pd-107	36,600	250,000
Cd-113m	40	230
Sn-121m	2,260 ^c	26,000
Sn-126	290 ^c	1,900
I-129	0.5	120
Cs-135	800	4,800
Sm-151	1,100	100,000
Ra-226	5	31
Th-229	15	8.6
Th-230	15	64
Th-232	15	7.1
Pa-231	2.4	2.3
U-232	4.3×10^{20} (20 µg/L) ^c	17
U-233	190,000 (20 µg/L) ^c	125
U-234	124,000 (20 µg/L) ^c	132
U-235	42.8 (20 µg/L) ^c	139

I-29
Table I3-3. (continued)

WSRC-RP-94-218

Radionuclide	MCL, ^a pCi/L	Allowable Concentration Based on 25 mrem per year, ^b pCi/L
U-236	1,270 (20 µg/L) ^c	139
U-238	6.66 (20 µg/L) ^c	139
Np-237	15	8.9
Pu-238	15	8.9
Pu-239	15	8.1
Pu-240	15	8.1
Pu-241	(based solely on Np-237) ^d	(based solely on Np-237) ^d
Pu-242	15	8.3
Pu-244	15	8.6
Am-241	15	7.6
Am-242m	1.27 ^e	8.1
Am-243	15	7.6
Cm-242	(based solely on Pu-238) ^e	(based solely on Pu-238) ^e
Cm-243	(based solely on Pu-239) ^e	(based solely on Pu-239) ^e
Cm-244	(based solely on Pu-240) ^e	(based solely on Pu-240) ^e
Cm-245	15	7.6
Cm-246	15	7.6
Cm-247	15	8.3
Cm-248	15	2.1
Bk-249	(based solely on Cm-245) ^e	(based solely on Cm-245) ^e
Cf-249	15	3.4
Cf-250	(based solely on Cm-246) ^e	(based solely on Cm-246) ^e
Cf-251	15	7.4
Cf-252	(based solely on Cm-248) ^e	(based solely on Cm-248) ^e

^a Option 1, Table 3.2-1, unless otherwise noted.

^b Calculated by dividing 25 mrem per year performance objective by EDE in Table 4.1-7.

^c Option 3, Table 3.2-1.

^d Np-237 daughter has significantly higher calculated groundwater concentration than Am-241 or Pu-241, due to greater mobility, long half-life, and conservative method of accounting for daughters. Therefore, MCL and allowable concentrations based solely on this daughter.

^e EDE not provided in Table 4.1-7 because groundwater concentration of parent is negligible.

Table I3-4. Groundwater-based disposal limits for the suspect soil trenches^a

Radionuclide	Compliance Point Groundwater Concentration (pCi/cc-CI)	Allowable Groundwater Concentration ^a	Suspect Soil Trench Inventory Limit (Ci)
H-3	1.8	20,000 pCi/L	1.1×10^1
C-14	3.2×10^{-1}	6,400 pCi/L	2.0×10^1
Al-26	$9.6 \times 10^{-6}^b$	420 pCi/L ^c	4.4×10^6
Ni-59	$1.9 \times 10^{-4}^b$	530 pCi/L	2.8×10^3
Ni-63	1.8×10^{-16}	80 pCi/L	4.4×10^{14}
Se-79	9.2×10^{-2}	660 pCi/L ^d	7.2
Rb-87	9.2×10^{-3}	270 pCi/L	2.9×10^1
Sr-90	2.6×10^{-5}	8 pCi/L	3.1×10^2
Zr-93	$3.3 \times 10^{-5}^b$	2,100 pCi/L	6.4×10^4
Tc-99	8.8×10^{-1}	800 pCi/L	9.1×10^{-1}
Pd-107	9.8×10^{-3}	36,600 pCi/L	3.7×10^3
Cd-113m	1.0×10^{-10}	40 pCi/L ^e	4.0×10^8
Sn-121m	3.4×10^{-11}	2,260 pCi/L ^e	6.6×10^{10}
Sn-126	4.3×10^{-3}	290 pCi/L ^e	7.4×10^1
I-129	7.6×10^{-1}	0.5 pCi/L	6.6×10^{-4}
Cs-135	$4.4 \times 10^{-4}^e$	800 pCi/L	1.8×10^3
Sm-151	7.7×10^{-12}	1,100 pCi/L	1.4×10^{11}
Ra-226	4.1×10^{-5}	5 pCi/L ^f	1.2×10^2
Th-229	$1.4 \times 10^{-10}^b$	8.6 pCi/L	6.1×10^7
Th-230 ^e Ra-226	$3.4 \times 10^{-10}^b$ $2.0 \times 10^{-6}^b$	15 pCi/L 5 pCi/L ^f	2.5×10^3
Th-232	$3.6 \times 10^{-10}^b$	7.1 pCi/L	2.0×10^7
Pa-231	$4.1 \times 10^{-5}^b$	2.3 pCi/L	5.6×10^1
U-232	2.1×10^{-6}	17 pCi/L	8.1×10^3
U-233 ^e Th-229	1.2×10^{-2} $8.8 \times 10^{-5}^b$	125 pCi/L 8.6 pCi/L	8.9

I-31
Table L3-4. (continued)

WSRC-RP-94-218

Radionuclide	Compliance Point Groundwater Concentration (pCi/cc-Ci)	Allowable Groundwater Concentration ^a	Suspect Soil Trench Inventory Limit (Ci)
U-234 ^e Th-230 Ra-226	1.4×10^{-2} $1.2 \times 10^{-5} \text{ }^b$ $3.8 \times 10^{-5} \text{ }^b$	132 pCi/L 15 pCi/L 5 pCi/L ^f	9.4
U-235 ^e Pa-231	1.4×10^{-2} $1.3 \times 10^{-4} \text{ }^b$	20 µg/L ^{ca} 23 pCi/L	3.1
U-236	1.4×10^{-2}	139 pCi/L	9.9
U-238	1.4×10^{-2}	20 µg/L ^{ca}	4.8×10^{-1}
Np-237	8.1×10^{-2}	8.9 pCi/L	1.1×10^{-1}
Pu-238 ^e U-234	8.1×10^{-9} 5.0×10^{-6}	8.9 pCi/L 132 pCi/L	2.6×10^4
Pu-239	4.2×10^{-3}	8.1 pCi/L	1.9
Pu-240	2.6×10^{-3}	8.1 pCi/L	3.1
Pu-241 ^e Am-241 Np-237	4.8×10^{-15} 6.7×10^{-16} 5.5×10^{-7}	--- --- 8.9 pCi/L	1.6×10^4
Pu-242	5.0×10^{-3}	8.3 pCi/L	1.7
Pu-244	5.1×10^{-3}	8.6 pCi/L	1.7
Am-241 ^e Np-237	2.0×10^{-14} 1.6×10^{-5}	7.6 pCi/L 8.9 pCi/L	5.6×10^2
Am-242m ^e U-234	8.3×10^{-19} 8.7×10^{-6}	1.27 pCi/L ^e 132 pCi/L	1.5×10^4
Am-243 ^e Pu-239	$6.7 \times 10^{-9} \text{ }^b$ $4.6 \times 10^{-4} \text{ }^b$	7.6 pCi/L 8.1 pCi/L	1.8×10^1
Cm-242 ^e Pu-238	--- ⁱ 4.1×10^{-11}	--- 8.9 pCi/L	2.2×10^8
Cm-243 ^e Pu-239	--- ⁱ 5.0×10^{-6}	--- 8.1 pCi/L	1.6×10^3
Cm-244 ^e Pu-240	--- ⁱ 7.2×10^{-6}	--- 8.1 pCi/L	1.1×10^3
Cm-245	$7.6 \times 10^{-9} \text{ }^b$	7.6 pCi/L	1.0×10^6

I-32
Table I3-4. (continued)

WSRC-RP-94-218

Radionuclide	Compliance Point Groundwater Concentration (pCi/cc-Ci)	Allowable Groundwater Concentration ^a	Suspect Soil Trench Inventory Limit (Ci)
Cm-246 [§] Pu-242	$3.9 \times 10^{-9} \text{ }^b$ $3.0 \times 10^{-5} \text{ }^b$	7.6 pCi/L 8.3 pCi/L	2.8×10^2
Cm-247 [§] Am-243 Pu-239	$1.9 \times 10^{-8} \text{ }^b$ $7.8 \times 10^{-9} \text{ }^b$ $1.6 \times 10^{-4} \text{ }^b$	8.3 pCi/L 7.6 pCi/L 8.1 pCi/L	5.1×10^1
Cm-248	$1.9 \times 10^{-8} \text{ }^b$	2.1 pCi/L	1.1×10^5
Bk-249 [§] Cf-249 Cm-245	— ⁱ 7.8×10^{-18} 7.8×10^{-13}	— 3.4 pCi/L 7.6 pCi/L	1.0×10^{10}
Cf-249 Cm-245	3.1×10^{-15} 3.1×10^{-10}	3.4 pCi/L 7.6 pCi/L	2.5×10^7
Cf-250 [§] Cm-246	— ⁱ $1.1 \times 10^{-11} \text{ }^b$	— 7.6 pCi/L	6.9×10^8
Cf-251 Cm-247 Am-243 Pu-239	7.2×10^{-12} $7.6 \times 10^{-13} \text{ }^b$ $4.1 \times 10^{-13} \text{ }^b$ $6.3 \times 10^{-9} \text{ }^b$	7.4 pCi/L 8.3 pCi/L 7.6 pCi/L 8.1 pCi/L	1.3×10^6
Cf-252 [§] Cm-248	— ⁱ $1.5 \times 10^{-13} \text{ }^b$	— 2.1 pCi/L	1.4×10^{11}

- ^a Limit on inventory in all five trenches; total volume of trenches is assumed to be $2.6 \times 10^4 \text{ m}^3$.
- ^b Selected from Table I3-3 as the lower of either the MCL or 25 mrem-per-year based allowable concentration.
- ^c Peak occurred after 10,000 year. Value given is the 10,000-year concentration.
- ^d Option 3, Table 3.2-1.
- ^e Not available in reference for Option 3. Calculated from CEDE in U.S.DOE 1988b to be 660 pCi/L.
- ^f Not available in reference for Option 3. Calculated from CEDE in U.S.DOE 1988b to be 40 pCi/L.
- ^g MCL is 5 pCi/L for Ra-226 *plus* Ra-228, but the inventory limit is calculated separately here.
- ^h Inventory limit reflects contribution of daughters listed.
- ⁱ Limit applies to total uranium.
- ^j Insignificant (less than $10^{-26} \text{ pCi/cc-Ci}$).

Table I3-5. Suspect soil disposal limits based on the air pathway*

Radionuclide	Flux from Soil (Ci m ⁻² yr ⁻¹) per Ci in trenches	Dose per unit radioactivity (mrem/year-Ci inventory)	Performance Objective (mrem/yr)	Inventory Limit (Ci)
H-3				
Off-site	4.8×10^{-6}	6.5×10^{-6}	10	1.5×10^6
Intruder	1.7×10^{-8}	4.1×10^{-4}	100	2.4×10^5
C-14				
Off-site	1.7×10^{-4}	1.2×10^{-2}	10	8.3×10^2
Intruder	1.7×10^{-4}	1.6	100	6.3×10^1
Rn-222				
Flux limit	23 pCi m ⁻² s ⁻¹	—	20 pCi m ⁻² s ⁻¹	44 (of U-234)

* Limit on inventory in all five trenches; total volume of trenches is assumed to be 2.6×10^4 m³.

Table I3-6. Results of dose analysis for intruder
agriculture scenario for suspect soil trenches

Radionuclide	SDCF ^b (rem/year per $\mu\text{Ci}/\text{m}^3$)	F ^c	Concentration Limit ^{a,d} ($\mu\text{Ci}/\text{m}^3$)	Inventory Limit ^{a,e} (Ci)
H-3	3.9×10^{-6}	1.5×10^{-12}	--	--
C-14	1.5×10^{-5}	6.9×10^{-2}	1.6×10^5	4.2×10^3
Al-26	3.9×10^{-3}	9.4×10^{-1}	4.5×10^1	1.2
Co-60	3.5×10^{-3}	2.0×10^{-6}	2.4×10^7	6.2×10^5
Ni-59	6.8×10^{-4}	8.8×10^{-1}	2.8×10^6	7.2×10^4
Ni-63	1.8×10^{-7}	4.5×10^{-1}	2.1×10^6	5.3×10^4
Sc-79	1.2×10^{-6}	2.1×10^{-1}	6.6×10^5	1.7×10^4
Rb-87	1.9×10^{-6}	6.8×10^{-1}	1.3×10^5	3.4×10^3
Sr-90	1.8×10^{-4}	4.4×10^{-2}	2.1×10^4	5.5×10^2
Zr-93	4.5×10^{-4}	9.1×10^{-1}	4.1×10^6	1.1×10^5
Nb-93m	1.9×10^{-4}	8.7×10^{-3}	1.0×10^9	2.6×10^7
Tc-99	1.1×10^{-5}	2.8×10^{-4}	5.4×10^7	--
Pd-107	3.2×10^{-4}	6.7×10^{-1}	7.8×10^6	2.0×10^5
Cd-113m	1.3×10^{-4}	6.3×10^{-3}	2.0×10^5	5.3×10^3
Sn-121m	4.7×10^{-7}	2.8×10^{-1}	1.3×10^6	3.3×10^4
Sn-126	2.6×10^{-3}	7.9×10^{-1}	8.1×10^1	2.1
I-129	8.3×10^{-5}	3.3×10^{-3}	6.1×10^5	---
Cs-135	1.2×10^{-6}	8.7×10^{-1}	1.6×10^5	4.2×10^3
Cs-137	7.7×10^{-4}	1.0×10^{-1}	2.2×10^3	5.6×10^1
Sm-151	1.0×10^{-4}	4.6×10^{-1}	3.6×10^7	9.4×10^5
Eu-154	1.7×10^{-3}	3.8×10^{-4}	2.6×10^5	6.7×10^3
Eu-155	4.0×10^{-5}	8.5×10^{-7}	4.9×10^9	1.3×10^8
Pb-210	3.0×10^{-4}	4.4×10^{-2}	1.3×10^4	3.3×10^2

Table L3-6. (continued)

Radionuclide	SDCF ^a (rem/year per $\mu\text{Ci}/\text{m}^3$)	F ^c	Concentration Limit ^{a,d} ($\mu\text{Ci}/\text{m}^3$)	Inventory Limit ^{a,e} (Ci)
Ra-226 ^a	1.2×10^{-1}	8.6×10^{-1}	1.6 ^a	4.2×10^{-2} ^a
Ra-226 ⁱ	2.7×10^{-3}	8.6×10^{-1}	7.2×10^1 ⁱ	1.9 ⁱ
Th-229	4.3×10^{-4}	9.5×10^{-1}	4.1×10^2	1.1×10^1
Th-230	1.1×10^{-5}	9.6×10^{-1}	1.6×10^4	4.1×10^2
Th-232 ^a	1.4×10^{-2}	9.6×10^{-1}	1.2×10^1 ^a	3.2×10^{-1} ^a
Th-232 ⁱ	3.6×10^{-3}	9.6×10^{-1}	4.8×10^1	1.3 ⁱ
Pa-231	8.3×10^{-4}	9.0×10^{-1}	2.2×10^2	5.8
U-232 ^a	1.2×10^{-2}	2.5×10^{-1}	5.6×10^1 ^a	1.4 ^a
U-232 ⁱ	2.3×10^{-3}	2.5×10^{-1}	2.9×10^2	7.5 ⁱ
U-233	1.1×10^{-5}	6.0×10^{-1}	2.5×10^4	6.6×10^2
U-234 ⁱ	1.1×10^{-5}	6.6×10^{-2}	5.1×10^3 ^a	1.3×10^2 ^a
Th-230	1.1×10^{-5}	9.4×10^{-4}	---	---
Ra-226 ^a	1.2×10^{-1}	2.6×10^{-4}	---	---
U-234 ⁱ	1.1×10^{-5}	6.0×10^{-1}	2.5×10^4 ⁱ	6.6×10^2 ⁱ
U-235	1.8×10^{-4}	6.0×10^{-1}	1.5×10^3	4.0×10^1
U-236	1.0×10^{-5}	6.0×10^{-1}	2.8×10^4	7.2×10^2
U-238	3.9×10^{-5}	6.0×10^{-1}	7.1×10^3	1.9×10^2
Np-237	5.0×10^{-4}	2.1×10^{-1}	1.6×10^2	4.1×10^1
Pu-238	3.4×10^{-5}	3.6×10^{-1}	1.4×10^4	3.5×10^2
Pu-239	4.0×10^{-5}	7.6×10^{-1}	5.5×10^3	1.4×10^2
Pu-240	4.0×10^{-5}	7.6×10^{-1}	5.5×10^3	1.4×10^2
Pu-241	7.7×10^{-7}	6.2×10^{-3}	1.1×10^{5a}	2.9×10^{3a}
Pu-242	3.8×10^{-5}	7.6×10^{-1}	5.8×10^3	1.5×10^2
Pu-244	3.7×10^{-5}	7.6×10^{-1}	5.9×10^3	1.5×10^2
Am-241	5.6×10^{-5}	8.1×10^{-1}	3.7×10^3	9.6×10^1

Table L3-6. (continued)

Radionuclide	SDCF ^b (rem/year per $\mu\text{Ci}/\text{m}^3$)	F ^c	Concentration Limit ^{a,d} ($\mu\text{Ci}/\text{m}^3$)	Inventory Limit ^{a,e} (Ci)
Am-242m	6.0×10^{-5}	6.2×10^{-1}	3.4×10^3 ^m	8.8×10^1 ^m
Am-243	2.5×10^{-4}	9.4×10^{-1}	7.1×10^2	1.8×10^1
Cm-243	1.6×10^{-4}	8.3×10^{-2}	1.3×10^4	3.3×10^2
Cm-244	2.0×10^{-5}	2.1×10^{-2}	4.0×10^5 ⁿ	--
Cm-245	1.1×10^{-4}	9.4×10^{-1}	1.6×10^3	4.2×10^1
Cm-246	4.0×10^{-5}	9.3×10^{-1}	4.5×10^3	1.2×10^2
Cm-247	4.4×10^{-4}	9.5×10^{-1}	4.0×10^2	1.0×10^1
Cm-248	1.4×10^{-4}	9.5×10^{-1}	1.3×10^3	3.3×10^1
Cf-249	4.6×10^{-4}	8.2×10^{-1}	4.4×10^2	1.1×10^1
Cf-250	1.7×10^{-5}	5.0×10^{-3}	8.2×10^6 ⁿ	--
Cf-251	1.6×10^{-4}	9.3×10^{-1}	1.1×10^3	2.9×10^1

- ^a Concentration and inventory limits are obtained from Eqs. (4.1-2) and (4.1-3). Limits are calculated for intrusion at 100 years after disposal, except as noted.
- ^b Values are obtained from Table 4.1-10.
- ^c Fraction of initial inventory of radionuclide remaining in disposal units at time scenario is assumed to occur.
- ^d Limit on average concentration in disposed waste.
- ^e Limit on inventory in all trenches; total volume of trenches is assumed to be $2.6 \times 10^4 \text{ m}^3$.
- ^f Value exceeds NRC's Class-C limit in 10 CFR Part 61 of $3 \times 10^6 \mu\text{Ci}/\text{m}^3$, which applies to individual waste packages at DOE sites (U.S.DOE 1988a).
- ^g Value exceeds NRC's Class-C limit in 10 CFR Part 61 of $8 \times 10^4 \mu\text{Ci}/\text{m}^3$, which applies to individual waste packages at DOE disposal sites (U.S.DOE 1988a).
- ^h Results include contribution to dose from radon decay product.
- ⁱ Results exclude contribution to dose from radon decay product.
- ^j Disposal limits are based on calculations at 1,600 years after disposal, taking into account buildup of long-lived decay products.
- ^k Disposal limits are based on buildup of Am-241 decay product.
- ^m Limit takes into account contribution to dose from ingrowth of Pu-238 decay product.
- ⁿ Limit for individual waste packages at DOE disposal sites is 100 nCi/g (about $2 \times 10^5 \mu\text{Ci}/\text{m}^3$) for all alpha-emitting transuranic radionuclides with half-lives greater than 5 years (U.S.DOE 1988a).

calculated using Eqs. 4.1-2 and 4.1-3. The SDCF for each radionuclide is obtained from Table 4.1-10, the geometrical reduction factor (G) for the suspect soil trenches of 0.6 is obtained from Table 4.1-13, and the fraction of the initial inventory of radionuclides remaining in the trenches at the time the agriculture scenario is assumed to occur, taking into account radioactive decay and mobilization and transport in water, was calculated using the PORFLOW computer code. For relatively mobile radionuclides (e.g., H-3 and Tc-99), the calculations indicate that the disposal limits are increased substantially when mobilization and transport in water is taken into account. Since the calculated concentration limit for H-3 exceeds the specific activity of this isotope, there are no limits for disposal based on a dose analysis for inadvertent intruders.

For Ra-226, Th-232, U-232, and U-234, two sets of concentration and inventory limits are calculated and listed in Table L3-6. The first set of results includes the contributions from radon decay products (i.e., Rn-222 for Ra-226 and U-234 and Rn-220 for Th-232 and U-232), but the second set of calculations excludes the contributions from radon. As described in Sects. 1.2.3 and 4.1.5.1, the two options for accounting for radon decay products are consistent with the present performance objective for protection of inadvertent intruders at DOE LLW disposal sites and a revision of the performance objective that is being considered at the present time.

For most radionuclides, the results in Table L3-6 are based on the SDCF for the radionuclide in disposed waste and depletion of the initial inventory of the radionuclide over 100 years due to radioactive decay and mobilization and transport in water, because the radionuclide concentrations, and thus the dose for the agriculture scenario, decrease monotonically with time after 100 years. However, there are a few exceptions to this case, which are described below.

For U-234, the calculations indicate that the maximum dose would occur at about 1,600 years after disposal, taking into account buildup of radiologically significant long-lived decay products, principally Ra-226 and its decay product Rn-222, as well as depletion of the initial inventory of the parent radionuclide due to mobilization and transport in water. However, for U-235, U-238, and Np-237, which also decay to radiologically significant long-lived decay

products, the maximum dose nonetheless is predicted to occur at 100 years after disposal and is due primarily to the parent radionuclide only, because depletion of the parent radionuclide due to mobilization and transport in water beyond 100 years more than compensates for any increase in dose due to buildup of the decay products. If the dose from Rn-222 is not included, the maximum dose for U-234 also occurs at 100 years.

The concentration and inventory limits for Am-242m take into account buildup of the Pu-238 decay product. Given the half-lives of 152 years for Am-242m, 87.75 years for Pu-238, and the assumed rate of depletion of Am-242m due to mobilization of water, the maximum dose in this case is predicted to occur at 100 years after disposal because the decrease in the inventory of Am-242m after 100 years more than compensates for the buildup of Pu-238. At this time, about 75% of the estimated dose is due to Am-242m with the remaining 25% due to Pu-238.

For Pu-241, Am-241, Cm-243, Cm-244, and Cf-250, the disposal limits are estimated taking into account buildup of the longer-lived decay products Am-241, Np-237, Pu-239, Pu-240, and Cm-246, respectively. For each of these radionuclides, the disposal limits are the more restrictive of the results obtained from two calculations. The first is a calculation for the parent radionuclide only at 100 years after disposal, taking into account radioactive decay and mobilization and transport in water. In the second calculation, the Bateman equations are used to estimate the maximum inventory of the decay product that would be produced in the decay of the parent radionuclide. This inventory is approximately equal to the initial unit inventory of the parent radionuclide times the ratio of the half-lives of the parent and decay product. This inventory of the decay product then is conservatively assumed to be produced at time $t = 0$, and the disposal limits for the decay product only are calculated for 100 years after disposal. This procedure is the same as that used by the NRC in calculating the concentration limits for Pu-241 and Cm-242 in 10 CFR Part 61.

If the procedure described above is applied to the radionuclides that produce longer-lived radiologically significant isotopes, only for Pu-241 are the disposal limits based on buildup of the decay product. In this case, the maximum inventory of the decay product Am-241 is about 30 times less than the initial inventory of the parent, but the dose per unit concentration of the decay product is nearly two orders of magnitude greater than the value for the

parent. For the other isotopes of concern, the parent radionuclide rather than the decay product determines the disposal limits for the parent radionuclide, because the maximum inventory of the decay product is at least two orders of magnitude less than the initial inventory of the parent but the dose per unit concentration of the decay product is within an order of magnitude of the value for the parent.

I.3.2 Interpretation of Results

The results presented in Sect. I.3.1 are summarized in Table I.3-7. The most restrictive pathway is identified, along with the corresponding inventory limit for each radionuclide. Actinium-227 and Ra-228 were removed from further consideration for intruders because the dose is accounted for in the analysis for the parent radionuclides Pa-231 and Th-232, respectively. Of the 56 radionuclides listed, none are potentially limited by the air pathway, 30 are limited by considerations of inadvertent intruders, and 26 are limited by the groundwater pathway.

These derived inventory limits are generally believed to be low-end estimates of the allowable inventory in the suspect soil trenches, as uncertainties encountered in data or models were generally addressed by choosing a conservative assumption. For example, for the groundwater pathway, no credit was taken for reduced infiltration by the engineered cover due to uncertainties in the long-term performance of this cover.

I.4 PERFORMANCE EVALUATION

I.4.1 Comparison to Performance Objectives

The results of the suspect soil analysis are presented in terms of disposal limits, in lieu of reliable estimates of the expected inventory in the trenches. Therefore, if the disposal limits listed in Table I.3-7 are not exceeded, and if the cumulative dose from all radionuclides is considered, this PA provides reasonable assurance that performance objectives will be met.

Table I3-7. Summary of disposal limits for the suspect soil trenches^a

Radionuclide	Limiting Pathway	Suspect Soil Trench Inventory Limit (Ci)
H-3	Groundwater	1.1×10^1
C-14	Groundwater	2.0×10^1
Al-26	Intruder	1.2
Co-60	Intruder	6.2×10^5
Ni-59	Groundwater	2.8×10^3
Ni-63	Intruder	5.3×10^4
Sc-79	Groundwater	7.2
Rb-87	Groundwater	2.9×10^1
Sr-90	Groundwater	3.1×10^2
Zr-93	Groundwater	6.4×10^4
Nb-93m	Intruder	2.6×10^7
Tc-99	Groundwater	9.1×10^{-1}
Pd-107	Groundwater	3.7×10^3
Cd-113m	Intruder	5.3×10^3
Sn-121m	Intruder	3.3×10^4
Sn-126	Intruder	2.1
I-129	Groundwater	6.6×10^{-4}
Cs-135	Groundwater	1.8×10^3
Cs-137	Intruder	5.6×10^1
Sm-151	Intruder	9.4×10^5
Eu-154	Intruder	6.7×10^3
Eu-155	Intruder	1.3×10^5
Pb-210	Intruder	3.3×10^2
Ra-226	Intruder	$4.2 \times 10^{-2}{}^b$ 1.9 ^c
Th-229	Intruder	1.1×10^1
Th-230	Intruder	4.1×10^2
Th-232	Intruder	$3.2 \times 10^{-1}{}^b$ 13 ^c
Pa-231	Intruder	5.8
U-232	Intruder	1.4 ^b 7.5 ^c

I-41
Table L3-7. (continued)

WSRC-RP-94-218

Radionuclide	Limiting Pathway	Suspect Soil Trench Inventory Limit (Ci)
U-233	Groundwater	8.9
U-234	Groundwater	9.4
U-235	Groundwater	3.1
U-236	Groundwater	9.9
U-238	Groundwater	4.8×10^1
Np-237	Groundwater	1.1×10^1
Pu-238	Intruder	3.5×10^2
Pu-239	Groundwater	1.9
Pu-240	Groundwater	3.1
Pu-241	Intruder	2.9×10^3
Pu-242	Groundwater	1.7
Pu-244	Groundwater	1.7
Am-241	Intruder	9.6×10^1
Am-242m	Intruder	8.8×10^1
Am-243	Intruder/Groundwater	1.8×10^1
Cm-242	Groundwater	2.2×10^8
Cm-243	Intruder	3.3×10^2
Cm-244	Groundwater	1.1×10^3
Cm-245	Intruder	5.1×10^1
Cm-246	Intruder	1.4×10^2
Cm-247	Intruder	1.2×10^1
Cm-248	Intruder	3.9×10^1
Bk-249	Groundwater	1.0×10^{10}
Cf-249	Intruder	1.1×10^1
Cf-250	Groundwater	6.9×10^8
Cf-251	Intruder	2.9×10^1
Cf-252	Groundwater	1.4×10^{11}

- * Limit on inventory in all five trenches; total volume of trenches is assumed to be $2.6 \times 10^4 \text{ m}^3$.
- ^b Considers contribution to dose from radon decay product.
- ^c Neglects contribution to dose from radon decay product.

L4.2 Design Changes Required to Meet Performance Objectives

Because a reliable estimate of the expected inventory of the suspect soil trenches does not presently exist, design changes for the suspect soil trenches are not indicated. In general, the inventory limits for these trenches are estimated to be one to two orders of magnitude lower than for vault-disposed waste.

L4.3 Data and Research Needs

The most important information that would improve the assessment of performance of the suspect soil trenches is an estimate of the expected inventory. Because there are no engineered barriers designed for the suspect soil trenches, and credit was not taken for the engineered cover, analysis of performance of these trenches is a fairly straight-forward procedure involving fewer uncertain parameters than for vault disposal. One critical assumption is, however, that water flow through the trenches is similar to that in the surrounding soil. During and after emplacement of soil in trenches, care must be taken to test the validity of that assumption. If the trenches are more hydraulically conductive than surrounding geologic materials, an increased flux of water and radionuclides over that predicted in this analysis may result.

L5 PORFLOW Input Files

```

TITLE SUSPECT SOIL; 40 cm/yr infiltration
/ PORFLOW-3D, Version 2.50
/ File to establish flow field in vadose zone for suspect soil trenches
/
/ L. M. McDowell-Boyer, last revised January 20, 1994
/
GRID 38 x 39
/
COORDinate X:
-500. 500. 1500. 3000. 4500. 6000. 7500. 9000.
9500. 9750. 10000. 10250. 10500. 11000. 12500. 14000.
15500. 17000. 18500. 20000. 21500. 23000. 24500. 26000.
27500. 29000. 29500. 29750. 30000. 30250. 30500. 31000.
32500. 34000. 35500. 38500. 39500. 40500.
/
COORDinate Y:
-100. 100. 200. 300. 400. 500. 600. 700.
800. 850. 875. 885. 895. 900. 905. 915.
925. 950. 1000. 1100. 1200. 1300. 1350. 1375.
1380. 1385. 1400. 1450. 1500. 1550. 1650. 1700.
1750. 1800. 1850. 1900. 1950. 1995. 2005.
/
MATERIAL type 1 is from (1,34) to (38,39) &Top Permeable layer
MATERIAL type 2 is from (1,1) to (38,33) $Backfill
MATERIAL type 3 is from (11,14) to (29,29) $Suspect Soil Trench
/
DATUm = 0. 0.
/
FOR 1: $ Top permeable layer to allow infiltration into domain
ROCK bulk density 2.65 gm/cc, neff=0.38, ntot=0.38, ndif=0.38
HYDRaulic prop. ss=1.e-3, Kx=1.6e7, Ky=1.6e7 cm per yr
MULTIphase flow: VAN Genuchten: n=3.70, alpha = 0.0819, Sr = 0.01
/
FOR 2: $Backfill
ROCK bulk density 1.60 gm/cc, neff=0.439, ntot=0.439, ndif=0.439
HYDRaulic prop. ss=1.e-3, Kx=333., Ky=333. cm per yr
/ Moisture characteristic curves entered in table format
MULTIphase flow: TABLE option, 79 sets
/ saturation potential in cm
0.22 378.3312
0.23 366.3198
0.24 354.5856
0.25 343.125
0.26 331.9344

```

Fig. I.5-1. PORFLOW input file - flow in the vadose zone.

0.27	321.0102
0.28	310.3488
0.29	299.9466
0.3	289.8
0.31	279.9054
0.32	270.2592
0.33	260.8578
0.34	251.6976
0.35	242.775
0.36	234.0864
0.37	225.6282
0.38	219.3968
0.39	209.3886
0.4	201.6
0.41	194.0274
0.42	186.6672
0.43	179.5158
0.44	172.5696
0.45	165.825
0.46	159.2784
0.47	152.9262
0.48	146.7648
0.49	140.7906
0.5	135.
0.51	129.3894
0.52	123.9552
0.53	118.6938
0.54	113.6016
0.55	108.675
0.56	103.9104
0.57	99.3042
0.58	94.8528
0.59	90.5526
0.6	86.4
0.61	82.3914
0.62	78.5232
0.63	74.7918
0.64	71.1936
0.65	67.725
0.66	63.3824
0.67	61.1622
0.68	58.0608
0.69	55.0746
0.7	52.2
0.71	49.4334
0.72	46.7712

Fig. I.5-1. (cont.).

Rev. 0

0.73	44.2098
0.74	41.7456
0.75	39.375
0.76	37.0944
0.77	34.9002
0.78	32.7888
0.79	30.7566
0.8	28.8
0.81	26.9154
0.82	25.0992
0.83	23.3478
0.84	21.6576
0.85	20.025
0.86	18.4464
0.87	16.9182
0.88	15.4368
0.89	13.9986
0.9	12.6
0.91	11.2374
0.92	9.9072
0.93	8.6058
0.94	7.3296
0.95	6.075
0.96	4.8384
0.97	3.6162
0.98	2.4048
0.99	1.2006
1.0	0.0000

MULTIphase flow: COND TABLE option, 79 sets
 / saturation relative conductivity

0.22	0.0000e+00
0.23	2.7016e-08
0.24	4.3226e-07
0.25	2.1883e-06
0.26	6.9161e-06
0.27	1.6885e-05
0.28	3.5013e-05
0.29	6.4864e-05
0.3	1.1066e-04
0.31	1.7725e-04
0.32	2.7016e-04
0.33	3.9552e-04
0.34	5.6020e-04
0.35	7.7160e-04
0.36	1.0378e-03
0.37	1.3677e-03

Fig. L5-1. (cont.).

Rev. 0

0.38	1.7705e-03
0.39	2.2564e-03
0.4	2.8360e-03
0.41	3.5208e-03
0.42	4.3226e-03
0.43	5.2541e-03
0.44	6.3287e-03
0.45	7.5602e-03
0.46	8.9633e-03
0.47	1.0553e-02
0.48	1.2346e-02
0.49	1.4357e-02
0.5	1.6606e-02
0.51	1.9108e-02
0.52	2.1883e-02
0.53	2.4950e-02
0.54	2.8328e-02
0.55	3.2039e-02
0.56	3.6102e-02
0.57	4.0541e-02
0.58	4.5377e-02
0.59	5.0632e-02
0.6	5.6322e-02
0.61	6.2500e-02
0.62	6.9161e-02
0.63	7.6341e-02
0.64	8.4066e-02
0.65	9.2362e-02
0.66	1.0126e-01
0.67	1.1078e-01
0.68	1.2096e-01
0.69	1.3183e-01
0.7	1.4341e-01
0.71	1.5574e-01
0.72	1.6885e-01
0.73	1.8277e-01
0.74	1.9753e-01
0.75	2.1317e-01
0.76	2.2972e-01
0.77	2.4721e-01
0.78	2.6569e-01
0.79	2.8518e-01
0.8	3.0573e-01
0.81	3.2736e-01
0.82	3.5013e-01
0.83	3.7406e-01

Fig. I.5-1. (cont.).

Rev. 0

0.84	3.9920e-01
0.85	4.2558e-01
0.86	4.5325e-01
0.87	4.8225e-01
0.88	5.1262e-01
0.89	5.4440e-01
0.9	5.7764e-01
0.91	6.1238e-01
0.92	6.4865e-01
0.93	6.8652e-01
0.94	7.2602e-01
0.95	7.6721e-01
0.96	8.1012e-01
0.97	8.5480e-01
0.98	9.0131e-01
0.99	9.4970e-01
1.0	1.0000e+00

/

FOR 3: \$Suspect Soil

ROCK bulk density 1.60 cm/cc, neff=0.439, ntot=0.439, ndif=0.439

HYDRAulic prop. ss=1.e-3, Kx=333., Ky=333. zone 2

/ Moisture characteristic curves entered in table format

MULTIphase flow: TABLE option, 79 sets

/ saturation potential in cm

0.22	378.3312
0.23	366.3198
0.24	354.5856
0.25	343.125
0.26	331.9344
0.27	321.0102
0.28	310.3488
0.29	299.9466
0.3	289.8
0.31	279.9054
0.32	270.2592
0.33	260.8578
0.34	251.6976
0.35	242.775
0.36	234.0864
0.37	225.6282
0.38	219.3968
0.39	209.3886
0.4	201.6
0.41	194.0274
0.42	186.6672
0.43	179.5158

Fig. I.5-1. (cont.).

0.44	172.5696
0.45	165.825
0.46	159.2784
0.47	152.9262
0.48	146.7648
0.49	140.7906
0.5	135.
0.51	129.3894
0.52	123.9552
0.53	118.6938
0.54	113.6016
0.55	108.675
0.56	103.9104
0.57	99.3042
0.58	94.8528
0.59	90.5526
0.6	86.4
0.61	82.3914
0.62	78.5232
0.63	74.7918
0.64	71.1936
0.65	67.725
0.66	63.3824
0.67	61.1622
0.68	58.0608
0.69	55.0746
0.7	52.2
0.71	49.4334
0.72	46.7712
0.73	44.2098
0.74	41.7456
0.75	39.375
0.76	37.0944
0.77	34.9002
0.78	32.7888
0.79	30.7566
0.8	28.8
0.81	26.9154
0.82	25.0992
0.83	23.3478
0.84	21.6576
0.85	20.025
0.86	18.4464
0.87	16.9182
0.88	15.4368
0.89	13.9986

Fig. I.5-1. (cont.).

Rev. 0

0.9	12.6
0.91	11.2374
0.92	9.9072
0.93	8.6058
0.94	7.3296
0.95	6.075
0.96	4.8384
0.97	3.6162
0.98	2.4048
0.99	1.2006
1.0	0.0000
MULTIphase flow: COND TABLE option, 79 sets	
/ saturation relative conductivity	
0.22	0.0000e+00
0.23	2.7016e-08
0.24	4.3226e-07
0.25	2.1883e-06
0.26	6.9161e-06
0.27	1.6885e-05
0.28	3.5013e-05
0.29	6.4864e-05
0.3	1.1066e-04
0.31	1.7725e-04
0.32	2.7016e-04
0.33	3.9552e-04
0.34	5.6020e-04
0.35	7.7160e-04
0.36	1.0378e-03
0.37	1.3677e-03
0.38	1.7705e-03
0.39	2.2564e-03
0.4	2.8360e-03
0.41	3.5208e-03
0.42	4.3226e-03
0.43	5.2541e-03
0.44	6.3287e-03
0.45	7.5602e-03
0.46	8.9633e-03
0.47	1.0553e-02
0.48	1.2346e-02
0.49	1.4357e-02
0.5	1.6606e-02
0.51	1.9108e-02
0.52	2.1883e-02
0.53	2.4950e-02
0.54	2.8328e-02

Fig. I.5-1. (cont.).

Rev. 0

0.55	3.2039e-02
0.56	3.6102e-02
0.57	4.0541e-02
0.58	4.5377e-02
0.59	5.0632e-02
0.6	5.6322e-02
0.61	6.2500e-02
0.62	6.9161e-02
0.63	7.6341e-02
0.64	8.4066e-02
0.65	9.2362e-02
0.66	1.0126e-01
0.67	1.1078e-01
0.68	1.2096e-01
0.69	1.3183e-01
0.7	1.4341e-01
0.71	1.5574e-01
0.72	1.6885e-01
0.73	1.8277e-01
0.74	1.9753e-01
0.75	2.1317e-01
0.76	2.2972e-01
0.77	2.4721e-01
0.78	2.6569e-01
0.79	2.8518e-01
0.8	3.0573e-01
0.81	3.2736e-01
0.82	3.5013e-01
0.83	3.7406e-01
0.84	3.9920e-01
0.85	4.2558e-01
0.86	4.5325e-01
0.87	4.8225e-01
0.88	5.1262e-01
0.89	5.4440e-01
0.9	5.7764e-01
0.91	6.1238e-01
0.92	6.4865e-01
0.93	6.8652e-01
0.94	7.2602e-01
0.95	7.6721e-01
0.96	8.1012e-01
0.97	8.5480e-01
0.98	9.0131e-01
0.99	9.4970e-01
1.0	1.0000e+00

Fig. I.5-1. (cont.).

Rev. 0

```
/
/ Boundary Conditions for flow simulations
/
SET S = 0.7
BOUN P -1 FLUX= 0.0
BOUN P +1 FLUX= 0.0
BOUN P -2 NODE= 0.0
BOUN P +2 FLUX= -40.0
/
PROPERty for P is HARM mean
MATRIx for P in 3 sweeps using ADI
CONVERgence for P; GLOBal 1.0e-2 max 1 iterations
CONVERgence for FLOW REFE GLOB 1.0e-2 max 3 iterations
/
DIAGnostic node for P and V at (21,28) every 20 steps
OUTPut every 10000 steps
/
FLUX BALANCE for P in 'fluxp2.out' every 200 steps
/
/ Simulate steady state flow field
/
SOLVe P AUTO 50 1. 1.1 max 1 min 1.e-10 2.0 100000
SAVE U, V, P, S NOW in 'flow40.bkg'
/
END
```

Fig. I.5-1. (cont.).

```

TITLE SUSPECT SOIL; 40 cm/yr infiltration
/ PORFLOW-3D, Version 2.50 File 'u234d40.dat'
/ File to simulate mass transport out of suspect soil trenches
/ U-234 plus daughters
/
/ L. M. McDowell-Boyer, March 8, 1994
/
GRID 38 x 39
/
COORDinate X:
-500. 500. 1500. 3000. 4500. 6000. 7500. 9000.
9500. 9750. 10000. 10250. 10500. 11000. 12500. 14000.
15500. 17000. 18500. 20000. 21500. 23000. 24500. 26000.
27500. 29000. 29500. 29750. 30000. 30250. 30500. 31000.
32500. 34000. 35500. 38500. 39500. 40500.
/
COORDinate Y:
-100. 100. 200. 300. 400. 500. 600. 700.
800. 850. 875. 885. 895. 900. 905. 915.
925. 950. 1000. 1100. 1200. 1300. 1350. 1375.
1380. 1385. 1400. 1450. 1500. 1550. 1650. 1700.
1750. 1800. 1850. 1900. 1950. 1995. 2005.
/
/ read in flow field for 40 cm/yr infiltration
/
READ 'flow40.bkg'
/
MATERial type 1 is from (1,34) to (38,39) &Top Permeable layer
MATERial type 2 is from (1,1) to (38,33) $Backfill
MATERial type 3 is from (11,14) to (29,29) $Suspect Soil Trench
MATERial type 10 from (1,38) to (38,39) $No diffusion out top of domain
/
DATUM = 0. 0.
/
LOCAte MATERial type 1 in subregion ID=BKFL
LOCAte MATERial type 2 in subregion ID=BKFL
LOCAte subregion (11,14) to (29,29) with ID=SUSPect soil
LOCAte subregion (1,1) to (38,39) with ID=DOMAin
/
/Specification for mass species C; U-234
/
FOR 1:
TRANsport properties for C Kd = 35., md = 158., Ld = 300., Td= 30.
ROCK density = 2.65; porosity = .30, .40, .30 $entire domain
FOR 2:
TRANsport properties for C Kd = 35., md = 158., Ld = 300., Td= 30.
ROCK density = 2.65; porosity = .30, .40, .30 $entire domain

```

Fig. I.5-2. Example PORFLOW input file - mass transport in vadose zone.

```

FOR 3:
TRANsport properties for C Kd = 35., md = 158., Ld = 300., Td= 30.
ROCK density = 2.65; porosity = .30, .40, .30  Sentic domain
FOR 10:
TRANsport properties for C Kd = 35., md = 0., Ld = 0., Td= 0.
ROCK density = 2.65; porosity = .30, .40, .30  Sentic domain
/
DECAY half life of C is 2.45e5 years, branching ratio is 1.0
/
/Specification for mass species C2; Th-230
/
FOR 1:
TRANsport properties for C2 Kd = 3200., md = 158., Ld = 300., Td= 30.
ROCK density = 2.65; porosity = .30, .40, .30  Sentic domain
FOR 2:
TRANsport properties for C2 Kd = 3200., md = 158., Ld = 300., Td= 30.
ROCK density = 2.65; porosity = .30, .40, .30  Sentic domain
FOR 3:
TRANsport properties for C2 Kd = 3200., md = 158., Ld = 300., Td= 30.
ROCK density = 2.65; porosity = .30, .40, .30  Sentic domain
FOR 10:
TRANsport properties for C2 Kd = 3200., md = 0., Ld = 0., Td= 0.
ROCK density = 2.65; porosity = .30, .40, .30  Sentic domain
/
DECAY half life of C2 is 7.7e4 years, branching ratio is 1.0
/
/Specification for mass species C3; Ra-226
/
FOR 1:
TRANsport properties for C3 Kd = 500., md = 158., Ld = 300., Td= 30.
ROCK density = 2.65; porosity = .30, .40, .30  Sentic domain
FOR 2:
TRANsport properties for C3 Kd = 500., md = 158., Ld = 300., Td= 30.
ROCK density = 2.65; porosity = .30, .40, .30  Sentic domain
FOR 3:
TRANsport properties for C3 Kd = 500., md = 158., Ld = 300., Td= 30.
ROCK density = 2.65; porosity = .30, .40, .30  Sentic domain
FOR 10:
TRANsport properties for C3 Kd = 500., md = 0., Ld = 0., Td= 0.
ROCK density = 2.65; porosity = .30, .40, .30  Sentic domain
/
DECAY half life of C3 is 1.6e3 years
/
/ Initial and boundary conditions
/
SET C = 0.0 for ID=BKFL
SET C = 1.0 for ID=SUSP
BOUNDary C at -1 FLUX =0.0
BOUNDary C at +1 FLUX =0.0
BOUNDary C at -2 GRAD =0.0
BOUNDary C at +2 FLUX =0.0

```

Fig. I.5-2. (cont.).

Rev. 0

```

/
SET C2 = 0.0 for ID=BKFL
SET C2 = 0.0 for ID=SUSP
BOUNDary C2 at -1 FLUX =0.0
BOUNDary C2 at +1 FLUX =0.0
BOUNDary C2 at -2 GRAD =0.0
BOUNDary C2 at +2 FLUX =0.0
/
SET C3 = 0.0 for ID=BKFL
SET C3 = 0.0 for ID=SUSP
BOUNDary C3 at -1 FLUX =0.0
BOUNDary C3 at +1 FLUX =0.0
BOUNDary C3 at -2 GRAD =0.0
BOUNDary C3 at +2 FLUX =0.0
/
/   Specify flux output
/
FLUX for C ID=DOMA in 'flux.out' every 2 step
FLUX for C ID=SUSP in 'flux.out' every 2 step
FLUX for C2 ID=DOMA in every 2 step
FLUX for C2 ID=SUSP in every 2 step
FLUX for C3 ID=DOMA in every 2 step
FLUX for C3 ID=SUSP in every 2 step
/
/   Specify solution criteria
/
MATRIX in X and Y directions for C, C2, and C3 in 1 sweep using ADI
CONVergence for C REFE LOCAL 1.e-2, max iterations = 3
PROPERty for C, C2, C3 is HARM mean
/
/   Specify output
/
DIAGnostic U, C at (20,20) every 20 steps   Scenter of suspect soil
HISTory for C, C2, C3 TABLE at (20,20) (20,2) (20,30) frequency=5
OUTPUT C, C2, C3 every 1000 steps
TIME = 0.0
/
/   Simulate mass transport with 40 cm/yr infiltration
/
DISAbLe FLOW
SOLVe C, C2, C3 AUTO 10000 10. 1.01 max 10. min 1.e-10 2.0 100000
SAVE C, C2, C3 NOW in 'eu234d40.arc' $10000 years
/
END

```

Fig. I.5-2. (cont.).

Rev. 0

```

TITLE CONTAMINANT TRANSPORT FOR E-AREA
/ File u234dgw.dat March 17, 1994
/ PORFLOW version 2.50
/
/ Contaminant transport modeling for Suspect Soil - saturated zone
/ U-234 plus Th-230 and Ra-226 daughters
/
GRID 38 by 30 by 28
Units are in cm's
COORDinate X -10000, 0, 45000, 90000, 135000, 145000, 155000,
165000, 175000, 185000, 195000, 205000, 215000, 225000,
235000, 245000, 250000, 257500, 265000, 272500, 280000,
287500, 295000, 302500, 310000, 317500, 325000, 332500,
340000, 347500, 355000, 362500, 370000, 380000, 390000,
427500, 465000, 475000,
/
COORDinate Y -7500, 0, 7500, 15000, 22500, 30000, 37500,
45000, 52500, 60000, 67500, 75000, 82500, 90000,
97500, 105000, 115000, 125000, 135000, 145000, 155000,
165000, 175000, 185000, 195000, 215000, 242500, 292500,
342500, 352500,
/
COORDinate Z 610, 732, 2073, 3414, 3536, 3658, 3780,
3901, 4023, 4785, 5547, 5669, 5791, 5913,
6035, 6157, 6370, 6553, 6751, 6949, 7148,
7346, 7544, 7742, 7940, 8138, 8336, 8534,
/
/
READ 'eflow40.arc' $40 cm/yr through vault regions
/
/ Identify a no-diffusion zone at top of domain to allow mass conservation
MATERial type 10 from (1,1,21) to (38,30,28)
/
FOR 1:
ROCK density = 2.65; porosity = .30, .40, .30
TRANsport properties for C Kd = 35., md = 158., Ld = 300., Td = 30.
TRANsport properties for C2 Kd = 3000., md = 158., Ld = 300., Td = 30.
TRANsport properties for C3 Kd = 500., md = 158., Ld = 300., Td = 30.
FOR 2:
ROCK density = 2.65; porosity = .30, .40, .30
TRANsport properties for C Kd = 1600., md = 158., Ld = 300., Td = 30.
TRANsport properties for C2 Kd = 5800., md = 158., Ld = 300., Td = 30.
TRANsport properties for C3 Kd = 9100., md = 158., Ld = 300., Td = 30.
FOR 3:
ROCK density = 2.65; porosity = .30, .40, .30
TRANsport properties for C Kd = 35., md = 158., Ld = 300., Td = 30.
TRANsport properties for C2 Kd = 3000., md = 158., Ld = 300., Td = 30.
TRANsport properties for C3 Kd = 500., md = 158., Ld = 300., Td = 30.

```

Fig. I.5-3. Example PORFLOW input file - mass transport in groundwater.

FOR 4:
 ROCK density = 2.65; porosity = .30, .40, .30
 TRANsport properties for C Kd = 1600., md = 158., Ld = 300., Td= 30.
 TRANsport properties for C2 Kd = 5800., md = 158., Ld = 300., Td= 30.
 TRANsport properties for C3 Kd = 9100., md = 158., Ld = 300., Td= 30.
 FOR 5:
 ROCK density = 2.65; porosity = .30, .40, .30
 TRANsport properties for C Kd = 35., md = 158., Ld = 300., Td= 30.
 TRANsport properties for C2 Kd = 3000., md = 158., Ld = 300., Td= 30.
 TRANsport properties for C3 Kd = 500., md = 158., Ld = 300., Td= 30.
 FOR 8:
 ROCK density = 2.65; porosity = .30, .40, .30
 TRANsport properties for C Kd = 35., md = 158., Ld = 300., Td= 30.
 TRANsport properties for C2 Kd = 3000., md = 158., Ld = 300., Td= 30.
 TRANsport properties for C3 Kd = 500., md = 158., Ld = 300., Td= 30.
 FOR 10:
 ROCK density = 2.65; porosity = .30, .40, .30
 TRANsport properties for C Kd = 35., md = 158., Ld = 300., Td= 30.
 TRANsport properties for C2 Kd = 3000., md = 158., Ld = 300., Td= 30.
 TRANsport properties for C3 Kd = 500., md = 158., Ld = 300., Td= 30.
 /
 /Specification for mass species C; U-234
 /
 DECAy half life of C is 2.45e5 years, branching ratio is 1.0
 INITIAL C = 0.0 everywhere
 BOUNDary C at -1 FLUX =0.0
 BOUNDary C at +1 FLUX =0.0
 BOUNDary C at -2 FLUX =0.0
 BOUNDary C at +2 FLUX =0.0
 BOUNDary C at -3 FLUX =0.0
 BOUNDary C at +3 FLUX =0.0
 /
 /Specifications for mass species C2; Th-230
 /
 DECAy half-life of C2 is 7.7e4 years, branching ratio is 1.0
 INITIAL C2 = 0.0 everywhere
 BOUNDary C2 at -1 FLUX =0.0
 BOUNDary C2 at +1 FLUX =0.0
 BOUNDary C2 at -2 FLUX =0.0
 BOUNDary C2 at +2 FLUX =0.0
 BOUNDary C2 at -3 FLUX =0.0
 BOUNDary C2 at +3 FLUX =0.0
 /
 /Specifications for mass species C3; Ra-226
 /
 DECAy half-life of C3 is 1.6e3 years
 INITIAL C3 = 0.0 everywhere

Fig. I.5-3. (cont.).

```

BOUNDary C3 at -1 FLUX =0.0
BOUNDary C3 at +1 FLUX =0.0
BOUNDary C3 at -2 FLUX =0.0
BOUNDary C3 at +2 FLUX =0.0
BOUNDary C3 at -3 FLUX =0.0
BOUNDary C3 at +3 FLUX =0.0
/
DISABle FLOW
DIAGNostic U, C at (28,12,20)  Sunder Suspect soil trenches
/MATERial type 6 from (17,14,20) to (17,14,20)
/MATERial type 6 from (19,13,20) to (19,15,20)
/LOCAt material type 6 as ID=ILNT
/MATERial type 7 is LAW vaults
/MATERial type 7 from (21,14,20) to (23,14,20)
/MATERial type 7 from (21,12,20) to (27,13,20)
/MATERial type 7 from (27,9,20) to (27,9,20)
/MATERial type 7 from (28,7,20) to (28,10,20)
/MATERial type 7 from (29,6,20) to (29,9,20)
/MATERial type 7 from (30,4,20) to (30,8,20)
/MATERial type 7 from (31,3,20) to (31,6,20)
/LOCAt material type 7 as subregion ID=LAWV
/
/MATERial type 8 is Suspect Soil Trenches
/MATERial type 9 is Naval Reactor Components
MATERial type 8 from (28,12,20) to (28,13,20)
LOCAt material type 8 as subregion ID=SUS
/
*** U-234 parent ***
SOURCe C for ID=SUS per VOLUME TABLE 31 sets      Smole per yr per mole U-234
1.8750E+01      3.5650E-19
5.3750E+01      1.0155E-17
9.0000E+01      1.1504E-16
1.2625E+02      5.2530E-16
1.6250E+02      1.4269E-15
1.9875E+02      2.8602E-15
2.3500E+02      4.7421E-15
2.7125E+02      6.9266E-15
3.0625E+02      9.1811E-15
3.4564E+02      1.1739E-14
3.9312E+02      1.4679E-14
4.5151E+02      1.7891E-14
5.2491E+02      2.1118E-14
6.1410E+02      2.3827E-14
7.0743E+02      2.5406E-14
8.1689E+02      2.6016E-14
1.0143E+03      2.4939E-14
1.3069E+03      2.1094E-14
1.7991E+03      1.4069E-14
2.4277E+03      7.6597E-15
3.0749E+03      3.9274E-15

```

Fig. I.5-3. (cont.).

3.7409E+03	1.9402E-15
4.4177E+03	9.3957E-16
5.1193E+03	4.4166E-16
5.8069E+03	2.1051E-16
6.4973E+03	9.9937E-17
7.1878E+03	4.7443E-17
7.8964E+03	2.2080E-17
8.5869E+03	1.0484E-17
9.2842E+03	4.9396E-18
9.9999E+03	2.2818E-18
*** Th-230 daughter ***	
SOURCE C2 for ID=SUS per VOLUME TABLE 31 sets \$mole per yr per mole U-234	
1.8750E+01	1.1206E-25
6.1250E+01	6.9486E-24
1.0500E+02	1.3894E-22
1.4875E+02	9.2337E-22
1.9250E+02	3.3150E-21
2.3625E+02	8.3331E-21
2.8000E+02	1.6747E-20
3.2438E+02	2.9161E-20
3.7737E+02	4.9208E-20
4.4485E+02	8.2429E-20
5.3359E+02	1.3702E-19
6.4220E+02	2.1557E-19
7.6302E+02	3.1129E-19
9.2271E+02	4.4097E-19
1.1444E+03	6.1212E-19
1.4811E+03	8.3246E-19
2.0031E+03	1.0729E-18
2.5786E+03	1.2283E-18
3.1790E+03	1.3138E-18
3.7938E+03	1.3571E-18
4.4177E+03	1.3751E-18
5.0293E+03	1.3815E-18
5.5706E+03	1.3804E-18
6.1157E+03	1.3773E-18
6.6790E+03	1.3720E-18
7.2241E+03	1.3667E-18
7.7692E+03	1.3604E-18
8.3325E+03	1.3540E-18
8.8805E+03	1.3477E-18
9.4310E+03	1.3403E-18
9.9999E+03	1.3340E-18
*** Ra-226 daughter ***	
SOURCE C3 for ID=SUS per VOLUME TABLE 31 sets \$mole per year per mole U-234	
1.8750E+01	6.9302E-29
7.0000E+01	1.0438E-26
1.2125E+02	3.5701E-25
1.7250E+02	3.3822E-24
2.2375E+02	1.5822E-23
2.7500E+02	4.9185E-23

Fig. I.5-3. (cont.).

3.2848E+02	1.2226E-22
3.9312E+02	2.8787E-22
4.7976E+02	6.9109E-22
5.9848E+02	1.6720E-21
7.3258E+02	3.4647E-21
9.1221E+02	7.0469E-21
1.1835E+03	1.4775E-20
1.6314E+03	3.1796E-20
2.2786E+03	6.0067E-20
2.9712E+03	8.8795E-20
3.6880E+03	1.1357E-19
4.4177E+03	1.3291E-19
5.1732E+03	1.4760E-19
5.9159E+03	1.5763E-19
6.6608E+03	1.6448E-19
7.4058E+03	1.6891E-19
8.1508E+03	1.7165E-19
8.8988E+03	1.7311E-19
9.6512E+03	1.7374E-19
9.7063E+03	1.7373E-19
9.7614E+03	1.7373E-19
9.8164E+03	1.7373E-19
9.8715E+03	1.7373E-19
9.9265E+03	1.7373E-19
9.9999E+03	1.7373E-19

HISTory for C, C2, C3 TABLE at (28,12,20)(28,15,20)(28,15,18)

(28,15,17)(28,15,16)(28,15,10)(26,13,16)

(30,13,18)(30,13,16)(30,13,10) frequency=3 on 'utr.hst'

OUTPUT C, C2, C3

CONVergence for C REFE 1.e-3, max iterations = 3

DIAGnostic U, C at (28,12,20) Sunder Suspect soil trenches

SOLVE C, C2, C3 AUTO 1.e3,DT=1.,fac=2.,mx=10,mn=1.e-8,df=2,nx=100000

SAVE C, C2, C3 NOW in 'utr.arc' \$1000 yr

SOLVE C, C2, C3 AUTO 1.e3,DT=10.,fac=2.,mx=100,mn=1.e-8,df=2,nx=100000

SAVE C, C2, C3 NOW in 'utr.arc' \$2000 yr

SOLVE C, C2, C3 AUTO 2.e3,DT=50.,fac=2.,mx=100,mn=1.e-8,df=2,nx=100000

SAVE C, C2, C3 NOW in 'utr.arc' \$4000 yr

SOLVE C, C2, C3 AUTO 2.e3,DT=50.,fac=2.,mx=100,mn=1.e-8,df=2,nx=100000

SAVE C, C2, C3 NOW in 'utr.arc' \$6000 yr

SOLVE C, C2, C3 AUTO 2.e3,DT=50.,fac=2.,mx=100,mn=1.e-8,df=2,nx=100000

SAVE C, C2, C3 NOW in 'utr.arc' \$8000 yr

SOLVE C, C2, C3 AUTO 2.e3,DT=100.,fac=2.,mx=100,mn=1.e-8,df=2,nx=100000

SAVE C, C2, C3 NOW in 'utr.arc' \$10000 yr

SOLVE C, C2, C3 AUTO 4.e4,DT=100.,fac=2.,mx=1000,mn=1.e-8,df=2,nx=100000

SAVE C, C2, C3 NOW in 'utr.arc' \$50000 yr

END

Fig. I.5-3. (cont.).

Rev. 0

APPENDIX I

REFERENCES

- ACRL. 1993. *PORFLOW, A Model for Fluid Flow, Heat and Mass Transport in Multifluid, Multiphase Fractures or Porous Media, Version 2.50*. Draft User's Manual. Analytic & Computational Research, Inc., Bel Air, California.
- Baes, C. F., III, and R. D. Sharp. 1983. A proposal for estimation of soil leaching and leaching constants for use in assessment models. *Journal of Environmental Qual.*, 12:17.
- Cook, J. R. 1991. *Technical Basis for Non-Vault Disposal of Suspect Soil (U)*. WSRC-RP-91-58. Westinghouse Savannah River Company, Savannah River Site, Aiken, S.C.
- CRC Press, Inc. 1981. *CRC Handbook of Chemistry and Physics*. Robert C. Weast and Melvin J. Astle, eds. Boca Raton, FL.
- Freeze, R. A., and J. A. Cherry. 1979. *Groundwater*. Prentice-Hall, Inc., New Jersey.
- Gruber, P. 1980. *A Hydrologic Study of the Unsaturated Zone Adjacent to a Radioactive-Waste Disposal Site at the Savannah River Plant, Aiken, South Carolina*. M. S. Thesis, University of Georgia, Athens, Georgia.
- Hoeffner, S. L. 1985. *Radionuclide Sorption on Savannah River Plant Burial Ground Soil: A Summary and Interpretation of Laboratory Data*. DP-1702. E. I. du Pont de Nemours and Company, Savannah River Laboratory, Aiken, SC.
- McIntyre, P. F. 1988. *Sorption Properties of Carbon-14 on Savannah River Plant Soil*. DPST-88-900, E. I. du Pont de Nemours and Company, Savannah River Laboratory, Aiken, SC.
- NRC. 1989. *Quality Assurance Program Requirements for Nuclear Facilities*. ASME NQA-1-1989 edition. The American Society of Mechanical Engineers.
- Oblath, S. R. 1982. *Migration of TcO₄ in SRP Soil*. DPST-82-815. E. I. duPont de Nemours and Company, Savannah River Laboratory, Aiken, SC.
- Sheppard, M. L., and Thibault, D. H. 1990. Default Soil Solid/Liquid Partition Coefficients, K_d s, for Four Major Soil Types: A Compendium. *Health Physics*, 59:471-482.

Ticknor, K. V., and Ruegger, B. 1989. *A Guide to the NEA's Sorption Data Base.*

Version 2.0. Nuclear Energy Agency, Paris, France.

U.S.DOE. 1988a. *Radioactive Waste Management, Order 5820.2A.* U. S. Department of Energy, Washington, D.C.

U.S.DOE. 1988b. *Internal Dose Conversion Factors for Calculation of Dose to the Public.*

DOE/EH-0071. U. S. Department of Energy, Washington, D.C.

APPENDIX J

SENSITIVITY/UNCERTAINTY ANALYSIS

Rev. 0

J.1 INTRODUCTION

The sensitivity and uncertainty of the PORFLOW simulations of the ILNT vault system were evaluated in terms of the movement of ^{99}Tc from the vault area through the vadose zone and in groundwater. The movement of contaminated water through the system is principally governed by: 1) infiltration; 2) hydraulic properties of the waste form, vaults, and soil; 3) depth to the water table; and 4) retention of contaminants by various materials in the waste, vaults and soil. Sensitivity and uncertainty of PORFLOW simulations of vault-contained low-level radioactive waste were evaluated in the Z-Area Radiological Performance Assessment (WSRC 1992) with respect to variable infiltration rates and hydraulic and diffusive properties of the waste form, vaults, and soil. The results indicated a low sensitivity to infiltration rate, due to the flux-controlling nature of the low-conductivity concrete materials, and a high sensitivity to hydraulic conductivity. This study focusses on the sensitivity and uncertainty in model results with respect to the parameter representing retention of contaminants in the waste form, concrete, and soil, which is the solid/liquid partition coefficient, or K_d .

Since a radionuclide will move through each of the three media (i.e., waste form, concrete vault, and soil) differently according to its K_d in each material, three K_d s, and appropriate probability distributions, were specified for ^{99}Tc . In addition to the K_d s, the time to cracking and time to collapse of the vaults roof were specified. The time-to-roof collapse was the sum of the time-to-roof cracking and the time between roof cracking and roof collapse, both of which were varied.

The K_d and time parameters together resulted in five factors being specified for the PORFLOW simulations in this analysis. Since there is considerable uncertainty associated with these five factors, they are considered to be random variables and distributions were specified for each factor. Based on the available literature, the K_d s are assumed to be observations from log-normal distributions. The bounds of the K_d distributions were estimated from available literature. The times associated with roof cracking and time between cracking and roof collapse are assumed to be distributed uniformly. The bounds of the time-

to-failure distributions were estimated by assuming the baseline values in Appendix K are approximately the midpoint of the ranges, and by considering the sensitivity data provided in Table 10 of that appendix.

The distributions and their limits for the five factors were entered into a Latin Hypercube Sample (LHS) generation program (Iman and Shortencarier 1984), which creates a sample based on the principles of LHS Theory. Table J.1-1 provides the factor information needed for the sample generation routine.

Table J.1-1. Factor specification for Latin Hypercube Sample generation

Factor	Distribution	Lower Limit	Upper Limit
K_d ⁹⁹ Tc waste form	log normal	1.0	6.2
K_d ⁹⁹ Tc concrete	log normal	70	7000
K_d ⁹⁹ Tc soil	log normal	0.01	0.4
Time to roof cracking	uniform	150 years	950 years
Time between roof cracking and collapse	uniform	175 years	775 years

J.2 PRELIMINARY SAMPLE

Initially a data file containing the necessary information for a pre-sample of ten LHS runs was set up and electronically transferred to the PORFLOW program. These runs were given in terms of five parameters, three K_d s and the two vault failure times. The general purpose of these initial ten runs was the identification of sampling and analysis problems.

These results were analyzed using linear regression analysis. An examination of the data indicated the possibility of several linear trends in terms of log responses versus the logs of the K_d or the log response versus the time factors. So the data analysis was directed towards the log-transform of the response data.

The data vector consisted of three responses; the maximum groundwater concentration of ^{99}Tc observed, the number of years after vault disposal that the maximum occurred, and the location of the sampling point where the maximum was observed.

Since the analysis of the initial ten runs did not raise the possibility of any real data problems, the study proceeded with the 100 runs.

J.3 SENSITIVITY ANALYSIS

The analysis of the full 100 runs involved the consideration of a full five factor multiple regression model with all interaction terms and quadratic effects. The form of this multiple regression model was the following:

Multiple Regression Model

$$\begin{aligned} \text{Log(Response)} = & A_0 + A_1 \cdot X_1 + A_2 \cdot X_2 + A_3 \cdot X_3 + A_4 \cdot X_4 + A_5 \cdot X_5 + A_{12} \cdot X_1 \cdot X_2 \\ & + A_{13} \cdot X_1 \cdot X_3 + A_{14} \cdot X_1 \cdot X_4 + A_{15} \cdot X_1 \cdot X_5 + A_{23} \cdot X_2 \cdot X_3 + A_{24} \cdot X_2 \cdot X_4 + A_{25} \cdot X_2 \cdot X_5 \\ & + A_{34} \cdot X_3 \cdot X_4 + A_{35} \cdot X_3 \cdot X_5 + A_{45} \cdot X_4 \cdot X_5 + A_{11} \cdot X_1 \cdot X_1 + A_{22} \cdot X_2 \cdot X_2 + A_{33} \cdot X_3 \cdot X_3 \\ & + A_{44} \cdot X_4 \cdot X_4 + A_{55} \cdot X_5 \cdot X_5 + \text{error.} \end{aligned}$$

The definitions of these factors are given in Table J.3-1. An inspection of the data showed that 85 of the 100 ^{99}Tc results occurred at the same node within the simulation domain. Thus, the location of the response was not included as a variable in the analysis.

Table J3-1. Variable definitions for multiple regression model

Variable	Definition
X1	Log(K_d Waste Form)
X2	Log(K_d Concrete)
X3	Log(K_d Soil)
X4	Time to Roof Cracking
X5	Time Between Roof Cracking and Roof Collapse

The selection of the important factors combinations was done in terms of the amount of variation that a group of factors would explain. These groups of factor combinations were selected by the use of a statistical procedure called step-wise regression. This procedure selects factor combinations in groups of one, two, three, etc., that explain the largest portion of the existing variation in the data. The intent was to obtain the smallest set of factor combinations that would explain the most variation. The set of factors combinations was allowed to increase only if the additional factor combination showed a real increase in the amount of variation explained by the linear model.

For example, for the log(max GW ^{99}Tc) response, the linear model involving only the term $X2^*X2$ explains about 96% of the total variation in the data; the addition of any other factor combinations did not make any real increase in the amount of variation explained by the model. Thus one can say that the peak groundwater concentration of ^{99}Tc is most sensitive to $X2$, or the K_d in concrete, of the parameters considered.

The factors combinations that have the most influence on the log responses are given in Table J3-2.

Table J3-2. Important variable combinations

Response	Important Variable Combinations	Percent of Variation Explained by Important Variables
Max GW ^{99}Tc	$X2^*X2$	96%
Years to Max GW ^{99}Tc	$X4 \ X2^*X2$	96%

J.4 UNCERTAINTY ANALYSIS

The amount of variability present in the simulated response data has been illustrated in two ways. The widths of the 95% confidence intervals for the means of the response distributions, Table J.4-1, and the width of the tolerance intervals for the response distributions. The tolerance intervals were computed in terms of 95% coverage of the response distributions, with 95% confidence, as shown in Table J.4-2. In both cases the intervals were based on the entire sample of 100 simulations. While the limits for the means are relatively tight, the limits for distributions are rather broad.

Table J.4-1. Confidence intervals for mean

Response	95% Confidence Limits	
	Lower	Upper
Max GW ^{99}Tc	0.035	0.046
Years to Max GW ^{99}Tc	1897	2254

Table J.4-2. Tolerance limits on response distribution

Response	95% Confidence that 95% of Distribution Covered by Interval	
	Lower Limit	Upper Limit
Max GW ^{99}Tc	0.008	0.192
Years to Max GW ^{99}Tc	783	5460

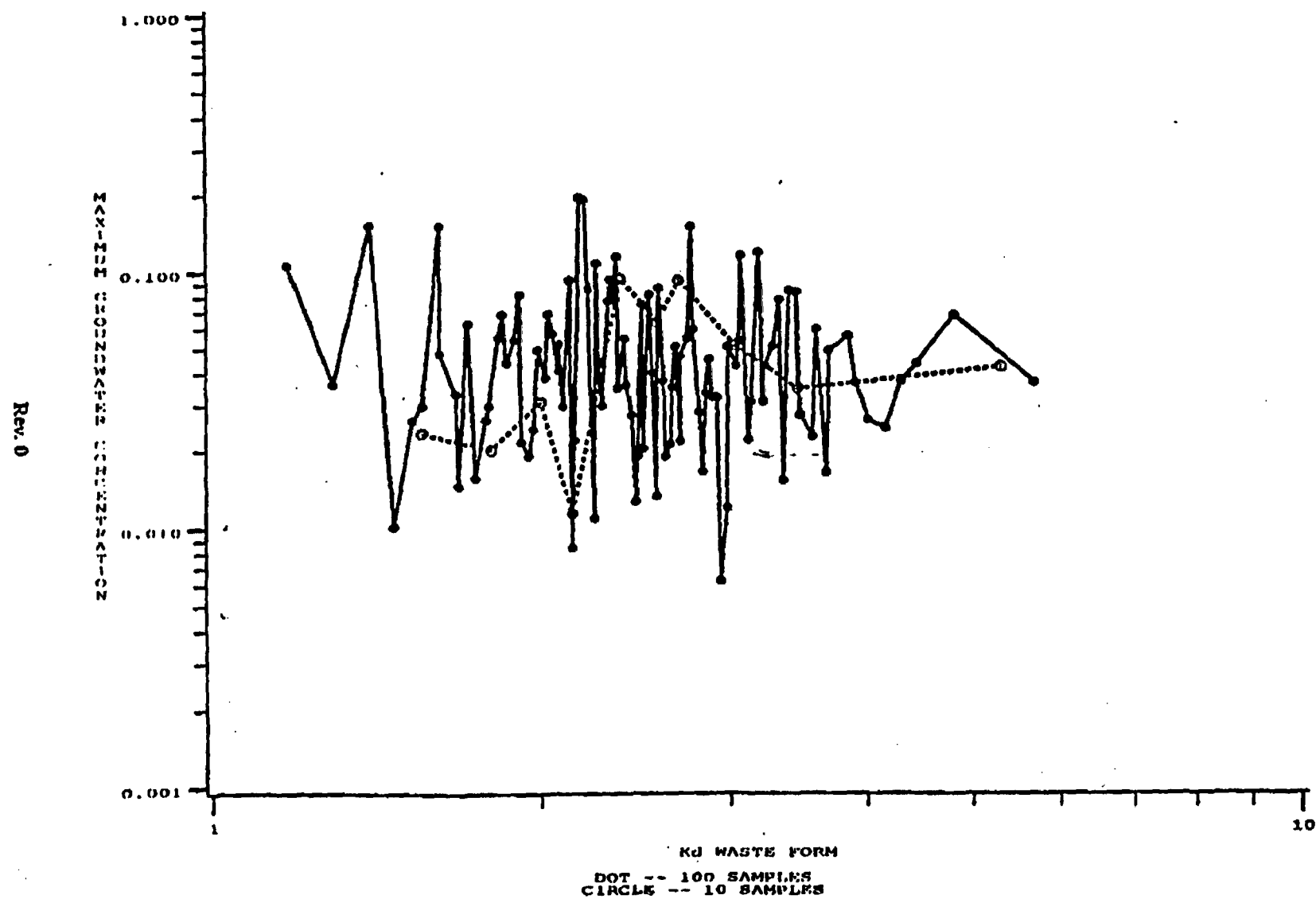
The plots of the response against the simulation variables, which are given in Sect. J.7, indicate that the variation in the ^{99}Tc groundwater results was dominated by the magnitude of the concrete K_g (X2) values. The dominance for the maximum groundwater concentration is total, while the time to occurrence of the maximum is also influenced by a small positive trend associated with the time to cracking of the roof (X4). The variation present in the ^{99}Tc concentrations are also illustrated by the estimated cumulative distribution functions (plus 95% confidence limits) of the concentrations (Sect. J.6).

J.5 SUMMARY

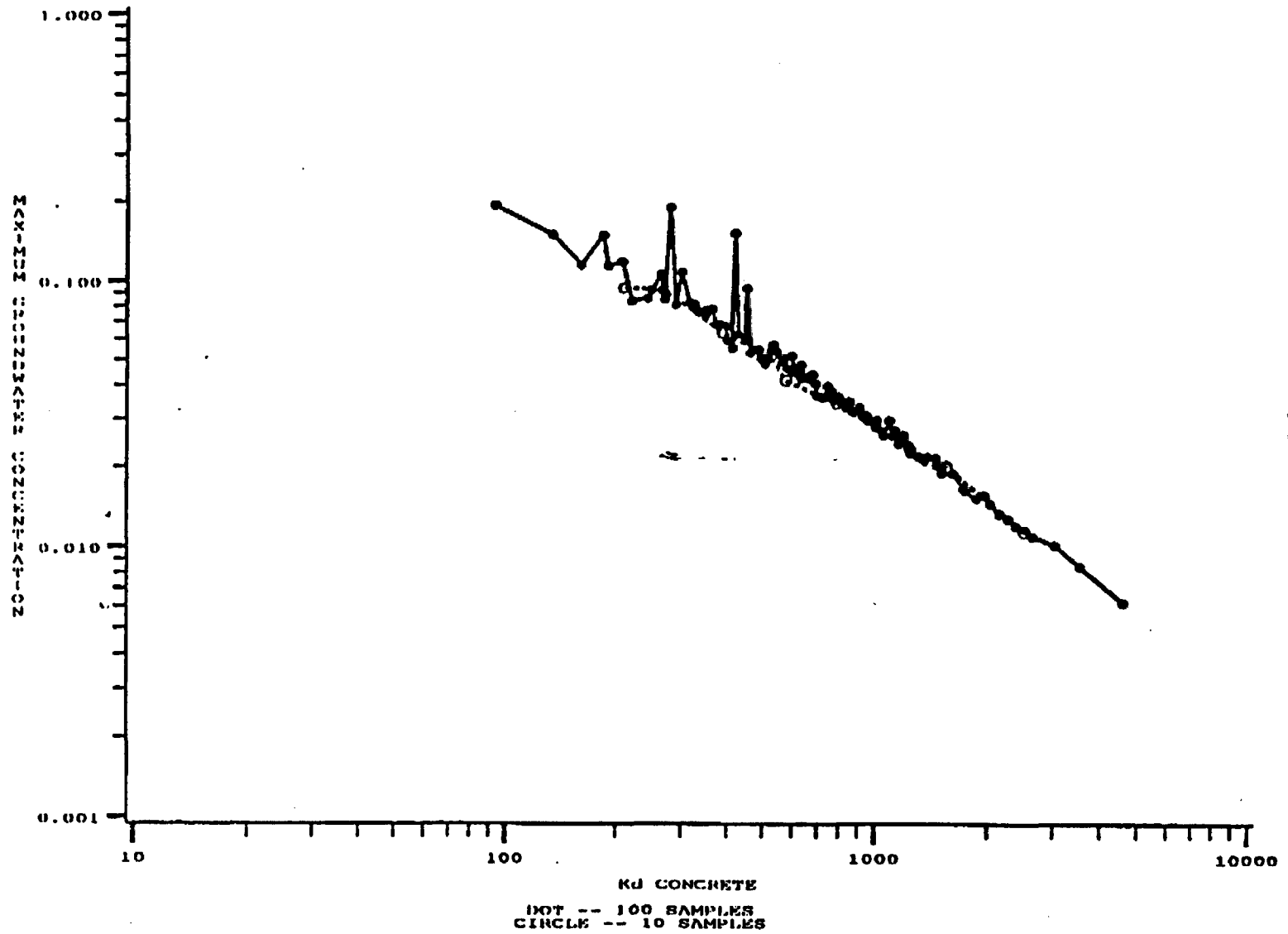
In general one can say that the ^{99}Tc responses are dominated by the concrete K_d , with some additional influence of the time-to-roof cracking. The K_d s for waste form and soil, along with the time between roof cracking and collapse do not seem to have any real effect on these responses.

J.6 RESPONSE PLOTS AND CUMULATIVE PROBABILITY DISTRIBUTION

MAXIMUM GROUNDWATER CONCENTRATION TC99



MAXIMUM GROUNDWATER CONCENTRATION TC99

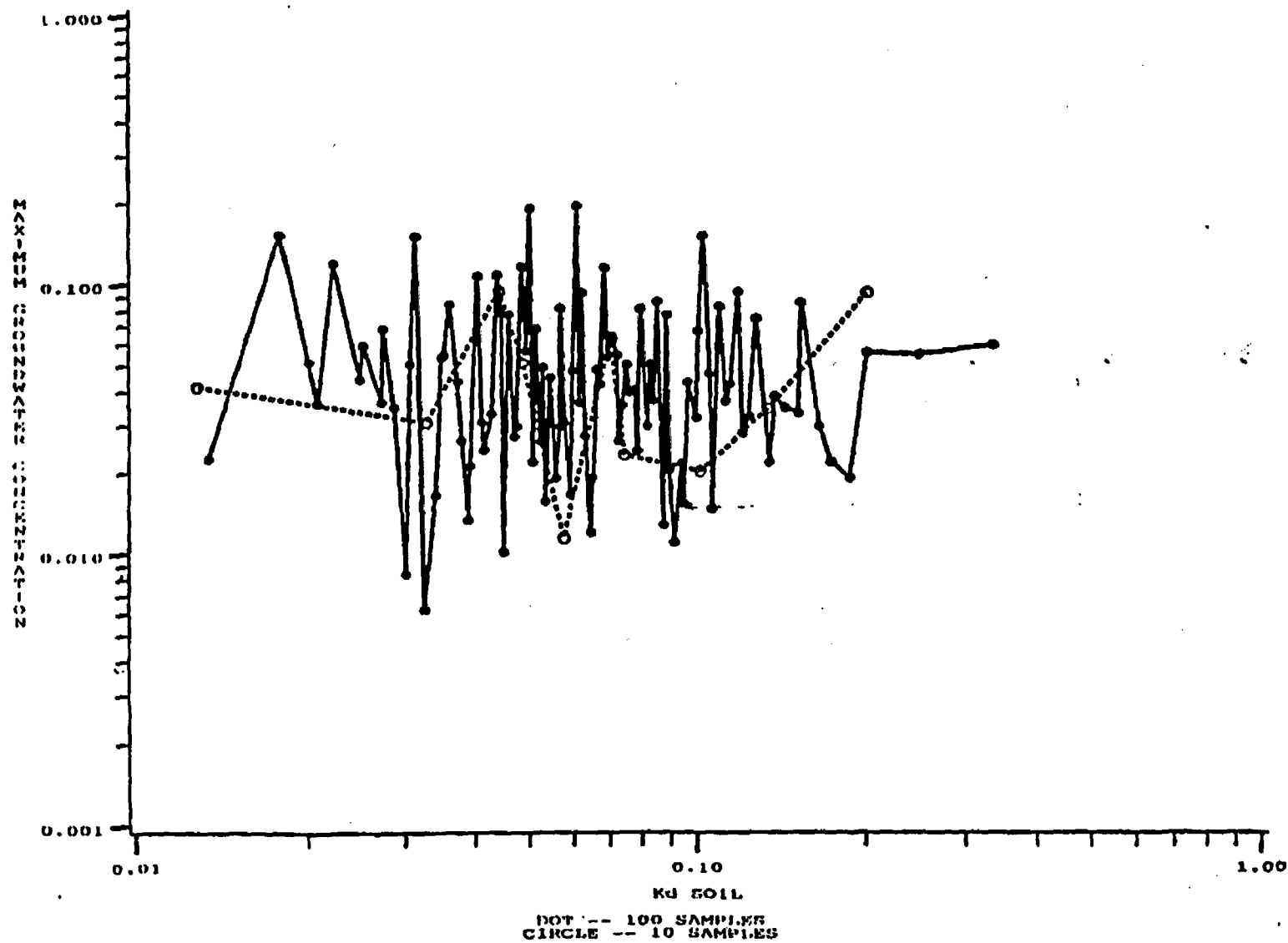


Rev. 0

J-8

WSRC-RP-94-218

MAXIMUM GROUNDWATER CONCENTRATION TC99

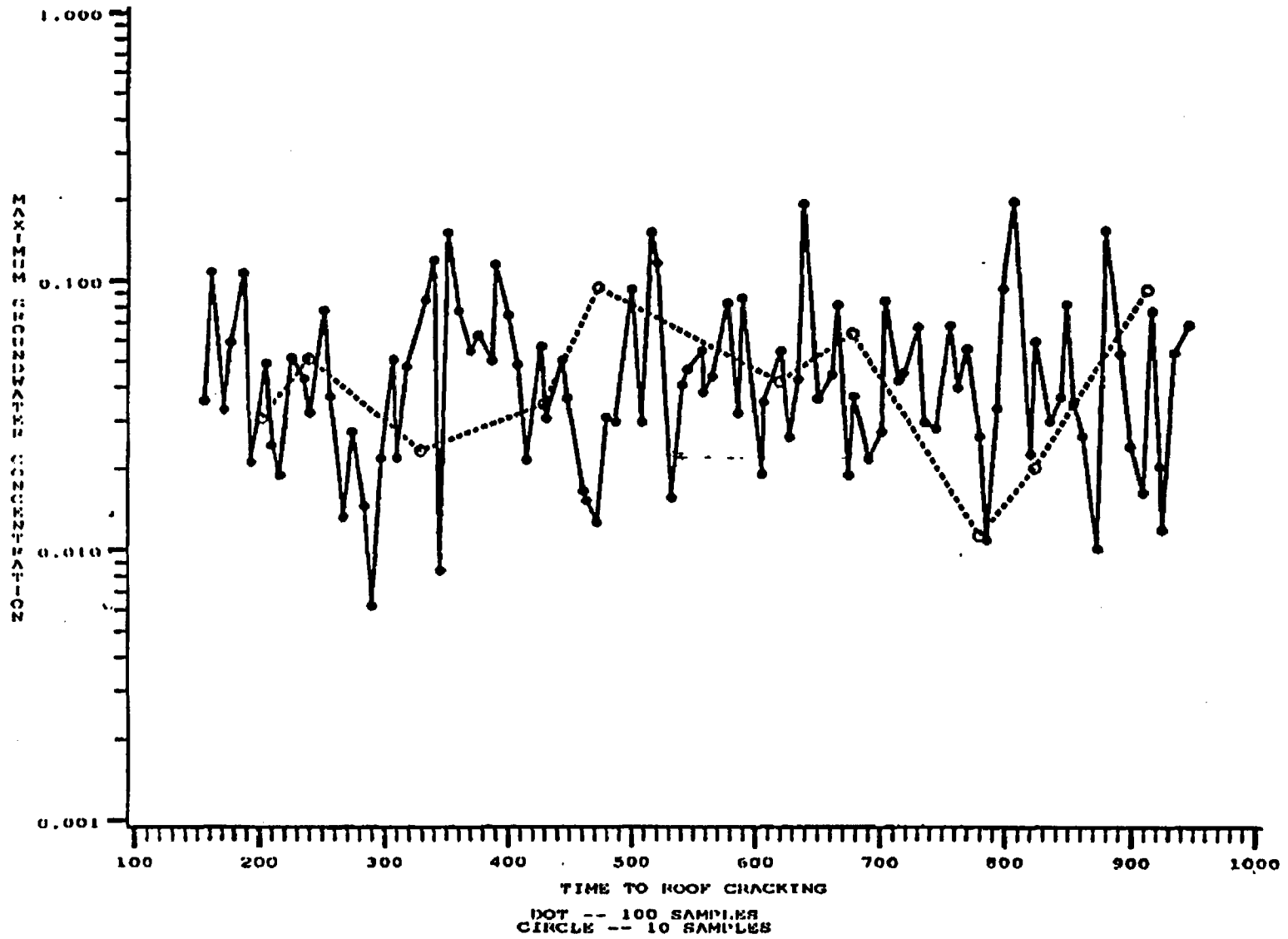


Rev. 0

J-9

WSRC-RF-94-218

MAXIMUM GROUNDWATER CONCENTRATION TC99

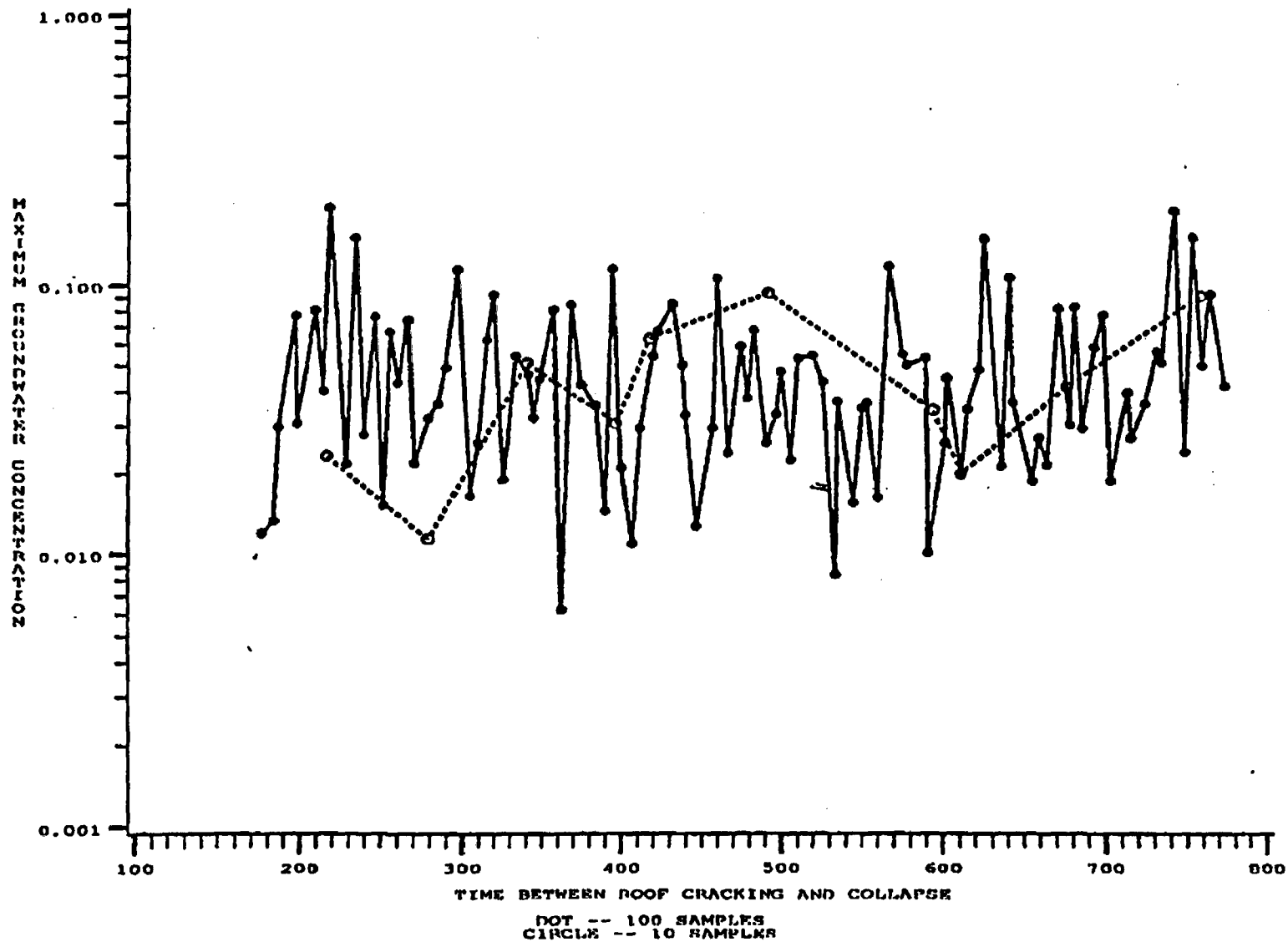


Rev. 0

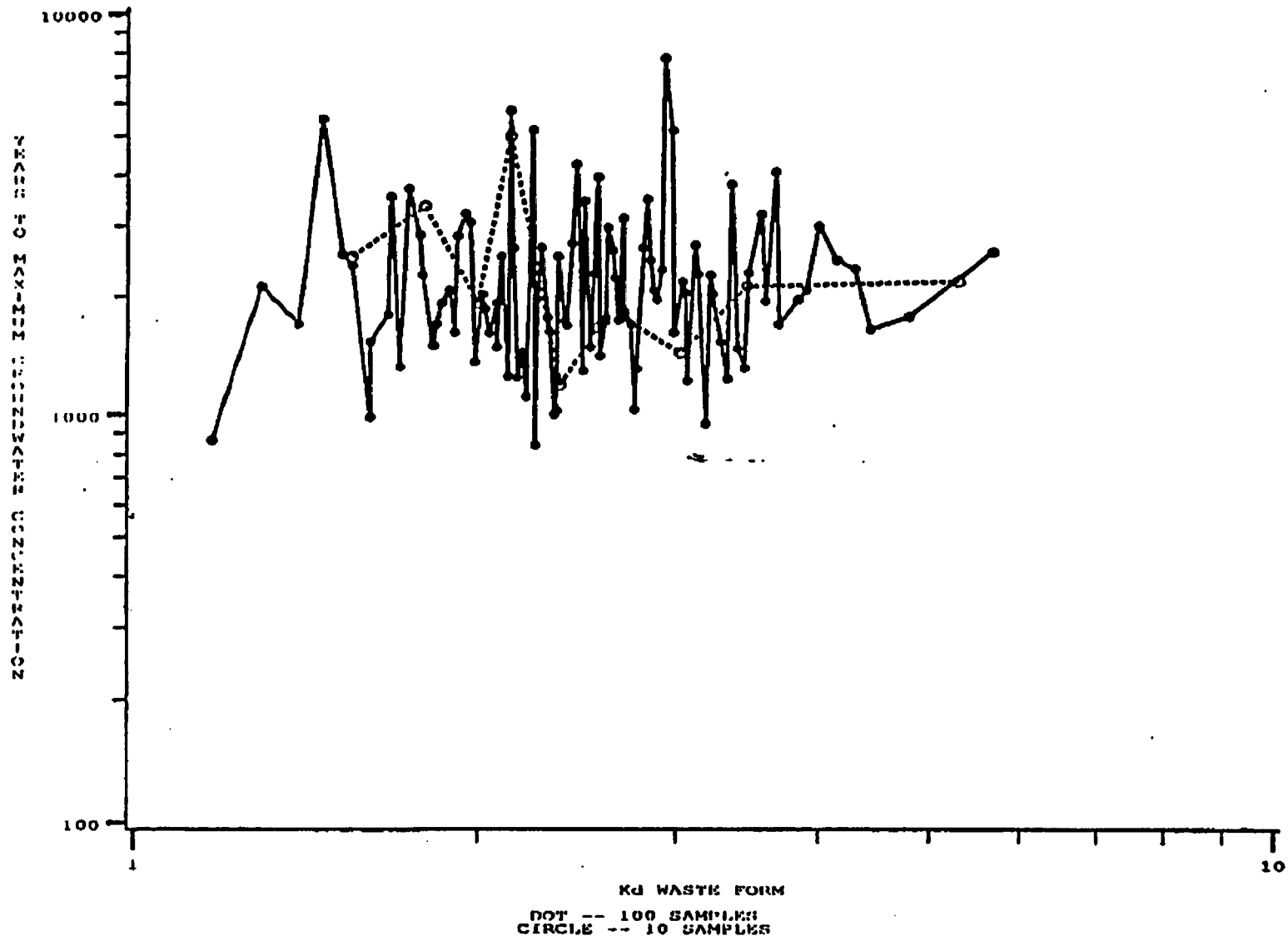
J10

WSRC-RP-94-218

MAXIMUM GROUNDWATER CONCENTRATION TC99



YEARS TO OCCURRENCE OF MAXIMUM TC99

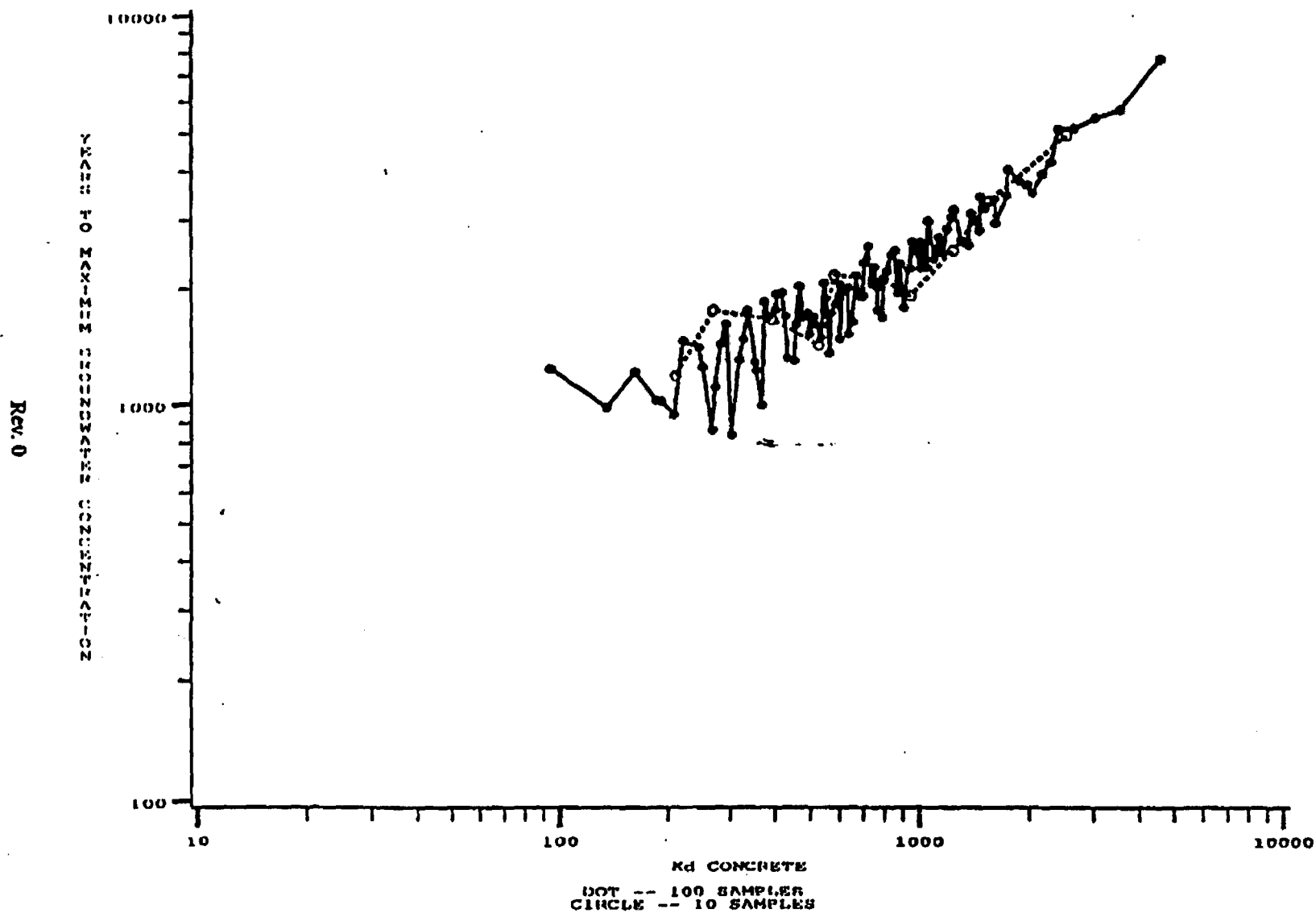


Rev. 0

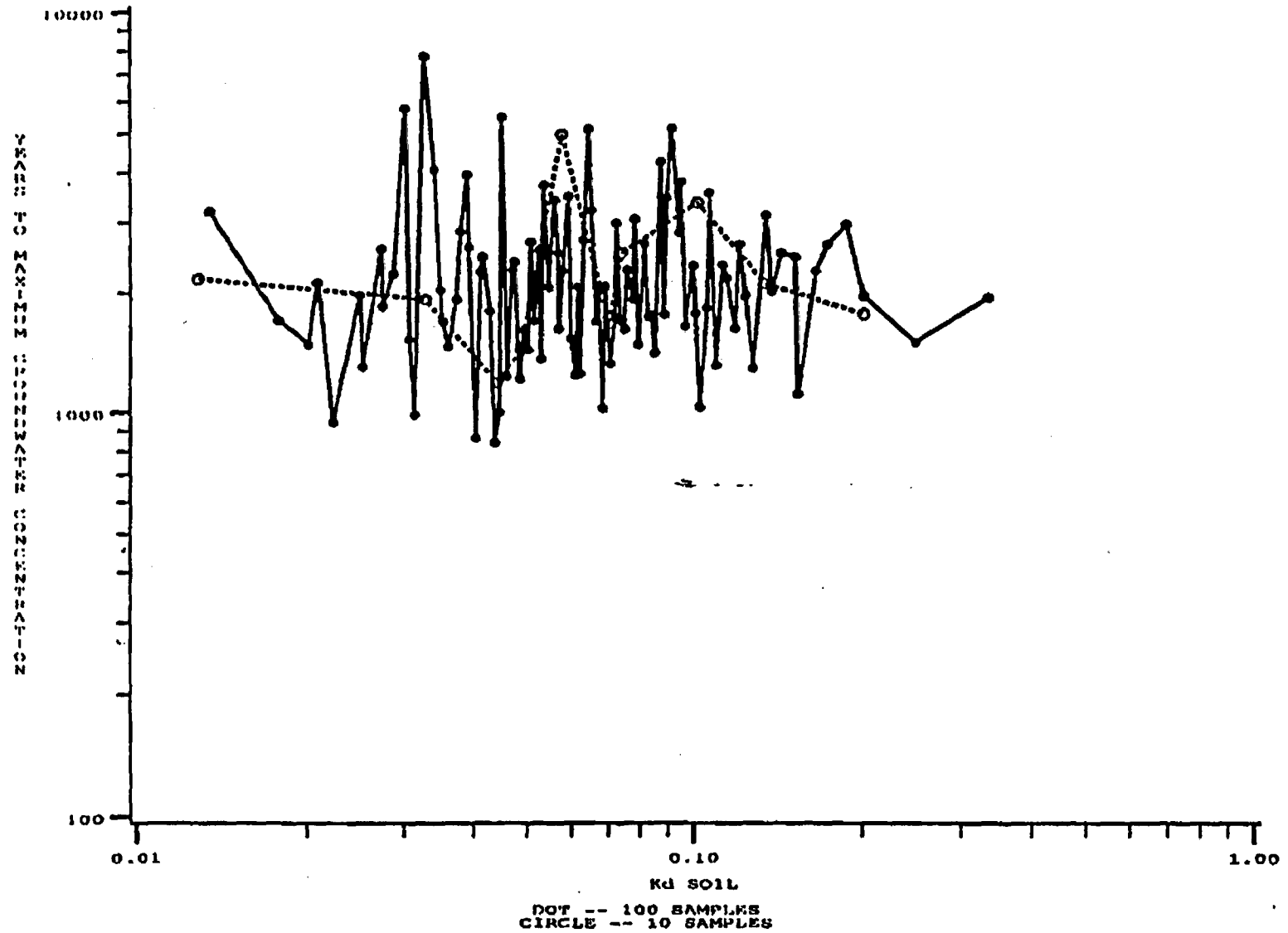
J-12

WSRC-RP-94-218

YEARS TO OCCURRENCE OF MAXIMUM TC99



YEARS TO OCCURRENCE OF MAXIMUM TC99

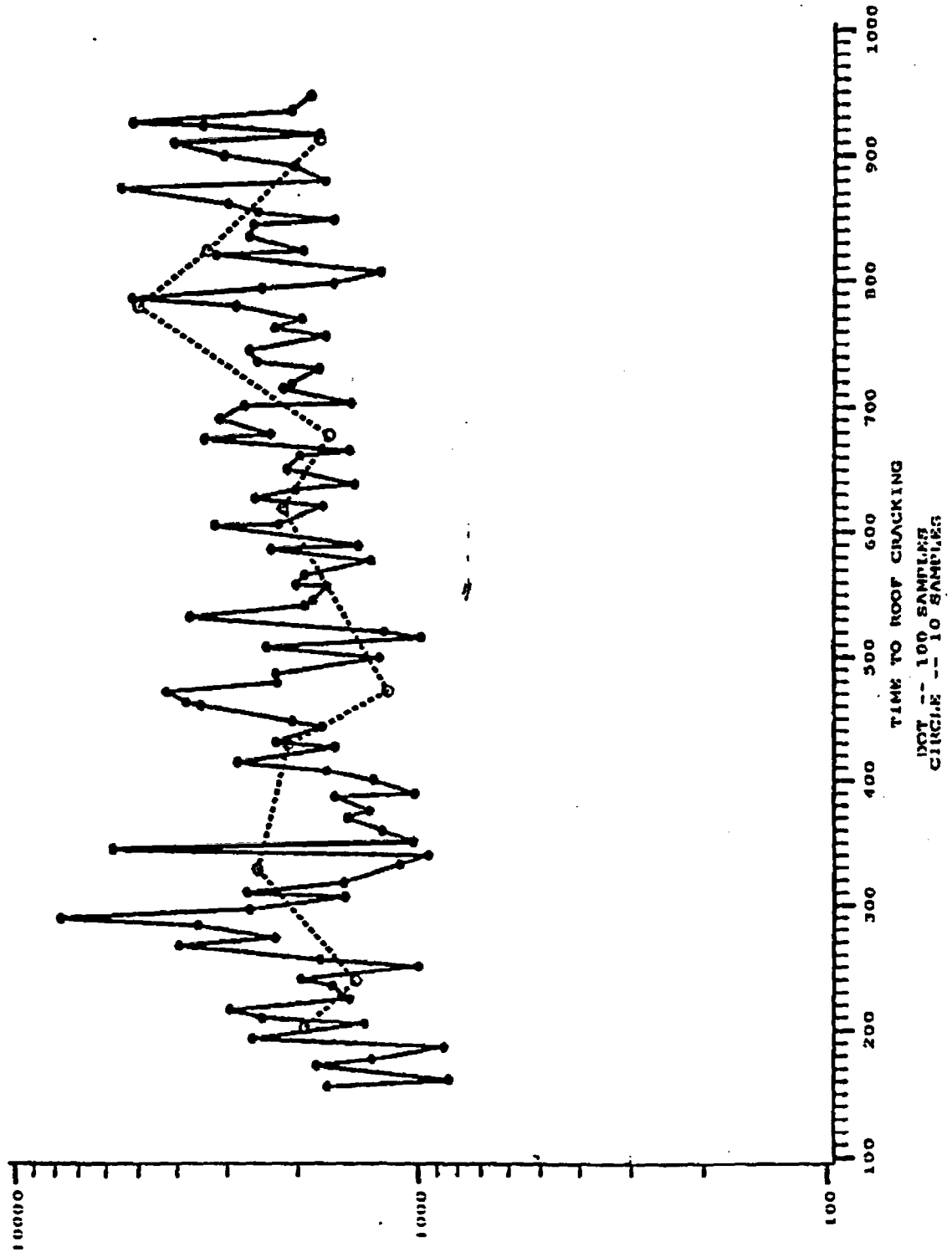


Rev. 0

J-14

WSRC-RP-94-218

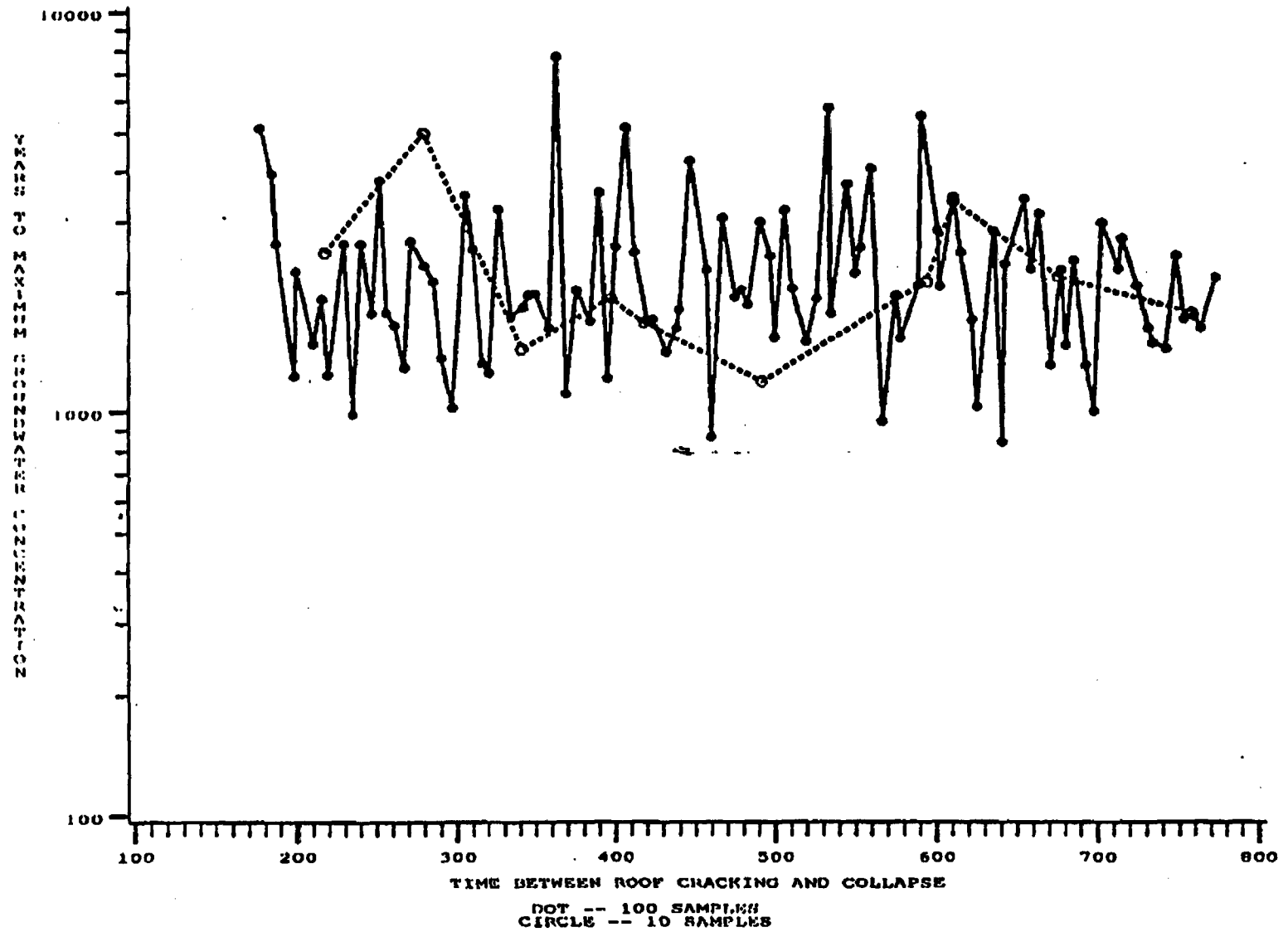
YEARS TO OCCURRENCE OF MAXIMUM TC99



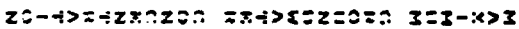
UOZUNZPZK1-CZ UOZUNZPZK1-CZ UOZUNZPZK1-CZ

YEARS TO OCCURRENCE OF MAXIMUM TC99

Rev. 0



95% CONFIDENCE LIMITS ON DISTRIBUTION



10,000

1. POLICY

APPENDIX J
REFERENCES

- Iman, R. L., and M. J. Shortencarier. 1984. *A Fortran 77 Program and User's Guide for the Generation of Latin Hypercube and Random Samples for Use with Computer Models.* NUREG/CR-3624, SAND83-2365. Sandia National Laboratory.
- WSRC. 1992. *Radiological Performance Assessment for the Z-Area Saltstone Disposal Facility.* WSRC-RP-92-1360. Savannah River Site, Westinghouse Savannah River Company, Aiken, SC.

APPENDIX K

**E-AREA VAULTS
VAULT DEGRADATION STUDY**

Rev. 0

E-AREA VAULTS VAULT DEGRADATION STUDY

FINAL REPORT

September 30, 1993



Prepared for Westinghouse Savannah River Company, Aiken, SC 29802

**E-AREA VAULTS
VAULT DEGRADATION STUDY
FINAL REPORT**

Prepared For:

Westinghouse Savannah River Company
Aiken, SC 29803

Prepared By
Erich R. Brandstetter
Jim L. Lolcama

INTERA Inc.
501 Greene Street, Suite 200-D
Augusta, GA 30901
Tel.: (706)722-2356
Fax: (706)724-2583

September 30, 1993

EXECUTIVE SUMMARY

The primary focus of this study was to determine the possible rates of roof and wall failure and the times to structural collapse of the roof and walls of three vault designs: the Intermediate Level Non-Tritium (ILNT), Intermediate Level Tritium (ILT) and Low Activity Waste (LAW) Vaults at the Department of Energy's Savannah River Site near Aiken, South Carolina. Failure was defined as a loss of ability to divert soil water around the vault. Collapse was defined as the total loss of structural integrity of the vault. Failure and eventual collapse of the three vault types results from concrete deterioration under stress, in the presence of corrosive soil water. Degradation rates for reinforced concrete were utilized, and the resultant changes in properties (such as strength, thickness, cracking and hydraulic conductivity) were evaluated. Baseline times to failure and collapse of the walls and roof components were modeled, and sensitivity analyses were conducted to provide boundaries on these estimated times. Thus, the goal of the project was to provide a bounding analysis of the time to roof and wall failure and potential collapse, rather than an actual prediction of the time to failure and collapse. The overall approach was to develop an executive model which linked various pre-existing models of degradation of reinforced concrete and to integrate that model with structural engineering models which estimate stress in the structure, for the bounding analysis of failure and collapse.

Degradation processes considered were magnesium and sulfate attack, calcium leaching, carbonation, and rebar corrosion due to both oxygen diffusion to the rebar (including breakdown of the passivating layer that initially prevents corrosion of rebar) and due to the "hydrogen evolution" reaction. Existing empirical models for the individual degradation processes were combined into a single model to create an overall model of the degradation of reinforced concrete. The state of stress in the concrete and rebar was calculated and the roof components and walls fractured in order to eliminate excessive stress which cannot be borne by the degraded structure. Crack aperture and spacing were computed and used to estimate hydraulic conductivity.

For each type of vault, a sensitivity analysis was performed to bound the predictions. After an initial rough sensitivity analysis on a large number of factors, six factors were selected for detailed sensitivity analysis: rate of rebar corrosion due to the "hydrogen evolution" reaction, rebar diameter, depth of concrete cover over the rebar, size of AASHTO "bridge" beams used to support the vault roof in the LAW vault design, and depth of soil cover over the vaults, and concrete strength.

The ILNT Vault design consists of 7 rectangular cells, each approximately 48.5' long by 27' wide by 29.75' high. The ILT is a similar design, the main differences being that it consists of only 2 cells and utilizes a slightly thicker roof. The LAW vault consists of 4 cells, each approximately 145' x 53' x 26'. It utilizes a significantly different design in that AASHTO "bridge" beams are used to support the roof span. Baseline times to failure and collapse for the ILNT vault were 570 and 1,045 years, respectively. The thicker roof and two-cell design of the ILT vault result in longer times to failure and collapse for the ILT vault; 790

and 1,300 years respectively. For the LAW vault, failure and collapse are predicted to occur in 1,420 and 3,100 years. The following table summarizes the baseline results for each vault type:

Summary of Baseline Results

Vault	Cracks Penetrate Roof/Failure (years)	Cracks Penetrate Walls (Mid-Height) (years)	Roof Collapse (years)
ILNT	570	800	1,045
ILT	790	1,080	1,300
LAW	1,420	2,235	3,100

Sensitivity analysis indicated that the rate of rebar corrosion due to the hydrogen evolution reaction is the most critical and uncertain model parameter. Variation within the bounds of acceptable values reported in the literature can result in the times to failure and collapse varying hundreds to thousands of years. For example, for the ILNT vault, the time to failure varied from 285 years to 2,775 years, based on variation in the hydrogen evolution corrosion rate. Similarly, the time to collapse varied from 525 years to beyond the 3,000-year duration of the simulation for the ILNT vault.

Variation in depth of concrete cover over rebar and in concrete strength within design constraints resulted in variation in times to failure and collapse of less than 100 years. Variation in depth of soil cover within design constraints resulted in variation in times to failure and collapse on the order of 100 to 400 years. Changing the rebar diameter has the potential to significantly impact the longevity of the vaults. For example, changing the bar designation by 1 (for example, from #8 to #7 or to #9) changes the time to failure and collapse on the order of 300 to 400 years. Changing the size of AASHTO beams has a similar impact on the time to collapse of the LAW vault. Utilizing a smaller beam, however, would result in cracks penetrating the vault (i.e., failure) immediately upon soil loading.

This study has combined pre-existing models for the degradation of reinforced concrete with proven structural engineering models to create a performance assessment code capable of predicting the time to failure (loss of ability to divert water) and collapse (loss of structural integrity) of buried concrete vaults. This code can also be used to estimate the impact of changes in design parameters on the longevity of reinforced concrete structures, and therefore has potential for application as a design aid tool for below-ground concrete storage facilities. The current mandate at DOE facilities to move in the direction of below-ground disposal in concrete-engineered structures makes this code a potentially important performance assessment tool.

TABLE OF CONTENTS

EXECUTIVE SUMMARY	ii
LIST OF TABLES	vi
LIST OF FIGURES	vii
1. INTRODUCTION	1
2. DESCRIPTION OF THE CLOSED ILT, ILNT AND LAW VAULTS	3
2.1 INTERMEDIATE-LEVEL VAULTS	3
2.1.1 ILNT Vaults	3
2.1.2 ILT Vaults	3
2.2 LAW VAULT	4
2.3 VAULT CLOSURE	4
3. MODELS OF CHEMICAL DEGRADATION AND STRUCTURAL ANALYSIS	5
3.1 CHEMICAL ATTACK	5
3.1.1 Sulfate and Magnesium Attack	5
3.1.2 Alkali and Calcium Hydroxide Leaching	6
3.1.3 Carbonation	7
3.1.4 Rebar corrosion	8
3.1.5 Vault Interiors	10
3.2 STRUCTURAL/ENGINEERING ANALYSIS	11
3.2.1 Application to the ILNT/ILT Vaults	12
3.2.2 Application to the LAW Vault	13
4. MODELING APPROACH	16
4.1 COMPUTER CODES	16
4.2 LINKING BETWEEN DEGRADATION AND STRUCTURAL MODELS	16
4.3 HYDRAULIC CONDUCTIVITY	16
4.3.1 Vault Roofs	16
4.3.2 Vault Walls	18
4.4 MODEL OUTPUT	18
4.5 DEFINITION OF FAILURE	18
4.6 SUMMARY OF CONSERVATIVISM	19
5. INPUT SUMMARY	21
6. MODEL RESULTS	22

7. SENSITIVITY ANALYSIS	24
7.1 SELECTION OF PARAMETERS AND VALUES	24
7.2 OUTPUT SUMMARY	25
7.2.1 ILNT Vault Sensitivity Analysis	26
7.2.2 ILT Vault Sensitivity Analysis	27
7.2.3 LAW Vault Sensitivity Analysis	27
7.3 SUMMARY OF THE IMPACT OF DESIGN CHANGES	29
8. FUTURE RESEARCH AREAS	32
9. SUMMARY AND CONCLUSIONS	34
REFERENCES	56
ACRONYMS AND ABBREVIATIONS	58
APPENDIX: QUALITY ASSURANCE	59
A.1 IMPLEMENTATION OF THE PROJECT QUALITY ASSURANCE PLAN	59
A.2 PROJECT QUALITY ASSURANCE PLAN	62

LIST OF TABLES

	Page
Table 1. Summary of Output Parameters	36
Table 2. Structural Input for the ILNT Vault	37
Table 3. Structural Input for the ILT Vault	38
Table 4. Structural Input for the LAW Vault	39
Table 5. Design Drawings Used	40
Table 6. Summary of Degradation Model Variables and Values	44
Table 7. Summary of Rebar Stress (ksi) in ILT Baseline Scenario	49
Table 8. Summary of Rebar Stress (ksi) in ILNT Baseline Scenario	50
Table 9. Summary of Baseline Results	51
Table 10. Summary of ILNT Vault Sensitivity Analyses	52
Table 11. Summary of ILT Vault Sensitivity Analyses	53
Table 12. Summary of LAW Vault Sensitivity Analyses	54
Table 13. Summary of Baseline Results Assuming High-pH Concrete	55

LIST OF FIGURES

- | | |
|------------------|--|
| Figure 1 | Schematic of ILNT Vault |
| Figure 2 | Schematic of ILT Vault |
| Figure 3 | Schematic of LAW Vault |
| Figure 4 | Portion of Vault Cross Section; Cracks Indicate Critical Stress Regions |
| Figure 5 | LAW Vault Roof, Showing Cracking Due to Curvature Over Wall |
| Figure 6 | Cross-Section of ILNT Vault Roof Showing Degradation at 400 Years |
| Figure 7 | Effective Hydraulic Conductivity of Vault Roof; ILNT Vault Design |
| Figure 8 | Effective Hydraulic Conductivity of Vault Roof; ILT Vault Design |
| Figure 9 | Effective Hydraulic Conductivity of Vault Roof; LAW Design |
| Figure 10 | ILNT Vault Time to Crack Penetration of Roof; Sensitivity to Hydrogen Evolution Corrosion Rate (cm/yr) |
| Figure 11 | ILNT Vault Time to Crack Penetration of Walls; Sensitivity to Hydrogen Evolution Corrosion Rate (cm/yr) |
| Figure 12 | ILNT Vault Time to Roof Collapse; Sensitivity to Hydrogen Evolution Corrosion Rate (cm/yr) |
| Figure 13 | ILNT Vault Time to Crack Penetration of Roof; Sensitivity to Depth of Soil Cover |
| Figure 14 | ILNT Vault Time to Crack Penetration of Walls; Sensitivity to Depth of Soil Cover |
| Figure 15 | ILNT Vault Time to Roof Collapse; Sensitivity to Depth of Soil Cover |
| Figure 16 | ILNT Vault Time to Crack Penetration of Roof; Sensitivity to Rebar Size |
| Figure 17 | ILNT Vault Time to Crack Penetration of Walls; Sensitivity to Rebar Size |
| Figure 18 | ILNT Vault to Roof Collapse; Sensitivity to Rebar Size |

LIST OF FIGURES (Continued)

- Figure 19** ILNT Vault Time to Crack Penetration of Roof; Sensitivity to Depth of Concrete Cover Over Rebar
- Figure 20** ILNT Vault Time to Crack Penetration of Walls; Sensitivity to Depth of Concrete Cover Over Rebar
- Figure 21** ILNT Vault Time to Roof Collapse; Sensitivity to Depth of Concrete Cover Over Rebar
- Figure 22** ILNT Vault Time to Crack Penetration of Roof; Sensitivity to Concrete Strength
- Figure 23** ILNT Vault Time to Crack Penetration of Roof; Sensitivity to Concrete Strength
- Figure 24** ILNT Vault Time to Roof Collapse; Sensitivity to Concrete Strength
- Figure 25** ILT Vault Time to Crack Penetration of Roof; Sensitivity to Hydrogen Evolution Corrosion Rate (cm/yr)
- Figure 26** ILT Vault Time to Crack Penetration of Walls; Sensitivity to Hydrogen Evolution Corrosion Rate (cm/yr)
- Figure 27** ILT Vault Time to Roof Collapse; Sensitivity to Hydrogen Evolution Corrosion Rate (cm/yr)
- Figure 28** ILT Vault Time to Crack Penetration of Roof; Sensitivity to Depth of Soil Cover
- Figure 29** ILT Vault Time to Crack Penetration of Walls; Sensitivity to Depth of Soil Cover
- Figure 30** ILT Vault Time to Roof Collapse; Sensitivity to Depth of Soil Cover
- Figure 31** ILT Vault Time to Crack Penetration of Roof; Sensitivity to Rebar Size
- Figure 32** ILT Vault Time to Crack Penetration of Walls; Sensitivity to Rebar Size
- Figure 33** ILT Vault Time to Roof Collapse; Sensitivity to Rebar Size
- Figure 34** ILT Vault Time to Crack Penetration of Roof; Sensitivity to Depth of Concrete Cover Over Rebar

LIST OF FIGURES (continued)

- Figure 35** **ILT Vault Time to Crack Penetration of Walls; Sensitivity to Depth of Concrete Cover Over Rebar**
- Figure 36** **ILT Vault Time to Roof Collapse; Sensitivity to Depth of Concrete Cover Over Rebar**
- Figure 37** **ILT Vault Time to Crack Penetration of Roof; Sensitivity to Concrete Strength**
- Figure 38** **ILT Vault Time to Crack Penetration of Walls; Sensitivity to Concrete Strength**
- Figure 39** **ILT Vault Time to Roof Collapse; Sensitivity to Concrete Strength**
- Figure 40** **LAW Vault Time to Crack Penetration of Roof; Sensitivity to Hydrogen Evolution Corrosion Rate (cm/yr)**
- Figure 41** **LAW Vault Time to Crack Penetration of Walls; Sensitivity to Hydrogen Evolution Corrosion Rate (cm/yr)**
- Figure 42** **LAW Vault Time to Roof Collapse; Sensitivity to Hydrogen Evolution Corrosion Rate (H₂rate; cm/yr) and Depth of Soil Cover**
- Figure 43** **LAW Vault Time to Crack Penetration of Walls; Sensitivity to Depth of Soil Cover**
- Figure 44** **LAW Vault Time to Crack Penetration of Roof; Sensitivity to Rebar Size**
- Figure 45** **LAW Vault Time to Crack Penetration of Walls; Sensitivity to Rebar Size**
- Figure 46** **LAW Vault Time to Roof Collapse; Sensitivity to Hydrogen Evolution Corrosion Rate (H₂rate; cm/yr) and Beam Type**
- Figure 47** **Cross-Section of Vault Roof Assuming Use of High-pH Concrete; Degradation at 50 Years**
- Figure 48** **Cross-Section of Vault Roof Assuming Use of High-pH Concrete; Degradation at 400 Years**

1. INTRODUCTION

The E-Area Vaults (EAV), which are the focus of this study, are located at the Savannah River Site (SRS) in South Carolina. The EAV designs which will be discussed in this report are the Intermediate Level Non-Tritium (ILNT), Intermediate Level Tritium (ILT) and Low Activity Waste (LAW) Vaults. Westinghouse Savannah River Company (WSRC) operates this site and is currently developing a Radiological Performance Assessment (RPA) for the EAV. The vault degradation study is a supporting study for this RPA.

The EAV site is located on a 200-acre site immediately north of Building 643-7E at the SRS. The original SRS Solid Waste Disposal Facility (SWDF) and the added EAV site are centrally located between the two chemical separations areas near the center of the SRS, between Upper Three Runs Creek on the north and Four Mile Creek on the south. Of this 200 acre tract, only 100 acres have been developed at this time. The nearest site boundary to the SWDF is about seven miles to the west. The SWDF is in a relatively level highland region of the SRS at about 300 ft above sea level.

The E-Area Vaults are reinforced concrete structures intended for below ground storage of low-activity and intermediate-level wastes. Each of the EAV designs are intended to house designated waste types. The LAW vaults, which are located at a separate facility from the ILT and ILNT vaults, are designed to receive and store low-activity waste radiating less than 200 mR/hr at 5 cm from an unshielded container and containing only incidental quantities of tritium. One section of the Intermediate Level facility is designated as the ILNT vault and receives waste radiating greater than 200 mR/hr at 5 cm in engineered metal containers. The remaining section is designated as the ILT vault and receives tritium-bearing waste contained in engineered metal containers or as overpacked tritium crucibles with most of the tritium removed. These two vault sections are adjacently located, share waste package handling equipment and are to be closed as one facility. The LAW vault facility will be closed separately. A third facility, also a part of the EAV Project, designated as the Long-Lived Waste Storage Building (LLWSB) has not been considered as part of this degradation study.

Closure of the vaults will be via below ground burial under about 8 feet of soil cover. The placement of the soil cover and soil backfill around the vaults will result in loading of the roof and walls of each unit. Chemical attack on the buried reinforced concrete will weaken the concrete, and the roof and walls of each vault type could be expected to fail and collapse over time. Failure is defined as a loss of ability to divert water around the vault. Degradation of concrete by sulfate attack can cause thinning, calcium hydroxide leaching results in weakening of the concrete, carbonation lowers the pH of the matrix-bound water, and oxic ("oxygen") and anoxic ("hydrogen evolution") rebar corrosion weakens the reinforced concrete mass. Failure of the vault would result in infiltrating ground water entering the interior of the vault rather than being diverted around its exterior.

INTERA's approach to this performance assessment problem for the E-Area Vaults has been to construct a mathematical model which integrates structural loading calculations with chemical degradation calculations. The model runs on a PC-platform and utilizes, as subroutines, pre-existing empirical models for the chemical degradation calculations, and an American Concrete Institute code for the design of reinforced concrete structures to calculate the state of stress within the structure. Adopting this modeling approach facilitates sensitivity analyses on different design components of the vaults.

This report presents the chemical degradation mechanisms which have been modeled for degradation of the concrete of each of the vault designs, describes the structural design model and the approach for integrating these models into one code, and finally, presents the results of the performance assessment calculations on the three vaults types for baseline (base case) and variant configurations of several of the design components. Further work which will likely be accomplished under a separate task will include evaluating the performance of the vault floors for the three vault designs, and extending the sensitivity analyses beyond six parameters.

2. DESCRIPTION OF THE CLOSED ILT, ILNT AND LAW VAULTS

The EAV Project consists of three types of facilities to house four designated waste types and the necessary roadways to allow waste container delivery. This section describes in brief the three vault types.

2.1 INTERMEDIATE-LEVEL VAULTS

The intermediate-level vaults consist of two separate, subsurface reinforced concrete vault structures. The individual vaults are adjacently located, share a similar design, and are closed as a single unit. The vaults are identified as the Intermediate Level Tritium (ILT) Vault, and the Intermediate Level Non-tritium (ILNT) Vault.

2.1.1 ILNT Vaults

Each ILNT Vault consists of seven cells or subdivided sections within the vault structure (Figure 1) and provides a total of approximately 200,000 ft³ of waste storage capacity. The vaults are subsurface concrete structures approximately 189 ft long, 48.5 ft wide, and 29.75 ft deep. Exterior end walls are 2½ ft thick, side walls are 2 ft thick, and interior walls (between the cells) are 1½ ft thick. All walls are structurally mated to a base slab which is approximately 2½ ft thick and extends past the outside of the exterior walls approximately 2 ft. The base slab rests on two layers of crushed stone placed on the compacted subsurface. The crushed stone drains to a collection sump to prevent a positive water head against the vault exterior.

Concrete is reinforced with deformed steel bars. All concrete construction joints are located at defined control joints with no horizontal joints in any vertical wall. All concrete joints include a waterstop seal which is continuous around all corners and intersections. All exterior concrete surfaces exposed to soil are coated with a coal tar-based waterproofing.

2.1.2 ILT Vaults

Each ILT Vault consists of two cells or subdivided sections within the vault structure (Figure 2) and provides approximately 57,000 ft³ of waste storage capacity. One cell will, in most cases be fitted with a silo system to permit the disposal of tritium crucibles. The ILT Vaults are structurally very similar to the ILNT, with slight differences such as wall height and thickness of the (proposed) roof slab. The ILT Vaults are approximately 57 feet long, 48.5 ft wide, and 28.5 feet deep. Wall arrangement, slab and slab base, and concrete are all identical for the two-cell configuration ILT vault and the seven-cell configuration ILNT vault.

2.2 LAW VAULT

Each LAW Vault consists of either two or three major subdivisions, or modules. Each module provides approximately 566,500 ft³ storage capacity and will accommodate more than 4,000 B-25 boxes. Figure 3 illustrates one module of a LAW Vault. Each module is approximately 214.5 ft long and 145 ft wide. Height of the vaults varies from approximately 26 to 27 feet. End, side, and interior walls of each module are all 2 ft thick. All walls are structurally mated to a 30-inch footer that is continuous under all cells in each module.

A reinforced concrete roof is supported by prestressed, concrete beams. The beams run between each wall the length of the vault. The end walls of each module have recessed beam seats to support a beam end, and the interior walls are equipped with bearing pads allowing beam ends to rest on the wall. The beams rest on elastomeric bearings which allow the bases of the beams to move towards each other as soil load and progressive deterioration of the structure causes the roof system to bend.

The slightly peaked roof is composed of 3½-inch thick, prestressed, concrete deck panels installed directly on the roof beams providing a base for a 16-inch, cast-in-place roof slab. The roof slab has 2-in. wide expansion joints between module walls. Each expansion joint has flashing installed to provide waterproofing. The roof slab is covered with a bonded-in-place layer of fiberboard insulation and a layer of waterproof membrane roofing.

2.3 VAULT CLOSURE

Final closure of the vaults consists of placing an earthen cover with an engineered clay cap over the entire 21-vault area. The final closure cap will consist of a 2-foot thick compacted clay layer, on top of which will be a clay geomembrane or clay/geotextile composite. This will be overlain with a 1-foot thick granular drainage layer. Above the drainage layer will be a geotextile filter fabric. The uppermost layer of the closure cap will be a 2-foot thick topsoil cover. The slope of each of these layers will be 3% over the ILNT and ILT Vaults, and 3% or 4.3% (depending on location) over the LAW Vaults. The total thickness of the soil layer will be between 8.5 and 9 ft. The "final closure cap" thus accounts for 5 ft of this thickness. The remaining volume will utilize compacted fill material. In addition, in order to reduce the hydraulic conductivity of the layered soil/vault system, a clay layer will be placed immediately adjacent to the vault roofs.

3. MODELS OF CHEMICAL DEGRADATION AND STRUCTURAL ANALYSIS

The selection of chemical degradation mechanisms for concrete was based on a process of eliminating mechanisms which demonstrated little or no effect under chemical conditions of the soil or concrete mix. The chemical degradation models which were included in the assessment were: SO_4 and Mg attack, $\text{Ca}(\text{OH})_2$ leaching, carbonation, and rebar corrosion in oxic and anoxic conditions. Below we have presented the models for chemical degradation processes, some empirical and some analytic, and have provided a description of the attack mechanisms for which the models were derived. These mechanisms have been modeled independently. For example, thinning of the concrete surface will not result in an increased rate of reinforcing steel corrosion due to faster diffusion of oxygen through the decreased cover. In addition, the structural analysis modeling is described.

3.1 CHEMICAL ATTACK

3.1.1 Sulfate and Magnesium Attack

Sulfate and magnesium are naturally occurring elements at the Savannah River Site, input to the soil water from rainfall and weathering of rock minerals. Sulfate reacts with tricalcium aluminate (C_3A) to form calcium aluminum sulfates leading to expansion and cracking of the surface of the concrete (Walton et al., 1990). A related problem is the reaction of magnesium with the cement to form Brucite [$\text{Mg}(\text{OH})_2$]. As the concrete cracks, its hydraulic conductivity increases, and water penetrates more easily into the interior, accelerating the deterioration of the concrete. Sulfate attack also results in a progressive loss of strength and mass due to deterioration in the cohesiveness of the cement hydration products. The reaction products have considerably greater volume than the reactants. This causes the expansion of the concrete which, in turn, results in cracking, spalling, and loss of strength. In addition, formation of gypsum causes a deterioration of the cement paste which results in a reduction in stiffness and strength, followed by more expansion, cracking, and loss of cohesiveness. Empirical studies indicate that the rate of attack by magnesium sulfate is twice that of sodium sulfate, and that the rate of attack is reduced by low water to cement ratio and by low C_3A content. The rate of surface loss due to sulfate attack was calculated according to:

$$X = 0.55 C_s (C_{\text{Mg}} + C_{\text{SO}_4}) t ,$$

where:

$X =$	distance of corrosion into concrete (cm),
$C_s =$	C_3A concentration in solid (mole/cm ³), and
$C_{\text{Mg}} =$	Mg concentration in solution (mole/cm ³),
$C_{\text{SO}_4} =$	SO_4 concentration in solution (mole/cm ³), and
$t =$	time (s).

3.1.2 Alkali and Calcium Hydroxide Leaching

When concrete is exposed to water, constituents in the concrete are leached. Alkalis are leached first, followed by calcium hydroxide. This process can be described in four stages:

1. Initially, the pH of standard concrete is approximately 13 due to the presence of alkali metal oxides and hydroxides. These alkali metals leach first.
2. After the alkali metals are leached, the pH is controlled at 12.5 by solid calcium hydroxide. Free (not bound by C-S-H gel) calcium hydroxide is leached first.
3. Following loss of free calcium hydroxide, calcium hydroxide is leached at a slower rate from the C-S-H gel. The C-S-H gel dissolves incongruously, while the pH drops to 10.5 and the calcium to silicon ratio drops to 0.85.
4. The pH is held to 10.5 by congruent dissolution of the C-S-H gel.

The loss of calcium results in a decrease in strength of approximately 1.5% for every 1% loss of total calcium content. The rate of calcium hydroxide leaching depends primarily on the flow of water through the concrete, but also on diffusion into the surrounding geology, and diffusion across a reaction zone in the concrete. Advective transport of leached calcium hydroxide from the concrete structure will dominate only under high rates of groundwater flow, and preferential flow of groundwater through the structure.

Atkinson and Hearne (1984) applied a shrinking core model to calcium hydroxide leaching. This model assumes that removal of calcium from the exterior of the concrete is rapid relative to movement of calcium through the concrete. Thus, leaching is controlled by conditions in the concrete and properties of the concrete, and so this process is referred to as "concrete-controlled leaching". As an alternative approach, Atkinson and Hearne also developed a leach model controlled by the surrounding geology ("geology-controlled leaching"). This model uses an equation for diffusion from a fixed concentration into a semi-infinite domain, with concentrations described by an error function (as in Crank, 1975), and allows for an analytic solution of the amount of calcium lost in a given amount of time. Both models predict that it will take over 1,000 years before calcium hydroxide leaching penetrates the upper 0.05 cm of the concrete. Both analytic models have been added to the degradation model. The equations used to approximate concrete-controlled and geology-controlled leaching, respectively, are:

$$X_c = \left(2 D_i \frac{C_i - C_{Fe}}{C_i} t \right)^{1/2}$$

and

$$X_G = 2\phi \frac{C_1 - C_{rw}}{C_s} \left(\frac{R_d D_E t}{\pi} \right)^{1/2} .$$

where,

$X_C =$	depth of leach penetration due to concrete-controlled leaching (cm),
$X_G =$	depth of leach penetration due to geology-controlled leaching (cm),
$D_i =$	intrinsic diffusion coefficient of Ca^{++} in concrete (cm^2/s),
$C_1 =$	Ca^{++} concentration in concrete pore water (mole/ cm^3),
$C_{rw} =$	Ca^{++} concentration in ground/soil water (mole/ cm^3),
$C_s =$	bulk Ca^{++} concentration in concrete solid (mole/ cm^3),
$\phi =$	porosity of soil (unitless),
$R_d =$	retardation coefficient (unitless), and
$D_E =$	effective dispersivity/diffusivity of Ca^{++} in the surrounding geologic material (cm^2/s).

A conservative estimate of the depth of leach penetration was obtained by summing X_C and X_G .

3.1.3 Carbonation

Carbonation is the reaction of carbon dioxide with cement to form calcium carbonate according to the reaction,



Sources of carbon dioxide are atmospheric gases and soil gases. Carbonation occurs most aggressively when the concrete is less than fully saturated with water, allowing CO_2 to diffuse through the air space in the concrete up to the reaction front within the concrete. At the reaction front, CO_2 dissolves in pore water and combines with calcium to precipitate calcium carbonate. From Walton et al. (1990), the depth of carbonation is proportional to the square root of time as shown in the equation below. The rate of carbonation depends on the moisture content of the concrete and its relative humidity, and ultimately on the type of cement used in the concrete mix.

Carbonation does not render the concrete less durable. Some fully-carbonated Roman concretes has survived to modern times. Shrinkage of the concrete may occur with carbonation as will a drop in the pH of the pore water. Carbonation of hydrated Portland-cement pastes also results in reduced hydraulic conductivity and increased hardness

(Verbeck, 1958). The pH shift can be from over 12 to about 8. At this lower pH, enhanced corrosion of steel reinforcing in the concrete may occur.

The rate of carbonation is dependent upon water saturation or relative humidity of the concrete. As relative humidity increases from 0 to 100%, the rate of carbonation passes through a maximum. Since water is required in the carbonation reaction, partially saturated conditions promote the reaction of CO_2 and $\text{Ca}(\text{OH})_2$ to form CaCO_3 , however increasing the water content above that required for this reaction to proceed will slow the diffusion rate of CO_2 through the concrete and limit the carbonation reaction. Typical subsurface environments approach 100% relative humidity, resulting in a water saturated concrete matrix. Therefore slow rates of carbonation are commonly found. The following analytic expression was employed for estimating carbonation rate in the degradation model:

$$X = (2D_i \frac{C_{rw}}{C_s} t)^{1/2}$$

where,

- X = depth of penetration of carbonation (cm)
- D_i = intrinsic diffusion coefficient of Ca^{++} in concrete (cm^2/s)
- C_{rw} = total inorganic carbon in ground water or soil moisture (mole/ cm^3)
- C_s = $\text{Ca}(\text{OH})_2$ bulk concentration in concrete solid (mole/ cm^3) and
- t = time (s)

Inherent in the use of this expression is the assumption that the concrete is water-saturated, and that the concrete is in direct contact with moisture containing a constant concentration of dissolved inorganic carbon.

3.1.4 Rebar corrosion

Corrosion of steel reinforcement results in a loss of strength due to loss of cross-sectional area of the rebar. In addition, a reinforced-concrete structure may suffer structural damage due to the loss of the bond between steel and concrete. Corrosion of the rebar produces a reaction product of greater volume than the rebar. Since the concrete surrounding the reinforcement prevents free expansion, this expansion exerts pressure on the concrete, and thus causes cracking and potentially spalling of the concrete structure, with consequent loss of strength. In the alkaline environment of standard concrete (low alkaline specialty concrete is used for the EAV construction), the rebar is protected from corrosion by the formation of a passivating layer around the rebar. This passivating layer, however, may be destroyed by the diffusion of chloride ions to the embedded steel (i.e., depassivation). Water to cement ratio and depth of concrete cover over the rebar are the most important factors in concrete construction that effect the time to depassivation. In the corrosion reaction, oxygen is electrochemically reduced and iron electrochemically oxidized, followed by conversion of the iron to iron oxides. The reaction rate is generally limited by diffusion of oxygen through

the concrete to the rebar, with oxygen diffusion increasing over time as processes, such as calcium hydroxide leaching and sulfate attack, decrease the diffusion limiting concrete cover over the rebar.

Thus, the corrosion of reinforcing steel due to oxygen diffusion occurs in two steps. First, the passivating layer must be broken down before the onset of corrosion. The time to onset of corrosion was approximated by:

$$t_c = \frac{129 X_c^{1.22}}{WCR + Cl^{0.42}} ,$$

where,

t_c = time to onset of corrosion (yr),
 X_c = thickness of concrete over rebar (inches),
 WCR = water-cement ratio in concrete (kg/kg), and
 Cl = chloride ion concentration in groundwater (ppm).

The reaction then proceeds, with a loss of reinforcing steel volume approximated by:

$$\% \text{ Rebar Remaining} = 100 \left(1 - \frac{4 * 9.4 \left(\frac{\text{cm}^3}{\text{mole}} \right) s D_i C_o (t - t_c)}{\pi d^2 \Delta X} \right) .$$

where,

s = spacing between reinforcement bars (cm),
 D_i = oxygen diffusion coefficient in concrete (cm²/s),
 C_o = oxygen concentration in groundwater (mole/cm³),
 t = time (s),
 d = diameter of rebar (cm), and
 ΔX = depth of rebar below surface (in).

Another mechanism of reinforcing steel corrosion is via the hydrogen evolution reaction. In this mechanism, H⁺ ion from the water molecule is used as the source of oxidant for corrosion. H₂ is a by-product of this reaction. If we assume a low, constant rate of hydrogen evolution corrosion (i.e., a number from the low end of the literature range is adopted), then the relative volume of steel remaining is:

where,

$$\frac{V_{H_2}}{V_{in}} = \frac{2at - d^2}{d^2}$$

- a** = corrosion rate from hydrogen evolution reaction (cm/yr),
t = time (yr), and
d = diameter of rebar (cm).
V_{H₂} = volume of steel after H₂ corrosion
V_{in} = initial volume of steel

Literature review of hydrogen evolution corrosion rates indicated a pH-dependance in the reaction rate. In the high pH range of typical concrete, the reaction rate is on the order of 1.5E-4 to 1E-5 cm/yr. If the pH drops below approximately 9, the reaction rate increases to values on the order of 1E-3 to 1E-4 cm/yr.

A bounding analysis for corrosion will be utilized by combining the rates due to oxygen-based corrosion and hydrogen evolution corrosion.

3.1.5 Vault Interiors

The degradation mechanisms that were considered for the walls and roof in contact with site soil are: Mg + SO₄ attack, Ca(OH)₂ leaching, concrete carbonation, and oxic and anoxic corrosion of the re-bar. Several of these mechanisms will not operate under the conditions anticipated inside the vaults or will occur so slowly that their net effect over the life of the vaults will be insignificant. Only anoxic ("hydrogen evolution") corrosion is anticipated as significant degradation process originating inside the vault, as discussed below.

Magnesium and sulfate attack requires a source of dissolved Mg and SO₄ in contact with the concrete such as would be provided by a moist soil. There is no continuous source of Mg and SO₄ in contact with the concrete in the vault interior, and therefore this mechanism is not anticipated to operate.

Two forms of calcium hydroxide leaching were considered: concrete controlled and geology controlled leaching. The concrete controlled leaching mechanism assumed a zero-concentration boundary condition at the surface of the concrete, a condition which would require ground water to flow over the concrete surface and "sweep" the calcium away from the surface as it diffuses out of the concrete. Inside the vaults, during the period of performance prior to collapse, there is no recognizable mechanism to create this zero-concentration boundary. As a result, a chemical diffusion gradient from the interior of the concrete towards the concrete surface will not be established and diffusion will not occur.

Geology controlled leaching assumes that a concentration gradient can be established into the (soil) material adjacent to the concrete. This is physically impossible in the LAW vault because of the lack of in-filling material and in the case of the ILT and ILNT vaults, where cement grout will contact the walls, the calcium concentration in the grout porewater will be identical to that in the concrete at all times. These conditions prevent a concentration gradient from forming outwards away from the concrete.

Concrete carbonation occurs in the presence of dissolved carbonate and calcium in the porewater of the concrete. Leaching of calcium hydroxide provides a source of calcium and diffusion of carbonate ion from soil water in contact with the concrete provides a source of carbonate. The carbonate in the soil water is replenished from dissolution of CO_2 gas from the soil air. Inside the LAW vault, the air space will contain CO_2 , although most likely at concentrations much less than in a biologically-active soil; differences of one to two orders of magnitude would be a reasonable estimate. Carbonation would most likely occur, however with only atmospheric levels of CO_2 driving the reaction, the carbonation front would advance at a much slower rate than for the outer surfaces of the vaults. From the empirical relationship that INTERA has been using to describe carbonation, a slowing of the movement of the carbonation front by an order of magnitude would be possible.

Corrosion of the reinforcing bar in concrete under oxygenated conditions requires an initial depassivation of the steel surface. The mechanism that has been invoked in our modeling relies on diffusion of chloride to the passivating layer. Depassivation is followed by oxidation of the exposed steel. The interior of the vaults does not provide a source of chloride for the depassivation mechanism. Degradation modeling of the interior of the vaults should therefore not include oxic corrosion of rebar, unless the concrete mix is such that the pH of the concrete is below 9.

Anoxic corrosion of rebar will occur in the presence of moisture in the concrete. Since water-saturated concrete has been assumed for the modeling of degradation, this mechanism would proceed at a rate approximately the same as for the exterior surfaces of the vault. Adjustments to the rate caused by a decrease in pH at the corroding surface following carbonation of the local concrete will not be required.

In summary, the dominant degradation mechanism for the interior surfaces of the vaults will likely be anoxic corrosion of re-bar. Carbonation is also likely to occur, however, the rate of advance of the carbonation front will be significantly less than for exterior surfaces. The effect of carbonation on anoxic corrosion will likely not be an important consideration.

3.2 STRUCTURAL/ENGINEERING ANALYSIS

The RCPC.DHelper models (Furlong, 1991) used as the basis for the structural analysis portion of this study are available commercially through the American Concrete Institute

Software Sales Department. The programs have been in use for the past 4 years by approximately 300 engineering offices. The programs are intended to serve as a design aid in accordance with governing design documents, the principle one of which is the Building Code of the American Concrete Institute ACI 319-89. The Building Code is a strength design document with considerations for serviceability, but the major consideration for design is the limit strength of reinforced concrete members. Consequently, the computer design aids focus on decisions related to strength design instead of service load performance.

Strength design employs results from elastic analyses of frame response to the many different types and configurations of load that concrete structures support. An analytic routine known as the Portland Cement Association Two-Cycle Method is used for the interpretation of worst effects from pattern loading on beams. The analytic tools in RCPC.DHelper are just as appropriate for serviceability analyses as for strength design. The RCPC.DHelper programs apply required load factors and incorporate appropriate reliability factors in the logic required for design. These programs were modified to bypass load factors and reliability factors in order simply to use response to service load forces (load and reliability factors = 1) for estimates of service load stress in steel reinforcement and shear stress in concrete slabs. Steel stress was computed assuming that the concrete had cracked.

The program most appropriate for Vault Study is the Continuous Beam program in RCPC.DHelper. That program was prepared for design of floor beams in two-dimensional rigid frames. The Vault study involved two structures that consisted of roof slabs cast as rigid and monolithic with supporting walls. The structure represented by a unit width of wall and roof slab is a two-dimensional rigid frame. Distances between supports were adjusted such that the actual clear distances between faces of framing elements remained the same as those in the finished structure.

3.2.1 Application to the ILNT/ILT Vaults

Because the ILNT and ILT vaults are virtually identical in their design, the same approach was used to analyze the two structures. The only changes required were changes in input parameters such as height of the structure and roof thickness. The structures were represented by a 1-ft wide span of walls and roof in the direction of maximum stress. The direction of maximum stress in the short direction of each cell, or, for example, along the 189-ft length of the ILNT vault. Hand calculations indicated that this approach is accurate to within approximately 3% of the full 2-way slab analysis (Furlong, 1993). Parameter values were selected to correspond to the respective height, thickness, amount of rebar, etc. in the walls and roof of each vault.

Stress in concrete and rebar was computed at the locations which experience the maximum stress. Maximum stress occurs over the walls, in the exterior face rebar, and at midspan, in the interior face rebar (Figure 4). After the stress in the rebar was calculated, the roof components and walls may fracture in order to eliminate excessive stress which cannot be borne by the degraded structure. When the stress in the rebar at a particular location

exceeds 40 ksi, cracks are assumed to penetrate the concrete. The approach to the calculation of stress in rebar assumes that the concrete has cracked. Crack width and spacing were computed as functions of the distance between the neutral axis¹ and the lower face of the concrete, the distance between the neutral axis and the center of the reinforcing steel, the diameter of the reinforcing steel, the concrete cover over the reinforcing steel, and the strain on the reinforcing steel.

When the stress in the rebar at a particular location reaches the yield strength of the rebar (60 ksi), the rebar will yield. In most cells, yield strength is reached first at the midspan region. Excess moment is then transferred to other regions in the cell. In the case of the midspan region reaching yield strength first, excess moment is transferred to the regions over the walls. This, in turn, increases the stress levels in the rebar over the walls. When the rebar reaches its yield strength at all three locations, a "hinge" is created. This will allow the roof to sag, and it is presumed that structural integrity will be lost at this point. Therefore, the point in time at which this occurs has been defined as the time of collapse. This process can be summarized as follows:

1. Rebar at center of span reaches yield strength.
2. Excess moment (and corresponding stress) transferred to region over walls.
3. Rebar over walls reaches yield strength, resulting in severe cracking and collapse.

For cells 3, 4, and 5 of the ILNT vault, the rebar reaches yield strength in the regions over the walls before reaching yield strength at midspan. In this case, the order is reversed:

1. Rebar over walls reaches yield strength.
2. Excess moment (and corresponding stress) transferred to midspan.
3. Rebar at midspan reaches yield strength, resulting in severe cracking and collapse.

3.2.2 Application to the LAW Vault

The 3" thick prestressed slabs in the LAW Vault roof design serve to hold the cast-in-place slab, and are therefore ignored in subsequent calculations. The soil and self weight (of the slab and the AASHTO beams) will cause the beams to move on the elastomeric bearings. As the beams move, the upper ends of the precast girders remain separated by a fixed distance at the slab atop the girders (Figure 5). Only the bases of the beams move toward each other, leaving at the end of each beam an angle of rotation each side of the supporting

¹When a slab deforms under loading, part of the slab will be in compression and part of the slab will be in tension (e.g., at mid-span, the upper portion of the slab is in compression, and the lower portion in tension). The neutral axis is the location in the slab where compression changes to tension; it is therefore an axis of zero strain.

wall. The angle of rotation remains essentially constant as long as the flexural stiffness of the girders remains constant under soil loading. Based upon the soil load and self load of the slab and beams, a curvature (in the roof, over the walls) of 0.35 radians/inch was calculated. This will result in a stress of 2.8 ksi in the concrete, sufficient to crack the concrete. The curvature was then used to calculate the moment in the slab, and stresses in the cracked concrete and rebar. In the LAW Vault design, the stress level in the rebar increases relatively slowly as the structure degrades, and generally does not reach the 40-ksi limit. Therefore, the depth of the neutral axis was calculated in order to approximate the depth of crack penetration. As the structure degrades, the neutral axis, and therefore the cracks, penetrate further into the concrete. When the depth of the neutral axis moves to within 1 inch of the interior surface of the roof, cracks are assumed to penetrate the roof slab.

Due to the difference in roof design, the LAW Vault roof could not be analyzed in the same manner as the intermediate level vaults. The roof slab has only 5 ft of unsupported span between the AASHTO beams. Preliminary calculations indicated that the 16-inch concrete slab can support soil loads across the slab even after significant degradation of the steel. Therefore, collapse of the vault will be determined by the ability of the AASHTO beams to support the structure. A moment arm calculation was used to calculate the moment at mid-span of the beams after soil loading. This was then compared to the ultimate moment² of the beams. Because the moment is approximately proportional to the steel area, the ratio of actual moment to ultimate moment is approximately equal to the amount of steel area that can be lost before collapse:

$$A_{\text{crk}} = A_{\text{init}} * \frac{M_{\text{pred}}}{M_u}$$

where:

- A_{crk} = critical steel area (the minimum area of steel in the AASHTO beams which is capable of supporting the soil load),
- A_{init} = initial steel area in the AASHTO beams (7.01 inch²),
- M_{pred} = predicted moment in beam after soil loading, and
- M_u = ultimate moment in beam.

In the model, then, collapse occurs when the steel area in the beams is reduced to A_{crk} .

The NAWY models (Nawy, 1989) were used to calculate loss in prestress in the beams due to elasticity loss, creep, shrinkage and relaxation. The model predicted that 90% of the prestress loss occurs in the first 10 years after release, and was in agreement with the prestress loss calculations by Tindall Concrete Georgia, Inc. (hereafter referred to as

²The ultimate moment is the maximum moment that the system can support before collapse.

"Tindall Concrete"). A value of 22% prestress loss was used as a conservative upper bound in the above calculations.

The LAW Vault walls were analyzed using the same RCPC-based code that was used for the intermediate level vaults. To do so, an equivalent roof slab was formulated for input into the code. After the roof slab of the LAW vault is cast, the system gains redundancy as a continuous, composite beam. The earth load was analyzed with the RCPC model using end span and wall models similar to that used for the intermediate level vaults. An equivalent roof slab width was computed to use a rectangular beam of 70-inch depth (the depth of the composite roof slab/AASHTO beam system) and produce the same moment as the composite slab and beam:

$$b = \frac{886200 \times 12}{70^3} = 31 \text{ in.}$$

where:

b = equivalent slab width;

886200 = I value of composite slab and beam system (from Tindall, 1993).

In this manner the RCPC-based code can be used to analyze stresses in the LAW vault walls.

4. MODELING APPROACH

4.1 COMPUTER CODES

The RCPC code (Furlong, 1991), as it is commercially available, is an interactive program; all input is typed in as the program runs, and output can be directed to the screen and/or a printer. In order to facilitate multiple model runs during the sensitivity analysis, and to maintain adequate Quality Assurance, the model was first modified to a file-based input/output system. In addition, minor modifications were added to compute stresses in rebar.

The NAWY models (Nawy, 1989) were used to evaluate prestress loss in the AASHTO beams and to confirm various calculations performed by Tindall Concrete. In addition to calculating time-dependent prestress loss, the NAWY models capabilities include service load analysis, strength analysis and design in flexure, shear reinforcement selection, and time dependent deflection of prestressed concrete beams.

4.2 LINKING BETWEEN DEGRADATION AND STRUCTURAL MODELS

The degradation model and structural model (modified RCPC) were combined, and a time loop was added so that the state of the structure through time could be modeled. The time loop was implemented as follows: First, the structural model is run at time zero on the (undegraded) structure. Next, the degradation model is run to determine the impact of degradation mechanisms on the physical state (thickness of concrete, diameter of reinforcing rebar, etc.) of the structure using a user-specified time step. After the degradation model is run, a temporary file is created that contains the modified concrete and reinforcing steel specifications. This file is then used as input for the next run of the structural model. Following the structural model run, the degradation model is run again, and the temporarily file is updated. This process of alternating between the structural and degradation models continues until the user-specified end of the simulation (e.g., 1,000 years). The state of the structure is printed at a user-specified time interval (e.g., 50 years).

4.3 HYDRAULIC CONDUCTIVITY

4.3.1 Vault Roofs

Walton (1993), presents a calculational method for Effective Hydraulic Conductivity (K_{eff}) of the vault roof. This method considers the adjacent porous media overlying the concrete roof. We have applied Walton's method in our K_{eff} determination. The closure design for each of the three vault designs considered in this report places a clay barrier over the roof to divert infiltration away from the roof. The infiltration flows laterally away from the vault through a granular drain layer which directly overlies the clay barrier. Only a very small amount of the infiltration will penetrate the intact clay barrier. During the period of

performance in which the concrete contains no cracks or during which the cracks do not fully penetrate the roof, the infiltration which penetrates the clay barrier will drain off of the sloped roof. The limiting barrier to flow will be the reinforced concrete. With cracking of the roof under applied stresses, the clay barrier will limit the infiltration to the roof, and any infiltration passing through the clay will likely enter the vault through penetrating cracks. The clay barrier is assumed to stay intact until collapse of the vault structure.

K_{eff} of the clay barrier and the concrete roof of the vault were derived using separate equations. The calculation of K_{eff} assumes steady, saturated flow through a set of equally spaced, parallel fractures in the concrete. The following equations after Walton (1993) derive the K_{eff} of the clay layer in the presence of fully penetrating cracks in the concrete.

$$K_{eff} = \zeta K_{clay} , \text{ and}$$

$$\zeta = \left\{ \frac{1}{2} + \frac{\tanh \left[a + b \ln \left(\frac{1}{x} \right) + c \ln (z) \right]}{2} \right\}^d ,$$

where

- K_{clay} = hydraulic conductivity of the clay layer (m/s),
- ψ = 1/2 of crack width (m),
- x = X/ψ = dimensionless crack spacing,
- z = Z/ψ = dimensionless thickness of the clay layer,
- H = depth of perched water on top of the vault (m),
- X = 1/2 of the crack spacing (m),
- Z = thickness of the clay layer (m),
- a = 0.0477, b = 0.606, c = 0.479, and d = 0.845.

The assumption of steady saturated flow through the clay layer can be demonstrated by calculating the depth of perched water above the clay layer in the granular drain. The analytic solutions for these equations are provided by McEnroe (1993). For the EAV geometry and hydraulic conductivity of the clay and granular drainage layer, a perched water table equal to the thickness of the granular drain was calculated, thereby verifying our assumptions.

The calculations of K_{eff} assume that the cracks are not infilled with porous material. Infilling of the cracks would result in much lower hydraulic conductivity of the clay/concrete layered system when the cracks have fully penetrated the concrete.

4.3.2 Vault Walls

The model for the hydraulic conductivity of the vault roofs assumes that the soil adjacent to the roof will be saturated. This will generally not be the case for the vault walls. Similar models to estimate the hydraulic conductivity of a cracked vault/unsaturated soil system are not available at this time. Nevertheless, the hydraulic conductivity of the walls will be limited by the conductivity of the adjacent material. Therefore, the unsaturated hydraulic conductivity of the adjacent backfill material can be used as an upper bound for the hydraulic conductivity of the cracked wall/soil system (just as the saturated hydraulic conductivity of the adjacent clay was the limiting value for the hydraulic conductivity of the cracked roof/soil system). The unsaturated hydraulic conductivity of the backfill material (or any soil) is a function of its moisture content. The Idaho National Engineering Laboratory is in the process of conducting flow and transport modeling for the vaults. They utilized a VanGenuchten approach to generate a moisture characteristic curve for the backfill material. This curve provides the relationship between moisture content and hydraulic conductivity. Model results indicate that the backfill will have a greater moisture content near the top of the vault, and therefore it will have a correspondingly greater hydraulic conductivity. For the intermediate level vaults, the unsaturated hydraulic conductivity of the backfill material adjacent to the walls was estimated as $7.5\text{E-}4$ cm/s near the top of the walls, $6.7\text{E-}4$ cm/s at mid-height of the walls, and $6.9\text{E-}4$ cm/s near the bottom of the walls. For the LAW Vault, the unsaturated hydraulic conductivity was estimated as $7\text{E-}4$ cm/s near the top of the walls, and $6.3\text{E-}4$ cm/s at mid-height and at the bottom of the walls. Thus, a value of $7.5\text{E-}4$ cm/s can be taken as a worst-case assumption for the hydraulic conductivity of the vault walls.

4.4 MODEL OUTPUT

Model output can be divided into two broad classes; degradation output and structural output. Structural output for the LAW vault includes additional parameters specific to the calculation of stress and cracking in the roof slab due to curvature over the walls. Output parameters are summarized in Table 1. Output is directed to two files. One file contains a summary of all structural parameters at each print interval. In order to facilitate plotting and interpretation, the second file contains one line per print interval. Rebar stress in the first 4 spans (for example, the first wall and the first three cell roof spans) and all degradation parameters are sent to this file.

4.5 DEFINITION OF FAILURE

Failure of a vault can be defined in three ways:

- Loss of ability to resist penetration from drilling.
- Loss of ability to divert water around the vault.

- **Structural failure (collapse) of the vault.**

Resistance to drill penetration is necessary to avoid accidental intrusion after the period of institutional control, for example, from a future resident attempting to put in a drinking water well. The geology in the vicinity of the vaults, to depths of approximately 200 ft, is made up of soft sediments only. Therefore, drill equipment is not outfitted for hard rock penetration. In the event that an attempt was made to drill over the vaults, the supervising geologist would almost certainly pull up and move over until a normal amount of resistance was encountered. Even in the event that the vault was highly degraded (for example, without rebar and with the consistency of limestone), the supervising geologist would again probably decide to pull up and move. This information on drilling equipment and procedures was obtained through a phone conversation with an experienced geologist in drilling oversight at the Savannah River Site (Asquith, 1993). Thus, drill penetration of the vaults is not expected to be of concern.

Intact concrete generally has a very low hydraulic conductivity; the E-Area Vaults concrete has a hydraulic conductivity of at most 10^{-12} m/s. Therefore, virtually all of the conductivity of the degraded structure will be through fractures. Calculations by INTERA indicate that, once fractures have penetrated the roof slab, the hydraulic conductivity will be very close to that of the clay overlying the vaults, or 10^{-9} m/s. Thus, loss of ability to divert water coincides with crack penetration of the roof.

The modeling approach to collapse of the vaults has been described previously. When a vault roof collapses, the engineered soil cap will also be compromised due to subsidence of the vault roof. This, in turn, will result in a very dramatic increase in hydraulic conductivity of the vault/soil cap system.

4.6 SUMMARY OF CONSERVATIVISM

This section summarizes the conservative assumptions made and approaches taken during the development and application of the performance assessment model. One of the assumptions having the greatest impact on model results was that the concrete was at a relatively low pH (at most 9.5). This results in more rapid degradation of the structure (basically due to more rapid rebar corrosion rates), and causes the estimated service life (i.e., time to crack penetration and collapse) to be several hundred years less than that of high-pH concrete. The sulfate attack rate is based upon empirical experiments using blocks of concrete. The equation was based on the observed attack rate at the location of greatest corrosion (at the corners of the blocks). Rebar corrosion will generally proceed via either anoxic or oxic corrosion. However, because it is not known at this time which mechanism will dominate at any given time, the rates were summed to estimate the rebar corrosion rate. This is clearly conservative because the sum will be greater than either rate individually. The soil cover was assumed to be of constant depth throughout the simulation. In reality, some erosion will take place in the 1,000 to 3,000-year period simulated, resulting in less load on the vaults and therefore lower stress levels and longer service life. In the structural model,

a 1-way analysis was used. This examines the stress in a beam supported at each end (Figure 4). Because the roof is supported by four walls, a cross-section receives some support from adjacent walls as well as the walls at each end. Thus, estimated stress levels will be slightly (approximately 3%) higher than those estimated by a 2-way analysis. The structural analysis also assumed that there would be no interior support provided by the contents. Clearly, if the contents provided some support, there would be less deflection and therefore less stress in the concrete members. In examining the prestressed bridge beams in the LAW vault, a 22% loss in prestressing was assumed. This was estimated to be a maximum loss of prestress. Actual losses can be expected to be less, particularly in the first 5-10 years after release. Cracks were assumed to penetrate the ILNT and ILT vault roofs and walls, and the LAW walls, when stress in rebar reached 40 ksi. This was estimated to be a conservative estimation of when crack depth would be sufficient to penetration the concrete members. For the LAW vault roof, crack depth was based upon a calculation of the depth of the neutral axis. To add conservatism to the estimation, cracks were assumed to penetrate when the depth of the neutral axis reached within 1 inch of the bottom of the roof slab. The approach for estimating the hydraulic conductivity of the cracked concrete assumed that cracks were evenly spaced across the entire surface of the concrete. In reality, the concrete can be expected to crack in fairly localized regions. This is particularly evident in the LAW vault roof, which is expected to crack only within a less than 2-foot wide region over the walls. This assumption is not expected to have a large impact on the calculated hydraulic conductivity, however, because a few cracks are sufficient to cause large changes in hydraulic conductivity. In contrast to the model assumptions, most of the input parameters for the baseline case utilized on average or typical values. For example, all chemical concentrations in groundwater were based on average values, reaction rates were based on the midpoint of the range of values found in the literature, and roof thickness and wall height used were the average (where variation existed).

5. INPUT SUMMARY

Model input for the structural analyses are listed in Table 2 - Table 4 for the three vault types. Structural input essentially consisted of the dimensions of the vaults (wall height and thickness, roof span and thickness), the size and spacing of the rebar, the depth of cover over the rebar, the compressive strength of the concrete, and the yield strength of the rebar. The required information was obtained from the design drawings for the E-Area Vaults. A list of the drawings used is provided in Table 5.

Input required by the degradation portion of the model is listed in Table 6. Where available and applicable, ranges of values for the input parameters are presented. Input requirements include concentrations of corrosive components of the adjacent groundwater, concentrations of components in the concrete, and reaction rates.

A baseline run was defined to determine a best estimate of the times to crack penetration and failure of the three vault designs. In the baseline case, average values of environmental parameters were used (for example, sulfate concentration of the groundwater). Actual or proposed design parameters (such as rebar size or depth of soil cover) were used. Where design parameters were variable (such as roof thickness in the intermediate level vaults), average values were used.

Soil loading in the baseline case assumed a 9-foot depth of soil cover. A value of 1.7 g/cm^3 (106 lb/ft^3) was used for the density of soil. In order to calculate the self-weight of the vault roofs, a concrete density of 2.34 g/cm^3 (146 lb/ft^3) was used. Lateral soil pressure on the walls was computed using a modified Rankine approach (Das, 1985).

6. MODEL RESULTS

Figure 6 is a cross-section of the ILNT Vault after 400 years of simulated degradation. The sulfate attack mechanism has removed an average of 0.19 cm from the surface of the concrete, and the rebar radius has been reduced from 1.25 cm to 1.05 cm, from a #8 bar to a radius somewhat less than that of a # 7 bar. Figures 7 through 9 present the effective hydraulic conductivity of the three vault designs. Prior to crack penetration, the hydraulic conductivity remains that of intact concrete, 10^{-12} m/s. When cracks penetrate the roof of the vault, the hydraulic conductivity of the (cracked) concrete increases to a conductivity near that of the surrounding clay, 10^{-9} m/s, followed by a gradual increase in hydraulic conductivity as crack apertures and the number of cracks increase, up to a theoretical maximum of 10^{-9} m/s.

Table 7 and Table 8 present summaries of the rebar stress for the baseline cases of the ILT and ILNT vaults, respectively. Each column in the tables represents a particular location in the vault. In this summary presentation, rebar stresses are tabulated at each time step for which an "event" occurs, with an event defined as crack penetration at some location in the vault, or collapse of a cell. Shading in the tables indicates that cracks have penetrated at that location. A box created with thick table lines indicates the time of roof collapse for each cell.

The ILT scenario is fairly straight-forward. Maximum rebar stress occurs at mid-span in the roof, due to the fact that there is twice as much rebar in the region over the walls as there is at mid-span. Rebar stress is slightly less over the interior wall than at midspan. Thus, crack penetration occurs first at mid-span in the roof (year 790), and soon thereafter over the interior wall (year 850). Rebar stress in the walls is much less than that in the roof, primarily because the lateral soil pressure on the walls is much less than the vertical soil pressure on the roof (lateral pressure is approximately one-third that of vertical). Thus, cracks do not penetrate the center region of the wall, or mid-height of the wall, until year 1,080. The rebar stress level in the roof rebar at mid-span and over the interior wall reaches its yield strength in years 1,125 and 1,150, respectively (not shown). As moment is transferred to the remaining rebar stress point at the exterior wall, this causes a rapid increase in rebar stress levels at this point, and cracks penetrate the roof over the exterior wall at year 1,225. The rapid increase in roof rebar stress over the exterior wall continues, and collapse of the roof occurs in year 1,300. With the loss of support from the roof, it is reasonable to assume that, although rebar stress in the walls near the roof and floor have not reached the levels indicative of crack penetration, the walls at this point will also fail and collapse.

Stress patterns in the ILNT Vault are similar to those in the ILT Vault, in that the rebar stress in the roof span of the exterior cells (cells 1 and 7 of Figure 1) over the exterior wall is much less than that over the interior wall of the same cell. In the first interior cell (cells 2 and 6), this effect is mediated somewhat, and in the remaining cells the rebar stress levels

are equal over each wall for a given cell. The lower stress level over the exterior wall results in higher rebar stress levels at mid-span of the exterior cell. Thus, crack penetration occurs first at mid-span of the exterior cell (year 570), followed by the first interior wall (year 675). Next cracks penetrate over the remaining walls (year 750), followed soon thereafter by crack penetration at mid-span of the remaining cells (year 775). Cracks do not penetrate the roof over the exterior walls until year 1,000. The first cells to collapse are the first interior cells (cells 2 and 6), in year 1,045, followed soon by the remaining interior cells in year 1,075. The exterior cells collapse in year 1,125. In the ILNT vault, the walls are slightly higher than the ILT vault, so the stress levels are correspondingly greater, with the result that cracks penetrate at mid-height in year 800, and near the top of the vault in year 1,050. Stress levels at the bottom of the walls have not reached the levels indicative of crack penetration at the point at which the roof has collapsed in all cells (year 1,125).

Due to the different design and consequent different approach to the analysis, the same type of table cannot be generated to summarize the LAW vault progression through failure and collapse. While crack penetration in the walls is indicated in the same manner (i.e., rebar stress above 40 ksi) as in the intermediate level vaults, crack penetration in the roof is indicated by depth of the neutral axis. Collapse is indicated by the area of prestressed steel in the AASHTO beams dropping below a critical level. The scenario can be described as follows: Cracks penetrate the roof due to curvature over the walls in year 1,420. Next, cracks penetrate at the top, mid-height, and bottom of the walls in years 2,015, 2,235 and 2,300, respectively. Finally, prestress steel loss is sufficient to cause collapse of the roof in year 3,110.

7. SENSITIVITY ANALYSIS

There are three classes of model input that could be considered in the sensitivity analysis. First, sensitivity analysis could be conducted for physical parameters, such as water chemistry or infiltration rates, which are represented by mean values, and are used in the models for the degradation of concrete. Second, sensitivity analysis could be performed for concrete degradation model parameters, such as reaction rates for any of the various degradation reactions. Finally, sensitivity analysis could be conducted on design parameters, such as depth of soil cover, thickness of roof slab, or diameter of rebar. All sensitivity analyses were conducted by varying a single parameter from the baseline case and leaving all other parameters unchanged. This section presents the rationale behind the selection of parameters to be included in the sensitivity analysis, and the results of the analysis.

7.1 SELECTION OF PARAMETERS AND VALUES

Calcium hydroxide is one of the primary buffers that contribute to the high pH of concrete. Based on an X-ray diffraction analysis of a sample of the E-Area Vault concrete, the concrete used for the E-Area Vaults contains no calcium hydroxide. This can be explained by a combination of two factors. First, the cement used in the concrete has a very low calcium hydroxide content. Second, the concrete is designed so that the calcium hydroxide will be removed via a reaction with slag in the concrete. Calculations by Chris Langton of the Savannah River Technology Center determined that the pH of the E-Area Vault concrete is approximately 8, that it is at most around 9 to 9.5, and that it may be as low as 7. Because the E-Area Vault concrete has essentially no calcium hydroxide content and a relatively low pH, the only degradation mechanisms that apply to the concrete are oxic and anoxic ("hydrogen evolution") corrosion of rebar, and sulfate attack. While varying the parameters relevant to the sulfate attack mechanism caused noticeable changes in the amount of surface loss due to sulfate attack, the impact on steel stress was minimal. The oxic corrosion rate has a slightly greater impact on steel stress, but the anoxic corrosion rate by far dominates the rebar corrosion. Thus, for low-pH concrete in the Savannah River Site environment, the only degradation process of interest in terms of the sensitivity analysis is hydrogen evolution corrosion of rebar. This process is modeled using only one parameter, the hydrogen evolution corrosion rate. Therefore, this parameter was selected for inclusion in the uncertainty analysis. Based on a literature review, the low-pH hydrogen evolution corrosion rate was varied between $1\text{E-}3$ and $1\text{E-}4$ cm/yr, and the high-pH of hydrogen evolution corrosion between $1.5\text{E-}4$ and $1\text{E-}5$ cm/yr. It is important to note that the low-pH assumption is generally conservative, in that most degradation mechanisms proceed at higher rates in the low-pH environment. The only exception is that, with calcium hydroxide leaching, there can be some decrease in concrete strength. Since the E-Area Vault concrete has no calcium hydroxide available for leaching, the concrete strength is assumed to remain constant throughout the simulation.

A preliminary sensitivity analysis was performed to help determine parameters for which to conduct a detailed sensitivity analysis. Of the parameters included in the initial sensitivity analysis, hydrogen evolution corrosion rate (discussed above) and depth of concrete cover over rebar was selected for detailed analysis. Design constraints limited the range of allowable cover to between 1½ and 3 inch. In addition, thickness of vault roofs and numerous parameters related to degradation mechanisms were considered in the initial sensitivity analysis, but not selected for detailed analysis.

New parameters selected for detailed analysis were rebar diameter, size of AASHTO beams (LAW Vault only), concrete strength, and depth of soil cover over the vaults. Rebar diameter was varied approximately to the minimum and maximum allowable according to ACI 318. The limits varied between vaults and between walls and roofs depending on the values of the relevant design parameters. Standard AASHTO beam sizes were used in the sensitivity analysis. Because changing the size by only one increment is very significant both in cost and in strength of beam, only types III, IV, and V beams were analyzed for the sensitivity analysis. Finally, a minimum soil cover of 8 ft is required to meet performance requirements. This was varied up to a maximum of 16 ft. For all parameters, intermediate values (i.e., between the extremes and the baseline) were selected as appropriate.

7.2 OUTPUT SUMMARY

In the sensitivity analysis, the first time of crack penetration of the roof and wall of the intermediate level vaults are reported, and, for the ILNT vault, the first cell to collapse. The first crack penetration occurs at mid-span of the exterior cell (for the ILT vault, the two cells are equivalent). The first cells to collapse in the ILNT vault are the first interior cells towards each end (cells 2 and 6). Collapse in a cell is indicated when the rebar reaches yield strength at mid-span and over the adjacent walls of that cell. In cells 2 and 6, the first location at which the rebar reaches yield is at mid-span, followed by the wall towards the exterior end of the vault. Collapse, then, occurs when the rebar in the roof reaches yield strength at the remaining location, over the wall towards the interior of the vault. Thus, for the sensitivity analysis of the ILNT Vault, this is the location of interest. By observing the stress in the roof rebar at this location, the time to collapse can be determined. Similarly, for the ILT vault, the last location in the cells to reach yield strength in the rebar is over the exterior wall. Finally, crack penetration of the walls at mid-height was used to indicate crack penetration of walls.

For the LAW Vault, collapse is indicated by prestress steel in the AASHTO beams reaching a critical level. Therefore, observing changes in the area of prestress steel will provide the determination of time to collapse. Crack penetration of the roof is indicated by the neutral axis approaching to within 1 inch of the bottom of the roof slab. As in the case of the intermediate-level vaults, crack penetration at mid-height of the walls was selected to indicate crack penetration of the walls.

Thus, for each vault, three critical output parameters have been selected on which to base the sensitivity analysis of the six input parameters. The output parameters can be used to determine the time to crack penetration of the roof, time to crack penetration of the walls, and collapse of the vaults. These pivotal times are summarized for the baseline case in Table 9.

Table 10 through Table 12 summarize the same pivotal times for each sensitivity run. For the LAW Vault, differences existed in some of the parameters between the different vault components, and these differences are indicated in the left-hand column of Table 12. For example, the AASHTO beams are made of a high-pH concrete. Therefore, they will be subject to the slower, high-pH rate of hydrogen evolution rebar corrosion. Furthermore, since they are on the interior of the vault, there are no corrosive processes available to lower the pH of the beam concrete and thereby increase the reaction rate. In addition, the rebar used in the roof and walls are different. In order to understand the dynamics of the vaults in greater detail, plots of steel stress vs. time are also presented for most of the sensitivity runs.

7.2.1 ILNT Vault Sensitivity Analysis

Pivotal times (time to crack penetration of the roof, time to crack penetration of the walls, and time to collapse) for the ILNT vault are summarized in Table 10.

All pivotal times are sensitive to hydrogen evolution corrosion rate (Figures 10, 11 and 12). Varying the corrosion rate over a range of one order of magnitude changed the pivotal times by an order of magnitude as well. The change in pivotal times is very close to proportional to the ratio of the baseline corrosion rate divided by the new corrosion rate. Increasing the corrosion rate from $5E-4$ to $1E-3$ changed the time to crack penetration (of the roof) from 570 years to 285 years, a decrease of 285 years, and decreasing the corrosion rate to $1E-4$ increased the time to crack penetration to 2,775 years, an increase of over 280%. Decreasing the corrosion rate to only $2.5E-4$ almost doubled the time to crack penetration of the roof.

Altering the depth of the soil has less impact on the pivotal times (Figures 13, 14 and 15). Decreasing the soil cover from 9 ft to 8 ft increases the pivotal times by approximately 50 to 100 years. Increasing the soil cover to 12 ft decreases the pivotal times by approximately 200 years, and increasing to 16 ft decreases the pivotal times by 300 to 400 years from the baseline values.

Changing the rebar size has the potential to create large changes in the pivotal times. Reducing the bar size to #6 would result in cracks penetrating the roof immediately upon soil loading (Figure 16), and the wall after 175 years (Figure 17); collapse would occur in 425 years (Figure 18). Using a #7 instead of the present #8 would result in crack penetration of the roof after 250 years, and collapse after 735 years. Increasing the rebar size has

similarly dramatic effects. Using #9 rebar would increase the pivotal times to on the order of 1,000 years, and #11 to on the order of 2,000 years.

Depth of concrete cover over the rebar has little impact on the longevity of low-pH vaults (Figures 19, 20 and 21). Note that this statement applies to the range of 1½- to 3-inch depth of concrete cover. Further decreasing the depth of cover further could have significant effects. Also, concrete cover over rebar can have very significant impacts if high-pH concrete is used; with increased cover reducing corrosion and thus extending the service life of the vault. Stress is slightly higher with greater depth of cover, and remains so throughout the simulation. Analysis of high-pH concrete (not shown) by INTERA demonstrated that depth of concrete cover over rebar can be very important. In high-pH concrete, several diffusion-limited processes become important. The result is that rebar with greater depth of cover degrades at significantly slower rates, and therefore, in the long term, experiences lower stress levels.

Concrete strength also has little impact on the longevity of the vault (Figures 22, 23, and 24). The reason for this is that concrete has very low tensile strength, and the rebar therefore provides the majority of the tensile strength in reinforced concrete. Thus, increasing the concrete strength decreases the stress levels in the rebar only slightly. High-strength concrete provides other advantages, however, such as resistance to shear stress and reduced hydraulic conductivity.

7.2.2 ILT Vault Sensitivity Analysis

Pivotal times for the ILT Vault are summarized in Table 11. The results are qualitatively very similar to those of the ILNT vault, with quantitative differences caused by the slight differences in some of the design parameters. Again, changes in pivotal times are roughly proportional to changes in hydrogen evolution corrosion rates. At the lowest rate, cracks did not penetrate the ILT Vault prior to the end of the 3,000-year simulation (Figures 25, 26 and 27). At the minimum depth of soil cover, pivotal times decreased by approximately 50 years, and at the maximum, decreased by 300 to 400 years (Figures 28, 29 and 30). Due to the thicker roof in the ILT Vault, #6 rebar did not result in crack penetration of the roof until year 155 (Figure 31). Otherwise (Figures 32 and 33), changing rebar size had similarly dramatic effects on the ILT Vault as was the case with the ILNT vault. Due to the overall more conservative design of the ILT Vault, depth of concrete cover over rebar (Figures 34, 35 and 36) and concrete strength (Figures 37, 38 and 39) had even less impact on the ILT vault than on the ILNT vault.

7.2.3 LAW Vault Sensitivity Analysis

Pivotal times for the LAW Vault sensitivity analysis are summarized in Table 12. Figure 40 shows the location of the neutral axis as a function of time for various rates of hydrogen evolution rebar corrosion. The depth is given in terms of the distance from the interior surface of the slab. This is done for two reasons. First, at the same time that the neutral

axis is moving to lower positions in the slab, sulfate attack is removing surface material from the top of the slab. Therefore, indicating the depth of the neutral axis as a distance from the exterior could be misleading, and, at best, confusing. Second, cracks are assumed to penetrate the roof slab when the depth of the neutral axis reaches 1 inch. Thus, displaying the depth of the neutral axis in this manner provides a graphical interpretation of the time to crack penetration. In spite of the differences in design between the LAW and intermediate level vaults, and the resultant differences in the structural calculations, the changes in the time to crack penetration of the roof remain roughly proportional to the changes in the corrosion rate. Crack penetration of the LAW walls also maintains this proportionality (Figure 41).

Figure 42 shows the results of the sensitivity of time to roof collapse of the LAW vault for both hydrogen evolution corrosion rate and depth of soil. The curves represent the area of prestressed steel remaining for different hydrogen evolution corrosion rates, as a function of time. The horizontal lines indicate the area of prestressed steel required to support different depths of soil. The intersection of a curve with a line, then indicates the point in time at which collapse will occur for a given combination of corrosion rate and soil depth. To interpret the impact of hydrogen evolution corrosion rate, consider the horizontal line corresponding to the baseline soil depth (9 ft); and disregard the other horizontal lines. This line indicates the rebar area necessary to support the weight of the vault and 9 ft of soil. When a particular curve crosses that line, that point in time is the time of collapse for that hydrogen evolution rate and the baseline (9 ft) depth of soil. These are the times that are presented under "Hydrogen Evolution Corrosion Rate" in Table 12. The proportionalities is maintained here as well, but not quite as close as in the other cases. At the highest corrosion rate, collapse is predicted at 1,600 years, and, at the lowest rate, the vault did not collapse prior to the end of the 10,000-year simulation.

Because crack penetration of the roof is based upon a neutral axis calculation, and the depth of the neutral axis is not calculated as a function of loading, soil loading does not change the time to crack penetration of the roof. In reality, because increased soil loads will increase the stress level in the rebar, changing soil depth would be expected to have a small impact on the depth of cracks, and therefore on the time to crack penetration. It may appear from the graph of wall stress for different soil depths (Figure 43) that soil load has less impact on LAW walls than on the walls of the intermediate-level vaults. The absolute change, however, remains close to that of the intermediate level vaults: pivotal times are approximately 100 years greater than baseline times for the minimum depth of soil, and 200 to 300 years less for the maximum depth of soil. To examine the impact of soil depth on collapse of the vault, return to Figure 42. This time, consider the baseline hydrogen evolution rate ($8E-5$) curve only, and neglect the other curves. When the baseline curve crosses the horizontal line for a particular soil depth, that indicates the time to collapse for that depth of soil. These are the values tabulated in Table 12 under "Depth of Soil Cover" (of course, other corrosion rate/soil depth combinations can also be interpreted from this graph). Depth of soil has a much more dramatic impact on time to LAW Vault collapse than on any other pivotal time (for the LAW Vault and the intermediate level vaults). At the

minimum depth of soil, roof collapse increases by almost 200 years, and at the maximum, decreases by over 1,000 years.

Figure 44 shows the impact of changing rebar size on the time to crack penetration of the roof, using the same format as Figure 40. Because the rebar in the roof slab is close to the ACI minimum, only one increment smaller (from #6 to #5) was used in the sensitivity analysis. Again, the effects are significant, decreasing the time to crack penetration by approximately 300 years. Nevertheless, this is still several hundred years greater than the time to crack penetration of the roof in the intermediate level vaults. Increasing the rebar size also has a significant impact on the time to crack penetration of the roof. Increasing to a #8 bar increases the time to crack penetration by 600 years, and, to #14, by approximately 2,400 years. Note that, in this case, the roof will collapse due to structural failure of the AASHTO beams before cracks penetrate the roof. Changes in crack penetration of the walls (Figure 45) are similarly dramatic, with a change of approximately 300 years for every unit increment in bar size. Because roof collapse is determined by the AASHTO beams, changing the bar size in the roof slab has no impact on time to collapse.

Increasing the size of the AASHTO beams from the current Type IV to Type V will have a relatively slight impact on the depth of cracks and therefore on the time to crack penetration. This is due to the neutral axis' lack of dependence on load factors and on the moment in the AASHTO beams. Due to the decreased stress levels in the roof slab rebar (not shown), some decrease in the time to crack penetration would be expected. Decreasing to Type III beams will result in increased stress levels in the roof slab rebar, caused by increased curvature over the walls. Stress levels will be sufficient to cause cracks to penetrate the roof slab (that is, greater than 40 ksi) immediately upon soil loading. Therefore, use of smaller beams is not recommended unless spacing between beams is decreased to compensate. Figure 46 illustrates the impact of using different sized AASHTO beams on the time to collapse, using the same format as Figure 42. The curves for various hydrogen evolution corrosion rates have been retained in order to maximize the amount of information available in the graph. In Figure 46, however, the horizontal lines represent the area of prestress steel required to maintain the structure for the different sizes of AASHTO beams. Using a larger beam results in a smaller requirement in terms of the area of prestress steel required. Using the baseline hydrogen evolution corrosion rate, changing the beam size changes the time to collapse by approximately 300 to 400 years.

7.3 SUMMARY OF THE IMPACT OF DESIGN CHANGES

Within the range of values selected (3,000 to 6,000 psi), concrete strength has little impact on the service life of the vaults, due to the fact that it is predominately the rebar that resists tensile stresses. It is important to note that concrete strength has other important contributions to the vaults, such as reducing permeability and resisting shear stress. Depth of concrete cover over rebar also had little impact on the service life of the vaults. There are two significant caveats to this statement, however. First, this statement applies to the range of 1½- to 3-inch depth of concrete cover. Further decreasing the depth of cover

further could have significant effects. Second, concrete cover over rebar can have very significant impacts if high-pH concrete is used, with increased cover reducing corrosion and thus extending the service life of the vault.

Rebar size has notable impacts on the service life of the vaults. Increasing or decreasing the rebar by one increment (for example, from #8 to #9 or #7) will increase or decrease, respectively, the service life of the vaults by from 200 to 300 years. Further increments in rebar size have similar effects. This is due to the increased cross-sectional area of the rebar. Thus, increasing or decreasing the rebar spacing would be expected to have impacts of the same type and magnitude.

The size of the AASHTO bridge beams that are used for the roof system in the LAW vaults has a significant influence on serviceability. In addition to the Type IV beams now used, smaller Type III and larger Type V beams were considered for this study. It was assumed that the spacing, amount of prestress steel, and amount of prestress applied were the same for each beam type. The nominal stiffness of beams is reflected by the I value. The ratio between Type III and Type IV beams is $125,390/260,741 = 0.48$. After the 16-inch slab is cast for composite action with the girders, the relative stiffness ratios will be higher, perhaps 0.6 to 0.7. The curvature of the slab over supports will be 30 to 40% larger as the smaller girders rotate at supports more than the Type IV girders when soil is placed over the hardened slabs. Consequent cracking will result in larger and deeper cracks over supports, and probable crack penetration upon soil loading. The limit strength at midspan will be proportional to the overall depth from the top surface of the slab to the centroid of prestressed strands at midspan. As a consequence, roof collapse is predicted to occur approximately 400 years earlier if the smaller beams are used. The ratio between the nominal stiffness of Type V and Type IV beams is $521,100/260,741 = 2.0$. After the 16-inch roof slab is added, the stiffness ratio will become 1.6 to 1.8. With greater stiffness, the deeper girders will rotate at supports through smaller angles than will Type IV beams, and the curvature in the slabs will be smaller for slabs supported on deeper girders. Cracking from such smaller curvatures will be smaller and less deep than those for the slabs supported on Type IV beams, although the neutral axis calculation indicates the same depth of cracking. The time to collapse is extended by slightly over 300 years using the larger girders. In summary, the use of the smaller Type III beams is not recommended. Although some of the increased curvature could be compensated for by closer spacing of the beams, it is not likely that this will be practical, as the beam spacing is already relatively small. On the other hand, increasing the beam size will likely have only a slight impact on the time to crack penetration, and a relatively small impact on the time to collapse (increased from 3,110 years to 3,430 years, or by about 10%). Thus, the present beam size seems to be appropriate. It may be possible to alter the beam spacing, however, and retain adequate service life. Larger beam spacing would result in greater curvature and thus decrease the time to crack penetration; and, of course, decrease the time to collapse. In addition, consideration would need to be given to whether the 16-inch roof span could support the larger distance between girders, particularly as the structure degrades. Nevertheless, it

seems likely that beam spacing could be altered and the vaults still satisfy the performance criteria.

Finally, depth of soil cover has significant impacts on the service life of the vaults. Decreasing the soil cover from the assumed 9 ft to the minimum of 8 ft increased the service life of the vaults by 50 to 100 years. Increasing the soil cover to the maximum considered, 16 ft, decreased the service life by approximately 200 to 400 years. The notable exception to this is the time to collapse of the LAW Vault, which decreased by over 1,000 years when the soil cover was increased.

8. FUTURE RESEARCH AREAS

This study was limited to the roof and walls of the ILT, ILNT and LAW vault types. If cracks penetrate the roof or walls of a vault before cracks penetrate the floor, there is the potential for infiltration water to enter and accumulate in the vault, resulting in leaching of the vault contents. When the floor does crack, toxic substances could then be released. Clearly, in order to accurately assess flow out of the vaults, it is necessary to estimate the time to crack penetration of the vault floors. This should be the first priority for additional work in this area.

This project has demonstrated the ability of the model to evaluate the impact of changes in design parameters on the longevity of reinforced concrete structures. A number of other design parameters were not considered in this study due to time and budget limitations. Additional sensitivity analyses could be conducted for structural parameters such as roof thickness, rebar spacing, AASHTO beam spacing, length, width and height of the vaults, and wall thickness, as well as degradation model inputs such as oxygen diffusion rate in the concrete, leach rate, carbonation rate, or time to depassivation of the rebar.

One issue that has not been addressed in this project is the potential for loss of bonding between the concrete and rebar as the rebar degrades. Corrosion products have greater volume than the rebar, and this can result in cracking or spalling of the concrete, or other mechanisms may result in loss of bonding.

If high-pH concrete is to be considered, sensitivity analysis should be conducted for other corrosion processes as well. Figures 47 and 48 demonstrate the importance of other processes in the corrosion of high-pH concrete. Figure 47 shows a worst-case degradation scenario at 50 years after burial. Sulfate attack has caused some surface loss. Oxidic corrosion has caused the exterior face rebar to corrode at a slightly greater rate than the interior face rebar, which will remain passivated (and thus not subject to oxidic corrosion) throughout the simulation. Leaching has resulted in a low-pH zone to a depth of 5.9 cm into the concrete. At 400 years (Figure 48), the low-pH zone has encompassed the exterior face rebar. This causes the hydrogen evolution corrosion reaction to proceed at an accelerated rate, resulting in significant corrosion of the exterior face rebar. The interior face rebar, still protected from oxidic corrosion, corrodes much more slowly, at the high-pH rate of hydrogen evolution corrosion. In a low-pH concrete, both exterior and interior rebar corrode at the higher hydrogen evolution corrosion rate. Thus, the high-pH concrete has two basic differences in terms of its corrosion rates: First, there is a delay, both before the onset of oxidic corrosion (minor impact) and before the high rate of hydrogen evolution corrosion (major impact). Second, the interior rebar corrodes only at the lower rate of hydrogen evolution corrosion throughout the simulation (major impact). Because of this, carbonation (which, in some scenarios, may be the mechanism for lowering pH), leach penetration, and time to depassivation of the rebar all become important. Table 13 presents the results of a baseline analysis of baseline results for the different vault types, under the assumption that

high-pH concrete is used. This can be compared to Table 9. LAW Vault results for high-pH concrete are not presented because changes were made to the LAW approach such that the initial high-pH results are not directly comparable with the final low-pH results. With high-pH concrete, the time to crack penetration of the roof increases by approximately 600 years for both intermediate level vaults, and the time to collapse increases by approximately 800 years.

An issue that was beyond the scope of this project was the performance of the clay layer overlying the vault. It may be worthwhile to investigate whether cracks in the concrete can result in cracks in the clay. This would increase the hydraulic conductivity of the clay layer and therefore of the clay/roof system. Furthermore, the clay layer is assumed to maintain the same thickness and size over the long time frames of the simulation. The accuracy of this should be investigated, as well as the impact of changes in the clay layer on the performance of the vaults.

Other issues not addressed in this project include the long-term performance of waterstops and control joints, of waterproof coatings placed on the exterior of the vaults, and the longevity of the sealed shrinkage cracks.

Finally, the hydrogen evolution corrosion rate is a significant source of uncertainty in the model. Any work that could determine this rate with greater accuracy would decrease the uncertainty in the model predictions.

9. SUMMARY AND CONCLUSIONS

This study has demonstrated a capability to estimate the degradation of the E-Area Vault structures and to utilize information on the degraded vaults to predict the times to failure (loss of ability to divert water) and collapse of the structures. The primary source of uncertainty in the model is the rate of rebar corrosion due to the anoxic hydrogen evolution reaction, which results in uncertainty of approximately one order of magnitude.

Degradation processes considered were magnesium and sulfate attack, calcium leaching, carbonation, and rebar corrosion due to both oxygen diffusion to the rebar (including breakdown of the passivating layer that initially prevents corrosion of rebar) and due to the "hydrogen evolution" reaction. Existing empirical models for the individual degradation processes were combined into a single model to create an overall model of the degradation of reinforced concrete. The degradation processes were used to predict the condition of the concrete, including its strength, thickness and hydraulic conductivity. The evaluation of structural response to loads and other influences (e.g., slow and steady degradation of reinforced concrete) is made on the basis of the equilibrium of forces and compatibility of deformation within the structure and in the surrounding media using the RCPC computer code as a foundation. In addition, the NAVY models were used to calculate loss in prestress in the beams due to elasticity loss, creep, shrinkage and relaxation. The state of stress in the concrete was calculated and the roof components and walls fractured in order to eliminate excessive stress which cannot be borne by the degraded structure. Crack width and spacing were also computed. By combining the degradation and structural models into a single performance assessment tool, sensitivity analysis can be conducted to determine the impact both of variation in important degradation processes and of changes in design parameters on the service life of the vaults.

Structural data for each vault type was based on a review of design drawings provided to INTERA by WSRC. Relevant environmental data (such as sulfate concentration in groundwater) were obtained through the Idaho National Engineering Laboratory (INEL). Corrosion rates were based upon an extensive literature review. All structural and degradation parameters were reviewed by WSRC and INEL. Structural analysis and calculations were reviewed by an expert structural engineer who specializes in the field of design of reinforced concrete structures.

For each type of vault, sensitivity analysis was performed to bound the predictions. After an initial rough sensitivity analysis on a large number of factors, six factors were selected for detailed sensitivity analysis: rate of rebar corrosion due to the "hydrogen evolution" reaction, rebar diameter, depth of concrete cover over the rebar, size of AASHTO "bridge" beams used to support the vault roof in the LAW vault design, and depth of soil cover over the vaults, and concrete strength. Output parameters for the sensitivity analysis were the time to first crack penetration of the vault roof, time to first crack penetration of the vault walls, and time to structural failure (collapse) of the vault roof. Times to crack penetration

are important because the hydraulic conductivity increases by approximately 3 orders of magnitude (over that of intact concrete) upon crack penetration.

From the calculations in this study, we have concluded:

That concrete strength, and, for the low-pH concrete being used in the E-Area vaults, depth of concrete cover over the rebar, have little impact on the vault performance. Depth of soil cover can alter the service life of the vaults on the order of hundreds of years, and rebar size can alter the service life of the vaults on the order of hundreds to thousands of years. Changing the size of the AASHTO beams in the LAW Vaults will change the time to collapse of the vaults on the order of several hundred years. Using a smaller beam, however, is not recommended (unless beam spacing is decreased appropriately), as stress levels in the roof-slab-rebar over the walls will result in crack penetration of the roof upon soil loading.

Future work should include a similar analysis of cracking of the vault floors; in order to accurately assess flow out of the vaults, it is necessary to estimate the time to crack penetration of the vault floors. Sensitivity analyses beyond those conducted for this study could be conducted for structural parameters such as roof thickness, rebar spacing, AASHTO beam spacing, length, width and height of the vaults, and wall thickness, as well as degradation model inputs such as oxygen² diffusion rate in the concrete, leach rate, carbonation rate, or time to depassivation of the rebar. In addition, if high-pH concrete is used, additional sensitivity analysis should be conducted on degradation mechanisms important in high-pH concrete. Mechanisms that may result in loss of bonding between rebar and concrete should be investigated and quantified. In addition, performance of the clay layer overlying the vault, of waterstops and control joints, of waterproof coatings placed on the exterior of the vaults, and the longevity of the sealed shrinkage cracks all could warrant further study. Finally, any work that could determine the anoxic (hydrogen evolution) corrosion rate in rebar with greater accuracy would decrease the uncertainty in the model predictions.

This project has demonstrated the ability of the code to estimate the impact of changes in design parameters on the longevity of reinforced concrete structures. The code therefore has potential for application as a design aid tool for below-ground concrete storage facilities. The current mandate at DOE facilities to move in the direction of below-ground disposal in concrete-engineered structures makes this code a potentially important performance assessment tool.

Table 1. Summary of Output Parameters

Parameter Description	Units
Degradation Parameters	
rebar volume lost due to the oxygen-diffusion limited reaction	%
% of rebar volume lost due to the hydrogen evolution reaction	%
total loss of rebar at the exterior and interior face of the slab	% volume loss remaining diameter (cm)
depth of SO ₄ penetration	cm
Ca(OH) ₂ leach penetration via the concrete-controlled assumption	cm
Ca(OH) ₂ leach penetration via the geology-controlled assumption	cm
total leach Ca(OH) ₂ penetration	cm
depth of carbonation penetration	cm
fracture aperture	mm
fracture spacing	m
effective hydraulic conductivity	m/s
Structural Parameters	
moments at critical stress regions	ft-kip
shear at critical stress regions	kip
concrete stresses at critical stress regions	psi
rebar stress at critical stress regions	ksi
concrete cracking stress	psi
concrete shear limit stress	psi
LAW Vault Curvature Parameters	
curvature over walls	radians/in
depth of neutral axis	inch and cm
stress in rebar due to curvature	ksi

Table 2. Structural Input for the ILNT Vault

Variable	"mean"	range	justification
Spans			
wall floor to roof center	32.5 ft ⁽¹⁾	32 - 33 ft	variable roof thickness
roof center to first wall center	27 ft		
inner wall center to center	26.5 ft		
roof thickness	33 inches	27 - 39 inches	
columns			
outer wall thickness	30 inches		
inner wall thickness	18 inches		
misc			
concrete cover over rebar	2.375 inches	1.5 - 3 inches	2.375 actual on blueprint, 2-3 accepted range; may want to go to 4
exterior face bar area	1.58 in ²		
interior face bar area	.79 in ²		
concrete compressive strength	4750 psi		midpoint of minimum spec (4,000) and minimum test (5,500)
rebar yield strength	60 ksi		
degradation			
maximum spacing (outside, at stress points)	12 inches		
rebar diameter	1 inches = 2.5cm		

(1) based on 29'8" wall and 2'3" to 3'3" roof thickness

Table 3. Structural Input for the ILT Vault

Variable	baseline	range	justification
Spans			
wall floor to roof center	30.5 ft ⁽¹⁾	30.25 - 30.75 ft	variable roof thickness
roof center to first wall center	27 ft		
inner wall center to center	N.A.		
roof thickness	48 inches	42 - 54 inches	
columns			
outer wall thickness	30 inches		
inner wall thickness	18 inches		
misc			
concrete cover over rebar	2.375 inches	1.5 - 3 inches	allowable range
exterior face rebar area	1.58 in ²		
interior face rebar area	.79 in ²		
concrete compressive strength	4750 psi		midpoint of minimum spec (4,000) and minimum test (5,500)
rebar yield strength	60 ksi		
degradation			
maximum spacing (outside, at stress points)	12 inches		
rebar diameter	1 inches = 2.5cm		

(1) based on 28'6" wall and 3'6" to 4'6" roof thickness

Table 4. Structural Input for the LAW Vault

Variable	Value	Source
AASHTO I-Beams		
Length of I-beam	52'	Tindall
Top flange width	20"	Tindall
Top flange depth	11"	Tindall
Bottom flange width	26"	Tindall
Bottom flange depth	8"	Tindall
Total depth	54"	Tindall
Web width	8"	Tindall
Concrete compressive strength at 28 days	6,000 psi	Tindall
Concrete compressive strength at prestress	5,000 psi	Tindall
Eccentricity at midspan	17.13	Tindall
Eccentricity at support	12	Tindall
Ultimate strength of prestress steel	250,000 psi	Tindall
Initial prestress	202,500 psi	Tindall
Yield strength of prestress steel	240,000 psi	Tindall
Young's modulus of prestress steel	28,700,000	Tindall
Area of prestress steel	7.01 inch ²	Tindall
Number of tendons	42	Tindall
Thickness of roof panels	3"	Design drawings
Thickness of roof slab	16"	Design drawings
rebar area in roof slab	0.88 in ² /foot	Design drawings
prestress loss	22%	Tindall, confirmed by NAWY10

Table 5. Design Drawings Used

Drawing Number	Revision Number	Title
AA98143C-11-A-TC3		AASHTO BEAMS AND ROOF PANELS (BY TINDALL CONCRETE, INC.)
SE5-6-2003303	2	BURIAL GROUND EXPANSION ILT VAULT JOINTS LOCATIONS & DETAILS (U) CONCRETE
SE5-6-2003304	1	BURIAL GROUND EXPANSION ILT VAULT BASE SLAB PLANS (U) CONCRETE
SE5-6-2003305	0	BURIAL GROUND EXPANSION ILT VAULT WALLS REINFORCING ELEVATIONS CONCRETE
SE5-6-2003306	0	BURIAL GROUND EXPANSION ILT VAULT WALLS SECTIONS & DETAILS CONCRETE
SE5-6-2003307	0	BURIAL GROUND EXPANSION ILT VAULT WALLS & CRANE RUNWAY PLAN AND SECTIONS CONCRETE
SE5-6-2003308	2	BURIAL GROUND EXPANSION ILNT VAULT JOINTS LOCATIONS & DETAILS (U) CONCRETE
SE5-6-2003309	0	BURIAL GROUND EXPANSION ILNT VAULT BASE SLAB PLANS CONCRETE
SE5-6-2003310	1	BURIAL GROUND EXPANSION ILNT VAULT WALLS REINF'G ELEVATIONS (U) CONCRETE
SE5-6-2003311	1	BURIAL GROUND EXPANSION ILNT VAULT WALLS SECTIONS & DETAILS (U) CONCRETE
SE5-6-2003315	0	BURIAL GROUND EXPANSION ILT VAULT PERMANENT ROOF SLAB PLAN & SECTIONS (FUTURE) CONCRETE

Drawing Number	Revision Number	Title
SE5-6-2003317	0	BURIAL GROUND EXPANSION ILNT VAULT PERMANENT ROOF SLAB PLAN & SECTIONS (FUTURE) CONCRETE
SE5-6-2003318	2	BURIAL GROUND EXPANSION ILT & ILNT VAULTS GENERAL NOTES AND LEGEND (U) CONCRETE
SE5-6-2008800	1	BURIAL GROUND EXPANSION LAW VAULT JOINTS LOCATIONS & DETAILS CONCRETE
SE5-6-2008801	1	BURIAL GROUND EXPANSION LAW VAULT GENERAL NOTES AND LEGEND CONCRETE
SE5-6-2008802	0	BURIAL GROUND EXPANSION LAW VAULT FOUNDATION, SLAB & ROOF FRAMING KEY PLANS CONCRETE
SE5-6-2008803	1	BURIAL GROUND EXPANSION LAW VAULT FOUNDATION & FLOOR SLAB PLAN - MODULE 1 CONCRETE
SE5-6-2008806	0	BURIAL GROUND EXPANSION LAW VAULT ROOF FRAMING & SLAB PLAN - MODULE 1 CONCRETE
SE5-6-2008809	0	BURIAL GROUND EXPANSION LAW VAULT WALLS ELEVATIONS SHEET 1 CONCRETE
SE5-6-2008810	1	BURIAL GROUND EXTENSION LAW VAULT WALLS ELEVATIONS SHEET 2 CONCRETE
SE5-6-2008811	0	BURIAL GROUND EXPANSION LAW VAULT WALLS ELEVATIONS SHEET 3 CONCRETE
SE5-6-2008812	1	BURIAL GROUND EXPANSION LAW VAULT WALLS SECTIONS & DETAILS SHEET 1 CONCRETE

Drawing Number	Revision Number	Title
SE5-6-2008813	1	BURIAL GROUND EXPANSION LAW VAULT WALLS SECTIONS & DETAILS SHEET 2 CONCRETE
SE5-6-2008814	1	BURIAL GROUND EXPANSION LAW VAULT WALLS SECTIONS & DETAILS SHEET 3 (FUTURE) CONCRETE
SE5-6-2008815	1	BURIAL GROUND EXPANSION LAW VAULT WALLS SECTIONS & DETAILS SHEET 4 CONCRETE
SE5-6-2008816	0	BURIAL GROUND EXPANSION LAW VAULT ROOF FRAMING & SLAB SECTIONS & DETAILS CONCRETE
SE5-6-2008817	0	BURIAL GROUND EXPANSION LAW VAULT PRESTRESSED ROOF BEAMS SECTIONS & DETAILS CONCRETE
W2017824	C	BURIAL GROUND EXPANSION ILT, ILNT & LAW VAULTS CLOSURE CONCEPT SITE PLAN CIVIL
W2017825		BURIAL GROUND EXPANSION ILT & ILNT VAULTS CLOSURE CONCEPT SITE CROSS SECTIONS CIVIL
W2017826	B	BURIAL GROUND EXPANSION LAW VAULTS CLOSURE CONCEPT SITE CROSS SECTIONS CIVIL
W2017827		BURIAL GROUND EXPANSION ILT & ILNT VAULTS CLOSURE CONCEPT PLAN AND SECTIONS CIVIL
W2017828	B	BURIAL GROUND EXPANSION LAW VAULTS CLOSURE CONCEPT PLAN & SELECTIONS CIVIL
W2020320	1	BURIAL GROUND EXPANSION ILT VAULT CRUCIBLE SILOS PLAN AND SECTIONS CONCRETE

Drawing Number	Revision Number	Title
W2020372	B	BURIAL GROUND EXPANSION LAW VAULTS CONSTRUCTION STRATEGY SITE CROSS SECTIONS CIVIL
W2020422	1	BURIAL GROUND EXPANSION ILT VAULT CRUCIBLE SILOS DETAILS CONCRETE

Table 6. Summary of Degradation Model Variables and Values

Variable	Definition	Scenario	Min/ Mean/ Median/ Maximum	Reference
Hydrogen Evolution Rebar Corrosion				
H2RATE1	Rate of rebar corrosion due to hydrogen evolution (cm/yr) at high pH (before calcium leaching or carbonation penetrate to rebar).	Minimum	1E-5	(6)
		Baseline	8E-5	(6)
		Maximum	1.5E-4	(6)
H2RATE2	Rate of rebar corrosion due to hydrogen evolution (cm/yr) at low pH (after calcium leaching or carbonation penetrate to rebar).	Minimum	1E-4	(6)
		Baseline	5E-4	(6)
		Maximum	1E-3	(6)
Chloride Initiation of Oxygen-based Rebar Corrosion				
COV	Required clear cover over bars (cm).	Minimum	7.62	design drawings
		Baseline	6.03	design drawings
		Maximum	5.08	design drawings
CLSOIL	Chloride ion concentration in groundwater (ppm).	Minimum	0.44	(1), p.2
		Baseline	1.3	(1), p.2
		Maximum	5.3	(1), p.2

WCR	Water to cement ratio (kg/kg).	Minimum	0.40	Assumed
		Baseline	0.44	(2), p.4
		Maximum	0.48	Assumed
Oxygen Corrosion of Rebar				
COV	Required clear cover over bars (cm).	Minimum	7.62	design drawings
		Baseline	6.03	design drawings
		Maximum	5.08	design drawings
O2DICONC	Oxygen diffusion coefficient in concrete (cm ² /s).	Minimum	2E-8	(1), p.4; from (2)
		Baseline	1E-7	(2), p.4
		Maximum	2E-6	(2), p.4
O2SOIL	Oxygen concentration in groundwater (mole/cm ³).	Minimum	1.25E-7	(1), p.4
		Baseline	2.47E-7	(1), p.4
		Maximum	3.125E-7	(1), p.4
Concrete-Controlled Leaching				
CADICONC	Intrinsic diffusion coefficient of Ca++ in concrete (cm ² /s).	All	1E-7	(2), p.4

CASOIL	Ca++ concentration in ground-soil water (mole/cm³).	Minimum	4.82E-7	(1), p.7
		Baseline	2.35E-8	(1), p.7
		Maximum	2.5E-9	(1), p.7
CASOLID	Bulk Ca++ concentration in concrete solid (mole/cm³).	Minimum*	0.0035	(2), p.4
		Baseline*	0.003	(2), p.4
		Maximum*	0.0025	(2), p.4
Geology-Controlled Leaching				
CADICONC	Intrinsic diffusion coefficient of Ca++ in concrete (cm²/s).	All	1E-7	(2), p.4
CAPORE	Ca++ concentration in concrete pore liquid (mole/cm³).	All	2.7E-6	(2), p.4
CASOIL	Ca++ concentration in ground-soil water (mole/cm³).	Minimum	4.82E-7	(1), p.7
		Baseline	2.35E-8	(1), p.7
		Maximum	2.5E-9	(1), p.7
CASOLID	Bulk Ca++ concentration in concrete solid (mole/cm³).	Minimum*	0.0025	(2), p.4
		Baseline*	0.003	(2), p.4
		Maximum*	0.0035	(2), p.4
DE	Effective dispersivity/diffusivity of Ca in geologic material (cm²/s).	Minimum	1E-6	(2), p.5
		Baseline	2E-6	(2), p.5
		Maximum	3E-6	(2), p.5

RD	Retardation factor of Ca in geologic material (ml/cm³).	Minimum	2	(2), p.4
		Baseline	3	(2), p.4
		Maximum	5	(2), p.4
Carbonation				
CODICONC	Diffusion coefficient of CO ₂ in concrete (cm²/s)	all	1E-7	(2)
CSOIL	Inorganic carbon content in the soil (mole/cm³)	minimum	1.88E-7	(7)
		baseline	4.33E-7	(7)
		maximum	6.78E-7	(7)
CAOHCONC	Ca(OH) ₂ concentration in concrete (mole/cm³)	minimum	0.0072	(2)
		baseline	.001485	average
		maximum	0.00225	(2)
Sulfate Attack				
C3A	C3A content in concrete (weight %; e.g. 8 for 8%).	minimum	7	assumed
		baseline	8	(1), p.6; (2), p.4
		maximum	9	assumed
SO4MGSOL	Sum of SO4 and Mg concentrations in soil solution (mole/l).	minimum	1.51E-5	(1), p.6
		baseline	1.08E-4	(1), p.6
		maximum	3.77E-4	(1), p.6

- (1) Dicke, 1993.
- (2) Walton and Dicke, 1993.
- (3) Walton, Plansky, and Smith, 1990.
- (4) Walton, J.C. 1993. Unpublished.
- (5) Langton, Chris. 1993. Personal communication.
- (6) Summarized from Grauer, *et al.*, 1991, Hansson, 1985, Marsh and Taylor, 1988, and Morley, 1986.
- (7) Seitz, 1993.
- * CASOLID acts in opposite directions for geology-controlled and concrete-controlled leaching; therefore it is not possible to maximize or minimize both leach rates in the same simulation run.

Table 7. Summary of Rebar Stress (ksi) in ILT Baseline Scenario

Time (years)	Walls			Roof Spans		
	Bottom	Mid-Height	Top	Over Exterior Wall	Mid-Span	Over Interior Wall
800	14.2	27.9	16.9	16.9	40.8	38.1
850	15.1	29.6	18.0	18.0	43.3	40.4
1,100	20.9	41.0	24.9	24.9	59.8	56
1,225	25.3	49.3	30.0	44.0	60.0	60.0
1,300	28.5	55.6	33.9	61.4	60.0	87.4

Table 8. Summary of Rebar Stress (ksi) in ILNT Baseline Scenario

Time (years)	Walls			Exterior Cell			First Interior Cell			Central Cells ⁽¹⁾		
	Bottom	Mid-Height	Top	Over Exterior Wall	Mid-Span	Over Interior Wall	Over Wall Towards Exterior	Mid-Span	Over Wall Towards Interior	Over Wall	Mid-Span	Over Wall
575	16.0	31.3	23.4	23.4	40.3	36.7	36.2	33.1	33.9	33.9	33.1	33.9
675	17.8	34.8	25.9	25.9	44.7	40.7	40.1	36.8	37.6	37.6	36.8	37.6
750	19.3	37.8	28.1	28.1	48.6	44.1	43.6	39.9	40.8	40.8	39.9	40.8
775	19.8	38.9	28.9	28.9	50	45.4	44.8	41.1	42.0	42.0	41.1	42.0
800	20.4	40.0	29.8	29.8	51.4	46.7	46.1	42.3	43.2	43.2	42.3	43.2
1,000	26.1	51.2	38.1	41.0	60.0	60.0	58.9	54.1	55.2	55.2	54.1	55.2
1,050	27.9	54.7	40.7	49.4	60.0	60.0	62.0	60.0	61.0	59.0	57.8	59.0
1,075	28.8	56.6	42.1	54.9	60.0	60.0				61.8	60.0	61.8
1,125	31.4	60.0	45.6	65.1	60.0	79.9						

(1) "Central Cells" refers to cells 3, 4, and 5 in Figure 1.

Table 9. Summary of Baseline Results

Vault	Cracks Penetrate Roof (years)	Cracks Penetrate Walls (Mid-Height) (years)	Roof Collapse (years)
ILNT	570	800	1,045
ILT	790	1,080	1,300
LAW	1,420	2,235	3,100

Table 10. Summary of ILNT Vault Sensitivity Analyses

Scenario	Cracks Penetrate Roof	Cracks Penetrate Walls (Mid-Height)	Roof Collapse
Baseline	570	800	1,045
Hydrogen Evolution Corrosion Rate (Baseline = 5E-4 cm/yr)			
1E-3	285	400	525
7.5E-4	380	535	700
2.5E-4	1,130	1,590	2,075
1E-4	2,775	3,000+	3,000+
Depth of Soil Cover (Baseline = 9 feet)			
8 feet	680	850	1,130
12 feet	400	590	925
16 feet	130	360	725
Rebar Size (Baseline = #8)			
#6	0	175	425
#7	250	485	735
#9	875	1,105	1,350
#11	1,785	1,965	2,150
#18	3,000+	3,000+	3,000+
Depth of Concrete Cover Over Rebar (Baseline = 2 3/8")			
1 1/2"	600	825	1,060
3"	550	780	1,030
Concrete Strength (Baseline = 4,750 psi)			
3,000 psi	570	800	1,040
6,000 psi	570	800	1,045

A "+" indicates that the event did not occur prior to the end of the simulation.

Table 11. Summary of ILT Vault Sensitivity Analyses

Scenario	Cracks Penetrate Roof	Cracks Penetrate Walls (Mid-Height)	Roof Collapse
Baseline	790	1,080	1,300
Hydrogen Evolution Corrosion Rate (Baseline = 5E-4 cm/yr)			
1E-3	395	535	655
7.5E-4	525	725	865
2.5E-4	1,560	2,155	2,565
1E-4	3,000+	3,000+	3,000+
Depth of Soil Cover (Baseline = 9 feet)			
8 feet	850	1,140	1,340
12 feet	625	940	1,180
16 feet	415	735	1,035
Rebar Size (Baseline = #8)			
#6	155	460	680
#7	470	770	985
#9	1,190	1,380	1,600
#11	1,950	2,185	2,340
#18	3,000+	3,000+	3,000+
Depth of Concrete Cover Over Rebar (Baseline = 2 3/8")			
1 1/2"	800	1,100	1,300
3"	775	1,075	1,290
Concrete Strength (Baseline = 4,750 psi)			
3,000 psi	790	1,080	1,300
6,000 psi	790	1,080	1,300

A "+" indicates that the event did not occur prior to the end of the simulation.

Table 12. Summary of LAW Vault Sensitivity Analyses

Scenario	Cracks Penetrate Roof	Cracks Penetrate Walls			Roof Collapse
		Top	Mid-Height	Bottom	
Baseline	1,420	2,015	2,235	2,300	3,110
Beam/Roof & Walls	Hydrogen Evolution Corrosion Rate (Baseline = 8E-5/5E-4 cm/yr)				
1.5E-4/1E-3	710	1,010	1,150	1,150	1,600
1.15E-4/7.5E-4	950	1,350	1,550	1,550	2,100
4.5E-5/2.5E-4	2,820	4,000	4,480	4,550	5,400
1E-5/1E-4	6,900	9,750	10,000+	10,000+	10,000+
Depth of Soil Cover (Baseline = 9 feet)					
8 feet	1,420	2,100	2,360	2,410	3,290
12 feet	1,420	1,900	2,185	2,235	2,610
16 feet	1,420	1,730	2,050	2,115	2,060
Walls/Roof Slab	Rebar Size (Baseline = #10/#6)				
#7/#5	1,120	1,100	1,325	1,400	3,110
#9/-	-	1,700	1,940	2,000	3,110
#14/#8	2,020	(3,150)	(3,410)	(3,450)	3,110
#18/#14	(3,800)	(4,440)	(4,710)	(4,750)	3,110
AASHTO Beam Size (Baseline = Type IV)					
Type III	0	2,015	2,235	2,300	2,700
Type V	1,420	2,015	2,235	2,300	3,430
Depth of Concrete Cover Over Rebar (Baseline = 2 3/8")					
1 1/2"	1,420	2,015	2,250	2,300	3,110
3"	1,415	2,015	2,250	2,300	3,110
Concrete Strength (Baseline = 4,750 psi)					
3,000 psi	1,420	2,015	2,235	2,300	3,110
6,000 psi	1,420	2,015	2,235	2,300	3,110

A "+" indicates that the event did not occur prior to the end of the simulation.
 Values in parentheses () indicate that roof collapse will occur prior to the indicated crack penetration.

Table 13. Summary of Baseline Results Assuming High-pH Concrete

Vault	Cracks Penetrate Roof (years)	Roof collapse (years)
ILNT	1,200	1,840
ILT	1,375	2,225
LAW	Not Available	

REFERENCES

- Asquith, S. 1993. Personal Communication. Conversation June 29, 1993 between Jim L. Lolcama of INTERA, Inc. and Shawn Asquith of Rust E and I.
- Atkinson, A. and Hearne, J.A. 1984. "An Assessment of the Long-Term Durability of Concrete in Radioactive Waste Repositories". AERE-R11465, Harwell, UK.
- Crank, J. 1975. *The Mathematics of Diffusion*. Oxford University Press, Oxford.
- Das, B.M. 1985. *Principles of Geotechnical Engineering*. PWS Puvliahwea, Boston, MA. 571p.
- Dicke, C. 1993. FAX of 3/29/93.
- Furlong, R.W. 1991. *Reinforced Concrete Personal Computer Design Handbook*. Prince, Davidson, & Wilson. Austin, TX. 77 pages.
- Furlong, R.W. 1993. "Uniform Loading of Rectangular Flat Plates." Unpublished correspondence, June 3, 1993.
- Grauer, P., Knecht, B., Kreiss, P. and Simpson, J.P. 1991. "Hydrogen Evolution from Corrosion of Iron and Steel in Intermediate Level Waste Repositories." *Material Research Society Symposium Proceedings* 212:295-302.
- Hansson, C.M. 1985. "The Corrosion of Steel and Zirconium in Anaerobic Concrete." *Material Research Society Symposium Proceedings* 50:475-482.
- Harrison, W.H. and Teychenne, D.C. 1981. *Sulphate Resistance of Buried Concrete: Second Interim Report on Long Term Investigation at Northwick Park*. Building Research Establishment, Her Majesty's Stationery Office, London.
- Marine, I.W. 1976. *Geochemistry of Groundwater at the Savannah River Plant*. DP-1356. September, 1976. E. I. du Pont de Nemours and Company, Savannah River Laboratory, Aiken, SC.
- Marsh, G.P. and Taylor, K.J. 1988. "An Assessment of Carbon Steel Containers for Radioactive Waste Disposal." *Corrosion Science* 28.3:289-320.
- McEnroe, B.M. 1993. "Maximum Saturated Depth Over Landfill Liner." *Journal of Environmental Engineering* 119.2.
- Morley, J. 1986. "Corrosion of Steel Foundation Caissons from the Old Redheugh Bridge in Newcastle upon Tyne." *British Corrosion Journal* 21.3:177-183.

- Nawy, E.G. 1989. *Prestressed Concrete Computer Programs in BASIC*. Prentice Hall. New Jersey.
- Seitz, R.R. 1993. FAX of March 22, 1993.
- Tindall Concrete. 1993. "Design Calculations for LAW Vault Expansion Modules Two and Three. Prepared for the United States Department of Energy, Savannah River Site. February 12, 1993, P.O. AA98143C, Project S-2890/4466, Job No. 52-106.
- Walton, J.C. 1993. "E-Area Vault Effective Permeability and Reinforcement Corrosion". Unpublished correspondence, July 6, 1993.
- Walton, J.C. 1993. "Degradation of Reinforced Concrete." Unpublished.
- Walton, J.C. and Dicke, C. 1993. "E-Area Notebook for ILNT/ILT Vaults: Degradation Calculations, (4-13-93) latest mix design data."
- Walton, J.C., Plansky, L.E. and Smith, R.W. 1990. *Models for Estimation of Service Life of Concrete Barriers in Low-Level Radioactive Waste Disposal*. Idaho National Engineering Laboratory. NUREG/CR-5542, EGG-2597.

ACRONYMS AND ABBREVIATIONS

ACI	American Concrete Institute
cm	centimeter
C ₃ A	tri-calcium aluminate
EAV	E-Area Vaults
ft	feet
in	inch
ILNT	intermediate-level non-tritium
ILT	intermediate-level tritium
INEL	Idaho National Engineering Laboratory
kip	1,000 pounds
ksi	1,000 pounds per square inch
LAW	low-activity waste
LLWSB	Long-Lived Waste Storage Building
m	meter
mm	millimeter
ppm	parts per million
psi	pounds per square inch
s	second
SRS	Savannah River Site
WSRC	Westinghouse Savannah River Company
yr	year

APPENDIX: QUALITY ASSURANCE

This Appendix is divided into three parts. First, the implementation of the Project Quality Assurance Plan is discussed. Next, the letter report describing INTERA's plan and procedures for software and technical reporting quality assurance for the E-Area Vaults Degradation Study is provided. Finally, forms used in maintaining Quality Assurance Control during the project are provided.

A.1 IMPLEMENTATION OF THE PROJECT QUALITY ASSURANCE PLAN

The RCPC.DHelper models (Furlong, 1991) used as the basis for the structural analysis portion of this study are available commercially through the American Concrete Institute Software Sales Department. The programs have been in use for the past 4 years by approximately 300 engineering offices.

The RCPC computer software for the analysis of reinforced concrete structures has formed the basis for this project. This software has been validated by the author. The software is divided into five main subroutines which do not interact, with each subroutine appropriate for a particular application. For the E-Area Vaults, the "Continuous Beams" program was utilized. This program was tested by using a sample data set available in the manual (Furlong, 1991), and comparing the computed results with results printed in the manual. All results were identical. Another program, NAWY10, was used to analyze the time-dependant loss of prestress in the AASHTO beams. In the same way, a sample data set available in the manual (Nawy, 1989) was used for testing the program. Computed results matched results printed in the manual.

There were four main revisions to the RCPC code:

1. Original program was designed for screen-based input and output. In order to facilitate the multiple runs necessary for the sensitivity analysis and calculation of stress levels through time, the program was modified to utilize file-based input and output.
2. Degradation subroutine was added.
3. A time loop was added to recursively calculate the vault condition through time.
4. For the LAW vault case, a section was added to compute the stress due to curvature and the depth of the neutral axis in the roof slab.

After the code was modified to utilize file-based input and output, an additional test was performed using the manual-supplied input and output. In addition, a data set was created appropriate for the E-Area Vaults. This data set was run in both the original model and in the modified model. Again, all results were identical.

Next the degradation subroutine and time loop were added. Degradation model components included:

- Time to depassivation of rebar.
- Oxidic corrosion of rebar.
- Anoxic ("hydrogen-evolution") corrosion of rebar.
- Sulfate attack.
- Calcium hydroxide leaching.
- Carbonation.
- Calculation of fracture aperture and spacing.

Testing of this modification consisted of two phases. First, results of the degradation model were compared to results obtained by modeling performed at INEL. There were extremely slight differences between INEL model results and INTERA results, easily attributed to rounding error. Next, testing was performed on the structural component of the code. The time zero results for the code were compared to the results obtained from the unmodified RCPC code. Because no degradation has taken place at time zero, these results should be, and were, the same. For the LAW vault modifications to calculate stress due to curvature in the roof, testing was performed by comparing model results to spreadsheet calculations.

All changes are documented in detail within the modified code, both at the point of modification and, in chronological order, at the top of the code.

Performance and Design Specifications were generated for the modifications to the RCPC.DHelper code, in order to incorporate concrete degradation, and were established as controlled documents (i.e., they were approved by the program manager and quality assurance manager and had a control date assigned). Performance and Design Specifications for RCPC.DHelper and NAWY10 were taken from the documentation for these codes and established as controlled documents. Performance Specifications for both acquired codes and modifications included the following components:

- a general description of RCPC.DHelper, NAWY10, and modifications to the RCPC.DHelper code, and the intended use of information expected from the codes, including relevant contract specifications.
- a description of physical and chemical phenomena accounted for and any important phenomena neglected.
- statement of relevant mathematical equations and derivations.

- statement and rationalization of applicable assumptions, limitations and simplifications.
- a general description of the type of output information.
- a general description of the type of input information.
- references.

Design Specifications for both acquired codes and modifications included the following components:

- Description of numerical techniques used to solve governing equations.
- Statement of relevant discretized (or otherwise transformed for numerical solution) equations and derivations.
- Statement and rationalization of applicable assumptions and limitations.
- Description of the structure and organization of the computer programs, including logic flow.
- Description of program input and output.
- Description of code/system interfaces.
- Glossary of model variables.

RCPC.DHelper and NAWY10 software was baselined (i.e., entered into the Control File Index at our Austin, TX headquarters). Modifications to software were identified, documented, and tracked through the Control File Index. All data and results which were used in formal code testing and applications were baselined. The project report was baselined and subjected to internal (i.e., within INTERA) review before being submitted to WSRC. The review was documented in the form of required changes, recommended changes and other observations, in writing on a copy of the draft document. After changes were made in response to the internal review, the report was again baselined and submitted to WSRC with the subtitle "Draft Report." All comments in response to WSRC review were received verbally only. Therefore, INTERA prepared a memo summarizing the review comments and distributed copies to WSRC and to the Control File Index at INTERA headquarters. After response to WSRC comments was completed, the report was again baselined and submitted to WSRC as the final report for this Task #7.

A.2 PROJECT QUALITY ASSURANCE PLAN

Mr. Shawn Reed
WSRC
Savannah River Technology Center
Solid Waste Engineering
#742-7G
Aiken, SC 29802

May 20, 1993

Re: Quality Assurance Procedures for Software and Technical Reports Under Contract #AA20180P-Task Order 7

Dear Mr. Reed:

The following letter report describes INTERA's plan and procedures for software and technical reporting quality assurance for the E-Area Vaults Degradation Study. This letter report is intended to satisfy Paul Lowe's request at the May 10 status meeting for a summary QA plan for the structural analysis software currently being used on this project and report deliverables. Software for this project has been developed primarily outside of INTERA. The software is two structural analysis codes for concrete structures obtained from the University of Texas at Austin and Rutgers University. Through a co-operative effort between the code authors and INTERA-AUGUSTA the codes are currently being modified to allow, (1) input of concrete thickness and re-bar spacing, (2) the use of file handling for input and output rather than the interactive default mode, and (3) chemical degradation of the reinforced concrete.

The QA plan and procedures for computer software and report deliverables have been taken from INTERA's Project Quality Assurance Manual prepared for the Westinghouse Savannah River Company (Draft; December 20, 1990). This NQA-1 manual has been submitted for approval with WSRC, however this approval is pending. We anticipate a review of the manual prior to the end of the current fiscal year.

PART A PROJECT QUALITY ASSURANCE PLAN

Quality assurance calls for baselining software and supporting documentation through the assignment of Control Identification Numbers (CIN's) and entry into the project Control File Index (CFI). The QA plan requires, for codes developed outside of INTERA, review, verification, validation (when possible) and documentation of software modification activities. Changes to baselined software shall also be identified and tracked through the CFI and shall be subject to review, approval, verification and validation as appropriate. Changes to baselined software shall require documentation and this documentation shall be entered into the CFI. In addition, procedures for the revision of baselined software shall require

identification of any baselines which might require changes as a result of the revision, and that users of affected software be notified of any revisions.

INTERA shall verify the suitability of previously developed computer codes by:

1. Reviewing previous applications of the code(s);
2. Performing a validation of the code(s) for the contract application by inputting data representative of the application;
3. Exercising the code(s) under expected use conditions; and
4. Evaluating the limitations of the code(s).

Results of the validation process shall be documented and entered into the project CFI. A summary report of the results shall be provided to the client.

The structural analysis code(s) adapted for this project are considered proprietary to the author, Dr. Richard Furlong, University of Texas at Austin and Dr. Edward Nawy, Rutgers University. The source code and documentation have been provided to INTERA for adaptation and use on this project without cost to WSRC.

PART B PROJECT QUALITY ASSURANCE PROCEDURES

TITLE: QA Control File and Index

The INTERA - AUGUSTA staff will be responsible for preparing and documenting records that will enter the QA Control File at our Corporate Headquarters in Austin. We will also be responsible for filing QA documents and documentation of client communications with the QA Administrator in Austin.

The INTERA - AUSTIN QA Administrator will be responsible for reviewing control documents, maintaining proper records storage, and maintaining the Control File Index.

TITLE: Baselining and Revising Baselined Specifications

Performance, Design, and Test Specifications shall be baselined for the major codes acquired and applied on this project.

When revising a code, Performance, Design, and Test Specifications shall be developed, baselined, and established as controlled documents (i.e., be approved by the program manager and quality assurance manager and have a control date assigned).

An example of a QA Control Document which shall be completed for Specifications has been included as an attachment.

TITLE: Baselineing and Revising Baselined Codes

All structural analysis codes shall be documented following acquisition for the project and during modification and testing. The documentation of the unmodified code(s) shall include: Test Data, Test Results, Validation History (if any), Code Abstract and Users Manual. Modifications which are completed by INTERA-AUGUSTA to the codes to allow, (1) the use of file handling for input and output rather than the interactive default mode, and (2) chemical degradation of the reinforced concrete will be documented with brief performance specifications, design specifications, and a comparison of the code output with empirical results from INEL.

In addition, each code should be accompanied by the following documentation, as appropriate: Code Name and Version Number, Brief Description of Code, Original Source Code and Original Author(s), Brief History of Major Modifications, Proprietary Details, Disclaimer, Language and Level, Machine Where Operative, and References.

An example of a QA Control Document which shall be completed for Computer Codes has been included as an attachment.

TITLE: Baselineing and Revising Baselined Test, Application and Other Data

All data which are to be used in formal (i.e., documented) code testing or in code applications shall be baselined. Data should be characterized in detail. The documentation should include, at a minimum, the following: source and method of acquisition, appropriateness for the intended model application, and derivation of input data (processed data) from raw data.

All test and application data baselines shall be written to diskette with copies furnished to the QA Administrator.

Baseline data shall be revised as necessary to correct problems or to improve/ensure quality. Revised baselines shall include justification for the revision.

An example of a QA Control Document which shall be completed for Test/Application/Other Data has been included as an attachment.

TITLE: Baselineing and Revising Baselined Test Results

All output data from the code testing phase shall be baselined. Testing of the unmodified structural analysis codes shall be limited to execution of the test problem provided with the code on the PC with which the structural analysis is to be completed. A formal review by the project engineer of the Test Results shall be completed to ensure the accuracy of the installed code.

Testing of the code modifications concerning deterioration of the reinforced concrete shall be limited to accurate reproduction of empirical data provided by INEL. Formal testing shall be reviewed by person(s) not involved in the modification of the code(s). Test Results shall be analyzed for satisfaction of Test Specifications.

The Test Results, and the analyses thereof, must be documented and baselined. A print-out of the Test Results and the Test Data shall be filed with the QA Administrator when Results are baselined.

An example of a QA Control Document which shall be completed for Test/Application Results has been included as an attachment.

TITLE: Baselineing Application Results

The results of all code applications to be transmitted outside of, or relied upon by, INTERA or which yield significant information about the code's capabilities or limitations, or about measured data, or about the system or process being modeled shall be baselined.

Where possible input data should be printed in conjunction with the corresponding Application Results output. A copy of the Application Results and Application Data shall be filed with the QA Administrator when results are baselined.

TITLE: Baselineing and Revising Baselined Technical Reports and Code Documentation

All Reports which are considered deliverables shall be baselined before transmission outside of INTERA. Code Documentation shall be baselined for internal control. For proprietary reasons, these Baselines will not be allowed outside of INTERA.

Topical Reports and Letter Reports which are specified as contract deliverables shall undergo formal technical review. Baselined reports shall be revised as necessary to correct problems, improve quality, or expand scope.

An example of a QA Control Document which shall be completed for Report/Code Documentation has been included as an attachment.

TITLE: Technical Reviews

Each Technical Report, Model Documentation Report, Letter Report, or other document containing technical information that is a project deliverable prepared to satisfy contract requirements shall be the subject of one of more technical reviews before being transmitted outside INTERA.

Documents and data shall be baselined before being submitted for technical review.

Reviews of reports and other documents should consider, as a minimum, the following items:

- Organization, clarity, and conciseness of the material presented;
- Correctness of any assumptions that are made;
- Adequacy of the discussion of variables;
- Validity of the conclusions and recommendations;
- Adequacy of illustrations, graphs, tabular data, etc.; and
- Appropriate acknowledgement of contributions and referenced material.

Reviews shall be documented with written comments in the form of required changes, recommended changes, and other observations. The review shall also document the material being reviewed (title or description), the author of the material, date of the review, and persons performing the review.

Review comments must be stated in terms which will clearly convey the meaning of the comment to others knowledgeable on the subject.

Review comments may be in the form of annotations on the document being reviewed if the comment can be adequately recorded in this manner. When such annotation is inadequate or inappropriate, the comment(s) shall be recorded on separate sheets.

Each review comment shall be responded to and resolved and the response/resolution shall be documented. When review comments are recorded on the document being reviewed, responses may also be recorded on the document.

All review comments recorded on separate sheets shall be responded to either on the review sheets or on separate sheets.

Editorial recommendations may be acknowledged in summary fashion, e.g., "implemented where possible".

When the technical reviewer is unable to accept the task manager's response to one or more required changes, the program manager shall be called upon to resolve the issue unless the program manager is involved in the disagreement, in which case one of the program manager's peers shall resolve the issue.

An example of a QA Control Document which shall be completed for Technical Reviews has been included as an attachment.

cc: Paul Lowe
Jim Cook
Keith Dykes

YY MM DD

Control Date (QAAA Only):

--	--	--
----	----	----

SPECIFICATION BASELINE

- ☐ Original Baseline (Complete Section 1 only)
- ☐ Revision to Previous Baseline (Complete Sections 1 and 2)

Project Title:

Project Number:

Contract No.:

CFI Description: _____

Section 1 - Baseline

1. Code Name: _____ Code CIN: _____

2. Source (Check one and complete):

This ☐ baseline ☐ revision was developed by: _____

Signature/Printed Name: _____

This ☐ baseline ☐ revision was acquired from: _____

Printed Name/Organization _____

3. Specification Type (check one only):

- ☐ A. Performance Specs.
- ☐ B. Design Specs.
- ☐ D. Test Specs.

4. Reference and Location of Specification (if not attached): _____

5. Cross-Reference to other Specifications for this code: (where possible):

QA CIN _____

Control Date: _____

QA CIN _____

Control Date: _____

00/00/00

QA CIN:

---	-	---	-	---	-
-----	---	-----	---	-----	---

YY MM DD

Control Date (QAAA Only):

--	--	--
----	----	----

Section 2 - Baseline Revision

1. Reason for Revision:

- a. ☐ Response to Review QA CIN: _____ Control Date: _____
- b. ☐ Problem Report/
Corrective Action QA CIN: _____ Control Date: _____
- c. ☐ Code Enhancement
- d. ☐ Other: _____

2. Description of Revision:

3. Baselines which may require revision as a result of this revision:

Recommended by: _____ PM

Date:

YY MM DD		
--	--	--

Approved by: _____ QAM

Date:

YY MM DD		
--	--	--

08/15/90

QA CIN:

---	-	---	C	---	-
-----	---	-----	---	-----	---

Y Y M M D D

Control Date (QAAA Only):

--	--	--
----	----	----

CODE (C)

- ☐ Original Baseline (Complete Section 1 only)
- ☐ Revision to Baseline (Complete Sections 1 and 2)

Project Name:
Contract No.:

Project Number:

CFI Description: _____

Section 1: Code Baseline

1. Code Name: _____

- ☐ Major Code ☐ Minor Code ☐ Commercial Utility Code

2. Source (check one and complete):

a. This ☐ baseline ☐ revision was developed by: _____
Signature(s)/Printed Name

b. This ☐ baseline ☐ revision was acquired from: _____
Printed Name

3. References:

a. ☐ Performance Specs. QA CIN: _____ Control Date: _____

b. ☐ Design Specs. QA CIN: _____ Control Date: _____

c. ☐ Test Specs. QA CIN: _____ Control Date: _____

d. ☐ Test Data QA CIN: _____ Control Date: _____

e. ☐ Test Results QA CIN: _____ Control Date: _____

5. Hardware:

a. ☐ PC b. ☐ Other (Specify): _____

c. Special Requirements: _____

6. Compiler/Linker Options:

a. ☐ FORTRAN a. ☐ PASCAL c. ☐ Other (Specify): _____

d. Compiler & Options: _____ e. Linker & Options: _____

08/15/90

QA CIN.

---	-	--	-	---	-
-----	---	----	---	-----	---

7. Code Storage:

- a. ☐ Tape Tape No: _____ Source File Title: _____
Executable File Title: _____ Format: _____
- b. ☐ Disk Disk No: _____ Source File Title: _____
Executable File Title: _____ Format: _____
- c. ☐ Other (give details): _____

Section 2: Code Revision

1. Reason for Revision:

- a. ☐ Response to Review QA CIN: _____ Control Date: _____
- b. ☐ Problem Report/
Corrective Action QA CIN: _____ Control Date: _____
- c. ☐ Code Enhancement/Evolution
- d. ☐ Other: _____

2. Description of Revision:

This revision was made to the code to correct a problem reported from the testing of the code. The problem was that the code was not working as intended. The code was revised to correct the problem and to improve the code's performance.

3. Baselines which may require changes as a result of this revision:

4. Revision approved by Code Custodian: _____ Date: _____
Signature

Recommended by: _____ PM

Date:

YY MM DD		
--	--	--

Approved by: _____ QAM

Date:

YY MM DD		
--	--	--

08/15/90

QA CIN:

---	-	---	E	---	-
-----	---	-----	---	-----	---

YY MM DD

Control Date (QAAA Only):

---	---	---
-----	-----	-----

TEST/APPLICATION/OTHER DATA (E)

- ☐ Original Baseline (Complete Section 1 only)
- ☐ Revision to Previous Baseline (Complete Sections 1 and 2)

Project Title:

Project Number:

Contract No.:

CFI Description: _____

Section 1 - Data Baseline**1. Data Type (check one):**

- a. ☐ Test Data Code Name: _____
- b. ☐ Application Data QA CIN: _____ Control Date: _____
- c. ☐ Library Data
- d. ☐ Generic Data (describe): _____

2. Source of Data:

- a. ☐ Documented internally by: _____
Signature/Printed Name

Signature/Printed Name

References made to:

☐ Laboratory☐ Field☐ Model☐ Literature☐ Judgement

Reference(s) to source(s) (if not attached): _____

- b. ☐ Acquired From: _____
Printed Name

1. Data Storage

- a. ☐ Tape/Disk
- i. Tape/Disk Number: _____
- ii. File Names: _____
- iii. Format: _____
- b. ☐ Other: _____

---	-	---	E	---	-
-----	---	-----	---	-----	---

4. Data Documentation Description (if not attached):

Section 2: Data Revision

1. Reason for Revision

a. ☐ Response to Review

QA CIN: _____

Control Date: _____

b. ☐ Problem Report/
Corrective Action

QA CIN: _____

Control Date: _____

c. ☐ Other: -

2. Description of Revision:

3. Baselines which may require changes as a result of this revision:

Recommended by: _____ PM

Date:

YY MM DD					
---	---	---	---	---	---

Approved by: _____ QAM

Date:

YY MM DD					
---	---	---	---	---	---

QA Control Document

08/15/90

QA CIN:

---	-	---	F	---	-
YY	MM	DD			

Control Date (QAAA Only):

---	---	---
-----	-----	-----

TEST/APPLICATION RESULTS (F)

- ☐ Test Results (Complete Section 1 only)
- ☐ Application Results (Complete Section 2)

Project Name:

Project Number:

Contract No.:

CFI Description: _____

Section 1: Test Results

1. Code Name: _____

2. Code QA CIN: _____ Control Date: _____

3. Test Data QA CIN: _____ Control Date: _____

4. Library Data QA CIN: _____ Control Date: _____
(if applicable)

5. Description of Test(s) (if not attached):

6. Analysis and Interpretation of Results (if not attached):

7. Storage of Results:

- a. ☐ Tape/Disk
- i. Tape/Disk Number: _____
- ii. File Names: _____
- iii. Format: _____

- b. ☐ Other: _____

08/15/90

QA CIN:

---	-	--	F	---	-
-----	---	----	---	-----	---

8. Test Performed by: _____ Date: _____
Signature/Printed Name

9. Results and Analysis Verified by: _____ Date: _____
Signature/Printed Name

Section 2: Application Results

1. Code Name: _____

2. Code QA CIN: _____ Control Date: _____

3. Test Data QA CIN: _____ Control Date: _____

4. Test Results QA CIN: _____ Control Date: _____

5. Application Data QA CIN: _____ Control Date: _____

6. Description of Application (if not attached):

7. Analysis and interpretation of results (if not attached):

8. Storage of Results:

a. ☐ Tape/Disk i. Tape/Disk Number: _____
ii. File Names: _____
iii. Format: _____

b. ☐ Other: _____

9. Application Performed by: _____ Date: _____
Signature/Printed Name

10. If known, give references to documents where results will be presented:

Description	QA CIN (if known)
a. _____	_____
b. _____	_____
c. _____	_____

YY MM DD

Recommended by: _____ PM

Date:

--	--	--
----	----	----

YY MM DD

Approved by: _____ QAM

Date:

--	--	--
----	----	----

QA Control Document

08/15/90

QA CIN:

---	-	---	G	---	-
-----	---	-----	---	-----	---

YY. MM DD

Control Date (QAAA Only):

--	--	--
----	----	----

REPORT/CODE DOCUMENTATION (G)

- ☐ Original Baseline (Complete Section 1 only)
- ☐ Revision to Baseline (Complete Sections 1 and 2)

Project Name:

Project Number:

Contract No.:

CFI Description: _____

Section 1: Baseline

1. Report Type:

a. ☐ Topical Report

b. ☐ Letter Report

c. ☐ Model Documentation: Code QA CIN: _____ Control Date: _____

2. Title (or Subject): _____

3. This ☐ baseline ☐ revision was developed by: _____
Signature/Printed Name

Signature/Printed Name

Signature/Printed Name

4. This ☐ baseline ☐ revision was acquired from: _____
Printed Name

5. References:

a. ☐ No reference to baselined data or results

b. ☐ Reference is made to data/results with the following baseline QA CIN's:

08/15/90

QA CIN:

---	-	---	6	---	-
-----	---	-----	---	-----	---

Section 2: Baseline Revision

1. Reason for Revision:

- a. ☐ Response to Review QA CIN: _____ Control Date: _____
- b. ☐ Corrective Action QA CIN: _____ Control Date: _____
- c. ☐ Other:

2. Description of Revision:**3. Baselines which may require changes as a result of this revision:**

Recommended by: _____ PM

Date:

YY	MM	DD
--	--	--

Approved by: _____ QAM

Date:

YY	MM	DD
--	--	--

QA Control Document

08/15/90

QA CIN:

---	-	---	I	---	-
-----	---	-----	---	-----	---

YY MM DD

Control Date (QAAA Only):

---	---	---
-----	-----	-----

REVIEW (I)

Project Name:

Project Number:

Contract No.:

CFI Description: _____

1. Title or Description of Baseline Reviewed: _____

2. Author/Originator: _____

3. QA CIN of Baseline Reviewed: _____

Control Date: _____

4. Location of Review Comments:

☐

On Document

☐

Review Form

Reviewed by: _____

Printed Name/Signature

Date: _____

5. Brief Review Comments:

The review was conducted on the basis of the information provided and the results are as follows. The review was conducted on the basis of the information provided and the results are as follows.

Recommended by: _____ PM

Date:

YY MM DD

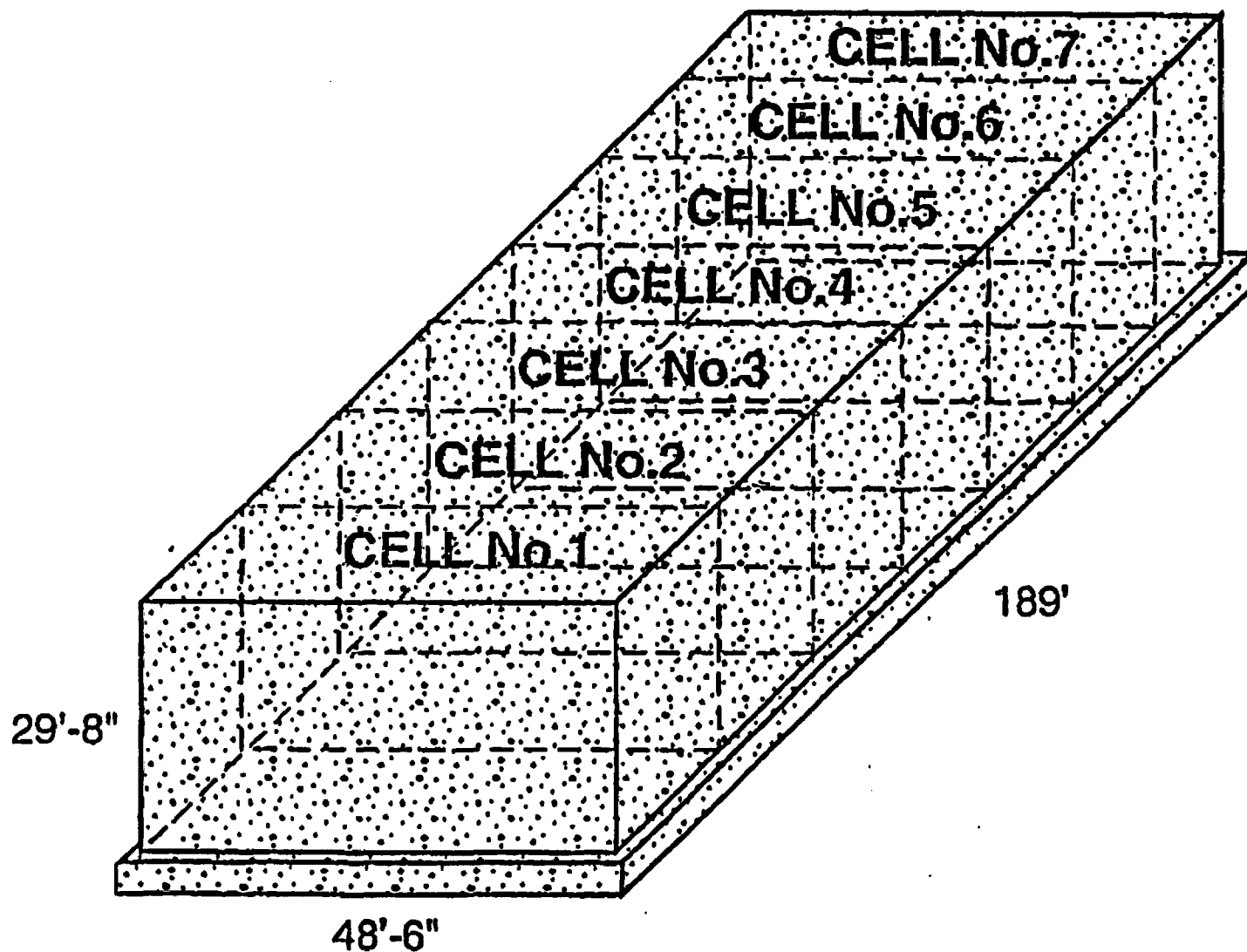
---	---	---
-----	-----	-----

Approved by: _____ QAM

Date:

YY MM DD

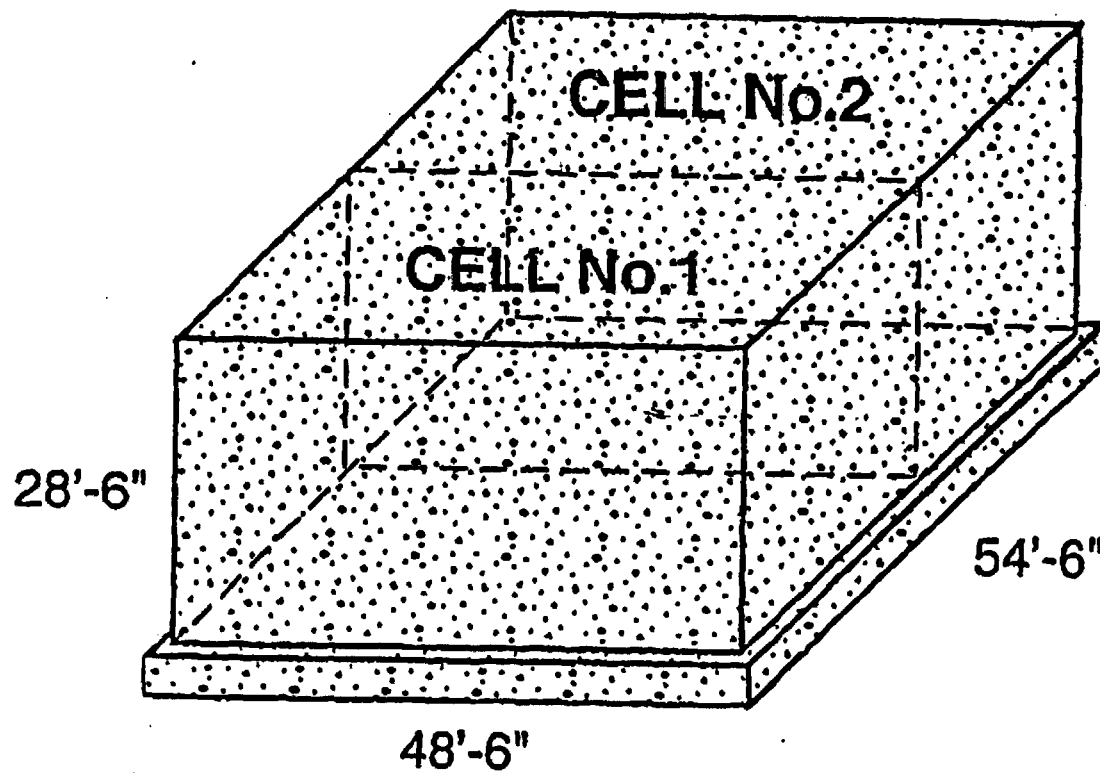
---	---	---
-----	-----	-----



INTERA

Schematic of ILNT Vault

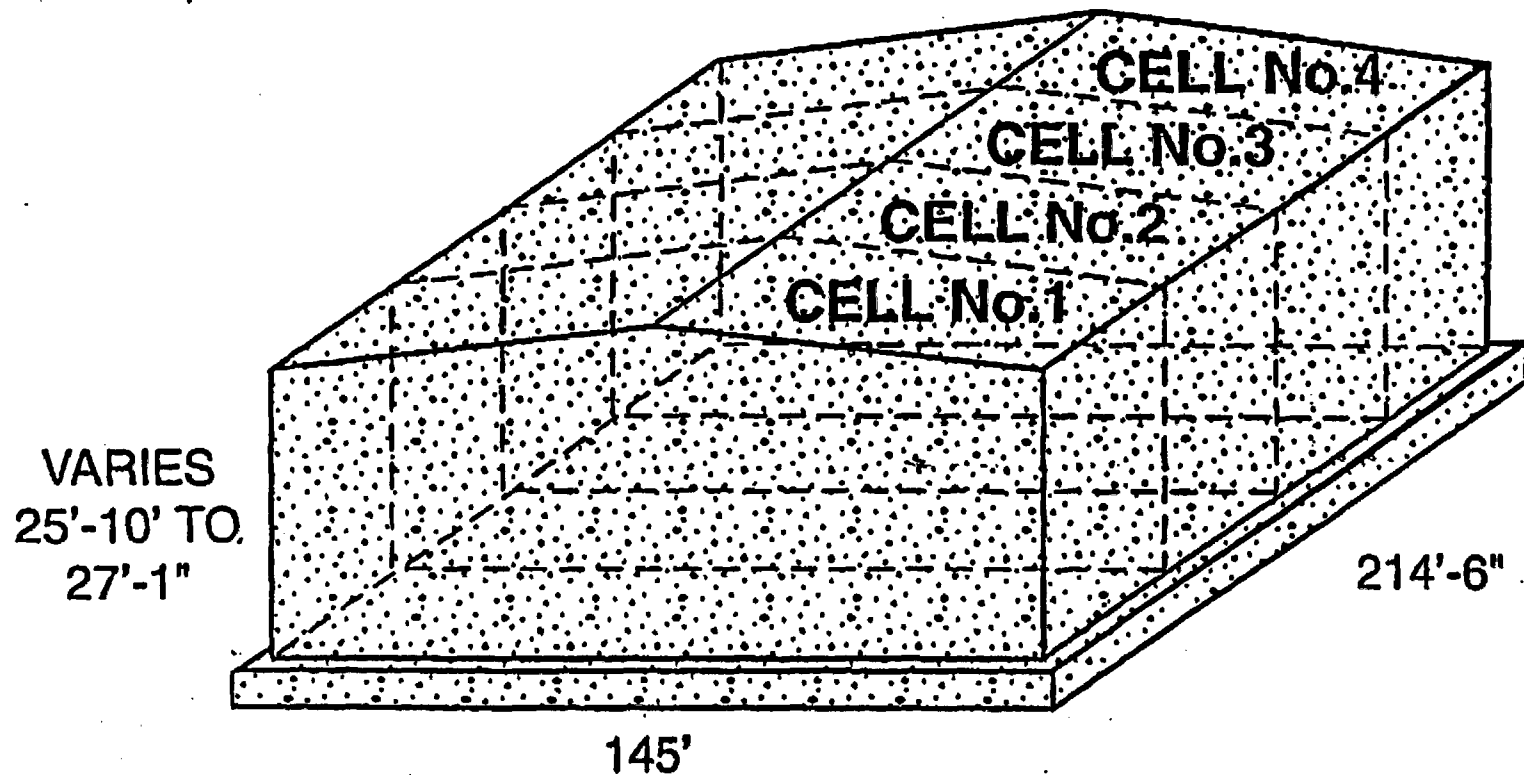
Figure 1



INTERA

Schematic of ILT Vault

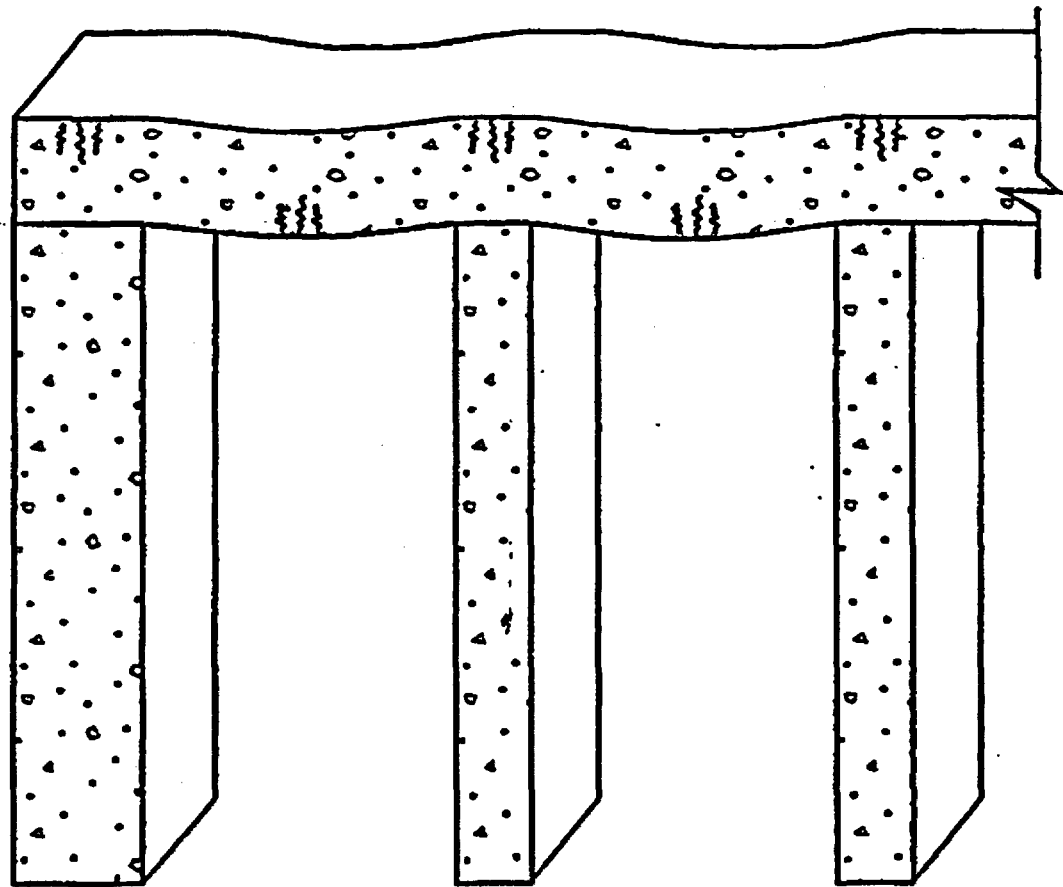
Figure 2



WETA

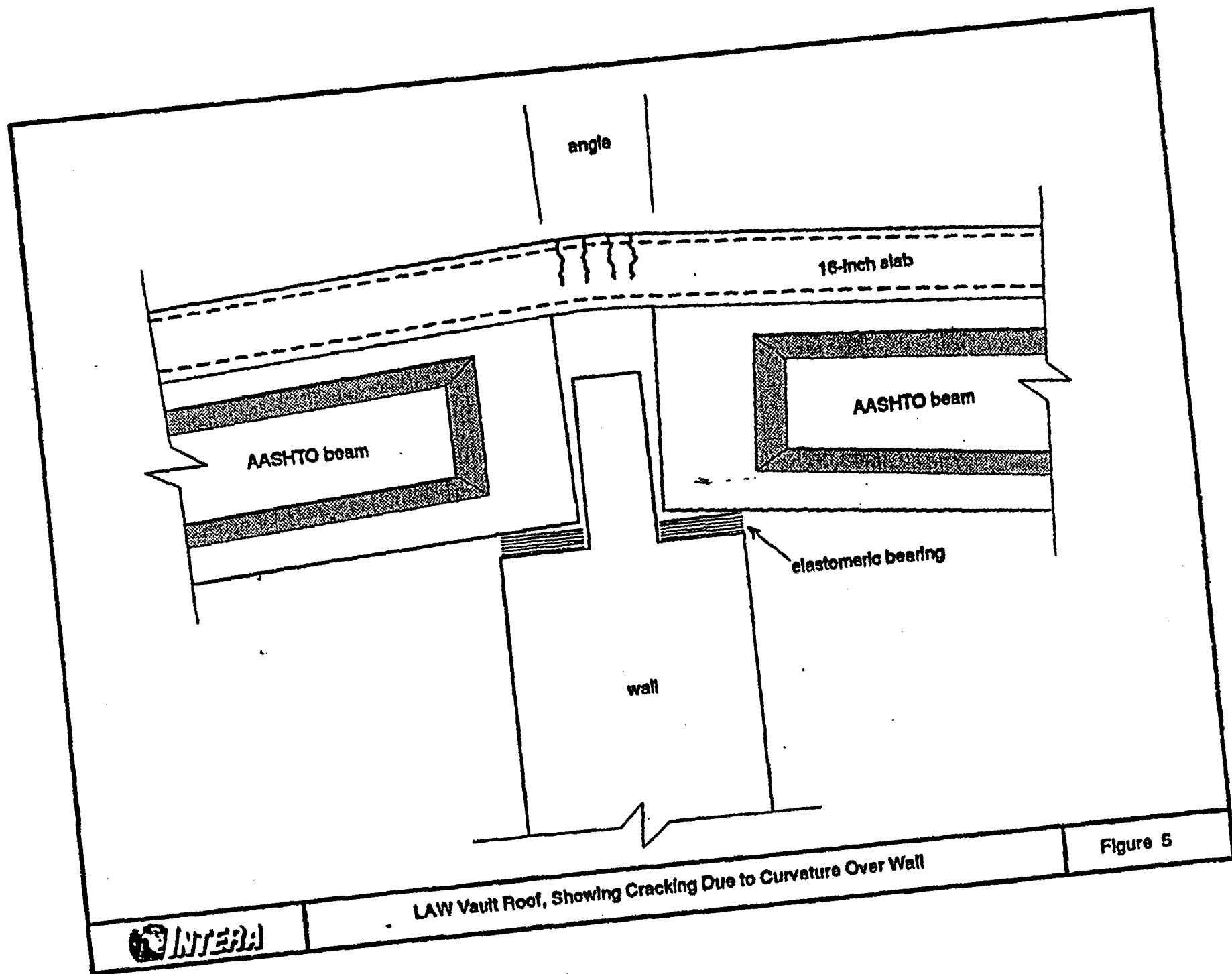
Schematic of LAW Vault

Figure 3



NOT TO SCALE
DEFLECTION HAS BEEN EXAGGERATED FOR EMPHASIS

DATE: 9/7/93	Portion of Vault Cross Section; Cracks Indicate Critical Stress Regions	
REF: #1025-007		
INTERA		Figure 4

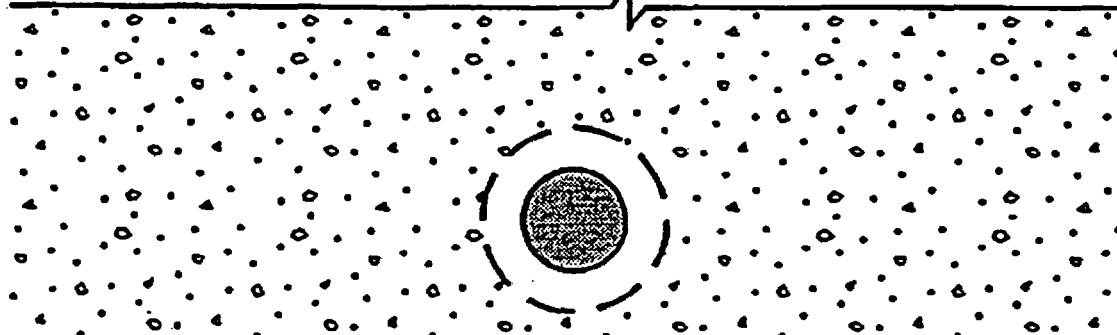
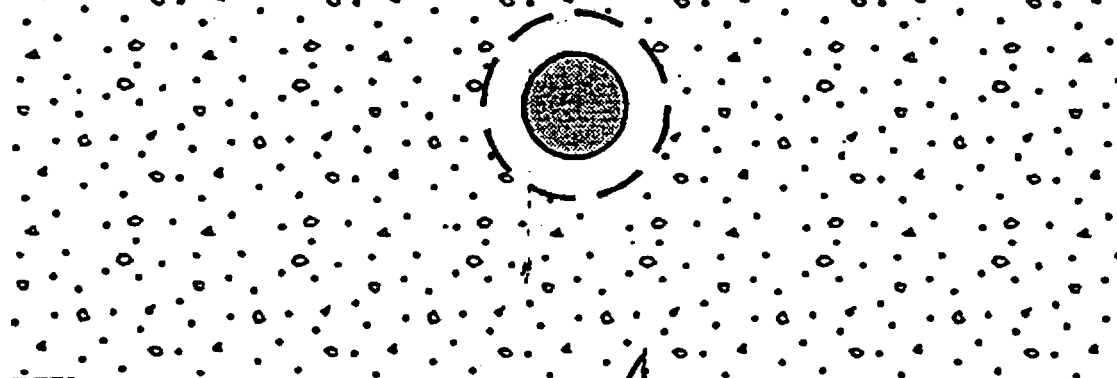


ORIGINAL CONCRETE ROOF SURFACE

CURRENT SURFACE DUE TO SO_2 ATTACK (0.19 cm LOSS)

ORIGINAL REBAR RADIUS: 1.25 cm

CURRENT REBAR RADIUS: 1.05 cm



ORIGINAL REBAR RADIUS: 1.25 cm

CURRENT REBAR RADIUS: 1.05 cm

VAULT INTERIOR

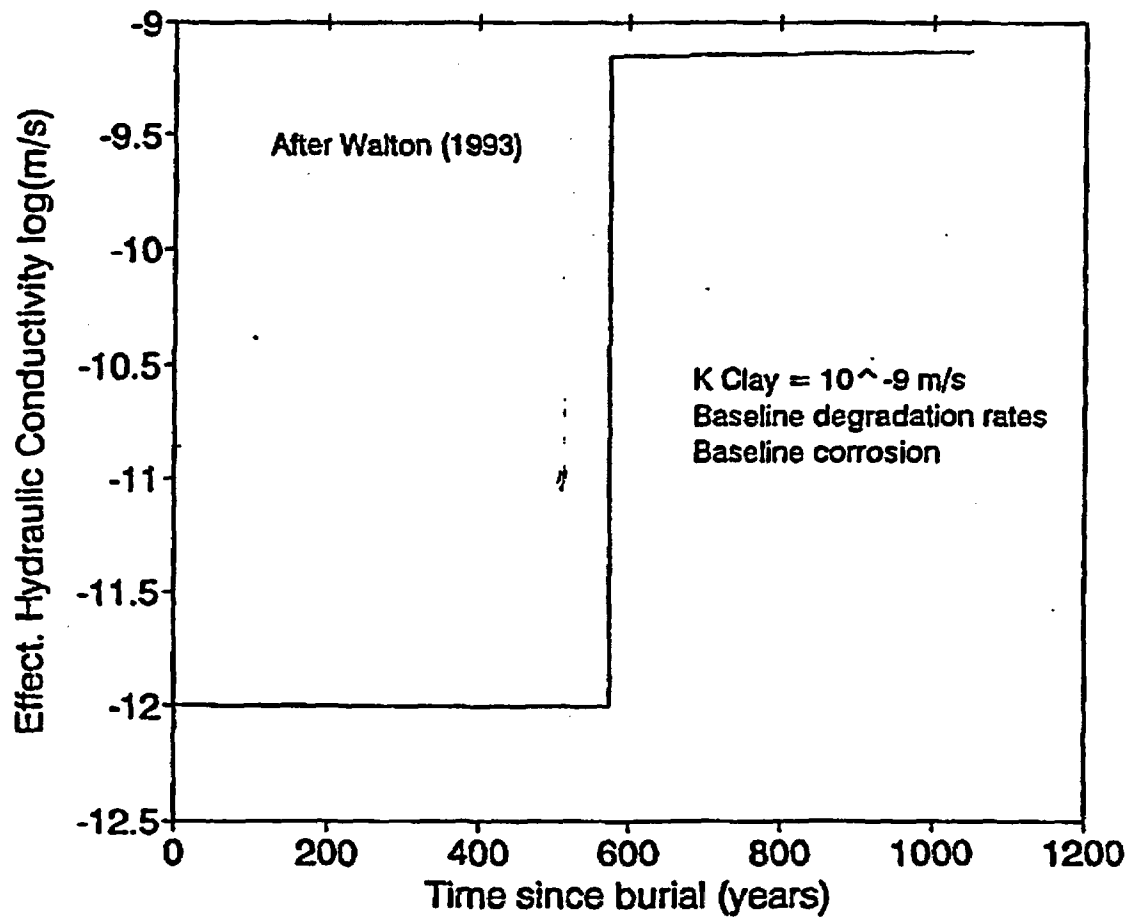
DATE: 9/7/93

REF: #1025-007

Cross-Section of ILNT Vault Roof
Showing Degradation at 400 Years

ATENA

Figure 6



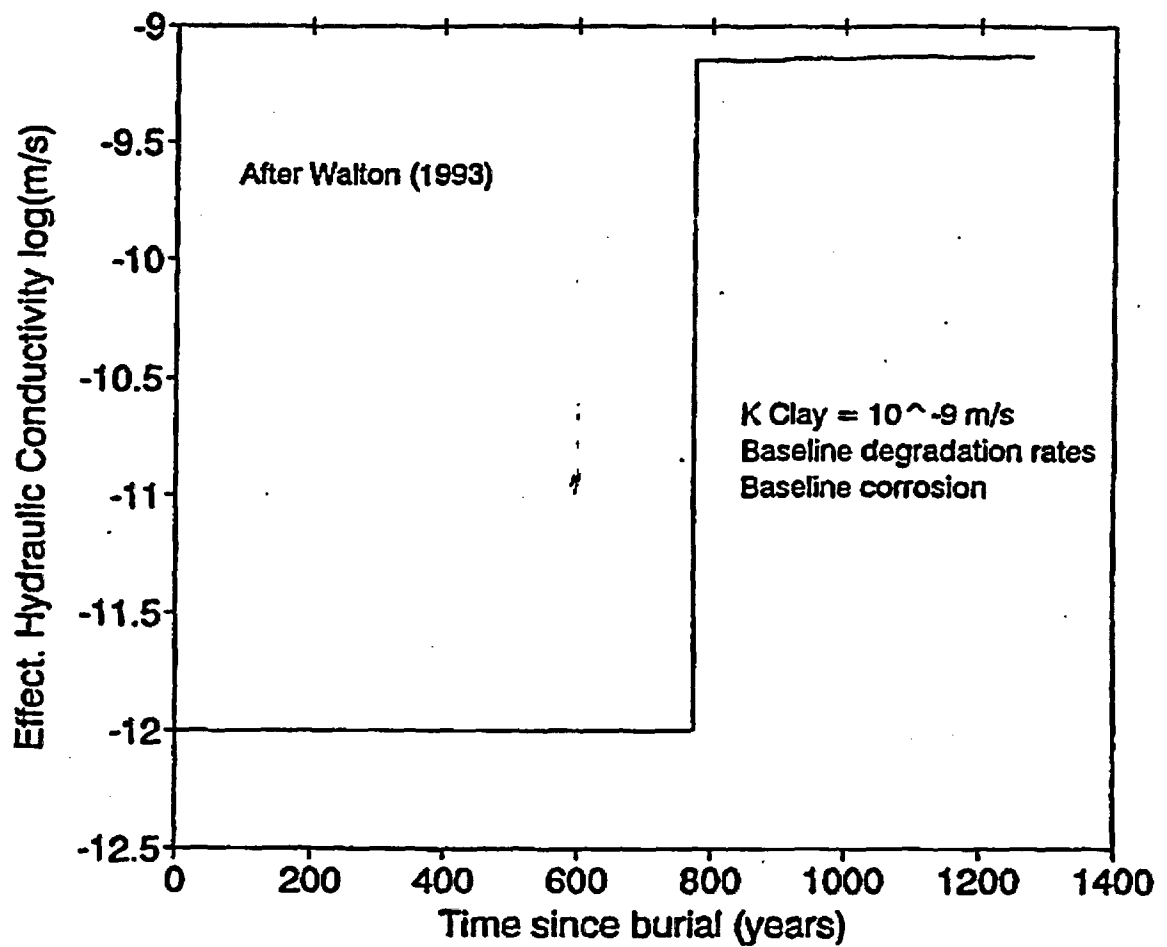
DATE: 9/7/93

REF: #1025-007

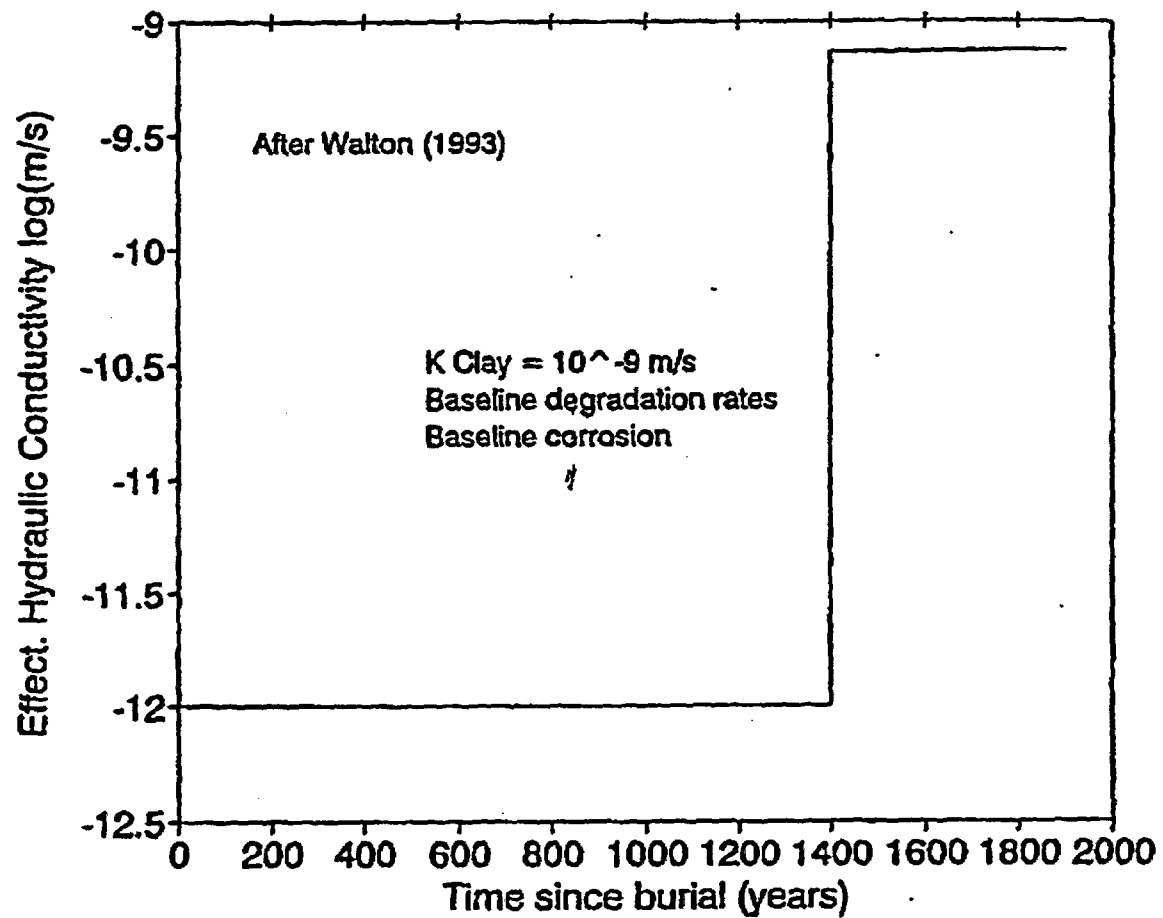
Effective Hydraulic Conductivity of Vault Roof;
ILNT Vault Design

INTERA

Figure 7



DATE: 9/7/93	Effective Hydraulic Conductivity of Vault Roof; ILT Vault Design	
REF: #1025-007		
INTERA		Figure 8



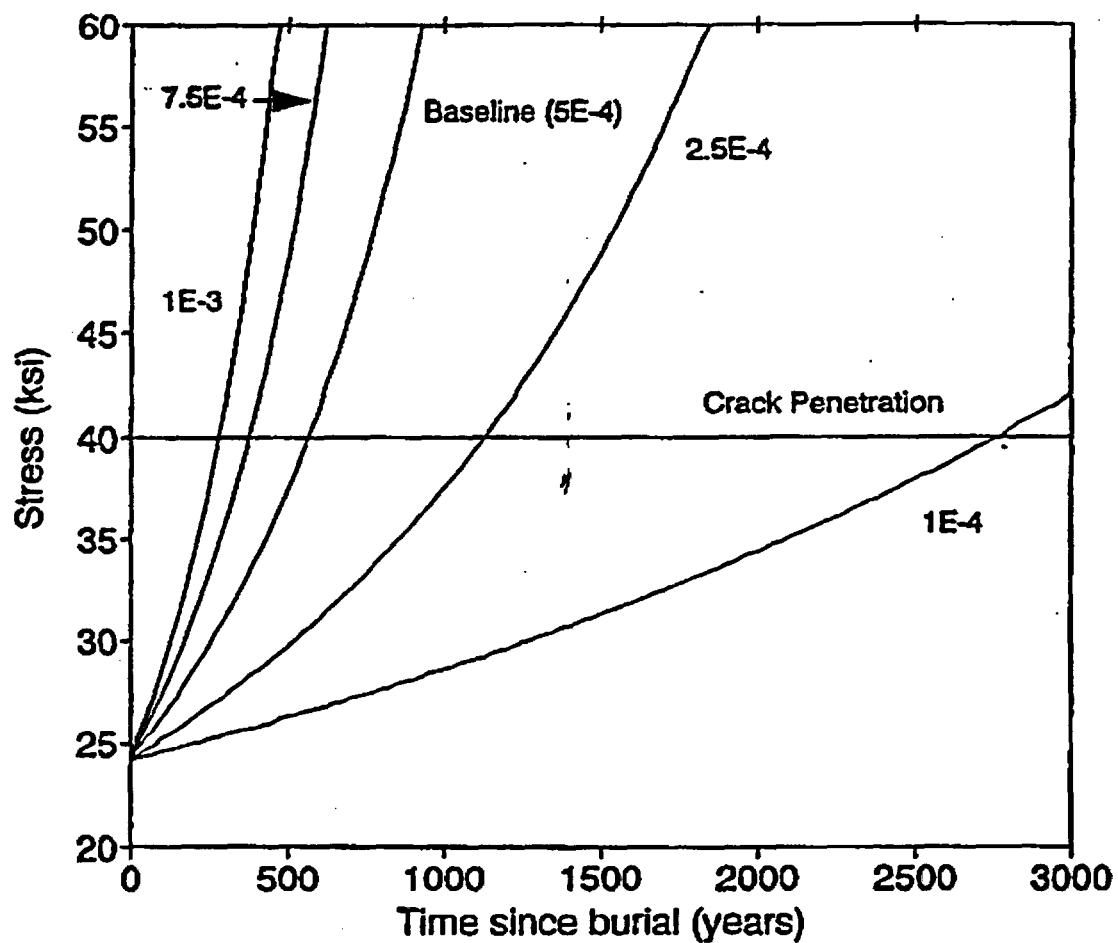
DATE: 9/7/93

REF: #1025-007

Effective Hydraulic Conductivity of Vault Roof;
LAW Vault Design

INTERA

Figure 9



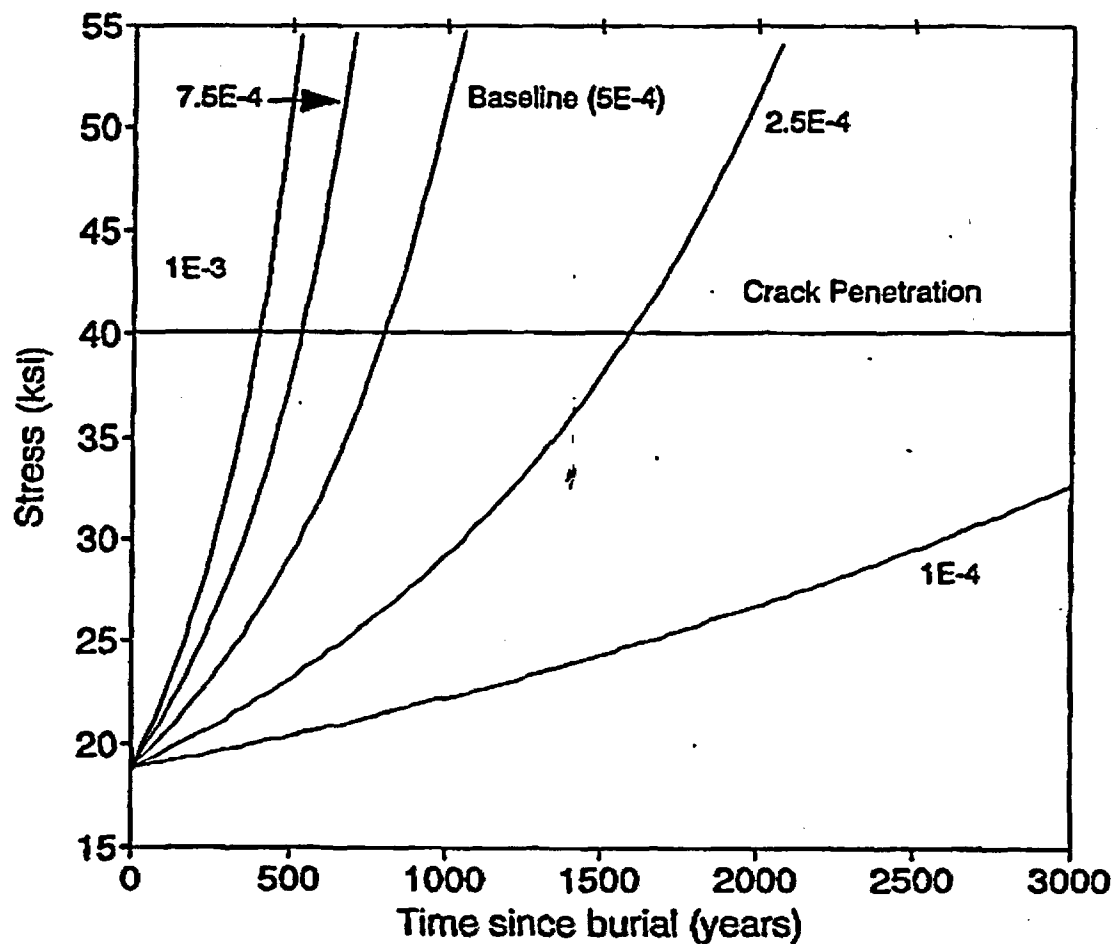
DATE: 9/7/93

REF: #1025-007

ILNT Vault Time to Crack Penetration of Roof;
Sensitivity to Hydrogen Evolution Corrosion Rate (cm/yr)

ITERA

Figure 10



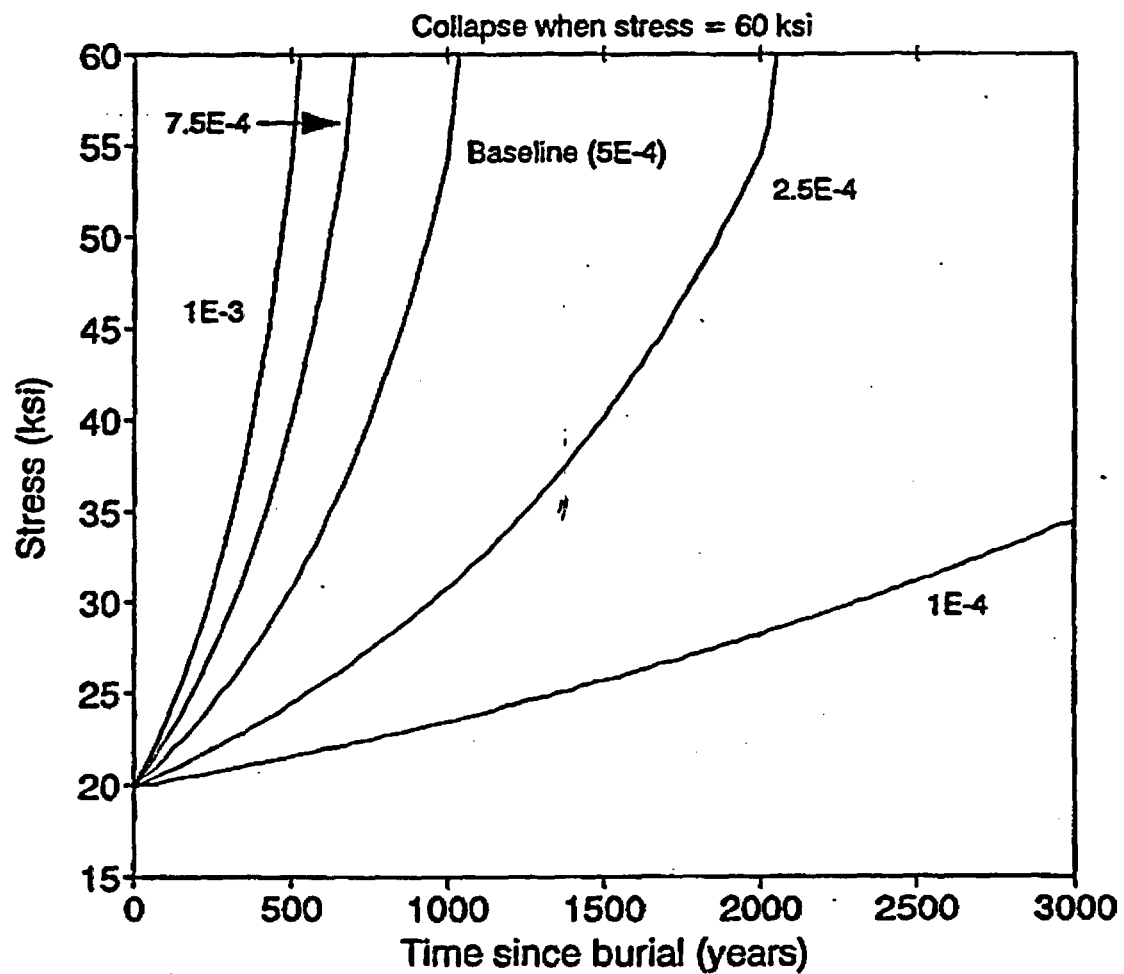
DATE: 9/7/93

REF: #1025-007

ILNT Vault Time to Crack Penetration of Walls;
Sensitivity to Hydrogen Evolution Corrosion Rate (cm/yr)

ITERA

Figure 11



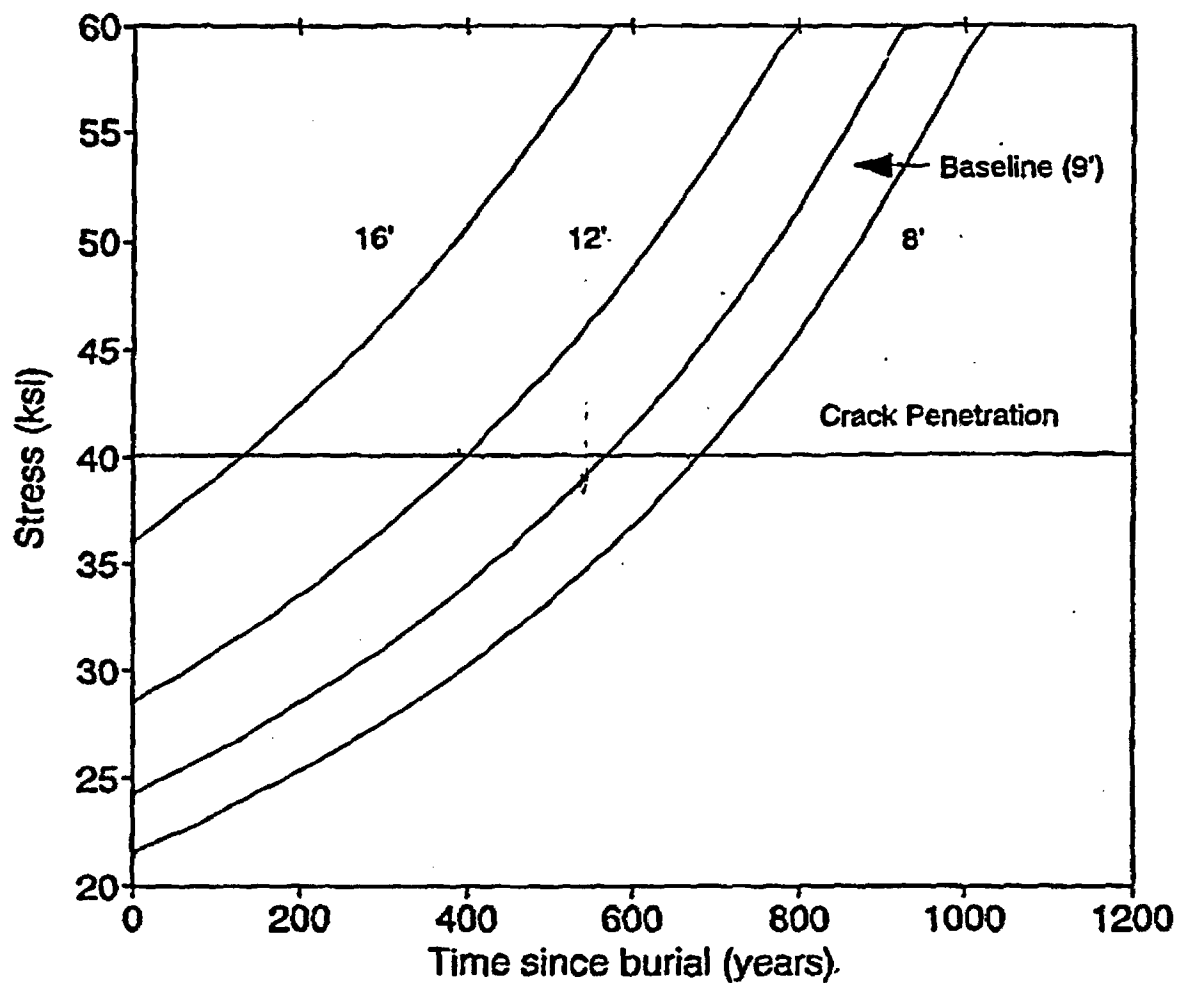
DATE: 9/7/93

REF: #1025-007

ILNT Vault Time to Roof Collapse;
Sensitivity to Hydrogen Evolution Corrosion Rate (cm/yr)

ITERA

Figure 12



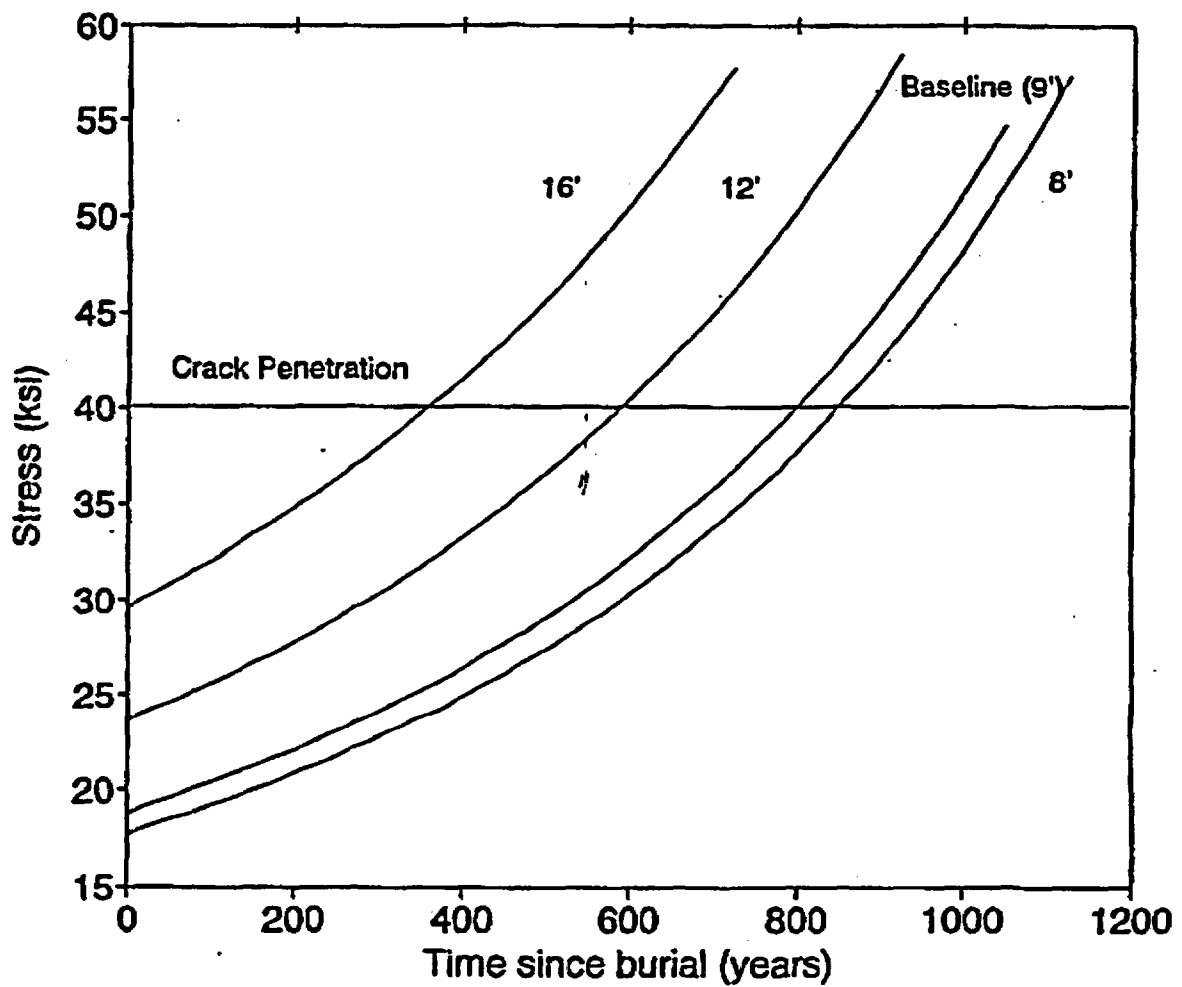
DATE: 9/7/93

REF: #1025-007

ILNT Vault Time to Crack Penetration of Roof;
Sensitivity to Depth of Soil Cover

ITERA

Figure 13



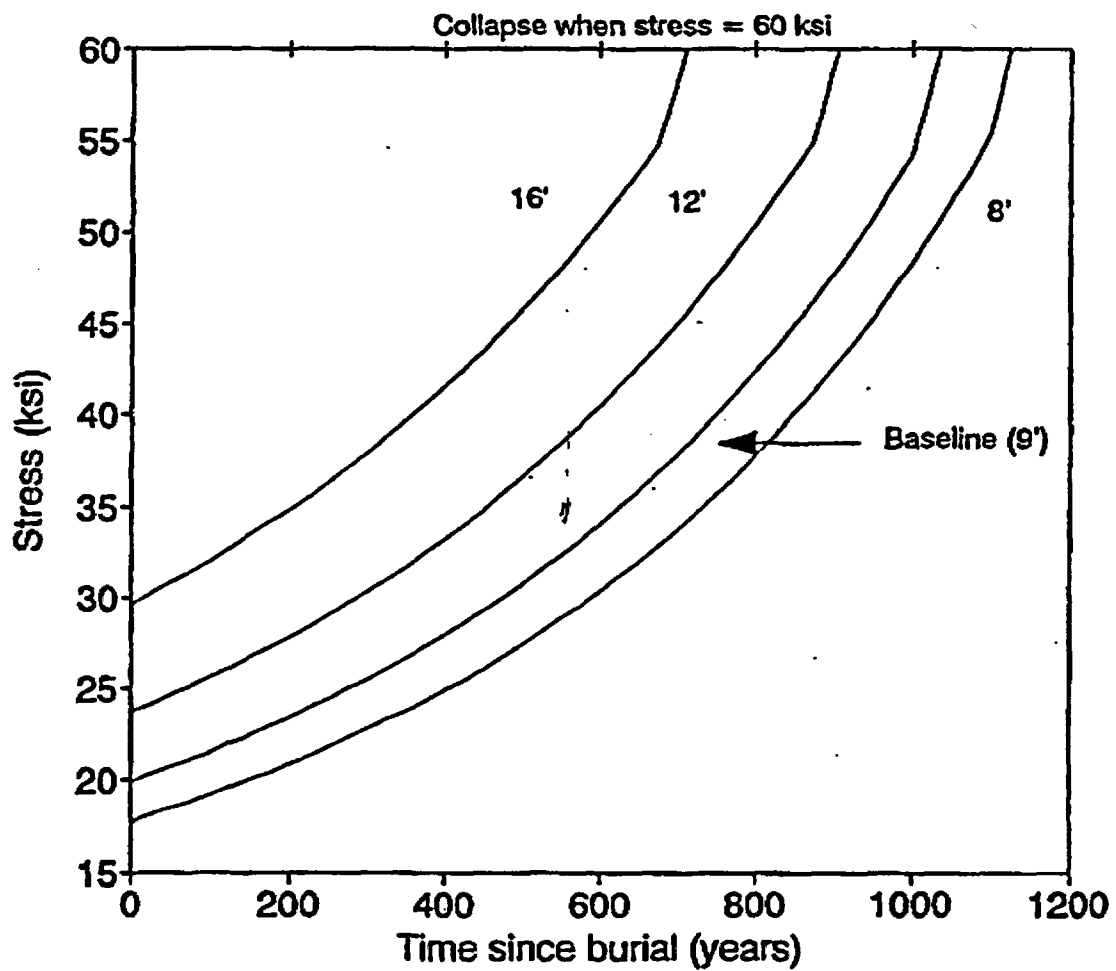
DATE: 9/7/93

REF: #1025-007

ILNT Vault Time to Crack Penetration of Walls;
Sensitivity to Depth of Soil Cover

ITERA

Figure 14



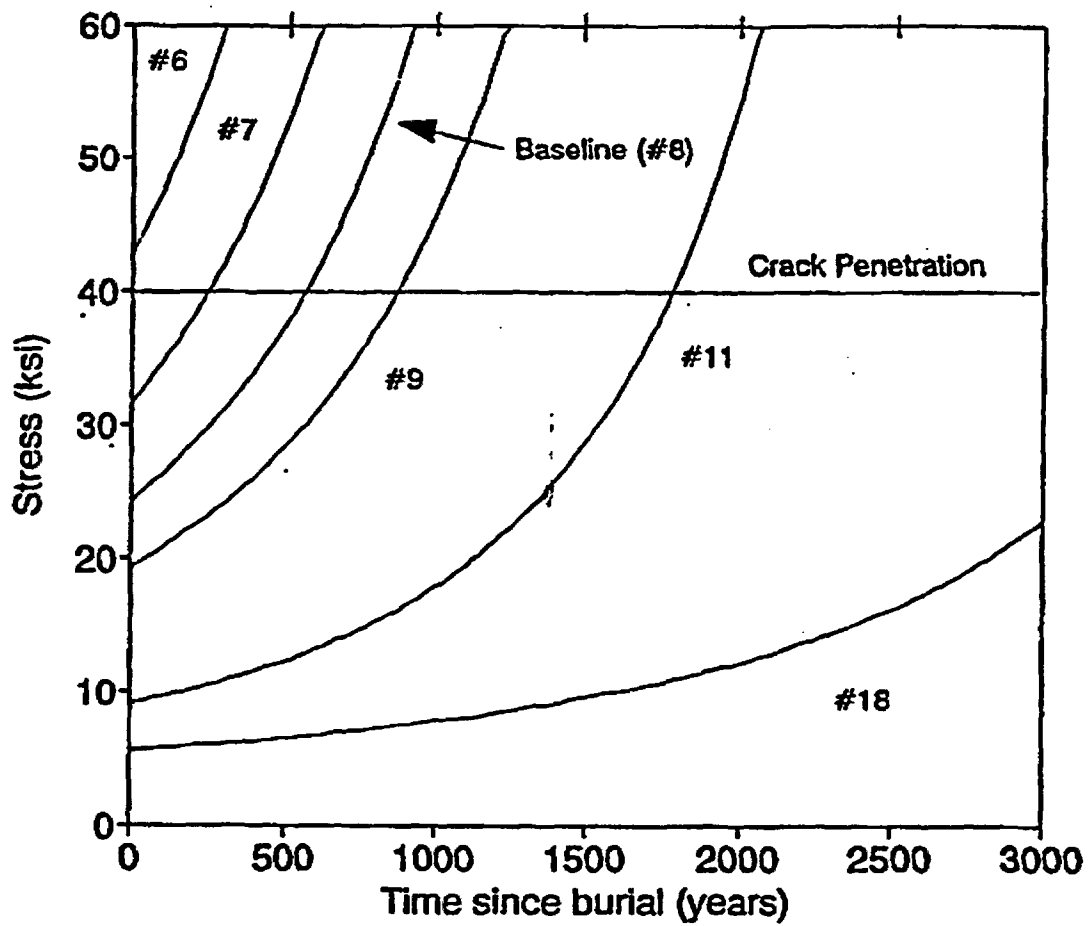
DATE: 9/7/93

REF: #1025-007

ILNT Vault Time to Roof Collapse;
Sensitivity to Depth of Soil Cover

ITERA

Figure 15



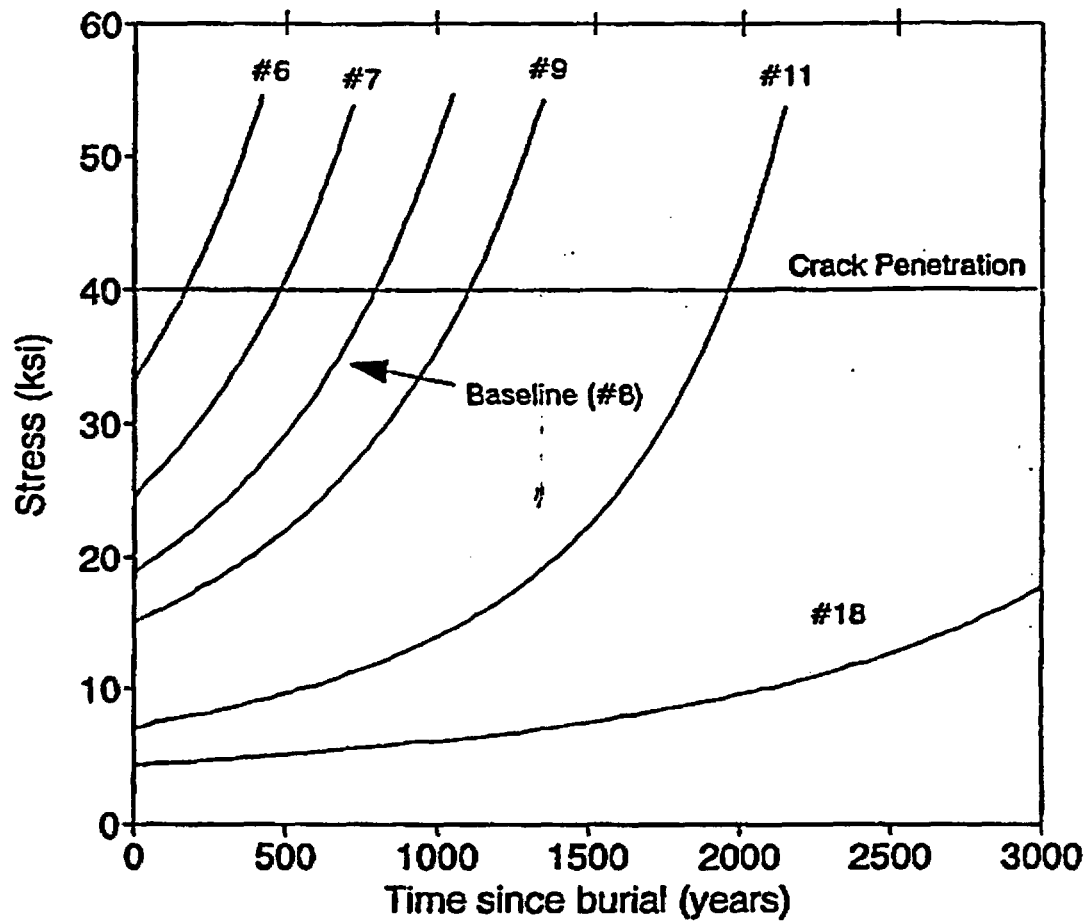
DATE: 9/7/93

REF: #1025-007

ILNT Vault Time to Crack Penetration of Roof;
Sensitivity to Rebar Size

INTERA

Figure 16



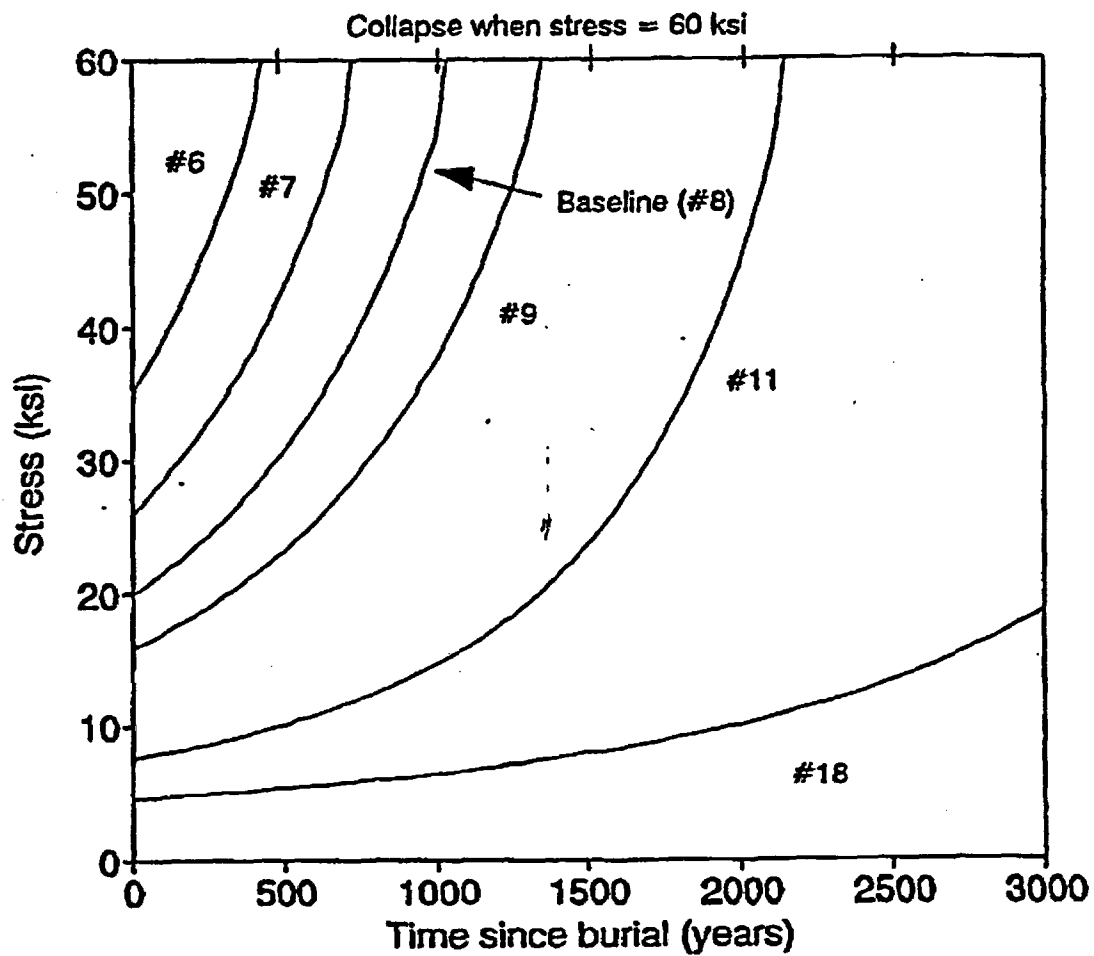
DATE: 9/7/93

REF: #1025-007

ILNT Vault Time to Crack Penetration of Walls;
Sensitivity to Rebar Size

ITERA

Figure 17



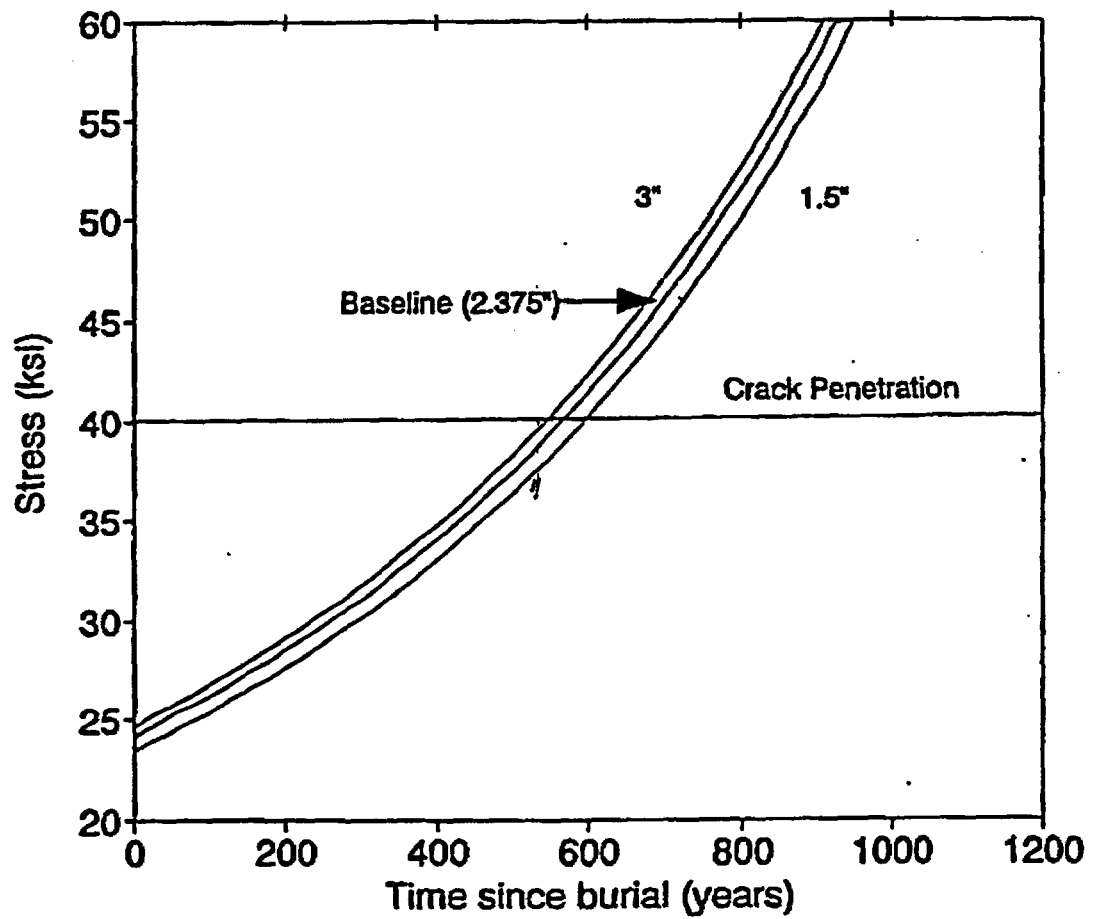
DATE: 9/7/93

REF: #1025-007

ILNT Vault Time to Roof Collapse;
Sensitivity to Rebar Size

INTERA

Figure 18



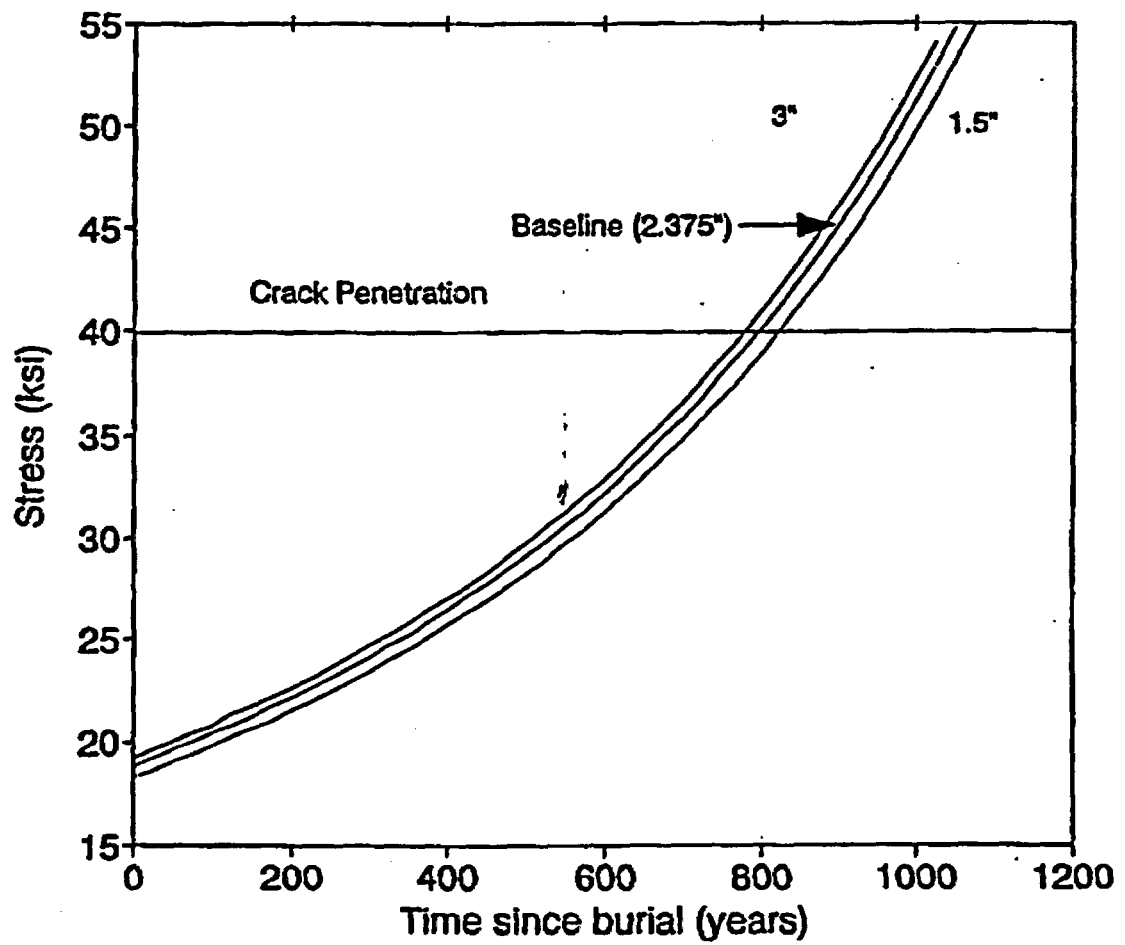
DATE: 9/7/93

REF: #1025-007

ILNT Vault Time to Crack Penetration of Roof;
Sensitivity to Depth of Concrete Cover Over Rebar

ITERA

Figure 19



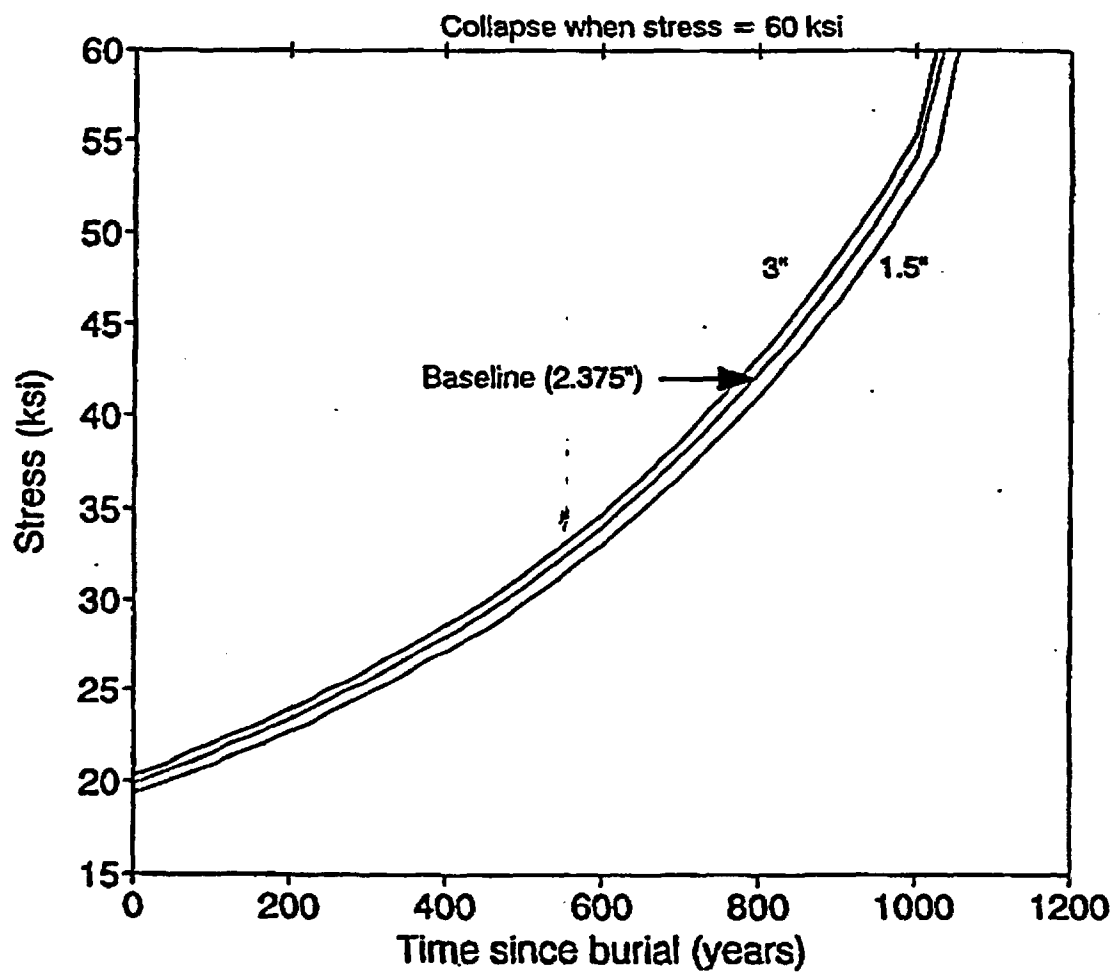
DATE: 9/7/93

REF: #1025-007

ILNT Vault Time to Crack Penetration of Walls;
Sensitivity to Depth of Concrete Cover Over Rebar

ITERA

Figure 20



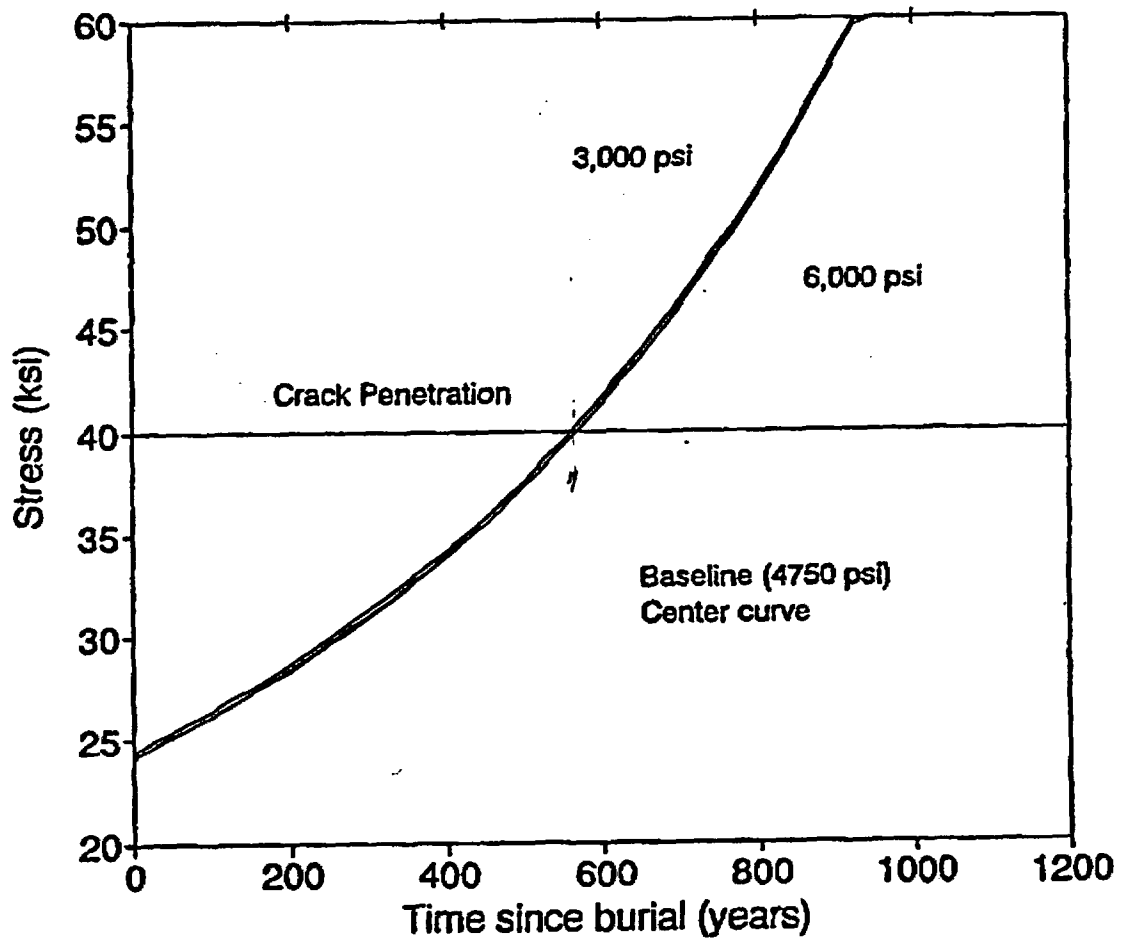
DATE: 9/7/93

REF: #1025-007

ILNT Vault Time to Roof Collapse;
Sensitivity to Depth of Concrete Cover Over Rebar

ILNT

Figure 21



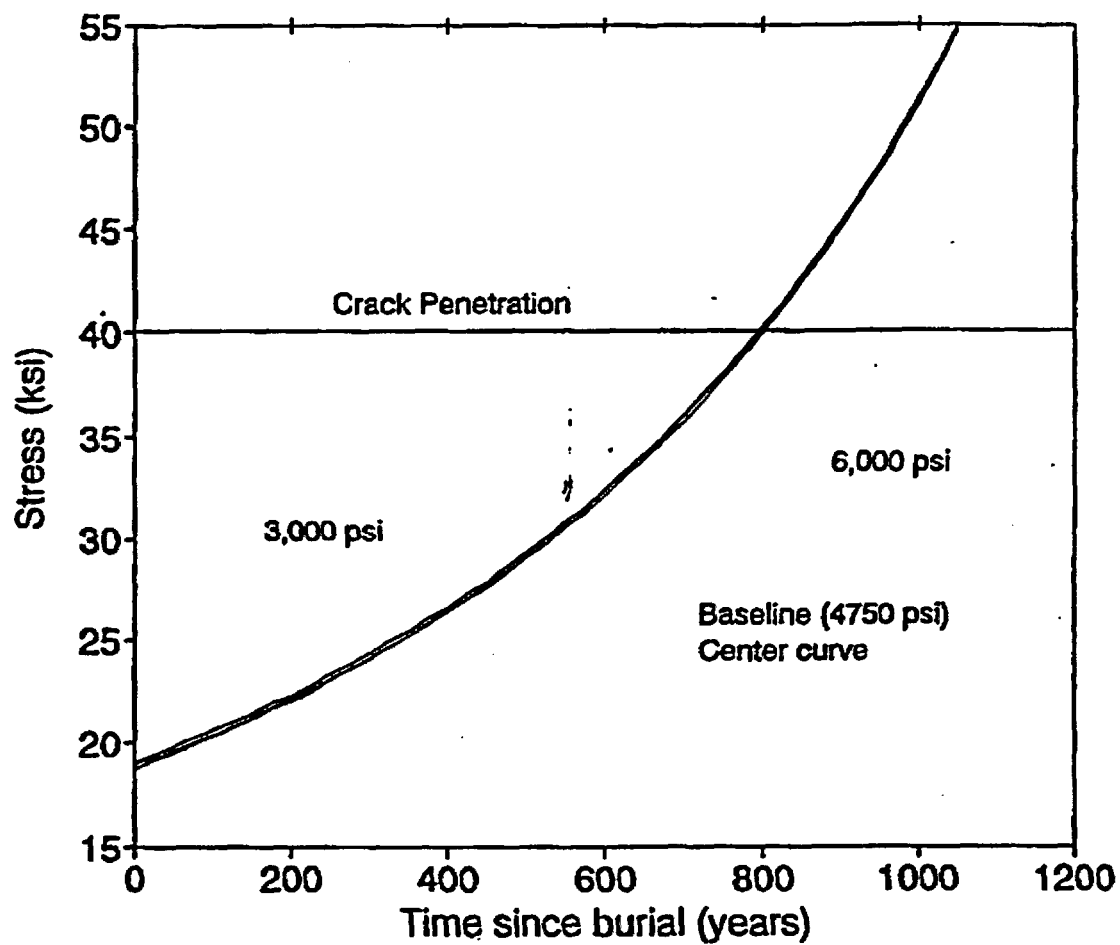
DATE: 9/7/93

REF: #1025-007

ILNT Vault Time to Crack Penetration of Roof;
Sensitivity to Concrete Strength

INTERA

Figure 22



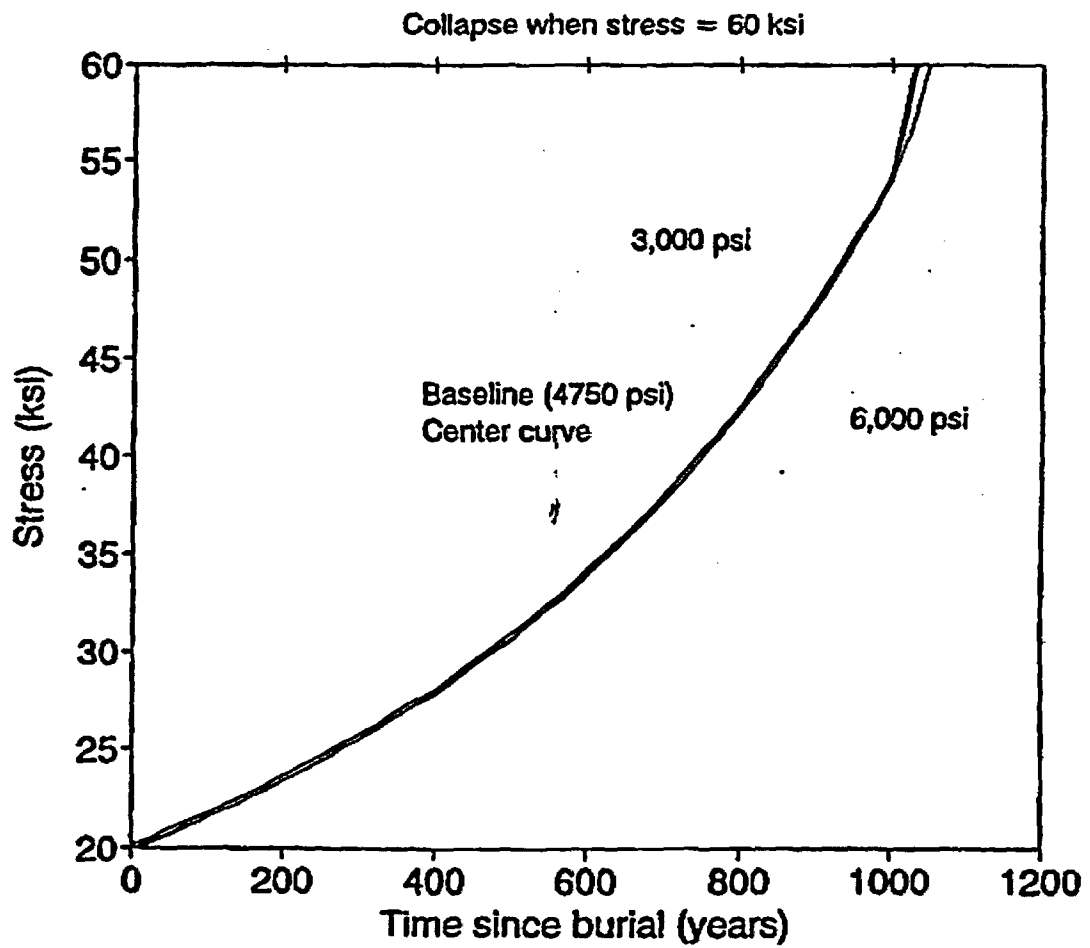
DATE: 9/7/93

REF: #1025-007

ILNT Vault Time to Crack Penetration of Walls;
Sensitivity to Concrete Strength

ILNT

Figure 23



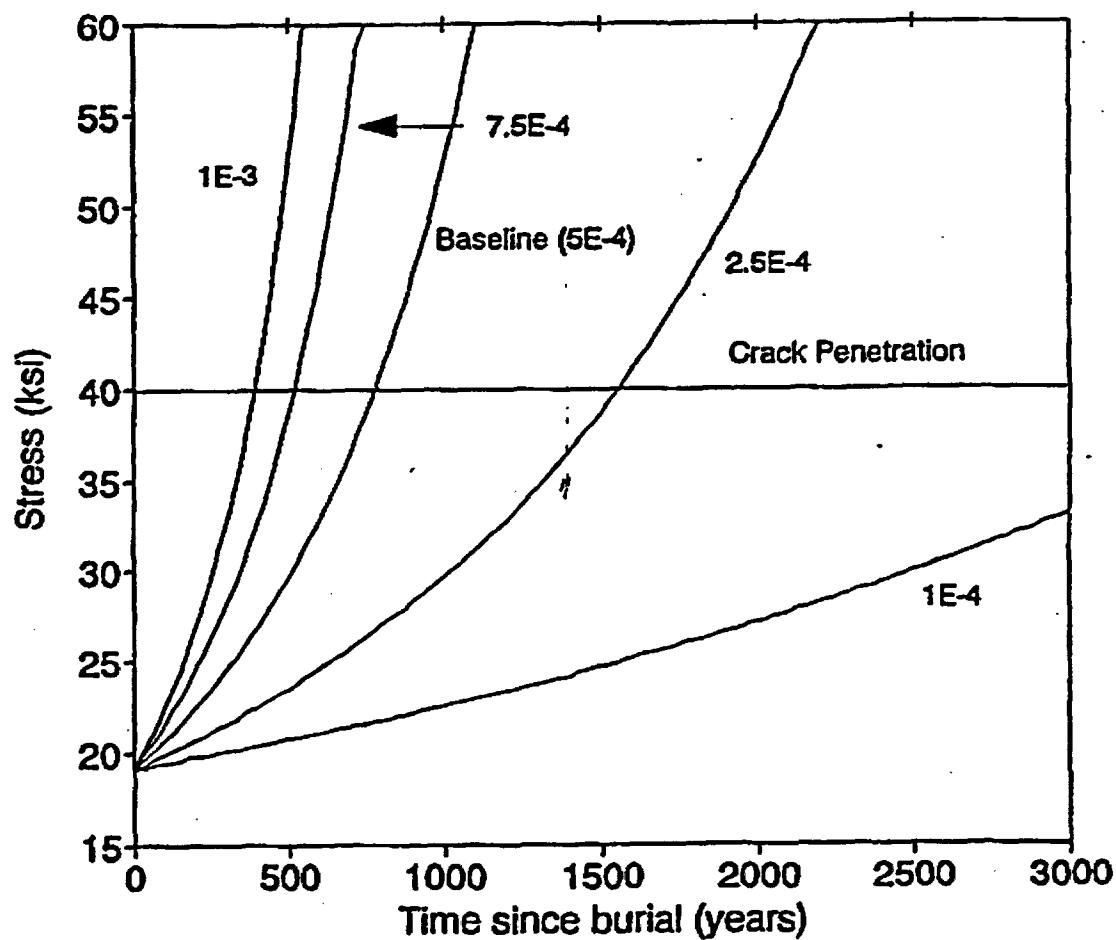
DATE: 9/7/93

REF: #1025-007

ILNT Vault Time to Roof Collapse;
Sensitivity to Concrete Strength

INTERA

Figure 24



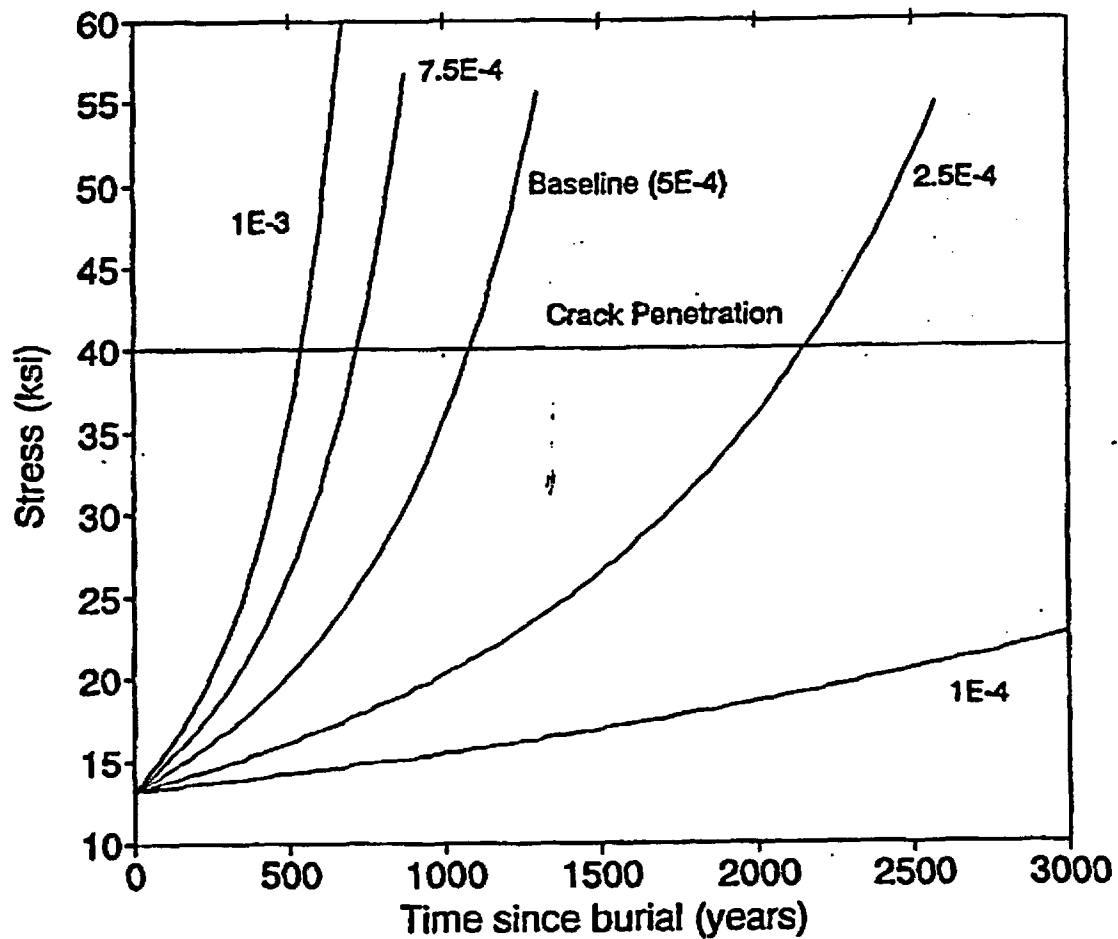
DATE: 9/7/93

REF: #1025-007

ILT Vault Time to Crack Penetration of Roof;
Sensitivity to Hydrogen Evolution Corrosion Rate (cm/yr)

INTERA

Figure 25



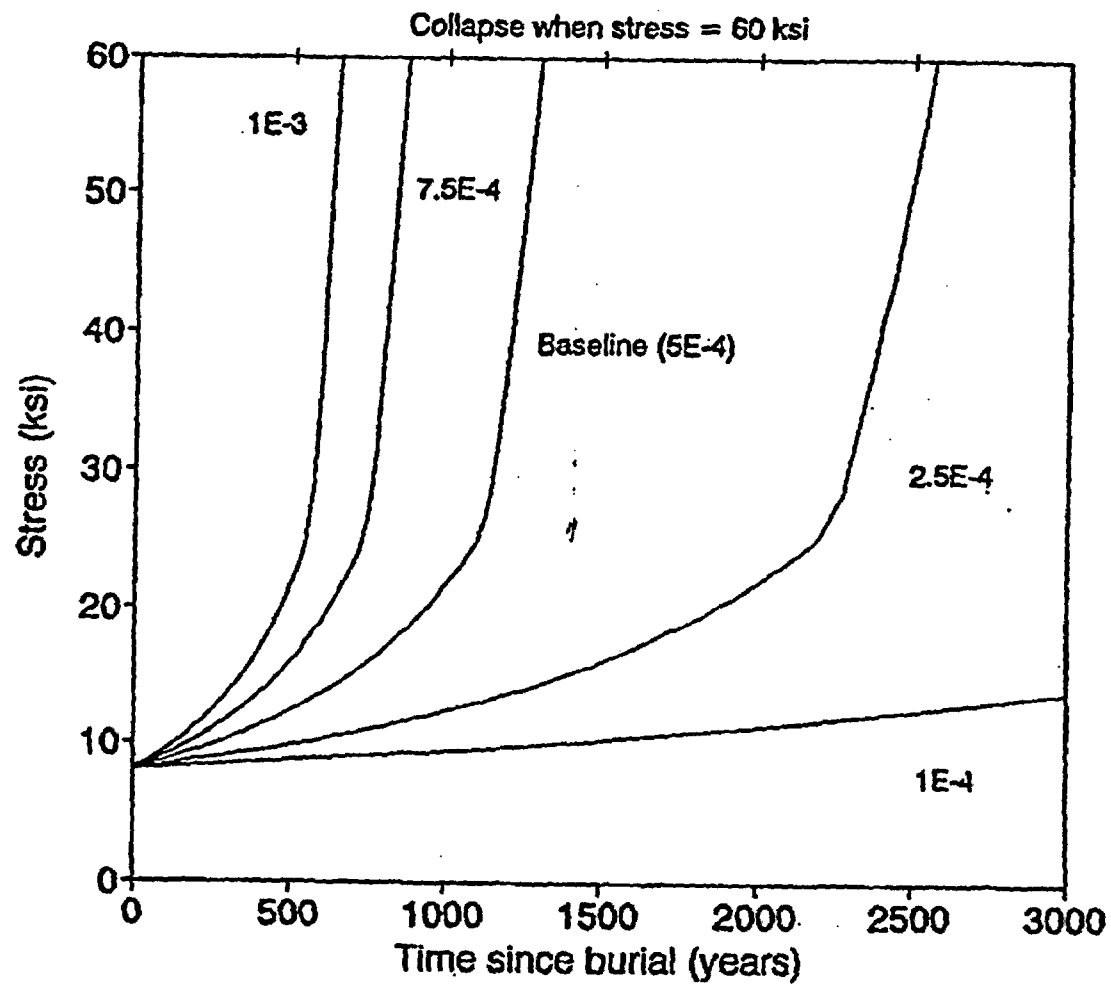
DATE: 9/7/93

REF: #1025-007

ILT Vault Time to Crack Penetration of Walls;
Sensitivity to Hydrogen Evolution Corrosion Rate (cm/yr)

ITERA

Figure 26



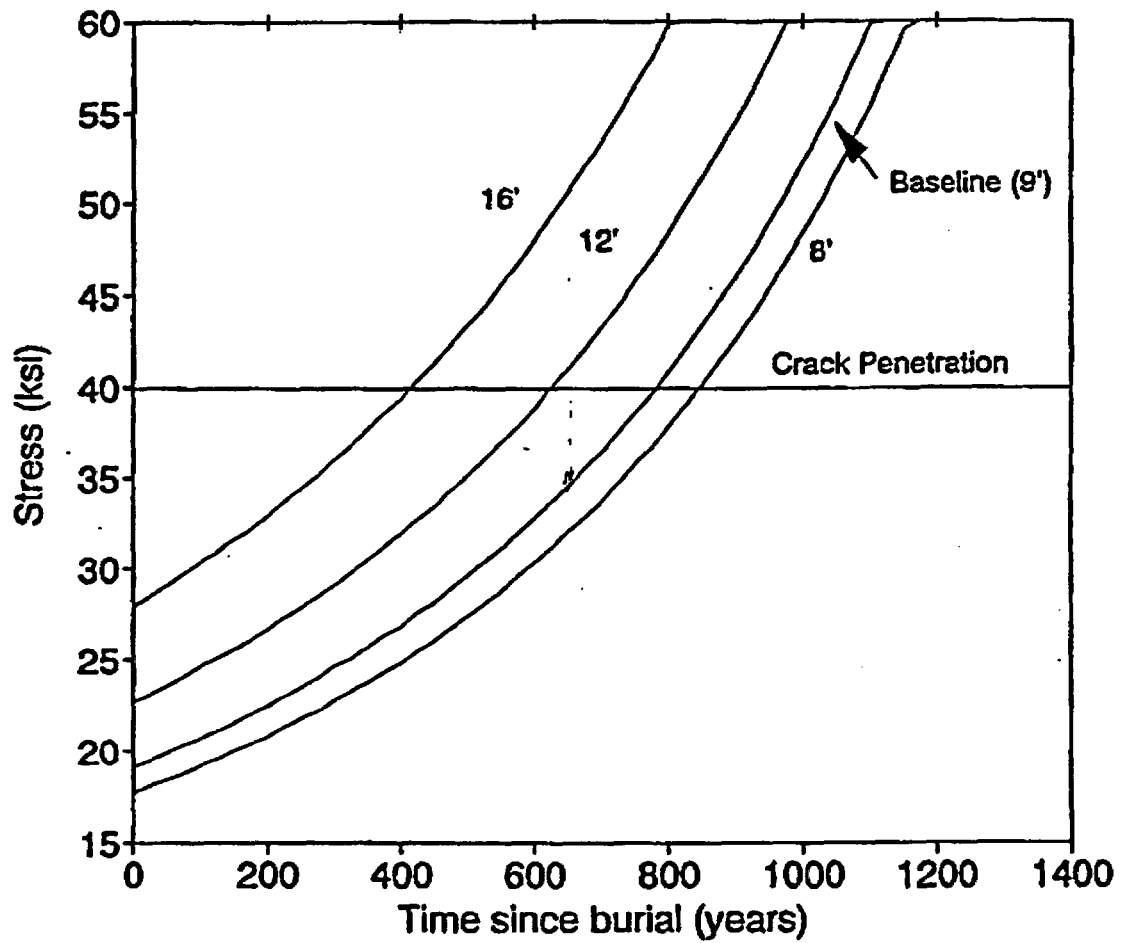
DATE: 9/7/93

REF: #1025-007

ILT Vault Time to Roof Collapse;
Sensitivity to Hydrogen Evolution Corrosion Rate (cm/yr)

INTEC

Figure 27



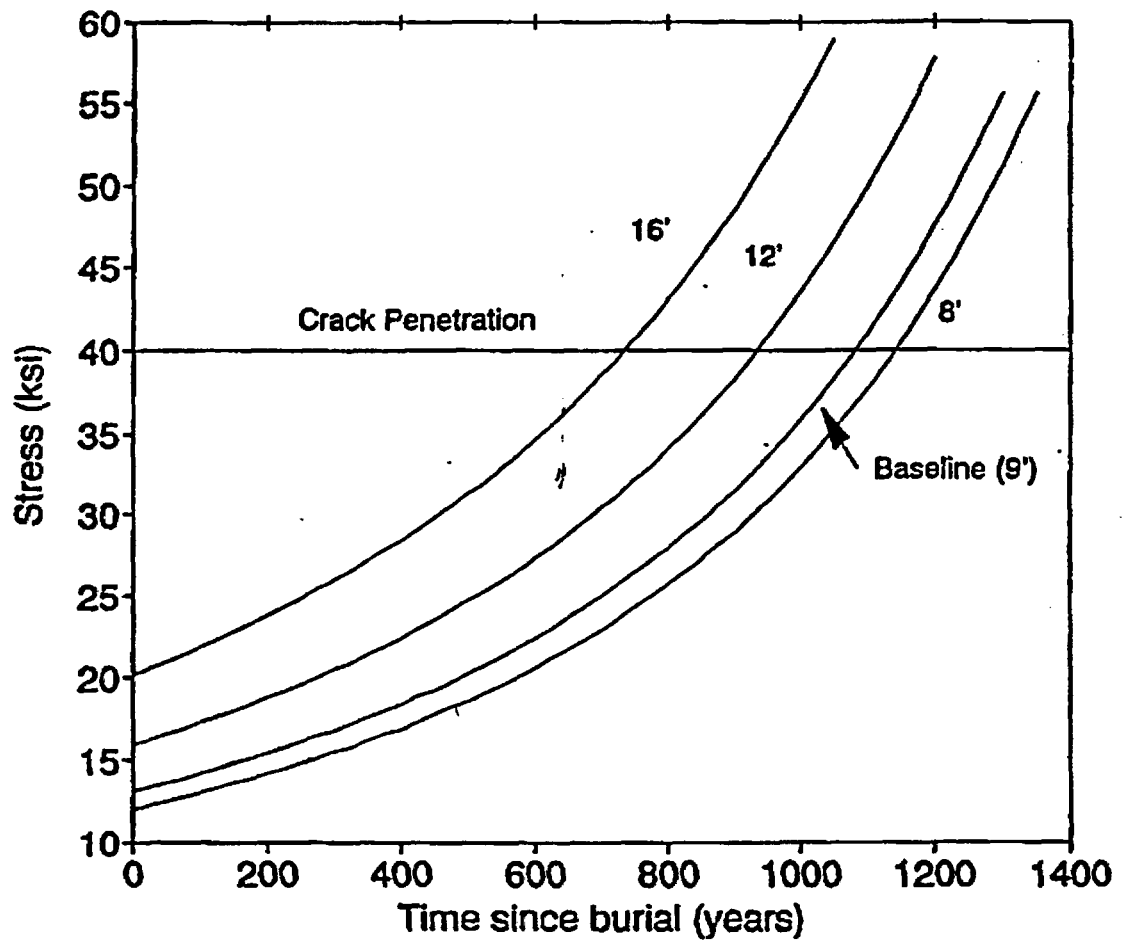
DATE: 9/7/93

REF: #1025-007

ILT Vault Time to Crack Penetration of Roof;
Sensitivity to Depth of Soil Cover

INTERA

Figure 28



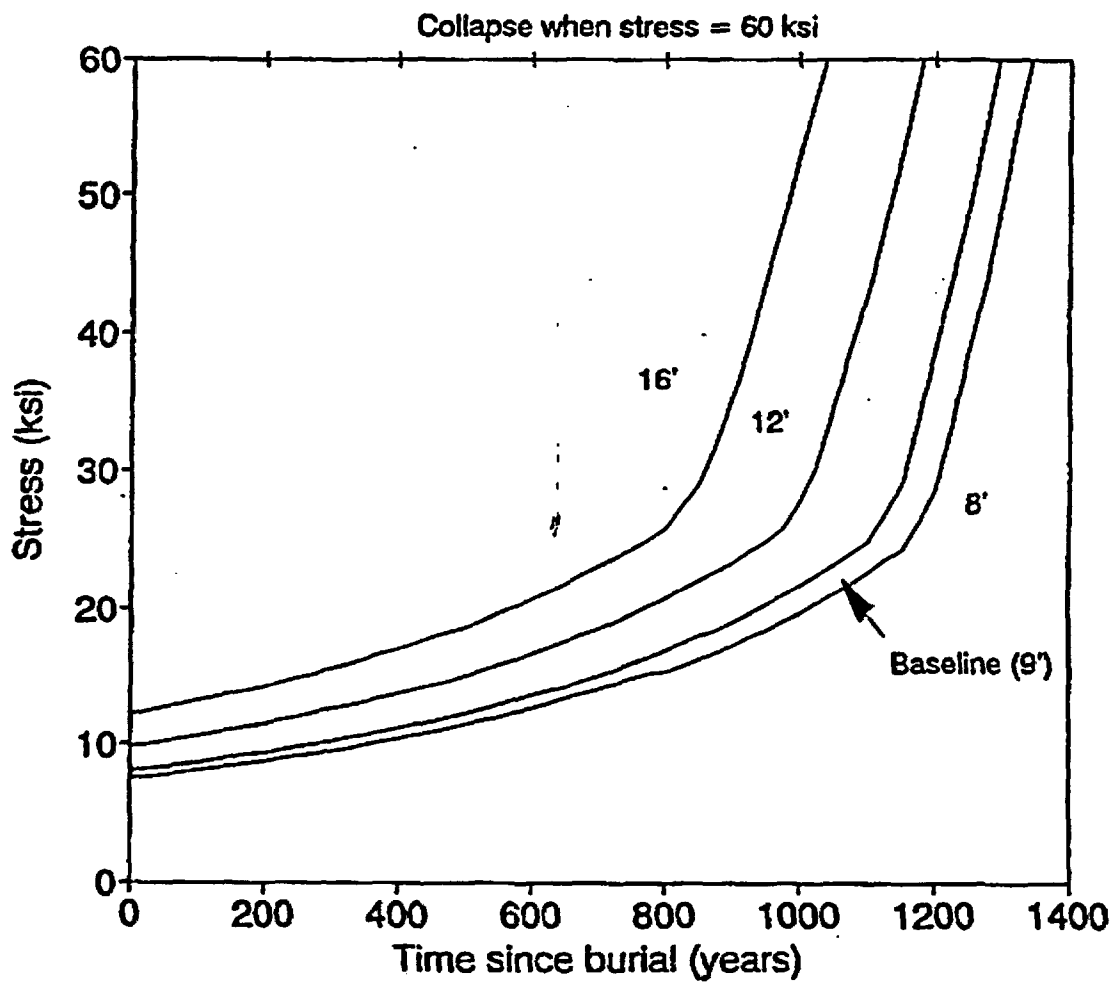
DATE: 9/7/93

REF: #1025-007

ILT Vault Time to Crack Penetration of Walls;
Sensitivity to Depth of Soil Cover

INTERA

Figure 29



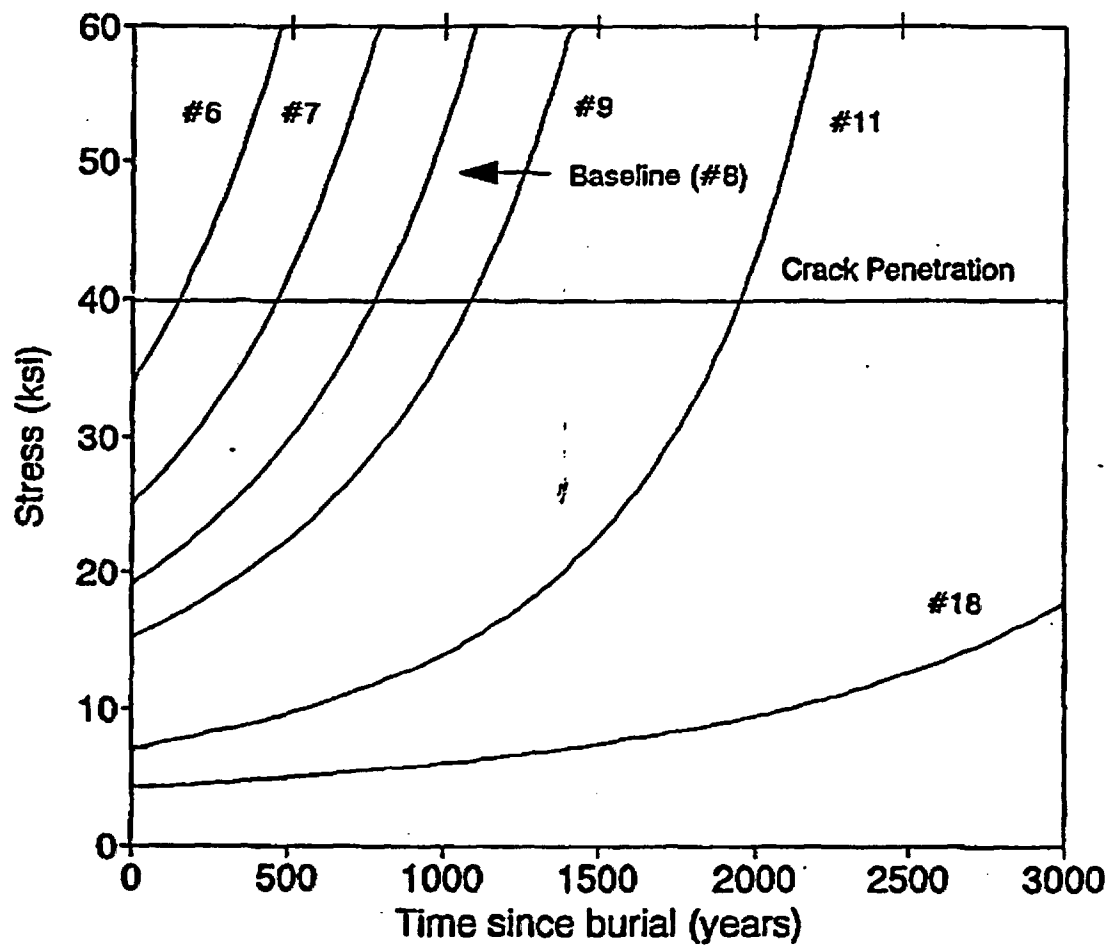
DATE: 9/7/93

REF: #1025-007

ILT Vault Time to Roof Collapse;
Sensitivity to Depth of Soil Cover

WETA

Figure 30



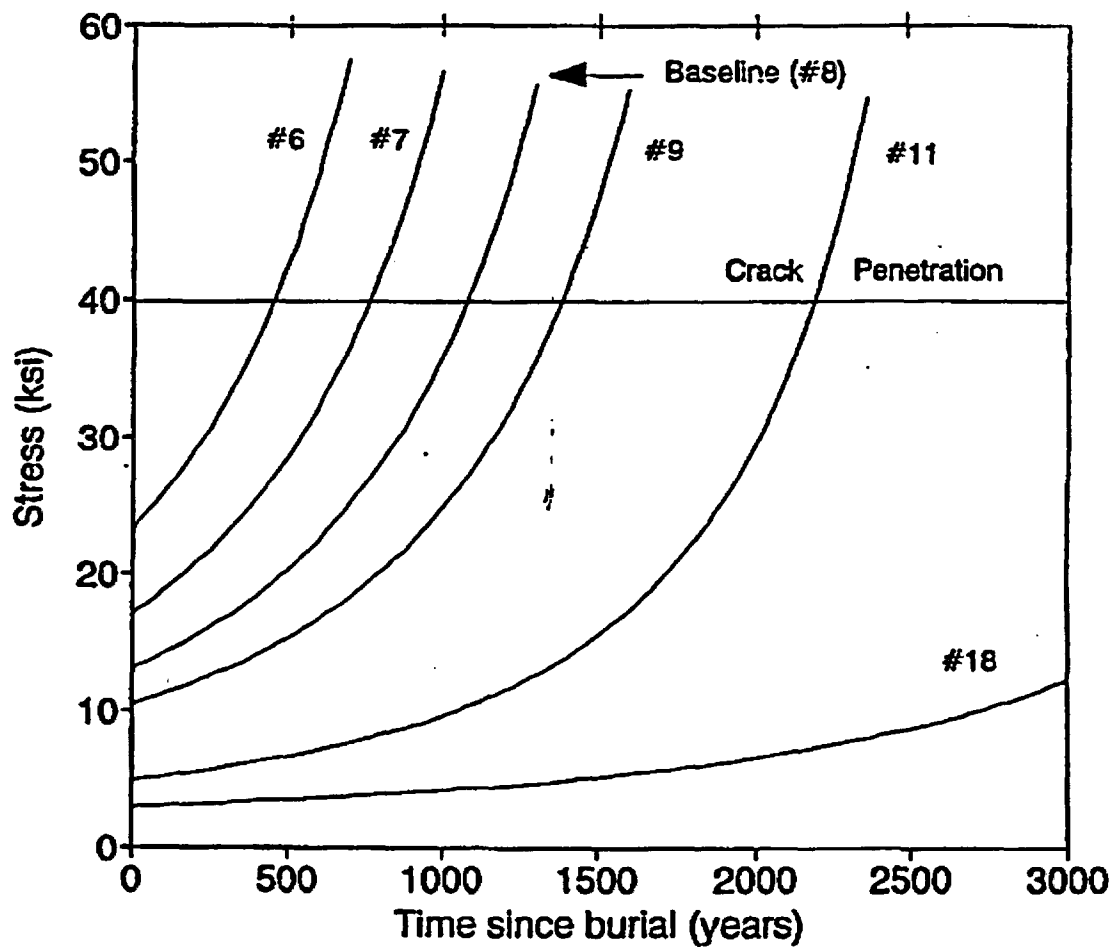
DATE: 9/7/93

REF: #1025-007

ILT Vault Time to Crack Penetration of Roof;
Sensitivity to Rebar Size

INTERA

Figure 31



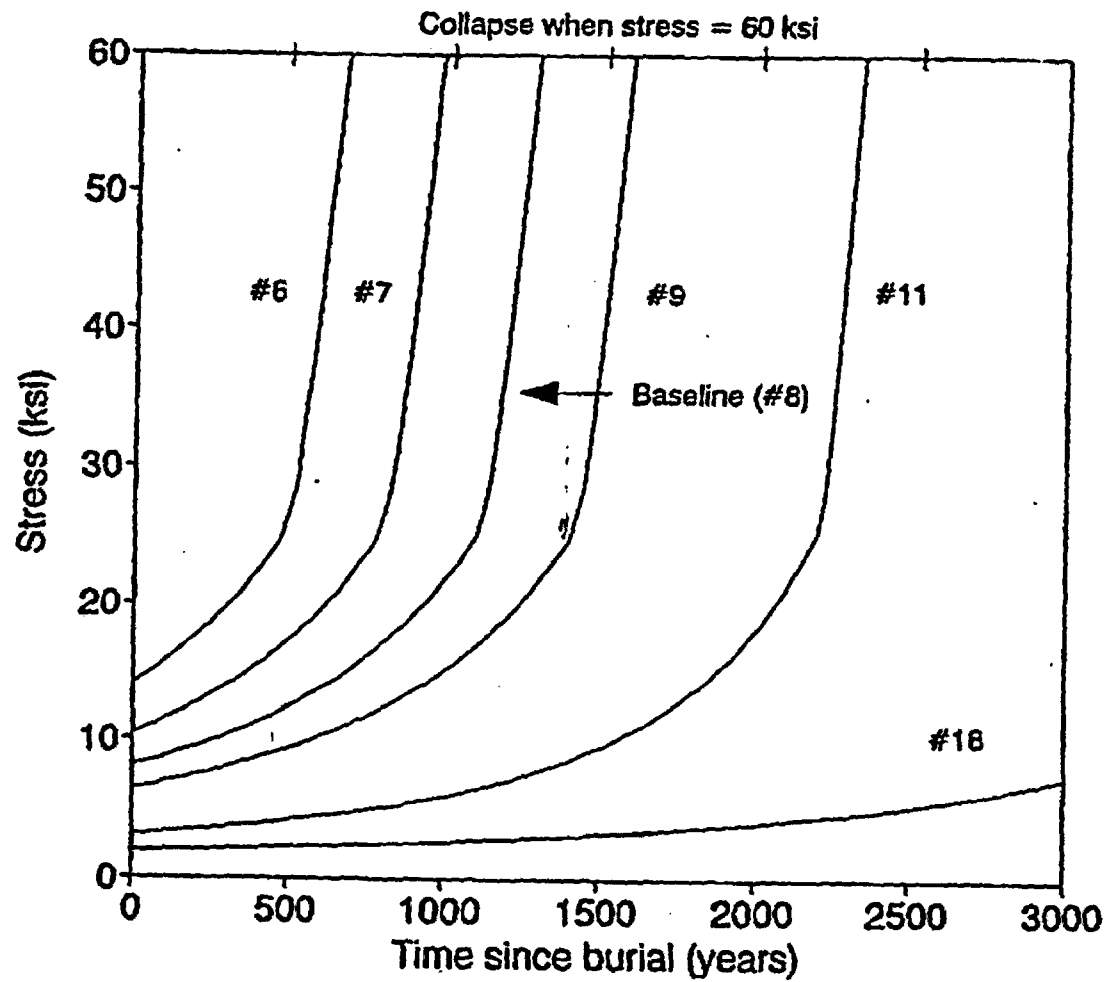
DATE: 9/7/93

REF: #1025-007

ILT Vault Time to Crack Penetration of Walls;
Sensitivity to Rebar Size

ITERA

Figure 32



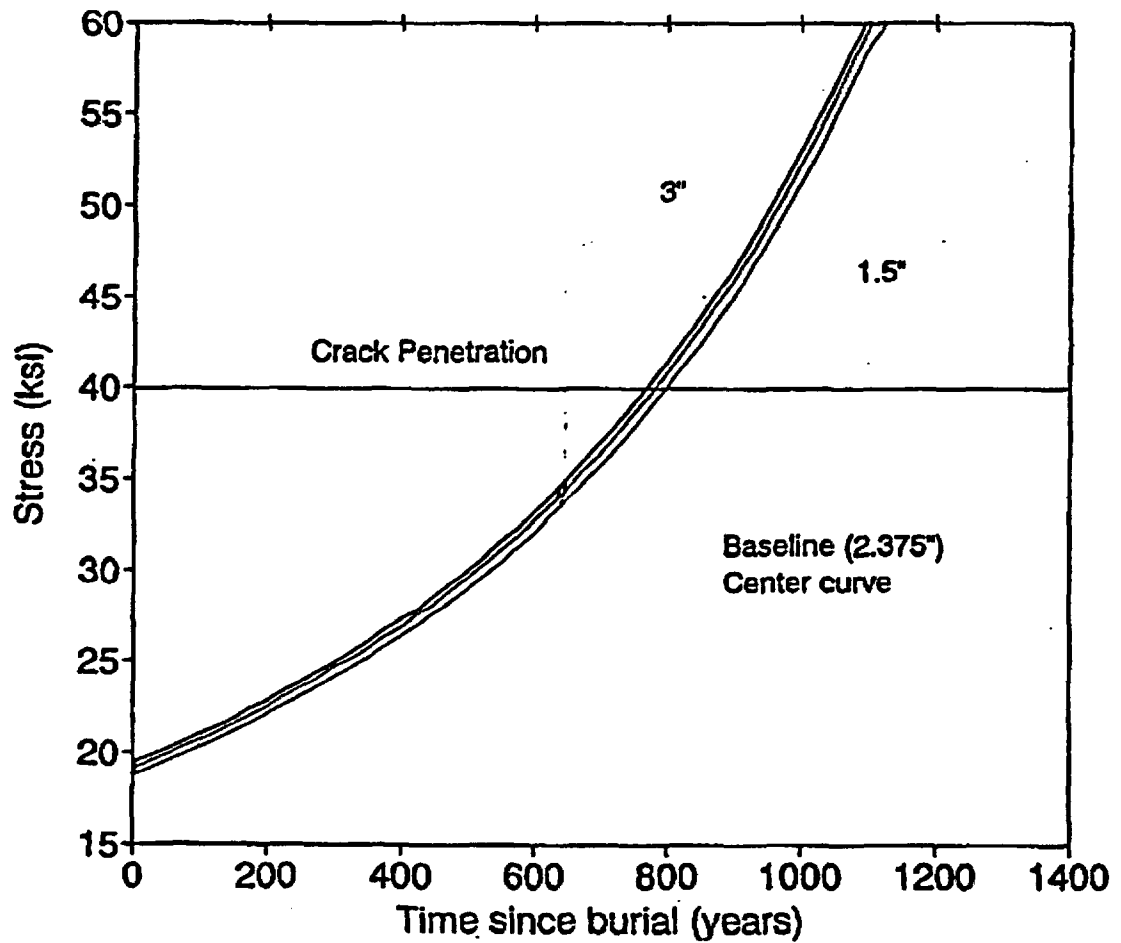
DATE: 9/7/93

REF: #1025-007

ILT Vault Time to Roof Collapse
Sensitivity to Rebar Size

INTERA

Figure 33



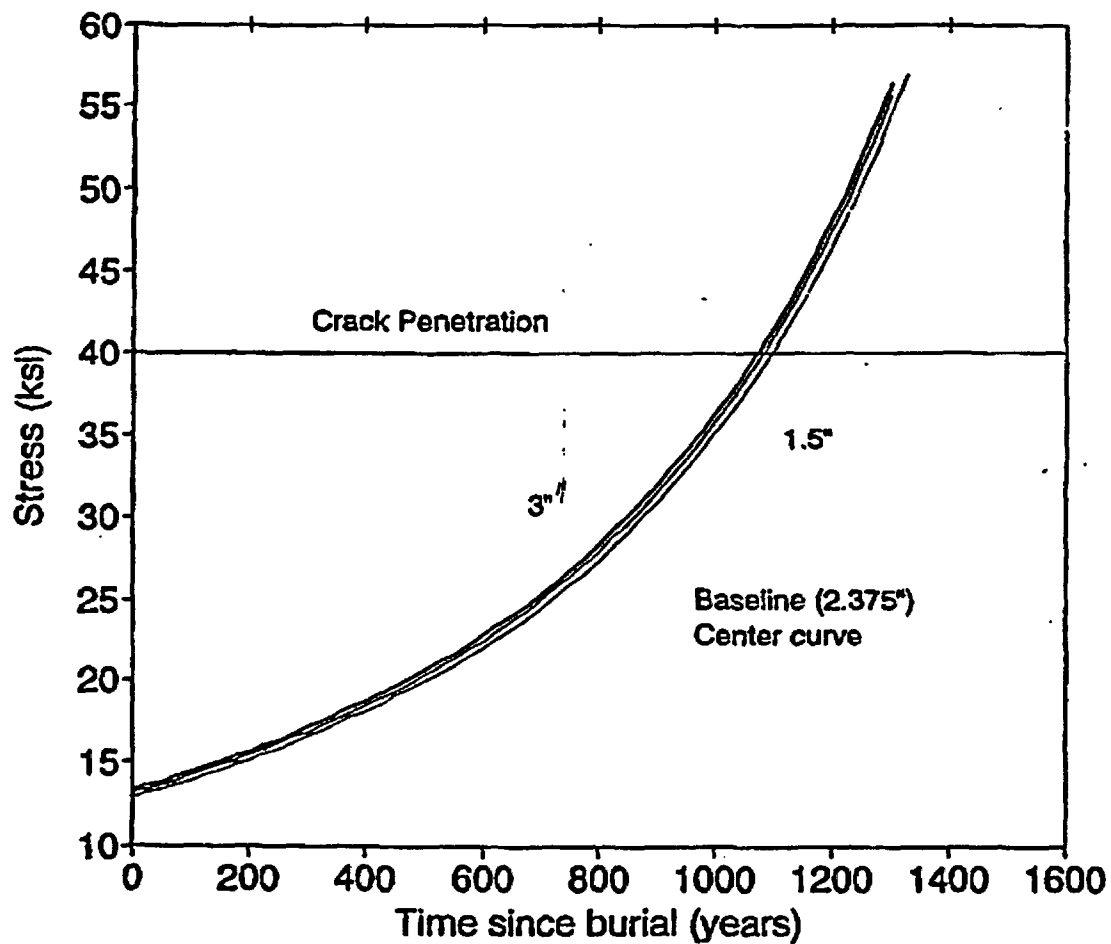
DATE: 9/7/93

REF: #1025-007

ILT Vault Time to Crack Penetration of Roof;
Sensitivity to Depth of Concrete Cover Over Rebar

INTERA

Figure 34



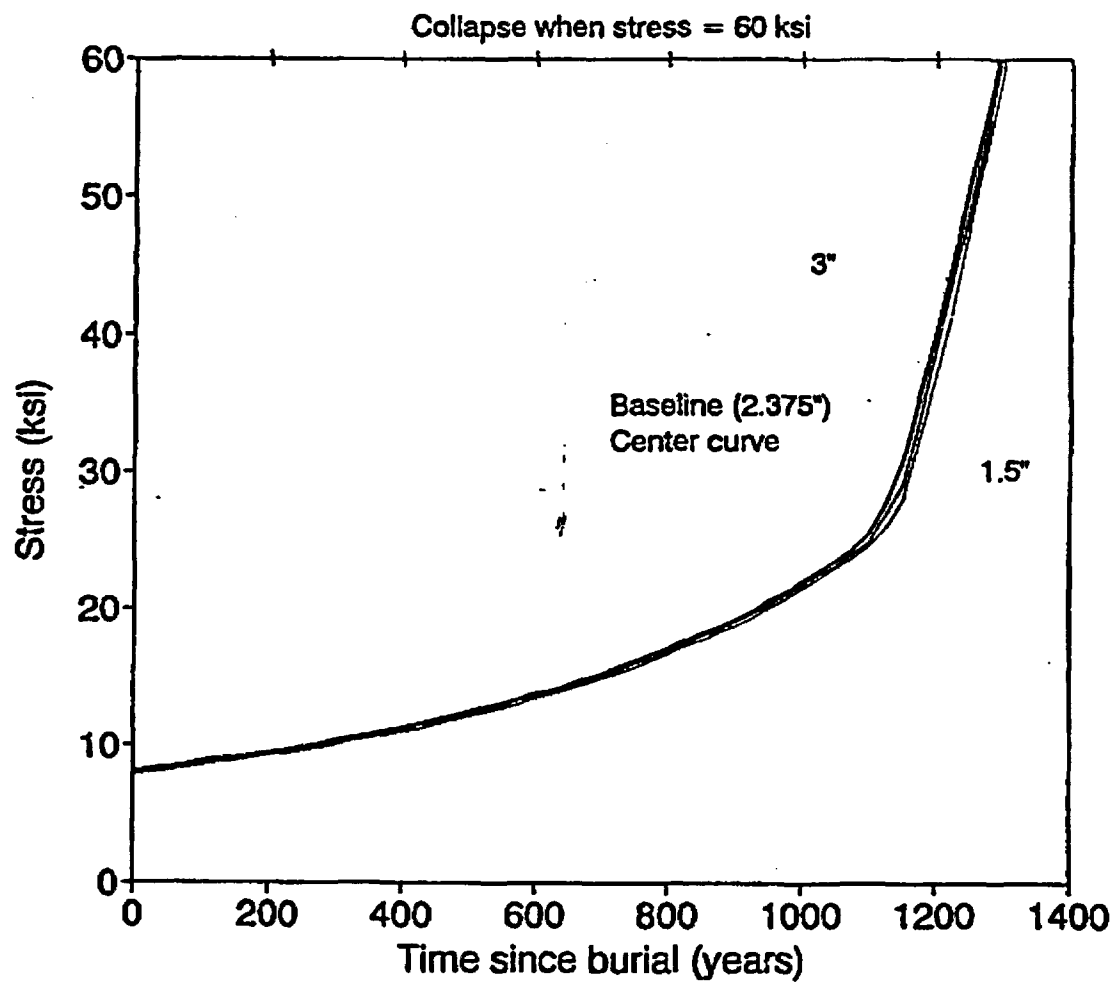
DATE: 9/7/93

REF: #1025-007

ILT Vault Time to Crack Penetration of Walls;
Sensitivity to Depth of Concrete Cover over Rebar

INTERA

Figure 35



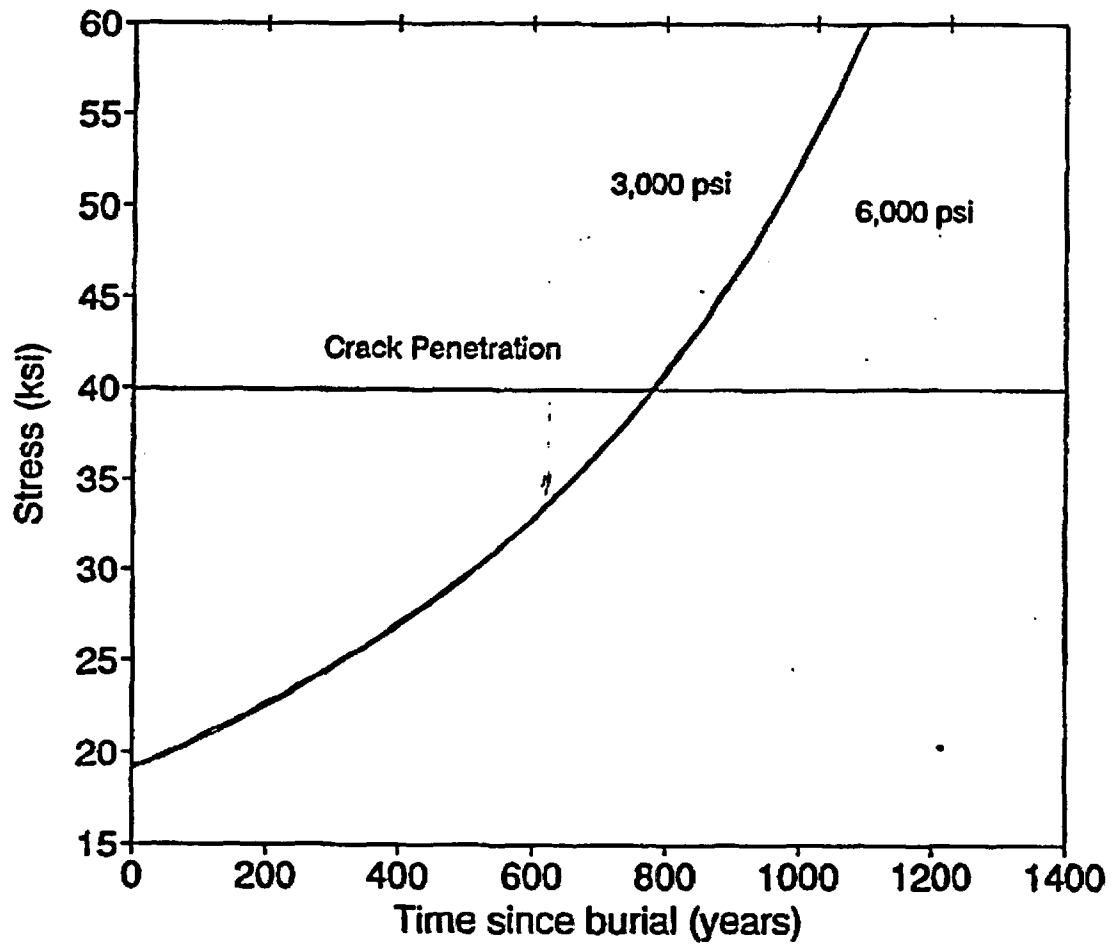
DATE: 9/7/93

REF: #1025-007

ILT Vault Time to Roof Collapse;
Sensitivity to Depth of Concrete Cover Over Rebar

INTERIA

Figure 36



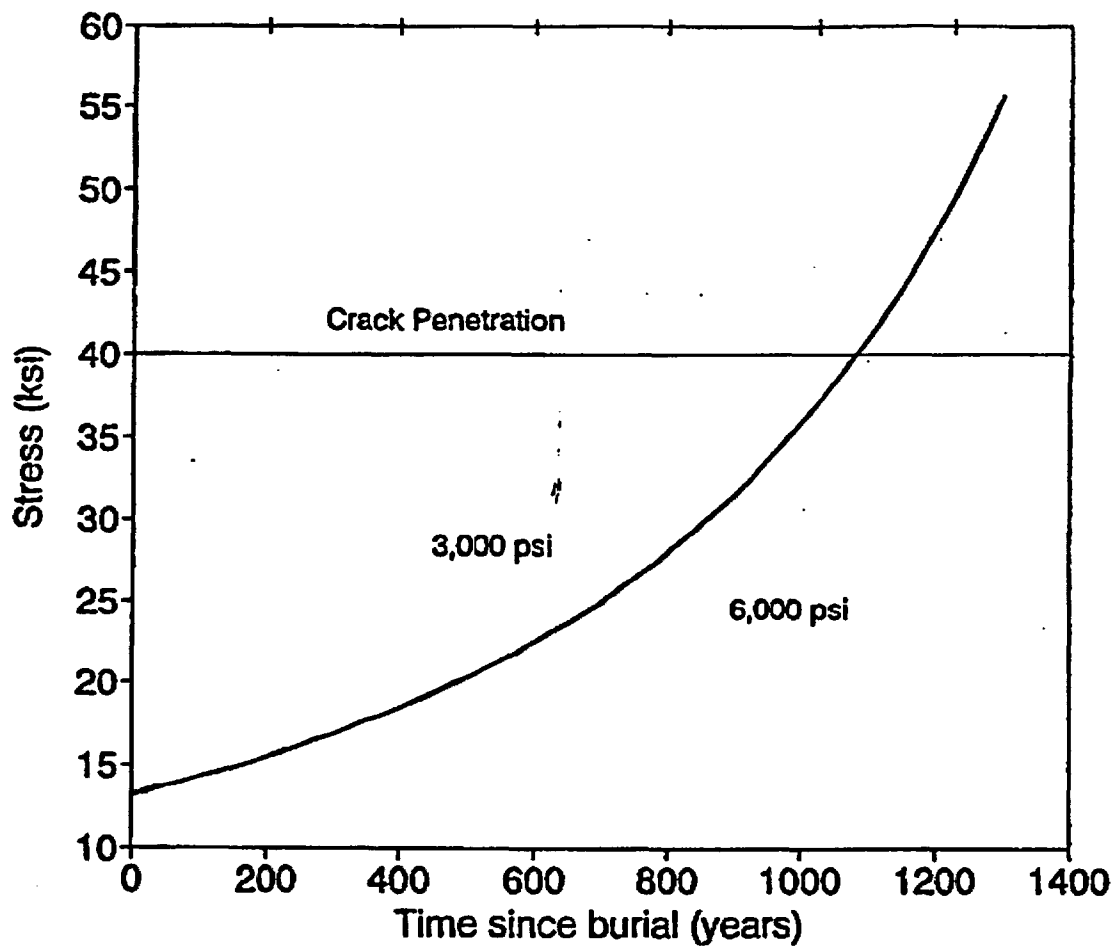
DATE: 9/7/93

REF: #1025-007

ILT Vault Time to Crack Penetration of Roof;
Sensitivity to Concrete Strength

INTERA

Figure 37



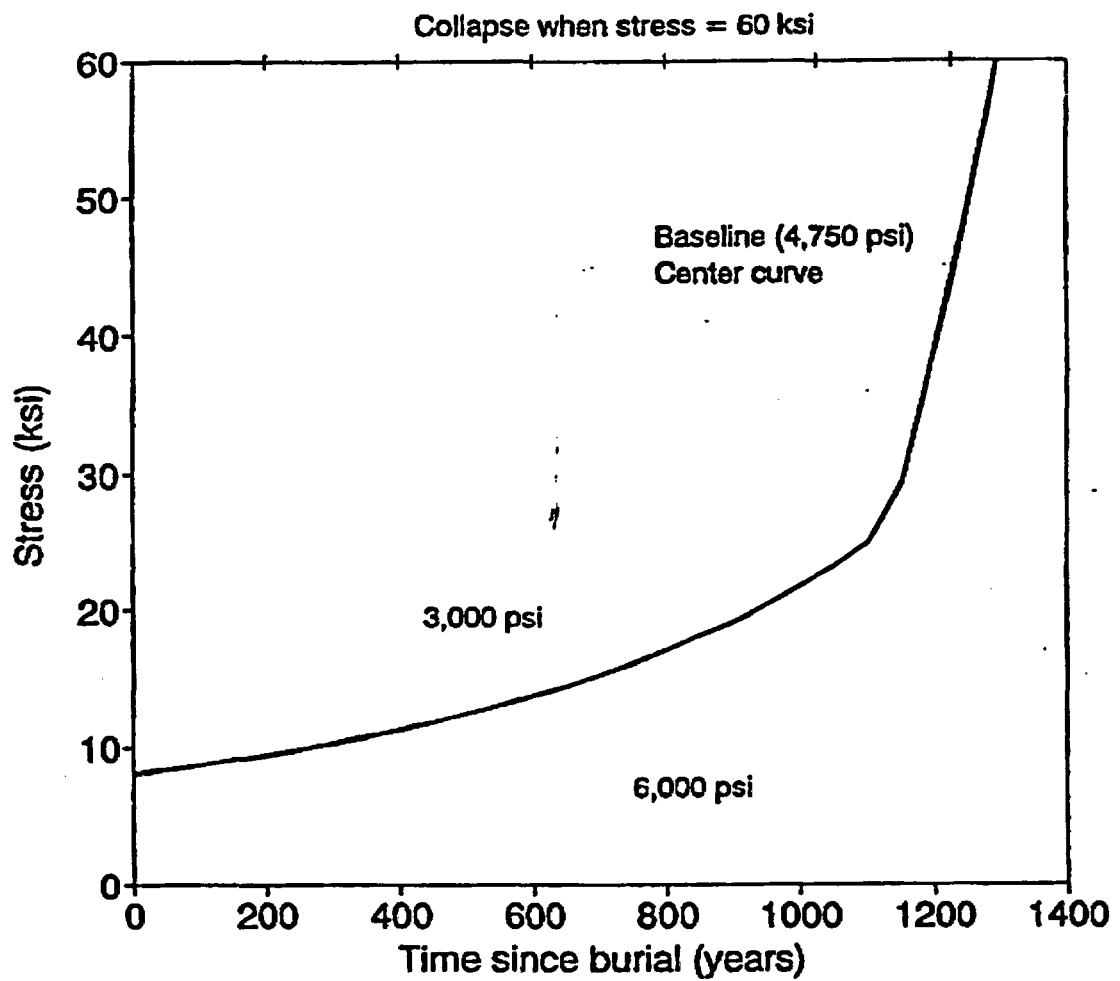
DATE: 9/7/93

REF: #1025-007

ILT Vault Time to Crack Penetration of Walls;
Sensitivity to Concrete Strength

INTERA

Figure 38



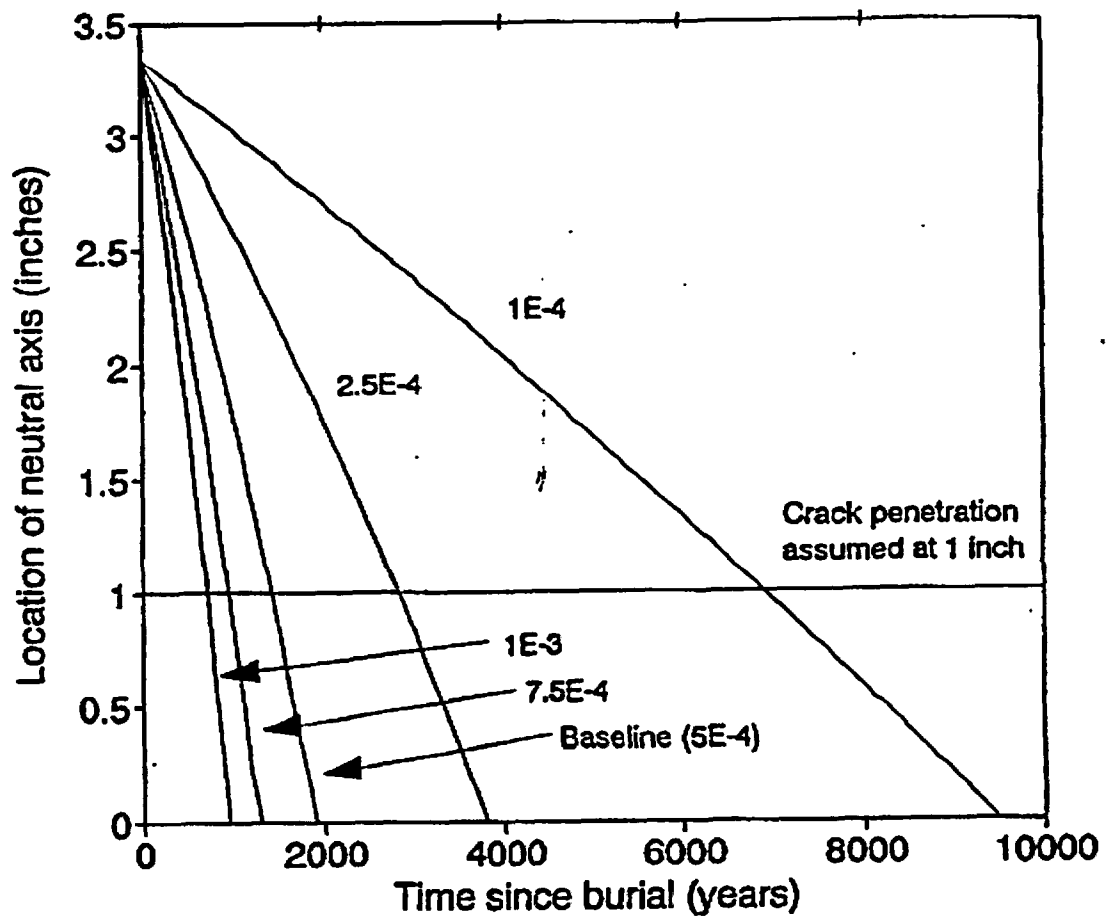
DATE: 9/7/93

REF: #1025-007

ILT Vault Time to Roof Collapse;
Sensitivity to Concrete Strength

ITERA

Figure 39



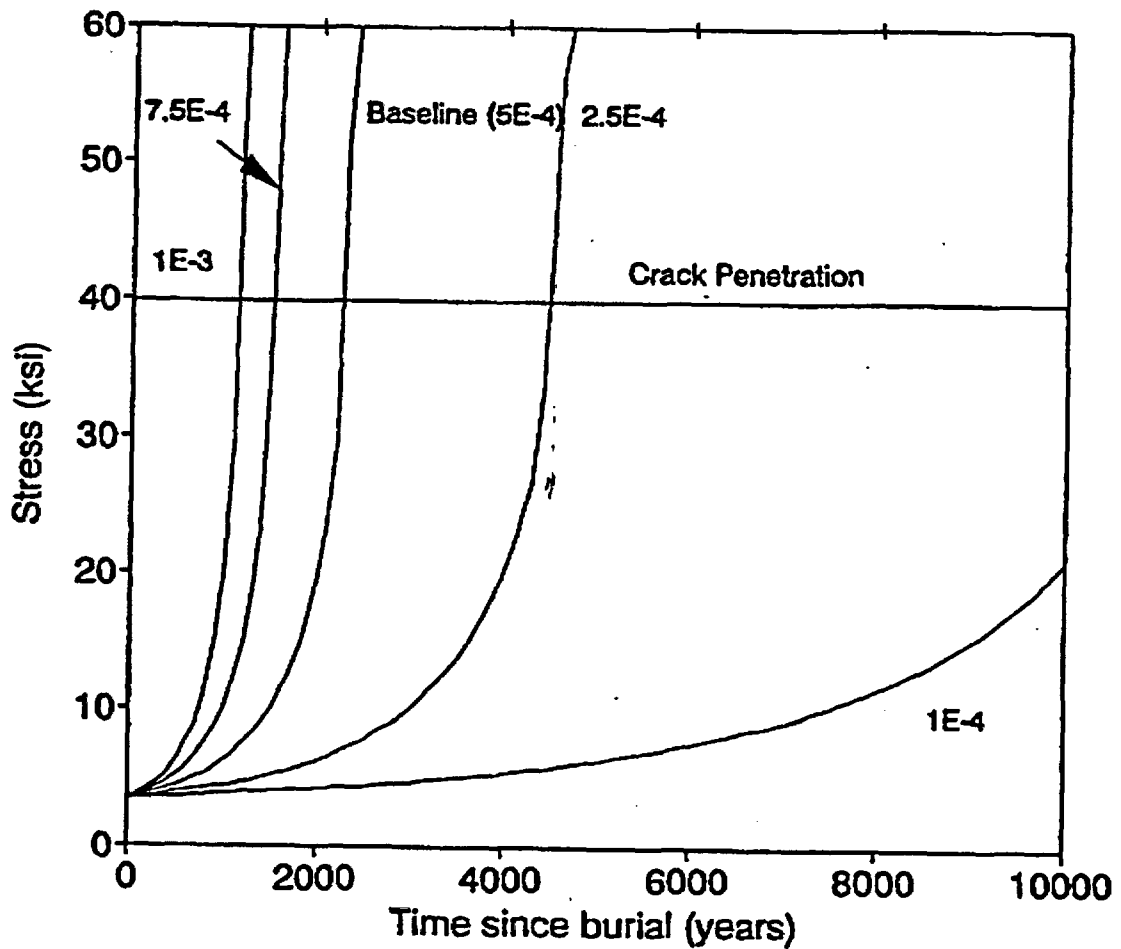
DATE: 9/7/93

REF: #1025-007

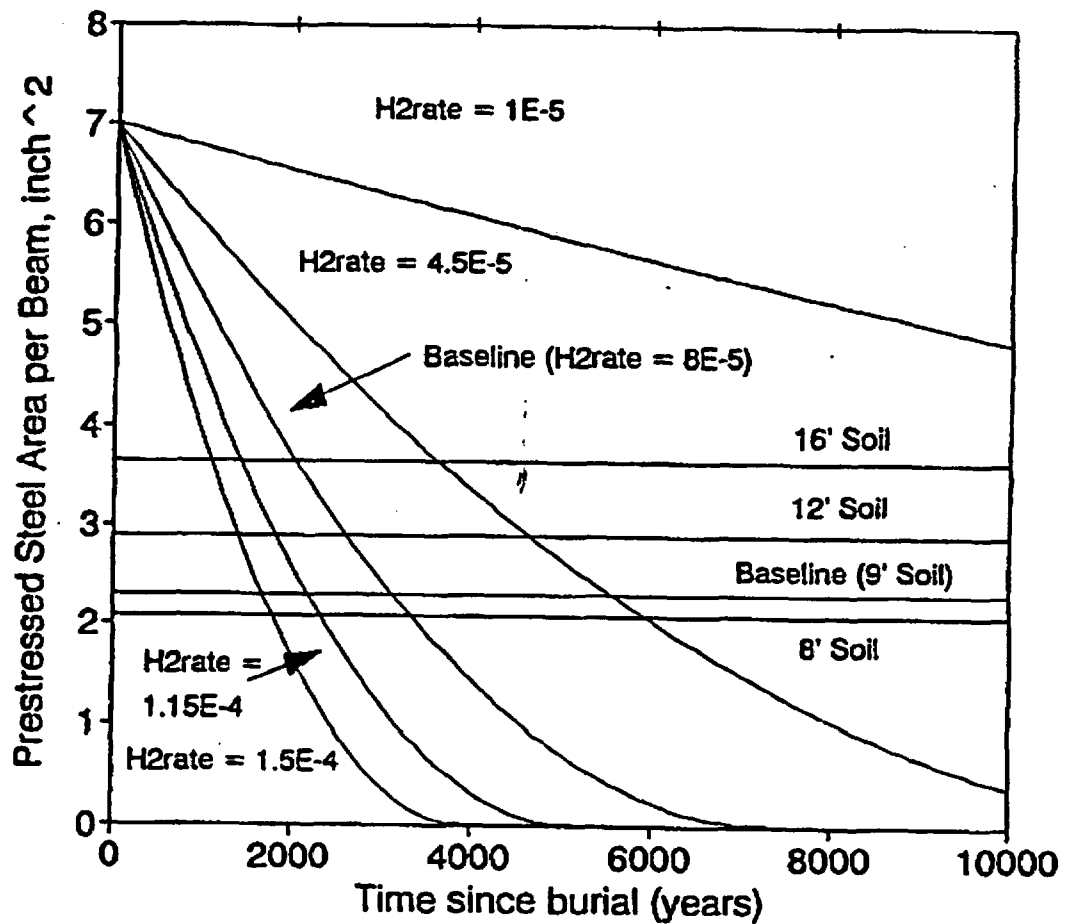
LAW Vault Time to Crack Penetration of Roof;
Sensitivity to Hydrogen Evolution Corrosion Rate (cm/yr)

INTERA

Figure 40



DATE: 9/7/93	LAW Vault Time to Crack Penetration of Walls; Sensitivity to Hydrogen Evolution Corrosion Rate (cm/yr)	
REF: #1025-007		
INTERA		Figure 41



Horizontal lines indicate minimum prestressed steel area required for various depths of soil cover.

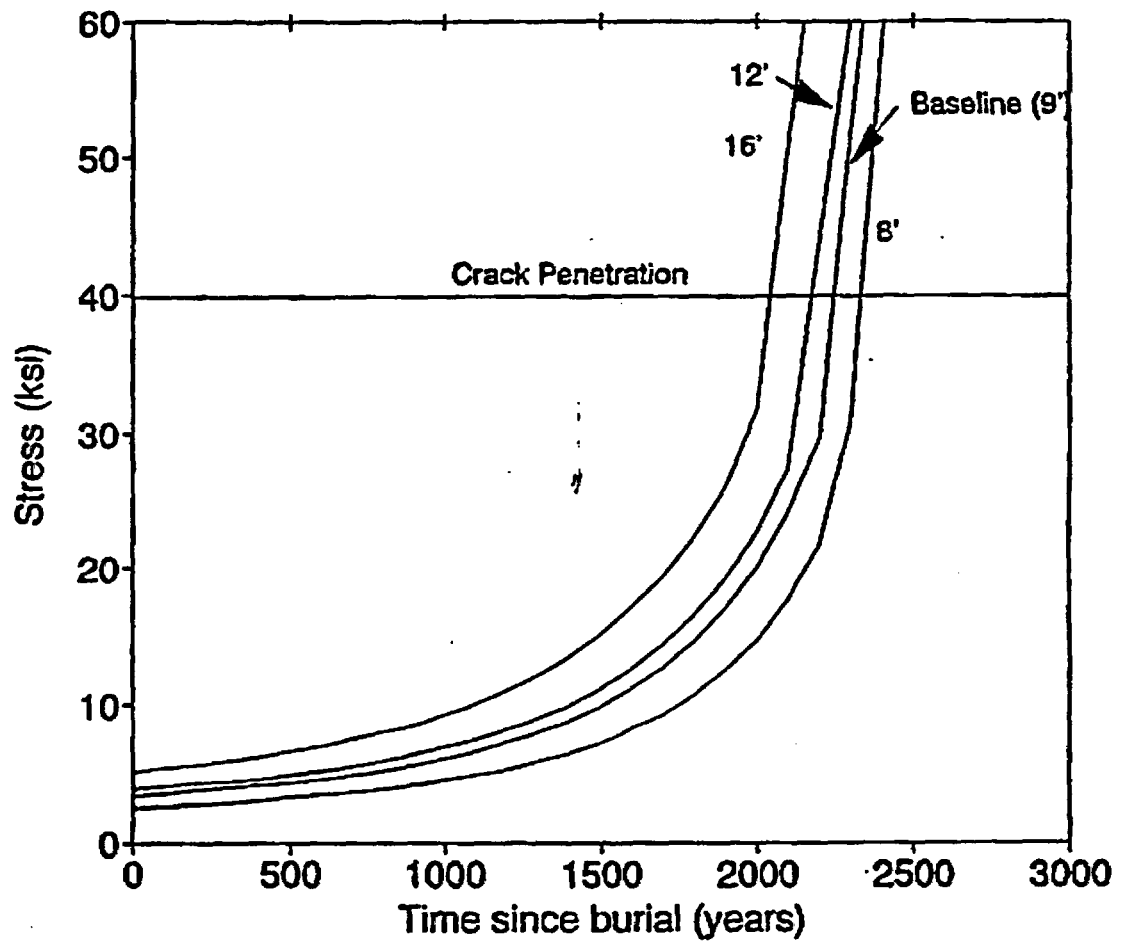
DATE: 9/7/93

REF: #1025-007

LAW Vault Time to Roof Collapse;
Sensitivity to Hydrogen Evolution Corrosion Rate
(H2rate; cm/yr) and Depth of Soil Cover

INTERA

Figure 42



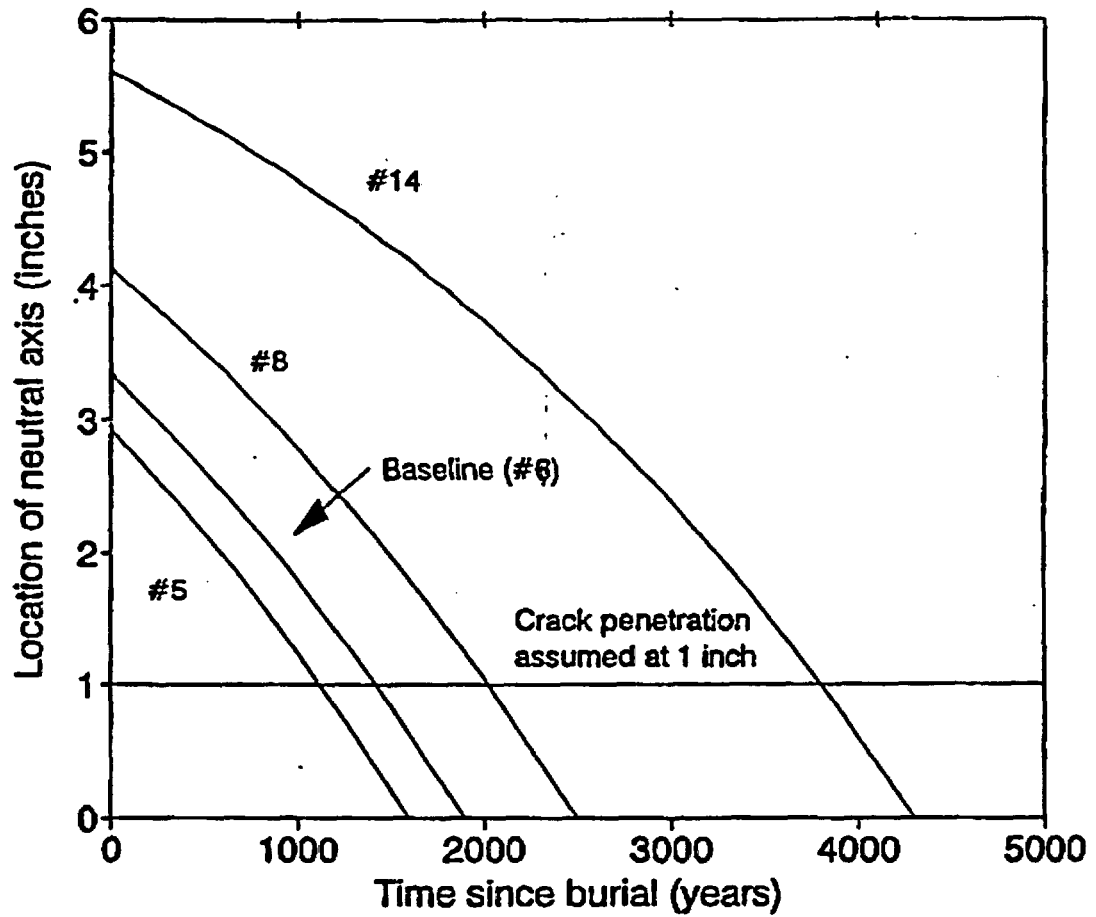
DATE: 9/7/93

REF: #1025-007

LAW Vault Time to Crack Penetration of Walls;
Sensitivity to Depth of Soil Cover

WETA

Figure 43



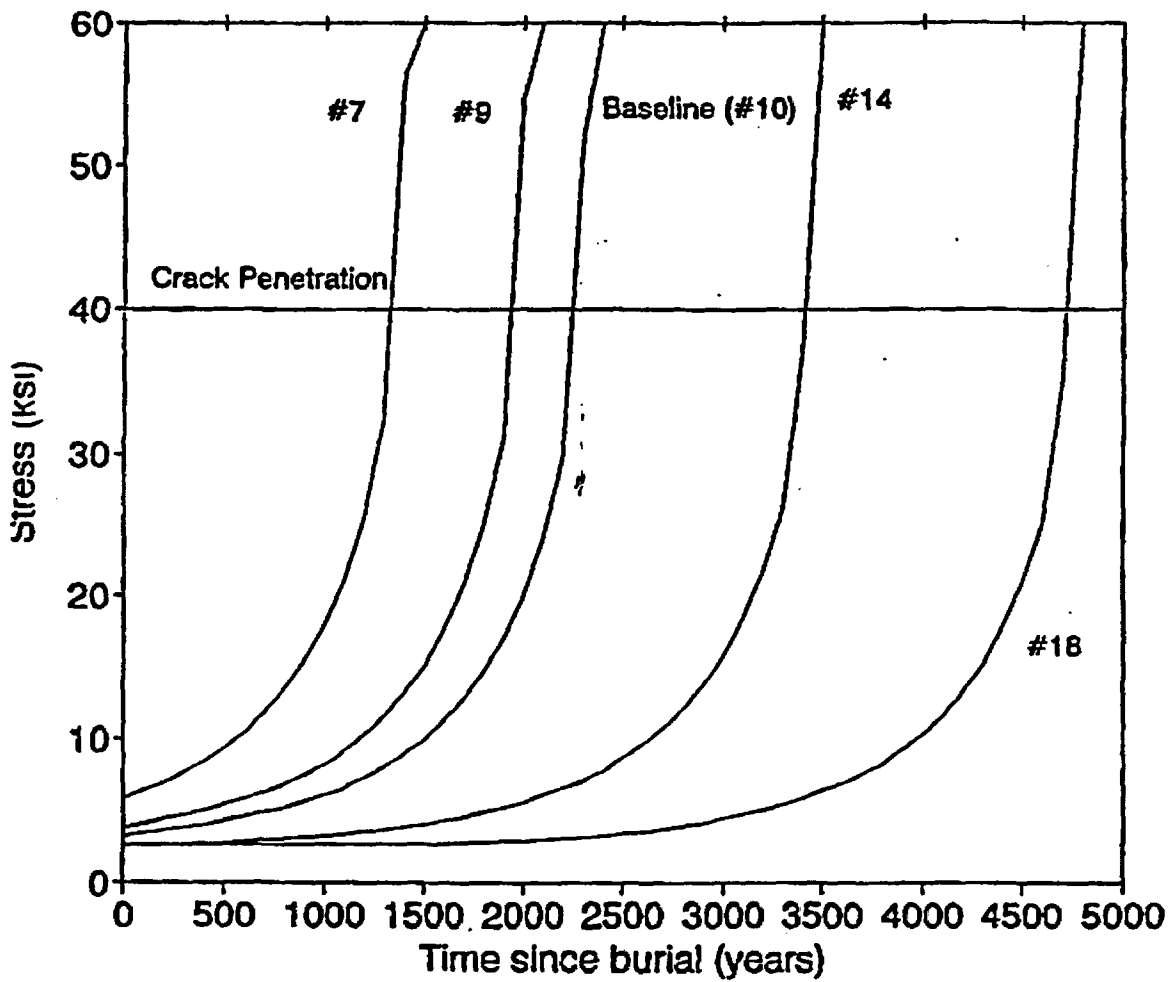
DATE: 9/7/93

REF: #1025-007

LAW Vault Time to Crack Penetration of Roof;
Sensitivity to Rebar Size

INTERA

Figure 44



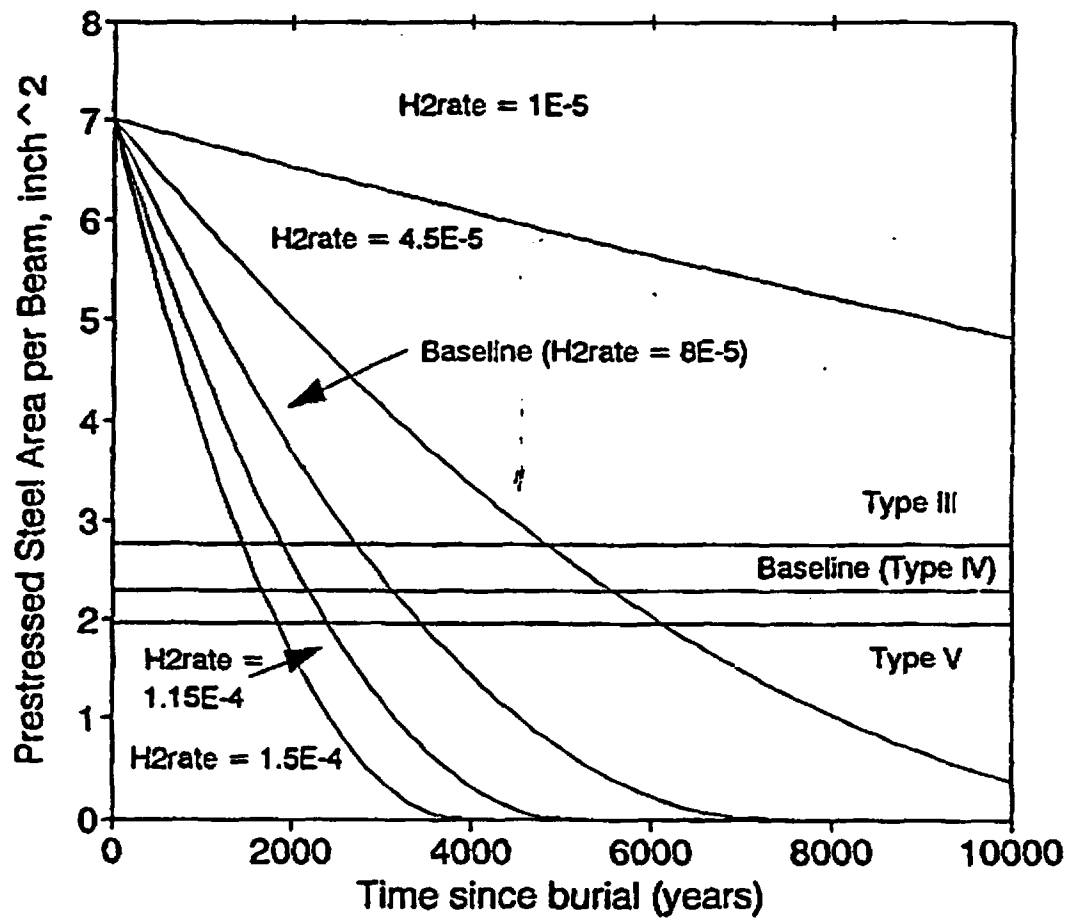
DATE: 9/7/93

REF: #1025-007

LAW Vault Time to Crack Penetration of Walls;
Sensitivity to Rebar Size

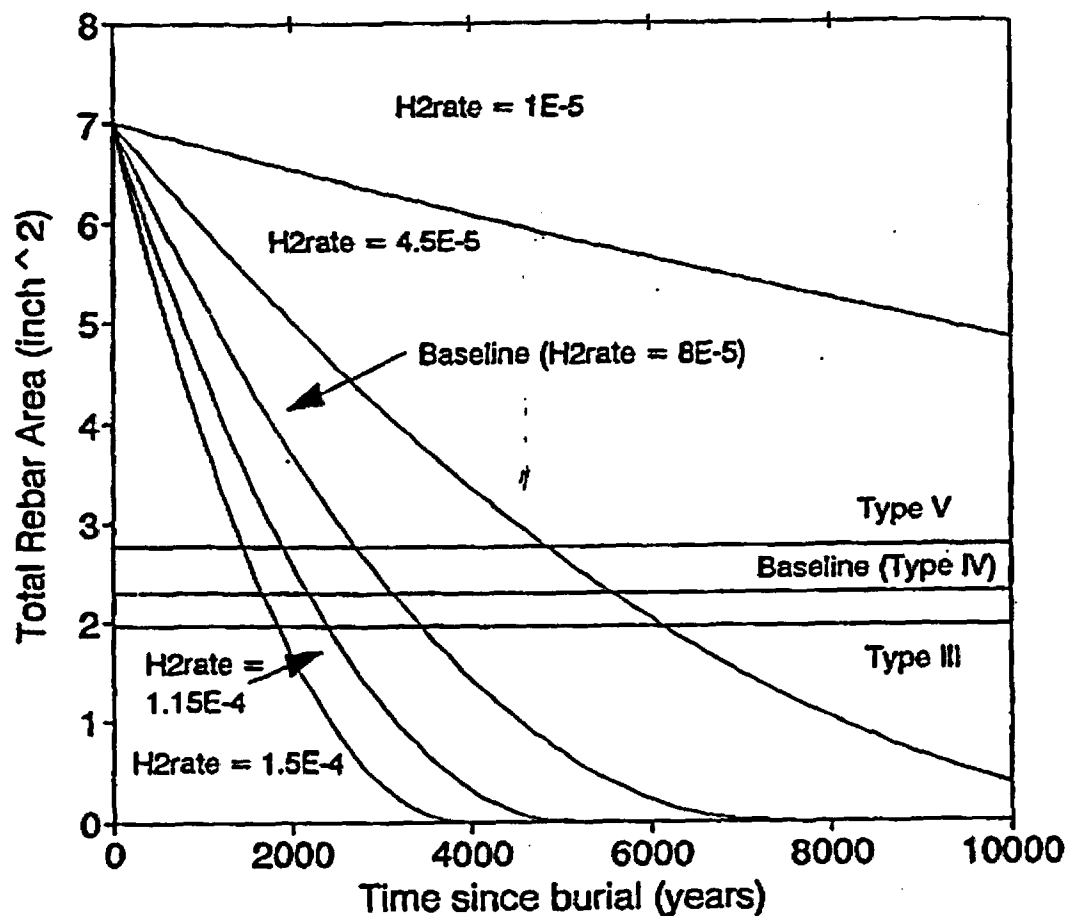
INTERA

Figure 45



Horizontal lines indicate minimum prestressed steel area required for various sized AASHTO beams.

DATE: 9/7/93	LAW Vault Time to Roof Collapse; Sensitivity to Hydrogen Evolution Corrosion Rate (H2rate; cm/yr) and Beam Type	
REF: #1025-007		
INTERA		Figure 46



Horizontal lines indicate minimum prestressed steel area required for various sized AASHTO beams.

DATE: 9/7/93	LAW Vault Time to Roof Collapse; Sensitivity to Hydrogen Evolution Corrosion Rate (H ₂ rate; cm/yr) and Beam Type	
REF: #1025-007		
INTERA		Figure 46

ORIGINAL CONCRETE ROOF SURFACE

CURRENT SURFACE DUE TO SO_2 ATTACK (0.1 cm LOSS)

THEORETICAL DEPTH OF CARBONATION (0.9 cm)

pH ZONE (≈ 9.5)

LEACH PENETRATION: 5.9 cm

pH ZONE (≈ 13)

ORIGINAL REBAR RADIUS: 1.27 cm

CURRENT REBAR RADIUS: 1.25 cm

pH ZONE (≈ 13)

ORIGINAL REBAR RADIUS: 1.27 cm

MINIMAL REBAR LOSS (0.006 cm)

VAULT INTERIOR

DATE: 9/7/93

REF: #1025-007

Cross-Section of Vault Roof Assuming Use of High-pH
Concrete; Degradation at 50 Years

INTERA

Figure 47

ORIGINAL CONCRETE ROOF SURFACE

CURRENT SURFACE DUE TO SO_2 ATTACK (0.7 cm LOSS)

THEORETICAL DEPTH OF CARBONATION (2.6 cm)

ORIGINAL REBAR RADIUS: 1.27 cm

CURRENT REBAR RADIUS: 0.7 cm

pH ZONE (≈ 9.5)

LEACH PENETRATION: 16.7 cm

pH ZONE (≈ 13)

pH ZONE (≈ 13)

ORIGINAL REBAR RADIUS: 1.27 cm

CURRENT REBAR RADIUS: 1.22 cm

VAULT INTERIOR

DATE: 9/7/93

REF: #1025-007

Cross-Section of Vault Roof Assuming Use of High-pH
Concrete; Degradation at 400 Years

INTERA

Figure 48

APPENDIX L

DESCRIPTION OF NAVAL REACTOR WASTE DISPOSAL

L.1 DESCRIPTION OF NAVAL REACTOR (NR) WASTE DISPOSAL

Heavily shielded shipping/disposal casks containing NR waste are planned to be disposed of in E-Area. Large quantities of activation products are associated with the metal matrix of the waste forms within the disposal containers. The purpose of this appendix is to assess the performance of the planned method of disposal of the NR waste.

L.1.1 Description of NR Waste Forms

Naval reactor waste consists of a variety of solid activated metal NR components, including core barrels, adapter flanges, closure heads, and other similar equipment. A concise description of the waste forms likely to be present in the disposal containers is not available because of the classified nature of this information. The total volume of the metal waste alone is expected to be about 3.5 m^3 per disposal container. About $3.8 \times 10^{-3} \text{ m}^3$ (1 gal) of water is expected to be present in each disposal cask.

The shipping/disposal containers in which the NR wastes are planned to be disposed are cylindrical in shape, and composed of carbon steel, with 304 stainless steel inner containers. The containers are Type B or Type-B equivalent, and thus, are designed to be impervious to water. A cross-section of a typical disposal container is illustrated in Fig. L.1-1 (WSRC 1992). The inner volume of this typical container is approximately 27 m^3 .

L.1.2 Layout and Capacity of NR Waste Disposal Site

In this assessment, it is assumed that 100 disposal casks containing NR waste will be disposed of in E-Area at grade. Given the dimensions provided in Fig. L.1-1, the minimum area for disposal of 100 casks is $1,024 \text{ m}^2$, which corresponds to the area required if 100 casks are placed immediately adjacent to each other in any type of rectangular arrangement. It is likely that there will be a spacing between casks at the time of disposal, and the layout assumed for this assessment is shown in Fig. L.1-2. Here, the spacing between casks is 1 m.

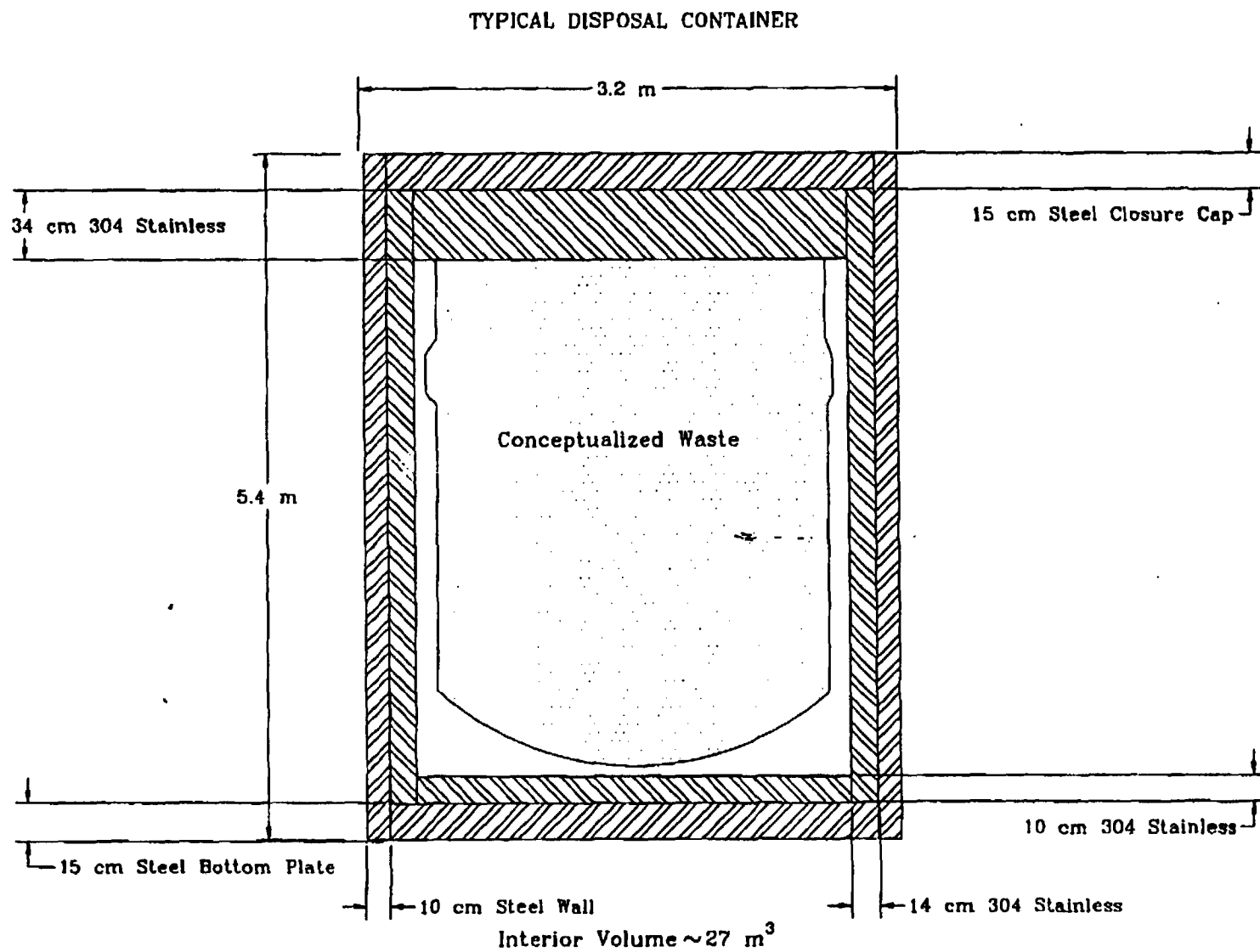


Fig. L1-1. Naval reactor waste disposal container.

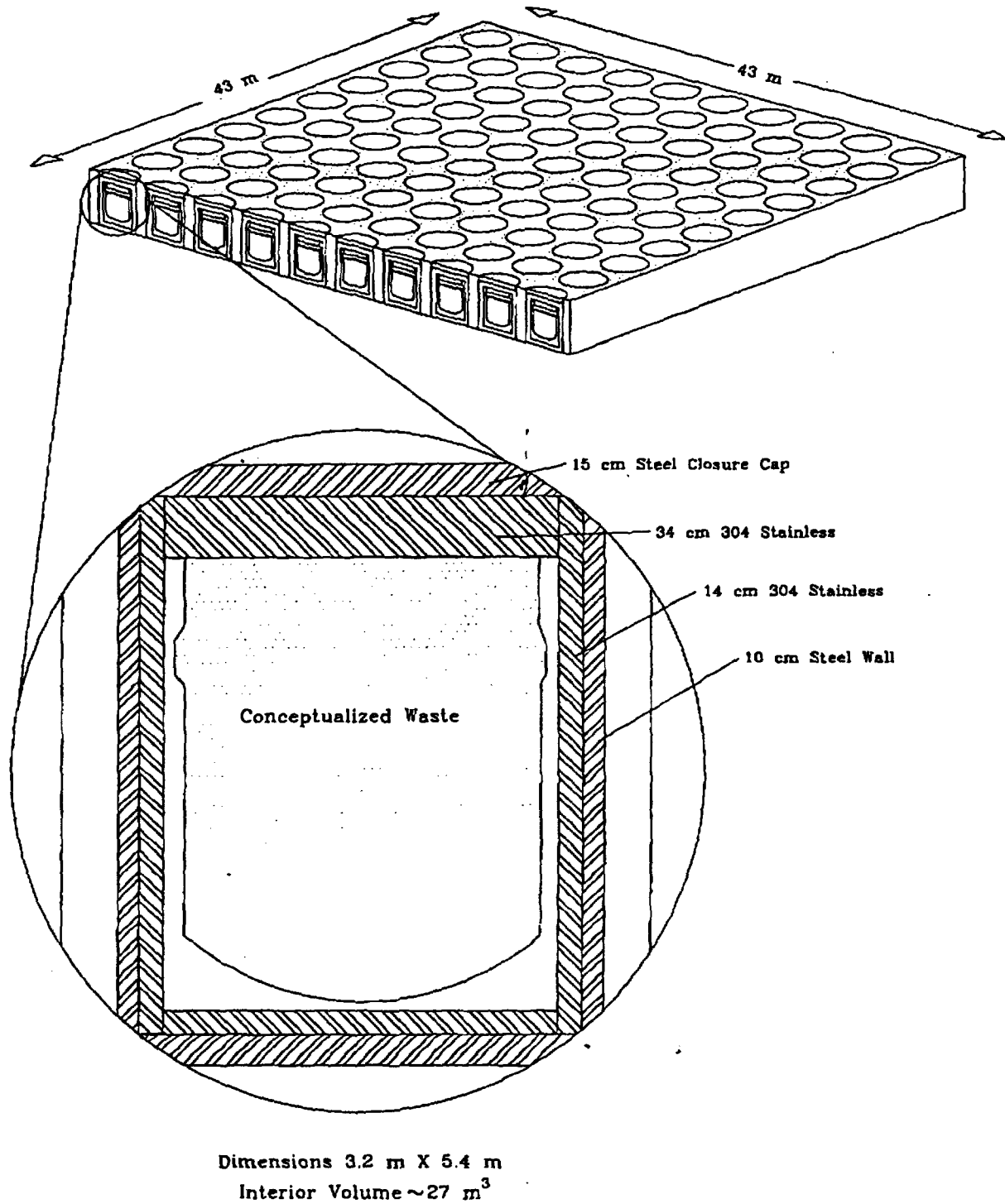


Fig. L.1-2. Proposed layout of Naval Reactor Waste Disposal Area in the EAV facility.

L.1.3 Radioactive Inventory of NR Waste

A radionuclide inventory supplied by the waste generators is presented in Table L.1-1 (WSRC 1992). This inventory applies to 41 casks of five different types that are planned to be delivered to E-Area. The total activity of these casks is estimated to be 5.84×10^6 Ci. This assessment considers, however, that up to 59 more disposal containers will be accepted, with the same general mix of cask types. Allowable inventories for 100 casks will be developed for the radionuclides listed in Table L.1-1.

L.1.4 Closure Concept

Because the NR waste disposal containers will be placed within the EAV facility, final closure will be similar to that for the entire facility. For the purposes of this assessment, the same closure concept as for the EAVs (Sect. 2.9) is assumed. Briefly, backfill of Burma Road sand is assumed to be placed over at-grade casks, above which a laterally extensive moisture barrier is assumed to be placed. The moisture barrier consists of 0.76 m of clay overlain by 0.3 m of gravel and a geotextile fabric. Over this moisture barrier, 0.76 m of backfill is assumed, followed by 0.15 m of topsoil. As a result, a minimum of 2.9 m of cover material is assumed to overlie the NR disposal casks at closure. This requires that the casks be placed in a topographically low spot so as not to project into the cover materials. Revegetation and drainage ditches are assumed to constitute final closure, for the purposes of stabilizing soil, preventing pine tree growth and diverting excess water from the gravel layer.

L.2 ANALYSIS OF PERFORMANCE OF NR WASTE

The methods used to analyze the long-term performance of the NR waste disposal unit within the EAV facility are described in this section. A description of the radionuclide source term posed by the disposal containers is provided in Sect. L.2.1. Pathways to exposure of human receptors are considered in Sect. L.2.2. The conceptual models developed and

Table L.1-1 Radioactive inventory for 41 NR disposal casks to be shipped to E-Area

Number of units: Description:	1 CBDC Hardware	8 Core Barrel	8 Holddown Barrels	16 CB/TS/CH Hardware	8 Adapter Flanges	Total all casks (Ci)
Isotopes:						
H-3	9.6×10^3	1.6	—	5.8×10^1	—	$2.2 \times 10^{+1}$
C-14	3.1×10^1	3.1×10^1	—	$1.1 \times 10^{+1}$	1.6×10^{-3}	$1.8 \times 10^{+2}$
Sc-46	3.3×10^3	—	—	—	—	3.3×10^{-3}
Cr-51	1.8×10^1	$1.5 \times 10^{+1}$	1.6×10^1	$8.1 \times 10^{+3}$	2.8×10^{-5}	$1.3 \times 10^{+5}$
Mn-54	3.1	$2.3 \times 10^{+1}$	1.8×10^1	$5.7 \times 10^{+2}$	8.5×10^{-3}	$9.3 \times 10^{+3}$
Fe-55	$2.1 \times 10^{+2}$	$3.7 \times 10^{+3}$	$2.2 \times 10^{+1}$	$2.1 \times 10^{+4}$	2.6×10^1	$3.7 \times 10^{+5}$
Co-58	$1.5 \times 10^{+1}$	$1.4 \times 10^{+2}$	1.8	$2.1 \times 10^{+4}$	3.8×10^2	$3.4 \times 10^{+5}$
Fe-59	5.1×10^{-2}	7.8×10^1	1.1×10^2	$1.5 \times 10^{+2}$	4.4×10^{-4}	$2.4 \times 10^{+3}$
Ni-59	2.8	$6.3 \times 10^{+1}$	7.8×10^1	$2.1 \times 10^{+2}$	4.8×10^{-4}	$3.9 \times 10^{+3}$
Co-60	$3.0 \times 10^{+2}$	$5.9 \times 10^{+3}$	$5.8 \times 10^{+1}$	$4.5 \times 10^{+4}$	1.5×10^1	$7.7 \times 10^{+5}$
Ni-63	$3.8 \times 10^{+2}$	$6.3 \times 10^{+3}$	$7.8 \times 10^{+1}$	$2.9 \times 10^{+4}$	4.8×10^2	$5.2 \times 10^{+5}$
Zn-65	1.3×10^1	—	—	—	—	1.3×10^1
Sr-90	1.2×10^{-2}	3.2×10^{-4}	2.8×10^{-4}	$2.9 \times 10^{+1}$	6.3×10^{-5}	$4.6 \times 10^{+2}$
Nb-94	6.4×10^{-3}	1.6×10^{-4}	1.4×10^1	3.2×10^1	3.2×10^{-3}	6.2
Nb-95	4.1×10^{-2}	2.4×10^{-3}	2.2×10^{-3}	$1.5 \times 10^{+5}$	4.7×10^{-4}	$2.4 \times 10^{+6}$
Zr-95	—	1.0×10^{-3}	9.4×10^{-4}	—	2.3×10^{-4}	1.7×10^{-2}
Tc-99	3.3×10^{-4}	3.7	—	—	—	$3.0 \times 10^{+1}$
In-113	—	—	—	$4.4 \times 10^{+3}$	—	$7.0 \times 10^{+4}$
Sn-113	—	—	—	$4.4 \times 10^{+3}$	—	$7.0 \times 10^{+4}$
In-114	—	—	—	$5.5 \times 10^{+2}$	—	$8.8 \times 10^{+3}$
Sn-119m	—	—	—	$5.5 \times 10^{+4}$	—	$8.8 \times 10^{+5}$
Sn-123	—	—	—	$1.5 \times 10^{+3}$	—	$2.4 \times 10^{+4}$
Sb-125	—	—	—	$1.2 \times 10^{+4}$	—	$1.9 \times 10^{+5}$
I-129	1.3×10^{-4}	—	—	—	—	1.3×10^{-4}
Cs-137	1.2×10^{-2}	3.2×10^{-4}	2.8×10^{-4}	6.3×10^{-3}	6.3×10^{-3}	1.2×10^1
Hf-181	4.5×10^{-3}	7.0×10^{-4}	6.3×10^{-4}	$2.6 \times 10^{+1}$	1.4×10^{-4}	$4.2 \times 10^{+4}$
Ta-182	2.9	—	—	$1.1 \times 10^{+3}$	—	$1.8 \times 10^{+4}$
Pu-239	2.5×10^{-5}	—	—	—	1.0×10^{-7}	2.6×10^{-5}
Pu-241	8.9×10^{-4}	2.3×10^{-5}	2.1×10^{-5}	4.7×10^{-4}	4.7×10^{-6}	8.8×10^{-3}

computational approach used to assess the performance of the NR waste unit are described in Sect. L.2.3.

L.2.1 Source Term

The NR waste provides a source of radionuclides to the geosphere. To characterize this source it is necessary to consider mechanisms of release. The NR waste is composed of solid activated metal, with less than 1% of the radionuclide inventory in the form of surface contamination (WSRC 1992). Release of radionuclides from the waste form to the interior of the casks will be governed by corrosion of the metal matrix. Corrosion rates are directly proportional to the surface area of the wastes, and are a strong function of the type of metal making up the waste and the chemistry of water contacting the waste. Release to the geosphere requires a breach of the disposal container, such that water contacts the waste, and requires the presence of corrosion products on the surface of the waste. Upon contact with water, radionuclides present in corrosion products are partitioned between pore water and the iron compounds constituting the corrosion products. The mechanisms relevant to partitioning include: 1) desorption from corrosion products; 2) dissolution of precipitated material within the corrosion product matrix; and/or 3) volatilization into soil gas. Transport in the geosphere occurs as a result of advective and diffusive processes. Advective processes arise as a consequence of the infiltration of water through the disposal unit. Diffusive processes are driven by the concentration gradient that exists between pore fluids of the waste matrix and pore fluids of the surrounding uncontaminated soil.

Corrosion of the steel disposal casks is an important consideration in developing a source term model. The disposal containers prevent release of radionuclides to the environment as a result of leaching until such time that the containers are no longer impervious to water. The outer carbon steel of the disposal casks (Fig. L.1-1) is less resistant to degradation than the inner stainless steel portion.

Degradation of the engineered cover will affect release to the geosphere through the effect on infiltration of water into the trenches. As was described in Sect. 3.1.3.1, a reasonable scenario for degradation of the cover is that the cover may be degraded to the

gravel layer approximately 900 years after closure of the E-Area Facility. Before that time, it is possible that infiltration may increase through the clay layer as a result of head build-up in the gravel layer, if for example the drains fail to divert sufficient water, or as a result of disturbance of the clay layer by roots or burrowing animals.

L.2.2 Pathways and Scenarios

In this section, the pathways to human exposure to potential NR waste constituents are addressed. The time periods of concern for human exposure are identical to those described in Sect. 3.2.1.

L.2.2.1 Transport Pathways

Radionuclides released from the NR wastes to the geosphere have the potential of reaching humans through numerous pathways. Most conceivable pathways for a buried LLW source such as the NR wastes are described in Sect. 3.2.2.1. The same rationale applied in pathway screening for the EAVs applies to the NR wastes, with the result that only pathways related to contaminated air or groundwater are considered to be of potential consequence for off-site exposures. For off-site exposures, pathways considered include leaching of corroded NR wastes, resulting in contamination of groundwater local to E-Area, and volatilization of H-3 and C-14. Intruder exposure scenarios are considered separately in Sect. L.2.2.3.

L.2.2.2 Exposures of Off-Site Members of the Public and Protection of Groundwater

From the discussion in Sect. 3.2.3.3, only the drinking water pathway needs to be considered for off-site releases of radionuclides in groundwater. In cases where the MCL in groundwater corresponds to a dose equivalent less than the performance objective for off-site individuals of 25 mrem per year from all exposure pathways, compliance with the MCL would ensure that the dose to off-site individuals would be substantially less than the performance objective. In cases where the MCL in groundwater corresponds to a dose equivalent greater

than the performance objective for off-site individuals, the dose from all exposure pathways, theoretically, should be considered. However, as discussed in Sect. 3.2.3.3, the dose from pathways other than drinking water would be insignificant compared with the dose from the drinking water pathway.

Other than the groundwater pathway, exposure to atmospheric concentrations of volatile radionuclides must be considered. For atmospheric releases of H-3 and C-14, the calculated dose is compared to the performance objective of 10 mrem per year EDE in this analysis.

L.2.2.3 Exposure Scenarios for Inadvertent Intruders

In Sect. 3.2.4, several exposure scenarios for inadvertent intruders that could be applied to disposal of LLW in concrete vaults were described. Two chronic exposure scenarios (the agriculture and post-drilling scenarios) and two acute exposure scenarios (the construction and drilling scenarios) were based on the assumption that an inadvertent intruder could access disposed waste while excavating or drilling at the disposal site. An additional chronic exposure scenario (the resident scenario) and an additional acute exposure scenario (the discovery scenario), were based on the assumption that an inadvertent intruder was prevented from accessing disposed waste while excavating at the disposal site by the presence of intact engineered barriers, but nonetheless, could receive an external exposure while residing or working at the site.

As described in Sect. L.1.1 and indicated in Fig. L.1-1, the NR wastes will be contained in thick-walled carbon steel and stainless steel casks. These casks presumably will degrade only very slowly by corrosion and, thus, reasonably can be presumed to prevent inadvertent intrusion into the waste for a considerable period of time after disposal. For as long as the casks maintain their integrity, an inadvertent intruder presumably could only receive an external exposure according to scenarios similar to the resident or discovery scenario used in the analysis for waste disposal in concrete vaults.

In the analysis for the NR wastes, three scenarios for exposure of inadvertent intruders are considered. The first is external exposure to waste inside an intact waste cask immediately upon loss of active institutional controls at 100 years after disposal, which is the earliest time

that inadvertent intrusion is assumed to be credible (U.S.DOE 1988a). At this time, a conservative, upper-bound estimate of external dose is obtained on the basis of (1) reported inventories of photon-emitting radionuclides in the waste given in Table L.1-1, (2) the known spectrum of photons in the decay of each radionuclide (Kocher 1981), (3) consideration of the shielding provided by the waste casks for different photon-emitting radionuclides in the waste, and (4) the assumption that the external dose rate at the surface of the waste casks at the present time does not exceed 200 mrem/h, which is an acceptance criterion for the waste casks specified in 49 CFR Part 173.

The second exposure scenario for inadvertent intruders considered in the analysis for the NR wastes is the agriculture scenario, which involves direct excavation into the waste itself. This scenario reasonably can occur only at times long after disposal when the waste casks have been degraded by corrosion. The agriculture scenario assumes that an inadvertent intruder constructs a home directly on top of disposed waste and that some of the waste is exhumed while constructing the foundation for the home. Some of the exhumed waste is mixed with native soil in the intruder's vegetable garden, and the intruder is assumed to receive exposures from ingestion of contaminated vegetables from the garden, direct ingestion of contaminated garden soil, external exposure while working in the garden, residing in the home on top of the waste, and inhalation exposure while working in the garden and residing in the home.

The third scenario considered is a post-drilling scenario which also could occur when the casks have failed. Although, as indicated in Sect. 3.2.4.1 and Appendix A.4, the dose from the post-drilling scenario will always be less than the dose from the agriculture scenario when the two scenarios are presumed to occur at the same time after disposal, the post-drilling scenario is considered because it could occur at an earlier time than the agriculture scenario. In this scenario, waste exhumed by drilling is assumed to be mixed with native soil in the intruder's vegetable garden, and the intruder is assumed to receive exposures from ingestion of contaminated vegetables from the garden, direct ingestion of contaminated garden soil, and external and inhalation exposures while working in the garden.

L.2.3 Models and Assumptions

In Sect. L.2.1 and L.2.2, the potential mechanisms of release of radionuclides from the NR wastes were defined and the relevant human exposure scenarios were described. In this section, the models adopted and assumptions made to carry out the computations necessary to estimate doses are described.

L.2.3.1 Near-Field Model

The near-field model for the NR wastes addresses release of radionuclides from the waste in the containers to the surrounding unsaturated soils of the vadose zone, and subsequent radionuclide transport to the water table. The conceptual models implemented to simulate flow and transport are described below.

Flow of water through the NR waste is limited by the integrity of the disposal container, the amount of infiltration through the overlying cover, and characteristics of the waste and surrounding soil. Using the disposal container design described in Sect. L.1.1, a two-dimensional computational grid was designed to represent a vertical cross-section through the NR waste disposal facility and surrounding soil. The model domain (Fig. L.2-1) forms the basis of the simulations carried out with PORFLOW, Version 2.5 (ACRI 1993), to estimate flow and mass transport through the waste to the water table. The waste is represented within this domain by a zone which is 43 m long and 5.4 m high. The thickness of the slice is assumed to be of unit thickness, or 1 cm in this case.

The amount of infiltration entering the top of the domain shown in Fig. L.2-1 was assumed to be 40 cm/year, which represents the average infiltration without an engineered cover over the waste. Although the cover will likely limit infiltration for hundreds of years if undisturbed, there is considerable uncertainty in the timing and extent of cover degradation. Furthermore, the simulations begin when the disposal containers are assumed to fail, at which time slumping of the cover may occur due to loss of integrity of these containers. Therefore, for this analysis, no credit was taken for reductions in infiltration brought about by the cover.

Rev. 0

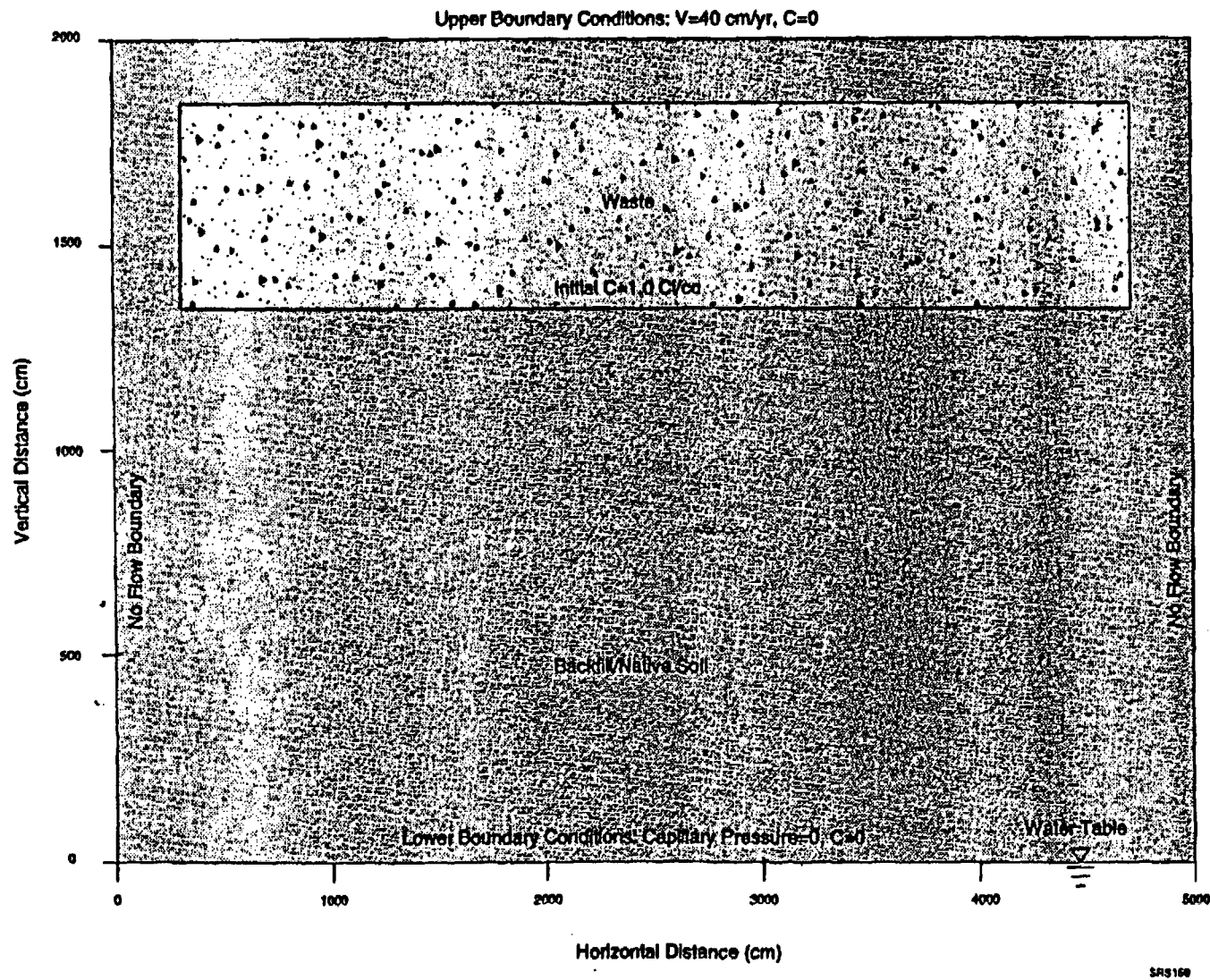


Fig. L2-1. Near-field simulation domain for NR waste.

L-11

WSRC-RF-94-218

Simulation of the path of water through the domain near profiles in the NR waste and surrounding soil. For this analysis, waste inside the disposal casks has achieved hydraulic equilibrium with surrounding soil at the time of disposal container failure. It is likely that water exists in the disposal cask at initial breaching. However, this is made because of the considerable uncertainty in modeling water flow over time. The simplified conceptual model might overestimate the time casks are intact for a relatively short period of time, if water readily collects in the casks before failure of the bottom portion of the cask. In the casks, the simplified model might briefly underestimate the time of failure of the bottom portion. However, this potential is more than compensated for by the conservative assumptions inherent in the model include: 1) that water enters the casks as readily as it flows through the waste is well-mixed within a porous matrix within the container and is displaced by pore water.

Simulation of radionuclide transport through the near-field waste at the time the disposal containers are considered breached. The rate of transport depends upon the time of breaching of the container and the activated metal wasteform. There is considerable uncertainty in the processes that affect both of these variables. With respect to the integrity of the welds and any crevices associated with the steel container, the timing and extent of this event. While the uniform corrosion rate is extremely slow, and at most 2×10^{-5} cm/year (Sullivan and others), the localized corrosion of welds is likely to allow water in and out of the container. The failure of the container is predicted with uniform corrosion. However, failure with localized corrosion is very difficult to predict with certainty. Corrosion of the wasteform is also uncertain due to the lack of information on the type of wasteform present in the wasteform.

is breached before significant radioactive decay has occurred. For the short-lived radionuclides, this assumes that the container breaches immediately (at $t = 0$). The second scenario assumes that the container breaches at 6,000 years and that the activated metal wasteform is completely in the form of corrosion products. The first scenario is not considered realistic, but rather a means of screening out radionuclides that are insignificant from the standpoint of potential groundwater contamination. The second scenario may be very conservative if the metal wasteform is a corrosion resistant material, like stainless steel.

Hydraulic properties described in Sect. 3.3.1.1 for native soil at the SRS are appropriate for the soil surrounding the NR disposal containers. The moisture characteristic data tabulated by Gruber (1980) were used to define the unsaturated hydraulic conductivity and matrix potential as a function of moisture content. Because the waste and surrounding backfill and native soil are assumed to have identical hydraulic properties, water is assumed to be neither diverted into or out of the NR waste following disposal container failure, but to flow vertically through all materials. Under steady-state hydrologic conditions, the amount of water flowing out of the domain at the water table is equal to the amount of water entering via infiltration; thus, the steady-state flux of water through the NR waste and surrounding soil was 40 cm/year. Flow simulations were carried out with PORFLOW for the two-dimensional domain described above. The PORFLOW input file for these simulations is provided in Fig. L5-1. The steady-state flow field was subsequently used in mass transport simulations to analyze the advective flux from the casks.

Release of radionuclides from corrosion products of the waste to the geosphere may result from desorption or dissolution processes, as noted in Sect. L2.1. Advective and diffusive processes act to mobilize the radionuclides in the pore waters of the corroded waste. For the NR waste analysis, radionuclides in the corrosion products are assumed to be completely soluble, and sorption is considered to be a fully-reversible linear process at equilibrium. Equilibrium partitioning between solid (sorbed) and liquid phases is characterized by the distribution coefficients (K_d s) listed in Table L2-2. The K_d values in this table are average values for sandy soil taken from site-specific literature, when available, and from a review article by Sheppard and Thibault (1990).

Table L2-2. Distribution coefficients assumed for subsurface transport simulations for radionuclides in NR waste.

Radionuclide	K _d Value Assumed (mL/g)	Literature Source
H-3	0	
C-14	2	McIntyre 1988
Sc-46	0	not available
Cr-51	70	Sheppard and Thibault 1990
Mn-54	50	Sheppard and Thibault 1990
Fe-55	220	Sheppard and Thibault 1990
Co-58	10	Hoeffner 1985
Fe-59	220	Sheppard and Thibault 1990
Ni-59	400	Sheppard and Thibault 1990
Co-60	10	Hoeffner, 1985
Ni-63	400	Sheppard and Thibault 1990
Zn-65	200	Sheppard and Thibault 1990
Sr-90	10	Hoeffner 1985
Nb-94	160	Sheppard and Thibault 1990
Nb-95	160	Sheppard and Thibault 1990
Zr-95	600	Sheppard and Thibault 1990
Tc-99	0.36	Oblath 1982
In-113	0	not available
Sn-113	130	Sheppard and Thibault 1990
In-114	0	not available
Sn-119m	130	Sheppard and Thibault 1990
Sn-123	130	Sheppard and Thibault 1990
Sn-125	130	Sheppard and Thibault 1990
I-129	0.6	Hoeffner 1994
Cs-137	330	Hoeffner 1985
Hf-181	450	Sheppard and Thibault 1990
Ta-182	220	Sheppard and Thibault 1990
Pu-239	100	Hoeffner 1985
Pu-241	100	Hoeffner 1985

The steady-state flow field from PORFLOW provided flow rates through the waste and to the water table (at the bottom of the domain, Fig. L.2-1), and K_d s, effective diffusion and dispersion coefficients, and radioactive decay constants provided the necessary information for simulating advective-diffusive transport. An example input file is shown in Fig. L.5-2. Effective diffusion (i.e., molecular diffusion corrected for tortuosity of a porous medium) and dispersion coefficients are not radionuclide-specific, and the values used for these parameters in the PORFLOW simulations were: 1) longitudinal dispersivity = 10 m; 2) transverse dispersivity = 2 cm; and 3) effective diffusion coefficient = $158 \text{ cm}^2 \text{ yr}^{-1}$. No data are available for dispersivities in the unconsolidated sediments of the SRS. In the unsaturated zone, where flow velocities are very low, dispersion, which is directly proportional to flow velocity, is likely to be fairly insignificant with respect to plume movement. The values chosen for these simulations are believed to be reasonable based on a discussion of field-scale dispersivity in a reputable groundwater textbook (Freeze and Cherry 1979).

L.2.3.2 Groundwater Transport Model

To simulate transport of radionuclides that are released from the NR component waste to the water table, the conceptual saturated zone transport model described in Sect. 3.3.2 was adopted. The flow field established by PORFLOW simulations, which implemented this conceptual model, was used in the NR waste analysis. Therefore, the groundwater transport model was identical to that described in Sect. 3.3.2 with the exceptions that the source zone was smaller (1 NR waste source node versus 4 nodes for the ILNT vaults and 35 nodes for the LAW vaults), and the K_d s listed in Table L.2-2 were used. The smaller source zone represents the relatively smaller source area presented by the NR waste. An example PORFLOW input file for four radionuclides is shown in Fig. L.5-3.

L.2.3.3 Atmospheric Release Model for Volatile Components

Potential atmospheric release of volatile forms of H-3 and C-14 must be considered in order to consider all potentially significant pathways of exposure to radionuclides from the NR waste. Inadvertent intruders may be exposed to air within residences built on top of the

soil above the waste, and off-site individuals may be exposed to concentrations transported to or beyond the SRS boundary.

To estimate fluxes of potentially volatile radionuclides, H-3 and C-14, from the NR wastes, the model developed to conservatively estimate fluxes of these radionuclides arising from the LAW vaults (Sect. A.3.5 and A.3.6) was used. The conservatism of this model lies mainly in the estimates for C-14 flux, because all of the C-14 available for volatilization (i.e., the C-14 in corrosion products of the waste form) is assumed to be in the form of gaseous $^{14}\text{CO}_2$. Tritium, on the other hand, is more realistically partitioned into water vapor in air according to the concentration of tritium in water calculated for the casks.

The flux calculations are normalized to a unit of *available* activity (Ci) of each radionuclide per disposal container. The availability of H-3 and C-14 after disposal is a function of the degree of corrosion of the steel waste form, and the amount of radioactive decay, that has occurred when release occurs.

For H-3, the vapor phase concentration in the NR waste is first calculated by assuming that the concentration of H-3 in water vapor in a disposal cask is the same as the H-3 concentration in any water contacting the wasteform. The ideal gas law is used to estimate the ambient concentration of water vapor in air in a disposal container, the results being 9.2 g m^{-3} at 10°C and 100% relative humidity. Converting to activity concentration units (Sect. A.2.3.1), the H-3 concentration in air in the disposal casks, in Ci m^{-3} , is 9.2×10^{-6} times the H-3 concentration in water. As noted above for C-14, all of the C-14 in corrosion products in the disposal casks is conservatively assumed to exist as $^{14}\text{CO}_2$ in the air in the disposal casks.

For off-site individuals, diffusion of H-3 and C-14 through soil overlying the NR disposal containers, and subsequent transport to the site boundary were considered. One meter of soil was assumed to cover the casks, although initially approximately 3 m of soil will overlie the casks with the engineered cover in place. Per Ci of available H-3 (i.e., undecayed H-3 in corrosion products) in each of the 100 disposal casks, the concentration in the air-filled voids of the casks is calculated from:

$$C_{T,H-3} = \frac{1 \text{ Ci}}{3.8 \times 10^{-3} \text{ m}^3} \times \frac{9.2 \times 10^{-6} \text{ Ci/m}^3_{(air)}}{1 \text{ Ci/m}^3_{(H_2O)}}$$

where $3.8 \times 10^3 \text{ m}^3$ (approximately one gal) represents the amount of pore fluid in a disposal container. This pore fluid content is based on amount of water expected for an average disposal container (Sect. L.1.1). The resulting air concentration of H-3 in the NR waste containers is $2.4 \times 10^3 \text{ Ci m}^{-3}$ for every Ci of H-3 in the corrosion products of a container. The flux of H-3 at the soil surface ($J_{\text{H-3}}$ in $\text{Ci m}^{-2} \text{ yr}^{-1}$) is calculated from:

$$J_{\text{H-3}} = D_a \left(\frac{C_{\text{H-3}}}{x} \right)$$

where D_a is the molecular diffusion coefficient in air ($754 \text{ m}^2 \text{ yr}^{-1}$ for water vapor, CRC 1981) and x is the soil thickness, assumed to be 1 m. The initial flux of H-3 (i.e., at closure) from the overlying soil is calculated to be $1.8 \text{ Ci m}^{-2} \text{ yr}^{-1}$ over an area of 800 m^2 (i.e., 8 m^2 per cask), per Ci of H-3 available for volatilization in each of the 100 NR waste disposal casks. With this flux rate, all of the available H-3 would be released from each disposal container in much less than one year. Therefore, to obtain an average annual flux rate, the total available H-3 in a disposal cask is assumed to be released in one year, and is divided by the individual cask area (8 m^2) to obtain a flux rate of H-3 from the NR waste disposal containers. The flux rate will depend strongly on when and how the disposal container is breached such that gaseous components can escape. If it is assumed that all H-3 is available for volatilization (i.e., corrosion of the waste form is instantaneous at closure), the flux rate from the disposal containers is calculated to be $0.13 \text{ Ci m}^{-2} \text{ yr}^{-1}$.

Similarly, for inadvertent intruders, H-3 flux from soil above the disposal containers is a function of the time that the gaseous components escape and whether there is a gradual release or instantaneous release. For intruders, however, exposure cannot occur prior to the 100 years of assumed institutional control, and thus, significant decay of H-3 has occurred by that time. Per Ci of total initial H-3 in each NR waste cask, no more than $3.6 \times 10^{-3} \text{ Ci}$ would remain at 100 years after closure based on consideration of radioactive decay alone. Leaching is neglected. If it is assumed that all undecayed H-3 is available for volatilization at 100 years, the flux rate of H-3 from the soil overlying the disposal containers is 3.6×10^{-3} times the initial flux rate ($0.13 \text{ Ci m}^{-2} \text{ yr}^{-1}$) calculated above, or $4.7 \times 10^{-4} \text{ Ci m}^{-2} \text{ yr}^{-1}$. This represents the maximum flux of H-3 assumed to enter the intruder's residence at any time.

For C-14, the concentration in the NR waste containers ($C_{T,C-14}$), in Ci m³ per Ci of available C-14 (i.e., C-14 in corrosion products) in each of the 100 containers, is calculated based on a 100-year Ci content of one; that is, decay has been insignificant and leaching is neglected. The ¹⁴CO₂ air concentration per Ci available C-14 is calculated for an unwetted void space of 23.5 m³ (27 m³ total minus 3.5 m³ of metal waste) in each cask to be 4.3×10^{-2} Ci m³. The flux of C-14 at the soil surface, J_{C-14} , is calculated in the same manner was done for H-3, using a diffusion coefficient of CO₂ in air of 440 m² yr⁻¹ (CRC 1981). The flux of C-14 from the soil overlying the NR waste containers, per Ci of available C-14 in corrosion products, is conservatively estimated to be 1.8×10^1 Ci m⁻² yr⁻¹ over a total cask area of approximately 800 m² (8 m² per cask). A C-14 flux of 1.8×10^1 Ci m⁻² yr⁻¹ over an area of 800 m² corresponds to a loss of the initial 1 Ci per cask available C-14 in much less than one year. Therefore, to obtain an average annual flux rate, the total available C-14 in a disposal cask is assumed to be released in one year, and is divided by the individual cask area (8 m²) to obtain a flux rate of C-14 from the NR waste disposal containers. The flux rate will depend strongly on when and how the disposal container is breached such that gaseous components can escape. If it is assumed that all C-14 is available for volatilization (i.e., corrosion of the waste form is complete at the time of volatile release), the flux rate from the disposal containers is calculated to be 0.13 Ci m⁻² yr⁻¹ per Ci of C-14 in each disposal cask. This flux rate represents the maximum flux, based on mass balance considerations, that can be assumed for determining off-site exposures and for estimating intruder exposures. Radioactive decay is assumed to be negligible at the time of release.

To more realistically estimate flux rates for H-3 or C-14, corrosion rates of the waste form and mode and time of release need to be considered. The worst case scenario would occur if the majority of the steel waste form corrodes before any release of volatile components, and if the release occurs before radioactive decay significantly diminishes the radionuclide content within the containers.

L2.3.4 Models for Dose Estimation

Doses to off-site members of the public resulting from use of contaminated groundwater beyond the 100-m buffer zone around all of the projected 100 NR disposal containers were not directly estimated. Rather, comparisons of maximum predicted groundwater concentrations with the more restrictive of either MCLs or allowable concentrations based on 25-mrem per year performance objective were made. The allowable concentrations were calculated by dividing 25 mrem per year by the EDE per unit concentration in drinking water (Table A.4-6, Sect. A.4). These calculations are simple, were performed by hand, and checked several times for accuracy.

Other than contaminated groundwater, the air pathway is the only potentially significant means of exposure that is considered for off-site individuals in the NR waste analysis (Sect. L.2.2.2). Doses to off-site individuals via the air pathway were calculated in the manner described in Sect. A.3.1.3. This methodology utilizes the source term described in Sect. L.2.3.3 above, in Ci yr⁻¹ of H-3 or C-14, and the AIRDOS-PC atmospheric dispersion model to estimate the all-pathway dose to an individual residing continuously at the SRS site boundary (5 km from E-Area).

To estimate dose to the intruder from potentially volatile H-3 and C-14 compounds released from the NR waste disposal containers, the same procedure described in Sect. A.3.1.2 was used. Assuming that the intruder's house resides directly on top of soil, 1 m in thickness, overlying the disposal containers, the steady-state air concentration (C_a), in Ci m⁻³, of H-3 or C-14 to which the intruder is exposed is estimated from:

$$C_a = \frac{J/a}{h}$$

where

- J = flux rate of volatile H-3 or C-14 into house, Ci m⁻² yr⁻¹,
- a = air exchange rate in house, assumed to be 8760 yr⁻¹, and
- h = height of the ceiling in house, 2.4 m.

The method for obtaining conservative estimates of the flux rates were provided in Sect. L2.3.3 above. The inhalation dose to the intruder (D_H) can be calculated from:

$$D_H = C_m \times B_r \times DCF_i$$

where

B_r = breathing rate ($8,000 \text{ m}^3 \text{ yr}^{-1}$), and

DCF_i = inhalation DCF for H-3 or C-14, (mrem Ci^{-1}).

Doses to inadvertent intruders from the external exposure, agriculture, and post-drilling scenarios were estimated according to the procedures described in Sect. L3.1.4 below.

L2.4 Performance Analysis Methodology

The models and assumptions described in Sect. L2.3 were applied to analyze the performance of the NR waste disposal containers. Doses to off-site individuals and inadvertent intruders and groundwater concentrations at the compliance point for groundwater resource protection per Ci of each radionuclide listed in Table L2-1 were estimated. The computational results are used to calculate inventory limits for each radionuclide based on performance objectives of the RPA.

Specifically, the near-field model was implemented, using the PORFLOW computer code, to estimate fluxes of radionuclides to the water table over time and to track the inventory in the disposal casks as a function of time. The results of the two-dimensional PORFLOW simulations are expressed in terms of fraction of the inventory in the simulation domain that leaves the bottom boundary of the domain over time, the bottom boundary representing the water table. The simulation domain represents a "slice" through the contents of the breached disposal containers and surrounding soil.

Following estimation of flux to the water table from the NR waste, the groundwater model was implemented, again using PORFLOW, to estimate the time-dependent groundwater concentrations of each radionuclide at the compliance point for groundwater resource

protection. The compliance point was selected from the groundwater simulation results as the node with the highest concentration which is at least 100 m from the edge of the 100 NR waste containers. Inventory limits based on groundwater protection requirements and the 25-mrem performance objective for off-site individuals were calculated from applicable MCLs and allowable inventories derived from dose estimates for the drinking water pathway.

The air pathway was considered by carrying out the calculations described in Sect. L.2.3.3 to calculate fluxes of H-3 and C-14 from the soil overlying the NR waste disposal containers, assuming the approximately 2 m of the engineered moisture barrier had been removed or eroded away. These fluxes were then used to conservatively estimate doses to intruders residing over the casks, or doses to off-site individuals per unit activity in each of the 100 disposal casks. Inventory limits were calculated for the air pathway based on the performance objectives of 10 mrem per year for off-site individuals, and 100 mrem per year for inadvertent intruders.

As described in Sect. L.2.2.3, three scenarios for exposure of inadvertent intruders are considered in the performance analysis for disposal of the NR wastes. The first scenario involves external exposure to intact waste casks at 100 years after disposal when the external dose that could be received would attain its maximum value. For this scenario, a simple model is developed to provide a conservative, upper-bound estimate of dose that might be received at this time, based essentially on the reported activities of photon-emitting radionuclides in the waste and the requirement that the external dose rate at the surface of a waste cask not exceed 200 mrem/h at the time of disposal. The second and third scenarios for inadvertent intrusion considered in this analysis are the agriculture and post-drilling scenarios, described in Sect. 3.2.4.1, which are assumed to occur only at a time long after disposal when the waste casks have been degraded by corrosion and excavation or drilling into the waste could occur. Estimates of potential doses to inadvertent intruders are provided on the basis of (1) the reported inventories of long-lived radionuclides in the waste given in Table L.1-1, (2) the scenario DCFs for the agriculture and post-drilling scenarios given in Tables 4.1-9 and 4.1-11, but modified to take into account those radionuclides that are in the form of activated metals, and (3) the total volume occupied by the waste casks after disposal, as obtained from Fig. L.1-2. However, the primary emphasis of the analysis for the agriculture

and post-drilling scenarios is the very long time after disposal at which the scenarios first would become credible, rather than the doses that might be received at that time.

L2.5 Quality Assurance

As described in Sect. 3.5, this analysis was conducted under the guidance of the provision of the ANSI/ASME NQA-1 Program Requirements for Nuclear Facilities (U.S.NRC 1989), as required by DOE Order 5820.2A (U.S.DOE 1988a). Pertinent elements of NQA-1 and relevant documentation are cited in that section of the RPA, and apply directly to the NR waste analysis.

L3 RESULTS OF NR WASTE ANALYSIS

The results of the analysis of performance of the NR waste disposal containers are presented in this section. Predicted releases to the environment (atmospheric releases and releases to the water table), resulting concentrations, results of dose analyses, and allowable inventories in the disposal casks are presented in Sect. L3.1. The results are interpreted in Sect. L3.2.

L3.1 Analysis Results

In this section, results are presented for the near-field model simulations, the groundwater transport simulations, the atmospheric transport calculations, and the intruder dose analysis.

L3.1.1 Near-Field Model Results

Table L3-1 lists the PORFLOW simulation results for the near-field model. The fluxes provided represent the peak flux to the water table per Ci inventory of radionuclides (in *available* form; i.e., as corrosion products of activated metal) in all of the 100 shipping casks

Table L3-1. Peak flux to the water table from NR waste.

Radionuclide	Predicted Fractional Flux (Ci/year-Ci)	Time of Peak Flux (year)
H-3	2.7×10^{-2}	1.4×10^1
C-14	2.8×10^{-2}	7.4×10^1
Sc-46	1.0×10^{-19}	3.1
Cr-51	--- ^a	---
Mn-54	7.7×10^{-71}	2.2×10^1
Fe-55	3.3×10^{-78}	5.0×10^1
Co-58	1.9×10^{-68}	4.1
Fe-59	--- ^a	---
Ni-59	1.0×10^{-4}	1.0×10^4
Co-60	1.2×10^{-20}	9.3×10^1
Ni-63	1.6×10^{-30}	2.1×10^3
Zn-65	1.6×10^{-98}	1.8×10^1
Sr-90	5.9×10^{-7}	1.6×10^2
Nb-94	3.1×10^{-4}	4.7×10^3
Nb-95	--- ^a	---
Zr-95	--- ^a	---
Tc-99	8.1×10^{-2}	2.5×10^1
In-113	--- ^a	---
Sn-113	--- ^a	---
In-114	--- ^a	---
Sn-119m	2.6×10^{-48}	2.1×10^1
Sn-123	--- ^a	---
Sb-125	1.8×10^{-74}	5.0×10^1
I-129	6.4×10^{-2}	3.2×10^1
Cs-137	7.7×10^{-45}	7.5×10^2
Hf-181	--- ^a	---
Ta-182	--- ^a	---
Pu-239	5.9×10^{-4}	2.9×10^3
Pu-241	1.4×10^{-37}	3.4×10^2

^a Less than 10^{-99} yr^{-1} .

which potentially will be disposed of in E-Area (i.e., peak fractional flux). These fluxes are based on a 40 cm/year infiltration rate through the NR waste, as was noted in Sect. L.2.3.1.

L.3.1.2 Groundwater Concentrations

The results of the groundwater transport simulations are listed in Table L.3-2. The values listed in this table represent peak groundwater concentration per Ci of radionuclide (assuming all of the radionuclide is *available* for leaching) in all of the 100 NR waste disposal casks, at the compliance point for groundwater protection. If the peak occurs at a time greater than 10,000 years after closure, the 10,000 year compliance point concentration is also provided. The compliance point is considered to be the point of maximum groundwater concentration at least 100 m from the edge of the disposal casks.

The groundwater concentrations per Ci inventory in all of the 100 NR disposal casks are compared to MCLs or allowable concentrations derived from the 25-mrem performance objective in Table L.3-3 below, to calculate total inventory limits for all 100 casks. Only the radionuclides in Table L.3-2 with peak groundwater concentrations exceeding 10^{-12} pCi/cc per Ci were considered further in this analysis. Inventory limits for individual casks were not determined because the results depend on the spacing of the casks at disposal, and thus, the limits calculated are only relevant to the spacing assumed (Fig. L.1-2) for this assessment. The MCLs listed in Table L.3-3 are those promulgated under the Safe Drinking Water Act, except where noted. Deviations occur only when current MCLs are not available. Allowable inventories for Pu-239 and Pu-241 (based on Am-241 daughter contributions) are calculated by dividing the 25 mrem per year performance objective by the EDEs per unit groundwater concentration for these isotopes (Table 4.1-7). This alternate to the MCLs is invoked because it results in a more restrictive requirement for groundwater concentration for Pu-239 and Pu-241 daughters.

The groundwater-based inventory limits were determined for the two scenarios assuming different times of breaching of the disposal container (Sect. L.2.3.1) by dividing the MCL or allowable concentration, by the compliance-point groundwater concentration per Ci of available inventory, after converting the concentration to appropriate units. The available

Table L3-2. Predicted groundwater compliance concentration for the NR waste.

Radionuclide	Groundwater Concentration at 10,000 years (pCi/cc-Ci) ^a	Peak Groundwater Concentration	
		pCi/cc-Ci	Time of peak (year)
H-3	---	6.7	1.7×10^1
C-14	---	2.2	1.1×10^2
Sc-46	---	9.0×10^{-13}	7.0
Mn-54	---	1.2×10^{-69}	2.5×10^1
Fe-55	---	---	---
Co-58	---	6.0×10^{-61}	1.1×10^1
Ni-59	1.2×10^{-3}	8.2×10^{-3}	1.5×10^4
Co-60	---	5.4×10^{-15}	1.5×10^2
Ni-63	---	5.8×10^{-23}	3.9×10^3
Zn-65	---	---	---
Sr-90	---	7.8×10^{-4}	2.4×10^2
Nb-94	---	2.4×10^{-2}	7.6×10^3
Tc-99	---	8.1	3.5×10^1
Sn-119m	---	---	---
Sb-125	---	---	---
I-129	---	5.8	4.7×10^1
Cs-137	---	4.8×10^{-37}	1.5×10^3
Pu-239	---	4.4×10^{-2}	4.8×10^3
Pu-241 Np-237	---	2.4×10^{-29} 1.3×10^{-6} ^c	6.5×10^2

^a If blank, peak occurs before 10,000 years.

^b Groundwater concentration less than 10^{-99} pCi/cc per Ci inventory in 100 casks.

^c Concentration reported for Np-237 is per Ci of Pu-241 originally present.

Table L3-3 Groundwater-based disposal limits for the NR waste

Radionuclide	Compliance Point Groundwater Concentration (pCi/cc-Ci)		Allowable Concentration Limit (pCi/L) ^a	Inventory Limit for 100 NR Waste Disposal Containers (Ci)	
	Container Breach at 0 years	Container Breach at 6,000 years		Container Breach at 0 years	Container Breach at 6,000 years
H-3	6.7	NA ^b	20,000	3.0	NA ^b
C-14	2.2	1.1	6,400	2.9	6.1
Ni-59	1.2×10^{-3}	3.8×10^{-10}	530	4.4×10^2	1.4×10^9
Sr-90	7.8×10^{-4}	NA ^b	8	1.0×10^1	NA ^b
Nb-94	2.4×10^{-2}	7.4×10^{-4}	707 ^c	2.9×10^1	9.6×10^2
Tc-99	8.1	8.0	800 ^d	9.9×10^{-2}	1.0×10^{-1}
I-129	5.8	5.8	0.5	8.6×10^{-5}	8.6×10^{-5}
Pu-239	4.4×10^{-2}	2.9×10^{-2}	8.1 ^d	1.8×10^{-1}	2.8×10^{-1}
Pu-241 Np-237	2.4×10^{-29} 1.3×10^{-6}	NA ^b 1.3×10^{-6}	530 8.9 ^d	6.8×10^3	6.8×10^3

^a Allowable concentrations are MCLs promulgated under Safe Drinking Water Act, except where noted.

^b Radionuclide decays to insignificant levels by 6,000 years.

^c No MCL given; value used is the new MCL proposed by the EPA in its modifications of DWS.

^d Value reflects the allowable concentration based on consideration of the 25 mrem per year performance objective, which is more restrictive than the MCL in this case.

NA = not applicable

inventory is considered to be the entire inventory for these calculations, which conservatively assumes that the wasteform is entirely corroded at the time of disposal cask breaching. The first, and most conservative, scenario assumes that breaching occurs instantaneously. The second scenario assumes that water does not enter and leave the cask until the year 6000. As expected, these results indicate that the assumed time of failure of the containers is very important in setting inventory limits for the relatively short-lived radionuclides (H-3 and Sr-90) in the NR waste based on considerations of potential groundwater contamination. For Ni-59 and Nb-94, delayed failure of the casks of at least 6,000 years delays the peak concentration of these more strongly sorbing radionuclides beyond the 10,000 year time at which groundwater concentrations are considered for compliance. For the more mobile radionuclides (C-14, Tc-99, I-129, and Np-237), the results indicate that if the casks fail prior to 10,000 years and if the waste form has entirely corroded by that time of cask failure, the inventory limits will not be significantly affected by the time of failure.

L3.13 Dose Analysis for Off-Site Releases of Radionuclides

As described in Sect. 3.2.3.3, the only performance objective of concern for off-site release of radionuclides is groundwater protection, provided doses from airborne release of radionuclides are insignificant. In order to evaluate the significance of the air pathway for the potentially volatile H-3 and C-14 radionuclides, doses were estimated using the fluxes derived in Sect. L2.3.3 and the inhalation exposure model described in Sect. L2.3.4. Flux rates above the soil were calculated assuming the entire waste form had corroded before release occurred, and that the entire inventory of H-3 and C-14 in corrosion products were released over a one year period. The estimated fluxes from the soil per Ci of H-3 and C-14 present in the vaults, the corresponding inhalation doses per unit activity (mrem/Ci), the appropriate performance objectives (mrem/year) and the inventory limits (Ci) based on the air pathway are given in Table L3-4. The doses are based on 50-year committed dose equivalent factors for inhalation of 6.3×10^4 mrem per Ci for $^3\text{H}_2\text{O}$ and 2.4×10^4 mrem per Ci for $^{14}\text{CO}_2$ (U.S.DOE 1988b).

Table L3-4. Disposal limits for NR waste based on the air pathway.

Radionuclide	Flux from Soil (Ci m ⁻² yr ⁻¹)	Dose per unit radioactivity (mrem/year-Ci in each cask)	Performance Objective (mrem/year)	Inventory Limit (Ci/cask)
H-3				
Off-Site	1.3×10^{-1}	2.2×10^{-1}	10	4.5×10^1
Intruder	4.7×10^{-4}	1.1×10^1	100	9.1
C-14				
Off-Site	1.3×10^{-1}	1.2	10	8.3
Intruder	1.3×10^{-1}	1.2×10^3	100	8.3×10^{-2}

L3.1.4 Dose Analysis for Inadvertent Intruders

As described in Sect. L2.2.3, three exposure scenarios for inadvertent intruders are considered in the PA for disposal of the NR wastes. The first scenario involves external exposure to photon-emitting radionuclides inside an intact waste cask and is assumed to occur at 100 years after disposal when the external dose to an inadvertent intruder would attain its maximum value. The second and third scenarios are the agriculture and post-drilling scenarios involving excavation or drilling into the waste. These scenarios are assumed to occur only at times long after disposal when the waste casks have been degraded by corrosion.

L3.1.4.1 Analysis of External Exposure of Inadvertent Intruders

This section discusses the analysis of potential external exposures of inadvertent intruders immediately upon loss of active institutional controls at 100 years after disposal. For the reasons described below, a conservative approach is used in estimating external dose at this time.

In principle, given information on the activities of photon-emitting radionuclides in the waste (see Table L.1-1) and the amount of shielding provided by the waste casks (see Fig. L.1-1), estimates of external dose rates near the surface of intact waste packages can be obtained. However, as illustrated by the following example, the available information on the disposed wastes appears to be insufficient to provide the basis for a reasonable estimate of external dose.

Based on the radionuclide inventory data in Table L.1-1 and the known spectrum of photons emitted in the decay of the various radionuclides, the most important photon-emitting radionuclide in the waste appears to be Co-60. That is, for an average waste cask at the present time, a substantial fraction of the external dose rate at the surface of an intact waste package should be due to the inventory of Co-60. From Table L.1-1, the maximum inventory of Co-60 in any waste cask is reported as 4.5×10^4 Ci. If we assume for simplicity that this activity is in the form of a point source at a distance of 1 m from the surface of the waste cask, then the external dose rate at the surface of the cask can be estimated from the known spectrum of photons emitted in the decay of Co-60 and the amount of shielding provided by the walls of the cask. At a distance of 1 m from a point source, the unshielded external dose rate in air per unit activity of Co-60 has been calculated from the decay data of Kocher (1981) as 1.4 rem/h per Ci (Unger and Trubey 1982). From Fig. L.1-1, the minimum thickness of shielding provided by the walls of a waste cask is 24 cm; and, from Fig. 13 of NCRP (1976), a thickness of 24 cm of iron, which is a reasonable approximation for the shielding provided by carbon and stainless steels, reduces the external dose rate from Co-60 by a factor of 6×10^4 . Thus, the estimated dose rate for the simplified case considered here is $(4.5 \times 10^4 \text{ Ci}) \times (1.4 \text{ rem/h per Ci}) \times (6 \times 10^4) = 38 \text{ rem/h}$. This estimate far exceeds an acceptance criterion for the waste casks, specified in 49 CFR Part 173, that the external dose rate at the surface not exceed 0.2 rem/h (200 mrem/h). Indeed, measurements on selected waste casks indicate that the external dose rate is less than 10 mrem/h.

There are two possible explanations for the unreasonably high estimate of external dose given above. The first is that the inventories of photon-emitting radionuclides in the waste could be greatly overestimated. The second, and perhaps more likely, explanation is that the waste is in the form of solid activated metals (see Sect. L.1.1), and the shielding provided by

the waste forms was not taken into account in the simple calculation given above. This shielding undoubtedly is substantial, but there is insufficient information on the waste forms themselves to provide the basis for any reasonable estimate of shielding they provide.

Given the inability to develop a reasonable estimate of external dose based on the available information on the waste forms, waste casks, and reported inventories of radionuclides, a simplified approach is used to obtain a conservative, upper-bound estimate of the external dose that could be received by an inadvertent intruder at 100 years after disposal, which is the earliest time that exposures could occur. This approach is described below.

The expected isotopes in the NR wastes are listed in Table L.1-1. A majority of the isotopes listed are photon-emitters. However, only three radionuclides—i.e., Co-60, Nb-94, and Cs-137 have half-lives sufficiently long that they could occur in substantial quantities in the waste after 100 years of decay. Most of the other radionuclides have half-lives of less than one year and, thus, would decay to minuscule levels within 100 years for any initial activity. The only other radionuclide that possibly could be of concern is Sb-125, which has a half-life of 2.77 years, but the inventory of this radionuclide is reduced by nearly eleven orders of magnitude after 100 years and, thus, would not be of concern for any reasonable levels of initial activity.

Conservative, upper-bound estimates of external doses from Co-60, Nb-94, and Cs-137 at 100 years after disposal are obtained as follows. As stated previously, Co-60 is the most important photon-emitting radionuclide in disposed waste, due to its high average activity in the waste casks (see Table L.1-1) and the high energies and intensities of the emitted photons (Kocher 1981). We first make the conservative assumption that the external dose rate at the surface of a waste cask at the present time is 200 mrem/h, which is the limit for any cask specified in 49 CFR Part 173 but apparently is not approached for any cask. We then assume that all of the dose rate of 200 mrem/h is due to Co-60. This assumption also is conservative (i.e., the dose rate from Co-60 is overestimated), because a substantial fraction of the external dose at the present time is due to other photon-emitting radionuclides in the waste.

Then, if the dose rate from Co-60 at the present time is assumed to be 200 mrem/h, the dose rate at 100 years after disposal would be reduced by a factor of 1.95×10^{-6} , based on the known half-life. Thus, a conservative, upper-bound estimate of the external dose rate from Co-60 at 100 years after disposal would be $(200 \text{ mrem/h}) \times (1.95 \times 10^{-6}) = 3.9 \times 10^{-4} \text{ mrem/h}$.

In order to estimate the contributions to external dose from Nb-94 and Cs-137 at 100 years after disposal, we assume that the activities of Co-60, Nb-94, and Cs-137 in disposed waste are in the same proportions as the total activities of these radionuclides in all casks given in Table L.1-1. That is, the activities of Co-60, Nb-94, and Cs-137 in an average cask are assumed to be in the ratios $(7.7 \times 10^5):(6.2):(0.12)$. Then, taking into account the decay of Co-60 and Cs-137 after 100 years (Nb-94 experiences negligible decay over this time), the activity ratios at 100 years would be $(1.5):(6.2):(0.012)$. We then assume that each radionuclide is a point source, in which case the dose rates per unit activity of each radionuclide calculated by Unger and Trubey (1982) can be used. The values in units of mrem/h per Ci are 1,400 for Co-60, 980 for Nb-94, and 380 for Cs-137. We further assume that the only shielding between the source and receptor locations is the 24 cm of steel at the sides of the casks (see Fig. L.1-1) and use the transmission curves for iron in Fig. 13 of NCRP (1976) to estimate the reduction in dose rate due to shielding for Nb-94 and Cs-137 relative to the reduction for Co-60. The latter assumption provides conservative overestimates of dose rate (i.e., underestimates of shielding) for Nb-94 and Cs-137, because the actual amount of shielding will be greater than 24 cm and the transmission of photons from Nb-94 and Cs-137 relative to the transmission of photons from Co-60 decreases as the amount of shielding increases. The transmission (shielding) factors for Co-60 and Cs-137 for 24 cm of iron are obtained directly from Fig. 13 of NCRP (1976) as 6×10^{-4} and 5×10^{-5} , respectively, and the value for Nb-94 is estimated by interpolation, based on the known photon spectrum for this radionuclide (Kocher 1981), as 1×10^{-4} .

With the information on dose rate per unit activity and transmission through 24 cm of iron given above, a conservative, upper-bound estimate of the external dose rate from Nb-94 can be obtained from the previous upper-bound estimate of the dose rate from Co-60 of 3.9×10^{-4} mrem/h as $(3.9 \times 10^{-4}) \times (6.2/1.5) \times (980/1,400) \times (1 \times 10^{-4})/(6 \times 10^{-4}) = 1.9 \times 10^{-4}$ mrem/h. A similar calculation for Cs-137 yields a dose rate of 7.1×10^{-5} mrem/h. Thus, the dose rate from Cs-137 apparently will be negligible relative to the dose rate from Co-60 and Nb-94.

From the calculations described above, we obtain a conservative, upper-bound estimate of external dose rate next to a waste cask at 100 years after disposal of 5.8×10^{-4} mrem/h, which is due essentially to Co-60 and Nb-94. This estimate is conservative because (1) the dose rate from Co-60 alone is overestimated by at least a factor of 20, based on the acceptance criterion on external dose rate for the waste casks of 200 mrem/h and measured dose rates for casks at the present time of less than 10 mrem/h, and (2) the transmission of photons from Nb-94 through all shielding materials relative to the transmission for Co-60 has been overestimated. The analysis would provide an underestimate of the dose rate only if the activity of Nb-94 in the waste relative to the activity of Co-60 has been greatly underestimated.

The conservative, upper-bound estimate of external dose rate obtained above corresponds to a dose from continuous exposure of 5 mrem per year. If an inadvertent intruder were located next to a waste cask continuously throughout the year, with no additional shielding assumed, the conservative, upper-bound estimate of the external dose rate indicates that the dose received from external exposure would be only a small fraction of the dose limit of 100 mrem per year in the performance objective for protection of inadvertent intruders (U.S.DOE 1988a). Thus, although the foregoing analysis is not intended to provide an accurate estimate of external dose at future times, the analysis clearly shows that the external dose to an inadvertent intruder due to exposure to intact waste casks should not be of concern in regard to meeting the performance objectives for disposal of the NR wastes. External dose to an inadvertent intruder could be of concern only if the inventory of Nb-94 in the waste casks relative to the inventory of Co-60 were much larger than reported in Table L.1-1.

L3.1.4.2 Analysis for Agriculture Scenario

At some distant time in the future, it is conceivable that the carbon steel and stainless steel waste casks will have degraded by corrosion and that the waste could be accessed by excavation, resulting in exposures of inadvertent intruders according to the agriculture scenario described in Sect. 3.2.4.1. This section considers potential doses to inadvertent intruders that could result from this scenario.

On the basis of the design of a typical waste cask shown in Fig. L.1-1 and estimates of corrosion rates of carbon steel and stainless steel, excavation into the waste would not be a credible occurrence for a very long time after disposal. For excavation into the waste to occur, the top of the casks would need to be degraded by corrosion, and Fig. L.1-1 indicates that the thicknesses of carbon steel and stainless steel on top of the casks is 15 cm and 34 cm, respectively. In this analysis, corrosion rates of 4×10^{-3} cm/year and 2×10^{-5} cm/year are assumed for carbon steel (Sullivan et al. 1988) and stainless steel (Sullivan and Suen 1989), respectively. Thus, the estimated time for complete corrosion of the carbon steel layer is about 4,000 years, and the estimated corrosion time for the layer of stainless steel is about 2×10^6 years. Unless the corrosion rate for stainless steel has been underestimated by more than two orders of magnitude, which does not appear likely, it seems reasonable to conclude that direct intrusion into the waste by excavation is not a credible occurrence for the first 10,000 years after disposal which, as described in Sect. 1.2.1, is the assumed time period for compliance with the performance objective for protection of inadvertent intruders. Therefore, on the basis of the agriculture scenario, no limits on average concentrations or inventories of radionuclides in waste casks need to be imposed to provide protection of future inadvertent intruders.

Simply for the purpose of providing a perspective on potential doses according to the agriculture scenario, a dose analysis for this scenario can be performed for the radionuclides listed in Table L.1-1. Only the long-lived radionuclides C-14, Ni-59, Nb-94, Tc-99, I-129, and Pu-239 possibly could be of concern at times far in the future. A dose analysis for these radionuclides can be performed taking into account the following factors: 1) the total inventory in all 41 casks reported in Table L.1-1, 2) the total volume of a waste cask, as estimated from Fig. L.1-1, of 43 m³, 3) the scenario DCFs for the agriculture scenario given in Table 4.1-9, 4) the assumption used in the NRC's 10 CFR Part 61 that the dose per unit concentration of a radionuclide should be reduced by a factor of ten if the radionuclide is in the form of an activated metal, and 5) the assumption based on Fig. L.1-2 that the waste casks will occupy about 40% of the total area of the disposal facility. A scenario DCF for Nb-94 is not given in Table 4.1-9. However, since this radionuclide is a high-energy photon

emitter, the analysis in Appendix A.4 for other such radionuclides indicates that the only important pathway in the agriculture scenario is external exposure while residing in the home. Using the model for this pathway described in Appendix A.4, the scenario DCF for Nb-94 is estimated to be 2.1×10^{-3} rem/year per $\mu\text{Ci}/\text{m}^3$.

If the calculations described above are carried out using Eq. (4.1-1), and a reduction in dose by a factor of ten is included for C-14, Ni-59, and Nb-94 in activated metals, as assumed in the NRC's 10 CFR Part 61, the following dose estimates in units of mrem per year are obtained: 60 for C-14, 6 for Ni-59, 290 for Nb-94, and 75 for Tc-99. The estimates for I-129 and Pu-239 are very low, due to the low inventories in the waste.

The dose estimates for the agriculture scenario given above are conservative because they do not take into account reductions in activity by radioactive decay, nor do they take into account any depletion of activity due to transport in infiltrating water. For example, if we assume that the lifetime of the waste casks is 2×10^6 years, as estimated previously, then the dose from the agriculture scenario at that time, taking into account depletion of the radionuclide inventories by radioactive decay only, would be about 0.1 mrem per year for Tc-99 and essentially zero for the other radionuclides listed above. If, as a more pessimistic alternative, we assume that the corrosion rate for the stainless steel on top of the waste casks could be as high as 10% of the assumed corrosion rate for carbon steel, the predicted lifetime of the casks would still be about 90,000 years. If the agriculture scenario could occur at this time and if only radioactive decay were taken into account in estimating depletion of radionuclide inventories over time, the estimated doses in mrem per year would be about 60 for Tc-99, 13 for Nb-94, 3 for Ni-59, and 0.001 for C-14.

The dose estimates for the agriculture scenario for times far beyond 10,000 years after disposal are provided only for the purpose of providing a perspective on the significance of the inventories of long-lived radionuclides in the waste. Because of the considerable thickness of the walls and top of the waste casks and the expected resistance of the casks to corrosion, especially the thick layer of stainless steel, excavation into the waste should not be a credible occurrence for a very long time after disposal, perhaps for as long as one million years or more. Even if the predicted lifetime of the casks is optimistic and excavation into the wastes could occur as soon as about 100,000 years, the estimated dose for the agriculture scenario,

based on the estimated inventories of radionuclides in the waste, would be less than the dose limit in the performance objective for protection of inadvertent intruders. The dose estimates at this time undoubtedly are conservative, because they do not take into account any depletion of radionuclide inventories by mobilization in infiltrating water. This should be a particularly important factor in reducing the inventory of Tc-99 in the waste at times after water could access the waste.

L3.1.4.3 Analysis for Post-Drilling Scenario

The analysis of exposures of inadvertent intruders according to the agriculture scenario considered in the previous section was based on the assumption that the scenario would not be credible until the top of the waste casks is degraded by corrosion and excavation into the waste could occur. However, it also is possible that, at some time before the casks have completely corroded away, the physical state of the casks would be such that drilling into the waste through a cask that is no longer completely intact could occur. For example, since the sides of the casks are thinner than the top, the top of the casks could collapse after the sides have mostly corroded away, thus providing openings through which drilling could occur.

Based on the thicknesses of carbon steel and stainless steel at the sides of the waste casks shown in Fig. L.1-1 and the estimated corrosion rates of the two materials given previously, we estimate that the lifetime of the sides of the casks should be about 7×10^5 years. Even if this estimate were optimistic and the casks lasted a considerably shorter period of time, the lifetime would be well in excess of 10,000 years even if the corrosion rate for the stainless steel were as high as 10% of the assumed corrosion rate for carbon steel. Therefore, only the long-lived radionuclides considered previously for the agriculture scenario could possibly be of concern for a scenario involving drilling into the waste, i.e., the post-drilling scenario described in Sect. 3.2.4.1.

The analysis of the post-drilling scenario presented in Appendix A.4 and summarized in Table 4.1-11 indicates the following. For radionuclides that do not emit significant intensities of high-energy photons, the dose from the post-drilling scenario would be approximately a factor of ten less than the dose from the agriculture scenario when the two scenarios would

occur at the same time (e.g., see Tables 4.1-9 and 4.1-11). Of the long-lived radionuclides of concern for the NR wastes, this result would apply to C-14, Ni-59, Tc-99, I-129, and Pu-239. For photon-emitting radionuclides, the dose from the post-drilling scenario is about three orders of magnitude less than the dose from the agriculture scenario, because the pathway involving external exposure during indoor residence, which is by far the most important pathway in the agriculture scenario, does not occur in the post-drilling scenario. Therefore, based on the estimates of dose for the agriculture scenario presented in the previous section, the dose for the post-drilling scenario, based on the inventories of radionuclides listed in Table L.1-1, would always be considerably less than the dose limit of 100 mrem per year in the performance objective for protection of inadvertent intruders (U.S.DOE 1988a), even if the post-drilling scenario could occur well before the agriculture scenario. Again, however, the post-drilling scenario is not expected to be a credible occurrence until well beyond 10,000 years after disposal, due to the expected lifetime of the waste casks.

L3.1.4.4 Other Considerations Related to Intruder Protection

In addition to the requirement for limiting potential doses to future inadvertent intruders, which the waste casks apparently would have no difficulty in meeting, the DOE requires that the concentrations of radionuclides in individual waste packages not exceed the Class-C limits established in the NRC's 10 CFR Part 61, which also are related to requirements for intruder protection. For the radionuclides listed in Table L.1-1, the NRC's Class-C limits in units of Ci/m³ are as follows: 80 for C-14 in activated metal, 220 for Ni-59 in activated metal, 7,000 for Ni-63 in activated metal, 0.2 for Nb-94 in activated metal, 3 for Tc-99, 0.08 for I-129, and 4,600 for Cs-137. In addition, the concentration limit for all alpha-emitting transuranic radionuclides with half-lives greater than five years, which would apply to Pu-239 in the NR wastes, is 100 nCi/g, and the limit for Pu-241 is 3,500 nCi/g.

For the radionuclides for which the NRC has specified Class-C limits, the maximum concentration in any waste cask can be estimated from the inventory data in Table L.1-1 and the assumption described in Sect. L.1-1 that the total volume of waste in each cask is 3.5 m³.

With these assumptions, we obtain the following estimates of maximum concentrations of radionuclides in the waste in units of Ci/m³: 3.1 for C-14, 60 for Ni-59, 8,300 for Ni-63, 0.091 for Nb-94, 1.1 for Tc-99, 3.7×10^{-7} for I-129, 3.4×10^{-3} for Cs-137, 7.1×10^{-6} for Pu-239, and 2.5×10^{-4} for Pu-241. If we assume that the average density of the waste form is approximately the same as the density of iron (7.86 g/cm³), the maximum concentrations of Pu-239 and Pu-241 correspond to 0.06 nCi/g and 2 nCi/g, respectively. Thus, if the inventory data in Table L.1-1 are reasonable, the maximum concentrations of Ni-63 slightly exceed the NRC's Class-C limit, which the DOE applies as a waste acceptance criterion for individual waste packages at its disposal sites (U.S.DOE 1988a), and the reported maximum concentrations of Ni-59, Nb-94, and Tc-99 are within a factor of 3-4 of the NRC's Class-C limits.

L3.1.4.5 Summary of Dose Analysis for Inadvertent Intruders

The analyses of potential exposures of inadvertent intruders to NR wastes contained in thick-walled steel casks may be summarized as follows.

First, on the basis of the acceptance criterion limiting the external dose rate at the surface of waste casks to 200 mrem/h at the present time and the available data on the inventories of short-lived and longer-lived photon-emitting radionuclides in the waste, external exposures of inadvertent intruders to intact waste casks at any time after loss of active institutional controls at 100 years after disposal could result in doses that are only a small fraction of the dose limits in the performance objective for protection of inadvertent intruders. The external dose to an inadvertent intruder could approach the dose limits only if the average inventory of the long-lived radionuclide Nb-94 in all waste casks were much greater than the maximum inventory reported in any of the waste casks. Furthermore, measurements on selected casks indicate that the dose rate at the present time is at least an order or magnitude less than the acceptance criterion, which provides an additional degree of confidence that the external dose to future inadvertent intruders would be considerably less than the dose limits and that the inventory of Nb-94 and any other long-lived photon-emitting radionuclides would have to be greatly underestimated in order for the external dose at future times to be of concern.

Second, because of the considerable thicknesses of carbon steel and stainless steel used in constructing the waste casks and the expected low rates of corrosion of these materials, there is a reasonable expectation that the waste casks will maintain their integrity and prevent direct intrusion into the waste, either by excavation or by drilling, for a time far in excess of 10,000 years, which is the assumed time period for compliance with the performance objective for protection of inadvertent intruders. That is, the available data on corrosion rates of steel indicate that the waste casks will be a highly effective barrier to intrusion into the waste for a very long time into the future, perhaps for one million years or more.

If excavation into the waste at some time beyond 10,000 years were a credible occurrence, calculations based on the agriculture scenario indicate that doses to inadvertent intruders could exceed the dose limit in the performance objective, due primarily to the estimated inventories of Nb-94 and Tc-99, but only if the scenario could occur within about 50,000 years. However, the agriculture scenario could occur at this time only if the corrosion rate of stainless steel has been greatly underestimated, which does not appear likely. If the scenario could reasonably occur only at times beyond 100,000 years, then the dose from the agriculture scenario would always be less than the dose limit in the performance objective, unless the inventory of Nb-94 and Tc-99 in the wastes has been underestimated.

Drilling intrusion into the waste also might become credible at some time far into the future. However, the post-drilling scenario could not reasonably occur for thousands of years after disposal, and the dose from this scenario at any such times, based on expected radionuclide inventories in the waste, would only be a small fraction of the dose limit in the performance objective. The post-drilling scenario also could be of concern only if the inventory of Nb-94 and Tc-99 in the wastes has been considerably underestimated.

The analysis of the inventories of long-lived radionuclides in the waste has indicated a concern in addition to the concerns about potential doses to future inadvertent intruders. In particular, the reported maximum concentration of Ni-63 in the waste slightly exceeds the NRC's Class-C limit in 10 CFR Part 61, which has been adopted as a waste acceptance criterion at DOE disposal sites. In addition, the reported maximum concentrations of Ni-59, Nb-94, and Tc-99 are within a factor of 3-4 of the NRC's Class-C limits, so these radionuclides also could be of concern with regard to meeting the DOE's waste acceptance criterion if the maximum concentrations in the waste have been underestimated by these amounts or more.

L3.2 Interpretation of Results

The results of the analysis of performance of the disposal casks for NR waste indicate that the groundwater pathway is the most limiting pathway for calculation of disposal limits, based on the conservative assumptions made. However, only nine of the 29 radionuclides listed in Table L.1-1 are of any concern with respect to the groundwater pathway. Of these nine, calculated inventory limits are lower than the expected inventory for 100 casks for five radionuclides; H-3, C-14, Ni-59, Sr-90 and Tc-99 (Table L.3-5). The intruder analyses indicated the following: 1) the external exposure to intact casks is not likely to result in doses that are significant with respect to dose limits; 2) the agriculture scenario is not likely to occur before 10,000 years, based on the corrosion resistance of the disposal containers, and thus is not likely to lead to doses exceeding the performance objectives before 10,000 years; 3) the post-drilling scenario would lead to doses that are only a small fraction of the dose limit in the performance objective for inadvertent intruders; and 4) the air pathway results for C-14 indicate a limiting inventory (8.3 Ci), which is less than the expected inventory (44 Ci) for 100 casks.

The derived inventory limits in Table L.3-5 are considered to be very low-end estimates of the allowable inventory in the NR waste, as uncertainties encountered in data or models were addressed by choosing a conservative assumption. In the groundwater pathway calculations, the activated metal waste form is assumed to be completely degraded at the time of disposal cask failure; an assumption necessitated by the lack of information on the composition and configuration of the waste form. Furthermore, no credit was taken for containment afforded by the disposal containers because of the uncertainty in the time that the welds might fail. For the air pathway calculations, all of the C-14 in the NR waste was assumed to be in the form of $^{14}\text{CO}_2$ to be released during a one-year period, and to be released at a time when radioactive decay has been insignificant; an obvious overestimate of the source term to the atmosphere.

Table L3-5 Groundwater-based disposal limits versus expected inventory for the NR waste

Radionuclide	Estimated NR Waste Inventory Limit (Ci/100 casks)			Expected NR Waste Inventory (Ci/100 Casks) ^d
	Air Pathway ^a	Breach at 0 years ^b	Breach at 6,000 years ^c	
H-3	9.1	3.0	NA ^e	5.4×10^1
C-14	8.3×10^{-2}	2.9	6.1	4.4×10^1
Ni-59		4.4×10^2	1.4×10^9	9.5×10^3
Sr-90		1.0×10^1	NA ^e	1.1×10^3
Nb-94		2.9×10^1	9.6×10^2	1.5×10^1
Tc-99		9.9×10^{-2}	1.0×10^{-1}	7.3×10^1
I-129		8.6×10^{-5}	8.6×10^{-5}	3.2×10^{-6}
Pu-239		1.8×10^{-1}	2.8×10^{-1}	6.3×10^{-5}
Pu-241 Np-237		6.8×10^3	6.8×10^3	2.1×10^{-2}

^a Inventory limit based on the air pathway (Table L3-4).

^b Inventory limit based on most conservative scenario, where breaching of disposal casks occurs at time 0 (Table L3-3).

^c Inventory limit based on scenario where breaching of disposal casks occurs at 6,000 years (Table L3-3).

^d Expected inventory for 100 casks based on Table L.1-1 inventory for 41 casks, scaled to 100 casks by assuming the same general mix of casks.

^e Radionuclide decays to insignificant levels by 6,000 years.

NA = not applicable.

L4 PERFORMANCE EVALUATION

L4.1 Comparison to Performance Objectives

The results of the NR waste analysis are summarized and interpreted in Sect. L3.2. The results of the intruder analysis suggested that the performance objectives for intruders will be met. The groundwater-based disposal limits, when compared to the expected inventory, suggest that the performance objectives for groundwater protection may not be met for this waste. However, the results in Table L3-5 do not indicate that the NR disposal casks are unsuitable for disposal in E-Area; rather, they indicate that the analysis must consider the containment provided by the casks *and* the corrosion rate of the waste form. The analysis is severely limited because of the lack of information available on the expected lifetime of welds in the disposal casks, and the composition and physical configuration of the waste form. If the wasteform is composed of stainless steel, the groundwater-based disposal limits would be considerably greater due to the corrosion resistance of stainless steel, and the fact that the uniform corrosion rate of stainless steel would control the source term.

L4.2 Design Changes Required to Meet Performance Objectives

Unless it can be assumed that no more than 1% of the C-14 in the casks is released as $^{14}\text{CO}_2$ in any one year, or that atmospheric releases will not occur before the time that 1% of the C-14 remains in the casks (i.e., about 38,000 years), a means of mitigating potential $^{14}\text{CO}_2$ release must be addressed. Venting of the casks would assure a slower release of any $^{14}\text{CO}_2$ produced during corrosion of the activated metal wasteform, but would likely contribute to faster breaching of the waste container.

L.4.3 Data and Research Needs

As was noted earlier, this assessment suffers from a lack of information on the composition and physical configuration of the waste form and on the expected lifetime of the welds in the disposal containers. In order to develop a defensible source term, an estimated rate of corrosion, based on composition and size and shape of the waste form is needed. If it is confirmed, as expected, that the waste form is composed of stainless steel, the release of radionuclides from even a breached cask would be significantly less than is estimated here. Other critical types of information needed to improve the assessment of performance of the NR waste are: 1) a means of estimating the chemical behavior of C-14 in air-tight casks, and 2) information pertinent to when the casks might fail with respect to release of volatile compounds in the containers.

The available data on inventories of long-lived radionuclides in the waste casks indicate that the maximum inventories of Ni-59, Ni-63, Nb-94, and Tc-99 in any cask could approach or slightly exceed the NRC's Class-C limits in 10 CFR Part 61, which are applied as WAC at DOE disposal sites (U.S.DOE 1988a). Thus, a re-evaluation of the inventories of these radionuclides in the waste is potentially important in ensuring that the NR wastes meet the DOE's WAC.

L5 PORFLOW INPUT FILES

TITLE E-AREA NR Unsaturated Flow Field

/

/ P. S. Lam & A. D. Yu

/ Feb 3, 1994

/

/=====

GRID 52 by 83

SCALE 1.0000

COORDINATE X

-25.0	25.0	75.0	125.0	175.0
225.0	275.0	325.0	375.0	425.0
475.0	525.0	575.0	625.0	675.0
725.0	775.0	825.0	875.0	925.0
975.0	1025.0	1075.0	1125.0	1175.0
1225.0	1275.0	1325.0	1375.0	1425.0
1475.0	1525.0	1575.0	1625.0	1675.0
1725.0	1775.0	1825.0	1875.0	1925.0
1975.0	2025.0	2075.0	2125.0	2175.0
2225.0	2275.0	2325.0	2375.0	2425.0
2475.0	2525.0			

SCALE 1.0000

COORDINATE Y

0.0	19.9	40.7	62.6	85.5
109.6	134.8	161.3	189.0	218.2
248.7	280.8	314.4	349.7	386.7
425.5	466.2	508.9	553.7	600.7
650.0	699.4	746.5	791.4	834.2
874.9	913.8	950.8	986.1	1019.7
1051.8	1082.3	1111.4	1139.1	1165.6
1190.7	1214.7	1237.6	1259.4	1280.2
1300.0	1320.0	1340.0	1360.0	1380.0
1400.0	1420.0	1440.0	1460.0	1480.0
1500.0	1520.0	1540.0	1560.0	1580.0
1600.0	1620.0	1640.0	1660.0	1680.0
1700.0	1720.0	1740.0	1760.0	1780.0
1800.0	1820.0	1840.0	1860.0	1880.0
1900.0	1920.0	1940.0	1960.0	1980.0
2000.0	2020.0	2040.0	2060.0	2080.0
2100.0	2120.0	2140.0		

/

ZONE 1 is from (1, 1) to (52, 83) \$ soil

ZONE 2 is from (1, 41) to (45, 68) \$ waste

/

DATUM = 0. 0.

GRAVity components are: 0.0, -1.

/

Fig. L5-1. PORFLOW input file - flow in the vadose zone for NR waste analysis.

```

DENSITY of fluid is constant and equal to 1. gm/cc
/
FOR 1 $soil
MATERIAL PROPERTIES: rho 1.60 gm/cc, neff = 0.439, ntot = 0.439, ndif = 0.439
MULT VAN n = 1.70 alpha = 7.5e-2 sr = 0.088
HYDR ss = 1e-3 kx = 315.0 ky = 315.0 kz = 315.0
/
FOR 2 $waste
MATERIAL PROPERTIES: rho 1.60 gm/cc, neff = 0.439, ntot = 0.439, ndif = 0.439
MULT VAN n = 1.70 alpha = 7.5e-2 sr = 0.088
HYDR ss = 1e-3 kx = 315.0 ky = 315.0 kz = 315.0
/
LOCate subregion ( 1, 1) to ( 52, 83) with ID=SOIL
LOCate subregion ( 1, 41) to ( 45, 68) with ID=WAST
/
SET S = 1.00 in ID=SOIL
/
BOUN P -1 FLUX = 0.
BOUN P +1 FLUX = 0.
BOUN P -2 VALU = 0.
BOUN P +2 FLUX = -40.
/
/ OPERATIONAL CONTROL
/
PROPERty for P is HARM mean
MATRIX in X and Y directions for P in 3 sweeps using ADI
RELAX P = 0.7
/
DIAGnostic node for V and S at (20, 20) every 5 steps
OUTPut every 900000 steps
/
FLUX BALANCE for P in 'run.flx' for ID=SOIL every 50 stps
FLUX BALANCE for P in 'run.flx' for ID=WAST every 50 stps
/
TIME=0.
/
CONV for P REFE; GLOB mode; value = 1.0e-04, max 5 iter, 2 4
SOLV P 100 init 1.e-7 inc 1.001 max 0.01 min 1.e-9 2.0 900000
/
SAVE U V P S in 'run.arc'
END

```

Fig. L.5-1. (cont.)

***** C-14 *****

/

/ E-Area NR Transport (Unsaturated)

/

/ P. S. Lam & A. D. Yu

/ Feb 4, 1994

/

/=====

GRID 52 by 83

SCALE 1.0000

COORDINATE X

-25.0	25.0	75.0	125.0	175.0
225.0	275.0	325.0	375.0	425.0
475.0	525.0	575.0	625.0	675.0
725.0	775.0	825.0	875.0	925.0
975.0	1025.0	1075.0	1125.0	1175.0
1225.0	1275.0	1325.0	1375.0	1425.0
1475.0	1525.0	1575.0	1625.0	1675.0
1725.0	1775.0	1825.0	1875.0	1925.0
1975.0	2025.0	2075.0	2125.0	2175.0
2225.0	2275.0	2325.0	2375.0	2425.0
2475.0	2525.0			

SCALE 1.0000

COORDINATE Y

0.0	19.9	40.7	62.6	85.5
109.6	134.8	161.3	189.0	218.2
248.7	280.8	314.4	349.7	386.7
425.5	466.2	508.9	553.7	600.7
650.0	699.4	746.5	791.4	834.2
874.9	913.8	950.8	986.1	1019.7
1051.8	1082.3	1111.4	1139.1	1165.6
1190.7	1214.7	1237.6	1259.4	1280.2
1300.0	1320.0	1340.0	1360.0	1380.0
1400.0	1420.0	1440.0	1460.0	1480.0
1500.0	1520.0	1540.0	1560.0	1580.0
1600.0	1620.0	1640.0	1660.0	1680.0
1700.0	1720.0	1740.0	1760.0	1780.0
1800.0	1820.0	1840.0	1860.0	1880.0
1900.0	1920.0	1940.0	1960.0	1980.0
2000.0	2020.0	2040.0	2060.0	2080.0
2100.0	2120.0	2140.0		

/

ZONE 1 is from (1, 1) to (52, 83) \$ soil

ZONE 2 is from (1, 41) to (45, 68) \$ waste

Fig. L.5-2. Example PORFLOW input file - mass transport of NR waste radionuclides in vadose zone.

```

/
DATUm = 0. 0.
/
READ record 1 'flowuns.arc'
/
GRAVity components are: 0.0, -1.
/
DENSity of fluid is constant and equal to 1. gm/cc
/
FOR 1 $soil
MATERial PROPerities: rho 1.60 gm/cc, neff = 0.439, ntot = 0.439 , ndif = 0.439
/MULT VAN n = 1.70 alpha = 7.5e-2 sr = 0.088
/HYDR ss = 1.e-3 kx = 315.0 ky = 315.0 kz = 315.0
TRANsport for C Kd= 2.00E+00 D= 158. al= 10. at= 2.
/
FOR 2 $waste
MATERial PROPerities: rho 1.60 gm/cc, neff = 0.439, ntot = 0.439 , ndif = 0.439
/MULT VAN n = 1.70 alpha = 7.5e-2 sr = 0.088
/HYDR ss = 1.e-3 kx = 315.0 ky = 315.0 kz = 315.0
TRANsport for C Kd= 2.00E+00 D= 158. al= 10. at= 2.
/
LOCAt subregion ( 1, 1) to ( 52, 83) with ID=SOIL
LOCAt subregion ( 1, 41) to ( 45, 68) with ID=WAST
/
SET C to 1.0 in ID=WASTE
/
DECAy half life for C is 5.73E+03
/
/BOUN P -1 FLUX = 0.
/BOUN P +1 FLUX = 0.
/BOUN P -2 VALU = 0.
/BOUN P +2 FLUX = -40.
/

BOUN C -1 FLUX = 0.
BOUN C +1 FLUX = 0.
BOUN C -2 VALU = 0.
BOUN C +2 VALU = 0.
/
/ OPERATIONAL CONTROL
/
PROPerity for C is HARM mean
MATRix in X and Y directions for C in 3 sweeps using ADI
RELAX P = 0.7
/
DIAGnostic node for V and C at (20, 5) every 5 steps
/OUTPut every 900000 steps
/

```

Fig. L.5-2. (cont.).


```

FLUX BALANCE for C in 'run.fix' for ID=SOIL every 10 stps
FLUX BALANCE for C in 'run.fix' for ID=WAST every 10 stps
/
TIME=0.
/
CONV for C REFE GLOB mode value = 1.0e-04 max 5 iter 2 4
HISTory for C (25, 50) every 20 in 'run.his'
//////////
DISABle FLOW
//////////
SOLV C    50 ini 1.0E-05 inc 1.05 max 1.0E-01 min 1.E-10 2.0 900000
SOLV C    50 ini 1.0E-05 inc 1.05 max 1.0E-01 min 1.E-10 2.0 900000
SOLV C    900 ini 1.0E-04 inc 1.05 max 1.0E+00 min 1.E-10 2.0 900000
/
OUTPut U V P S C NOW
/
SAVE      U V P S C in 'run.arc'
END

```

Fig. L5-2. (cont.).

```

*** C-14 ***
/
/ NAVAL REACTOR TRANSPORT IN THE SATURATED ZONE
/
/ ASSUMING TOTAL INITIAL INVENTORY = 1.E+12
/ PORFLOW version 2.50
/
/ P. S. LAM AND A. D. YU
/ 2/11/94
/
GRID 38 by 30 by 28
/units are in cm's
COORDinate X  -10000,  0, 45000, 90000, 135000, 145000, 155000,
                165000, 175000, 185000, 195000, 205000, 215000, 225000,
                235000, 245000, 250000, 257500, 265000, 272500, 280000,
                287500, 295000, 302500, 310000, 317500, 325000, 332500,
                340000, 347500, 355000, 362500, 370000, 380000, 390000,
                427500, 465000, 475000,
/
COORDinate Y  -7500,  0, 7500, 15000, 22500, 30000, 37500,
                45000, 52500, 60000, 67500, 75000, 82500, 90000,
                97500, 105000, 115000, 125000, 135000, 145000, 155000,
                165000, 175000, 185000, 195000, 215000, 242500, 292500,
                342500, 352500,
/
COORDinate Z   610,  732, 2073, 3414, 3536, 3658, 3780,
                3901, 4023, 4785, 5547, 5669, 5791, 5913,
                6035, 6157, 6370, 6553, 6751, 6949, 7148,
                7346, 7544, 7742, 7940, 8138, 8336, 8534,
/
/
READ 'eflow40.arc' $40 cm/year through vault regions
/
/Identify a no-diffusion zone at top of domain to allow mass conservation
MATERial type  9 from (1,1, 1) to (38,30,28)
MATERial type 10 from (1,1,21) to (38,30,28)
/
FOR 9
ROCK density = 2.65; porosity = .30, .40, .30
TRANsport for C Kd= 2.00E+00 D= 158. al= 10. at= 2.
FOR 10:
ROCK density = 2.65; porosity = .30, .40, .30
TRANsport for C Kd= 2.00E+00 D= 0. al= 0. at= 0.
/
DECAy half life for C is 5.73E+03
/
INITial C = 0.0 everywhere

```

Fig. L.5-3. Example PORFLOW input file - mass transport of NR waste radionuclides in groundwater.

```

/
BOUNDary C at -1 FLUX =0.0
BOUNDary C at +1 FLUX =0.0
BOUNDary C at -2 FLUX =0.0
BOUNDary C at +2 FLUX =0.0
BOUNDary C at -3 FLUX =0.0
BOUNDary C at +3 FLUX =0.0
/
DISAbLe FLOW
/
DIAGnostic C, V at (28,14,18) every 1 step $EXPECTED NAVY PEAK
/
HISTory for C TABLE at 'RUN.HIS'
  (28,14, 6) (28,14, 7) (28,14, 8) (28,14, 9) (28,14,10)
  (28,14,11) (28,14,12) (28,14,13) (28,14,14) (28,14,15)
  (28,14,16) (28,14,17) (28,14,18) (28,14,19) (28,14,20)
  (29,13,16) (29,13,17) (29,13,18) (29,13,19) (29,13,20)
  frequenCe=5
/
LOCAtE subregion (28,13,20) (28,13,20) as ID=NAVY
/
/Source Units in pCi/cc-year per Ci of inventory
/
*** C-14 ***
SOURCe C for ID=NAVY per VOLUMe TABLE 50 sets
  0.000E+00    0.000E+00
  3.014E-01    4.410E-67
  2.122E+00    3.479E-35
  6.122E+00    1.094E-21
  1.012E+01    1.372E-15
  1.412E+01    1.037E-11
  2.012E+01    6.833E-08
  2.412E+01    4.017E-06
  2.812E+01    9.338E-05
  3.212E+01    1.095E-03
  3.612E+01    7.593E-03
  4.012E+01    3.490E-02
  4.612E+01    1.893E-01
  5.000E+01    4.185E-01
  5.084E+01    4.840E-01
  5.422E+01    8.039E-01
  5.822E+01    1.266E+00
  6.222E+01    1.747E+00
  6.822E+01    2.316E+00
  7.022E+01    2.431E+00
  7.222E+01    2.500E+00
  7.422E+01    2.519E+00
  7.622E+01    2.491E+00
  7.822E+01    2.417E+00

```

Fig. L5-3. (cont.).

8.022E+01	2.303E+00
8.222E+01	2.155E+00
8.622E+01	1.789E+00
9.022E+01	1.384E+00
9.422E+01	9.993E-01
9.822E+01	6.757E-01
1.005E+02	5.270E-01
1.033E+02	3.736E-01
1.232E+02	1.799E-02
1.632E+02	4.383E-06
2.032E+02	1.617E-10
2.432E+02	1.895E-15
2.832E+02	1.051E-20
3.032E+02	2.018E-23
3.432E+02	5.509E-29
3.832E+02	1.108E-34
4.232E+02	1.786E-40
4.632E+02	2.448E-46
5.032E+02	2.971E-52
5.432E+02	3.292E-58
5.832E+02	3.405E-64
6.232E+02	3.338E-70
6.632E+02	3.142E-76
7.032E+02	2.863E-82
7.432E+02	2.545E-88
7.832E+02	2.219E-94

/

TIME = 0. years

CONVergence for C GLOB REFE 1.e-3, max iterations = 3

/

SOLV C 59 ini 1.2E-03 inc 1.05 max 1.2E-01 min 1.E-10 2.0 90000

SOLV C 29 ini 5.9E-04 inc 1.05 max 5.9E-02 min 1.E-10 2.0 90000

SOLV C 850 ini 1.7E-02 inc 1.05 max 1.7E+00 min 1.E-10 2.0 90000

/

END

Fig. L.5-3. (cont.).

APPENDIX L
REFERENCES

- ACRI. 1993. *PORFLOW, A Model for Fluid Flow, Heat and Mass Transport in Multifluid, Multiphase Fractures or Porous Media, Version 2.50*. Draft User's Manual. Analytic & Computational Research, Inc., Bel Air, California.
- CRC Press, Inc. 1981. *CRC Handbook of Chemistry and Physics*. Robert C. Weast and Melvin J. Astle, eds. Boca Raton, FL.
- Freeze, R. A., and J. A. Cherry. 1979. *Groundwater*. Prentice-Hall, Inc., New Jersey.
- Gruber, P. 1980. *A Hydrologic Study of the Unsaturated Zone Adjacent to a Radioactive-Waste Disposal Site at the Savannah River Plant, Aiken, South Carolina*. M. S. Thesis, University of Georgia, Athens, Georgia.
- Hoeffner, S. L. 1985. *Radionuclide Sorption on Savannah River Plant Burial Ground Soil: A Summary and Interpretation of Laboratory Data*. DP-1702. E. I. du Pont de Nemours and Company, Savannah River Laboratory, Aiken, SC.
- Kocher, D. C. 1981. *Radioactive Decay Data Tables*. DOE/TIC-11026. U. S. Department of Energy.
- McIntyre, P. F. 1988. *Sorption Properties of Carbon-14 on Savannah River Plant Soil*. DPST-88-900. E. I. du Pont de Nemours and Company, Savannah River Laboratory, Aiken, SC.
- NCRP. 1976. *Structural Shielding Design and Evaluation for Medical Use of X Rays and Gamma Rays of Energies up to 10 MeV*. NCRP Report No. 49. National Council on Radiation Protection and Measurements, Bethesda, MD.
- Oblath, S. B. 1982. *Migration of TcO₂ in SRP Soils*. DPST-82-815. E. I. Du Pont de Nemours and Company, Savannah River Laboratory, Aiken, SC.
- Sheppard, M. I., and Thibault, D. H. 1990. Default Soil Solid/Liquid Partition Coefficients, K_d s, for Four Major Soil Types: A Compendium. *Health Phys.*, 59:471-482.

- Sullivan, T. M., C. R. Kempf, C. J. Suen, and S. M. Mughabghab. 1988. *Low-Level Radioactive Waste Source Term Model Development and Testing*. NUREG/CR-5204, BNL-NUREG-52160. Brookhaven National Laboratory, Upton, NY.
- Sullivan, T. M., and C. J. Suen. 1989. *Low-Level Waste Shallow Land Disposal Source Term Model : Data Input Guides*. NUREG/CR-5387, BNL-NUREG-52206. Brookhaven National Laboratory, Upton, Long Island, NY.
- Unger, L. M., and D. K. Trubey. 1982. *Specific Gamma-Ray Dose Constants for Nuclides Important to Dosimetry and Radiological Assessment*. ORNL/RSIC-45/R1, Oak Ridge National Laboratory, Oak Ridge, Tennessee.
- U.S.DOE. 1988a. *Radioactive Waste Management, Order 5820.2a*. U. S. Department of Energy, Washington, D.C.
- U.S.DOE. 1988b. *Internal Dose Conversion Factors for Calculation of Dose to the Public*. DOE/EH-0071. U. S. Department of Energy, Washington, D.C.
- U.S.NRC. 1989. *Quality Assurance Program Requirements for Nuclear Facilities*. ASME NQA-1-1989 Edition. The American Society of Mechanical Engineers.
- WSRC. 1992. *Above Ground Storage of Naval Reactor Waste Forms in the SWDF*. Savannah River Site report no. WSRC-TA-92-00005-1. Westinghouse Savannah River Company, Aiken, SC.

APPENDIX M

PORFLOW INPUT FILES

M1 PORFLOW INPUT FILES - NEARFIELD

```

TITLE E-AREA ILNT vault post PA run, 4 cm rate flow run.
/
/ Intact flow run for the ILNT vault.
/
USER CS Cary S. Smith
/
GRID 46 by 72    $ initial grid based on z -area runs
/
SCREEn on
COORDinate X:
/
-25.0  25.0  100.0  200.0  300.0  400.0  500.0  590.0  650.0  690.0
720.0  740.0  755.0  $ <-- backfill
              765.0  780.0  800.0  830.0  870.0  910.0  950.0
990.0  1020.0  1040.0  1055.0  $ <-- sand
              1065.0  1078.0  1090.0  1102.0  1115.0  $ wall
                                      1125.0
1140.0  1160.0  1185.0  1225.0  1275.0  1325.0  1375.0  1425.0  1475.0  1525.0
1575.0  1625.0  1675.0  1725.0  1775.0  1825.0  $ <-- waste
/
COORDinate Y :
/
-10.0  10.0  35.0  65.0  105.0  155.0  215.0  295.0  380.0  460.0
535.0  600.0  655.0  700.0  735.0  760.0  780.0  795.0  $ <--backfill
              805.0  820.0
840.0  855.0  870.0  885.0  $ <--sand
              895.0  906.0  917.0  928.0  939.0  950.0
961.0  $ <--concrete
      971.0  985.0  1005.0  1030.0  1065.0  1110.0  1165.0  1230.0  1310.0
1400.0  1490.0  1560.0  1615.0  1660.0  1695.0  1720.0  1740.0  1753.0  $waste
              1763.0
1775.0  1787.0  1800.0  1812.0  1824.0  $ <--concrete
              1834.0  1844.0  1854.0  1864.0  $ <clay
                                      1874.0
1884.0  1894.0  1904.0  1914.0  $ <--sand
              1924.0  1939.0  1960.0  1985.0  2005.0  2040.0
2075.0  2125.0  $ <--backfill
/
READ 2 nd record from 'end.2'
/
ZONE 1 is from ( 1, 1) to ( 46, 72) $ BACKFILL
ZONE 2 is from ( 14, 19) to ( 46, 64) $ SAND
ZONE 3 is from ( 25, 50) to ( 46, 55) $ CONCRETE (roof)
ZONE 4 is from ( 30, 32) to ( 46, 49) $ WASTE
ZONE 5 is from ( 25, 56) to ( 46, 60) $ CLAY
ZONE 6 is from ( 25, 25) to ( 46, 31) $ CONCRETE (floor)
ZONE 7 is from ( 25, 25) to ( 29, 49) $ CONCRETE (walls)
/

```

Fig. M1-1. PORFLOW Input File - Flow simulation through intact ILNT vault.


```

DATUm = 0. 0.
GRAVity components are: -0.02, -1.
/
DENSity of fluid is constant and equal to 1. gm/cc
/
FOR 1 $BACKFILL
MATERial PROPERTIES: rho 1.60 gm/cc, neff = 0.439, ntot = 0.439 , ndif = 0.439
HYDRAulic properties: ss = 1.e-3, Kx = 315.4 Ky = 315.4 cm/yr
MULTiphase flow: VAN, n = 1.7 , alpha = 0.075 /cm, Swr = 0.2000
/
FOR 2 $SAND
MATERial PROPERTIES: rho 2.60 gm/cc, neff = 0.375, ntot = 0.375 , ndif = 0.375
HYDRAulic prop. ss = 1.e-7, Kx = 3.154e+4 Ky = 3.154e+4
MULTiphase flow: VAN, n = 2.5 , alpha = 0.055 /cm, Swr = 0.2000
/
FOR 3 $CONCRETE roof
MATERial PROPERTIES: rho 2.60 gm/cc, neff = 0.150, ntot = 0.150 , ndif = 0.150
HYDRAulic prop. ss = 1.e-7, Kx = 3.154e-3 Ky = 3.154e-3
MULTiphase flow: VAN, n = 3.43, alpha = 5.98e-4 /cm, Swr = 0.9800
/
FOR 4 $WASTE
MATERial PROPERTIES: rho 1.70 gm/cc, neff = 0.50, ntot = 0.50, ndif = 0.50
HYDRAulic properties: ss = 1e-7, Kx = 3.154e-3 Ky = 3.154e-3 cm/yr
MULTiphase flow: VAN, n = 3.43, alpha = 5.98e-4 /cm, Swr = 0.9800
/
FOR 5 $CLAY
MATERial PROPERTIES: rho 2.60 gm/cc, neff = 0.386, ntot = 0.386 , ndif = 0.386
HYDRAulic properties: ss = 6.e-4, Kx = 3.154 Ky = 3.154
MULTiphase flow: VAN, n = 1.51, alpha = 1.75e-3 /cm, Swr = 0.8800
/
FOR 6 $CONCRETE floor
MATERial PROPERTIES: rho 2.60 gm/cc, neff = 0.150, ntot = 0.150 , ndif = 0.150
HYDRAulic properties: ss = 1.e-7, Kx = 3.154e-3 Ky = 3.154e-3
MULTiphase flow: VAN, n = 3.43, alpha = 5.98e-4 /cm, Swr = 0.9800
/
FOR 7 $CONCRETE walls
MATERial PROPERTIES: rho 2.60 gm/cc, neff = 0.150, ntot = 0.150 , ndif = 0.150
HYDRAulic properties: ss = 1.e-7, Kx = 3.154e-3 Ky = 3.154e-3
MULTiphase flow: VAN, n = 3.43, alpha = 5.98e-4 /cm, Swr = 0.9800
/
LOCAt subregion ( 1, 1) to ( 46, 72) with ID=TOTL
LOCAt subregion ( 25, 25) to ( 46, 55) with ID=VALT
LOCAt subregion ( 30, 32) to ( 46, 49) with ID=WAST
LOCAt subregion ( 25, 56) to ( 46, 60) with ID=CLAY
/
/SET S for ID=TOTL to 0.70
/SET S for ID=VALT to 1.00
/SET S for ID=WAST to 1.00
/SET S for ID=CLAY to 1.00
/

```

Fig. M1-1. (continued).

```
BOUN P -1 FLUX = 0.
BOUN P +1 FLUX = 0.
BOUN P -2 VALU = 0.
BOUN P +2 FLUX = -4.
/
/ OPERATIONAL CONTROL
/
PROPerTy for P is HARM mean
MATRiX in X and Y directions for P in 2 sweeps using ADI
CONVergence for P; LOCAL mode; value = 1.0e-04, max of 1 iterations
CONVergence for FLOW REFERENCE; LOCAL mode; val = 1e-3, max of 5 iterations
/
DIAGnostic node at (30, 40) every 50 steps
OUTPut every 100000 steps
/
FLUX BALANCE for P in 'flux.out' for ID=TOTL every 500 stps
FLUX BALANCE for P          for ID=VALT every 500 stps
/
SOLV for P 500 in AUTO init 1e-4 inc 1.05 max 5 min 1e-9 2.0 900000
SAVE U V P S NOW in 'end.3'
SAVE S NOW in 'end.3'
/
END
```

Fig. M.1-1. (continued).

```

TITLE E-AREA ILNT vault post PA run, 4 cm rate flow run.
/
/ Intact flow run for the ILNT vault.
/
USER CS Cary S. Smith
/
GRID 46 by 72 $ initial grid based on z -area runs
/
SCREEN on
COORDinate X:
/
-25.0 25.0 100.0 200.0 300.0 400.0 500.0 590.0 650.0 690.0
720.0 740.0 755.0 $ <-- backfill
          765.0 780.0 800.0 830.0 870.0 910.0 950.0
990.0 1020.0 1040.0 1055.0 $ <-- sand
          1065.0 1078.0 1090.0 1102.0 1115.0 $ wall
                          1125.0
1140.0 1160.0 1185.0 1225.0 1275.0 1325.0 1375.0 1425.0 1475.0 1525.0
1575.0 1625.0 1675.0 1725.0 1775.0 1825.0 $ <-- waste
/
COORDinate Y:
/
-10.0 10.0 35.0 65.0 105.0 155.0 215.0 295.0 380.0 460.0
535.0 600.0 655.0 700.0 735.0 760.0 780.0 795.0 $ <--backfill
                          805.0 820.0
840.0 855.0 870.0 885.0 $ <--sand
          895.0 906.0 917.0 928.0 939.0 950.0
961.0 $ <--concrete
          971.0 985.0 1005.0 1030.0 1065.0 1110.0 1165.0 1230.0 1310.0
1400.0 1490.0 1560.0 1615.0 1660.0 1695.0 1720.0 1740.0 1753.0 $waste
                          1763.0
1775.0 1787.0 1800.0 1812.0 1824.0 $ <--concrete
          1834.0 1844.0 1854.0 1864.0 $ <clay
                          1874.0
1884.0 1894.0 1904.0 1914.0 $ <--sand
          1924.0 1939.0 1960.0 1985.0 2005.0 2040.0
2075.0 2125.0 $ <--backfill
/
ZONE 1 is from ( 1, 1) to ( 46, 72) $ BACKFILL
ZONE 2 is from ( 14, 19) to ( 46, 64) $ SAND
ZONE 3 is from ( 25, 50) to ( 46, 55) $ CONCRETE (roof)
ZONE 4 is from ( 30, 32) to ( 46, 49) $ WASTE
ZONE 5 is from ( 25, 56) to ( 46, 60) $ CLAY
ZONE 6 is from ( 25, 25) to ( 46, 31) $ CONCRETE (floor)
ZONE 7 is from ( 25, 25) to ( 29, 49) $ CONCRETE (walls)
/
DATUM = 0. 0.
GRAVity components are: -0.02, -1.
/
DENSity of fluid is constant and equal to 1. gm/cc
/

```

Fig. M.1-2. PORFLOW Input File - Flow simulation through cracked ILNT vault.

FOR 1 \$BACKFILL

MATERIAL PROPERTIES: rho 1.60 gm/cc, neff = 0.439, ntot = 0.439, ndif = 0.439

HYDRAULIC properties: ss = 1.e-3, Kx = 315.4 Ky = 315.4 cm/yr

MULTIphase flow: VAN, n = 1.7, alpha = 0.075 /cm, Swr = 0.2000

/

FOR 2 \$SAND

MATERIAL PROPERTIES: rho 2.60 gm/cc, neff = 0.375, ntot = 0.375, ndif = 0.375

HYDRAULIC prop. ss = 1.e-7, Kx = 3.154e+4 Ky = 3.154e+4

MULTIphase flow: VAN, n = 2.5, alpha = 0.055 /cm, Swr = 0.2000

/

FOR 3 \$CONCRETE roof

MATERIAL PROPERTIES: rho 2.60 gm/cc, neff = 0.150, ntot = 0.150, ndif = 0.150

HYDRAULIC prop. ss = 1.e-7, Kx = 3.154e-0 Ky = 3.154e-0

MULTIphase flow: VAN, n = 1.51, alpha = 1.75e-3 /cm, Swr = 0.8800

/

FOR 4 \$WASTE

MATERIAL PROPERTIES: rho 1.70 gm/cc, neff = 0.50, ntot = 0.50, ndif = 0.50

HYDRAULIC properties: ss = 1e-7, Kx = 315.4 Ky = 315.4 cm/yr

MULTIphase flow: VAN, n = 1.7, alpha = 0.075 /cm, Swr = 0.2000

/

FOR 5 \$CLAY

MATERIAL PROPERTIES: rho 2.60 gm/cc, neff = 0.386, ntot = 0.386, ndif = 0.386

HYDRAULIC properties: ss = 6.e-4, Kx = 3.154 Ky = 3.154

MULTIphase flow: VAN, n = 1.51, alpha = 1.75e-3 /cm, Swr = 0.8800

/

FOR 6 \$CONCRETE floor

MATERIAL PROPERTIES: rho 2.60 gm/cc, neff = 0.150, ntot = 0.150, ndif = 0.150

HYDRAULIC properties: ss = 1.e-7, Kx = 3.154e-3 Ky = 3.154e-3

MULTIphase flow: VAN, n = 3.43, alpha = 5.98e-4 /cm, Swr = 0.9800

/

FOR 7 \$CONCRETE walks

MATERIAL PROPERTIES: rho 2.60 gm/cc, neff = 0.150, ntot = 0.150, ndif = 0.150

HYDRAULIC prop. ss = 1.e-7, Kx = 3.154e+4 Ky = 3.154e+4

MULTIphase flow: VAN, n = 2.5, alpha = 0.055 /cm, Swr = 0.2000

/

LOCATE subregion (1, 1) to (46, 72) with ID=TOTL

LOCATE subregion (25, 25) to (46, 55) with ID=VALT

LOCATE subregion (30, 32) to (46, 49) with ID=WAST

LOCATE subregion (25, 56) to (46, 60) with ID=CLAY

/

SET S for ID=TOTL to 0.70

SET S for ID=VALT to 1.00

SET S for ID=WAST to 0.50

SET S for ID=CLAY to 1.00

/

BOUN P -1 FLUX = 0.

BOUN P +1 FLUX = 0.

BOUN P -2 VALU = 0.

BOUN P +2 FLUX = -4.

/

Fig. M.1-2 (continued).

```

/ OPERATIONAL CONTROL
/
PROPERty for P is HARM mean
MATRIX in X and Y directions for P in 2 sweeps using ADI
CONVergence for P; LOCAL mode; value = 1.0e-04, max of 1 iterations
CONVergence for FLOW REFERENCE; LOCAL mode; val = 1e-3, max of 5 iterations
/
DIAGnostic node at (30, 40) every 50 steps
OUTPut every 100000 steps
/
FLUX BALANCE for P in 'flux.out' for ID=TOTL every 500 stps
FLUX BALANCE for P          for ID=VALT every 500 stps
/
SOLV for P  0.1 in init 5e-4 inc 1.00 max 1 min 1e-9 2.0 900000
SOLV for P  0.9 in AUTO init 1e-7 inc 1.05 max 1 min 1e-9 2.0 900000
SAVE U V P S  NOW in 'end.0'
SAVE      S  NOW in 'end.0'
/
SOLV for P  4 in AUTO init 1e-7 inc 1.05 max 1 min 1e-9 2.0 900000
SAVE U V P S  NOW in 'end.0'
SAVE      S  NOW in 'end.0'
/
SOLV for P  5 in AUTO init 1e-6 inc 1.05 max 1 min 1e-9 2.0 900000
SAVE U V P S  NOW in 'end.0'
SAVE      S  NOW in 'end.0'
/
SOLV for P  10 in AUTO init 1e-6 inc 1.05 max 1 min 1e-9 2.0 900000
SAVE U V P S  NOW in 'end.1'
SAVE      S  NOW in 'end.1'
/
SOLV for P  30 in AUTO init 1e-5 inc 1.05 max 1 min 1e-9 2.0 900000
SAVE U V P S  NOW in 'end.1'
SAVE      S  NOW in 'end.1'
/
SOLV for P  50 in AUTO init 1e-5 inc 1.05 max 1 min 1e-9 2.0 900000
SAVE U V P S  NOW in 'end.1'
SAVE      S  NOW in 'end.1'
/
SOLV for P  100 in AUTO init 1e-4 inc 1.05 max 1 min 1e-9 2.0 900000
SAVE U V P S  NOW in 'end.2'
SAVE      S  NOW in 'end.2'
/
SOLV for P  300 in AUTO init 1e-4 inc 1.05 max 3 min 1e-9 2.0 900000
SAVE U V P S  NOW in 'end.2'
SAVE      S  NOW in 'end.2'
/
END

```

Fig. M.1-2. (continued).

TITLE E-AREA ILNT vault post PA run, 4 cm rate flow run.

/

/ Intact flow run for the ILNT vault.

/

USER CS Cary S. Smith

/

GRID 46 by 72 \$ initial grid based on z -area runs

/

SCREEn on

COORDinate X:

/

-25.0 25.0 100.0 200.0 300.0 400.0 500.0 590.0 650.0 690.0

720.0 740.0 755.0 \$ <- backfill

765.0 780.0 800.0 830.0 870.0 910.0 950.0

990.0 1020.0 1040.0 1055.0 \$ <- sand

1065.0 1078.0 1090.0 1102.0 1115.0 \$ wall

1125.0

1140.0 1160.0 1185.0 1225.0 1275.0 1325.0 1375.0 1425.0 1475.0 1525.0

1575.0 1625.0 1675.0 1725.0 1775.0 1825.0 \$ <- waste

/

COORDinate Y :

/

-10.0 10.0 35.0 65.0 105.0 155.0 215.0 295.0 380.0 460.0

535.0 600.0 655.0 700.0 735.0 760.0 780.0 795.0 \$ <-backfill

805.0 820.0

840.0 855.0 870.0 885.0 \$ <-sand

895.0 906.0 917.0 928.0 939.0 950.0

961.0 \$ <-concrete

971.0 985.0 1005.0 1030.0 1065.0 1110.0 1165.0 1230.0 1310.0

1400.0 1490.0 1560.0 1615.0 1660.0 1695.0 1720.0 1740.0 1753.0 \$waste

1763.0

1775.0 1787.0 1800.0 1812.0 1824.0 \$ <-concrete

1834.0 1844.0 1854.0 1864.0 \$ <clay

1874.0

1884.0 1894.0 1904.0 1914.0 \$ <-sand

1924.0 1939.0 1960.0 1985.0 2005.0 2040.0

2075.0 2125.0 \$ <-backfill

/

ZONE 1 is from (1, 1) to (46, 72) \$ BACKFILL

ZONE 2 is from (14, 19) to (46, 64) \$ SAND

ZONE 3 is from (25, 50) to (46, 55) \$ CONCRETE (roof)

ZONE 4 is from (30, 32) to (46, 49) \$ WASTE

ZONE 5 is from (25, 56) to (46, 60) \$ CLAY

ZONE 6 is from (25, 25) to (46, 31) \$ CONCRETE (floor)

ZONE 7 is from (25, 25) to (29, 49) \$ CONCRETE (walls)

/

DATUm = 0. 0.

GRAVity components are: -0.02, -1.

/

DENSity of fluid is constant and equal to 1. gm/cc

Fig. M1-3. PORFLOW Input File - Flow simulation through failed ILNT vault.

```

/
FOR 1 $BACKFILL
MATERial PROPERTIES: rho 1.60 gm/cc, neff = 0.439, ntot = 0.439 , ndif = 0.439
HYDRaulic properties: ss = 1.e-3, Kx = 315.4 Ky = 315.4 cm/yr
MULTIphase flow: VAN, n = 1.7 , alpha = 0.075 /cm, Swr = 0.2000
/
FOR 2 $SAND
MATERial PROPERTIES: rho 2.60 gm/cc, neff = 0.375, ntot = 0.375 , ndif = 0.375
HYDRaulic prop. ss = 1.e-7, Kx = 3.154e+4 Ky = 3.154e+4
MULTIphase flow: VAN, n = 2.5 , alpha = 0.055 /cm, Swr = 0.2000
/
FOR 3 $CONCRETE roof
MATERial PROPERTIES: rho 2.60 gm/cc, neff = 0.150, ntot = 0.150 , ndif = 0.150
HYDRaulic properties: ss = 1e-7, Kx = 315.4 Ky = 315.4 cm/yr
MULTIphase flow: VAN, n = 1.7 , alpha = 0.075 /cm, Swr = 0.2000
/
FOR 4 $WASTE
MATERial PROPERTIES: rho 1.70 gm/cc, neff = 0.50, ntot = 0.50, ndif = 0.50
HYDRaulic properties: ss = 1e-7, Kx = 315.4 Ky = 315.4 cm/yr
MULTIphase flow: VAN, n = 1.7 , alpha = 0.075 /cm, Swr = 0.2000
/
FOR 5 $CLAY
MATERial PROPERTIES: rho 2.60 gm/cc, neff = 0.386, ntot = 0.386 , ndif = 0.386
HYDRaulic properties: ss = 1e-7, Kx = 315.4 Ky = 315.4 cm/yr
MULTIphase flow: VAN, n = 1.7 , alpha = 0.075 /cm, Swr = 0.2000
/
FOR 6 $CONCRETE floor
MATERial PROPERTIES: rho 2.60 gm/cc, neff = 0.150, ntot = 0.150 , ndif = 0.150
HYDRaulic prop. ss = 1.e-7, Kx = 3.154e+4 Ky = 3.154e+4
MULTIphase flow: VAN, n = 2.5 , alpha = 0.055 /cm, Swr = 0.2000
/
FOR 7 $CONCRETE walls
MATERial PROPERTIES: rho 2.60 gm/cc, neff = 0.150, ntot = 0.150 , ndif = 0.150
HYDRaulic prop. ss = 1.e-7, Kx = 3.154e+4 Ky = 3.154e+4
MULTIphase flow: VAN, n = 2.5 , alpha = 0.055 /cm, Swr = 0.2000
/
LOCate subregion ( 1, 1) to ( 46, 72) with ID=TOTL
LOCate subregion ( 25, 25) to ( 46, 55) with ID=VALT
LOCate subregion ( 30, 32) to ( 46, 49) with ID=WAST
LOCate subregion ( 25, 56) to ( 46, 60) with ID=CLAY
/
SET S for ID=TOTL to 0.75
SET S for ID=VALT to 0.75
SET S for ID=WAST to 0.75
SET S for ID=CLAY to 0.75
/
BOUN P -1 FLUX = 0.
BOUN P +1 FLUX = 0.
BOUN P -2 VALU = 0.
BOUN P +2 FLUX = -40.
/

```

Fig. M1-3. (continued).

```

/ OPERATIONAL CONTROL
/
PROPERty for P is HARM mean
MATRIX in X and Y directions for P in 2 sweeps using ADI
CONVERgence for P; LOCAL mode; value = 1.0e-04, max of 1 iterations
CONVERgence for FLOW REFERENCE; LOCAL mode; val = 1e-3, max of 5 iterations
/
DIAGnostic node at (30, 40) every 50 steps
OUTPut every 100000 steps
/
FLUX BALANCE for P in 'flux.out' for ID=TOTL every 500 stps
FLUX BALANCE for P          for ID=VALT every 500 stps
/
SOLV for P  0.1 in init 5e-4 inc 1.00 max 1 min 1e-9 2.0 900000
SOLV for P  0.9 in AUTO init 1e-7 inc 1.05 max 1 min 1e-9 2.0 900000
SAVE U V P S  NOW in 'end.0'
SAVE      S  NOW in 'end.0'
/
SOLV for P  4 in AUTO init 1e-7 inc 1.05 max 1 min 1e-9 2.0 900000
SAVE U V P S  NOW in 'end.0'
SAVE      S  NOW in 'end.0'
/
SOLV for P  5 in AUTO init 1e-6 inc 1.05 max 1 min 1e-9 2.0 900000
SAVE U V P S  NOW in 'end.0'
SAVE      S  NOW in 'end.0'
/
SOLV for P  10 in AUTO init 1e-6 inc 1.05 max 1 min 1e-9 2.0 900000
SAVE U V P S  NOW in 'end.1'
SAVE      S  NOW in 'end.1'
/
SOLV for P  30 in AUTO init 1e-5 inc 1.05 max 1 min 1e-9 2.0 900000
SAVE U V P S  NOW in 'end.1'
SAVE      S  NOW in 'end.1'
/
SOLV for P  50 in AUTO init 1e-5 inc 1.05 max 1 min 1e-9 2.0 900000
SAVE U V P S  NOW in 'end.1'
SAVE      S  NOW in 'end.1'
/
SOLV for P  100 in AUTO init 1e-4 inc 1.05 max 1 min 1e-9 2.0 900000
SAVE U V P S  NOW in 'end.2'
SAVE      S  NOW in 'end.2'
/
SOLV for P  300 in AUTO init 1e-4 inc 1.05 max 3 min 1e-9 2.0 900000
SAVE U V P S  NOW in 'end.2'
SAVE      S  NOW in 'end.2'
/
END

```

Fig. M.1-3. (continued).


```

TITLE E-AREA ILNT vault post PA run, 4 cm rate flow run.
/
/ Transport run for H3, C14, Ni59, and Tc99
/
USER CS Cary S. Smith
/
GRID 46 by 72
/
SCREEN on
COORDinate X:
/
-25.0 25.0 100.0 200.0 300.0 400.0 500.0 590.0 650.0 690.0
720.0 740.0 755.0 $ <-- backfill
          765.0 780.0 800.0 830.0 870.0 910.0 950.0
990.0 1020.0 1040.0 1055.0 $ <-- sand
          1065.0 1078.0 1090.0 1102.0 1115.0 $ wall
          1125.0
1140.0 1160.0 1185.0 1225.0 1275.0 1325.0 1375.0 1425.0 1475.0 1525.0
1575.0 1625.0 1675.0 1725.0 1775.0 1825.0 $ <-- waste
/
COORDinate Y:
/
-10.0 10.0 35.0 65.0 105.0 155.0 215.0 295.0 380.0 460.0
535.0 600.0 655.0 700.0 735.0 760.0 780.0 795.0 $ <--backfill
          805.0 820.0
840.0 855.0 870.0 885.0 $ <--sand
          895.0 906.0 917.0 928.0 939.0 950.0
961.0 $ <--concrete
          971.0 985.0 1005.0 1030.0 1065.0 1110.0 1165.0 1230.0 1310.0
1400.0 1490.0 1560.0 1615.0 1660.0 1695.0 1720.0 1740.0 1753.0 $waste
          1763.0
1775.0 1787.0 1800.0 1812.0 1824.0 $ <--concrete
          1834.0 1844.0 1854.0 1864.0 $ <clay
          1874.0
1884.0 1894.0 1904.0 1914.0 $ <--sand
          1924.0 1939.0 1960.0 1985.0 2005.0 2040.0
2075.0 2125.0 $ <--backfill
/
READ 1 st record from 'start'
/
ZONE 1 is from ( 1, 1) to ( 46, 72) $ BACKFILL
ZONE 2 is from ( 14, 19) to ( 46, 64) $ SAND
ZONE 3 is from ( 25, 50) to ( 46, 55) $ CONCRETE (roof)
ZONE 4 is from ( 30, 32) to ( 46, 49) $ WASTE
ZONE 5 is from ( 25, 56) to ( 46, 60) $ CLAY
ZONE 6 is from ( 25, 25) to ( 46, 31) $ CONCRETE (floor)
ZONE 7 is from ( 25, 25) to ( 29, 49) $ CONCRETE (walls)
/

```

Fig. M.1-4. PORFLOW Input File - Mass transport simulation for intact ILNT vault.

DATUm = 0. 0.
 GRAVity components are: -0.02, -1.
 /
 DENSity of fluid is constant and equal to 1. gm/cc
 /
 FOR 1 \$BACKFILL
 MATERial PROPERTIES: rho 1.60 gm/cc, neff = 0.439, ntot = 0.439 , ndif = 0.439
 TRANsport for C kd = 0.0, D = 158.0, al = 10.0 at = 2.0 \$ C is H3
 TRANsport for C2 kd = 2.40, D = 158.0, al = 10.0, at = 2.0 \$ C2 is C14
 TRANsport for C3 kd = 300.0, D = 158.0, al = 10.0, at = 2.0 \$ C3 is Ni59
 TRANsport for C4 kd = 0.36, D = 158.0, al = 10.0, at = 2.0 \$ C4 is Tc99
 /
 FOR 2 \$SAND
 MATERial PROPERTIES: rho 2.60 gm/cc, neff = 0.375, ntot = 0.375 , ndif = 0.375
 TRANsport for C kd = 0.0, D = 158.0, al = 10.0 at = 2.0 \$ C is H3
 TRANsport for C2 kd = 5.0, D = 158.0, al = 10.0, at = 2.0 \$ C2 is C14
 TRANsport for C3 kd = 0.0, D = 158.0, al = 10.0, at = 2.0 \$ C3 is Ni59
 TRANsport for C4 kd = 0.1, D = 158.0, al = 10.0, at = 2.0 \$ C4 is Tc99
 /
 FOR 3 \$CONCRETE roof
 MATERial PROPERTIES: rho 2.60 gm/cc, neff = 0.150, ntot = 0.150 , ndif = 0.150
 TRANsport for C kd = 0.0, D = 0.315, al = 5.0 at = 2.0 \$ C is H3
 TRANsport for C2 kd = 5000.0, D = 0.315, al = 5.0, at = 2.0 \$ C2 is C14
 TRANsport for C3 kd = 1000.0, D = 0.315, al = 5.0, at = 2.0 \$ C3 is Ni59
 TRANsport for C4 kd = 700.0, D = 0.315, al = 5.0, at = 2.0 \$ C4 is Tc99
 /
 FOR 4 \$WASTE
 MATERial PROPERTIES: rho 1.70 gm/cc, neff = 0.50, ntot = 0.50, ndif = 0.50
 TRANsport for C kd = 0.0, D = 0.158, al = 5.0 at = 2.0 \$ C is H3
 TRANsport for C2 kd = 5000.0, D = 0.158, al = 5.0, at = 2.0 \$ C2 is C14
 TRANsport for C3 kd = 1000.0, D = 0.158, al = 5.0, at = 2.0 \$ C3 is Ni59
 TRANsport for C4 kd = 1.0, D = 0.158, al = 5.0, at = 2.0 \$ C4 is Tc99
 /
 FOR 5 \$CLAY
 MATERial PROPERTIES: rho 2.60 gm/cc, neff = 0.386, ntot = 0.386 , ndif = 0.386
 TRANsport for C kd = 0.0, D = 47.0, al = 5.0, at = 1.0 \$ C is H3
 TRANsport for C2 kd = 0.0, D = 47.0, al = 5.0, at = 2.0 \$ C2 is C14
 TRANsport for C3 kd = 650.0, D = 47.0, al = 5.0, at = 1.0 \$ C3 is Ni59
 TRANsport for C4 kd = 2.2, D = 47.0, al = 5.0, at = 2.0 \$ C4 is Tc99
 /
 FOR 6 \$CONCRETE floor
 MATERial PROPERTIES: rho 2.60 gm/cc, neff = 0.150, ntot = 0.150 , ndif = 0.150
 TRANsport for C kd = 0.0, D = 0.315, al = 5.0 at = 2.0 \$ C is H3
 TRANsport for C2 kd = 5000.0, D = 0.315, al = 5.0, at = 2.0 \$ C2 is C14
 TRANsport for C3 kd = 1000.0, D = 0.315, al = 5.0, at = 2.0 \$ C3 is Ni59
 TRANsport for C4 kd = 700.0, D = 0.315, al = 5.0, at = 2.0 \$ C4 is Tc99
 /

Fig. M.1-4. (continued).

```

FOR 7 $CONCRETE walls
MATERIAL PROPERTIES: rho 2.60 gm/cc, neff = 0.150, ntot = 0.150, ndif = 0.150
TRANsport for C kd = 0.0, D = 0.315, al = 5.0, at = 2.0 $ C is H3
TRANsport for C2 kd = 5000.0, D = 0.315, al = 5.0, at = 2.0 $ C2 is C14
TRANsport for C3 kd = 1000.0, D = 0.315, al = 5.0, at = 2.0 $ C3 is Ni59
TRANsport for C4 kd = 700.0, D = 0.315, al = 5.0, at = 2.0 $ C4 is Tc99
/
LOCAtE subregion ( 1, 1) to ( 46, 72) with ID=TOTL
LOCAtE subregion ( 25, 25) to ( 46, 55) with ID=VALT
LOCAtE subregion ( 30, 32) to ( 46, 49) with ID=WAST
LOCAtE subregion ( 25, 56) to ( 46, 60) with ID=CLAY
/
SET C to 1.0 in ID=WASTE
SET C2 to 1.0 in ID=WASTE
SET C3 to 1.0 in ID=WASTE
SET C4 to 1.0 in ID=WASTE
/
DECAy half life for C is 12.3
DECAy half life for C2 is 5730
DECAy half life for C3 is 75000
DECAy half life for C4 is 2.13e+5
/
BOUN C -1 FLUX = 0.
BOUN C +1 FLUX = 0.
BOUN C -2 VALU = 0.
BOUN C +2 VALU = 0.
/
BOUN C2 -1 FLUX = 0.
BOUN C2 +1 FLUX = 0.
BOUN C2 -2 VALU = 0.
BOUN C2 +2 VALU = 0.
/
BOUN C3 -1 FLUX = 0.
BOUN C3 +1 FLUX = 0.
BOUN C3 -2 VALU = 0.
BOUN C3 +2 VALU = 0.
/
BOUN C4 -1 FLUX = 0.
BOUN C4 +1 FLUX = 0.
BOUN C4 -2 VALU = 0.
BOUN C4 +2 VALU = 0.
/
/ OPERATIONAL CONTROL
/
PROPERty for C C2 C3 C4 is HARM mean
MATRIX in X and Y directions for C C2 C3 C4 in 1 sweeps using ADI
CONVergence for C REFERENCE; LOCAL mode; value = 1.0e-04, max of 5 iterations
CONVergence for C2 REFERENCE; LOCAL mode; value = 1.0e-04, max of 5 iterations
CONVergence for C3 REFERENCE; LOCAL mode; value = 1.0e-04, max of 5 iterations
CONVergence for C4 REFERENCE; LOCAL mode; value = 1.0e-04, max of 5 iterations
/

```

Fig. M.1-4. (continued).

```

DIAGnostic node for C2 and C3 at (30, 40) every 4 steps
OUTPUt every 900000 steps
/
FLUX BALAnce for C in 'flux.out' for ID=TOTL every 20 stps
FLUX BALAnce for C          for ID=VALT every 20 stps
FLUX BALAnce for C2         for ID=TOTL every 20 stps
FLUX BALAnce for C2         for ID=VALT every 20 stps
/
FLUX BALAnce for C3         for ID=TOTL every 20 stps
FLUX BALAnce for C3         for ID=VALT every 20 stps
FLUX BALAnce for C4         for ID=TOTL every 20 stps
FLUX BALAnce for C4         for ID=VALT every 20 stps
/
HISTory for C C2 C3 C4 (31, 33) (40, 33) (45, 33) every 20 in 'hist.out'
DISAbLe FLOW
/
SOLV for  C C2 C3 C4  100 init 0.050 inc 1.000 max 0.100 mn 1.e-4 1.1 900000
SAVE      C C2 C3 C4  NOW in 'end.0'
/
SOLV for  C C2 C3 C4  100 init 0.100 inc 1.001 max 0.100 mn 1.e-4 1.1 900000
SAVE      C C2 C3 C4  NOW in 'end.0'
/
SOLV for  C C2 C3 C4  100 init 0.200 inc 1.001 max 0.100 mn 1.e-4 1.1 900000
SAVE      C C2 C3 C4  NOW in 'end.0'
/
SOLV for   C2 C3 C4  100 init 0.100 inc 1.001 max 0.100 mn 1.e-4 1.1 900000
SAVE      C2 C3 C4  NOW in 'end.1'
/
SOLV for   C2 C3 C4  100 init 0.100 inc 1.001 max 0.100 mn 1.e-4 1.1 900000
SAVE      C2 C3 C4  NOW in 'end.1'
/
SOLV for   C2 C3 C4   75 init 0.100 inc 1.001 max 0.100 mn 1.e-4 1.1 900000
SAVE      C2 C3 C4  NOW in 'end.1'
/
END

```

Fig. M1-4. (continued).

```

TITLE E-AREA ILNT vault post PA run, 4 cm rate flow run.
/
/ Solubility limited run for Pu239, Pu240, Pu242
/
USER CS Cary S. Smith
/
GRID 46 by 72
/
SCREEn on
COORDinate X:
/
-25.0  25.0  100.0  200.0  300.0  400.0  500.0  590.0  650.0  690.0
720.0  740.0  755.0  $ <-- backfill
              765.0  780.0  800.0  830.0  870.0  910.0  950.0
990.0  1020.0  1040.0  1055.0  $ <-- sand
              1065.0  1078.0  1090.0  1102.0  1115.0  $ wall
                                      1125.0
1140.0  1160.0  1185.0  1225.0  1275.0  1325.0  1375.0  1425.0  1475.0  1525.0
1575.0  1625.0  1675.0  1725.0  1775.0  1825.0  $ <-- waste
/
COORDinate Y :
/
-10.0  10.0  35.0  65.0  105.0  155.0  215.0  295.0  380.0  460.0
535.0  600.0  655.0  700.0  735.0  760.0  780.0  795.0  $ <--backfill
                                      805.0  820.0
840.0  855.0  870.0  885.0  $ <--sand
              895.0  906.0  917.0  928.0  939.0  950.0
961.0  $ <--concrete
              971.0  985.0  1005.0  1030.0  1065.0  1110.0  1165.0  1230.0  1310.0
1400.0  1490.0  1560.0  1615.0  1660.0  1695.0  1720.0  1740.0  1753.0  $waste
                                      1763.0
1775.0  1787.0  1800.0  1812.0  1824.0  $ <--concrete
              1834.0  1844.0  1854.0  1864.0  $ <clay
                                      1874.0
1884.0  1894.0  1904.0  1914.0  $ <--sand
              1924.0  1939.0  1960.0  1985.0  2005.0  2040.0
2075.0  2125.0  $ <--backfill
/
READ 1 st record from 'start'
/
ZONE 1 is from ( 1, 1) to ( 46, 72) $ BACKFILL
ZONE 2 is from ( 14, 19) to ( 46, 64) $ SAND
ZONE 3 is from ( 25, 50) to ( 46, 55) $ CONCRETE (roof)
ZONE 4 is from ( 30, 32) to ( 46, 49) $ WASTE
ZONE 5 is from ( 25, 56) to ( 46, 60) $ CLAY
ZONE 6 is from ( 25, 25) to ( 46, 31) $ CONCRETE (floor)
ZONE 7 is from ( 25, 25) to ( 29, 49) $ CONCRETE (walls)
/

```

Fig. M1-5. PORFLOW Input File - Mass transport simulation for intact ILNT vault, solubility-limited source.

DATUm = 0. 0.

GRAVity components are: -0.02, -1.

/

DENSity of fluid is constant and equal to 1. gm/cc

/

FOR 1 \$BACKFILL

MATERial PROPERTIES: rho 1.60 gm/cc, neff = 0.439, ntot = 0.439, ndif = 0.439

TRANsport for C kd = 100.0, D = 158.0, al = 10.0 at = 2.0 \$ C is Pu239

TRANsport for C2 kd = 100.0, D = 158.0, al = 10.0, at = 2.0 \$ C2 is Pu240

TRANsport for C3 kd = 100.0, D = 158.0, al = 10.0, at = 2.0 \$ C3 is Pu242

/

FOR 2 \$SAND

MATERial PROPERTIES: rho 2.60 gm/cc, neff = 0.375, ntot = 0.375, ndif = 0.375

TRANsport for C kd = 550.0, D = 158.0, al = 10.0 at = 2.0 \$ C is Pu239

TRANsport for C2 kd = 550.0, D = 158.0, al = 10.0, at = 2.0 \$ C2 is Pu240

TRANsport for C3 kd = 550.0, D = 158.0, al = 10.0, at = 2.0 \$ C3 is Pu242

/

FOR 3 \$CONCRETE roof

MATERial PROPERTIES: rho 2.60 gm/cc, neff = 0.150, ntot = 0.150, ndif = 0.150

TRANsport for C kd = 5000.0, D = 0.315, al = 5.0 at = 2.0 \$ C is Pu239

TRANsport for C2 kd = 5000.0, D = 0.315, al = 5.0, at = 2.0 \$ C2 is Pu240

TRANsport for C3 kd = 5000.0, D = 0.315, al = 5.0, at = 2.0 \$ C3 is Pu242

/

FOR 4 \$WASTE

MATERial PROPERTIES: rho 1.70 gm/cc, neff = 0.50, ntot = 0.50, ndif = 0.50

TRANsport for C kd = 0.0, D = 0.158, al = 5.0 at = 2.0 \$ C is Pu239

TRANsport for C2 kd = 0.0, D = 0.158, al = 5.0, at = 2.0 \$ C2 is Pu240

TRANsport for C3 kd = 0.0, D = 0.158, al = 5.0, at = 2.0 \$ C3 is Pu242

/

FOR 5 \$CLAY

MATERial PROPERTIES: rho 2.60 gm/cc, neff = 0.386, ntot = 0.386, ndif = 0.386

TRANsport for C kd = 5100.0, D = 47.0, al = 5.0, at = 1.0 \$ C is Pu239

TRANsport for C2 kd = 5100.0, D = 47.0, al = 5.0, at = 2.0 \$ C2 is Pu240

TRANsport for C3 kd = 5100.0, D = 47.0, al = 5.0, at = 1.0 \$ C3 is Pu242

/

FOR 6 \$CONCRETE floor

MATERial PROPERTIES: rho 2.60 gm/cc, neff = 0.150, ntot = 0.150, ndif = 0.150

TRANsport for C kd = 5000.0, D = 0.315, al = 5.0 at = 2.0 \$ C is Pu239

TRANsport for C2 kd = 5000.0, D = 0.315, al = 5.0, at = 2.0 \$ C2 is Pu240

TRANsport for C3 kd = 5000.0, D = 0.315, al = 5.0, at = 2.0 \$ C3 is Pu242

/

FOR 7 \$CONCRETE walls

MATERial PROPERTIES: rho 2.60 gm/cc, neff = 0.150, ntot = 0.150, ndif = 0.150

TRANsport for C kd = 5000.0, D = 0.315, al = 5.0 at = 2.0 \$ C is Pu239

TRANsport for C2 kd = 5000.0, D = 0.315, al = 5.0, at = 2.0 \$ C2 is Pu240

TRANsport for C3 kd = 5000.0, D = 0.315, al = 5.0, at = 2.0 \$ C3 is Pu242

/

Fig. M1-5. (continued).

```

LOCAtE subregion ( 1, 1) to ( 46, 72) with ID=TOTL
LOCAtE subregion ( 25, 25) to ( 46, 55) with ID=VALT
LOCAtE subregion ( 30, 32) to ( 46, 49) with ID=WAST
LOCAtE subregion ( 25, 56) to ( 46, 60) with ID=CLAY
/
SOURCe C ; SOLUb. lim CONST = 1.0e-13 g/cc, s= 4.0214e-1 g, t= 0.0 in ID=WASTe
SOURCe C2; SOLUb. lim CONST = 1.0e-13 g/cc, s= 1.2354e-1 g, t= 0.0 in ID=WASTe
SOURCe C3; SOLUb. lim CONST = 1.0e-13 g/cc, s= 7.1335e-0 g, t= 0.0 in ID=WASTe
/
DECAy half life for C is 2.41e+4
DECAy half life for C2 is 6.56e+3
DECAy half life for C3 is 3.75e+5
/
BOUN C -1 FLUX = 0.
BOUN C +1 FLUX = 0.
BOUN C -2 VALU = 0.
BOUN C +2 VALU = 0.
/
BOUN C2 -1 FLUX = 0.
BOUN C2 +1 FLUX = 0.
BOUN C2 -2 VALU = 0.
BOUN C2 +2 VALU = 0.
/
BOUN C3 -1 FLUX = 0.
BOUN C3 +1 FLUX = 0.
BOUN C3 -2 VALU = 0.
BOUN C3 +2 VALU = 0.
/
/
/ OPERATIONAL CONTROL
/
PROPERty for C C2 C3 is HARM mean
MATRIX in X and Y directions for C C2 C3 in 1 sweeps using ADI
CONVergence for C REFERENCE; LOCAL mode; value = 1.0e-04, max of 5 iterations
CONVergence for C2 REFERENCE; LOCAL mode; value = 1.0e-04, max of 5 iterations

CONVergence for C3 REFERENCE; LOCAL mode; value = 1.0e-04, max of 5 iterations
/
DIAGNostic node for C2 and C3 at (39, 3) every 4 steps
OUTPUt every 900000 steps
/
FLUX BALANCE for C in 'flux.out' for ID=TOTL every 20 stps
FLUX BALANCE for C for ID=VALT every 20 stps
FLUX BALANCE for C2 for ID=TOTL every 20 stps
FLUX BALANCE for C2 for ID=VALT every 20 stps
/
FLUX BALANCE for C3 for ID=TOTL every 20 stps
FLUX BALANCE for C3 for ID=VALT every 20 stps
/

```

Fig. M.1-5. (continued).

```

DISABle FLOW
HISTory for C C2 C3 (39, 29) (39, 21) (39, 3) every 20 in 'hist.out'
/
SOLV for C C2 C3 100 init 0.050 inc 1.000 max 0.100 mn 1.e-4 1.1 900000
SAVE C C2 C3 NOW in 'end.0'
/
SOLV for C C2 C3 100 init 0.100 inc 1.001 max 0.100 mn 1.e-4 1.1 900000
SAVE C C2 C3 NOW in 'end.0'
/
SOLV for C C2 C3 100 init 0.200 inc 1.001 max 0.100 mn 1.e-4 1.1 900000
SAVE C C2 C3 NOW in 'end.0'
/
SOLV for C C2 C3 100 init 0.100 inc 1.001 max 0.100 mn 1.e-4 1.1 900000
SAVE C C2 C3 NOW in 'end.1'
/
SOLV for C C2 C3 100 init 0.100 inc 1.001 max 0.100 mn 1.e-4 1.1 900000
SAVE C C2 C3 NOW in 'end.1'
/
SOLV for C C2 C3 75 init 0.100 inc 1.001 max 0.100 mn 1.e-4 1.1 900000
SAVE C C2 C3 NOW in 'end.1'
/
END

```

Fig. M.1-5. (continued).

M2 PORFLOW INPUT FILES - GROUNDWATER

```

TITLE Flow Code for Contaminant Transport Modeling
/File Eflow40.dat September 14, 1993
/PORFLOW-3D Version 2.50
/Base flow file for E-Area simulations
/Version for constant heads along internal streams
/Recharge=40cm/yr
GRID 38 by 30 by 28
/
/Note: Length units are in cm, time units are in years
/
COORDinate X -10000, 0, 45000, 90000, 135000, 145000, 155000,
165000, 175000, 185000, 195000, 205000, 215000, 225000,
235000, 245000, 250000, 257500, 265000, 272500, 280000,
287500, 295000, 302500, 310000, 317500, 325000, 332500,
340000, 347500, 355000, 362500, 370000, 380000, 390000,
427500, 465000, 475000,
/
COORDinate Y -7500, 0, 7500, 15000, 22500, 30000, 37500,
45000, 52500, 60000, 67500, 75000, 82500, 90000,
97500, 105000, 115000, 125000, 135000, 145000, 155000,
165000, 175000, 185000, 195000, 215000, 242500, 292500,
342500, 352500,
/
COORDinate Z 610, 732, 2073, 3414, 3536, 3658, 3780,
3901, 4023, 4785, 5547, 5669, 5791, 5913,
6035, 6157, 6370, 6553, 6751, 6949, 7148,
7346, 7544, 7742, 7940, 8138, 8336, 8534,
/
/Note: Boundary conditions for Upper Three Runs
LOCAte region (1,1,6) to (1,2,6) ; ID=UT1
LOCAte region (1,3,6) to (1,5,6) ; ID=UT2
LOCAte region (2,5,6) to (2,7,6) ; ID=UT3
LOCAte region (2,8,7) to (2,11,7); ID=UT4
LOCAte region (2,12,7) to (2,15,7); ID=UT5
LOCAte region (2,16,8) to (2,19,8); ID=UT6
LOCAte region (3,19,8) to (3,22,8); ID=UT7
LOCAte region (4,22,8) to (4,23,8); ID=UT8
LOCAte region (5,23,9) to (5,24,9); ID=UT9
LOCAte region (6,24,9) to (6,25,9); ID=UT10
LOCAte region (7,25,9) to (9,25,9); ID=UT11
LOCAte region (10,25,9) to (14,25,9); ID=UT12
LOCAte region (15,25,9) to (16,25,9); ID=UT13
LOCAte region (16,24,9) to (20,24,9); ID=UT14
LOCAte region (21,24,9) to (21,25,9); ID=UT15
LOCAte region (22,25,9) to (24,25,9); ID=UT16
LOCAte region (24,26,9) to (28,26,9); ID=UT17

```

Fig. M2-1. PORFLOW-3D input files for the groundwater flow field.

```

LOCAtc region (29,26,9) to (32,26,9); ID=UT18
LOCAtc region (32,27,9) to (33,27,9); ID=UT19
LOCAtc region (33,28,9) to (35,28,9); ID=UT20
LOCAtc region (35,29,9) to (37,29,9); ID=UT21
LOCAtc region (37,30,9) to (38,30,9); ID=UT22
/
//Note: Boundary Conditions for the "Unnamed Branch"
LOCAtc region (6,22,9) to (6,23,9); ID=UB1 $Reach 18-19 #2
LOCAtc region (7,21,9) to (7,21,9); ID=UB2 $Reach 18-19 #1
LOCAtc region (7,20,10) to (8,20,10); ID=UB3 $Reach 18-19 #2
LOCAtc region (8,19,10) to (9,19,10); ID=UB4 $Reach 19-20 #2
LOCAtc region (9,18,10) to (10,18,10); ID=UB5 $Reach 19-20 #2
LOCAtc region (10,17,11) to (11,17,11); ID=UB6 $Reach 19-20 #2
LOCAtc region (11,16,16) to (11,16,16); ID=UB7 $Reach 19-20 #1
LOCAtc region (11,15,16) to (11,15,16); ID=UB8 $Reach 20-POE #1
LOCAtc region (12,15,17) to (12,15,17); ID=UB9 $Reach 20-POE #1
LOCAtc region (12,14,18) to (12,14,18); ID=UB10 $Reach 20-POE #1
LOCAtc region (13,14,19) to (13,14,19); ID=UB11 $Reach 20-POE #1
LOCAtc region (13,13,20) to (13,13,20); ID=UB12 $Reach 20-POE #1
LOCAtc region (13,12,21) to (13,12,21); ID=UB13 $Reach 20-POE #1
LOCAtc region (14,12,22) to (14,12,22); ID=UB14
/
//Note: Boundary Conditions for Crouch Branch
LOCAtc region (24,23,9) to (24,24,9); ID=CB1 $Reach 1-2 #2
LOCAtc region (25,22,9) to (26,22,9); ID=CB2 $Reach 2-12 #2
LOCAtc region (27,21,9) to (28,21,9); ID=CB3 $Reach 12-13 #2
LOCAtc region (28,20,10) to (29,20,10); ID=CB4 $Reach 12-13 #2
LOCAtc region (30,19,10) to (32,19,10); ID=CB5 $Reach 13-14 #3
LOCAtc region (32,18,10) to (32,18,10); ID=CB6 $Reach 13-14 #1
LOCAtc region (33,15,11) to (33,17,11); ID=CB7 $Reach 14-16 #3
LOCAtc region (34,15,16) to (34,15,16); ID=CB8 $Reach 14-16 #1
LOCAtc region (34,14,16) to (34,14,16); ID=CB9 $Reach 14-16 #1
LOCAtc region (34,12,16) to (34,13,16); ID=CB10 $Reach 16-4 #2
LOCAtc region (35,12,17) to (35,12,17); ID=CB11 $Reach 16-4 #1
LOCAtc region (35,11,18) to (35,11,18); ID=CB12 $Reach 16-4 #1
LOCAtc region (35,10,19) to (35,10,19); ID=CB13 $Reach 16-4 #1
/
//Central tributary
LOCAtc region (17,22,9) to (17,23,9); ID=CENT $Reach 17-POE #2
/
//Regions of initial head conditions for problem domain
/
LOCAtc region (2,2,12) to (38,30,28); ID=dom1
LOCAtc region (2,2,5) to (38,30,11); ID=dom2
LOCAtc region (2,1,1) to (38,30,4); ID=dom3
LOCAtc region (1,25,1) to (35,30,28); ID=dom4
LOCAtc region (1,1,1) to (2,24,28); ID=dom5
/

```

Fig. M.2-1. (continued).

MATERIAL type 1 from (1,1,1) to (38,30,28) \$Barnwell
 MATERIAL type 2 from (1,1,12) to (38,30,15) \$Tan Clay
 MATERIAL type 3 from (1,1,9) to (38,30,11) \$McBean Formation
 MATERIAL type 4 from (1,1,5) to (38,30,8) \$Green Clay
 MATERIAL type 5 from (1,1,1) to (38,30,4) \$Congaree Formation
 MATERIAL type 5 from (1,5,1) to (2,30,28) \$Congaree Formation
 MATERIAL type 5 from (2,22,1) to (4,30,28) \$Congaree Formation
 MATERIAL type 5 from (5,25,1) to (25,30,28) \$Congaree Formation
 MATERIAL type 5 from (23,23,1) to (24,24,28) \$Congaree Formation
 MATERIAL type 5 from (25,26,1) to (31,30,28) \$Congaree Formation
 MATERIAL type 5 from (32,26,1) to (33,30,28) \$Congaree Formation
 MATERIAL type 5 from (34,28,1) to (35,30,28) \$Congaree Formation
 MATERIAL type 5 from (36,29,1) to (36,30,28) \$Congaree Formation

/

/INITIAL Head conditions for problem domain

/

SET LINEar func P = 7.224e3 -0.01 * Y for ID=dom1

SET LINEar func P = 6.888e3 -0.01 * Y for ID=dom2

SET LINEar func P = 5.090e3 -0.0047 * Y for ID=dom3

SET LINEar func P = 4.115e3 +0.00106 * X for ID=dom4

SET LINEar func P = 3.962e3 +0.00076 * Y for ID=dom5

/

/Note: Boundary conditions for Upper Three Runs

FIXEd P is 3.627e3 for ID=UT1

FIXEd P is 3.657e3 for ID=UT2

FIXEd P is 3.719e3 for ID=UT3

FIXEd P is 3.780e3 for ID=UT4

FIXEd P is 3.840e3 for ID=UT5

FIXEd P is 3.901e3 for ID=UT6

FIXEd P is 3.962e3 for ID=UT7

FIXEd P is 3.993e3 for ID=UT8

FIXEd P is 4.023e3 for ID=UT9

FIXEd P is 4.054e3 for ID=UT10

FIXEd P is 4.084e3 for ID=UT11

FIXEd P is 4.145e3 for ID=UT12

FIXEd P is 4.176e3 for ID=UT13

FIXEd P is 4.206e3 for ID=UT14

FIXEd P is 4.237e3 for ID=UT15

FIXEd P is 4.267e3 for ID=UT16

FIXEd P is 4.328e3 for ID=UT17

FIXEd P is 4.389e3 for ID=UT18

FIXEd P is 4.450e3 for ID=UT19

FIXEd P is 4.511e3 for ID=UT20

FIXEd P is 4.572e3 for ID=UT21

FIXEd P is 4.633e3 for ID=UT22

/

Fig. M2-1. (continued).

/Note: Boundary Conditions for the "Unnamed Branch"

FIXED P = 4.267e3 for ID=UB1
 FIXED P = 4.572e3 for ID=UB2
 FIXED P = 4.876e3 for ID=UB3
 FIXED P = 5.182e3 for ID=UB4
 FIXED P = 5.486e3 for ID=UB5
 FIXED P = 5.791e3 for ID=UB6
 FIXED P = 6.096e3 for ID=UB7
 FIXED P = 6.248e3 for ID=UB8
 FIXED P = 6.401e3 for ID=UB9
 /FIXED P = 6.553e3 for ID=UB10
 /FIXED P = 6.767e3 for ID=UB11
 /FIXED P = 7.010e3 for ID=UB12
 /FIXED P = 7.163e3 for ID=UB13
 /SET P = 7.346e3 for ID=UB14
 /

/Note: Boundary Conditions for Crouch Branch

FIXED P = 4.267e3 for ID=CB1
 FIXED P = 4.420e3 for ID=CB2
 FIXED P = 4.572e3 for ID=CB3
 FIXED P = 4.785e3 for ID=CB4
 FIXED P = 5.029e3 for ID=CB5
 FIXED P = 5.151e3 for ID=CB6
 FIXED P = 5.791e3 for ID=CB7
 FIXED P = 6.035e3 for ID=CB8
 FIXED P = 6.248e3 for ID=CB9
 FIXED P = 6.350e3 for ID=CB10
 FIXED P = 6.401e3 for ID=CB11
 FIXED P = 6.553e3 for ID=CB12
 FIXED P = 6.767e3 for ID=CB13
 /

BOUNDary P for -1 FLUX = 0

BOUNDary P for +1 FLUX = 0

BOUNDary P for +2 FLUX = 0

LOCAtc region (2,1,5) to (37,1,28); ID=DIV

BOUNDary P for -2 FLUX = 0 for ID=DIV \$Drainage divide for the McBean/Barnwell

LOCAtc region (2,1,1) to (37,1,4); ID=REG

BOUNDary P for -2 FLUX = 9.0e2 cm/yr for ID=REG \$ Regional Congaree flow

BOUNDary P for -3 FLUX = 3.65e-5 cm/yr \$ Recharge from the Ellenton

BOUNDary P for +3 FLUX = -4.00e1 cm/yr \$ Recharge from precipitation
 /

FOR 1:

HYDRaulic ss=0.0001, Kx = 4.0e4, Ky = 4.0e4, Kz = 1.0e4 cm/yr

FOR 2:

HYDRaulic ss=0.0001, Kx = 6.4e1, Ky = 6.4e1, Kz = 4.3e1 cm/yr

FOR 3: \$Barnwell/McBean

HYDRaulic ss=0.0001, Kx = 4.1e4, Ky = 4.1e4, Kz = 3.1e4 cm/yr

FOR 4:

HYDRaulic ss=0.0001, Kx = 3.0, Ky = 3.0, Kz = 2.0 cm/yr

Fig. M.2-1. (continued).

```

FOR 5:
HYDRaulic ss=0.0001, Kx = 4.2e5, Ky = 4.2e5, Kz = 4.2e4 cm/yr
/
/Note: Flux Balance for Unnamed Branch
FLUX BALance for P for ID=UB1 every 500 steps
FLUX BALance for P for ID=UB2 every 500 steps
FLUX BALance for P for ID=UB3 every 500 steps
FLUX BALance for P for ID=UB4 every 500 steps
FLUX BALance for P for ID=UB5 every 500 steps
FLUX BALance for P for ID=UB6 every 500 steps
FLUX BALance for P for ID=UB7 every 500 steps
FLUX BALance for P for ID=UB8 every 500 steps
FLUX BALance for P for ID=UB9 every 500 steps
FLUX BALance for P for ID=UB10 every 500 steps
FLUX BALance for P for ID=UB11 every 500 steps
FLUX BALance for P for ID=UB12 every 500 steps
FLUX BALance for P for ID=UB13 every 500 steps
/
/Note: Flux Balance for Crouch Branch
FLUX BALance for P for ID=CB1 every 500 steps
FLUX BALance for P for ID=CB2 every 500 steps
FLUX BALance for P for ID=CB3 every 500 steps
FLUX BALance for P for ID=CB4 every 500 steps
FLUX BALance for P for ID=CB5 every 500 steps
FLUX BALance for P for ID=CB6 every 500 steps
FLUX BALance for P for ID=CB7 every 500 steps
FLUX BALance for P for ID=CB8 every 500 steps
FLUX BALance for P for ID=CB8 every 500 steps
FLUX BALance for P for ID=CB9 every 500 steps
FLUX BALance for P for ID=CB10 every 500 steps
FLUX BALance for P for ID=CB11 every 500 steps
FLUX BALance for P for ID=CB12 every 500 steps
FLUX BALance for P for ID=CB13 every 500 steps
/
/Note: Flux Balance for entire domain
FLUX BALance for P everywhere every 500 steps
/
/Note: Flux Balance for entire domain
/
CONVergence for P; GLOBal mode; value=1.e-5, 3 iterations
DIAGnostic for P and U at node (33,16,11)
/
MATRix P = 3
/
SOLVe in STEADy state mode: maximum steps 1000
OUTPut: P,U,V,W
/OUTPUT P, U, V, W in XZ plane
SAVE on file 'eflow40.arc'
END

```

Fig. M.2-1. (continued).

```

TITLE CONTAMINANT TRANSPORT FOR E-AREA
/FILE Erun1.dat January 18, 1994
/PORFLOW version 2.50
/
/Contaminant transport modeling LAW, ILTV, ILNTV
/C-14, Tc-99
/
GRID 38 by 30 by 28
/units are in cm's
COORDinate X -10000, 0, 45000, 90000, 135000, 145000, 155000,
165000, 175000, 185000, 195000, 205000, 215000, 225000,
235000, 245000, 250000, 257500, 265000, 272500, 280000,
287500, 295000, 302500, 310000, 317500, 325000, 332500,
340000, 347500, 355000, 362500, 370000, 380000, 390000,
427500, 465000, 475000,
/
COORDinate Y -7500, 0, 7500, 15000, 22500, 30000, 37500,
45000, 52500, 60000, 67500, 75000, 82500, 90000,
97500, 105000, 115000, 125000, 135000, 145000, 155000,
165000, 175000, 185000, 195000, 215000, 242500, 292500,
342500, 352500,
/
COORDinate Z 610, 732, 2073, 3414, 3536, 3658, 3780,
3901, 4023, 4785, 5547, 5669, 5791, 5913,
6035, 6157, 6370, 6553, 6751, 6949, 7148,
7346, 7544, 7742, 7940, 8138, 8336, 8534,
/
/
READ 'eflow40.arc' $40 cm/yr through vault regions
/
/Identify a no-diffusion zone at top of domain to allow mass conservation
MATERial type 10 from (1,1,21) to (38,30,28)
/
FOR 1:
ROCK density = 2.65; porosity = .30, .40, .30
TRANsport properties for C Kd = 2.0, md = 158., Ld = 300., Td= 30.
TRANsport properties for C3 Kd = 2.0, md = 158., Ld = 300., Td= 30.
TRANsport properties for C2 Kd = 0.36, md = 158., Ld = 300., Td= 30.
TRANsport properties for C4 Kd = 0.36, md = 158., Ld = 300., Td= 30.
FOR 2:
ROCK density = 2.65; porosity = .30, .40, .30
TRANsport properties for C Kd = 2.0, md = 158., Ld = 300., Td= 30.
TRANsport properties for C3 Kd = 2.0, md = 158., Ld = 300., Td= 30.
TRANsport properties for C2 Kd = 1., md = 158., Ld = 300., Td= 30.
TRANsport properties for C4 Kd = 1., md = 158., Ld = 300., Td= 30.
FOR 3:
ROCK density = 2.65; porosity = .30, .40, .30
TRANsport properties for C Kd = 2.0, md = 158., Ld = 300., Td= 30.
TRANsport properties for C3 Kd = 2.0, md = 158., Ld = 300., Td= 30.
TRANsport properties for C2 Kd = 0.36, md = 158., Ld = 300., Td= 30.
TRANsport properties for C4 Kd = 0.36, md = 158., Ld = 300., Td= 30.

```

Fig. M2-2. PORFLOW-3D input file for the groundwater mass transport of C-14 and Tc-99.

FOR 4:

ROCK density = 2.65; porosity = .30, .40, .30

TRANsport properties for C Kd = 2.0, md = 158., Ld = 300., Td = 30.

TRANsport properties for C3 Kd = 2.0, md = 158., Ld = 300., Td = 30.

TRANsport properties for C2 Kd = 1., md = 158., Ld = 300., Td = 30.

TRANsport properties for C4 Kd = 1., md = 158., Ld = 300., Td = 30.

FOR 5:

ROCK density = 2.65; porosity = .30, .40, .30

TRANsport properties for C Kd = 2.0, md = 158., Ld = 300., Td = 30.

TRANsport properties for C3 Kd = 2.0, md = 158., Ld = 300., Td = 30.

TRANsport properties for C2 Kd = 0.36, md = 158., Ld = 300., Td = 30.

TRANsport properties for C4 Kd = 0.36, md = 158., Ld = 300., Td = 30.

FOR 6:

ROCK density = 2.65; porosity = .30, .40, .30

TRANsport properties for C Kd = 2.0, md = 158., Ld = 300., Td = 30.

TRANsport properties for C3 Kd = 2.0, md = 158., Ld = 300., Td = 30.

TRANsport properties for C2 Kd = 0.36, md = 158., Ld = 300., Td = 30.

TRANsport properties for C4 Kd = 0.36, md = 158., Ld = 300., Td = 30.

FOR 7:

ROCK density = 2.65; porosity = .30, .40, .30

TRANsport properties for C Kd = 2.0, md = 158., Ld = 300., Td = 30.

TRANsport properties for C3 Kd = 2.0, md = 158., Ld = 300., Td = 30.

TRANsport properties for C2 Kd = 0.36, md = 158., Ld = 300., Td = 30.

TRANsport properties for C4 Kd = 0.36, md = 158., Ld = 300., Td = 30.

FOR 10:

ROCK density = 2.65; porosity = .30, .40, .30

TRANsport properties for C Kd = 2.0, md = 0., Ld = 0., Td = 0.

TRANsport properties for C3 Kd = 2.0, md = 0., Ld = 0., Td = 0.

TRANsport properties for C2 Kd = 0.36, md = 0., Ld = 0., Td = 0.

TRANsport properties for C4 Kd = 0.36, md = 0., Ld = 0., Td = 0.

/

/Specification for mass species C; C-14

/

DECAy half life of C is 5730. years

INITIAL C = 0.0 everywhere

BOUNDary C at -1 FLUX = 0.0

BOUNDary C at +1 FLUX = 0.0

BOUNDary C at -2 FLUX = 0.0

BOUNDary C at +2 FLUX = 0.0

BOUNDary C at -3 FLUX = 0.0

BOUNDary C at +3 FLUX = 0.0

/

/Specifications for mass species C3; C-14

/

DECAy half-life of C3 is 5730. years

INITIAL C3 = 0.0 everywhere

BOUNDary C3 at -1 FLUX = 0.0

BOUNDary C3 at +1 FLUX = 0.0

BOUNDary C3 at -2 FLUX = 0.0

BOUNDary C3 at +2 FLUX = 0.0

BOUNDary C3 at -3 FLUX = 0.0

BOUNDary C3 at +3 FLUX = 0.0

/

Fig. M2-2. (continued).

```
/Specifications for mass species C2; Tc-99
/
DECAY half-life of C2 is 2.13e5 years
INITIAL C2 = 0.0 everywhere
BOUNDary C2 at -1 FLUX =0.0
BOUNDary C2 at +1 FLUX =0.0
BOUNDary C2 at -2 FLUX =0.0
BOUNDary C2 at +2 FLUX =0.0
BOUNDary C2 at -3 FLUX =0.0
BOUNDary C2 at +3 FLUX =0.0
/
/Specifications for mass species C4; Tc-99
/
DECAY half-life of C4 is 2.13e5 years
INITIAL C4 = 0.0 everywhere
BOUNDary C4 at -1 FLUX =0.0
BOUNDary C4 at +1 FLUX =0.0
BOUNDary C4 at -2 FLUX =0.0
BOUNDary C4 at +2 FLUX =0.0
BOUNDary C4 at -3 FLUX =0.0
BOUNDary C4 at +3 FLUX =0.0
/
DISABLE FLOW
DIAGNOSTIC U, C at (19,14,20) $under ILT/ILNT vaults
/DIAGNOSTIC U and C at 26,11,20
/Material type 6 is ILT/ILNT vaults
Material type 6 from (17,14,20) to (17,14,20)
Material type 6 from (19,13,20) to (19,15,20)
LOCATE material type 6 as ID=ILNT
/Material type 7 is LAW vaults
MATERIAL type 7 from (21,14,20) to (23,14,20)
MATERIAL type 7 from (21,12,20) to (27,13,20)
MATERIAL type 7 from (27,9,20) to (27,9,20)
MATERIAL type 7 from (28,7,20) to (28,10,20)
MATERIAL type 7 from (29,6,20) to (29,9,20)
MATERIAL type 7 from (30,4,20) to (30,8,20)
MATERIAL type 7 from (31,3,20) to (31,6,20)
LOCATE material type 7 as subregion ID=LAWV
/
/MATERIAL type 8 is Suspect Soil Trenches
/MATERIAL type 9 is Naval Reactor Components
/
```

Fig. M.2-2. (continued).

*** C-14 ***

SOURCE C for ID=ILNT per VOLUME TABLE 30 sets SpCi/cc-yr per pCi inventory

0.0000E+00	0.0000E+00	
3.2400E+02	2.5565E-49	\$too low
5.3600E+02	4.5313E-47	\$too low
7.4700E+02	6.0532E-32	
9.6100E+02	1.0934E-27	
1.1720E+03	2.8703E-24	
1.3840E+03	3.1634E-23	
1.6610E+03	3.0947E-22	
3.2775E+03	3.2781E-19	
1.2003E+04	3.7479E-17	
1.2739E+04	3.7194E-17	
1.3552E+04	3.6233E-17	
1.4451E+04	3.4615E-17	
1.5444E+04	3.2400E-17	
1.6542E+04	2.9672E-17	
1.7756E+04	2.6593E-17	
1.9096E+04	2.3300E-17	
2.0568E+04	1.9975E-17	
2.2068E+04	1.6954E-17	
2.3568E+04	1.4326E-17	
2.5060E+04	1.2081E-17	
2.6643E+04	1.0051E-17	
2.8393E+04	8.1957E-18	
3.0326E+04	6.5288E-18	
3.2463E+04	5.0716E-18	
3.4824E+04	3.8321E-18	
3.7323E+04	2.8456E-18	
3.9823E+04	2.1102E-18	
4.2323E+04	1.5631E-18	
4.5323E+04	1.0894E-18	

*** TC-99 ***

SOURCE C2 for ID=ILNT per VOLUME TABLE 30 sets SpCi/cc-yr per pCi inventory

0.0000E+00	0.0000E+00	
2.4400E+02	4.3160E-40	\$too low
4.1600E+02	1.1503E-38	\$too low
5.8700E+02	6.4031E-36	\$too low
7.5900E+02	8.6662E-20	
9.3100E+02	2.8593E-17	
1.1020E+03	1.6113E-15	
1.2740E+03	6.4433E-15	
1.4460E+03	1.2834E-14	
1.7318E+03	1.7823E-14	
1.8478E+03	1.7147E-14	
1.9949E+03	1.5001E-14	
2.1674E+03	1.1852E-14	
2.4008E+03	8.0364E-15	
2.7158E+03	4.6094E-15	
3.1409E+03	2.3118E-15	

Fig. M.2-2. (continued).

3.7147E+03	1.1117E-15
4.4891E+03	5.9122E-16
5.4129E+03	3.8314E-16
6.6992E+03	2.3791E-16
8.1896E+03	1.2646E-16
9.6896E+03	5.8195E-17
1.1336E+04	2.1068E-17
1.3552E+04	4.2110E-18
1.6542E+04	3.3684E-19
2.0568E+04	7.9468E-21
2.5060E+04	7.4467E-23
3.0326E+04	2.8667E-25
3.7323E+04	9.8763E-28
4.5323E+04	1.2356E-29
*** C-14 ***	
SOURCE C3 for ID=LAWV per VOLUME TABLE 30 sets SpCi/cc-yr per pCi inventory	
0.0000E+00	0.0000E+00
3.0400E+02	5.7979E-34
5.5600E+02	2.0641E-32
8.0800E+02	1.3554E-31
1.0600E+03	4.7169E-31
1.3120E+03	1.1846E-30
1.8788E+03	2.1227E-20
2.6348E+03	8.7186E-19
3.9246E+03	2.5340E-16
4.8129E+03	3.5774E-16
4.9329E+03	3.5656E-16
5.3992E+03	3.3065E-16
6.3208E+03	2.3462E-16
7.5696E+03	1.1693E-16
8.8696E+03	4.8546E-17
1.0065E+04	1.9969E-17
1.1569E+04	6.1735E-18
1.3349E+04	1.5338E-18
1.5827E+04	2.8952E-19
1.9040E+04	8.2027E-20
2.2608E+04	3.5230E-20
2.6577E+04	1.4225E-20
3.1071E+04	4.6617E-20
3.7223E+04	9.0923E-22
4.3723E+04	1.2840E-22
4.9723E+04	1.8533E-23
5.7033E+04	1.5780E-24
6.5716E+04	7.4287E-26
7.7725E+04	9.1264E-28
9.0725E+04	6.4513E-30
*** TC-99 ***	

Fig. M.2-2. (continued).

SOURCE C4 for ID=LAWV per VOLUME TABLE 30 sets SpCi/cc-yr per pCi inventory

0.0000E+00	0.0000E+00
2.3600E+02	2.6308E-30
4.5600E+02	4.4868E-29
6.7400E+02	2.1524E-28
8.9400E+02	6.5177E-28
1.1120E+03	1.5236E-27
1.3300E+03	3.0497E-27
1.8368E+03	5.5216E-17
2.4908E+03	2.9471E-16
3.2046E+03	4.5871E-15
3.5106E+03	2.4235E-15
3.8166E+03	7.1396E-16
4.0146E+03	2.8688E-16
4.0609E+03	2.3003E-16
4.1261E+03	1.6834E-16
4.2175E+03	1.0851E-16
4.3460E+03	5.9049E-17
4.5129E+03	2.8162E-17
4.6829E+03	1.4811E-17
4.8529E+03	9.1349E-18
5.1380E+03	5.6391E-18
6.4080E+03	1.9519E-18
8.0696E+03	3.1007E-19
9.7696E+03	2.6895E-20
1.1701E+04	1.1990E-21
1.4413E+04	9.1349E-24
1.8223E+04	6.2253E-27
2.3208E+04	2.9453E-31
2.8689E+04	4.2633E-36
3.6723E+04	3.4483E-43

Stoo low
Stoo low

HISTORY for C, C2, C3, C4 TABLE at (17,14,20)(19,17,18)(19,17,16)

(19,17,20)(30,11,10)(23,16,20)(23,16,18)(22,16,20)

(22,16,18) frequency=3 on 'ctc.hst'

OUTPUT C, C2, C3, C4

CONVERGENCE for C2 REFE 1.e-3, max iterations = 3

DIAGNOSTIC U, C2 at (19,14,20) Sunder ILT/ILNT vaults

SOLVE C, C2, C3, C4 AUTO 1.7e32,DT=1.,fac=2.,mx=100,mn=1.e-8,df=2,nx=100000

SAVE C2, C4 NOW in 'ctc.arc'

SOLVE C, C2, C3, C4 AUTO 1.e2,DT=1.,fac=2.,mx=100,mn=1.e-8,df=2,nx=100000

SAVE C2, C4 NOW in 'ctc.arc'

SOLVE C, C2, C3, C4 AUTO 1.e2,DT=1.,fac=2.,mx=100,mn=1.e-8,df=2,nx=100000

SAVE C2, C4 NOW in 'ctc.arc'

SOLVE C, C2, C3, C4 AUTO 1.1e3,DT=1.,fac=2.,mx=100,mn=1.e-8,df=2,nx=100000

SAVE C2, C4 NOW in 'ctc.arc'

SOLVE C, C2, C3, C4 AUTO 2.0e2,DT=1.,fac=2.,mx=100,mn=1.e-8,df=2,nx=100000

SAVE C2, C4 NOW in 'ctc.arc'

SOLVE C, C2, C3, C4 AUTO 1.0e2,DT=1.,fac=2.,mx=100,mn=1.e-8,df=2,nx=100000

SAVE C2, C4 NOW in 'ctc.arc'

SOLVE C, C2, C3, C4 AUTO 1.0e2,DT=1.,fac=2.,mx=100,mn=1.e-8,df=2,nx=100000

SAVE C2, C4 NOW in 'ctc.arc' \$3.4e3

Fig. M.2-2. (continued).

CONvergence for C3 REFE 1.e-3, max iterations = 3
DIAGnostic U, C3 at (19,14,20) \$under ILT/ILNT vaults
SOLVE C, C2, C3, C4 AUTO 1.4e3,DT=1.,fac=2.,mx=100,mn=1.e-8,df=2,nx=100000
SAVE C, C2, C3, C4 NOW in 'etc.arc' \$4.8e3
SOLVE C, C2, C3, C4 AUTO 1.2e3,DT=1.,fac=2.,mx=100,mn=1.e-8,df=2,nx=100000
SAVE C, C2, C3, C4 NOW in 'etc.arc' \$6.0e3 years
SOLVE C, C2, C3, C4 AUTO 6.e3,DT=1.,fac=2.,mx=100,mn=1.e-8,df=2,nx=100000
SAVE C, C2, C3, C4 NOW in 'etc.arc' \$1.2e4 years
SOLVE C, C3 AUTO 1.0e3,DT=1.,fac=2.,mx=100,mn=1.e-8,df=2,nx=100000
SAVE C, C3 NOW in 'etc.arc' \$1.3e4 years
SOLVE C, C3 AUTO 1.0e4,DT=1.,fac=2.,mx=1000,mn=1.e-8,df=2,nx=100000
SAVE C, C3 NOW in 'etc.arc' \$2.3e4 years
SOLVE C, C3 AUTO 1.0e4,DT=1.,fac=2.,mx=1000,mn=1.e-8,df=2,nx=100000
SAVE C, C3 NOW in 'etc.arc' \$3.3e4 years
SOLVE C, C3 AUTO 1.0e4,DT=1.,fac=2.,mx=1000,mn=1.e-8,df=2,nx=100000
SAVE C, C3 NOW in 'etc.arc' \$4.3e4 years
END

Fig. M2-2. (continued).

Rev. 0